THE JOURNAL
OF
CHEMICAL PHYSICS

VOLUME 20, NUMBER 10 OCTOBER, 1952

Nuclear Electric Quadrupole Spectra in Solids

R. BERSOHN
Department of Chemistry, Cornell University, Ithaca, New York

(Received April 9, 1952)

Recent experiments have demonstrated the feasibility of observing nuclear electric quadrupole interactions of widely varying magnitudes in solids. While these effects can often be observed in powdered samples, the most complete information is obtainable from the Zeeman pattern of a single crystal. To facilitate interpretation of these experiments, the nuclear spin energy levels are derived for different relative magnitudes of quadrupole interaction and external magnetic field. Besides the knowledge of the gradient of the electric field tensor, in principle, low frequency molecular rotation should be detectable by means of the quadrupole spectra.

A NUCLEUS interacts with the charged particles surrounding it principally as if it were a point charge. Nonspherically symmetric nuclei possess in addition an energy of interaction that is (nuclear radius/atomic radius)^2 smaller than the principal interaction but has the virtue of being dependent on the orientation of the nucleus. This interaction can be studied by measuring the magnetic dipole transition spectrum of a solid, and in this way simultaneous information[1–6] has been obtained about the departure from spherical symmetry of the electric field surrounding the nucleus and of the nucleus itself.

The underlying physical theory has been discussed by Pound,[1] and using this theory several relations will be derived that are intended to help in the interpretation of these experiments. In practice, three situations have arisen:

1. The electric quadrupole interactions are comparable with magnetic interactions due to surrounding magnetic dipoles.[4]
2. The electric quadrupole interaction is rather less than the energy of the nucleus in the external magnetic field.[4,5,6]
3. The electric quadrupole interaction is rather greater than the energy of the nucleus in the external magnetic field.[1,2,3,7]

I. SECOND MOMENT OF ABSORPTION CURVE

When the electric interactions are so feeble that they are comparable with magnetic interactions due to surrounding dipoles, the absorption curve may show no structure but may be considerably broadened. The line width may still be analyzed by the determination of its moments as was done by Van Vleck.[8] The Hamiltonian for a system of spins will consist of three parts:

$$\mathcal{H}=\mathcal{H}_{\text{Zeeman}}+\mathcal{H}_{\text{dipole-dipole and exchange}}+\mathcal{H}_{\text{electrostatic}}$$

$$=\beta H\Big(g\sum_{j=1}^{N}S_{zj}+g'\sum_{j'=1}^{N'}S_{zj'}\Big)+\sum_{j>k}\left(A_{jk}\mathbf{S}_j\cdot\mathbf{S}_k+B_{jk}S_{zj}S_{zk}\right)+\sum_{j'<k'}\left(A_{j'k'}\mathbf{S}_{j'}\cdot\mathbf{S}_{k'}+B_{j'k'}S_{zj'}S_{zk'}\right)+\sum_{j,k'}C_{jk'}S_{zj}S_{zk'}+\sum_{j=1}^{N}\left(E_jS_{zj}^2+F_jS_{zj}^4\right). \quad (1)$$

Aside from the standard notation

$$A_{jk}=\tilde{A}_{jk}+g^2\beta^2/r_{jk}^3(\tfrac{3}{2}\gamma_{jk}^2-\tfrac{1}{2}),$$
$$B_{jk}=-3g^2\beta^2/r_{jk}^3(\tfrac{3}{2}\gamma_{jk}^2-\tfrac{1}{2}), \quad (2)$$
$$C_{jk'}=\tilde{A}_{jk'}+(1-3\gamma_{jk'}^2)(gg'\beta^2/r_{jk}^3),$$

z is the direction of the external field; γ_{jk} is the cosine of the angle between the external field and the vector r_{jk} connecting spins j and k. The $\tilde{A}$'s are coefficients of interactions of exchange form.

If the resonant spin is a nuclear spin,

$$E_j=\tfrac{3}{4}[eQ/S(2S-1)](\partial^2V/\partial z^2)_j, \quad (3)$$

the quadrupole coupling constant of th jth nucleus, and F_j is the electric sixteen pole coupling constant. On the

[1] R. V. Pound, Phys. Rev. **79**, 685 (1950); **82**, 343 (1951).
[2] H. G. Dehmelt and H. Kruger, Naturwiss. **37**, 111 (1950); **38**, 921 (1951).
[3] R. Livingston, J. Chem. Phys. **20**, 1170 (1952).
[4] N. A. Schuster and G. E. Pake, Phys. Rev. **81**, 157, 886 (1951).
[5] Hattin, Rollin, and Seymour, Phys. Rev. **83**, 672 (1951).
[6] Petch, Smellie, and Volkoff, Phys. Rev. **84**, 602 (1951).
[7] C. Dean and R. V. Pound, J. Chem. Phys. **20**, 195 (1952).
[8] J. H. Van Vleck, Phys. Rev. **74**, 1168 (1948).

other hand, if the spin is electronic, E_j is the z component of the second-order potential and F_j is the z component of the fourth-order potential. This discussion is not relevant to a paramagnetic system in which spin-orbit coupling has to be introduced explicitly.

As Van Vleck has shown, the mean square frequency of the absorption curve is given by the relation

$$h^2\langle\nu^2\rangle=-\frac{Tr[\mathcal{H},S_x]^2}{TrS_x^2}, \tag{4}$$

where S_x is the x component of the total spin of the resonant spins. The commutator is

$$[\mathcal{H},S_x]=ig\beta H\sum_{j=1}^{N}S_{yj}+i\sum_{k>j}B_{jk}(S_{yj}S_{zk}+S_{zj}S_{yk})+i\sum_{j=1}^{N}\sum_{k'=1}^{N'}C_{jk'}S_{yj}S_{zk'}-i\sum_{j=1}^{N}E_j\{S_{yj},S_{zj}\}-i\sum_{j=1}^{N}F_j\{S_{zj}^2,\{S_{yj},S_{zj}\}\}, \tag{5}$$

where the face brackets are anticommutators.

The mean square frequency can be calculated from this commutator, and the mean square line width can be found from the relations

$$\langle\nu^2\rangle=\langle(\Delta\nu)^2\rangle+\nu_0^2, \tag{6}$$

where $h\nu_0$ is $g\beta H$.

$$\begin{aligned}h^2\langle(\Delta\nu)^2\rangle&=\tfrac{2}{3}\sum_{j>k}\frac{B_{jk}^2}{N}S(S+1)+\sum_{j=1}^{N}\sum_{k'=1}^{N}\frac{C_{jk'}^2}{3N}S(S+1)\\&\quad+\sum_{j=1}^{N}\frac{E_j^2}{N}(\tfrac{4}{5}S(S+1)-\tfrac{3}{5})\\&\quad+\sum_{j=1}^{N}\frac{E_jF_j}{N}\left(\frac{48}{35}S^2(S+1)^2-\frac{76}{35}S(S+1)+\frac{6}{7}\right)\\&\quad+\sum_{j=1}^{N}\frac{F_j^2}{N}\left(\frac{16}{21}S^3(S+1)^3-\frac{268}{105}S^2(S+1)^2+\frac{112}{35}S(S+1)-\frac{9}{7}\right).\end{aligned} \tag{7}$$

In computing these traces the following relations (in addition to those given by Van Vleck) are helpful:

$$\sum_{M=-S}^{S}M^6=\frac{1}{21}[3S^3(S+1)^3-3S^2(S+1)^2+S(S+1)](2S+1), \tag{8}$$

$$\sum_{M=-S}^{S}M^8=\frac{1}{45}[5S^4(S+1)^4-10S^3(S+1)^3+9S^2(S+1)^2-3S(S+1)](2S+1). \tag{9}$$

The first two magnetic interaction terms are just those obtained by Van Vleck. A check on the electric terms results from noticing that when S is one-half, they must vanish and when S is one, the contribution of the jth spin must be $(E_j+F_j)^2$. Van Vleck's conclusion that isotropic exchange coupling only enters in the fourth moment is unaltered by the introduction of electric interactions.*

While the second- and fourth-order potentials appear in the same way, they can be distinguished from each other in a single crystal by the different dependence of E and F on angle which would lead to a different dependence of the mean square line width on angle. When measurements are made on a powder the essential information can still be derived if the electric field is purely tetragonal (and fourth-order terms do not have to be included) or if the electric field is purely cubic. In these cases the average over all magnetic field orientations of E_j^2 and F_j^2 will be $\frac{1}{5}(E_j^0)^2$ and $41/105(F_j^0)^2$, where E_j^0 and F_j^0 are coupling constants referred to the tetragonal axis or one of the cube normals, respectively.

II. QUADRUPOLE SPLITTING OF THE MAGNETIC RESONANCE LINE

If the quadrupole interaction is small compared to the Zeeman energy but large compared to the dipole-dipole interactions, hyperfine structure can be observed. Neglecting the dipole-dipole interactions, each nucleus can be considered separately. The relevant Hamiltonian will be

$$\mathcal{H}=g\beta HI_z+F, \tag{10}$$

where

$$F=Q\cdot\nabla E \tag{11}$$

is the scalar product of the nuclear electric quadrupole moment tensor with the gradient of the electric field tensor and is regarded as a small perturbation. The gradient of the electric field tensor, being irreducible, has five components:

$$\begin{aligned}(\nabla E)_0&=-\tfrac{1}{2}(\partial E_z/\partial z),\\(\nabla E)_{\pm1}&=\frac{1}{\sqrt{6}}\left[\frac{\partial E_x}{\partial z}\pm i\frac{\partial E_y}{\partial z}\right],\\(\nabla E)_{\pm2}&=-\frac{1}{2\sqrt{6}}\left[\frac{\partial E_x}{\partial x}-\frac{\partial E_y}{\partial y}\pm 2i\frac{\partial E_x}{\partial y}\right].\end{aligned} \tag{12}$$

In a representation that diagonalizes the Zeeman energy the matrix elements of F are

$$\begin{aligned}(m|F|m)&=A[3m^2-I(I+1)](\nabla E)_0,\\(m|F|m\pm1)&=\mp(\sqrt{6}/2)A(2m\pm1)\times[(I\pm m+1)(I\mp m)]^{\frac{1}{2}}(\nabla E)_{\mp1},\\(m|F|m\pm2)&=(\sqrt{6}/2)A\{(I\mp m)(I\mp m-1)\times(I\pm m+1)(I\pm m+2)\}^{\frac{1}{2}}(\nabla E)_{\mp2}\\&=\sqrt{6}Af^{\frac{1}{2}}(I,m\pm1)(\nabla E)_{\pm2},\end{aligned} \tag{13}$$

* *Note added in proof.*—Ishiguro, Kambe, and Usui, Physica **17**, 310 (1951) showed that if the exchange and dipolar interactions are very small compared to the quadrupole energy, individual unsymmetrical lines will appear whose second moments depend on the exchange integral.

where $A=eQ/2I(2I-1)$ and Q is the nuclear electric quadrupole moment. $f(I, m)$ is $\frac{1}{4}(I^2-m^2)((I+1)^2-m^2)$.

This situation has been discussed by Carr and Kikuchi,[9] when the electric field surrounding the nucleus has tetragonal symmetry, and more generally by Petch, Smellie, and Volkoff.[6] The same problem will be treated here using different mathematical techniques.

The data to be obtained from this experiment consist of the derivative of the electric field $\partial E_z/\partial z$, an asymmetry parameter $\eta=[(\partial E_x/\partial x)-(\partial E_y/\partial y)]/(\partial E_z/\partial z)$ where x, y, z are the principal axes of the tensor ∇E, and the orientation of these principal axes with respect to the crystallographic axes.

To third order in the quadrupole coupling, the energy of the nuclear state with magnetic quantum number m is

$$E_m=mg\beta H+A[3m^2-I(I+1)](\nabla E)_0+3A^2\frac{(\nabla E)_1(\nabla E)_{-1}}{g\beta H}m[4I(I+1)-1-8m^2]$$
$$+3A^2\frac{(\nabla E)_2(\nabla E)_{-2}}{g\beta H}m[2I(I+1)-1-2m^2]+\tfrac{3}{2}\sqrt{6}\frac{A^3}{g^2\beta^2H^2}\{(\nabla E)_1{}^2(\nabla E)_{-2}+(\nabla E)_{-1}{}^2(\nabla E)_2\}$$
$$\times[2I^2(I+1)^2-3I(I+1)+m^2(-24I(I+1)+15)+30m^4]-9A^3\frac{(\nabla E)_0(\nabla E)_{-1}(\nabla E)_1}{g^2\beta^2H^2}$$
$$\times[I(I+1)+m^2(12I(I+1)-7)-20m^4]+9A^3\frac{(\nabla E)_0(\nabla E_2)(\nabla E)_{-2}}{g^2\beta^2H^2}$$
$$\times[I^2(I+1)^2-2I(I+1)+m^2(-6I(I+1)+7)+5m^4]. \quad (14)$$

Equation (11) relates the observed frequencies to the components of the tensor $(\nabla E)_p$ in an orthogonal system x, y, z whose z axis is the magnetic field. To exhibit explicitly the dependence of the frequencies on the orientation of the crystal in the magnetic field, let a convenient orthogonal axis system X, Y, Z be chosen in the crystal and let the orientation of $\mathbf{H}$ in this system be given by the polar coordinates θ, ϕ. For convenience, let the x axis lie in the X, Y plane.

The components $(\nabla E)_p$ in the x, y, z system are related to the components $(\nabla E)_q'$ in the X, Y, Z system by the equation

$$(\nabla E)_p=\sum_{q=-2}^{2}\mathfrak{D}^{(2)}(\{0\theta\phi\})_{qp}(\nabla E)_q', \quad (15)$$

where the matrix $\mathfrak{D}_{qp}{}^{(j)}$ is the irreducible representation of the rotation group discussed by Wigner.[10]

When Eq. (15) is substituted into Eq. (14), the explicit dependence of the nuclear energy levels on crystal orientation is obtained. The results of an experiment are essentially the five components $(\nabla E)_q'$. In order to relate $(\nabla E)_q'$ to the principal axis components $(\nabla E)_r{}^*$, the (usually unknown) principal axis transformation must be carried out:

$$(\nabla E)_p=\sum_{r=-2}^{2}\mathfrak{D}^{(2)}(\{\alpha\beta\gamma\})_{rp}(\nabla E)_r{}^*. \quad (16)$$

α, β, γ are the Eulerian angles of the principal axis system with respect to the axis system X, Y, Z.

In the principal axis system $\nabla\epsilon$ has the form

$$(\nabla E)_0{}^*=-\tfrac{1}{2}(\partial E_z{}^*/\partial z^*),$$
$$(\nabla E)_{\pm1}{}^*=0, \quad (17)$$
$$(\nabla E)_{\pm2}{}^*=-\frac{1}{2\sqrt{6}}\eta(\partial E_z{}^*/\partial z^*).$$

Consequently $(\nabla E)_q'$ can be expressed in terms of the principal axis components $(\nabla E)_n{}^*$ by means of the relations

$$(\nabla E)_0'=(\tfrac{3}{2}\cos^2\beta-\tfrac{1}{2})(\nabla E)_0{}^*-6^{\frac{1}{2}}\sin^2\beta\cos2\alpha(\nabla E)_2{}^*,$$
$$(\nabla E)_{\pm1}'=\pm(6^{\frac{1}{2}}/2)\sin\beta\cos\beta e^{\pm i\gamma}(\nabla E)_0{}^*$$
$$+\tfrac{1}{2}(1\pm\cos\beta)\sin\beta e^{2i\alpha\pm i\gamma}(\nabla E)_2{}^*$$
$$-\tfrac{1}{2}(1\mp\cos\beta)\sin\beta e^{-2i\alpha\pm i\gamma}(\nabla E)_2{}^*, \quad (18)$$
$$(\nabla E)_{\pm2}'=(6^{\frac{1}{4}}/4)\sin^2\beta e^{\pm2i\gamma}(\nabla E)_0{}^*$$
$$+\tfrac{1}{4}(1\pm\cos\beta)^2e^{\pm2i\gamma+2i\alpha}(\nabla E)_2{}^*$$
$$+\tfrac{1}{4}(1\mp\cos\beta)^2e^{\pm2i\gamma-2i\alpha}(\nabla E)_2{}^*.$$

The price paid for the ease of transformation has been to introduce complex components $(\nabla E)_q'$. Actually, only the real combinations

$$i((\nabla E)_1'+(\nabla E)_{-1}'), \quad i((\nabla E)_2'-(\nabla E)_{-2}'),$$
$$(\nabla E)_1'-(\nabla E)_{-1}', \quad (\nabla E)_2'+(\nabla E)_{-2}', \quad (\nabla E)_0$$

enter, and once these combinations are formed all quantities are explicitly real.

It should be emphasized that α, β, γ, $(\partial E_z/\partial z)$, and η represent the expectation values of dynamical variables taken over all motions in the solid whose period is shorter than the period associated with the line width.[11] In molecular solids in which intermolecular forces are

[9] E. F. Carr and C. Kikuchi, Phys. Rev. **78**, 470 (1950).

[10] E. Wigner, Gruppentheorie, etc., Friedr. Vieweg, Braunschweig (1931), reprinted by J. W. Edwards, Ann Arbor.

[11] Bloembergen, Purcell, and Pound, Phys. Rev. **73**, 679 (1948).

TABLE I. Energy levels for successive approximations in powers of η^2.

	m	E_0	E_1	E_2	E_3	E_4	E_∞
$\eta^2=1$	5/2	10	10.5556	10.5848	10.5832	10.5830	10.5830
	3/2	−2	1.0000	−0.9167	1.1620	−1.7106	0
	1/2	−8	−11.5556	−9.6681	−11.7453	−8.8725	−10.5830
$\eta^2=1/4$	5/2	10	10.1389	10.1407	10.1407	10.1407	10.1407
	3/2	−2	−1.2500	−1.3698	−1.3373	−1.3485	−1.3455
	1/2	8	−8.8889	−8.7709	−8.8034	−8.7922	−8.7952

much weaker than intramolecular forces, $\partial E_z/\partial z$ and η would be approximately temperature independent, but the temperature dependence of α, β, γ would be a measure of the low frequency motion occurring in the solid.

III. MAGNETIC SPLITTING OF THE QUADRUPOLE RESONANCE LINE

A. The Energy Levels in the Absence of a Field

If the quadrupole interaction is large enough, no constant magnetic field is required to observe transitions. For this case it is suggestive to write the Hamiltonian simply

$$\mathcal{H}=\frac{-eQ}{2I(2I-1)}\left[\frac{\partial E_x}{\partial x}I_x^2+\frac{\partial E_y}{\partial y}I_y^2+\frac{\partial E_z}{\partial z}I_z^2\right].$$

In this form it is clear that the system admits the rhombic group whose axes are the principal electric axes. There is a striking resemblance between this Hamiltonian and the Hamiltonian for a rigid rotating top,

$$\mathcal{H}=\frac{1}{2I_a}J_a^2+\frac{1}{2I_b}J_b^2+\frac{1}{2I_c}J_c^2.$$

For integral spin the two problems are identical and full solutions are available.[12]

If I is half-integral, the $(2I+1)$ states of orientation contain $I+\frac{1}{2}$ doubly degenerate representations of the rhombic group so that the secular equation of degree $2I+1$ factors into two identical equations of degree $I+\frac{1}{2}$. The difficulty of solving the latter equations combined with the accurate frequency measurements possible makes imperative accurate approximations to the energy levels.

In principle, the energy levels should be obtainable by perturbation theory. In order to be at all successful, the axis of quantization z must be chosen to be the principal axis along which the magnitude of the electric field gradient is largest.

The matrix elements of the quadrupole interaction in this representation are

$$\begin{aligned}(m|\mathcal{H}|m)&=(3m^2-I(I+1))A(\nabla E)_0,\\ (m|\mathcal{H}|m\pm2)&=6^{\frac{1}{2}}f^{\frac{1}{2}}(I,m\pm1)A(\nabla E)_{\pm2}\\ &=f^{\frac{1}{2}}(I,m\pm1)\eta A(\nabla E)_0.\end{aligned}\tag{19}$$

[12] King, Hainer, and Cross, J. Chem. Phys. **11**, 27 (1943).

In the absence of a field the eigenvalues are assumed to be expanded in a power series in η:

$$E_m{}^0=A(\nabla E)_0\sum_{n=0}^{\infty}c_n(m)\eta^n,$$

where it is clear from the form of the matrix elements and the fact that I is half-integral that the coefficients of all odd powers of η vanish.

Using fourth-order perturbation theory[13] one finds that

$$\begin{aligned}c_0&=3_m{}^2-I(I+1),\\ c_2&=\frac{1}{12}\left\{\frac{f(I,m-1)}{m-1}-\frac{f(I,m+1)}{m+1}\right\},\\ c_4&=\frac{1}{864}\left\{\frac{f(I,m+1)f(I,m-1)}{(m-1)^2(m+1)^2}+\frac{1}{2}\frac{f^2(I,m+1)}{(m+1)^3}\right.\\ &\quad-\frac{1}{2}\frac{f^2(I,m-1)}{(m-1)^3}-\frac{1}{4}\frac{f(I,m+1)f(I,m+3)}{(m+1)^2(m+2)}\\ &\quad\left.+\frac{1}{4}\frac{f(I,m-1)f(I,m-3)}{(m-1)^2(m-2)}\right\}.\end{aligned}\tag{20}$$

Some of the fourth-order terms can be checked by expanding in powers of η^2 the exact solutions for a spin of three halves. These particular expansions suggest that the perturbation expansion converges rapidly. The convergence of the perturbation theory can perhaps be better judged by considering the spin five-halves secular equation, which is just

$$E^3-(84+28\eta^2)E-160+160\eta^2=0.$$

The roots of this equation can be expanded in powers of η^2 more easily by an iteration procedure than by perturbation theory. The three eigenstates are then labeled for convenience by $\pm m$, the states which they become when η adiabatically vanishes:

$$E_{\pm\frac{1}{2}}=10+(5/9)\eta^2+(85/2916)\eta^4-(715/473{,}392)\eta^6-(62{,}935/306{,}110{,}016)\eta^8,\tag{21a}$$

$$E_{\pm\frac{3}{2}}=-2+3\eta^2-(23/12)\eta^4+(449/216)\eta^8-(44{,}675/15{,}552)\eta^8,\tag{21b}$$

$$E_{\pm\frac{5}{2}}=-8-(32/9)\eta^2+(1376/729)\eta^4-(122{,}656/59{,}049)\eta^6+(13{,}740{,}640/4{,}782{,}969)\eta^8.\tag{21c}$$

The second-order terms of Eq. (21) have been obtained by Townes and Dailey[14] and the fourth-order terms check with the general perturbation theory expansion Eq. (20). An over-all check on these expansions is that the trace of the Hamiltonian is identically zero.

[13] K. F. Niessen, Phys. Rev. **34**, 253 (1929).

[14] C. H. Townes and B. P. Dailey, J. Chem. Phys. **20**, 35 (1952).

The speed with which these series converge may be judged from Table I.

It shows that for $|\eta|<\frac{1}{2}$ the series will give fairly accurate values of the roots. Near $|\eta|=1$ only one of the series [Eq. (21a)] converges rapidly while the others are useless. For high precision if η is not small, it will suffice to compute one root by means of Eq. (21a) and obtain the other two from a quadratic equation.

B. The First-Order Zeeman Effect

In the absence of a magnetic field the spectrum yields the principal axis components of the gradient of the electric field tensor times the quadrupole moment. Actually this statement is not true if the spin is three-halves because then only one frequency can be observed. Moreover, only the magnitude of η is obtained.† The study of the first-order Zeeman effect enables η, $|(\nabla E)_0|$, and the orientation of the principal axes to be determined whenever the nuclear spin is half-integral. Knowing the orientation of the molecule in the crystal from x-ray crystallography and deriving the orientation of the principal axes in the crystal from the nuclear quadrupole experiments, one can then compute the orientation of the principal axes with respect to the molecule.‡

The linear Zeeman effect can be obtained readily when η is small enough so that the term second order in η is a sufficient approximation to the energy levels. The energy of the state m is then given by

$$E_m=E_m{}^0+mg\beta H_z+\frac{\eta^2g\beta H_z(m+2)f(I,m+1)}{144(m+1)^2}+\eta^2g\beta H_z\frac{(m-2)f(I,m-1)}{144(m-1)^2}\quad\text{for}\quad|m|\geq 5/2,$$

$$E_{\pm\frac{1}{2}}=E_{\pm\frac{1}{2}}{}^0\pm g\beta\left\{\frac{9}{4}H_z{}^2+\frac{7}{600}\eta^2f(I,5/2)H_z{}^2-\frac{1}{24}\eta^2H_z{}^2f(I,\tfrac{1}{2})+\frac{1}{36}\eta^2(H^2-H_z{}^2)(I-\tfrac{1}{2})(I+\tfrac{3}{2})f(I,\tfrac{1}{2})\right\}^{\frac{1}{2}},$$

$$E_{\pm\frac{3}{2}}=E_{\pm\frac{3}{2}}{}^0\pm g\beta\Big\{\tfrac{1}{4}H_z{}^2-\tfrac{1}{6}\eta(H_x{}^2-H_y{}^2)(I+\tfrac{1}{2})(I+\tfrac{3}{2})^{\frac{1}{2}}(I-\tfrac{1}{2})^{\frac{1}{2}}f^{\frac{1}{2}}(I,\tfrac{1}{2})+\tfrac{1}{4}(I+\tfrac{1}{2})^2(H^2-H_z{}^2)$$
$$+\frac{5}{648}\eta^2f(I,\tfrac{3}{2})H_z{}^2-\frac{1}{24}\eta^2f(I,\tfrac{1}{2})H_z{}^2+\frac{\eta^2}{36}(H^2-H_z{}^2)(I+\tfrac{3}{2})(I-\tfrac{1}{2})f(I,\tfrac{1}{2})$$
$$+\frac{\eta^2}{108}(H^2-H_z{}^2)(I+\tfrac{1}{2})(I+5/2)^{\frac{1}{2}}(I-\tfrac{3}{2})^{\frac{1}{2}}f^{\frac{1}{2}}(I,\tfrac{1}{2})f^{\frac{1}{2}}(I,\tfrac{3}{2})\Big\}^{\frac{1}{2}}.$$

The states $m=\pm\frac{1}{2}$ and $m=\pm\frac{3}{2}$ must be treated separately because the external field produces transitions between these previously degenerate states. The choice of linear combinations which will be energy eigenstates depends on the orientation of the external field.

By considering a special case one can see in detail what the effect of applying a magnetic field will be. Dean[15] has investigated the case of a spin of three-halves in a strong external electric field of arbitrary symmetry but in a weak magnetic field. Weiss[16] has treated the case of an axial electric field but a magnetic field of various strengths and orientations. Dean was able to obtain the parameters η and $(\nabla E)_0$ independently in several crystals containing nuclei with spin three-halves.

The nuclear electric quadrupole spectra become most meaningful when measured in single crystals. A complicating feature is that in each unit cell the identical nuclei may be in nonequivalent positions, i.e., there will be two or more different (∇E) tensors. The resulting multiplicity of lines will decrease the average intensity and may make analysis impossible. This fact plus the difficulty of preparing large single crystals are the most serious limitations to the entire method.

The author has benefited from discussions with Professors Pound and Van Vleck of Harvard where this work was begun.

† The sign of $(\nabla E)_0$ is not obtainable in this type of experiment because of the inversion symmetry of the magnetic field.

‡ Dean and Pound (reference 7) showed conversely that if the orientation of the principal axes with respect to the molecule is apparent from symmetry, the orientation of the molecule in the crystal can be determined.

[15] C. Dean, Phys. Rev. **86**, 607 (1952).
[16] P. R. Weiss, Phys. Rev. **73**, 470 (1948); **74**, 1478 (1948).

THE JOURNAL OF CHEMICAL PHYSICS VOLUME 20, NUMBER 10 OCTOBER, 1952

Inter- and Intramolecular Energy Transfer Processes. 2. Hydrocarbon-Hydrocarbon Systems

MARGARET M. MOODIE AND C. REID
University of British Columbia, Vancouver, British Columbia, Canada
(Received February 14, 1952)

The transfer of energy from one species of hydrocarbon to another has been observed. The conditions under which such transfer occurs indicate that one aromatic hydrocarbon may be adsorbed onto crystals of the other forming a surface complex with a binding energy of a few hundred calories. Transfer of energy occurs readily between the components of this complex but not between molecules of different hydrocarbons when both are in solution. However, evidence for resonance transfer of energy between pairs of molecules of the same substance when both are in solid solution has been found.

INTRODUCTION

THE transfer of electronic energy absorbed by crystals of aromatic hydrocarbons to "impurity" hydrocarbons within the crystal is a well-known phenomenon.[1–4] In view of the calculations and experiments of Förster[5] which suggest that long-range energy transfer processes should occur in solution, the behavior under irradiation of pairs of hydrocarbons in solution is of interest. It has already been shown[6] that energy transfer can occur if the solvent itself is an absorber, as in the case of hydrocarbon solutions irradiated with x-rays; but this is clearly a "short-range" phenomenon.

Our experiments are designed to investigate systems in which the solvent has energy levels too high for it to be excited by the radiation used. It is clear at the outset that in such solutions transfer of energy does not occur with an efficiency at all comparable with that of the process occurring in crystals. Thus anthracene crystals, contaminated with sufficient naphthacene (1 part in 10^5) to show strongly the characteristic naphthacene green emission, fluoresce only in the blue when dissolved and show no trace of naphthacene emission even after quite long exposure times. In order to examine this qualitative observation more carefully, we have used solutions of pairs of hydrocarbons in inert solvents which form glassy solids at −180°C. Under these conditions collision quenching is eliminated and fluorescence yields are high. Transfer of electronic energy during collisions is also prevented, and it is thus possible to estimate the average distance between molecules of the two components, assuming a random distribution. It will be shown that under our experimental conditions no evidence for long-range intermolecular transfer of energy between two different molecules in solution has been observed. In heterogeneous systems, where one component is present in microcrystalline form and the other is dissolved in the glassy matrix, highly efficient transfer of energy from the dissolved to the solid component has been observed[7] and is the principal subject investigated in this paper.

EXPERIMENTAL METHOD

Aromatic hydrocarbons were dissolved or suspended in solvents of varying polarity which formed clear glasses when cooled in liquid nitrogen contained in an unsilvered Dewar vessel. The resulting systems were irradiated with monochromatic light from a General Electric AH6 mercury arc with suitable filters. The fluorescence from the solution and any scattered mercury light were photographed using an E2 Hilger quartz prism spectrograph. The resulting plates were scanned with a Kipp and Zonen densitometer equipped with a paper recorder.

The solvents used, in order of decreasing polarity, were (1) eight parts of methanol, one of ethanol, and one of isopropanol, (2) EPA or five parts of ether, five of isopentane, and two of ethanol, (3) one part of ether to five of isopentane, (4) one part each of ether and methyl cyclohexane to four of isopentane, (5) one part of isopentane and four of methyl cyclohexane, and (6) one part of methyl cyclohexane to four of isopentane.

Suspensions were made by rapid cooling of supersaturated solutions or, when high concentrations were required, by mechanical dispersion. As reproducibility in particle size and density was difficult to attain small variations from experiment to experiment were inevitable.

For studies at −70°C the coolant was a mixture of ether and isopentane cooled with liquid nitrogen. (Dry ice baths gave cloudy, fluorescent coolants unsuitable for our purposes.) Suspensions at −70°C and at 20°C

[1] E. J. Bowen, Nature **142**, 1081 (1938); **153**, 652 (1944); J. Chem. Phys. **13**, 306 (1945); E. J. Bowen and E. Mikiewicz, Nature **159**, 706 (1947); Bowen, Mikiewicz, and Smith, Proc. Phys. Soc. (London) **A62**, 26 (1949); E. J. Bowen and P. D. Lawley, Nature **164**, 572 (1949).

[2] F. Weigert, Trans. Faraday Soc. **36**, 1033 (1940).

[3] J. A. Miller and C. A. Baumann, Cancer Research **3**, 217 (1943).

[4] S. C. Ganguly, Proc. Ind. Assoc. for Cultivation of Sci. **26**, 7 (1943); Nature **151**, 673 (1943); **153**, 652 (1944); Ind. J. Phys. **18**, 347 (1944); **19**, 222 (1945); J. Chem. Phys. **13**, 128 (1945).

[5] Th. Förster, Ann. Physik **2**, 55 (1948); Z. Naturforsch. **4a**, 321 (1949); Z. Elektrochem. **53**, 93 (1949). A general survey of energy transfer mechanisms is given by J. Franck and R. Livingston, Revs. Modern Phys. **21**, 505 (1949) and by Th. Förster, *Fluoreszenz Organischer Verbindungen* (Vandenhoeck & Ruprecht, Göttingen, 1951).

[6] H. Kallmann and M. Furst, Phys. Rev. **79**, 857 (1950); **81**, 853 (1951).

[7] M. M. Moodie and C. Reid, J. Chem. Phys. **19**, 986 (1951).

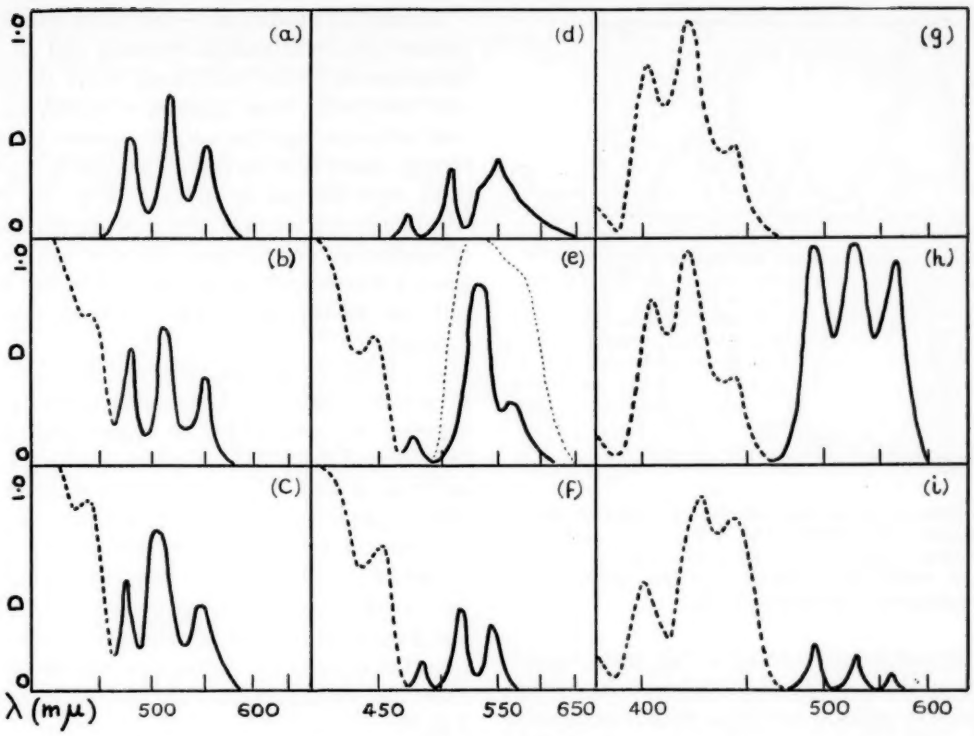

FIG. 1. Anthracene-naphthacene system. (In all emission spectra traces the ordinate D represents optical density, while the abscissa represents the wavelength in millimicrons.) Dashed curves show anthracene emission; solid and dotted curves naphthacene emission. First column, naphthacene in solution: (a) naphthacene alone; (b) same naphthacene concentration as (a) with added anthracene, also in solution at −180°C; (c) as (b) at 20°C. Second column, naphthacene in suspension: (d) naphthacene alone at −180°; (e) Same naphthacene concentration as (d) with added anthracene in solution, also at −180°. Upper dotted curve shows the effect of a threefold increase in anthracene concentration, the naphthacene concentration remaining unchanged; (f) as (e) at 20°C. Third column, anthracene in suspension: (g) anthracene alone at −180°; (h) same anthracene concentration as (g) with naphthacene in solution to give a naphthacene-anthracene ratio of $1:10^5$ at −180°; (i) as (h) at 20°C. The solvent used in all cases is EPA.

were stirred continuously during the exposure time to prevent settling out.

Low temperature absorption studies were made using the same spectrograph and the same general arrangement.

As in all fluorescence work, high purity of both solvents and solutes was essential since impurities might act as acceptors of energy absorbed by the major components. The solvents were redistilled frequently and sometimes chromatographed. The hydrocarbons were finally purified by chromatographing through an alumina column with a benzene-petroleum ether mixture as solvent. It will be shown later that it is almost impossible to obtain hydrocarbons completely free of minute traces of other hydrocarbons.

RESULTS

(a) In both polar and nonpolar solvents and at temperatures of −180°C and 20°C, there is no observable interaction between molecules of naphthacene and molecules of anthracene, chrysene, 1,2,5,6 dibenzanthracene, 9,10 dichloroanthracene, or pyrene when both substances are in true solution (Figs. 1(a) and 1(b)). Several hundred exposures under different conditions of solvent polarity, temperature, and hydrocarbon concentration have confirmed this fact, subject to the limitation of concentration imposed by the maximum solubility of the hydrocarbons used. It is estimated that a systematic 10 to 20 percent increase in intensity would have been detected, and in systems consisting of a tenfold excess of "donor" over "receiver" molecules this could be achieved with a transfer efficiency of only 1 to 2 percent. Concentration ratios of donor to receiver as high as 1000:1 still showed no detectable effect, so that "less than 5 percent" is a very conservative estimate of the efficiency of the transfer process in solution under the conditions of our experiments.

(b) Energy transfer occurs in systems containing a microcrystalline suspension of one of the hydrocarbon components. At −180° the addition of an anthracene solution to a suspension of naphthacene produces a new, rather broad and intense emission band at 5330A (Figs. 1(d) and 1(e)) whose intensity is proportional to the anthracene concentration. Replacement of the anthracene solution with a chrysene solution shifts the band center to 5440A, while with 1,2,5,6 dibenzanthracene solution the band occurs at 5500A.

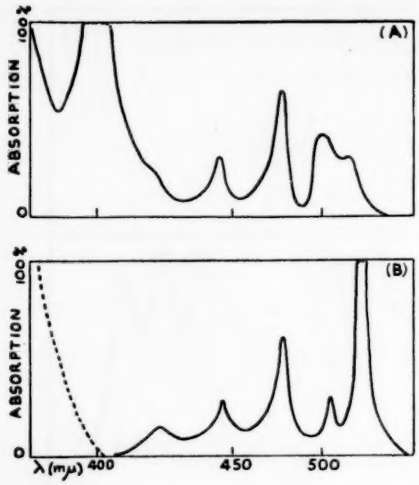

FIG. 2. Absorption of anthracene solution-naphthacene suspension transfer system at −180°C. (A) A combined anthracene solution-naphthacene suspension in EPA showing the new absorption band at 4030A; (B) absorption of the separate components at the same concentrations as in (A).

The occurrence or nonoccurrence of this new emission band depends on the polarity of the solvent. In systems with anthracene in solution and naphthacene suspension the band appears with the same intensity in both EPA and methyl cyclohexane-isopentane solvents, but not in the more polar alcohol glass where the fluorescence is just the sum of those of the separate components. Similarly, only in the less polar methyl cyclohexane-isopentane glasses is there any appreciable interaction in systems containing chrysene or 1,2,5,6 dibenzanthracene solution and naphthacene suspension. That these effects are not simply due to solubility changes was established by using an amount of the crystalline hydrocarbon well in excess of its solubility in any of the solvents and a constant amount of the dissolved hydrocarbon in each case.

No energy transfer between pyrene or 9,10 dichloroanthracene in solution and microcrystals of naphthacene could be detected in any of the glassy solvents used.

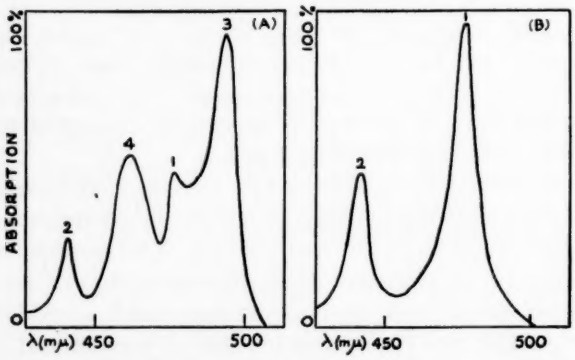

FIG. 3. New absorption bands of an anthracene suspension-naphthacene solution system. (A) Anthracene suspension and naphthacene solution in EPA at −180°C; (B) naphthacene solution alone at −180°C. The new bands are marked (3) and (4) while (1) and (2) are the normal naphthacene solution bands.

Absorption studies at −180° were made both on the various two hydrocarbon systems and on the separate components. Under conditions where transfer occurs, a new absorption band appears at 4030A for the anthracene solution-naphthacene suspension system and the strong absorption maximum at 5330A characteristic of solid naphthacene disappears (Fig. 2.) The new absorption bands for the corresponding chrysene or 1,2,5,6 dibenzanthracene systems are too weak or lie at too short a wavelength to be detected by the method used, but the 5330A band does diminish considerably in intensity.

(c) Table I and Figs. 1(g) and 1(h) show the results of similar experiments in which naphthacene in EPA solution has been added to suspensions of anthracene, chrysene, 1,2,5,6 dibenzanthracene, or 9,10 dichloroanthracene and the resulting system cooled to −180°. The naphthacene bands are shifted to longer wavelengths and are greatly enhanced in intensity, but they do retain the character of "solution" rather than "solid" bands. One part of naphthacene in 3×10^9 parts of anthracene or in 1.2×10^7 parts of chrysene have been detected in this way. Absorption bands corresponding to these new emission bands are also observed (Table I and Fig. 3).

Dry crystals of anthracene contaminated by small amounts of naphthacene show similar emission bands. If the contaminating naphthacene concentration rises above 1 part in 10^5 the band at 5330A characteristic of a solid naphthacene transfer system appears.[8] At this point it seems that the naphthacene molecules are no longer isolated from each other, but are beginning to form aggregates within the anthracene crystal. In the dry crystals the minimum detectable concentration of naphthacene is about 1 part in 10^6. The higher quantum yield of naphthacene emission in the suspension system indicates again the presence of an efficient solution-solid energy transfer process.

(d) Figure 4 shows the emission characteristic of dry anthracene crystals compared with that of suspensions of anthracene alone in solvents of decreasing polarity at −180°. In the most polar solvent (Fig. 4(b)) the series of sharp bands with high energy limit at 3770A characteristic of anthracene solution are apparent and mask the weaker emission from the suspended solid. As the polarity decreases these bands decrease in intensity and are replaced by a new type of emission in the region of the emission bands of the dry solid, but much more diffuse than the latter. In solutions in the nonpolar solvents, without suspended solid, the characteristic solution bands reappear and the emission spectrum looks essentially like Fig. 4(b).

In the nonpolar suspension it appears that energy which would have been emitted as "solution bands" has been transferred to the solid. The diffuseness of the emission may be attributed to variable interaction

[8] F. R. Lipsett, Master's Thesis (University of British Columbia, 1951).

energy between the dissolved molecules and the crystal. Similar behavior is shown by chrysene (Fig. 5), 1,2,5,6 dibenzanthracene, 9,10 dichloroanthracene, and naphthacene.

All the experiments reported in sections (a), (b), (c) and (d) have been repeated at −70°C and at 20°C in liquid solutions and suspensions. With both substances in true solution the results remained negative (Fig. 1(c)). In (b), (c), and (d) the same phenomena occurred with lower efficiency at −70°, but at 20° energy transfer ceased entirely in type (b) and (d) experiments (Fig. 1(f)), while the shifted naphthacene bands described in (c) retained 20–25 percent of their low temperature intensity (Fig. 1(i)).

At this point it is interesting to note that pentacene fluoresces so weakly that negative results were obtained when it was used as the crystalline receiver molecule in type (b) and (d) experiments, but that it showed a brilliant emission in the red in type (c) experiments with

TABLE I. Absorption and emission band maxima for transfer systems containing naphthacene solution and a second hydrocarbon in suspension at −180° in EPA.

Naphthacene solution +	Absorption band maxima in A	Emission band maxima in A	Origin of band system
Alone	4210, 4460, 4750	4750, 5130, 5550	4750
Anthracene suspension	4590, 4940	4970, 5350, 5780	4955
Chrysene suspension	4850	4860, 5190, 5620	4855
1,2,5,6 Dibenzanthracene suspension	4690, 4890	4900, 5270, 5660	4895
9,10 Dichloroanthracene suspension		4840,	4840(?)

anthracene, chrysene, or 1,2,5,6 dibenzanthracene as the host crystal. The polyacenes are exceptional among the hydrocarbons in behaving in this manner. Anthracene also shows up in trace quantities in naphthalene or phenanthrene crystals.

DISCUSSION

Our failure to detect any appreciable energy transfer in the systems containing only dissolved molecules does not contradict the work of Förster.[5] The very low solubility of aromatic hydrocarbons at −180°C in the solvents used severely limited the concentration range over which we could work. In EPA the approximate concentrations attainable at −180°C are for anthracene 3.56×10^{-4} mole per liter, for chrysene 1.18×10^{-4} moles per liter, and for naphthacene 1.54×10^{-5} moles per liter. (These are the highest concentrations at which no separation of solid was visible on cooling to −180°C with cross illumination. Usually the appearance of visible turbidity and the observation of a characteristic

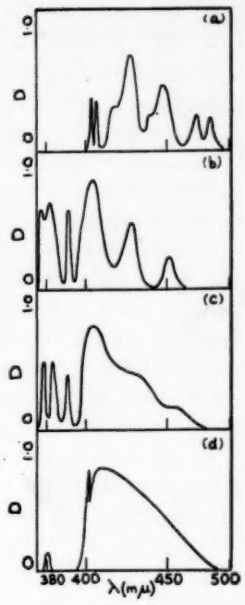

FIG. 4. Self transfer in anthracene. (a) emission from dry anthracene crystals at −180°C, (b) emission of a solution of anthracene containing excess suspended anthracene crystals in 12 cc of isopentane-methyl cyclohexane glass with 0.6 cc of alcohol added to increase the solvent polarity, (c) as (b) with only 0.1 cc of alcohol, (d) as (b) with no added alcohol. The "solution" bands have disappeared and have been replaced by a continuum different to the emission of dry crystals or solution. The "solution" bands reappeared in solution (d) when the suspended solid was removed.

"solid" emission could be correlated.) Thus in an anthracene solution-naphthacene solution system the average distance between the solute molecules is 165A, while in a chrysene-naphthacene system the average distance is 232A. These distances are considerably greater than the maximum of 60A over which Förster found interaction between molecules of trypaflavin and rhodamine B.

We will now consider possible interaction mechanisms for the systems in which we have found energy transfer. Although the solvent influences the transfer process, it remains throughout in its ground state as the incident radiation (maximum energy used was 33,000 cm^{-1}) is insufficient to excite it. Thus the possible mechanisms are:

1. Reabsorption of the energy donor's emission by the acceptor substance.
2. Transfer from one component of a molecular complex to another.
3. Long-range dipole-dipole interaction of the type predicted by Förster.

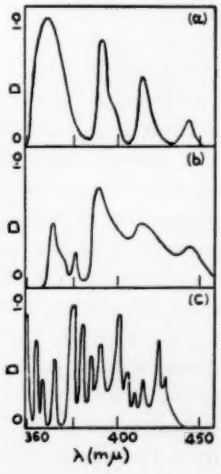

FIG. 5. Self transfer in chrysene. (a) emission from dry crystalline chrysene at −180°C, (b) emission of a chrysene suspension in methyl cyclohexane-isopentane. The spectrum shows a trend towards the continuum found for anthracene under similar conditions. The "solution" bands are also missing, (c) emission of chrysene in methyl cyclohexane-isopentane solution.

4. "Resonance transfer" of energy between identical molecules, before the excited molecule loses its vibrational energy.

It will be noted that the interaction term in Förster's expression is zero unless the emission band of the donor overlaps the absorption band of the acceptor. This is a consequence of the assumption that the energy transfer process, like the emission of radiation, is slow compared with the rate at which vibrational energy is lost, so that both processes occur from the lowest vibrational level in the excited electronic state. Since this is not the case in process 4, the latter must be considered separately from type 3. Furthermore, since complex formation may involve orbital overlap or even electron transfer, the mechanism for type 2 may be quite different to that involved in any long-range processes.

In the three types of system in which we have found energy transfer the emission region of one component overlaps, at least in part, the absorption of the second component. Thus, the possibility of energy transfer by means of a reabsorption of the energy donor's emission must not be overlooked. However, that this mechanism is unimportant is shown by the following five observations.

A. Equal weights of anthracene and naphthacene were dissolved in EPA and in methyl cyclohexane-isopentane-ethanol so that at −180°C the anthracene remained in solution in both solvents, while the naphthacene formed a suspension in the second solvent but remained in solution in the EPA. Transfer was detectable only when microcrystalline naphthacene was present. This fact coupled with the observation that naphthacene solution and dry naphthacene crystals have almost identical absorption coefficients in the region of the anthracene solution emission (wavelengths up to 4800A) indicates that transfer occurs by a process other than that of re-absorption of the anthracene emission by the naphthacene microcrystals.

B. Further evidence for a nonradiative process comes from the observation that the transfer does not produce the same intensity increase in all the vibrational bands of the acceptor molecule. For example, transfer from various hydrocarbons in solution to naphthacene suspension produces an intensity increase in what appears to be a slightly shifted O−O band. In the case of systems containing various hydrocarbon suspensions and naphthacene in solution, the transferred energy is emitted in a set of bands displaced by 100 to 200A from the normal naphthacene solution emission. Even in some of the systems in which energy is transferred from molecules in solution to microcrystals of the same substance, the resulting emission shows slight shifts in band positions or slight differences in the relative band intensities when comparisons with the emission of dry solid are made. On the other hand, the emission of the donor substance usually suffers the same intensity decrease in all the vibrational bands rather than a decrease only in the region where it overlaps the absorption bands of the acceptor substance.

C. The occurrence of transfer depends on the solvent even though hydrocarbon absorption is the same in all the solvents used.

D. Additional absorption bands appear in the transfer systems.

E. The great decrease in transfer efficiency at 20°C is not comparable with the relatively small change in the absorption coefficients in going from −180° to 20°.

None of these phenomena would be expected if a simple absorption, emission, re-absorption, re-emission process were involved.

Varying the solvent polarity does not change the interaction energy in a continuous manner. As the polarity of the solvent falls the interaction between molecules in solutions of anthracene, chrysene, or 1,2,5,6 dibenzanthracene and the naphthacene microcrystals shows a sudden appearance after which it remains approximately constant. This and the appearance of a new absorption band in the transfer system suggest the formation of a molecular complex and a consequent short-range interaction. If the solvent molecules are more polar than the inductively polarized hydrocarbon molecules, preferential adsorption of solvent on the crystal surface occurs and hydrocarbon complex formation is prevented. A similar type of complex is formed between naphthacene molecules and microcrystals of anthracene, chrysene, 1,2,5,6 dibenzanthracene, and 9,10 dichloroanthracene.

Complex formation is thus dependent on the magnitude of the dipole induced in the hydrocarbon molecule compared to the dipole of the solvent. Consequently it should be possible to arrange the hydrocarbon molecules in order of decreasing ease of polarizability of their π-electron system on the basis of transfer efficiency. For the hydrocarbons studied, this gives (1) naphthacene and anthracene, (2) chrysene and 1,2,5,6 dibenzanthracene, and (3) 9,10 dichloroanthracene and pyrene. This order is what one might expect from considerations of the susceptibility of these molecules to attack by electropositive reagents.

The increased efficiency of microcrystals over single molecules as one component of a transfer system is presumably due to "adsorption" (i.e., the binding force between the single molecule and the crystal is greater than that between two single molecules). The lack of single molecule transfer indicates that the intermolecular attractive forces are so weak that even at −180°C they are largely overcome by thermal agitation. This suggests that the energy of such single-pair attraction cannot be much greater than 50 calories/mole. However, since transfer in systems with microcrystals is still readily discernable at 200K, the "adsorption" force between the interacting molecules and microcrystals must be at least 300 calories/mole.

In view of the behavior of the hydrocarbon-aromatic nitro compound complexes in solution,[9] it seems probable

[9] C. Reid, J. Chem. Phys. (to be published).

that at lower temperatures than those available to us, complexes between hydrocarbon molecules in solution might be stable, and transfer would be observable.

Since solution fluorescence disappears in transfer systems containing only a suspension of one hydrocarbon, there must be a succession of energy transfers from one molecule in solution to another with a final transfer to the microcrystal (Figs. 4 and 5). As the emission band of the transfer system is not exactly identical with that of the dry crystals or with the sum of that from dry crystals and solution, the last step probably involves the formation of a type of complex in which there is an oriented surface layer of molecules not packed in the same way as in the crystal. Energy transfer in solution thus occurs quite readily between identical hydrocarbon molecules, while under similar conditions no transfer between different hydrocarbon molecules is observable. This leads us to the important conclusion that strong overlap of the emission region of molecule A and the absorption region of molecule B is not essential, and therefore that process 4 is more important than process 3 under the conditions of our experiments (i.e., no collisions). In this case Förster's[5] expression for the probability of the transfer process between molecules A and B at a distance R_{AB} apart,

$$P_{AB}=\frac{2c}{\pi^4 n^2 \bar{N}^2 \bar{\nu}^2 R_{AB}{}^6}\int_0^\infty f^A \epsilon^B d\bar{\nu},$$

where $\bar{N}=6.06\times10^{20}$, $\bar{\nu}$ = frequency in cm^{-1}, ϵ^B = molar extinction coefficient of B, f^A = molar emission intensity of A at frequency $\bar{\nu}$, and n = refractive index of medium, should be modified. The integral, which makes the expression dependent on the emission-absorption overlap should be replace by

$$\int_0^\infty (\epsilon^A)^2 d\bar{\nu}$$

for identical molecules. The justification for this, if the transfer process is rapid compared to vibrational deactivation, is clear from Fig. 6. Use of this formula gives transfer times ranging from about 10^{-8} sec for $R=100$A down to 10^{-13} sec for $R=25$A, showing that the process may in fact be fast enough to compete with vibrational deactivation, which may be quite slow in the solid state at −180°C.

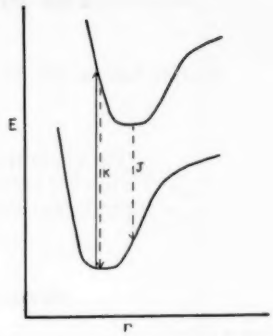

FIG. 6. K represents the energy available for transfer if the process is more rapid than vibrational deactivation and is identical with the absorbed energy. J represents the energy available for processes slower than vibrational deactivation such as emission of radiation.

The effect of temperature, solvent polarity, etc. on transfer between molecules of the same species is a phenomenon difficult to study without introducing some other detecting transfer step. Lifetime and depolarization studies of this phenomenon would be of great value.

We would like to suggest that a wider recognition of "dispersion force" complexes[10] may help to explain a wide variety of phenomena. The extreme difficulty encountered in the preparation of hydrocarbons absolutely free of each other doubtless results from the formation of such complexes. Fluorescence quenching may also be satisfactorily explained by such complex formation.[11] In fact, many instances of apparent quenching may involve the formation of complexes emitting in the infrared. It is clear that claims that long-range energy transfer processes have been observed in which average distances are calculated from concentrations must be examined very carefully to ensure that the possibility of complex formation has been ruled out.

ACKNOWLEDGMENTS

One of us (M.M.M.) is indebted to the National Research Council of Canada for a bursary. The authors also wish to thank the National Research Council of Canada and the President's Committee on Research of the University of British Columbia for grants in aid of research. A sample of pentacene was kindly furnished by Professor E. Clar; use of a densitometer in the Anatomy Department of the University of Washington is also gratefully acknowledged.

[10] M. J. S. Dewar, *The Electronic Theory of Organic Chemistry* (Oxford University Press, Cambridge, England, 1949).
[11] E. J. Bowen, Quart. Revs., London **1**, 1 (1947).

The Properties of *n*-Butforane and Its Mixtures with *n*-Butane

J. H. SIMONS* AND J. W. MAUSTELLER†
Fluorine Laboratories, State College, Pennsylvania, and Fluorine Research Center, the University of Florida, Gainesville, Florida
(Received March 31, 1952)

The physical properties of *n*-butforane C_4F_{10} were determined and also these mixtures of it with *n*-butane, C_4H_{10}. The properties of these two-component systems parallel very closely the system previously reported, *n*-pentforane and *n*-pentane. The necessity of a concept such as that of "interpenetration" is confirmed.

INTRODUCTION

THE study of the two-component system n-C_5F_{12} $-n$-C_5H_{12}[1] showed deviations from Raoult's law far greater than could be explained on the basis of the then existing solubility theories. To effect a correlation, a new concept was invented. This was named interpenetration and envisioned an interlocking of the attractive force fields between hydrocarbon molecules far greater than between fluorocarbon molecules or between a fluorocarbon and hydrocarbon molecule. It is desirable to confirm this phenomenon by further experimental data and check the theory with another pair of substances. The next lower member of the straight chain homologous series of both fluorocarbon and hydrocarbon was chosen, n-C_4F_{10} and n-C_4H_{10}. The differences in boiling points and heats of vaporization of this pair are even smaller than the previously studied pair of substances, so that a large deviation from Raoult's law would be even more striking.

TABLE I. Some physical properties of *n*-butforane and *n*-butane.

Property	n-C_4F_{10}	n-C_4H_{10}
Molecular weight	238.0	58.12
Boiling point	270.96°K	272.61°K[a]
Freezing point	144.96±0.05°K	134.86±0.15°K[a]
Vapor pressure	$\log_{10}P=-2039.6/T$ $-2.8024\ln T$ $+26.1077$ P is in mm Hg at 0°C and $g=980.665$ T is in °K	$\log_{10}P=6.83029^{a}$ $-\frac{945.90}{(240.00+t)}$ P is in mm Hg t is in °C
Liquid density	$D=1.6484$ $+10^{-3}\alpha(259.88-T)$ $+10^{-6}\beta(259.88-T)^2$ $\alpha=3.18$ $\beta=-0.0003$ T is in °K	$D=0.601+10^{-3}\alpha t^{b}$ $+10^{-6}\beta t^2$ $\alpha=-1.28$ $\beta=-0.6$ t is in °C
Molal volume at 259.95°K	144.4 cc/mol	94.1 cc/mol
E_v at 259.95°K (uncorrected)	5.48 kcal/mol	5.28 kcal/mol
$\Delta E/V$ at 259.95°K	37.95 cal/cc	55.1 cal/cc
$\frac{dE/dt}{dV/dt}$ at 259.95°K	54.90 cal/cc	45.4 cal/cc[c]
Electron polarizability	9.47A[d]	8.51A[d,e]

[a] F. D. Rossini *et al*, Selected Values of Properties of Hydrocarbons, National Bureau of Standards Circular C-461, Nov. (1947).
[b] International Critical Tables *III*, 28.
[c] Calculated from vapor pressure and liquid density equations.
[d] See reference 1.
[e] Extrapolated from values of this property of higher molecular weight members of these homologous series.

SOURCE OF SUBSTANCES

Pure grade *n*-butane 99 percent minimum was obtained from a petroleum company. After degassing, freezing point determinations confirmed its purity sufficient for the present studies. The *n*-butforane was obtained electrochemically[2] from *n*-dibutyl ether. It was fractionated in a column, which in operation had about one hundred theoretical plates. Analysis of cooling curves at the freezing point showed both substances to be 99.8 mol percent pure, if the impurity were liquid soluble and solid insoluble.

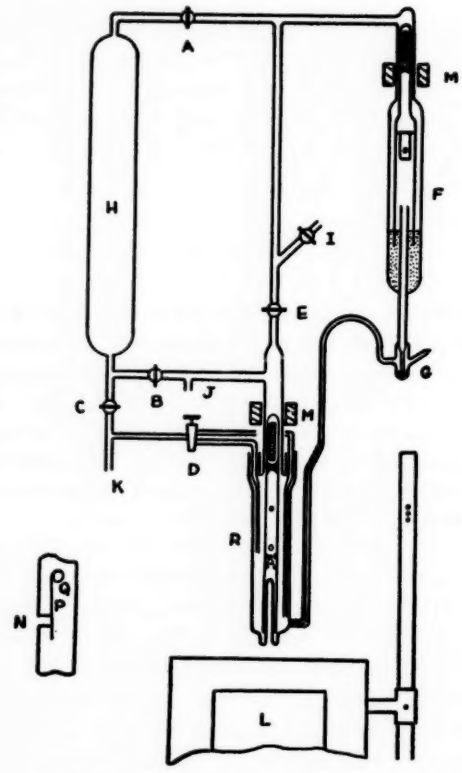

FIG. 1. Liquid-vapor equilibrium apparatus.

* Present address: College of Engineering, University of Florida, Gainesville, Florida.
† Present address: Mars, Pennsylvania.
[1] J. H. Simons and R. D. Dunlap, J Chem. Phys. **18**, 335 (1950).
[2] J. H. Simons and co-workers, J. Electrochem. Soc. **95**, 47 (1949).

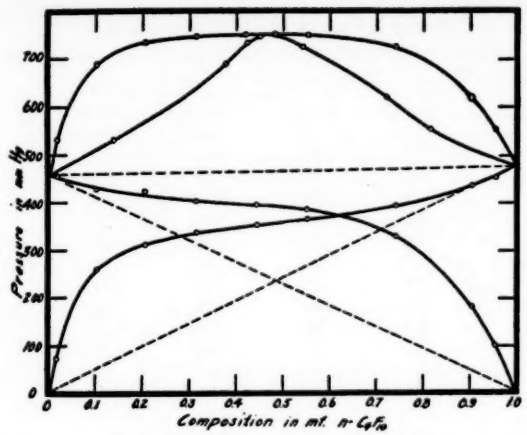

FIG. 2. Pressure-composition diagram for n-C_4F_{10} and n-C_4H_{10} at 259.95°K.

PROPERTIES OF n-BUTFORANE

The freezing points, vapor pressures, and liquid density of n-butforane were determined in similar manners to those used for n-pentforane.[1] The values are shown in Table I, where they are compared with the properties of n-butane.

APPARATUS

The equipment used for liquid-vapor and liquid-liquid equilibrium determinations was similar to that used in the previous study[1] with modifications to adjust to equipment for use of lower boiling components. The equilibrium apparatus shown in Fig. 11 of reference 3 was used, but a vapor pump was attached to it for use in liquid-vapor determinations. This is shown in Fig. 1. The auxiliary apparatus of the equipment is shown in Fig. 4, reference 3.

The vapor circulating pump F consists of a glass cylinder closed at the top and extending at the open bottom end into a pool of mercury in which it floats. A polyethylene flap valve is the inlet port. This is shown in detail in the insert where N is the entry port, P the

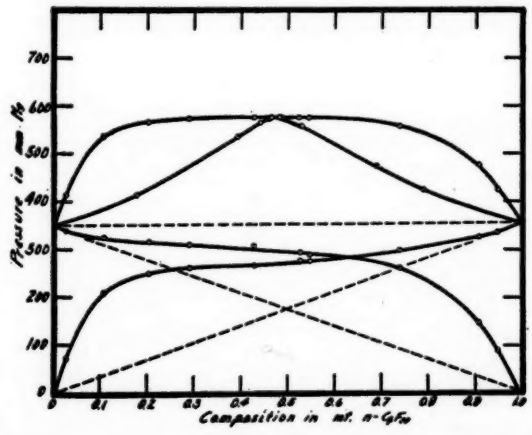

FIG. 3. Pressure-composition diagram for n-C_4F_{10} and n-C_4H_{10} at 253.62°K.

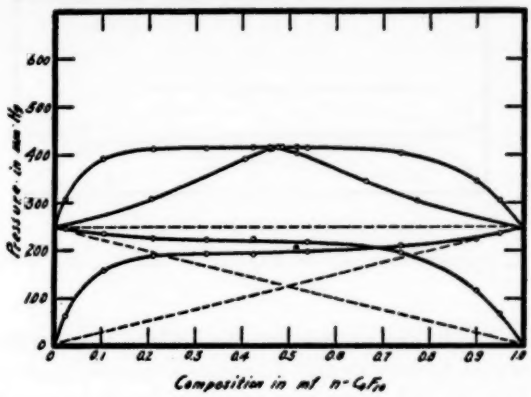

FIG. 4. Pressure-composition diagram for n-C_4F_{10} and n-C_4H_{10} at 246.35°K.

polyethylene flapper, and Q the support for it. The solenoid M, operating on a piece of iron on the top of the glass cylinder, provides for its vertical motion. G is a mercury check valve in which the minimum amount of mercury is used as to impose the minimum back pressure. Between G and the equilibrium apparatus fine capillary tubing is used to reduce the volume. For trapping vapor samples a vapor holder H of 500-cc capacity is provided. This is isolated by the stopcocks A, B, and C. Stopcock D provides for sampling either of the two liquid phases, and stopcock E provides a by-pass of the holder to allow free circulation of vapor through the pump and equilibrium apparatus. To opening I is attached storage bulbs for holding samples. Openings I and K connect to the auxiliary system as shown in Fig. 4, reference 3. The solenoids which operated both the liquid stirrer and the vapor pump were motivated by current supplied from a motor-driven commutator. The constant temperature bath had water-methanol for the fluid, a vessel of dry ice for cooling, and a light bulb for heating.

PROCEDURE

Two procedures were used: one for the liquid-vapor and the other for liquid-liquid equilibrium. For the former, a sample was prepared by mixing the two vapors in a large bulb on the apparatus and transferring 50 cc of it as liquid to a storage bulb held in dry ice attached to outlet I. The constant temperature bath was raised to

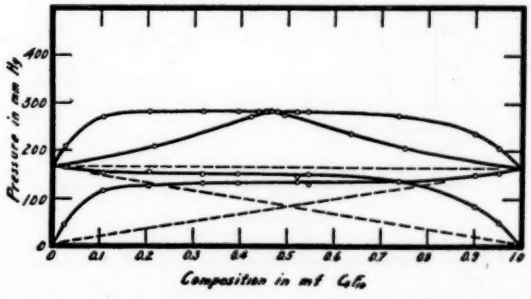

FIG. 5. Pressure-composition diagram for n-C_4F_{10} and n-C_4H_{10} at 238.45°K.

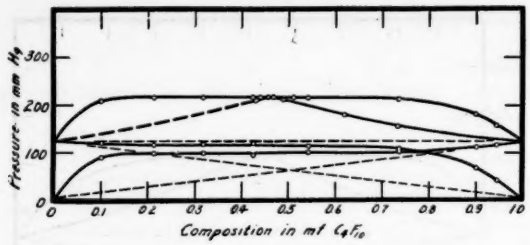

FIG. 6. Pressure-composition diagram for n-C_4F_{10} and n-C_4H_{10} at 233.23°K.

position, and the sample condensed into the solubility apparatus. Stopcocks E and I were closed; and stopcocks A and B opened. The vapor pump was started, and after about one hour was stopped; A and B closed, and E opened. Samples of 100 cc of vapor were then taken from both liquid and vapor phases, and vapor densities determined by direct weighing. Triplicate determinations were made at each temperature, and a sample of liquid was taken for a density measurement. This was repeated at different temperatures.

For liquid-liquid equilibrium measurements, holder H was evacuated, stopcocks A and B were closed, and stopcock E opened. The liquid pump on the equilibrium apparatus was operated for about one hour, and then samples were taken of each of the liquid phases for vapor density determinations.

RESULTS

The properties of pure n-butforane as determined are given in Table I.

Raoult's law diagrams at five temperatures are shown in Figs. 2–6 and smoothed out data from these curves in Table II. The original experimental data can be found elsewhere.[3] A minimum boiling point at 260.2°K and 760 mm at 0.57-mol fraction fluorocarbon was observed. This compares with a minimum at 0.53 for the five carbon atom system previously studied.[3]

The liquid-liquid phase diagram is shown in Fig. 7 and the smoothed out data in Table III. The critical unmixing temperature is found experimentally to be

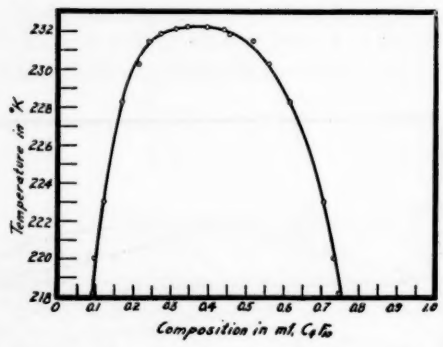

FIG. 7. Mutual solubilities of n-C_4F_{10} and n-C_4H_{10}.

[3] J. W. Mausteller, Ph.D. thesis, 1951, The Pennsylvania State College, State College, Pennsylvania.

TABLE II. Partial pressures of n-C_4F_{10} and n-C_4H_{10} over solution. Partial pressures of n-C_4F_{10} in mm Hg.

Mole fraction of C_4F_{10}	Temperatures in °K 259.95	253.62	246.35	238.43	233.23
0.1	257	203	156	112	91
0.2	311	251	187	128	100
0.3	335	264	192	132	100
0.4	348	268	194	133	100
0.5	361	273	198	135	100
0.6	373	282	202	136	100
0.7	388	294	207	137	102
0.8	407	308	214	141	105
0.9	436	326	226	151	112
1.0	477	356	249	163	121

Partial pressures of n-C_4H_{10} in mm Hg

Mole fraction of C_4H_{10}	Temperatures in °K 259.95	253.62	246.35	238.43	233.23
0.1	189	156	117	86	69
0.2	293	235	176	126	101
0.3	349	274	204	144	112
0.4	378	288	213	150	116
0.5	393	295	216	151	117
0.6	400	303	218	152	118
0.7	406	311	222	153	118
0.8	416	317	227	154	118
0.9	434	327	233	158	121
1.0	459	348	249	168	127

232.2°K at a composition of 0.39-mol fraction fluorocarbon. The calculated value using Hildebrand's equation[4] is 41°K at a composition of 0.39-mol fraction.

The densities of the liquid mixtures were determined over a 25 range for 9 different compositions. At two temperatures °K the total volume V is given in the equation below as a function of the mol fraction of the fluorocarbon n:

$$V_{259.95}=96.18+61.40n-12.94n^2,$$
$$V_{233.23}=91.39+56.74n-10.67n^2.$$

The change in volume on mixing the pure components is a maximum at 49.8-mol percent butforane at 259.95°K and 50.9-mol percent at 233.23°K; the percentage increase in volume at these points are 2.9 and 2.4, respectively.

TABLE III. Smoothed mutual solubility data.

Temperature °K	Concentration as mol fraction Solubility of n-C_4F_{10} in n-C_4H_{10}	Solubility of n-C_4H_{10} in n-C_4F_{10}
232.2 is the consolute temperatures with a composition of 0.37-mf n-butforane		
232	0.291	0.554
231	0.225	0.479
230	0.195	0.439
228	0.165	0.379
226	0.144	0.337
224	0.129	0.306
222	0.115	0.273
220	0.102	0.262
218	0.901	0.245
216	0.079	0.230

[4] J. H. Hildebrand, J. Am. Chem. Soc. **51**, 66 (1929).

TABLE IV. Heats and energies of mixing.

Mol fract. n-C_4F_{10}	$\bar{H}_1-\bar{H}_1^i$ cal	$F_1-\bar{F}_1^i$ cal	$\bar{E}_1-E_1^0$ cal	$\bar{E}_1-(v/\bar{v})E_1^0$ cal	At 233.23°K $\bar{v}_1$ cc	At 233.23°K $\phi_2^2\bar{v}_1$ cc	At 239.95°K $\bar{v}_1$ cc	At 239.95°K $\phi_2^2\bar{v}_1$ cc
0.1	1455	899	171	290	155	109.4	160	114.5
0.2	1062	639	123	171	149	74.9	157	79.3
0.3	786	459	86	101	144	51.7	153	54.7
0.4	638	325	57	57	142	35.1	149	37.3
0.5	513	225	37	29	141	22.6	148	24.3
0.6	386	145	21	15	139	13.8	146	15.1
0.7	138	83	11	7	138	7.5	145	8.1
0.8	0	36	5	3	137	3.3	145	3.5
0.9	0	10	1	1	137	0.8	144	0.9
Mol fract. n-C_4H_{10}								
0.1	1185	776	133	66	102	87.1	108	91.9
0.2	992	611	114	61	101	71.9	106	75.8
0.3	696	482	94	55	98	57.7	105	61.1
0.4	574	375	75	47	96	45.1	104	47.7
0.5	495	275	56	43	94	33.8	101	35.7
0.6	403	195	39	38	94	23.6	99	24.9
0.7	222	121	24	29	92	14.8	97	15.7
0.8	69	66	12	17	91	7.7	96	8.0
0.9	49	25	3	6	90	1.8	95	2.3

$$\phi_2=(n_2v_2)/(n_1v_1+n_2v_2)$$

DISCUSSION

The properties of this two component liquid system of a fluorocarbon and a hydrocarbon parallel very closely those of the system reported previously[1] and confirm the measurements. Calculations of significance for this system can be made from the experimental determination, using the equations in the previous paper. Thermodynamic quantities can be calculated from the experimental data. A summation of these is given in Table IV, with the calculations made as previously reported and the partial molal volumes obtained by the method of intercepts from the relationship between molal volume and mol fraction. The thermodynamic functions of mixing are plotted against the volume fraction in Fig. 8. The solubility parameters calculated in several ways are shown in Table V. Using the same method for calculating the interpenetration factor for butane as was used for pentane, the value at 259.95°K is 0.37A and that at 233.23°K is 0.32A.

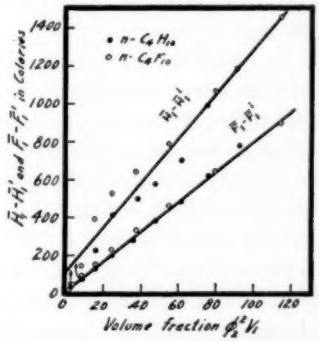

FIG. 8. Heats and free energies of mixing *vs* volume fraction at 259.95°K.

TABLE V. Solubility parameters.

	259.95°K C_4F_{10}	259.95°K C_4H_{10}	233.23°K C_4F_{10}	233.23°K C_4H_{10}
Volume in cc/mol	144.4	94.1	137.3	88.3
E_v in kcal/mol	5.48	5.28	5.88	5.42
$(E_v/V)^{\frac{1}{2}}$	6.16	7.44	6.55	7.84
	$(\Delta E_1/V_1)^{\frac{1}{2}}-(\Delta E_2/V_2)^{\frac{1}{2}}$			
From the physical properties	1.28 at 259.95°K 1.29 at 233.23°K			
From the plot of $\bar{H}_1-\bar{H}_1^i$ *vs* $\phi_2^2\bar{V}_1$	3.58			
From the plot of $\bar{F}_1-\bar{F}_1^i$ *vs* $\phi_2^2\bar{V}_1$	2.78			
From the observed consolute temperature	2.90			

CONCLUSION

The two-component liquid system of butforane-butane parallels in its properties the system pentforane-pentane very closely. The necessity for a concept like that of interpenetration seems to be confirmed.

The Entropy of Solution of Nonelectrolytes

J. H. HILDEBRAND, *Department of Chemistry, University of California, Berkeley, California*

AND

R. L. SCOTT, *Department of Chemistry, University of California, Los Angeles, California*

(Received April 7. 1952)

The linear relation between the logarithm of the solubility of a solid nonelectrolyte and the logarithm of the absolute temperature, recently set forth by one of us, makes possible a rather accurate calculation of the partial molal entropy of transfer of the solute from solid to saturated solution. By subtracting from this the calculated entropy of fusion of the solid, one obtains the entropy of transfer from pure liquid to solution. This is several entropy units in excess of the ideal entropy in the case of solutions with high activity coefficients, but this difference is satisfactorily accounted for by the entropy involved in the expansion which accompanies the formation of such solutions under constant pressure. The entropy of mixing at constant volume seems to conform closely to the ideal (or Flory-Huggins) entropy.

IN the treatment of the problem of the solubility of nonelectrolytes, which now is widely applied, the free energy of mixing is expressed in terms of the entropy and the energy of mixing.[1] One of the simplifying assumptions made in the course of deriving the final expression was to neglect changes in volume on mixing. That this involved an error was early recognized,[2] but, fortunately for calculating solubility equilibria, the errors thus introduced into the entropy and energy largely cancel each other so that the free energy of mixing thus calculated is more accurate than either.[3] It is desirable nevertheless, for the refinement of theory, to consider more fully the effect of volume changes upon mixing.

In order to study the effect of a certain factor it is wise to select systems in which it plays a predominant role rather than systems in which it can be masked by other factors of similar magnitude. We therefore turn, as so often before, to iodine solutions, which offer enormous deviations from Raoult's law; in a saturated solution in carbon tetrachloride at 25°, for example, its activity coefficient referred to pure liquid is 22.5, far greater than that of a component of any pair of miscible liquids. On the other hand, both molecules have high symmetry and do not differ greatly in molal volume, and the solution is purely "physical"; therefore the entropy of a solution cannot be seriously affected by such factors. It would be very difficult to determine calorimetrically the heat of dilution of such a dilute solution, but we may use for our purpose the temperature coefficient of solubility. One of us[4] has called attention to the fact that remarkably straight lines are obtained, except in concentrated solutions, when the logarithm of the mole fraction of a solute x_2 is plotted against $\log T$. This permits $(\partial \log x_2/\partial \log T)_{\bar{F}_2-F_2^s}$ to be fixed quite accurately. It was shown, also, that the entropy of change from solid to saturated solution is given by

$$\bar{S}_2-S_2^s=R\left(\frac{\partial \ln a_2}{\partial \ln x_2}\right)_T\left(\frac{\partial \ln x_2}{\partial \ln T}\right)_{\bar{F}_2-F_2^s}, \qquad (1)$$

where a_2 is the activity of the solute in the solution referred to its pure liquid. The factor $\partial \ln a_2/\partial \ln x_2$ approaches unity as x_2 approaches zero, Henry's law, and the small departure from unity can be calculated with sufficient accuracy for our purpose by differentiating the equation

$$\ln a_2=\ln x_2+\bar{V}_2\phi_1^2(\delta_2-\delta_1)^2/RT, \qquad (2)$$

which holds well for violet iodine solutions. (Here ϕ_1 is the volume fraction of the solvent, v_2 the molal volume of liquid iodine, 59.0 cc, δ_2 its "solubility parameter," 14.1, and δ_1 that of the solvent, 8.6 for carbon tetrachloride. x_2 in this case is 0.01147). We obtain in this way $\partial \ln a_2/\partial \ln x_2=0.96$. The measured solubilities give $\partial \ln x_2/\partial \ln T=10.93$, and Eq. (1) gives $\bar{S}_2-S_2^s=20.80$.

We wish, next, to calculate the entropy involved in transferring liquid iodine to a solution of composition x_2 and to ascertain how well it agrees with the postulated entropy of transfer to a "regular" solution, $-R\ln x_2$. Since $\bar{S}_2-S_2^0=(\bar{S}_2-S_2^s)-(S_2^0-S_2^s)$, we will find the value of the entropy of fusion by aid of the measurements of Frederick and Hildebrand,[5] who gave for the heat of fusion $H_2^0-H_2^s=3740$ cal/mole at the melting point, $T_m=386.75$, and values for the heat capacity of liquid and solid which give a mean value of $\Delta C_p=5.5$ in the interval 25° to the melting point. (This involves a long extrapolation of C_p for the liquid, and the subsequent figures involve a corresponding uncertainty.) From these figures we calculate the entropy of fusion at 25° to be 8.24, and hence $\bar{S}_2-S_2^0=12.56$. But $-R\ln x_2=8.88$, less by 3.68. The Flory-Huggins expression,

$$\bar{S}_2-S_2^0=-R\ln\varphi_2+\varphi_1\left(1-\frac{V_2}{V_1}\right), \qquad (3)$$

[1] J. H. Hildebrand and R. L. Scott, *Solubility of Nonelectrolytes* (Reinhold Publishing Corporation, New York, 1950).
[2] J. H. Hildebrand, J. Am. Chem. Soc. **51**, 661 (1929).
[3] See reference 1, Chap. VIII.
[4] J. H. Hildebrand, J. Chem. Phys. **20**, 190 (1952).
[5] K. J. Frederick and J. H. Hildebrand, J. Am. Chem. Soc. **60**, 1436 (1938).

designed to take account of different molal volumes of the pure constituents, gives 9.07, which reduces the discrepancy only to 3.49.

A regular solution was originally defined by the senior author[2] as "one involving no entropy change when a small amount of one of its components is transferred to it from an ideal solution of the same composition" (i.e., mole fraction), "the total volume remaining unchanged." It was further stated that the equation $(\partial S/\partial V)_T=(\partial P/\partial T)_V$ could be used to calculate the contribution made by the change in volume. Scatchard[6] was the first to determine the magnitude of this effect by considering the process of solution as split into two steps; first, mixing at constant volume, then expanding the solution to 1 atmos pressure. This process has been further discussed in our monograph, and we apply it to the second case below.

For the first case here considered we reverse the order and first expand the liquid solute from V_2^0 to $\bar{V}_2$, its partial molal volume in the solution; then transfer to the solution at the new constant volume. For $\bar{V}_2$ we use the figure 65.8 cc at 18° for iodine in carbon tetrachloride, obtained by Dawson.[7] We use for V_2^0 our own extrapolated value, 59.0 cc. Starting with the thermodynamic equation

$$\left(\frac{\partial S}{\partial V}\right)_T=\left(\frac{\partial P}{\partial T}\right)_V=\frac{1}{T}\left(\frac{\partial E}{\partial V}\right)_T-\frac{P}{T}, \qquad (4)$$

we may neglect P/T for a liquid, and we may write[8] $(\partial E/\partial V)_T=\Delta E^V/V=\delta^2$, where δ is the solubility parameter of the solute. Integrating between the limits V_2^0 and $\bar{V}_2$, we get

$$\bar{S}_2(\bar{V}_2)-\bar{S}_2(V_2^0)=\int_{V_2^0}^{\bar{V}_2}\left(\frac{\partial S_2}{\partial V_2}\right)_T dV$$

$$=\left(\frac{\partial S_2}{\partial V_2}\right)_T(\bar{V}_2-V_2^0)=(\bar{V}_2-V_2^0)\delta_2^2/T. \qquad (5)$$

For iodine $\delta_2=14.1$ and the volume change is 6.8 cc, so the entropy difference due to the volume expansion should be about 4.5 eu. This is sufficiently close to the observed discrepancy 3.68 to make it rather clear that the ideal entropy applies to mixing at constant volume.

Another example, that of iodine in perfluoro *n*-heptane, is even more extreme. At 25°C, the solubility[9] is only 0.018 mole percent, corresponding to an activity coefficient γ_2 with the huge value of 1400. From the solubilities at 0°, 25°, and 35°, we calculate $(\partial \log x_2/\partial \log T)_{\bar{P}_2-P_2^s}$ as 17.0±0.6. The correction factor $(\partial \ln a_2/\partial \ln x_2)_T$ is for this very dilute solution essentially unity (0.999) so $\bar{S}_2-S_2^s$ is 33.7 eu. Subtracting $S_2^0-S_2^s=8.2$ from this we obtain $\bar{S}_2-S_2^0=25.5$ eu. The entropy change at constant volume is only 17.2 eu if it is taken as ideal ($-R\ln x_2$) and 18.4 if the Flory-Huggins equation (Eq. (3)) is used, leaving a discrepancy of 7–8 eu.

The partial molal volume of iodine in the fluorocarbon solution is unknown, so we must fall back upon more approximate methods of calculating the change in entropy on expansion from V_2^0 to $\bar{V}_2$. According to elementary theory[3] the change in volume is directly proportional to the nonideal part of the free energy of mixing, and the change in entropy can be shown to be

$$\bar{S}_2(\bar{V}_2)-\bar{S}_2(V_2^0)=\alpha RT\ln\gamma_2, \qquad (6)$$

where γ_2 is the activity coefficient of the iodine and α is the coefficient of thermal expansion. If α is different for the solute and solvent, the α which appears in Eq. (6) is a complex average, but it can be shown that in dilute solutions ($x_2\to 0$) one should use α_1, the coefficient of thermal expansion of the solvent. Using $\gamma_2=1400$ and $\alpha_1=1.6\times10^{-3}$ deg^{-1} for the fluorocarbon,[10] we calculate this entropy difference to be 6.9 eu, in excellent agreement with the experimental data.

This approximate method gives for the case of iodine in carbon tetrachloride ($\alpha_1=1.2\times10^{-3}$ deg^{-1}), an entropy difference of 2.2 eu, somewhat low by comparison with the observed value of 3.68 eu.

It may be emphasized that these two solutions deviate enormously from Raoult's law, and therefore greatly enhance the difference between the entropy of mixing at constant pressure and at constant volume. The solutions for which this effect has heretofore been studied show expansions of the order of one percent or less, while for iodine in carbon tetrachloride $\bar{V}-V^0$ is 11.5 percent.

It is evident from the foregoing discussion that the experimental entropy of mixing at constant pressure is markedly different from the entropy of mixing at constant volume, which should be approximately ideal. It is obviously important not to omit this restriction in defining the regular solution.[11] We repeat, however, that the volume expansion has little effect on the free energy, a fact which is demonstrated by the conspicuous success of Eq. (2) in computing solubility of iodine in nonpolar solvents, even in the fluorocarbon C_7F_{16} for which a very marked entropy discrepancy was observed. Neglect of this volume correction is not serious for small deviations from Raoult's law, nor even for large deviations so far as solubility equilibria are concerned.

It seems evident that further refinements in the theory of solubility require studies, both experimental and theoretical, of changes of volume upon mixing.

This work is part of a project supported by the AEC.

[6] G. Scatchard, Trans. Faraday Soc. **33**, 160 (1937). See also Scatchard, Wood and Mochel, J. Phys. Chem. **43**, 119 (1939); S. E. Wood and J. P. Brusie, J. Am. Chem. Soc. **65**, 1891 (1943); S. E. Wood and A. E. Austin, J. Am. Chem. Soc. **67**, 480 (1945); S. E. Wood, J. Chem. Phys. **15**, 358 (1947).

[7] H. M. Dawson, J. Chem. Soc. (London) **97**, 1041 (1910).

[8] J. H. Hildebrand and J. M. Carter, J. Am. Chem. Soc. **54**, 3592 (1932); R. L. Scott, J. Chem. Phys. **16**, 256 (1948); see also Reference 1, pp. 96–99 and pp. 427–429.

[9] Hildebrand, Benesi, and Mower, J. Am. Chem. Soc. **72**, 1017 (1950).

[10] A. V. Grosse and G. H. Cady, Ind. Eng. Chem. **39**, 367 (1947).

[11] J. H. Hildebrand, Nature **168**, 868 (1951).

THE JOURNAL OF CHEMICAL PHYSICS VOLUME 20, NUMBER 10 OCTOBER, 1952

Hydrogen Overvoltage and Atomic Hydrogen Electrodes

PIERRE VAN RYSSELBERGHE
Department of Chemistry, University of Oregon, Eugene, Oregon
(Received May 19, 1952)

The fundamental thermodynamics and kinetics of hydrogen overvoltage are re-examined and improved. A precise definition of the transfer coefficient is given, the significance of the free energy of activation is discussed, and additional theoretical support is given for the interpretation of hydrogen overvoltage as being due to the establishment of reversible atomic hydrogen electrodes.

IN a previous paper in this Journal[1] we treated the electrochemical thermodynamics and kinetics of hydrogen overvoltage through the use of electrochemical potentials in a more detailed and explicit manner than had been done previously by other authors. In a more recent paper[2] certain aspects of our treatment were improved, and in particular, a more detailed interpretation of overvoltage as due to the establishment of atomic hydrogen electrodes was presented. The effect of adsorption of the activated complex was examined through the formal introduction of a Freundlich exponent, which was shown to enter into the constants of the Tafel equation (see Hickling and Salt).[3]

In view of the fact that other authors[4,5] are now using electrochemical potentials in their discussions of hydrogen overvoltage and in view of the fact that our own treatment was meant to provide a general frame within which more detailed considerations of mechanism should find their logical place, it appears important to present again the main steps of our reasoning and to add to them a number of theoretical refinements. For the sake of simplicity and brevity we shall consider the Freundlich exponent as equal to one and shall indicate, at the end of the discussion, what modifications an exponent different from one would introduce.

Positions 1, 2, 3, 4, and 5 are, respectively, the surface of the electrode, the locus of the activated H^+ ions, the average position of all adsorbed H^+ ions, the locus of the activated H^+ ions involved in the adsorption process, the free solution. The cathodic current corresponding to the discharge of H^+ ions is (see notations in previous paper)[1]

$$I=(kTF/h)\cdot C_2. \tag{1}$$

The electrochemical equilibrium condition between H^+ in positions 2 and 5 is

$$\bar{\mu}_2=\bar{\mu}_5 \quad \text{or} \quad m_2^0+\ln(C_2f_2)+s_2=m_5^0+\ln a_5+s_5. \tag{2}$$

Hence

$$I=(kTF/hf_2)\cdot a_5\cdot\exp(m_5^0-m_2^0)\cdot\exp(s_5-s_2). \tag{3}$$

The activity a_5 is connected with the reversible potential difference between positions 1 and 5 by the formula

$$s_1^r-s_5^r=s_1^0-s_5^0+\ln a_5, \tag{4}$$

in which $s_1^0-s_5^0$ corresponds to the reversible potential difference when $a_5=1$ and the pressure of molecular hydrogen is equal to 1 atmosphere.

The overvoltage is the difference between the reversible potential difference for $p_{H_2}=1$ atmos and the actual potential difference:

$$v=s_1^r-s_5^r-(s_1-s_5). \tag{5}$$

Combining (3), (4), and (5),

$$I=(kTF/hf_2)\cdot\exp(m_5^0-m_2^0+s_5^0-s_1^0)\cdot\exp(v+s_1-s_2). \tag{6}$$

This formula will become of the Tafel type if we set

$$v+s_1-s_2=\alpha v+s_1^r-s_2^r. \tag{7}$$

Formulas (7) and (5) show that

$$\alpha=[s_2^r-s_5^r-(s_2-s_5)]/[s_1^r-s_5^r-(s_1-s_5)], \tag{8}$$

which is the ratio of the overvoltage between positions 2 and 5 to the total one between positions 1 and 5. Formula (8) constitutes a precise definition of α.

From (6) and (7) we deduce

$$I=I_0\cdot\exp(\alpha v) \tag{9}$$

with

$$I_0=(kTF/hf_2)\cdot\exp(m_5^0-m_2^0+s_5^0-s_1^0+s_1^r-s_2^r), \tag{10}$$

and (taking the activity coefficient of the complex equal to unity)

$$m_5^0-m_2^0+s_5^0-s_1^0+s_1^r-s_2^r=-(\Delta F^\ddagger/RT). \tag{11}$$

The free energy of activation $\Delta F^\ddagger$, obtainable by extrapolation of the Tafel line, is thus seen not to be merely the difference $\mu_2^0-\mu_5^0$ but to include also electric potential differences multiplied by the Faraday. Similarly the enthalpy of activation $\Delta H^\ddagger$ includes these differences and their temperature coefficients; it is obtainable from the temperature coefficient of overvoltage.

Since

$$\psi_1^0-\psi_2^0=(\mu_5^0+\mu_{e1}-\tfrac{1}{2}\mu_{H_2}^0)/F, \tag{12}$$

in which μ_{e1} represents the chemical potential of the electron in the metal, we have also

$$\Delta F^\ddagger=\mu_2^0+\mu_{e1}-\tfrac{1}{2}\mu_{H_2}^0+F(\psi_2^r-\psi_1^r), \tag{13}$$

[1] P. Van Rysselberghe, J. Chem. Phys. **12**, 1226 (1949).
[2] P. Van Rysselberghe, J. chim. phys. **49**, C47 (1952).
[3] A. Hickling and F. W. Salt, Trans. Faraday Soc. **38**, 474 (1942).
[4] R. Parsons and J. O'M. Bockris, Trans. Faraday Soc. **47**, 914 (1951).
[5] J. O'M. Bockris and E. C. Potter, J. Electrochem. Soc. **99**, 169 (1952).

a formula whose correctness can also be checked through the fact that

$$\Delta F^{\ddagger} = -RT \ln a_{20}, \tag{14}$$

a_{20} being the activity of the complex corresponding to the exchange current I_0. The potential difference $\psi_1 - \psi_2$ would be given by

$$\psi_1 - \psi_2 = (\mu_2^0 + \mu_{e1} - \tfrac{1}{2}\mu_{H_2}^0)/F + (RT/F) \cdot \ln(a_2/p_{H_2}^{\frac{1}{2}}), \tag{15}$$

if we had reversibility with respect to molecular hydrogen at pressure p_{H_2}, and by

$$\psi_1 - \psi_2 = (\mu_2^0 + \mu_{e1} - \mu_H^0)/F + (RT/F) \cdot \ln(a_2/p_H), \tag{16}$$

if we had reversibility with respect to atomic hydrogen at pressure p_H. Formulas (15), (13), and (10) would lead to

$$\omega = vRT/F = (RT/F) \cdot \ln(p_{H_2}^{\frac{1}{2}}), \tag{17}$$

while formulas (16), (13), and (10) would lead to

$$\omega = (RT/F) \cdot \ln p_H + (\mu_H^0 - \tfrac{1}{2}\mu_{H_2}^0)/F, \tag{18}$$

or, at 25°C,

$$\omega = 0.06 \log p_H + 2.11 \text{ volts}. \tag{19}$$

An overvoltage of 1 volt would make p_{H_2} in formula (17) equal to $10^{33.4}$ atmos and p_H in formula (19) equal to $10^{-18.5}$ atmos. The latter value is a plausible one,* while the former is obviously to be ruled out. Atomic hydrogen resulting from the discharge process would remain in the adsorbed state at the surface of the metal and, in the steady state of constant overvoltage for a constant current density, would escape at a pressure appreciably larger than its equilibrium pressure of $10^{-35.2}$ atmos with molecular H_2 at 1 atmos. At low overvoltages corresponding to small currents or to metals favoring the combination $2H \rightarrow H_2$, the pressure of atomic H approaches this equilibrium value. It is, however, to be expected that, in the steady state, an equilibrium between adsorbed H, H_2, and possible hydrides is established for each set of values of ω and I. The chemical potential per mole of adsorbed H_2 in equilibrium with H at a pressure of $10^{-18.5}$ atmos corresponding to an overvoltage of 1 volt is

$$\mu_2 = 2(\mu_H^0 + RT \ln p_H) = 46 \text{ kilocalories}. \tag{20}$$

The chemical potential per mole of hydride MH would be 23 kilocalories. For any overvoltage ω one would have $\mu_{H_2} = 2\omega F$ and $\mu_{HM} = \omega F$. The composition of the electrode surface is thus a function of the overvoltage. From (9) and (18) we get

$$p_H = 10^{-35.2} \cdot (I/I_0)^{1/\alpha}. \tag{21}$$

Since α is often close to 0.5, we see that the pressure of atomic H is practically proportional to the square of the current density. Vice versa, I is proportional to the square root of p_H, a plausible result since I is proportional to the rate of production of gaseous H_2 and hence to the square of the surface concentration of H, this latter concentration being proportional to a fractional power $1/m$ of the pressure p_H. This fractional power must be $\frac{1}{4}$ to make I proportional to $p_H^{\frac{1}{2}}$. In general, one would have $\alpha m = 2$.

The foregoing considerations apply to high overvoltages. At low overvoltages formula (9) is replaced by

$$I = I_0(\exp(\alpha v) - \exp(-\beta v)), \tag{22}$$

with

$$\alpha + \beta = 1, \tag{23}$$

or, expanding the exponentials as power series,

$$I = I_0 v = (I_0 F/RT) \cdot \omega. \tag{24}$$

If we still consider ω as due to the establishment of a reversible atomic hydrogen electrode in accordance with (19), we now have, in place of (21),

$$p_H = 10^{-35.2} \cdot \exp(I/I_0). \tag{25}$$

For $\omega = 0.1$ volt formula (9) is nearly as accurate as (22) or (24) and p_H is $10^{-33.5}$ atmos, i.e., 50 times the equilibrium pressure with H_2 at 1 atmos.

If we had introduced, as in our second paper on hydrogen overvoltage,[2] a Freundlich exponent z in the adsorption equilibrium condition between positions 2 and 5, we would have found that

$$(\alpha + \beta) \cdot z = 1, \tag{26}$$

a relation whose experimental test would require the separate determination of α and β at large cathodic and anodic overvoltages, respectively, or the determination of the sum $\alpha + \beta$ at very low overvoltages [the right-hand side of (24) is multiplied by $(\alpha + \beta)$], provided the exchange current I_0 applying there is the same as that obtained by the extrapolation of either the cathodic or the anodic Tafel line (see discussion of our previous paper).[2]

Summing up the contents of our three papers[1,2] on hydrogen overvoltage we may say that, in steady overvoltage states, the discharge process $H^+ + e^- \rightarrow H$ and the combination process $H + H \rightarrow H_2$ occurring at the same rate, it is immaterial whether one selects a slow discharge or a slow combination theory to calculate this rate. It appears highly probable that the step $H^+ + e^- \rightarrow H$ is reversible, the apparent overvoltage being thus due to the establishment of a reversible atomic hydrogen electrode. The activity of adsorbed H at the surface of the electrode is in equilibrium with the pressure of the escaping H and with the activities of adsorbed H_2 and of hydrides. The irreversibility of the whole process resides then in the difference of chemical potential between adsorbed H_2 and the escaping gas. As overvoltage decreases with current on a particular electrode or as metals of increasing catalytic effect on the combination $H + H \rightarrow H_2$ are being considered, the pressure of atomic H approaches its equilibrium value with H_2 at 1 atmos and the electrode behaves more and more like a reversible H_2 electrode.

* J. O'M. Bockris (Chem. Revs. **43**, 525 (1948), see p. 564) states that such pressures have little physical meaning. A considerably larger amount of atomic hydrogen than the surface concentration which would be in equilibrium with such pressures could be present in the electrode surface under the form of hydrides.

Molecular Structure of Bromoform*

QUITMAN WILLIAMS,† JOHN T. COX, AND WALTER GORDY
Department of Physics, Duke University, Durham, North Carolina
(Received April 14, 1952)

The structure of bromoform has been evaluated entirely from microwave spectroscopy. The B_0 values in Mc/s of the isotopic species studied are: 1247.61±0.025 for $CHBr_3^{79}$; 1217.30±0.025 for $CHBr_3^{81}$; 1239.45 ±0.025 for $CDBr_3^{79}$; 1209.51±0.025 for $CDBr_3^{81}$. These constants yield the structure as follows: d_{CH} =1.07A±0.01A, d_{CBr}=1.930A±0.003A, angle BrCBr=110°48′±16′.

INTRODUCTION

ALTHOUGH several approximate measurements of the BrBr and CBr distances in bromoform have been made from electron diffraction,[1] no value for the CH distance has been previously obtained. Recent microwave results[2] indicate that the CH distance in chloroform is shorter than the tetrahedral value for methane and that angle ClCCl is larger than the tetrahedral value of 109°28′. The present study reveals that the corresponding dimensions in bromoform are similar.

Preliminary results of the present investigation have been reported previously.[3] Japanese workers[4] have recently reported the observation of the 0→1 rotational transition of $CHBr_3$. An unexpectedly large value of the stretching constant D_J is required to bring our B_0 values into agreement with the ones which they report.

TABLE I. Frequencies of rotational transitions and derived rotational constants of different isotopic species of bromoform.

	$J\rightarrow J$	ν (Mc/s)	B_0 (Mc/s)[a]	I (gm-cm² ×10⁴⁰)[b]
$CHBr_3^{79}$	10→11	27,447.9±0.5		
	11→12	29,942.7±0.5	1247.61±0.025	672.4_{11}
	12→13	32.438.2±0.5		
	14→15	37,427.8±0.5		
$CHBr_3^{81}$	10→11	26,781.1±0.5		
	11→12	29,215.4±0.5	1217.30±0.025	689.1_{54}
	12→13	31,649.9±0.5		
	13→14	34,084.1±0.5		
$CDBr_3^{79}$	11→12	29,747.2±0.5		
	12→13	32,225.6±0.5	1239.45±0.025	676.8_{38}
	13→14	34,704.6±0.5		
$CDBr_3^{81}$	11→12	29,028.2±0.5		
	12→13	31,447.3±0.5	1209.51±0.025	693.5_{95}
	13→14	33,866.2±0.5		

[a] Obtained from the observed frequencies by neglecting centrifugal distortion effects.
[b] h=6.623773×10⁻²⁷ erg-sec from DuMond and Cohen, Revs. Modern Phys. 21, 651 (1949).

ROTATIONAL CONSTANTS

The rotational frequencies were observed with a 100 Kc square-wave Stark-modulation spectrograph and measured in the usual manner with frequencies monitored by station WWV. The nuclear hyperfine structure expected because of the Br quadrupole moment was not resolved. This limited somewhat the accuracy of the evaluations of the spectral constants but did not effectively limit the structural determinations beyond that imposed by the differences in zero point vibrational energies of the different isotopic species. Despite the relatively large quadrupole moments of Br^{79} and Br^{81}, the stronger components of the hyperfine structure would, for the high J transition observed in the present study, be expected to fall very near the position of the hypothetical unsplit rotational line. The appearance of the spectrum was in accordance with this behavior. A moderately sharp and strong line was observed for each transition.

In Table I values of the observed rotational frequencies together with the B_0 values and moments of inertia I_B derived from them are given for the four symmetric-top configurations investigated. Groups of lines caused by asymmetric-top species such as $HCBr^{79}Br_2^{81}$ were observed but because of their complexity were not analyzed. The centers of gravity of these partially resolved groups fell, however, at the positions calculated by treating these slightly asymmetric species as symmetric rotors. Additional confirmation for the assignments was thus obtained. Sufficient information was obtained from the completely symmetric species listed in Table I for a complete evaluation of the molecular structure.

The accuracy of the B_0 values was estimated from the internal consistency of the results derived from the different rotational transitions and from a consideration of the sharpness and shape of the observed lines which are comprised of unresolved hyperfine multiplets. Relative values of the frequencies for the same transition in the different isotopic species are measured to a somewhat higher accuracy than are the absolute B_0 values listed.

* The research reported in this paper has been sponsored by the Geophysics Research Division of Air Force Cambridge Research Center under Contract W19-122-ac-35.
† Texas Company Fellow. Present address: Department of Physics, Georgia Institute of Technology, Atlanta, Georgia.
[1] For reference see L. R. Maxwell, J. Opt. Soc. Am. 30, 374 (1940).
[2] Ghosh, Trambarulo, and Gordy, J. Chem. Phys. 20, 605 (1952).
[3] J. Q. Williams and W. Gordy, Phys. Rev. 79, 225A (1950).
[4] Kojima, Tsukada, and Hagiwara (privately communicated by Dr. M. Mizushima).

STRUCTURE

One more isotopic species was measured than is required to evaluate the structure. This additional parameter allows a partial check on the accuracy of the determination through the internal consistency test. Values of the structural parameters obtained from the different isotopic combinations are given in Table II. In the last column averaged values are given with error limits chosen so as to take in the maximum deviations from the mean values. These limits are about the same as those obtained from the internal consistency test in other similar molecules, and we believe that they approximate the errors which may be caused by zero point vibrations. However, these limits may not represent the maximum deviations which might be obtained with any possible isotopic combination, and are not to be regarded as precise estimates of the errors.

TABLE II. Molecular dimensions of bromoform as derived from different isotopic combinations.

Combinations used	d_{C-H}	d_{C-Br}	Angle BrCBr
$CHBr_3^{79}$ $CHBr_3^{81}$ $CDBr_3^{79}$	1.0579	1.9324	110°32.6′
$CHBr_3^{79}$ $CHBr_3^{81}$ $CDBr_3^{81}$	1.0601	1.9329	110°33.2′
$CHBr_3^{79}$ $CDBr_3^{79}$ $CDBr_3^{81}$	1.0750	1.9273	111°1.8′
$CHBr_3^{81}$ $CDBr_3^{79}$ $CDBr_3^{81}$	1.0777	1.9271	111°3.2′
Averages	1.068±0.010	1.930±0.003	110°48′±16′

Table III presents a comparison of the structural parameters obtained for bromoform with the corresponding ones in chloroform and fluoroform. As might be expected from steric factors, the Hal−C−Hal angle increases in the series from fluoroform to bromoform. The surprising feature is that the CH distance decreases in the same sequence. It is of interest also to compare the structures of these molecules with those of the methyl halides. The microwave investigations of Gordy, Simmons, and Smith[5] revealed that the CH distance in the methyl halides is slightly longer than the tetrahedral value 1.093A of methane, and that the HCH angles are slightly greater than the tetrahedral value 109°28′. Therefore, the H−C−Hal angles deviate in the same direction (smaller) from the tetrahedral value in the methyl halides as in the haliforms, while the CH distances in the two classes of molecules lie on opposite sides of the tetrahedral value in methane, 1.093A.

[5] Gordy, Simmons, and Smith, Phys. Rev. **74**, 243 (1948).

TABLE III. Comparison of molecular structures of fluoroform, chloroform and bromoform.

	d_{CH}	d_{C-Hal}	Angle Hal−C−Hal
F_3CH [a]	1.09_8	1.332	108°48′
Cl_3CH [a]	1.07_3	1.767	110°24′
Br_3CH	1.06_8	1.930	110°48′

[a] Values for these molecules from Ghosh, Trambarulo, and Gordy, J. Chem. Phys. **20**, 605 (1952).

The fact that the CH distance decreases with the increasing number of halogens attached to the central carbon might be largely an effect of the increasing positive charge on the carbon caused by the ionic character contributed by structures of type I. Presumably

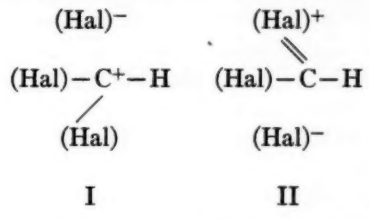

I II

in fluoroform, and to a lesser extent also in chloroform, contributions from I would be largely replaced by contributions from structures of type II. This might account for the appreciably shorter CF distance in fluoroform than that in methyl fluoride as well as the approximately normal value of the CH distance in fluoroform. The fact that the CBr distance in bromoform is almost identical to that in methyl bromide shows that structures of type II are relatively unimportant in bromoform. The CH distance in iodoform would be of help in interpreting these results, but unfortunately this parameter has not yet been evaluated for iodoform.

We wish to thank Professor R. B. Bernstein of the Illinois Institute of Technology for supplying the sample of deuterated bromoform and Dr. R. F. Trambarulo for his interest and help.

THE JOURNAL OF CHEMICAL PHYSICS VOLUME 20, NUMBER 10 OCTOBER, 1952

Cooperative Orientation Effects in Solutions

J. A. BARKER
Division of Industrial Chemistry, C.S.I.R.O., Melbourne, Australia
(Received January 15, 1952)

A general theoretical method for evaluating the effect on thermodynamic properties of cooperative orientation in solutions is developed. The theory is applied to the systems methanol+benzene, methanol carbon tetrachloride, and chloroform+ethanol. Theoretical curves for excess free energy of mixing, heat of mixing, and excess entropy of mixing as functions of composition are presented and are in reasonable quantitative agreement with experimental values for the first two systems and qualitatively similar to the experimental curves for the third. It is concluded that the method provides a useful approach to the theory of solutions of associated liquids in general.

I. INTRODUCTION

THE thermodynamic properties of solutions of associated liquids show considerable complexity in their dependence on concentration and temperature. In a previous paper[1] an attempt was made to relate the thermodynamic behavior of solutions of alcohols in nonpolar solvents with the molecular interactions occurring in the solutions. In the present paper a general theoretical method is discussed for problems of this type, in which the interaction energies of neighboring molecules depend on their relative orientations.

The general viewpoint adopted is similar to that of regular solution theory and the theory of polymer solutions in that a quasi-lattice picture of the liquid is used, each molecule occupying a certain number of sites on a well-defined lattice. However, the interaction energies of neighboring molecules are supposed to depend on the parts of the molecular surface which are in contact. The mathematical treatment is based throughout on the Bethe quasi-chemical approximation.

The theory is developed with full generality in Secs. II and III, and is applied to particular problems in Secs. IV and V.

II. THE BETHE APPROXIMATION AND QUASI-CHEMICAL EQUATIONS

The Bethe approximation method is here used to construct a grand partition function from which quasi-chemical relations between the numbers of interactions of various types in the equilibrium configuration may be derived.

Molecules of types $A, B \cdots$ are to be arranged on a z-coordinated lattice, of which a molecule of type A occupies r_A sites. A type A molecule has q_Az neighboring sites,[2] where $q_Az=r_Az-2r_A+2$.

It is supposed that the surface of an A molecule, for example, is divided into q_Az contact points, each of which has a specific interaction energy with the neighboring part of the surface of another molecule. Thus if an A molecule and a B molecule occupy neighboring sites in such a way that the kth contact point of the A molecule is in contact with the lth contact point of the B molecule then the interaction energy is defined to be ${}^*U_{kl}{}^{AB}$ (k and l may take the values 1 to q_Az and 1 to q_Bz, respectively). The further definitions are made:

$$U_{kl}{}^{AB}={}^*U_{kl}{}^{AB}-\tfrac{1}{2}{}^*U_{kk}{}^{AA}-\tfrac{1}{2}{}^*U_{ll}{}^{BB},$$

$${}^*\eta_{kl}{}^{AB}=\exp[-{}^*U_{kl}{}^{AB}/kT],\quad \eta_{kl}{}^{AB}=\exp[-U_{kl}{}^{AB}/kT].$$

The grand partition function is constructed by considering the modes of occupation of a definite pair of neighboring sites PQ, the remainder of the assembly being represented by averaged terms.[3] Let $N_\kappa{}^A$ represent the number of ways in which an A molecule may be placed on the site P with its kth contact point in contact with whatever molecule occupies the site Q. It is assumed that $N_k{}^A$ is independent of the mode of occupation of Q (this is accurately true if either the molecule A on P or the molecule on Q occupy only a single site; if both are long-chain molecules it is an approximation, though probably a good one). It is also assumed that the molecules are not so flexible that a remote segment of the molecule A on P can "fold back" and occupy the site Q.

"Occupation factors" $\epsilon_k{}^A$ and factors $\eta_k{}^A$ for the interaction of the kth contact point of an A molecule with the averaged environment are also introduced.[3] Then the approximate grand partition function is

$$\Xi_2=f[\sum_{\substack{ik\\AB}}{}^*\eta_{ik}{}^{AB}\epsilon_i{}^A\epsilon_k{}^BN_i{}^AN_k{}^B\prod_{j\neq i}\eta_j{}^A\prod_{l\neq k}\eta_l{}^B+C]. \quad (1)$$

In the summation the term involving ${}^*\eta_{ik}{}^{AB}$ has coefficient l if $({}_i{}^A)\equiv({}_k{}^B)$, and 2 otherwise.

The factor f includes the effect of all pairs of sites other than PQ, while C represents the contribution of configurations in which P and Q are occupied by adjacent segments of the same molecule. The point of the method is that neither f nor C depends on the quantities ${}^*\eta_{ik}{}^{AB}$.

If now $N_{ik}{}^{AB}$ denotes the number of interactions of $({}_i{}^A)$ and $({}_k{}^B)$ surface, then $N_{ik}{}^{AB}$ is given in terms of the grand partition function by

$$N_{ik}{}^{AB}={}^*\eta_{ik}{}^{AB}\partial\ln\Xi/\partial{}^*\eta_{ik}{}^{AB}.$$

[1] J. Barker, J. Chem. Phys. **19**, 1430 (1951).
[2] A. R. Miller, *Theory of High Polymer Solutions* (Oxford University Press, New York, 1948), p. 18.
[3] See reference 2, Chapter III.

If the approximate expression (1) for the grand partition function is used, the quasi-chemical conditions (2) are readily deduced:

$$(N_{ik}{}^{AB})^2/N_{ii}{}^{AA}N_{kk}{}^{BB}=4(*\eta_{ik}{}^{AB})^2/(*\eta_{ii}{}^{AA}*\eta_{kk}{}^{BB})$$
$$=4(\eta_{ik}{}^{AB})^2. \qquad (2)$$

Since all lattice sites are assumed to be occupied, there are necessary relations between the $N_{ik}{}^{AB}$ of the form

$$2N_{ii}{}^{AA}+\sum_{\substack{B,\,k\\(_k{}^B)\not\equiv(_i{}^A)}} N_{ik}{}^{AB}=N_A. \qquad (3)$$

Suppose that the q_Az contact points of an A molecule may be divided into a number of classes, the number in the μth class being $Q_\mu{}^A$, such that the members of a class are equivalent with respect to interaction energies, i.e.,

$$*\eta_{il}{}^{AB}=*\eta_{kl}{}^{AB}$$

and

$$*\eta_{ii}{}^{AA}=*\eta_{ik}{}^{AA}=*\eta_{kk}{}^{AA},$$

for all values of i, k in the same class and for all values of B and l.

Then (2) and (3) may be replaced by the equations*

$$(N_{\mu\nu}{}^{AB})^2/(N_{\mu\mu}{}^{AA})(N_{\nu\nu}{}^{BB})=4(\eta_{\mu\nu}{}^{AB})^2, \qquad (2')$$

$$2N_{\mu\mu}{}^{AA}+\sum_{\substack{B,\,\nu\\(_\nu{}^B)\not\equiv(_\mu{}^A)}} N_{\mu\nu}{}^{AB}=Q_\mu{}^AN_A. \qquad (3')$$

In these equations the Greek suffixes μ, ν represent classes and

$$N_{\mu\nu}{}^{AB}=\sum_{i\text{ in }\mu}\sum_{k\text{ in }\nu} N_{ik}{}^{AB}.$$

If the substitutions

$$N_{\mu\nu}{}^{AB}=2X_\mu{}^AX_\nu{}^B\eta_{\mu\nu}{}^{AB}N \quad \text{for} \quad (_\mu{}^A)\not\equiv(_\nu{}^B),$$
$$=(X_\mu{}^A)^2N \quad \text{for} \quad (_\mu{}^A)\equiv(_\nu{}^B)$$

are made, the quasi-chemical Eq. (2′) are automatically satisfied. The Eqs. (3′), which determine the parameters $X_\mu{}^A$, then take the form

$$X_\mu{}^A\sum_{B,\nu}\eta_{\mu\nu}{}^{AB}x_\nu{}^B=\frac{Q_\mu{}^A}{2}\frac{N_A}{N}.$$

In the particular problems of later sections, N is taken to be $\sum N_A$.

III. THE CONFIGURATIONAL FACTOR AND PARTITION FUNCTION

A method due to Guggenheim[4] is used to calculate the number $g(N_{\mu\nu}{}^{AB}\cdots, N_A\cdots)$ of configurations corresponding to a given set of values of $N_{\mu\nu}{}^{AB}$. The method by which the thermodynamic functions for the solution may be calculated is then indicated.

The partition function for the solution is given by

$$Q=\sum_{N_{\mu\nu}{}^{AB}} g(N_{\mu\nu}{}^{AB}\cdots, N^A\cdots)\prod\exp(N_{\mu\nu}{}^{AB}\ln{}^*\eta_{\mu\nu}{}^{AB}). \qquad (4)$$

The equilibrium values of $N_{\mu\nu}{}^{AB}$ are determined by maximizing the logarithm of the term under summation in (4), subject to the restrictions imposed by Eq. (3′). The maximizing conditions are

$$2\partial\ \ln g/\partial N_{\mu\nu}{}^{AB}-\partial\ \ln g/\partial N_{\mu\mu}{}^{AA}$$
$$-\partial\ \ln g/\partial N_{\nu\nu}{}^{BB}+2\ \ln\eta_{\mu\nu}{}^{AB}=0. \qquad (5)$$

The device used by Guggenheim was to assume that Eq. (5) was identical with the quasi-chemical condition (2′). This assumption is made here also.

If the sets of Eqs. (5) and (2′) are to be identical it is required that

$$\partial\ \ln g/\partial N_{\mu\nu}{}^{AB}=-\ln N_{\mu\nu}{}^{AB}+\ln 2+\varphi(N_A{}^*, N_B\cdots) \quad \text{for} \quad (_\mu{}^A)\not\equiv(_\nu{}^B),$$
$$\partial\ \ln g/\partial N_{\mu\mu}{}^{AA}=-\ln N_{\mu\mu}{}^{AA}+\varphi(N_A, N_B\cdots),$$

where $\varphi(N_A, N_B\cdots)$ may be any function of $N_A, N_B\cdots$. Integration of these expressions leads to the result

$$\ln g=-\sum \ln N_{\mu\nu}{}^{AB}!+\ln 2\sum{}' N_{\mu\nu}{}^{AB}+\varphi'(N_A, N_B\cdots),$$

in which $\sum'$ means summation for $(_\mu{}^A)\not\equiv(_\nu{}^B)$, and φ' is related to φ by $\varphi'=\varphi\cdot\frac{1}{2}z\sum q_AN_A$.

The arbitrary function φ' is determined by the requirement that when all $\eta_{\mu\nu}{}^{AB}$ are unity, $\ln g$ must reduce to $\ln g_0$, where g_0 is the number of configurations available to N_A molecules occupying r_A sites, N_B molecules occupying r_B sites, etc., regardless of the types of interaction.

Thus the final result is

$$\ln g=\ln g_0+\sum \ln(*N_{\mu\nu}{}^{AB}!/N_{\mu\nu}{}^{AB}!)$$
$$+\ln 2\sum{}'(N_{\mu\nu}{}^{AB}-*N_{\mu\nu}{}^{AB}), \qquad (6)$$

where the quantities $*N_{\mu\nu}{}^{AB}$ are determined by solving Eq. (2) and (3′) with all $\eta_{\mu\nu}{}^{AB}$ set equal to unity. An approximate result for g_0 is given by Guggenheim:[5]

$$g_0=\left[\frac{(\sum q_AN_A)!}{(\sum r_AN_A)!}\right]^{\frac{1}{2}z}\frac{(\sum r_AN_A)!}{\prod N_A!}\prod\rho_A{}^{N_A}, \qquad (7)$$

where ρ_A is the number of configurations available to an A molecule which has one segment constrained to lie on a specified site.

Using the results (6) and (7) it is possible to calculate the thermodynamic functions for the solution.

The free energy is given by

$$G\doteq A=-kT\ \ln Q$$
$$=-kT[\ln g+\sum{}' N_{\mu\nu}{}^{AB}\ln\eta_{\mu\nu}{}^{AB}$$
$$+\tfrac{1}{2}\sum_A N_A\sum_\mu Q_\mu{}^A\ln{}^*\eta_{\mu\mu}{}^{AA}] \qquad (8)$$

* The proof of this uses relations of the type

$$(N_{ik}{}^{AB}N_{il}{}^{AC})/(N_{ii}{}^{AA}N_{kl}{}^{BC})=2(*\eta_{ik}{}^{AB}*\eta_{il}{}^{AC})/(*\eta_{ii}{}^{AA}*\eta_{kl}{}^{BC}),$$

which may be derived from the grand partition function (1).

[4] E. A. Guggenheim, Proc. Roy. Soc. (London) **A183**, 213 (1944).

[5] E. A. Guggenheim, Proc. Roy. Soc. (London) **A183**, 203 (1944).

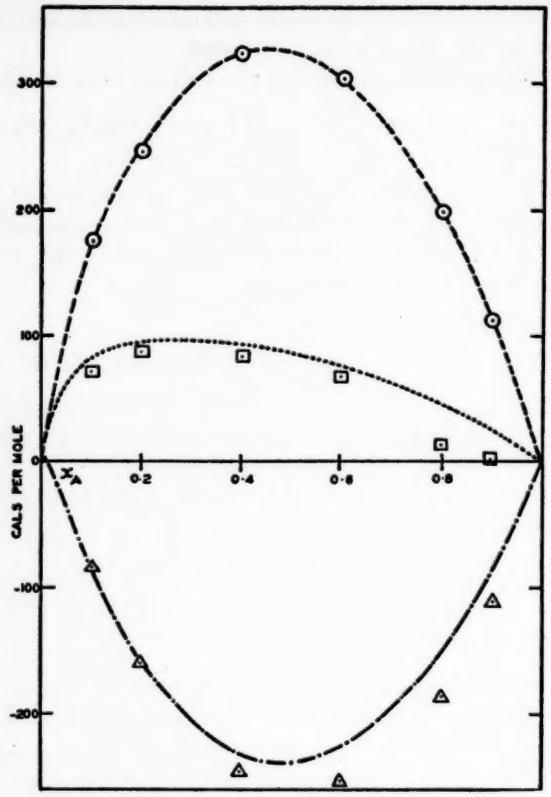

FIG. 1. Methanol-carbon tetrachloride at 35°C. $z=4$, $r_A=2$, $r_s=4$, $Q_H{}^A=1$, $Q_O{}^A=2$, $Q_I{}^A=3$. $U_1=-4700$ cals/mole, $U_2=-1345$ cals/mole, $U_3=+17.4$ cals/mole. – – – – – – – – Theoretical $G_x{}^E$. ····· Theoretical $H_x{}^M$. –·–·–·–·– Theoretical $TS_x{}^E$. ⊙ Experimental $G_x{}^E$. ⊡ Experimental $H_x{}^M$. △ Experimental $TS_x{}^E$. Experimental points calculated from equation given by Scatchard and Ticknor (see reference 6).

and the heat content by

$$H \doteq E = -kT[\sum{}' N_{\mu\nu}{}^{AB} \ln\eta_{\mu\nu}{}^{AB} + \tfrac{1}{2}\sum_A N_A \sum_\mu Q_\mu{}^A \ln{}^*\eta_{\mu\mu}{}^{AA}]. \quad (9)$$

In both (8) and (9) the last term cancels in the calculation of changes of thermodynamic functions on mixing, and the term is omitted in what follows. The trivial differences between Gibbs free energy G and Helmholtz free energy A, and between heat content H and energy E, have been neglected.

In terms of the parameters $X_\mu{}^A$ of Sec. II and of further parameters defined by

$${}^*X_\mu{}^A = \frac{Q_\mu{}^A N_A}{2N}\left(\frac{2N}{\sum q_A z N_A}\right)^{\frac{1}{2}}.$$

Equations (8) and (9) take the simpler forms (8′) and (9′):

$$G \doteq A = -kT \ln g_0 + kT\sum_{A,\mu} N_A Q_\mu{}^A \ln(X_\mu{}^A/{}^*X_\mu{}^A), \quad (8')$$

$$H \doteq E = -2NkT\sum{}' X_\mu{}^A X_\nu{}^B \eta_{\mu\nu}{}^{AB} \ln\eta_{\mu\nu}{}^{AB}. \quad (9')$$

By setting all N_A except one equal to zero the thermodynamic functions for the pure components of the solution may be found. The changes in the thermodynamic functions on mixing, and hence the changes in excess of those for an ideal solution, may then be calculated.

Make the identification $N=\sum N_A$ and carry out the foregoing program. We find the following results for the total molar excess free energy of mixing $G_x{}^E$, the excess chemical potentials $\mu_A{}^E$, and the total molar heat of mixing $H_x{}^M$:

$$G_x{}^E = \sum x_A \mu_A{}^E, \quad (10)$$

$$\mu_A{}^E = RT[\sum_\mu Q_\mu{}^A \ln(X_\mu{}^A/x_A X_\mu{}^{A1}) + r_A(\tfrac{1}{2}z-1)\ln(\sum_B r_B x_B/r_A)], \quad (11)$$

$$H_x{}^M = -2RT[\sum_A \sum_{\mu,\nu} (X_\mu{}^A X_\nu{}^A - x_A{}^1 X_\mu{}^{A1} X_\nu{}^{A1})\eta_{\mu\nu}{}^{AA} \ln\eta_{\mu\nu}{}^{AA} + \sum_{A\neq B}\sum_{\mu\nu} X_\mu{}^A X_\nu{}^B \eta_{\mu\nu}{}^{AB} \ln\eta_{\mu\nu}{}^{AB}]. \quad (12)$$

In these equations x_A represents the mole fraction of the component A. The parameters $X_\mu{}^A$ are determined by Eqs. (13) below, and $X_\mu{}^{A1}$ is the value of $X_\mu{}^A$ for $x_A=1$:

$$X_\mu{}^A \sum \eta_{\mu\nu}{}^{AB} X_\nu{}^B = (Q_\mu{}^A/2)x_A. \quad (13)$$

The Eqs. (10)–(13) contain in summarized form the useful theoretical results of Secs. II and III. The most laborious step in applications is the solution of the sets of Eq. (13). The methods used to obtain solutions are set out in the appendix.

IV. SOLUTIONS OF ALCOHOLS IN NONPOLAR SOLVENTS

(a) Comparison with a Previous Method of Calculation

As a check on the approximate method used in this paper, thermodynamic functions have been calculated for a model of a solution of an alcohol in a nonpolar solvent used in a previous paper,[1] and the results obtained by the method of this paper and by the different method of the previous paper have been compared.

This model may be specified as follows:

Lattice: $z=4$.
Alcohol molecules (A):

$$r_A=1,\ Q_H{}^A=Q_O{}^A=1,\ Q_I{}^A=2.$$

H, O, I, represent, respectively, hydroxyl hydrogen, oxygen, and hydrocarbon surface.
Solvent molecules (S):

$$r_S=1,\ Q_S{}^S=4.$$

Interaction energies: $U_{HO}=-4700$ cals/mole, others zero.
Temperature: $T=308.16$°K.

The values of G_x^E, H_x^M, and TS_x^E calculated for this model by the two methods agree over the whole composition range to within 0.1 cals/mole. The values are shown in Fig. (2a) of reference 1.

Since the approximations in the two calculations are at least superficially quite different, this agreement is a satisfactory check on the present method, which can deal with a wider range of problems than the previous method.

(b) Comparison with Experimental Data

The theory has been tested by comparison with experimental data for the systems methanol+carbon tetrachloride and methanol+benzene, which have been studied in detail by Scatchard *et al.*[6] The comparison was made at 35°C. It was first necessary to decide the models to be used for the various molecules and to choose values for the interaction energies.

The geometrical models† were chosen to give a reasonable picture of the actual molecules. They were not adjusted to give the best agreement with experiment, and in fact equally good agreement could be obtained with different models (see below). The methanol molecules were supposed to have contact-points representing hydroxyl hydrogen (H), oxygen (O), and hydrocarbon (I) parts of the surface of the molecule. In the main series of calculations it was assumed that there were 2 oxygen contacts and 1 hydroxyl hydrogen contact per molecule. The values assigned to the geometrical parameters for this model were:

Lattice: $z=4$.
Methanol molecules (A):
$r_A=2$, $q_Az=6$, $Q_H{}^A=1$, $Q_O{}^A=2$, $Q_I{}^A=3$.
Solvent molecules (S):
$r_S=4$, $q_Sz=10$, $Q_S{}^S=10$.

The values for r_A, r_S were chosen to give a roughly correct value for the ratios of the molar volumes of the liquids.

Calculations were also made for a different model, the parameters for which are set out below.

The interactions considered in the calculations were the hydrogen bond, represented by $H-O$ interaction; an interaction between hydroxyl hydrogen and solvent molecule, represented by $H-S$ interaction; and an alcohol-solvent interaction independent of orientation, represented by $H-S$, $O-S$, and $I-S$ interaction. Thus there were three interaction energies U_1, U_2, and U_3 to be determined, where

$$U_{HO}{}^{AA}={}^*U_{HO}{}^{AA}-\tfrac{1}{2}{}^*U_{HH}{}^{AA}-\tfrac{1}{2}{}^*U_{OO}{}^{AA}=U_1,$$
$$U_{HS}{}^{AS}=U_2+U_3,$$
$$U_{OS}{}^{AS}=U_{IS}{}^{AS}=U_3.$$

The hydrogen-bond strength U_1 is known only approximately, while U_2 and U_3 were completely unknown *a priori*. It was, therefore, necessary to determine the values which fitted the experimental data best.

In practice it was found that the data could be fitted equally well for any value of U_1 between -3000 and -5000 cal/mole. It also appeared that the excess entropy of mixing depended only slightly on U_3. The following procedure was therefore adopted. A value of U_1 was chosen; U_2 was then determined to give approximately the correct value of TS_x^E for the equimolal mixture, and finally U_3 was determined to give the correct value of G_x^E for the equimolal mixture.

Figures 1 and 2 show the results of one attempt to fit the data for methanol+carbon tetrachloride and methanol+benzene, respectively. The theoretical results indicate that for methanol+carbon tetrachloride the excess entropy of mixing should be positive for sufficiently low alcohol concentrations ($x_A<0.01$ in Fig. 1). This behavior is not confirmed by experimental results, but since measurements have not been made at such low concentrations, this does not necessarily imply disagreement between theory and experiment. The experimental data indicate that the heat of mixing for

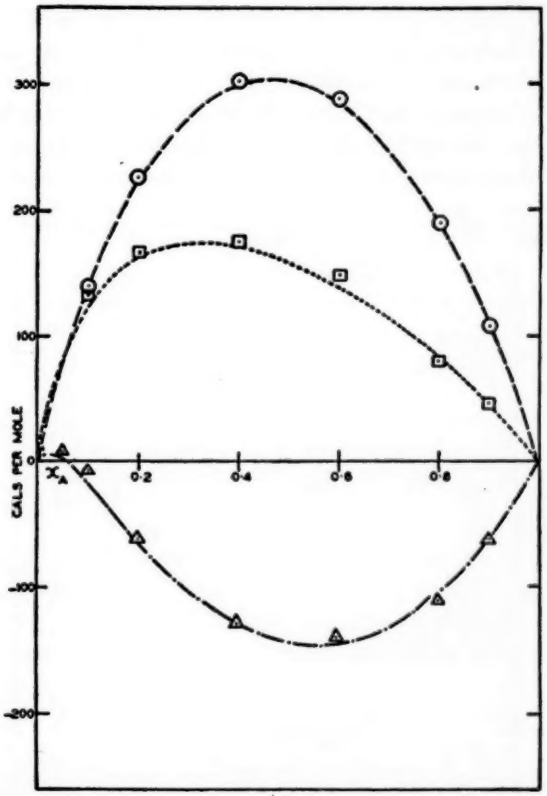

FIG. 2. Methanol-benzene at 35°C. $z=4$, $r_A=2$, $r_s=4$, $Q_H{}^A=1$, $Q_O{}^A=2$, $Q_I{}^A=3$. $U_1=-4700$ cals/mole, $U_2=-2040$ cals/mole, $U_3=+17.4$ cals/mole. – – – – – – – – Theoretical G_x^E. ····· Theoretical H_x^M. –·–·–·–·– Theoretical TS_x^E. ⊙ Experimental G_x^E. ⊡ Experimental H_x^M. △ Experimental TS_x^E. Experimental points calculated from equation given by Scatchard and Ticknor (see reference 6).

[6] G. Scatchard and L. B. Ticknor, J. Am. Chem. Soc. (to be published).

† The author is indebted to Professor E. A. Guggenheim and Professor G. Scatchard for suggestions as to the detailed form of the model for the alcohol molecules.

the same system becomes slightly negative at very high alcohol concentrations. This behavior could be reproduced by taking U_3 negative, but the agreement between theory and experiment over the bulk of the concentration range was then less satisfactory. Apart from this point the theoretical curves reproduce the characteristics of the experimental data in a satisfactory way.

A similarly good fit of the experimental data could be obtained with the following different sets of parameters.

Methanol+carbon tetrachloride:

(a) $z=4$, $r_A=2$, $r_S=4$, $Q_H{}^A=1$, $Q_O{}^A=2$, $Q_I{}^A=3$. $U_1=-3800$ cals/mole, $U_2=-424$ cals/mole, $U_3=+12.4$ cals/mole.
(b) $z=12$, $r_A=1$, $r_S=2.2$, $Q_H{}^A=Q_O{}^A=1$, $Q_I{}^A=10$. $U_1=-4700$ cals/mole, $U_2=+737$ cals/mole, $U_3=+6.8$ cals/mole.

Methanol+benzene:

(a) $z=4$, $r_A=2$, $r_S=4$, $Q_H{}^A=1$, $Q_O{}^A=2$, $Q_I{}^A=3$. $U_1=-3800$ cals/mole, $U_2=-1190$ cals/mole, $U_3=+12.4$ cals/mole.
(b) $z=12$, $r_A=1$, $r_S=2.2$, $Q_H{}^A=Q_O{}^A=1$, $Q_I{}^A=10$. $U_1=-4700$ cals/mole, $U_2=-137$ cals/mole, $U_3=+8.7$ cals/mole.

The experimental data could be fitted by using only two *disposable* constants for each system (U_2 and U_3). This compares favorably with the application of regular solution theory to solutions of nonpolar liquids, where two disposable constants (an interaction energy and its temperature derivative) are required to give similar agreement.

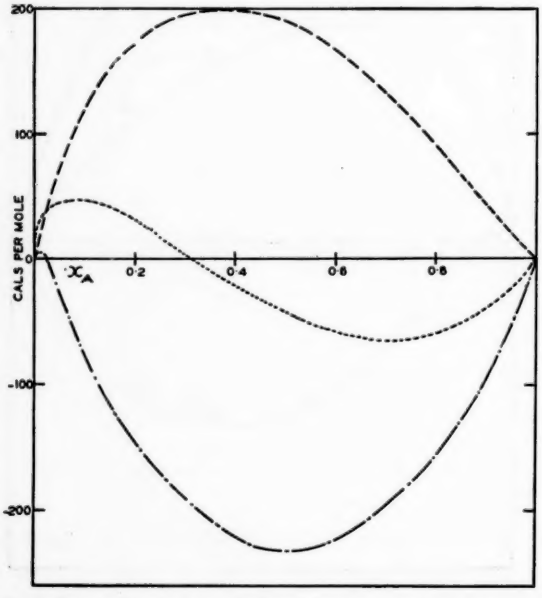

FIG. 3. Ethanol-chloroform at 35°C, theoretical results. $z=4$, $r_A=3$, $r_C=4$, $Q_H{}^A=1$, $Q_O{}^A=2$, $Q_I{}^A=5$, $Q_{Cl}{}^C=7$, $Q_h{}^C=3$. $U_{HO}=-4700$ cals/mole, $U_{HCl}=-1345$ cals/mole, $U_{Hh}=U_{OCl}=U_{Icl}=U_{Ih}=17.4$ cals/mole, $U_{Oh}=-672$ cals/mole. – – – – – – – Theoretical $G_x{}^E$. ····· Theoretical $H_x{}^M$. –·–·–·– Theoretical $TS_x{}^E$.

The qualitative reasons for the behavior shown in Figs. 1 and 2 are of interest. The positive $TS_x{}^E$ values shown at low alcohol concentrations by methanol+benzene (and, according to the theory, by methanol+carbon tetrachloride) are due to the breaking of hydrogen bonds and the resulting gain in orientational freedom of the methanol molecules. If this breaking of hydrogen bonds is due purely to a dilution effect, it is significant only at very low alcohol concentrations (compare with methanol+carbon tetrachloride). But in methanol+benzene the stronger interaction between hydroxyl hydrogen and solvent molecule promotes the breaking of the hydrogen bonds at higher concentrations, and so the positive values of $TS_x{}^E$ extend to higher concentrations, and $TS_x{}^E$ is less negative over the remainder of the concentration range. The negative values of $TS_x{}^E$ at higher concentrations are due to the tendency of the methanol molecules to cluster together. The partial molar excess entropy of mixing of the unassociated component at infinite dilution is negative because, for energetic reasons, a benzene or carbon tetrachloride molecule tends to replace one of the comparatively few methanol molecules which are not involved in hydrogen bonds.

The largest contribution to the heat of mixing is that due to the breaking of hydrogen bonds. The interaction between hydroxyl hydrogen and solvent molecule would of itself give rise to exothermic mixing, but this is outweighed by the increase in the number of hydrogen bonds broken. The heat of mixing is therefore more positive for methanol+benzene than for methanol+carbon tetrachloride.

V. THE SYSTEM ETHANOL+CHLOROFORM

As an example of systems in which more complicated interactions occur, an attempt was made to explain the experimental results of Scatchard and Raymond[7] for the system ethanol+chloroform. The model used for the ethanol molecule was similar to that for methanol, but with $r_A=3$, corresponding to the extra methyl group. The chloroform molecule was supposed to have chlorine (Cl) and hydrogen (h) points of contact. The geometrical parameters were:

Lattice: $z=4$.
Ethanol molecules (A):
$r_A=3$, $Q_H{}^A=1$, $Q_O{}^A=2$, $Q_I{}^A=5$.
Chloroform molecules (C):
$r_S=4$, $Q_{Cl}{}^C=7$, $Q_h{}^C=3$.

The result of one attempt to fit the data is shown in Fig. 3. Experimental data for comparison are shown in Fig. 4. The $H-O$, $H-$Cl, $I-$h, and $O-$Cl interactions were given the same values as were found for methanol+carbon tetrachloride, and the h$-O$ interaction energy

[7] G. Scatchard and C. L. Raymond, J. Am. Chem. Soc. **60**, 1278 (1938).

(representing a "hydrogen bond" from chloroform hydrogen to ethanol oxygen) was adjusted to give a qualitative fit of the experimental data. The agreement between theory and experiment is by no means quantitative in this case, but the theoretical results show similar qualitative behavior to that shown by the experimental data. Models for the chloroform molecule with one and two hydrogen points of contact were also tried, but that with three hydrogen points of contact, as above, gave better results than either. This agrees with the conclusion of Scatchard and Raymond that the associated complexes in the solution contained at least three alcohol molecules to each chloroform molecule.

Qualitatively speaking, the negative values of H_x^M at high ethanol concentrations are due essentially to the $O-$h interaction between the ethanol oxygen and the chloroform hydrogen. The $H-$Cl interaction works in the opposite direction (cf. the qualitative discussion of the methanol systems). The difference is due to the fact that there are two effective oxygen spots per alcohol molecule but only one effective hydrogen spot, so that an h$-O$ link can be formed without breaking an alcohol-alcohol hydrogen bond, while an $H-$Cl link cannot. The formation of h$-O$ links also limits the orientational freedom of the chloroform molecules, thus making TS_x^E strongly negative so that G_x^E remains positive even at high ethanol concentrations. The positive values of H_x^M and TS_x^E at low ethanol concentrations are due to the breaking of alcohol-alcohol hydrogen bonds, as in the methanol systems.

VI. DISCUSSION

The theory of this paper gives a method for calculating the configurational contribution to the thermodynamic functions of solutions of associated liquids, provided that the molecules of the liquids considered can be represented by certain models. The approach will be a useful one if the configurational contribution to the thermodynamic functions is the major one. The detailed way in which the theory can reproduce the rather complicated concentration dependence of the thermodynamic functions for the systems studied indicates that both of these requirements are at least partially satisfied. The model set up in Sec. II is rather artificial for some molecules (e.g., benzene, carbon tetrachloride). Nevertheless, it does give some representation of the volume and surface relations of the molecules, and since it is the only model for which simple and general theoretical results can be found, it is the logical choice for preliminary investigations of the field.

The treatment of mixtures of alkanes given by Tompa[8] may be regarded as a special case of the present theory, in which there are only two kinds of points of contact on the molecule.

[8] H. Tompa, Trans. Faraday Soc. **45**, 101 (1949).

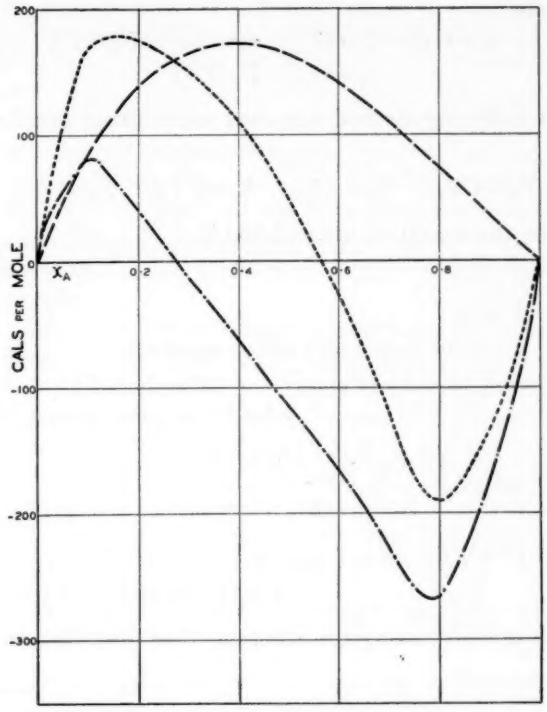

FIG. 4. Experimental thermodynamic functions for system of ethanol-chloroform at 45°C, after Scatchard and Raymond (see reference 7). – – – – – – G_x^E. ····· H_x^M. –·–·–·– TS_x^E.

The number of systems for which sufficient accurate data are available to test theories of this kind is not large. This is particularly true in regard to the heat and entropy changes on mixing. While there are a reasonable number of systems for which the free energy change on mixing is known to within a few calories per mole, there are very few for which the heat of mixing is known to similar accuracy. More extensive calorimetric measurements of heats of mixing would be of great benefit to the theory of solutions.

ACKNOWLEDGMENTS

The author wishes to thank Professor E. A. Guggenheim for some helpful suggestions, Professor G. Scatchard for communicating prior to publication the data on methanol systems used in this paper and for some helpful remarks, and Miss P. C. Miller for performing quickly and accurately much of the heavy numerical work involved.

APPENDIX

For the methanol systems (Sec. IV) the equations to be solved were

$$X_H[X_H+\eta_1X_O+X_I+\eta_2\eta_3X_S]=x_A/2,$$
$$X_O[\eta_1X_H+X_O+X_I+\eta_3X_S]=x_A,$$
$$X_I[X_H+X_O+X_I+\eta_3X_S]=3x_A/2,$$
$$X_S[\eta_2\eta_3X_H+\eta_3X_O+\eta_3X_I+X_S]=5x_S,$$

where

$$\eta_1=\exp[-U_1/kT],\quad \eta_2=\exp[-U_2/kT],\quad \eta_3=\exp[-U_3/kT].$$

The following method was used to construct solutions. Set

$$X_H=CY_H,\quad X_O=CY_O,\quad X_I=CY_I,\quad X_S=CY_S.$$

Then the equations are satisfied if

(i) $Y_H=1$.

(ii) $Y_O=\alpha$.

(iii) Y_I is the larger root of the quadratic

$$Y_I^2[2\eta_2-2]-Y_I[\alpha(\eta_1+\eta_2-2)-2\eta_2+2]+3\alpha[1-\eta_1\eta_2+\alpha(\eta_1-\eta_2)]=0.$$

(iv) $$\eta_3 Y_S=\frac{2+\alpha\eta_1-\alpha^2-Y_I(\alpha-2)}{\alpha-2\eta_2}.$$

(v) $$C^2=5/[Y_S(\eta_2\eta_3+\eta_3\alpha+\eta_3Y_I+Y_S)+10(1+\eta_1\alpha+Y_I+\eta_2\eta_3Y_S)].$$

Any one of the original equations then serves to determine the mole fraction x_A. As α varies between the limits $2\eta_2$ and $(\eta_1+9)/8+[(\eta_1+9)^2/64-1]^{\frac{1}{2}}$ the composition range from $x_A=0$ to $x_A=1$ is covered.

For ethanol chloroform the equations were

$$X_H[X_H+\eta_1X_O+X_I+\eta_2\eta_3X_{Cl}+\eta_3X_h]=x_A/2 \quad (a)$$

$$X_O[\eta_1X_H+X_O+X_I+\eta_3X_{Cl}+\eta_4\eta_3X_h]=x_A \quad (b)$$

$$X_I[X_H+X_O+X_I+\eta_3X_{Cl}+\eta_3X_h]=3x_A/2 \quad (c)$$

$$X_{Cl}[\eta_2\eta_3X_H+\eta_3X_O+\eta_3X_I+X_{Cl}+X_h]=7x_C/2 \quad (d)$$

$$X_h[\eta_3X_H+\eta_4\eta_3X_O+\eta_3X_I+X_{Cl}+X_h]=3x_C/2. \quad (e)$$

For these equations a successive approximation method was used. Starting with approximate values for X_{Cl}, X_h and X_I the Eqs. (a) and (b) were solved for X_H and X_O by using (b) to calculate X_H for a number of values of X_O and then substituting in (a) to determine the appropriate X_O value. Then with these values for X_H and X_O the Eqs. (c), (d), and (e) were solved in turn as quadratics in X_I, X_{Cl}, and X_h, respectively. The values obtained by this procedure converged reasonably rapidly to solutions of the whole set of equations.

THE JOURNAL OF CHEMICAL PHYSICS VOLUME 20, NUMBER 10 OCTOBER, 1952

Some Crystal Energetic Relationships in Oxysalts

H. RAMBERG
Department of Geology, University of Chicago, Chicago 37, Illinois

(Received March 17, 1952)

A regularity exists between the heat of formation of alkali and alkaline earth oxysalts and the acidity and basicity of the oxides involved. The more basic an alkali or an alkaline earth oxide, the larger is the exothermic heat of formation of its oxysalts from the component oxides. Likewise, the more acidic the nonmetal oxide, the larger is the exothermic heat of formation of its salts from the component oxides. Although this is expectable in a general way, the regularity and consistency of these rules are rather surprising.

The exothermic heat of formation from the oxides of different oxysalts of the same metal increases when the nonmetal changes through the sequences: B, C, N, and Si, P, S, Cl. This is explained in light of the increasing covalent character (or increasing polarization) of the oxygen-nonmetal bonds through the same series of elements.

The exothermic heat of formation of polymerized oxysalts from the component oxides (borates, silicates, phosphates, pyrosulfates) is larger per equivalent than for the corresponding simple oxysalts. This is qualitatively explained as a result of the oxygen-nonmetal bond being less polarized or more ionic in a polymerized salt than in the nonpolymerized salt with the same central atom in the oxyanion.

The heat of salt formation per equivalent increases numerically when the metal changes from Li to Cs, or from Mg to Ra. This is related to the increase of the crystal energy of the corresponding metal oxides.

THE EXCHANGE OF CATIONS BETWEEN PAIRS OF OXYSALTS OR BETWEEN OXIDES AND OXYSALTS

CERTAIN thermochemical parameters of chemical compounds show more or less regularity with respect to the position of the constituent elements in the periodic table. Most remarkable in this respect is perhaps the heat of formation per gram equivalent of some oxysalts from their constituent acidic and basic oxides. These relationships were pointed out recently by G. H. Cartledge[1] who gave simple empiric equations between the heat of salt formation and the ionic potential of the cations based upon their corrected univalent radii. In this paper we shall discuss some of the consequences to be drawn from these regularities between thermochemical properties of oxysalts and the position of the cations in the periodic table. Figure 1 shows the heat of formation per two gram equivalents of salt formed from the acidic and basic oxides.[2] The

[1] G. H. Cartledge, J. Phys. Colloid Chem. 55, 248 (1951).

[2] The data necessary for this figure are taken from (a) F. R. Bichowsky and D. R. Rossini, *The Thermochemistry of Chemical Substances* (Reinhold Publishing Corporation, New York, 1936); (b) O. Kubaschewski and E. L. L. Evans, *Metallurgical Thermochemistry* (Butterworth-Springer, London, 1951); (c) *Tables of Selected Values of Chemical Thermodynamic Properties* (U. S. National Bureau of Standards, 1947).

diagram was constructed in the following way. First, the ΔH values of all sulfates were plotted on a line which made an arbitrary angle with the abscissa. By this arrangement the several metals become spaced in a certain manner along the vertical axis. Horizontal lines were then drawn through the points on the sulfate line, each line referring to a given metal. On these horizontal lines were plotted the heat of formation of all other salts such that all salts of a given metal were plotted on the horizontal line representing this metal. It then appeared that the ΔH-points fell close to straight inclined lines, each line connecting all the ΔH-points of the salts of a given acid. After this was done some of the lines were displaced a little in order to make the scattering of the ΔH-values as small as possible.

From this figure two general facts come out clearly: (1) Salts of the same basic oxide have lower heat of formation (from oxides in their standard state) the stronger the acidity of the acidic oxide. (2) Salts of the same acidic oxide exhibit lower heat of formation, the stronger the basicity of the metal oxide.

In other words, the heat of formation of oxysalts from the constituent oxides is a measure on the strength of the acids if salts of the same metal are compared, and a measure on the strength of the bases if salts of the same acid are compared.

It is noticeable that most of the lines in Fig. 1 converge toward the upper right-hand side. This feature shows that base exchange reactions of metals between two solid salts are exothermic if the most acidic anion combines with the most basic metal oxide at the same time as the less acidic anion combines with the less basic metal. There are some exceptions (note, for example, the nitrates relative to the sulfates), but they are not numerous enough to make the general principle invalid. Discussion regarding the reason for the different slopes of the ΔH-lines in Fig. 1 follows later in this paper.

Reactions between a metal oxide and an oxysalt will proceed exothermally in such a direction that the most basic metal combines with the oxyanion to form a salt, while the less basic or less electropositive metal combines with oxygen to form simple oxide. There is no exception from this rule among the oxides and salts in question.

There are other conspicuous features of Fig. 1 and Table I which shall be discussed, namely, (1) the fact that the heat of salt formation (per gram equivalent from oxides in their standard state) is lower for strong acids than for weak acids; (2) that the heat of salt formation is lower for pyrosalts or polymerized salts than for *ortho* or simple salts (see Table I); (3) that the heat of salt formation decreases from Mg salts toward Cs salts.

THE RELATIONSHIP BETWEEN HEAT OF SALT FORMATION AND STRENGTH OF THE ACID

The energy ΔH of reaction between acidic and basic oxides may be separated into three parts: (1) the energy ΔH_{ox} required to separate the metallic oxide into an ionic gas of M^{n+} and O^{2-}; (2) the energy $\Delta H'$ involved in the reaction between the gaseous O^{2-} ions and acidic oxide by which gaseous oxyanions are formed; (3) the energy ΔH_s released when the metal ions combine with the oxyanions forming the crystalline salt.

ΔH is then given by the following equation:

$$\Delta H = \Delta H_{ox} + \Delta H' + \Delta H_s. \qquad (1)$$

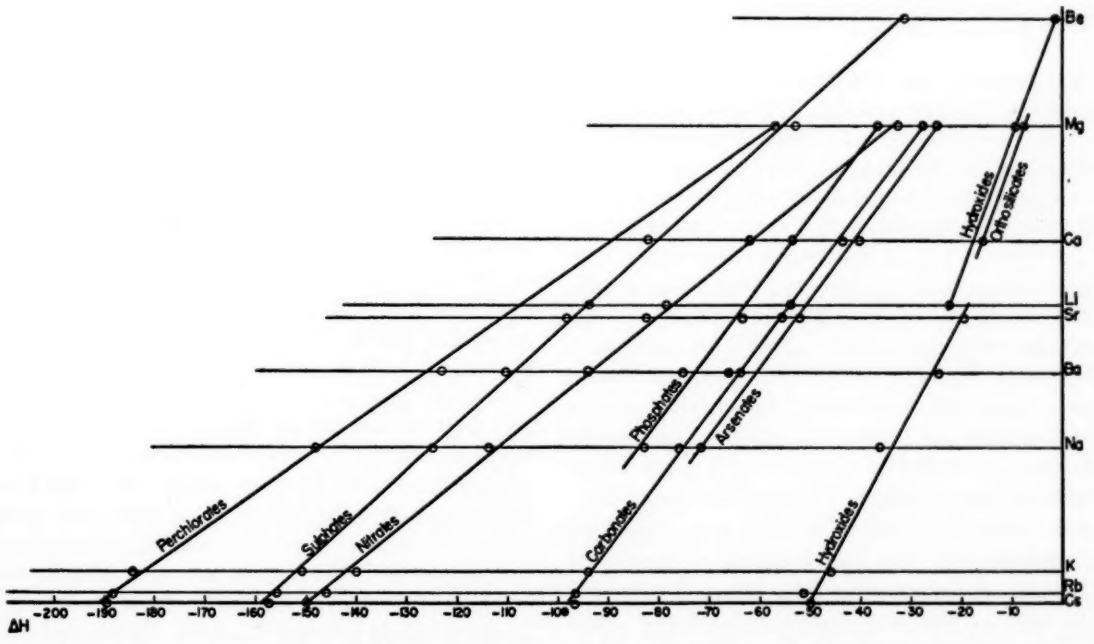

FIG. 1. ΔH of formation of some oxysalts from their basic and acidic oxides; given in kcal per two equivalents. The black solid circle on the Ba line refers to barium arsenate.

TABLE I. Heat of formation of simple and polymerized oxysalts.[a]

Compound	Heat of formation from oxides, in kcal per 2 equivalents
$Ca_3(BO_3)_2$	$-20.\ \pm1.$
$Ca_2B_2O_5$	$-22.9\pm1.$
CaB_2O_4	$-29.4\pm1.$
CaB_4O_7	$-42.9\pm1.$
Li_4SiO_4	$-24.5\pm5.$
Li_2SiO_3	$-28.0\pm4.$
$Li_2Si_2O_5$	$-38.0\pm5.$
Na_2SiO_3	$-63.2\pm7.$
$Na_2Si_2O_5$	$-65.2\pm7.$
Zn_2SiO_4	$+10.\ -$
$ZnSiO_3$	$+4.0\pm5.0$
Ba_2SiO_4	$-23.0\pm7.$
$BaSiO_3$	$-25.5\pm7.$
Ca_2SiO_4	-16.4 ± 0.5
$CaSiO_3$	-21.5 ± 0.5
Fe_2SiO_4	-4.2 ± 1.3
$FeSiO_3$	-7.2 ± 2.5
K_4SiO_4	-43.8 ± 7.0
K_2SiO_3	$-64.5\pm7.$
$K_2Si_2O_5$	$-74.5\pm7.$
$K_2Si_4O_9$	$-81.0\pm7.$
Na_3PO_4	-82.8
$Na_4P_2O_7$	-94.5
K_2SO_4	-150.5
$K_2S_2O_7$	-177.2
K_2CrO_4	-108.8
$K_2Cr_2O_7$	-125.5
K_3PO_4 aq.	-110.4
$K_4P_2O_7$ aq.	-119.9

[a] Data from references 2(a) and 2(b).

ΔH_{ox} is a positive quantity; ΔH_s is always negative; so is ΔH in the cases in question. $\Delta H'$ may perhaps be positive in a few cases, but most likely it is negative.

For the carbonates, sulfates, nitrates, and perchlorates the ΔH_s-values are less in numerical magnitude than the corresponding ΔH_{ox}-values. This is due to the large size and the low total charge of these oxyanions. It is a well-known rule from crystal chemistry of ionic crystals that the crystal energy per equivalent rises if the size of the ions increases, or if the charge on the ions decreases.[3] Thus, for example, ionic sulfides have higher crystal energy per equivalent than corresponding oxides; and the crystal energy per equivalent rises rather rapidly from nitrides with triply charged nitrogen, over oxides with doubly charged oxygen, to univalent fluorides.

It is less certain whether or not the ΔH_s-values for borates, phosphates, and silicates are numerically smaller than the corresponding ΔH_{ox}-values. The borate anions as well as the *ortho*phosphate and the *ortho*-silicate anions are much larger than the oxygen ion, but the oxyanions here considered have 3 and 4 charges such that an increase of dissociation energy per equivalent (ΔH_s) caused by the large size of the anions as compared with the oxygen ion may perhaps be compensated for by the higher charge on the complex oxyanions. It is evident, though, that the ΔH_s-value increases through the sequences: borates (BO_3^{3-})→carbonates (CO_3^{2-})→nitrates (NO_3^{1-}); and silicates (SiO_4^{4-})→phosphates (PO_4^{3-})→sulfates (SO_4^{2-})→perchlorates (ClO_4^{1-}) because of the decreasing negative charge on the oxyanions. On the other hand, it is established that the ΔH-value decreases through the same sequences of salts (if salts of the same metal are considered, see Fig. 1). According to Eq. (1) then, it can be concluded that the $\Delta H'$-value must decrease faster than the ΔH_s-value increases through the sequences: $BO_3^{3-}\rightarrow CO_3^{2-}\rightarrow NO_3^{1-}$; and $SiO_4^{4-}\rightarrow PO_4^{3-}\rightarrow SO_4^{2-}\rightarrow ClO_4^{1-}$. This last conclusion is strongly supported if the energetics of the reactions involving the term $\Delta H'$ are considered:

$$\underset{\text{solid}}{\tfrac{1}{3}B_2O_3}+\underset{\text{gas}}{O^{2-}}=\underset{\text{gas}}{\tfrac{2}{3}BO_3^{3-}}+\Delta H'_{BO_3}, \quad (2)$$

$$\underset{\text{gas}}{CO_2}+\underset{\text{gas}}{O^{2-}}=\underset{\text{gas}}{CO_3^{2-}}+\Delta H'_{CO_3}, \quad (3)$$

$$\underset{\text{solid}}{N_2O_5}+\underset{\text{gas}}{O^{2-}}=\underset{\text{gas}}{2NO_3^{1-}}+\Delta H'_{NO_3}, \quad (4)$$

$$\underset{\text{solid}}{\tfrac{1}{2}SiO_2}+\underset{\text{gas}}{O^{2-}}=\underset{\text{gas}}{\tfrac{1}{2}SiO_4^{4-}}+\Delta H'_{SiO_4}, \quad (5)$$

$$\underset{\text{solid}}{\tfrac{1}{3}P_2O_5}+\underset{\text{gas}}{O^{2-}}=\underset{\text{gas}}{\tfrac{2}{3}PO_4^{3-}}+\Delta H'_{PO_4}, \quad (6)$$

$$\underset{\text{gas (or solid)}}{SO_3}+\underset{\text{gas}}{O^{2-}}=\underset{\text{gas}}{SO_4^{2-}}+\Delta H'_{SO_4}, \quad (7)$$

$$\underset{\text{gas}}{Cl_2O_7}+\underset{\text{gas}}{O^{2-}}=\underset{\text{gas}}{2ClO_4^{1-}}+\Delta H'_{ClO_4}. \quad (8)$$

According to the considerations above the following relationships are valid: $\Delta H'_{ClO_4}<\Delta H'_{SO_4}<\Delta H'_{PO_4}<\Delta H'_{SiO_4}$; and $\Delta H'_{NO_3}<\Delta H'_{CO_3}<\Delta H'_{BO_3}$.

It is conspicuous that the $\Delta H'$-values decrease with increasing valency of the central atom (ion) in the oxyanion (if the AO_3^{n-} and the AO_4^{n-} ions are considered separately). That is, *the $\Delta H'$-value decreases with increasing polarizing power of the central ion or with increasing covalent character of the* A—O *bonds in the oxyanions*. This is particularly interesting in view of the fact that the energy of the A—O bond in the oxides increases with increasing valency of the A atom or ion, as shown in Table II. Now to form the oxides from the elements in their atomic gaseous state the electrons of the A atoms must either be completely loosened from the A atoms if the bonds are 100 percent ionic, or activated to a level at which the electrons can constitute covalent bonds between A and O. The ionization energy per electron for maximum valency stage increases from B^{III} to N^{V} and from Si^{IV} to Cl^{VII}. This increment in

[3] E. E. van Arkel, *Molecules and Crystals* (Interscience Publishers, New York, 1949).

ionization energy is not fully regained by the bond formation in the oxides; hence the bond strength A—O decreases as A changes from B to N or from Si to Cl.[4] When the acidic oxides change into oxyanions by reaction with O^{2-}, however, the activation of the A atom has already taken place in the formation of the oxide, and a part of the activation energy is actually regained when the oxyion is formed. It appears that the part of the activation energy which is regained when the oxyanions are formed is larger, the larger the activation energy itself.

When the acidic oxides in question are compared with the corresponding simple oxyions it is seen that the chief constitutional difference is that the *oxides have* A—O—A *bridges* (disregarding for the moment CO_2), *the simple oxyions have no such shared oxygen atoms*. When the acidic oxides form oxyions, it means that A—O—A bridges in the oxides are broken to form one-sidedly bonded oxygen in the oxyions

$$A-O-A+O^{2-}\rightleftharpoons A-O+O-A+\Delta H'.$$

There are two reasons why an A—O—A bridge has higher energy than two single A—O bonds. (1) The two rather highly charged A ions will repel one another. (2) In the oxyion the oxygen is one-sidedly polarized by the A ion; hence the strength of the A—O link is increased significantly by the polarization. The shared oxygen in the A—O—A bridge is polarized by the two A ions from opposite sides such that each of the O—A bonds in an A—O—A bridge is less strengthened by the polarization.

Thus, if an ionic model is applied it follows naturally that the *energy of the reaction of acidic oxides with* O^{2-} *will decrease when the charge of the central ion increases and thus its polarizing power increases*, provided oxyanions with the same coordination number of oxygen are compared. The same conclusion follows from a covalent model. The covalent character becomes gradually more dominating from B—O toward N—O, and from Si—O toward Cl—O. It is now likely that the less ionic and the more covalent the A—O bond, the greater is the difference in energy between a symmetric A—O—A link and two unsymmetric single A—O bonds, because in the A—O—A link there will be a competition among two A atoms for the valency electrons of one oxygen atom, whereas in a single unsymmetric A—O bond the A atom can utilize more freely the valency electrons of the oxygen atom.

The relationship between the heat of salt formation and the acidity of the acidic oxide is thus due to the condition that the $\Delta H'$-values are closely related to the acidity of the acidic oxide because the strength of an oxyacid is determined by the bonds between the central atom (ion) and oxygen such that the more polarized, or more covalent the O—A bond, the weaker is the attraction between oxygen and hydrogen and hence the stronger is the acid.

[4] See reference 3.

Returning to the ionic picture it is realized that the polarizing power of a given central ion in an oxyion does not only depend upon its charge and radius, but also upon the number of oxygen ions which surround the central ion. The oxygen ions will partly neutralize the polarizing power of the central positive ion. Therefore, for example, the polarizing power of C^{4+} in CO_3^{2-} is larger than that of Si^{4+} in

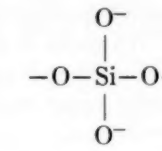

or the polarizing power of N^{5+} in —ONO— is larger than that of P^{5+} in

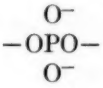

because of the greater number of oxygen ions in the *ortho* ions. It is therefore reasonable that the $\Delta H'_{CO_3}$-value is lower than the $\Delta H'_{SiO_4}$-value, and that the $\Delta H'_{NO_3}$-value is lower than the $\Delta H'_{PO_4}$-value, as is indicated by the relative ΔH-values of corresponding salts (Fig. 1).

The model above is not directly applicable to the formation of carbonate ion from CO_2, nor to the formation of sulfate ion from gaseous SO_3. In these cases it is a question of increasing the coordination number of C and S from 2 to 3, and from 3 to 4, respectively. Yet the ΔH-values for the carbonates fall where one would expect on account of the strength of the carbonic acid as compared with boric and nitric acids (Fig. 1). The ΔH of the sulfates here applied are based on solid SO_3 which is polymerized by means of S—O—S bridges; but if gaseous SO_3 is used instead, the ΔH-values for the sulfates will only be displaced some 12 kcal which will not disturb significantly the relative position of the sulfate line in Fig. 1.

The reason for not finding any significant disturbance of the ΔH- or $\Delta H'$-values depending upon whether the oxyions form by breaking A—O—A bridges or by changing coordination number in the case of CO_2 and SO_3, must be that there is only a relatively insignificant energy difference between the molecular and polymerized forms of these oxides. It is known that the energy difference between solid polymerized S_nO_{3n} and gaseous SO_3 is only some 10–12 kcal per mol.[5] The energy

TABLE II. Bond energy in kcal per equivalent of some oxides based upon gaseous monatomic elements representing zero level.[a]

Compound:	B_2O_3	CO_2	N_2O_5		
Bond energy:	−135.	−80.5	−47.6		
Compound:	Al_2O_3	SiO_2	P_2O_5	SO_3	Cl_2O_7
Bond energy:	−114.5	−102.2	−72.6	−58.3	−29.1

[a] Data from references 2(a) and 2(c).

[5] See reference 2(a).

difference between molecular O=C=O and some possible polymerized form:

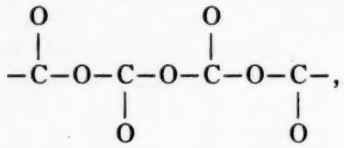

is not known, but most likely it is small because the energy of two single C−O bonds is about the same as the energy of one double C=O bond[6] and polymerization of O=C=O would chiefly mean transfer of a certain number of double C=O bonds into twice as many single C−O bonds. Hence, it becomes likely that the energy of reaction in the following two cases would be rather similar:

$$nO{=}C{=}O+nO^{2-}=nCO_3^{2}+n\Delta H'_{CO_3},$$

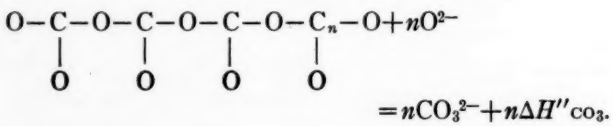

$$=nCO_3^{2-}+n\Delta H''_{CO_3}.$$

HEAT OF FORMATION OF POLYMERIZED OXYSALTS

It is an experimental fact that the ΔH-values per gram equivalent of pyrosalts or polymerized salts are lower than for the corresponding simple salts. Some examples on that are shown in Table I. Silicates and borates are unique in their ability to form salts of different degree of polymerization. In these cases the ΔH-values per equivalent decreases rather regularly with increasing degree of polymerization. It is evident that the low ΔH-values of polymerized salts are not due to any energy of polymerization simply because the acidic oxides from which the salts are formed are polymerized to start with, such that the salt formation goes on by breaking A−O−A bridges rather than by building such links. It is interesting that the model as applied above on the simple oxyanions, leads to the conclusion that the $\Delta H'$-values will decrease with increasing degree of polymerization. Most likely this is the chief cause of the decrease of the ΔH-values with increasing degree of polymerization. The structure of silicates are well known. *Ortho*silicates contain the independent

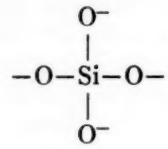

ion. Pyrosilicates contain the double ion with one oxygen bridge:

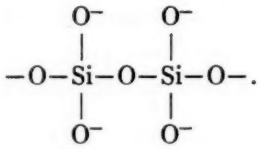

The metasilicates have a polymerized silicon-oxygen chain, each SiO_4 tetrahedron containing two shared and two unshared oxygen ions:

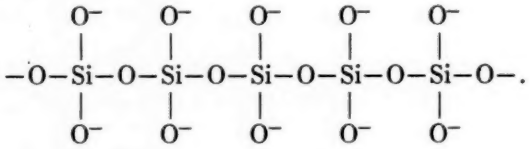

In so-called phyllosilicates the polymerization has gone one step further to give sheets of composition $Si_{2n}O_{5n}^{-2n}$ where each SiO_4 tetrahedron has three bridging or shared oxygen ions, only one oxygen in each SiO_4 group being one-sidedly bonded to silicon.

In an oxygen bridge, A−O−A, the displacement of the electrons of the oxygen ion or atom toward either of the two A ions (A=Si, B, P etc.) is partly hindered by the presence of the other A ion. For that reason the electron density between O and A is lower in an A−O−A bridge than in a single A−O binding. Now the *low electron density along the* O−A *bond in an* A−O−A *bridge causes the polarizing power of the* A *ion to increase as compared with an A ion attached to only nonbridging oxygen* because the closer the electrons of the oxygen are pulled toward the A ion, the more they neutralize the excess positive charge on the A ion. It has been found that the energy connected with transferring an A−O−A link in oxides to two A−O− bonds in oxyions, decreases with increasing polarizing power of the A ion. It therefore follows, that the $\Delta H'$-value for breaking *one* A−O−A bridge after the scheme: $-A-O-A+O^2=-A-O-+-O-A-+\Delta H'$, is lower the greater the number of unbroken oxygen bridges which remain around the A ion. In phyllosilicates *three* oxygen bridges remain around each silicon, only one is broken. Hence, the $\Delta H'$-value for phyllosilicates should be low. In

TABLE III. Crystal energy in kcal per two equivalent of oxides and fluorides.[a]

Metal	Crystal energy of oxides	Crystal energy of fluorides
Mg	−933.	−691.
	Δ=93	Δ=70
Ca	−840.	−621.
	Δ=46	Δ=39
Sr	−794.	−582.
	Δ=40	Δ=35
Ba	−754.	−547.
Li	−693.	−485.
	Δ=77	Δ=55
Na	−616.	−430.
	Δ=57	Δ=42
K	−559.	−378.
	Δ=14	Δ=12
Rb	−545.	−366.
	Δ=17	Δ=16
Cs	−528.	−350.

[a] Data from reference 2(a).

[6] Y. K. Syrkin and M. E. Dyatkina, *Structure of Molecules and the Chemical Bond* (Interscience Publishers, Inc., New York, 1950).

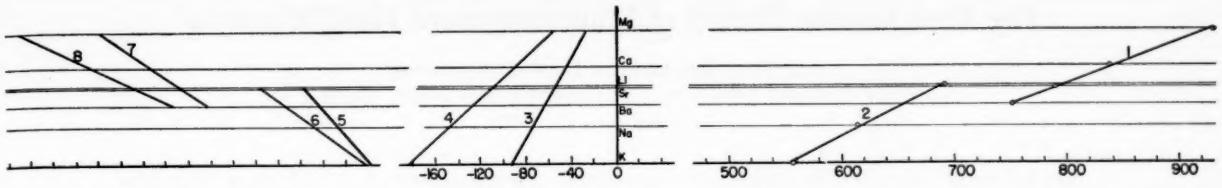

FIG. 2. Line 1 gives the dissociation energy ΔH_{ox} in kcal per mol of alkaline earth oxides; line 2 gives the same for the alkali oxides. Line 3 gives the ΔH of formation of carbonates from oxides, and line 4 the same for perchlorates. Lines 5 and 7 give the energy released when gaseous metal ions combine with gaseous perchlorate ions and form crystals. Lines 6 and 8 give the energy released when metal ions and carbonate ions form crystals. The slopes of lines 5, 6, 7, and 8 are correct, but their positions in the energy diagram are uncertain. All values are in kcal per two equivalents.

metasilicates *two* oxygen bridges remain around the silicon ion, and the $\Delta H'$-value should be correspondingly higher. In pyrosilicates only *one* bridging oxygen remains around each silicon, the other three are broken and in consequence the $\Delta H'$-value should be still higher. For *ortho*silicates all oxygen bridges are broken, each silicon being bonded to four unshared oxygen ions; the $\Delta H'$-value of the *ortho*silicates should hence be the highest. As seen from Table I, this fits exactly the experimental results provided ΔH is changing sympathetically with $\Delta H'$, which is a likely assumption.

The reason why polymerized acids are generally stronger than corresponding simple acids[7] is evidently connected with the change of the $\Delta H'$-value with polymerization as discussed here.

THE RELATIONSHIP BETWEEN HEAT OF SALT FORMATION AND TYPES OF CATION

ΔH for salts of the same acid decreases with increasing basicity of the metal oxides, the Mg salts having the highest, the Cs salts the lowest ΔH-values. For salts of the same acid the $\Delta H'$-value is constant, such that any change in ΔH is caused by changes in ΔH_{ox} and/or ΔH_s according to the equation: $\Delta H = \Delta H_{ox} + \Delta H' + \Delta H_s$.

The crystal energies, ΔH_{ox}, which are well known for the oxides here considered, are plotted in a diagram with the same relative spacing between the metals as in Fig. 1. ΔH_{ox} falls on two reasonably straight lines, one for the alkali metals, another for the earth alkali metals (Fig. 2).

Because the ΔH-values and the ΔH_{ox}-values are linear functions in Figs. 1 and 2, it follows that the ΔH_s-values must also be linear functions in a diagram with the same spacing between the metals. The ΔH_s-values for the several salts of a certain acid must fall on two straight lines, one for the alkali salts, another for the alkaline earth salts, the horizontal distance between these two lines being the same as the distance between the two ΔH_{ox}-lines.

The slope of an ΔH_s-line for salts of a certain acid is determined by the slopes of the corresponding ΔH-line, and of the two ΔH_{ox}-lines. The absolute positions of the ΔH_s-lines (in Fig. 2), however, are not determined unless the $\Delta H'$-values are known, or a ΔH_s-value for one salt for each of the acids is known.

The empiric fact that the ΔH-value of salts of the same acid decreases from Mg salts to Cs salts requires that the corresponding ΔH_s-value changes more slowly with change of metal than the ΔH_{ox}-value. This is visualized in Fig. 2. The last relation is in harmony with the low effective charge of the oxygen in the oxysalts. The lower the average negative charge on the oxygen in the oxyanions, the less should ΔH_s change when the metal changes from Mg to Ba, or from Li to Cs. See the ΔH_s-lines 5, 6, 7, 8 in Fig. 2. This effect is also illustrated by comparing the crystal energies of oxides and fluorides (Table III). The difference in crystal energy per equivalent of metal oxides is somewhat larger than the difference between corresponding fluorides

The slopes of the ΔH and corresponding ΔH_s-lines in Fig. 2 are related such that the steeper the slope of the ΔH-line, the smaller is the slope of the corresponding ΔH_s-lines. The relative slopes of the several ΔH-lines can be expressed by taking the distance K—Mg in Fig. 1 as unity. The slopes of the several ΔH-lines are then as follows:

perchlorates: $-1/126$;
nitrates: $-1/109$;
sulfates: $-1/94$;
phosphates: $-1/65$;
arsenates: $-1/65$;
carbonates: $-1/67$;
*ortho*silicates: $-1/33$.

Thus, the steepness of the ΔH_s-lines decreases from perchlorates to *ortho*silicates. Now the average charges of the oxygen in the several oxyions are: SiO_4^{4-}: $1e$, CO_3^{2-}: $\frac{2}{3}e$, AsO_4^{3-}: $\frac{3}{4}e$, PO_4^{3-}: $\frac{3}{4}e$, SO_4^{2-}: $\frac{1}{2}e$, NO_3^{-}: $\frac{1}{3}e$, ClO_4^{-}: $\frac{1}{4}e$. Hence the steepness of the ΔH_s-lines in Fig. 2 is related to the average charge on the oxygen in the oxyanion in such a way that the lower the charge, the steeper is the ΔH_s-lines, which is in agreement with general relation between crystal energy and charge of the anion.

[7] B. Eistert, *Chemismus und Konstitution* (Ferdinand Enke, Stuttgart, 1948).

The Free Volume Theory of Multicomponent Fluid Mixtures*

ZEVI W. SALSBURG AND JOHN G. KIRKWOOD
Sterling Chemistry Laboratory, Yale University, New Haven, Connecticut

(Received May 15, 1952)

The free volume theory of the liquid state is extended to multicomponent mixtures by using the method of moments in the treatment of the order-disorder problem. Retention of only the first moment yields an approximation to the partition function which has recently been studied by Prigogine and Garikian and by Prigogine and Mathot. An approximation equivalent to retaining the third moment is given, and the calculation of the thermodynamic functions from the first moment approximation is discussed.

ALTHOUGH in principle an exact theory of the liquid state can be given within the framework of statistical mechanics, the mathematical difficulties encountered in trying to obtain explicit results have prompted the use of intuitively plausible models. One of these models in the form of the free volume theory developed by Eyring[1] and co-workers and by Lennard-Jones and Devonshire[2] has provided a useful approximate description of the thermodynamic properties of pure liquids.

One[3] of us has shown that the free volume theory can be derived from the general principles of statistical mechanics by means of well-defined approximations. This general insight into the nature of the free volume theory has provided the basis for extending the theory to multicomponent fluid mixtures. The results of this extension are given in this article.

Recently, Prigogine[4,5] and co-workers have given expressions for the excess thermodynamic properties of binary liquid solutions by extending the Lennard-Jones and Devonshire cell method. In their derivation they assumed, as a first approximation, a random mixing and thus neglected short-range order. In general the cooperative phenomena exhibited by fluid mixtures can be treated (within the framework of the free volume theory) by the order-disorder methods developed in the theory of the solid state. The expansion given by the method of moments[6,7] will be used in the following development.

We consider a closed system of N monatomic molecules and r different species. We let N_i denote the number of molecules of species i ($i=1, 2, \cdots, r$), where $\sum_i N_i=N$. We span the physical volume v by means of a virtual lattice which divides this volume into N cells of equal size. The partition function Q for this system is given by the theory of the classical canonical ensemble in the form

$$Q=\prod_{i=1}^{r}\left(\frac{2\pi m_i kT}{h^2}\right)^{3N_i/2}\frac{Z_{N_1,N_2,\cdots,N_r}}{\prod_{i=1}^{r}N_i!}, \tag{1}$$

where

$$Z_{N_1,N_2,\cdots,N_r}=\int^{v}\cdots\int^{v}e^{-\beta V}\prod_{k=1}^{N}dv_k,$$

$$\beta=1/kT.$$

$Z_{N_1,N_2,\cdots,N_r}$ is the Gibbs phase integral in configuration space, m_i is the mass of a molecule of species i, T the thermodynamic temperature, k the Boltzmann constant, h Planck's constant, and V the potential of intermolecular force.

If we denote the volume of each of the above virtual cells by Δ, the integral over the volume may be replaced by a sum of integrals over the cells. We then obtain for the Gibbs phase integral the expression

$$Z_{N_1,\cdots,N_r}=\sum_{l_1=1}^{N}\cdots\sum_{l_N=1}^{N}\int^{\Delta l_1}\cdots\int^{\Delta l_N}e^{-\beta V}\prod_{k=1}^{N}dv_k. \tag{2}$$

In general, Eq. (2) may be expressed in terms of integrals of the type

$$Z_{N_1,N_2,\cdots,N_r}^{(\xi_1^1,\cdots,\xi_N^1,\xi_1^2,\cdots,\xi_N^2,\cdots,\xi_1^r,\cdots,\xi_N^r)},$$

where ξ_s^i is the number of molecules of species i occupying the cell Δ_s. We may then write

$$\frac{Z_{N_1,\cdots,N_r}}{\prod_{i=1}^{r}N_i!}=\sum_{\xi_1^1,\cdots,\xi_N^1=0}^{N_1}\cdots\sum_{\xi_1^r,\cdots,\xi_N^r=0}^{N_r}\frac{Z_{N_1,\cdots,N_r}^{(\xi_1^1,\cdots,\xi_N^r)}}{\prod_{i=1}^{r}\prod_{s=1}^{N}\xi_s^i!} \tag{3}$$

$$\sum_s \xi_s^i=N_i \quad (i=1, 2, \cdots, r)$$

$$\sum_i \xi_s^i=\text{no. of molecules in cell } s.$$

We denote by $Z^{(1)}$ the sum containing the integrals for all distinguishable configurations corresponding to

* This work was carried out with support from the ONR under Contract Nonr-410(00) with Yale University.

[1] H. J. Eyring and O. Hirschfelder, J. Chem. Phys. **4**, 250 (1937).
[2] Lennard-Jones and Devonshire, Proc. Roy. Soc. (London) **A163**, 53 (1937); **165**, 1 (1938).
[3] J. G. Kirkwood, J. Chem. Phys. **18**, 380 (1950).
[4] I. Prigogine and Garikian, Physica **16**, 239 (1950).
[5] I. Prigogine and V. Mathot, J. Chem. Phys. **20**, 49 (1952).
[6] J. G. Kirkwood, J. Chem. Phys. **6**, 70 (1938).
[7] J. G. Kirkwood, J. Phys. Chem. **43**, 97 (1939).

single occupancy of each cell.

$$Z^{(1)}=\sum_{\xi_1{}^1,\cdots,\xi_N{}^1=0}^{1}\cdots\sum_{\xi_1{}^r,\cdots,\xi_N{}^r=0}^{1}\times\int^{\Delta_1}\cdots\int^{\Delta_N}e^{-\beta V(\mathbf{r}_1,\cdots,\mathbf{r}_N,\xi)}\prod_{k=1}^{N}dv_k \tag{4}$$

$$\sum_{s=1}^{N}\xi_s{}^i=N_i\quad(i=1,2,\cdots,r)$$

$$\sum_{i=1}^{r}\xi_s{}^i=1\quad(s=1,2,\cdots,N),$$

where $V(\mathbf{r},\xi)$ is the potential of intermolecular force for an arbitrary configuration, $\xi_1{}^1,\cdots,\xi_N{}^1,\cdots,\xi_1{}^r,\cdots,\xi_N{}^r$.

Formally we can define a parameter σ by the relation

$$(\sigma)^N=\sum_{\xi_1{}^1,\cdots,\xi_N{}^1=0}^{N_1}\cdots\sum_{\xi_1{}^r,\cdots,\xi_N{}^r=0}^{N_r}\frac{1}{\prod_{i=1}^{r}\prod_{s=1}^{N}\xi_s{}^i!}\times\frac{Z_{N_1,\cdots,N_r}^{(\xi_1{}^1,\cdots,\xi_N{}^r)}}{Z^{(1)}}, \tag{5}$$

$$\sum_{s=1}^{N}\xi_s{}^i=N_i\quad(i=1,2,\cdots,r),$$

and write

$$\frac{Z_{N_1,\cdots,N_r}}{\prod_{i=1}^{r}N_i!}=(\sigma)^N Z^{(1)}. \tag{6}$$

σ has the value 1 if, as at high densities, intermolecular repulsive forces exclude multiple occupancy by causing all

$$Z_{N_1,\cdots,N_r}^{(\xi_1{}^1,\cdots,\xi_N{}^r)}$$

except those corresponding to single occupancy to vanish. However, as the density tends to zero and all

$$Z_{N_1,\cdots,N_r}^{(\xi_1{}^1,\cdots,\xi_N{}^r)}$$

become equal, σ approaches the value e. The problem of obtaining the exact value of σ[8] is left open for the present and we will confine our attention to the analysis of the free volume approximation to $Z^{(1)}$.

Corresponding to a given configuration, $\xi_1{}^1,\cdots,\xi_N{}^r$, there will exist the phase integral $Z^{(1)}(\xi)$ which is related to a relative probability density in configuration space, $P^{(1)}(\xi,\mathbf{r}_1,\cdots,\mathbf{r}_N)$, in the following manner.

$$P^{(1)}(\xi,\mathbf{r}_1,\cdots,\mathbf{r}_N)=\exp[\beta(A^{(1)}(\xi)-V(\xi,\mathbf{r}_1,\cdots,\mathbf{r}_N))] \tag{7}$$

$$\exp[-\beta A_r{}^{(1)}(\xi)]=Z^{(1)}(\xi),$$

where

$$A^{(1)}(\xi)=E^{(1)}(\xi)-TS^{(1)}(\xi),$$

$$E^{(1)}(\xi)=\int^{\Delta_1}\cdots\int^{\Delta_N}V(\xi,\mathbf{r}_1,\cdots,\mathbf{r}_N)\times P^{(1)}(\xi,\mathbf{r}_1,\cdots,\mathbf{r}_N)\prod_{k=1}^{N}dv_k,$$

$$S^{(1)}(\xi)=-k\int^{\Delta_1}\cdots\int^{\Delta_N}P^{(1)}(\xi,\mathbf{r}_1,\cdots,\mathbf{r}_N)\times\log P^{(1)}(\xi,\mathbf{r}_1,\cdots,\mathbf{r}_N)\prod_{k=1}^{N}dv_k,$$

and

$$\sum_{\xi_1{}^1,\cdots,\xi_N{}^1=0}^{1}\cdots\sum_{\xi_1{}^r,\cdots,\xi_N{}^r=0}^{1}\exp[-\beta A^{(1)}(\xi)]=Z^{(1)},$$

$$\sum_{i=1}^{r}\xi_s{}^i=1\quad(s=1,2,\cdots,N),$$

$$\sum_{s=1}^{N}\xi_s{}^i=N_i\quad(i=1,2,\cdots,r).$$

From Eqs. (1) and (6) we obtain the following expression for the total free energy, $A_{N_1,N_2,\cdots,N_r}$.

$$A_{N_1,\cdots,N_r}=-kT\log\left[\prod_{i=1}^{r}\left(\frac{2\pi m_i kT}{h^2}\right)^{3Ni/2}\right]-NkT\log\sigma-kT\log Z^{(1)}. \tag{8}$$

We now introduce the approximation[3]

$$\prod_{s=1}^{N}\varphi(\mathbf{r}_s,\xi)=P^{(1)}(\xi,\mathbf{r}_1,\cdots,\mathbf{r}_N). \tag{9}$$

$\varphi(\mathbf{r}_s,\xi)$ depends only on the position $\mathbf{r}_s$ of the molecule in the cell s, referred to some convenient origin in that cell, and on the given configuration $\{\xi\}$. $\varphi(\mathbf{r}_s,\xi)$ is also subject to the following normalization condition

$$\int^{\Delta}\varphi(r,\xi)dv=1.$$

We will now assume that the intermolecular potential $V(\xi,\mathbf{r}_1,\cdots,\mathbf{r}_N)$ for a given configuration $\{\xi\}$, can be expressed in the form

$$V(\xi,\mathbf{r}_1,\cdots,\mathbf{r}_N)=\sum_{k<s}\sum_{i,l=1}^{r}\xi_k{}^i\xi_s{}^l V_{il}(|\mathbf{R}_{sk}|) \tag{10}$$

$$\sum_{i=1}^{r}\xi_s{}^i=1\quad(s=1,\cdots,N).$$

$V_{il}|\mathbf{R}_{sk}|$ is the intermolecular potential for a pair of molecules of type i and l, respectively, located in cells s and k.

$$|\mathbf{R}_{sk}|=|\mathbf{R}_{sk}{}^0+\mathbf{r}_k-\mathbf{r}_s|,$$

where $\mathbf{R}_{sk}{}^0$ is the vector from the origin in the cell s to the origin in cell k.

Following the analysis outlined,[3] we extremalize $A^{(1)}(\xi)$ with respect to the functions $\varphi(\mathbf{r}_s,\xi)$, obtaining

[8] For a discussion of this problem for the case of a pure liquid see (a) J. A. Pople, Phil. Mag. **42**, 459 (1951). (b) P. Janssens and I. Prigogine, Physica **16**, 895 (1950).

the set of simultaneous integral equations

$$\varphi(\mathbf{r}_s, \xi)=e^{\beta[\alpha(\xi)-\psi(\mathbf{r}_s,\xi)]} \quad (s=1, \cdots, N),$$

where (11)

$$e^{-\beta\alpha(\xi)}=\int^{\Delta_s} e^{-\beta\psi(\mathbf{r},\xi)}dv$$

$$\psi(\mathbf{r}_s, \xi)=\int^{\Delta_s} w_s(\mathbf{r}-\mathbf{r}_s)e^{\beta[\alpha(\xi)-\psi(\mathbf{r},\xi)]}dv$$

$$w_s(\mathbf{r}-\mathbf{r}_s)=E(\mathbf{r}-\mathbf{r}_s)-\bar{E}_s$$

$$\bar{E}_s=\int^{\Delta_s}\int^{\Delta} E(\mathbf{r}-\mathbf{r}_s)\varphi(\mathbf{r}, \xi)dvdv_s$$

$$E(\mathbf{r})=\sum_{\substack{k=1\\ \neq s}}^{N}\sum_{i,l=1}^{r}\xi_k{}^i\xi_s{}^l V_{il}(|\mathbf{R}_{sk}{}^0+\mathbf{r}|)$$

$$\sum_{i=1}^{r}\xi_s{}^i=1 \quad (s=1, \cdots, N).$$

If $\varphi(\mathbf{r}, \xi)$ is sharply peaked in the vicinity of the cell origin, it may be set equal to $\delta(\mathbf{r})$, the Dirac delta function, in a zero approximation. It has been shown[3] that this approximation leads to the Lennard-Jones Devonshire theory.

Since

$$A^{(1)}(\xi)=\sum_{s=1}^{N}\left\{\alpha(\xi)+\frac{\bar{E}_s(\xi)}{2}\right\}, \tag{12}$$

$$Z^{(1)}=\int^{\Delta_1}\cdots\int^{\Delta_N}\sum_{\xi_1{}^1, \cdots, \xi_N{}^1=0}^{1}\cdots$$

$$\sum_{\xi_1{}^r, \cdots, \xi_N{}^r=0}^{1} e^{-\beta W(\xi,\mathbf{r}_1,\cdots,\mathbf{r}_N)}\prod_{k=1}^{N}dv_k, \tag{13}$$

$$\sum_{s=1}^{N}\xi_s{}^i=N_i \quad (i=1, \cdots, r),$$

$$\sum_{i=1}^{r}\xi_s{}^i=1 \quad (s=1, \cdots, N),$$

where

$$W(\xi, \mathbf{r}_1, \cdots, \mathbf{r}_N)=\sum_{s=1}^{N}\sum_{\substack{k=1\\ \neq s}}^{N}\sum_{i,l=1}^{r}\xi_k{}^i\xi_s{}^l\epsilon_{sk}{}^{il}(\mathbf{r}_s),$$

$$\sum_{i=1}^{r}\xi_s{}^i=1 \quad (s=1, \cdots, N),$$

$$\epsilon_{sk}{}^{il}(\mathbf{r}_s)=V_{il}(|\mathbf{R}_{sk}{}^0-\mathbf{r}_s|)-\tfrac{1}{2}V_{il}(|\mathbf{R}_{sk}{}^0|).$$

The integrand in Eq. (13) can be expanded by the method of moments[6,7] in the following manner, where it is to be understood that in this calculation the vectors of the set $\{\mathbf{r}_1, \cdots, \mathbf{r}_N\}$ are held fixed. Let the exponential $e^{-\beta W}$ in the integrand of Eq. (13) be expanded in powers of βW. Hence

$$\sum_{\xi_1{}^1, \cdots, \xi_N{}^1=0}^{1}\cdots\sum_{\xi_1{}^r, \cdots, \xi_N{}^r=0}^{1} e^{-\beta W}$$

$$=\frac{N!}{\prod_{i=1}^{r}N_i!}\sum_{n=0}^{\infty}\frac{M_n}{n!}(-\beta)^n,$$

$$\sum_{s=1}^{N}\xi_s{}^i=N_i \quad (i=1, \cdots, r), \tag{14}$$

$$\sum_{i=1}^{r}\xi_s{}^i=1 \quad (s=1, \cdots, N),$$

where

$$M_n=\frac{\prod_{i=1}^{r}N_i!}{N!}\sum_{\xi_1{}^1, \cdots, \xi_N{}^1=0}^{1}\cdots\sum_{\xi_1{}^r, \cdots, \xi_N{}^r=0}^{1}(W)^n,$$

$$\sum_{s=1}^{N}\xi_s{}^i=N_i \quad (i=1, \cdots, r),$$

$$\sum_{i=1}^{r}\xi_s{}^i=1 \quad (s=1, \cdots, N).$$

We can rewrite this expansion using the semi-invariants or cumulants, λ_n, of Thiele.

$$\frac{N!}{\prod_{i=1}^{r}N_i!}\sum_{n=0}^{\infty}\frac{M_n}{n!}(-\beta)^n=\frac{N!}{\prod_{i=1}^{r}N_i!}\exp\left[\sum_{n=1}^{\infty}\frac{\lambda_n}{n!}(-\beta)^n\right]. \tag{15}$$

The semi-invariants, λ_n, are expressible[6] in terms of the moments M_n. The first few are given by

$$\begin{aligned}\lambda_1&=M_1,\\ \lambda_2&=M_2-M_1{}^2,\\ \lambda_3&=M_3-3M_1M_2+2M_1{}^3.\end{aligned} \tag{16}$$

From Eqs. (13), (14), and (15) we obtain

$$Z^{(1)}=\frac{N!}{\prod_{i=1}^{r}N_i!}\int^{\Delta_1}\cdots\int^{\Delta_N}$$

$$\times\exp\left[\sum_{n=1}^{\infty}\left(\frac{\lambda_n}{n!}\right)(-\beta)^n\right]\prod_{k=1}^{N}dv_k. \tag{17}$$

From Eq. (14), we have

$$M_n=\langle W^n\rangle_{Av}, \tag{18}$$

where the average denotes an a priori average over all configurations. Since

$$\langle\xi_s{}^i\rangle_{Av}=x_i \quad (s=1, \cdots, N),$$

$$M_1=\sum_{s=1}^{N}\sum_{\substack{k=1\\ \neq s}}^{N}\sum_{i,l=1}^{r}x_ix_l\epsilon_{sk}{}^{il}(\mathbf{r}), \tag{19}$$

where x_i is the mole fraction of species i.

At sufficiently high temperatures or when the differences in interaction will not alter a random distribution of the r species among nearest neighbors, one is justified in retaining only the first moment in the above theory. Retention of only the first moment has been shown[6,7] to be equivalent to the Bragg-Williams approximation. Employing this approximation, a simplified extension of the Lennard-Jones and Devonshire smoothed potential is obtained by replacing the summation over k in Eq. (19) by an integral over a sphere of radius equal to the mean distance between molecules.[3] For a binary solution this procedure yields precisely the expression first used by Prigogine and Garikian.[4]

One[9] of us has given an alternative approach to the order-disorder problem. This method gives an approximation equivalent to retaining the third moment and has been shown[9] to be equivalent to the method of local configurations of Bethe[10] and the quasi-chemical method of Fowler and Guggenheim.[11,12]

Eq. (13) may be rewritten in the form

$$Z^{(1)}=\int^{\Delta_1}\cdots\int^{\Delta_N}\Phi(\mathbf{r},0)\times\exp\left[\int_0^1\frac{\partial\log\Phi(\mathbf{r},\lambda)}{\partial\lambda}d\lambda\right]\prod_{k=1}^{N}dv_k, \quad (20)$$

where

$$\Phi(\mathbf{r},\lambda)=\sum_{\xi_1',\cdots,\xi_N'=0}^{1}\cdots\sum_{\xi_1^r,\cdots,\xi_N^r=0}^{1}e^{-\beta\lambda W(\xi,r_1,\cdots,r_N)}$$

$$\sum_{s=1}^{N}\xi_s{}^i=N_i\quad(i=1,2,\cdots,r)$$

$$\sum_{i=1}^{r}\xi_s{}^i=1\qquad(s=1,\cdots,N).$$

$\Phi(\mathbf{r},0)$ reduces to the total number of configurations among the cells

$$\Phi(\mathbf{r},0)=\frac{N!}{\prod_{i=1}^{r}N_i!}.$$

The procedure for evaluating $\partial\log\Phi(\mathbf{r},\lambda)/\partial\lambda$ is given in detail[9] in the computation of $\partial\log f/\partial\alpha$, and in the case of a binary mixture yields the result

$$Z^{(1)}=\binom{N}{N_1}\prod_{s=1}^{N}\left\{\int^{\Delta_s}\exp\left[-\beta\sum_{\substack{k=1\\ \neq s}}^{N}U_{sk}(\mathbf{r})\right]dv_s\right\}, \quad (21)$$

where

$$U_{sk}(\mathbf{r})=\frac{1}{\beta[\epsilon_{sk}{}^{11}(\mathbf{r})-2\epsilon_{sk}{}^{12}(\mathbf{r})+\epsilon_{sk}{}^{22}(\mathbf{r})]}\times\left[\left\{q\log\frac{\varphi-q}{1-q}+\log\frac{\varphi+1}{2}\right\}\epsilon_{sk}{}^{11}(\mathbf{r})+\left\{(1+q)\log\frac{2(\varphi+q)}{(1+q)(\varphi+1)}+(1-q)\log\frac{2(\varphi-q)}{(1-q)(\varphi+1)}\right\}\epsilon_{sk}{}^{12}(\mathbf{r})+\left\{\log\frac{\varphi+1}{2}-q\log\frac{\varphi+q}{1+q}\right\}\epsilon_{sk}{}^{22}(\mathbf{r})\right]$$

$$\varphi=[q^2+(1-q^2)\exp-\beta\{\epsilon_{sk}{}^{11}(\mathbf{r})-2\epsilon_{sk}{}^{12}(\mathbf{r})+\epsilon_{sk}{}^{22}(\mathbf{r})\}]^{\frac{1}{2}}$$

$$q=x_1-x_2$$

$$\beta=1/kT.$$

Retaining only the first moment and using Eqs. (18), (17), and (19) we obtain for the total free energy

$$A_{N_1,\cdots,N_r}=NkT\sum_{i=1}^{r}x_i\log x_i+A^*{}_{N_1,\cdots,N_r}+A^E{}_{N_1,\cdots,N_r}$$

$$A^*{}_{N_1,\cdots,N_r}=-kT\sum_{i=1}^{r}N_i\log\left\{e\left(\frac{2\pi m_i kT}{h^2}\right)^{\frac{3}{2}}v\right\}$$

$$A^E{}_{N_1,\cdots,N_r}=-NkT\log\frac{\sigma}{e}-NkT\log\frac{1}{v}\int^{\Delta}e^{-\beta w_0(\mathbf{r})}dv+\frac{N}{2}E_0(N_1,\cdots,N_r) \quad (22)$$

$$w_0(r)=\sum_{k=2}^{N}\sum_{i,l=1}^{r}x_ix_l\{V_{il}(|\mathbf{R}_{1k}{}^0-\mathbf{r}|)-V_{il}(|\mathbf{R}_{1k}{}^0|)\}$$

$$E_0(N_1,\cdots,N_r)=\sum_{k=2}^{N}\sum_{i,l=1}^{r}x_ix_lV_{il}(|\mathbf{R}_{1k}{}^0|).$$

For spherical nonpolar molecules the intermolecular potential for a pair of molecules, $V_{il}(|\mathbf{R}_{1k}{}^0-\mathbf{r}_1|)$, can be represented by the Lennard-Jones potential

$$V_{il}(|\mathbf{R}_{1k}{}^0-\mathbf{r}_1|)=4\epsilon_{il}\left[\left(\frac{a_{il}}{R}\right)^{12}-\left(\frac{a_{il}}{R}\right)^{6}\right], \quad (23)$$

where $R=|\mathbf{R}_{1k}{}^0-\mathbf{r}_1|$ is the scalar distance between the molecule in cell 1 and the molecule in cell k, ϵ_{il} is the maximum energy of interaction, and a_{il} is the value of R for which $V_{il}(R)=0$.

[9] J. G. Kirkwood, J. Chem. Phys. **8**, 623 (1940).
[10] Bethe, Proc. Roy. Soc. (London) **A145**, 699 (1934).
[11] Guggenheim, Proc. Roy. Soc. (London) **A169**, 304 (1938).
[12] Fowler and Guggenheim, Proc. Roy. Soc. (London) **A174**, 189 (1940).

Following the procedure given by Wentorf, Buehler, Hirschfelder, and Curtiss,[13] we replace the sum over k in the definition of $w_0(\mathbf{r})$, Eq. (20), by an integral over the first, second, and third shells of nearest neighbors situated at distances a, $\sqrt{2}a$, and $\sqrt{3}a$, respectively. Then

$$w_0(r)=\sum_{i,l=1}^{r} x_i x_l 12\epsilon_{il}\left\{\left(\frac{v_{il}^0}{v}\right)^4 L(y) - 2\left(\frac{v_{il}^0}{v}\right)^2 M(y)\right\},$$

where (24)

$$L(y)=l(y)+\frac{1}{128}l\left(\frac{y}{2}\right)+\frac{2}{729}l\left(\frac{y}{3}\right)$$

$$M(y)=m(y)+\frac{1}{16}m\left(\frac{y}{2}\right)+\frac{2}{27}m\left(\frac{y}{3}\right)$$

$$l(y)=(1+12y+25.2y^2+12y^3+y^4)(1-y)^{-10}-1$$

$$m(y)=(1+y)(1-y)^{-4}-1$$

$$y=\left(\frac{r}{a}\right)^2$$

$$v_{il}^0=Na_{il}^3.$$

$w_0(r)$ can be written in the form

$$w_0(r)=12\bar{\epsilon}\left\{\left(\frac{\bar{v}^0}{v}\right)^4 L(y)-2\left(\frac{\bar{v}^0}{v}\right)^2 M(y)\right\}, \quad (25)$$

where $\bar{\epsilon}$ and $\bar{v}^0$ are determined by the two equations

$$\bar{\epsilon}\bar{v}^{0^4}=\sum_{i,l=1}^{r} x_i x_l \epsilon_{il} v_{il}^{0^4}$$

$$\bar{\epsilon}\bar{v}^{0^2}=\sum_{i,l=1}^{r} x_i x_l \epsilon_{il} v_{il}^{0^2}.$$

Formally the theory for a multicomponent system becomes identical in form with the Lennard-Jones and Devonshire theory for a pure liquid with constants $\bar{\epsilon}$ and $\bar{v}^0$. Extensive tables[13] are available for the calculations of thermodynamic functions of a pure liquid and can be used without modification to obtain the properties of solutions for which the first moment approximations are valid.

As a first approximation in determining $\bar{\epsilon}$ and $\bar{v}^0$, we adopt the familiar expressions

$$(\epsilon_{il})^2=\epsilon_{ii}\epsilon_{ll}$$
$$a_{il}=(a_{ii}+a_{ll})/2. \quad (26)$$

In the applications discussed by Prigogine[4,5] and his co-workers it was assumed that $a_{11}=a_{12}=a_{22}$. While the cells in this theory are taken to be equal in size, the limitation on the relative sizes of the molecules is not nearly as severe. The only complication introduced is in the definition of $\bar{\epsilon}$ and $\bar{v}^0$ which now have the form

$$\bar{v}^0=\left[\frac{\sum_{i,l=1}^{r} x_i x_l \epsilon_{il} v_{il}^{0^4}}{\sum_{i,l=1}^{r} x_i x_l \epsilon_{il} v_{il}^{0^2}}\right]^{\frac{1}{3}}$$

$$\bar{\epsilon}=\frac{\left[\sum_{i,l=1}^{r} x_i x_l \epsilon_{il} v_{il}^{0^2}\right]^2}{\sum_{i,l=1}^{r} x_i x_l \epsilon_{il} v_{il}^{0^4}}. \quad (27)$$

With these definitions the Helmholtz free energy A can be calculated from the expression

$$A^E{}_{N_1,\cdots,N_r}=-NkT\log\frac{\sigma}{e}-NkT\log\frac{2\pi\sqrt{2}G}{N}+\frac{N}{2}E_0(N_1,\cdots,N_r)$$

$$E_0=12\bar{\epsilon}\left\{1.0109\left(\frac{\bar{v}^0}{v}\right)^4-2.4090\left(\frac{\bar{v}^0}{v}\right)^2\right\}, \quad (28)$$

where

$$G=\int_0^{0.30544} y^{\frac{1}{2}}\exp[-\beta w_0(y)]dy.$$

The chemical potential μ_i of component i can be obtained from Eq. (28) and the relation

$$\mu_i=(\partial A/\partial N_i)_{T,V,N_j}.$$

The result is

$$\mu_i=\mu_i^*+kT\log x_i+\mu_i^E,$$

$$\mu_i^*=-kT\log\left\{\left(\frac{2\pi m_i kT}{h^2}\right)^{\frac{3}{2}}v\right\},$$

$$\mu_i^E=-kT\log\frac{2\pi\sqrt{2}G}{N}-kT\log\frac{\sigma}{e}-12\bar{\epsilon}\left[1.2045\left(\frac{\bar{v}^0}{v}\right)^2-\left(1.51635+\frac{2g_L}{G}\right)\left(\frac{\bar{v}^0}{v}\right)^4\right]-\sum_{l=1}^{r} x_l 12\epsilon_{li}\left[\left(2.4090+\frac{4g_M}{G}\right)\left(\frac{v_{li}^0}{v}\right)^2-\left(1.0109+\frac{2g_L}{G}\right)\left(\frac{v_{li}^0}{v}\right)^4\right], \quad (29)$$

$$g_L=\int_0^{0.30544} y^{\frac{1}{2}}L(y)\exp[-\beta w_0(y)]dy,$$

$$g_M=\int_0^{0.30544} y^{\frac{1}{2}}M(y)\exp[-\beta w_0(y)]dy.$$

[13] Wentorf, Buehler, Hirschfelder, and Curtiss, J. Chem. Phys. **18**, 1484 (1950).

Moments of higher order than the first can be computed by methods previously presented[4,5] and are limited only in so far as they necessitate extensive numerical computations. A more serious restriction is placed upon the relative sizes of the molecules, since the theory is limited to cells of equal size. In addition, we have bypassed the problem of calculating the communal entropy. Although the limitations of the free volume theory are evident, further modifications to this theory would be of minor practical importance without solutions to the two problems just mentioned.

THE JOURNAL OF CHEMICAL PHYSICS VOLUME 20, NUMBER 10 OCTOBER, 1952

Thermodynamic Properties of the Diatomic Interhalogens from Spectroscopic Data*

LELAND G. COLE† AND GERARD W. ELVERUM, JR.
Jet Propulsion Laboratory, California Institute of Technology, Pasadena, California
(Received March 31, 1952)

The thermodynamic functions C_p^0, S^0, $-(F^0-E_0^0)/T$, and $(H^0-E_0^0)/T$ of the six diatomic interhalogens, chlorine monofluoride, bromine monofluoride, iodine monofluoride, bromine monochloride, iodine monochloride, and iodine monobromide, have been evaluated as a function of temperature from 298.16°K to 2000°K by the application of statistical methods. These results have been combined with newly evaluated properties of the fluorine, chlorine, bromine, and iodine atoms and molecules to yield the heats and free energies of dissociation and dissociation constants for the equilibria between the interhalogens and their molecular and atomic dissociation products. The calculations are based on available experimental spectroscopic constants with the exception of the anharmonicity term and internuclear distance for bromine chloride and of the internuclear distances in iodine fluoride and iodine bromide. These quantities are estimated empirically.

1. INTRODUCTION

THE heat capacities, entropies, free energies, and heat contents of the gaseous diatomic interhalogens (chlorine monofluoride, bromine monofluoride, iodine monofluoride, bromine monochloride, iodine monochloride, and iodine monobromide) have been evaluated as a function of temperature from 298.16°K to 2000°K by application of statistical methods to the molecular constants derivable from spectroscopic data. The thermodynamic functions of the six diatomic interhalogens in the ideal gaseous state at 1-atmosphere pressure have been evaluated for the rigid-rotator, harmonic-oscillator, diatomic model for which the contributions to the functions from anharmonicity have been evaluated by use of the unexpanded form[1] of the high temperature corrections of Mayer and Mayer.[2] The reduced masses and molecular weights (Aston scale) were calculated from the isotope abundances and packing fractions of Mattauch and Fluegge[3]; the physical constants were taken from Dumond and Cohen.[4] Neither nuclear-spin entropy nor the entropy of isotope mixing has been included in the tabulations of entropy and free energy.

2. CHLORINE MONOFLUORIDE

Wahrhaftig[5] has observed $^3\Pi_0^+ \rightarrow {}^1\Sigma^+$ transition in chlorine monofluoride and obtained values for ω_e'' of 793.2 cm^{-1}, for $\chi_e''\omega_e''$ of 9.9 cm^{-1}, for B_e'' of 0.518 cm^{-1}, and for α_e of 0.006 cm^{-1}, whereas Schmitz and Schumacher[6] reported an ω_e'' of 780.4 cm^{-1} and an $\chi_e''\omega_e''$ of 4.0 cm^{-1} from an investigation of the vibration spectrum of this interhalogen. Potter[7] has employed the data of Wahrhaftig, for the sake of self-consistency in the vibrational and rotational contributions, and obtained the heat capacity, entropy, and free energy of Cl^nF from 298.16°K to 2000°K. Gilbert *et al.*[8] have subsequently observed the rotational transitions for $J=0\rightarrow1$ for $Cl^{35}F$ and $Cl^{37}F$ in the microwave region from which they have derived values for B_e of 15,483.688±0.026 mc and 15,189.221±0.026 mc, and for α of 130.666±0.029 mc for the two isotopic species.

* This paper presents the results of one phase of research carried out at the Jet Propulsion Laboratory under Contract No. DA-04-495 Ord 18, sponsored by the Department of the Army, Ordnance Corps.
† Present address: University of Michigan, Willow Run Research Center, Ypsilanti, Mich.
[1] Cole, Farber, and Elverum, J. Chem. Phys. **20**, 586 (1952).
[2] J. E. Mayer and M. G. Mayer, *Statistical Mechanics* (John Wiley and Sons, Inc., New York, 1940).
[3] J. Mattauch and S. Fluegge, *Nuclear Physics Tables* (Interscience Publishers, Inc., New York, 1946).
[4] J. W. M. Dumond and E. R. Cohen, *A Least Squares Adjustment of the Atomic Constants as of December 1950*, a report to the National Research Council, Committee on Constants and Conversion Factors of Physics, California Institute of Technology, 1951.
[5] A. L. Wahrhaftig, J. Chem. Phys. **10**, 248 (1942).
[6] H. Schmitz and H. Schumacher, Z. Naturforsch. **2a**, 358 (1947).
[7] R. L. Potter, J. Chem. Phys. **17**, 957 (1949).
[8] Gilbert, Roberts, and Griswold, Phys. Rev. **76**, 1723 (1949).

TABLE I. Vibrational and rotational constants for the diatomic interhalogens.

Isotopic species	ω_e cm^{-1}	$\chi_e\omega_e$ cm^{-1}	B_e cm^{-1}	$a_e\times10^3$ cm^{-1}	r_e A
$Cl^{35}F^{19}$	786.34	6.23	0.516509	4.35879	1.62811
$Cl^{37}F^{19}$	778.82	6.11	0.506686	4.33514	1.62811
$Br^{79}F^{19}$	671.0	3.0	0.357165	5.214	1.7555_5
$Br^{81}F^{19}$	669.4	3.0	0.355454	5.177	1.7555_5
$I^{127}F^{19}$	610.0	3.0	0.280785	···	1.90_6
$Br^{79}Cl^{35}$	436.3	1.70_3	0.1559_5	···	2.11
$Br^{79}Cl^{37}$	428.1	1.63_9	0.1501_1	···	2.11
$Br^{81}Cl^{35}$	434.7	1.69_0	0.1547_7	···	2.11
$Br^{81}Cl^{37}$	426.4	1.62_6	0.1489_2	···	2.11
$I^{127}Cl^{35}$	384.18	1.465	0.1141619	5.36	2.3207
$I^{127}Cl^{37}$	375.95	1.403	0.1093241	5.02	2.3207
$I^{127}Br^{79}$	268.4	0.78_0	0.05847	···	2.43
$I^{127}Br^{81}$	266.4	0.76_8	0.05758	···	2.43

Gilbert's values for D_e were based on the vibrational frequency of Wahrhaftig.[5] We have revised them in view of the recent results of Nielsen and Jones[9] on the vibration-rotation fine structure of the first overtone and fundamental of ClF and find $D_e(Cl^{35}F)=8.913\times10^{-7}$ cm^{-1} and $D_e(Cl^{37}F)=8.577\times10^{-7}$ cm^{-1}. The Nielsen and Jones constants for ω_e and for $\chi_e\omega_e$ and the new rotational constants for the ClF species are summarized in Table I, together with the values for these constants (as used in the present calculations) for the several isotopic species of the other five interhalogens.

The heat capacity, entropy, and free energy of $Cl^{35}F$ and of $Cl^{37}F$ of Potter[7] have been revised for these changes in the spectroscopic constants, and in addition the heat-content function has been evaluated from 298.16°K to 2000°K for use in evaluating the heats and free energies of dissociation of ClF as a function of temperature. The thermodynamic properties for Cl^nF were determined from an abundance ratio[3] of Cl^{35} to Cl^{37} of 3.07±0.03 and are summarized in Table II.

The heats and free energies of dissociation and dissociation constants for the reactions

$$ClF\rightleftharpoons\tfrac{1}{2}Cl_2+\tfrac{1}{2}F_2$$

and

$$ClF\rightleftharpoons Cl+F$$

were evaluated as a function of temperature, making use of the heat of dissociation of fluorine measured recently by Doescher,[10] the dissociation energy of chlorine,[11] the thermodynamic functions of molecular and atomic fluorine,[1] and the dissociation energies of chlorine monofluoride. The convergence limit[12] for ClF, combined with the foregoing quantities and the excitation energies of chlorine and fluorine,[11] leads to a value

TABLE II. Heat capacity, entropy, free energy, and heat content of chlorine monofluoride.

T °K	C_p^0 cal mole^{-1} deg^{-1}	S^0 cal mole^{-1} deg^{-1}	$-(F^0-E_0^0)/T$ cal mole^{-1} deg^{-1}	$(H^0-E_0^0)/T$ cal mole^{-1} deg^{-1}
298.16	7.669	52.080	44.936	7.143
300	7.678	52.127	44.980	7.146
400	8.068	54.392	47.061	7.331
500	8.335	56.223	48.716	7.507
600	8.515	57.760	50.099	7.661
700	8.633	59.083	51.290	7.793
800	8.731	60.243	52.338	7.905
900	8.800	61.275	53.274	8.001
1000	8.854	62.206	54.122	8.084
1200	8.932	63.828	55.609	8.219
1400	8.990	65.210	56.884	8.326
1600	9.037	66.414	58.001	8.412
1800	9.076	67.480	58.996	8.484
2000	9.111	68.439	59.894	8.545

of ΔE_0^0 for the formation of ClF of −13.995±0.2 kcal mole^{-1} if the dissociation products are assumed to be $F(^2P_{1/2})$ and $Cl(^2P_{3/2})$ and to a value of −12.637±0.2 kcal mole^{-1} if the products are assumed to be $F(^2P_{3/2})$ and $Cl(^2P_{1/2})$. The possibility of the products being $F(^2P_{3/2})$ and $Cl(^2P_{3/2})$ is excluded since there is a predissociation limit below the $A^3\Pi_0^+$ convergence limit. The dissociations to atomic products were calculated to have values of ΔE_0^0 of +58,947 and +60,305 cal mole^{-1}, respectively. The energy terms and dissociation constants for the two conditions of excitation are summarized in Table III. The free energies of the chlorine atom and molecule were taken from the work of Giauque and Overstreet[12] after slight revisions for subsequent changes in the physical constants.[4] The heat-content function for chlorine was obtained from the same spectral data used by Giauque since there has been no revision in these constants to date.[13,14]

3. BROMINE MONOFLUORIDE

Vibrational analyses of the BrF spectrum emitted by flames formed when fluorine was reacted with hydrogen bromide or bromine led Durie and Gaydon[15] to numerical values of ω_e and $\chi_e\omega_e$ of 673 cm^{-1} and 4 cm^{-1} for this interhalide. Broderson and Schumacher[16] had previously analyzed the absorption bands of BrF and arrived at the values of 671 cm^{-1} and 3 cm^{-1}, respectively, for these molecular constants. These are the constants recorded by Herzberg[13] for $Br^{79}F$ and are the values used in the present calculations. Both sets of data result in a ν of 665 cm^{-1} from which value the vibrational contributions to the thermodynamic func-

[9] A. H. Nielsen and E. A. Jones, J. Chem. Phys. **19**, 1117–1121 (1951).
[10] R. N. Doescher, J. Chem. Phys. **19**, 1070 (1951); J. Chem. Phys. (in publication).
[11] F. D. Rossini *et al.*, *Selected Values of Chemical Thermodynamic Properties*, U. S. National Bureau of Standards (1947).
[12] W. F. Giauque and R. Overstreet, J. Am. Chem. Soc. **54**, 1731–1744 (1932).
[13] G. Herzberg, *Molecular Spectra and Molecular Structure. I. Spectra of Diatomic Molecules* (D. Van Nostrand Company, Inc., New York, 1950).
[14] C. E. Moore, U. S. National Bureau of Standards, Circular No. 467 (1949).
[15] R. A. Durie and A. G. Gaydon, paper presented at the American Chemical Society Meeting, New York, September 3–7 (1951); R. A. Durie, Proc. Roy. Soc. (London) **207A**, 388–395 (1951).
[16] P. H. Broderson and H. J. Schumacher, Z. Naturforsch. **2a**, 358 (1947).

tions were obtained. The differences, resulting from the choice of one or the other anharmonicity constant, in the numerical values for the contributions from the anharmonicity of vibration and the increase of moment of inertia with increasing v and j values to the thermodynamic properties can be shown to be small. The differences in heat capacity, for example, of the $Br^{79}F$ species were calculated to be only 0.003 cal $mole^{-1}$ deg^{-1} at 298.16°K and 0.036 cal $mole^{-1}$ deg^{-1} at 2000°K. The rotational constants for $Br^{79}F$ and $Br^{81}F$ were taken from Smith, Tidwell, and Williams' observations on mixtures of BrF_3, BrF_5, Br_2, and F_2 in the microwave region.[17] The six lines observed in the 20.9×10^3 to 21.5×10^3 mc sec^{-1} region and the Stark shifts were interpreted as the $J=0\leftrightarrow1$ transition for BrF. The vibrational constants for $Br^{81}F$ were calculated from those of $Br^{79}F$ by the usual relationships, assuming that the force constants in the two species were equal. The thermodynamic properties C_p^0, S^0, $-(F^0-E_0^0)$, and $(H^0-E_0^0)/T$ reported in Table IV for Br^nF were obtained by adding the contributions from the two species in proportion to the relative abundances of the bromine isotopes.[3] A short graphical Birge-Sponer extrapolation for the upper state of BrF led Durie and Gaydon[15] to dissociation energies for the ground state of 2.16±0.02 ev if the upper state goes to excited bromine and normal fluorine, and of 2.58±0.02 ev if the upper state goes to excited fluorine and normal bromine. These data are in essential agreement with the values of Broderson and Schumacher[16] as reported by Herzberg.[13] Wahrhaftig[5] had concluded in the case of ClF that the dissociation products consisted of an excited fluorine atom and a normal chlorine atom since the lighter atom in ICl was excited on dissociation in the upper state. Durie,[15] on the basis of the lack of chemical evidence for the stability of iodine fluorides lower than IF_5 in molecular weight and commensurate with a D_0''(IF) of 2.87 ev (for $I^2P_{3/2}$ and $F^2P_{1/2}$), has concluded that the three fluorine-containing diatomic interhalogens dissociate to a $^2P_{1/2}X$ and $^2P_{3/2}F$. For the present purpose, in view of the uncertainty in the values of ΔE_0^0, the heats and free energies of dissociation and dissociation constants for BrF have been calculated for both dissociation energies; the results are summarized in Table V. These calculations were based on a dissociation energy for bromine[13] of 45.441 kcal $mole^{-1}$ and on the free energies for Br_2 and Br of Gordon and Barnes[18] which have been revised for subsequent

TABLE III. Heats, free energies, and equilibrium constants for the dissociation of chlorine monofluoride.

			$ClF \rightleftarrows Cl+F$			
		$\Delta E_0^0=58.947$ kcal	$K=\frac{P_{Cl}P_F}{P_{ClF}}$		$\Delta E_0^0=60.305$ kcal	$K=\frac{P_{Cl}P_F}{P_{ClF}}$
$\frac{T}{°K}$	$\Delta H^0/T$	$\Delta F^0/T$		$\Delta H^0/T$	$\Delta F^0/T$	
298.16	200.81	175.49	4.443×10^{-39}	205.37	180.04	4.492×10^{-40}
300	199.60	174.26	8.254×10^{-39}	204.12	178.78	8.463×10^{-40}
400	150.40	124.25	7.008×10^{-28}	153.80	127.64	1.270×10^{-28}
500	120.83	94.107	2.711×10^{-21}	123.54	96.82	6.914×10^{-22}
600	101.07	73.935	6.944×10^{-17}	103.33	76.198	2.223×10^{-17}
700	86.92	59.476	1.004×10^{-13}	88.861	61.416	3.782×10^{-14}
800	76.289	48.593	2.400×10^{-11}	77.987	50.290	1.022×10^{-11}
900	68.004	40.104	1.719×10^{-9}	69.512	41.613	8.047×10^{-10}
1000	61.363	33.295	5.291×10^{-8}	62.721	34.652	2.672×10^{-8}
1200	51.378	23.045	9.195×10^{-6}	52.509	24.177	5.203×10^{-6}
1400	44.224	15.692	3.720×10^{-4}	45.193	16.662	2.284×10^{-4}
1600	38.843	10.152	6.043×10^{-3}	39.692	11.001	3.943×10^{-3}
1800	34.649	5.8301	5.319×10^{-2}	35.403	6.5844	3.639×10^{-2}
2000	31.286	2.3582	3.052×10^{-1}	31.965	3.0370	2.169×10^{-1}
			$ClF \rightleftarrows \frac{1}{2}Cl_2+\frac{1}{2}F_2$			
		$\Delta E_0^0=12.637$ kcal	$K=\frac{P^{\frac{1}{2}}_{Cl_2}P^{\frac{1}{2}}_{F_2}}{P_{ClF}}$		$\Delta E_0^0=13.995$ kcal	$K=\frac{P^{\frac{1}{2}}_{Cl_2}P^{\frac{1}{2}}_{F_2}}{P_{ClF}}$
$\frac{T}{°K}$	$\Delta H^0/T$	$\Delta F^0/T$		$\Delta H^0/T$	$\Delta F^0/T$	
298.16	42.458	43.629	2.917×10^{-10}	47.012	48.183	2.950×10^{-11}
300	42.199	43.369	3.325×10^{-10}	46.558	47.895	3.410×10^{-11}
400	31.678	32.814	6.738×10^{-8}	35.072	36.208	1.221×10^{-8}
500	25.360	26.477	1.635×10^{-6}	28.075	29.192	4.169×10^{-7}
600	21.145	22.250	1.372×10^{-5}	23.407	24.513	4.393×10^{-6}
700	18.131	19.231	6.266×10^{-5}	20.071	21.171	2.361×10^{-5}
800	15.873	16.961	1.964×10^{-4}	17.570	18.658	8.363×10^{-5}
900	14.117	15.192	4.786×10^{-4}	15.626	16.700	2.240×10^{-4}
1000	12.712	13.784	9.718×10^{-4}	14.069	15.142	4.908×10^{-4}
1200	10.604	11.665	2.823×10^{-3}	11.735	12.796	1.597×10^{-3}
1400	9.0987	10.150	6.051×10^{-3}	10.068	11.119	3.715×10^{-3}
1600	7.9723	9.0107	1.073×10^{-2}	8.8208	9.8592	7.003×10^{-3}
1800	7.0967	8.1323	1.670×10^{-2}	7.8509	8.8865	1.143×10^{-2}
2000	6.3968	7.4142	2.397×10^{-2}	7.0756	8.0930	1.703×10^{-2}

[17] Smith, Tidwell, and Williams, Phys. Rev. **77**, 420 (1950).
[18] A. R. Gordon and C. Barnes, J. Chem. Phys. **1**, 692 (1933).

changes in physical constants and extended to 2000°K; in addition the heat-content function has been evaluated (for use in obtaining the data given in Table V) from 298.16°K to 2000°K; the properties of the normal isotopic mixture of bromine were assumed to be given adequately[12,18] by use of the spectral constants for $Br^{79}Br^{81}$ as recorded by Herzberg.[13]

4. IODINE MONOFLUORIDE

Of the three fluorine-containing diatomic interhalogens there appeared to be no physicochemical evidence for the existence of iodine monofluoride,[19] but the chlorine and bromine monofluorides had been known since their isolation, respectively, by Ruff and Ascher[20] in 1928 and by Ruff and Menzel[21] in 1931; their melting and boiling points had been determined by Ruff and his co-workers to be, respectively, -161 ± 0.5°C and -103 ± 3.0°C for the chlorine compound and approximately -33°C and 20°C for the bromine compound. On this basis one would expect iodine monofluoride, if stable, to be either a solid at room temperature or a liquid of relatively low vapor pressure. Ruff and Braida,[22] on the basis of vapor-pressure measurements of iodine and iodine penta- and heptafluorides, found no evidence for the existence of any lower fluorides of iodine. However, Durie, in a study of flames supported by fluorine,[23] found that methyl iodide, when burned in an atmosphere of fluorine, emitted a strong, banded spectrum which he provisionally attributed to iodine monofluoride; Durie subsequently observed this same emission spectrum when fluorine gas was caused to impinge on the surface of iodine crystals. Durie and Gaydon[15] in a more detailed study of these red-degraded bands (from 4350A to beyond 6900A) concluded, on the basis of the similarity of the rotational structure of the iodine monofluoride spectrum to the $^3\Pi_0{}^+\leftarrow{}^1\Sigma$ system of ICl, that the IF band system arises from corresponding states in the IF molecule; they found the following constants: $\nu_e=19{,}054$ cm^{-1}, $\omega_e''=610$ cm^{-1}, and $\chi_e\omega_e=3$ cm^{-1}; and $\nu_{00}=18{,}995$ cm^{-1}, $\omega_e'=412.5$ cm^{-1}, and $\chi_e\omega_e=3.8$ cm^{-1}. We have evaluated the vibrational contributions to the thermodynamic properties of gaseous IF in the ideal state from these constants. The rotational constants were based on an internuclear distance of 1.906A obtained from the covalent radii of iodine and fluorine, their electronegativities, and the additivity rule for partially ionic covalent radii.[24] The molecular weight was calculated from the data of Mattauch and Fluegge to be 145.949. The heat capacity, entropy, free energy, and heat content for iodine monofluoride calculated from these data are summarized in Table VI. With these data and the dissociation energy of iodine,[13] the dissociation energy of fluorine[1] obtained from its heat of dissociation,[10] the thermodynamic properties of the iodine atom and molecule,[25] and the dissociation energy of IF,[15] we obtained the heats and free energies of dissociation and dissociation constants for the equilibria

$$IF \rightleftharpoons \tfrac{1}{2}I_2+\tfrac{1}{2}F_2$$

and

$$IF \rightleftharpoons I+F.$$

The data of Murphy[25] on the free energy of iodine have been re-evaluated for subsequent changes in the physical constants;[4] use was made also of the more recently reported vibrational and rotational constants for the ground state of iodine obtained with high precision by Rank and Baldwin[26] from Wood's green-line resonance series. In addition, the heat content and free energy of the atom and molecule were calculated to 2000°F for use in evaluating the foregoing equilibria. The numerical results of these calculations (see Table VII) were obtained for dissociation energies of 1.98 ± 0.04 ev and 2.87 ± 0.04 ev corresponding to the two conditions of excitation assumed for the dissociation products obtained from IF. For lack of a chemical heat of formation these data were obtained from a Birge-Sponer extrapolation for the excited state of the IF molecule, and it is not possible to decide definitely between them now. Durie prefers a $D_0{}^0$ of 1.98 ev since the higher value would make IF a more stable molecule than is ClF or BrF; furthermore, he points out that there is a downward progression in force constant in going from ClF to IF, and a regular progression downward in $D_0{}^0$ results only if the dissociation products in all three fluorine-containing interhalogens consist of a

TABLE IV. Heat capacity, entropy, free energy, and heat content of bromine monofluoride.

T °K	$C_p{}^0$ cal mole^{-1} deg^{-1}	S^0 cal mole^{-1} deg^{-1}	$-(F^0-E_0{}^0)/T$ cal mole^{-1} deg^{-1}	$(H^0-E_0{}^0)/T$ cal mole^{-1} deg^{-1}
298.16	7.869	54.703	47.474	7.229
300	7.877	54.712	47.518	7.233
400	8.240	57.072	49.628	7.443
500	8.468	58.937	51.310	7.627
600	8.614	60.494	52.714	7.780
700	8.713	61.830	53.924	7.907
800	8.783	62.998	54.986	8.012
900	8.835	64.036	55.935	8.101
1000	8.876	64.969	56.793	8.176
1200	8.935	66.691	58.295	8.298
1400	8.978	67.974	59.581	8.392
1600	9.012	69.175	60.707	8.468
1800	9.040	70.238	61.708	8.694
2000	9.065	71.192	62.609	8.582

[19] H. S. Booth and J. T. Pinkston, Chem. Rev. **41**, 421 (1947).
[20] O. Ruff and E. Ascher, Z. anorg. u. allgem. Chem. **176**, 258 (1928).
[21] O. Ruff and W. Menzel, Z. anorg. u. allgem. Chem. **202**, 60 (1931); O. Ruff and A. Braida, Z. anorg. u. allgem. Chem. **214**, 81 (1933).
[22] O. Ruff and A. Braida, Z. anorg. u. allgem. Chem. **220**, 43 (1934).
[23] R. A. Durie, Proc. Phys. Soc. (London) **63A**, 1292 (1950).
[24] V. Schomaker and D. P. Stevenson, J. Am. Chem. Soc. **63**, 37 (1941).
[25] G. M. Murphy, J. Chem. Phys. **4**, 344 (1936).
[26] D. H. Rank and W. M. Baldwin, J. Chem. Phys. **19**, 1210 (1951).

TABLE V. Heats, free energies, and equilibrium constants for the dissociation of bromine monofluoride.

			$BrF \rightleftarrows Br + F$			
		$\Delta E_0^0 = 49.799$ kcal	$K = \frac{P_{Br}P_F}{P_{BrF}}$		$\Delta E_0^0 = 59.943$ kcal	$K = \frac{P_{Br}P_F}{P_{BrF}}$
T °K	$\Delta H^0/T$	$\Delta F^0/T$		$\Delta H^0/T$	$\Delta F^0/T$	
298.16	169.98	144.94	2.112×10^{-22}	204.01	178.96	7.749×10^{-40}
300	168.96	143.89	3.568×10^{-22}	202.77	177.71	1.454×10^{-39}
400	127.29	101.57	6.353×10^{-23}	152.65	126.93	1.822×10^{-28}
500	102.22	76.059	2.385×10^{-17}	122.51	96.347	8.783×10^{-22}
600	85.462	58.998	1.277×10^{-13}	102.37	75.904	2.578×10^{-17}
700	73.470	46.774	5.993×10^{-11}	87.962	61.265	4.079×10^{-14}
800	64.463	37.576	6.136×10^{-9}	77.143	50.256	1.039×10^{-11}
900	57.451	30.404	2.266×10^{-7}	68.722	41.675	7.799×10^{-10}
1000	51.838	24.652	4.096×10^{-6}	61.982	34.796	2.486×10^{-8}
1200	43.418	15.992	3.198×10^{-4}	51.871	24.445	4.545×10^{-6}
1400	37.405	9.7760	7.303×10^{-3}	44.650	17.022	1.905×10^{-4}
1600	32.897	5.0874	7.730×10^{-2}	39.237	11.427	3.181×10^{-3}
1800	29.229	1.4239	4.884×10^{-1}	34.864	7.0595	2.865×10^{-2}
2000	26.591	1.5241	2.153	31.663	3.5479	1.677×10^{-1}
			$BrF \rightleftarrows \frac{1}{2}Br_2 + \frac{1}{2}F_2$			
		$\Delta E_0^0 = 9.3834$ kcal	$K = \frac{P^{\frac{1}{2}}_{Br_2}P^{\frac{1}{2}}_{F_2}}{P_{BrF}}$		$\Delta E_0^0 = 19.528$ kcal	$K = \frac{P^{\frac{1}{2}}_{Br_2}P^{\frac{1}{2}}_{F_2}}{P_{BrF}}$
T °K	$\Delta H^0/T$	$\Delta F^0/T$		$\Delta H^0/T$	$\Delta F^0/T$	
298.16	31.679	32.797	6.796×10^{-8}	65.703	66.821	2.491×10^{-15}
300	31.486	32.603	7.494×10^{-8}	65.301	66.418	3.052×10^{-15}
400	23.648	24.725	3.948×10^{-6}	49.009	50.087	1.132×10^{-11}
500	18.933	19.995	4.268×10^{-5}	39.222	40.284	1.571×10^{-9}
600	15.787	16.839	2.089×10^{-4}	32.695	33.746	4.215×10^{-8}
700	13.539	14.570	6.543×10^{-4}	28.031	29.062	4.452×10^{-7}
800	11.852	12.889	1.524×10^{-3}	24.532	25.570	2.581×10^{-6}
900	10.543	11.565	2.968×10^{-3}	21.815	22.837	1.021×10^{-5}
1000	9.4949	10.517	5.031×10^{-3}	19.640	20.661	3.052×10^{-5}
1200	7.9249	8.9333	1.1160×10^{-2}	16.379	17.387	1.585×10^{-4}
1400	6.8054	7.8007	1.973×10^{-2}	14.052	15.047	5.147×10^{-4}
1600	5.9678	6.9486	3.030×10^{-2}	12.308	13.289	1.247×10^{-3}
1800	5.1535	6.2853	4.230×10^{-2}	10.789	11.921	2.481×10^{-3}
2000	4.7998	5.7521	5.532×10^{-2}	9.8720	10.824	4.309×10^{-3}

normal fluorine atom and an excited halogen atom.[15] That this progression may necessarily not be regular, however, can be appreciated by including the new dissociation energy and force constant for the F_2 molecule[1] in this interhalogen series. Need for further thermochemical data on the three fluorine-containing interhalides is clearly indicated.

5. BROMINE MONOCHLORIDE

The light-absorption measurements, by Barratt and Stein[27] and Gillam and Morton,[28] of bromine and chlorine solutions (in carbon tetrachloride) established the existence of bromine monochloride in solution. Subsequent spectroscopic studies of Gray and Style,[29] Jost,[30] Dickinson and Murdock as reported by Beeson and Yost,[31] Vesper and Rollefson,[32] and Brauer and Victor[33] definitely established the existence of BrCl in the gaseous state. Even though these absorption measurements resulted in dissociation constants which varied from 0.10 to 0.22, the spectroscopic studies ended a long-standing dispute over the existence[34–38] or non-

TABLE VI. Heat capacity, entropy, free energy, and heat content of iodine monofluoride.

T °K	C_p^0 cal mole^{-1} deg^{-1}	S^0 cal mole^{-1} deg^{-1}	$-(F^0-E_0^0)/T$ cal mole^{-1} deg^{-1}	$(H^0-E_0^0)/T$ cal mole^{-1} deg^{-1}
298.16	7.996	56.454	49.155	7.293
300	8.004	56.472	49.199	7.297
400	8.344	58.826	51.338	7.520
500	8.549	60.711	53.045	7.707
600	8.678	62.282	54.473	7.859
700	8.765	63.627	55.702	7.983
800	8.828	64.802	56.782	8.085
900	8.874	65.844	57.747	8.170
1000	8.911	66.781	58.621	8.242
1200	8.965	68.411	60.151	8.358
1400	9.006	69.796	61.462	8.448
1600	9.038	71.001	62.611	8.520
1800	9.067	72.071	63.634	8.579
2000	9.092	73.024	64.558	8.629

[27] S. Barratt and C. P. Stein, Proc. Roy. Soc. (London) **122A**, 582 (1929).
[28] A. E. Gillam and R. A. Morton, Proc. Roy. Soc. (London) **124A**, 604 (1929).
[29] L. T. M. Gray and D. W. G. Style, Proc. Roy. Soc. (London) **126A**, 603 (1930).
[30] W. Jost, Z. physik. Chem. **153**, 143 (1931).
[31] C. M. Beeson and D. M. Yost, J. Am. Chem. Soc. **61**, 1432 (1939).
[32] H. G. Vesper and G. K. Rollefson, J. Am. Chem. Soc. **56**, 620 (1934).
[33] G. Brauer and E. Victor, Z. Elektrochem. **41**, 508 (1935).
[34] M. Balard, Ann. chim. et phys. **32** (2), 337 (1826).
[35] C. F. Schönbein, J. prakt. Chem. **88** (1), 483 (1863).
[36] W. Bornemann, Ann. 189, 183 (1877).
[37] V. Thomas and P. Dupois, Compt. rend. **143**, 282 (1906).
[38] L. W. Andrews and H. A. Carlton, J. Am. Chem. Soc. **29**, 688 (1907).

UNIVERSITY OF MICHIGAN LIBRARIES

TABLE VII. Heats, free energies, and equilibrium constants for the dissociation of iodine monofluoride.

			$IF \rightleftharpoons I + F$			
	$\Delta E_0^0 = 45.649$ kcal			$\Delta E_0^0 = 66.168$ kcal		
T °K	$\Delta H^0/T$	$\Delta F^0/T$	$K = \frac{P_I P_F}{P_{IF}}$	$\Delta H^0/T$	$\Delta F^0/T$	$K = \frac{P_I P_F}{P_{IF}}$
298.16	156.00	131.32	1.999×10^{-29}	224.82	200.14	1.822×10^{-44}
300	155.06	130.36	3.235×10^{-29}	223.46	198.76	3.646×10^{-44}
400	116.84	91.519	9.970×10^{-21}	168.14	142.82	6.132×10^{-32}
500	93.839	68.115	1.299×10^{-15}	134.88	109.15	1.396×10^{-24}
600	78.466	52.462	3.425×10^{-12}	112.66	86.660	1.150×10^{-19}
700	67.462	41.246	9.679×10^{-10}	96.775	70.559	3.798×10^{-16}
800	59.195	32.807	6.763×10^{-8}	84.843	58.456	1.677×10^{-13}
900	52.754	26.229	1.852×10^{-6}	75.553	49.028	1.928×10^{-11}
1000	47.596	20.956	2.631×10^{-5}	68.115	41.475	8.625×10^{-10}
1200	39.848	13.023	1.425×10^{-3}	56.947	30.122	2.612×10^{-7}
1400	34.304	7.3354	2.494×10^{-2}	48.960	21.992	1.562×10^{-5}
1600	30.141	3.0536	2.151×10^{-1}	42.965	15.878	3.388×10^{-4}
1800	26.902	−0.2845	1.154	38.302	11.115	3.723×10^{-3}
2000	24.312	−2.9645	4.445	34.572	7.2950	2.545×10^{-2}
			$IF \rightleftharpoons \frac{1}{2}I_2 + \frac{1}{2}F_2$			
	$\Delta E_0^0 = 10.182$ kcal			$\Delta E_0^0 = 30.701$ kcal		
T °K	$\Delta H^0/T$	$\Delta F^0/T$	$K = \frac{P^{\frac{1}{2}}_{I_2} P^{\frac{1}{2}}_{F_2}}{P_{IF}}$	$\Delta H^0/T$	$\Delta F^0/T$	$K = \frac{P^{\frac{1}{2}}_{I_2} P^{\frac{1}{2}}_{F_2}}{P_{IF}}$
298.16	34.451	35.494	1.749×10^{-8}	103.27	104.31	1.594×10^{-23}
300	34.241	35.283	1.946×10^{-8}	102.64	103.68	2.194×10^{-23}
400	25.704	26.726	1.442×10^{-6}	77.002	78.024	8.873×10^{-18}
500	20.570	21.593	1.909×10^{-5}	61.608	62.631	2.052×10^{-14}
600	17.146	18.174	1.067×10^{-4}	51.344	52.372	3.583×10^{-12}
700	14.700	15.745	3.623×10^{-4}	44.012	45.058	1.422×10^{-10}
800	12.864	13.901	9.161×10^{-4}	38.513	39.550	2.272×10^{-9}
900	11.441	12.474	1.879×10^{-3}	34.240	35.273	1.955×10^{-8}
1000	10.302	11.343	3.319×10^{-3}	30.821	31.862	1.088×10^{-7}
1200	8.5957	9.6424	7.811×10^{-3}	25.695	26.742	1.431×10^{-6}
1400	7.3795	8.4294	1.438×10^{-2}	22.036	23.086	9.008×10^{-6}
1600	6.4696	7.5207	2.272×10^{-2}	19.294	20.345	3.578×10^{-5}
1800	5.7636	6.8188	3.234×10^{-2}	17.163	18.218	1.043×10^{-4}
2000	5.2007	6.2636	4.277×10^{-2}	15.460	16.523	2.449×10^{-4}

existence[39–41] of this diatomic halide. Blair and Yost[42] subsequently determined calorimetrically the heats of solution of bromine in carbon tetrachloride and of formation of BrCl (in CCl_4); making use of the heat of solution of chlorine in carbon tetrachloride derived from the temperature coefficient of solubility of Cl_2 in CCl_4,[43] they determined the heat of formation of BrCl(g) from gaseous bromine and chlorine to be 300 cal mole^{-1} and the standard entropy to be 57.1 cal mole^{-1} deg^{-1}; this latter value was based on a standard free energy of formation of BrCl(g) obtained from light-absorption measurements[44] and from dissociation measurements by Brass[45] on nitrosyl chloride and by Yost[45] on phosgene. Jellinek and Schutza[46] and Schutza[47] subsequently measured the dissociation of mixtures of molten potassium, silver, lead, and other halide pairs and obtained values of K for the reaction

$$2BrCl \rightleftharpoons Br_2 + Cl_2$$

in the range for 500°C to 800°C, which showed no consistent trend with temperature. Beeson and Yost,[31] from equilibrium measurements on the gaseous system

TABLE VIII. Heat capacity, entropy, free energy, and heat content of bromine monochloride.

T °K	C_p^0 cal mole^{-1} deg^{-1}	S^0 cal mole^{-1} deg^{-1}	$-(F^0-E_0^0)/T$ cal mole^{-1} deg^{-1}	$(H^0-E_0^0)/T$ cal mole^{-1} deg^{-1}
298.16	8.384	57.339	49.783	7.556
300	8.390	57.390	49.829	7.558
400	8.625	59.840	52.039	7.801
500	8.754	61.779	53.800	7.980
600	8.833	63.383	55.267	8.116
700	8.886	64.749	56.527	8.222
800	8.925	65.938	57.630	8.308
900	8.955	66.991	58.612	8.378
1000	8.979	67.936	59.499	8.437
1200	9.018	69.577	61.051	8.531
1400	9.050	70.969	62.366	8.603
1600	9.077	72.179	63.519	8.660
1800	9.103	73.250	64.542	8.708
2000	9.126	74.210	65.461	8.749

[39] M. Berthelot, Compt. rend. **94**, 1619 (1882).
[40] P. Lebeau, Compt. rend. **143**, 589 (1906).
[41] B. J. Karsten, Z. anorg. u. allgem. Chem. **53**, 365 (1907).
[42] C. M. Blair and D. M. Yost, J. Am. Chem. Soc. **55**, 4489 (1933).
[43] N. W. Taylor and J. H. Hildebrand, J. Am. Chem. Soc. **45**, 682 (1923).
[44] P. G. Murdoch, *The Dissociation Constant for Bromine Chloride at Room Temperature* (thesis, Part II), California Institute of Technology, Pasadena, California, 1932.
[45] P. D. Brass, *The Dissociation of Nitrosyl Chloride* (thesis, Part III), California Institute of Technology, Pasadena, California, 1932.
[46] K. Jellinek and H. Schutza, Z. anorg. u. allgem. Chem. **227**, 52 (1936).
[47] H. Schutza, Z. anorg. u. allgem. Chem. **239**, 245 (1938).

TABLE IX. Heats, free energies, and equilibrium constants for the dissociation of bromine monochloride.

	$BrCl \rightleftarrows Br + Cl$			$BrCl \rightleftarrows \frac{1}{2}Br_2 + \frac{1}{2}Cl_2$		
T °K	$\Delta H^0/T$	$\Delta F^0/T$	$K=\frac{P_{Br}P_{Cl}}{P_{BrCl}}$	$\Delta H^0/T$	$\Delta F^0/T$	$K=\frac{P^{\frac{1}{2}}_{Br_2}P^{\frac{1}{2}}_{Cl_2}}{P_{BrCl}}$
298.16	175.12	151.16	9.142×10^{-34}	0.80286	2.1578	0.3376
300	174.06	150.09	1.580×10^{-33}	0.80122	2.1527	0.3385
400	130.98	106.51	5.278×10^{-24}	0.59370	1.9542	0.3740
500	105.12	80.273	2.860×10^{-18}	0.47205	1.8356	0.3971
600	87.869	62.728	1.954×10^{-14}	0.39203	1.7574	0.4130
700	75.539	50.158	1.092×10^{-11}	0.33376	1.6913	0.4270
800	66.286	40.702	1.272×10^{-9}	0.29405	1.6590	0.4340
900	59.085	33.328	5.203×10^{-8}	0.26214	1.6244	0.4416
1000	53.321	27.412	2.777×10^{-6}	0.23675	1.6002	0.4470
1200	44.673	18.507	9.023×10^{-5}	0.19967	1.5653	0.4549
1400	38.495	12.104	2.263×10^{-3}	0.17303	1.5319	0.4626
1600	33.862	7.3397	2.488×10^{-2}	0.15498	1.5096	0.4678
1800	30.258	3.5080	1.711×10^{-1}	0.14109	1.5000	0.4701
2000	27.373	0.4741	7.878×10^{-1}	0.12995	1.4781	0.4753

NO, Br_2, Cl_2, NOBr, NOCl, and BrCl in the range from 372°K to 492°K, obtained a mean K of 0.148 (for a temperature of 462°K). These data, when combined with those of Vesper and Rollefson[32] and with available spectroscopic data, yielded a heat-content change for the reaction

$$\tfrac{1}{2}Br_2(g)+\tfrac{1}{2}Cl_2 \rightleftarrows BrCl(g)$$

of -233 cal as the most acceptable value. This value, in view of the experimental uncertainties, was assumed for the value of ΔE_0^0 in the present calculations in preference to the value of 750 ± 500 cal mole^{-1} of Jost[30] used by Butkow,[48] who has calculated the free energies and equilibrium constants for BrCl and its dissociation reactions to molecular and atomic bromine and chlorine. In addition to these properties we have also obtained the heat capacity, entropy, and heat content as a function of temperature. For these calculations ω was taken to be 430 cm^{-1},[13] and the anharmonicity constant was found, by interpolation from smooth curves obtained by plotting the available constants for the ten halogens and interhalogens as a function of reduced mass, to be 1.68_4 cm^{-1} from which a value of ω_e of 433.4 cm^{-1} was obtained for use in obtaining the high temperature corrections.[2] The molecular constants for the four isotopic species of BrCl were calculated from these values (Table I) and from an internuclear separation which was estimated to be 2.11A. The heat contents and free energies of bromine and chlorine needed for the evaluation of the results reported in Tables VIII and IX were obtained as described in the discussions of ClF and BrF. Calculations at the extreme limits of temperature were made to show that the errors in these data resulting from neglect of the relative abundances of the four species of BrCl were smaller than the uncertainties resulting from the several assumptions involved in obtaining working constants for this interhalide. At 298.16°K and 2000°K, respectively, the heat capacities for $Br^{79}Cl^{35}$ were calculated to be 8.378 and 9.126 cal mole^{-1} deg^{-1}, and for $Br^{81}Cl^{37}$, 8.392 and 9.128 cal mole^{-1} deg^{-1}.

[48] K. Butkow, Rec. trav. chim. **67**, 551 (1948).

6. IODINE MONOCHLORIDE

Iodine monochloride is a liquid up to 97.4°C and exhibits polymorphism; the dark-red, alpha form melts at 27.2°C, and the brown-red form melts at 13.92°C. The existence of ICl was established from phase studies of iodine-chlorine mixtures by Stortenbeker in 1889.[49] The entropy of ICl at 298.16°K was calculated by Brown and reported by McMorris and Yost,[50] whereas McMorris and Yost determined the free energy, heat content, and entropy experimentally from measurements of the decomposition pressures of barium chloroplatinate and nitrosyl chloride in the presence of gaseous iodine. The dissociation at 25°C and 100°C were found to be 0.42 percent and 1.58 percent, respectively. An experimental entropy at 298.16°K of 59.6 eu was determined from these data. Blair and Yost[42] subsequently determined the entropy of ICl(g) to be 59.2 eu from

TABLE X. Heat capacity, entropy, free energy, and heat content of iodine monochloride.

T °K	C_p^0 cal mole^{-1} deg^{-1}	S^0 cal mole^{-1} deg^{-1}	$-(F^0-E_0^0)/T$ cal mole^{-1} deg^{-1}	$(H^0-E_0^0)/T$ cal mole^{-1} deg^{-1}
298.16	8.492	59.123	51.468	7.655
300	8.497	59.175	51.514	7.661
400	8.697	61.650	53.753	7.898
500	8.805	63.604	55.535	8.069
600	8.871	65.216	57.018	8.198
700	8.917	66.587	58.289	8.297
800	8.950	67.780	59.403	8.377
900	8.977	68.835	60.393	8.442
1000	8.999	69.782	61.286	8.497
1200	9.035	71.426	62.843	8.584
1400	9.065	72.821	64.168	8.650
1600	9.092	74.033	65.330	8.704
1800	9.118	75.106	66.357	8.748
2000	9.141	76.068	67.281	8.787

[49] W. Stortenbeker, Z. physik. Chem. **3**, 11 (1889); Rec. trav. chim. Pays-Bas **7**, 152 (1889).

[50] J. McMorris and D. M. Yost, J. Am. Chem. Soc. **54**, 2247 (1932).

TABLE XI. Heats, free energies, and equilibrium constants for the dissociation of iodine monochloride.

	$ICl \rightleftharpoons I + Cl$			$ICl \rightleftharpoons \frac{1}{2}I_2 + \frac{1}{2}Cl_2$		
T °K	$\Delta H^0/T$	$\Delta F^0/T$	$K=\frac{P_I P_{Cl}}{P_{ICl}}$	$\Delta H^0/T$	$\Delta F^0/T$	$K=\frac{P^{\frac{1}{2}}_{I_2} P^{\frac{1}{2}}_{Cl_2}}{P_{ICl}}$
298.16	168.74	145.19	1.854×10^{-32}	11.186	12.507	1.848×10^{-3}
300	167.72	144.16	3.123×10^{-32}	11.117	12.437	1.914×10^{-3}
400	126.20	102.17	4.695×10^{-23}	8.3304	9.6598	7.743×10^{-3}
500	101.29	76.889	1.571×10^{-17}	6.6597	7.9943	1.790×10^{-2}
600	84.668	59.983	7.779×10^{-13}	5.5475	6.8845	3.129×10^{-2}
700	72.788	47.870	3.453×10^{-11}	4.7524	6.1070	4.627×10^{-2}
800	63.870	38.760	3.381×10^{-9}	4.1601	5.4978	6.288×10^{-2}
900	56.926	31.654	1.208×10^{-7}	3.6987	5.0353	7.935×10^{-2}
1000	51.415	25.954	2.127×10^{-6}	3.3799	4.6657	9.558×10^{-2}
1200	43.010	17.373	1.596×10^{-4}	2.7779	4.1104	1.264×10^{-1}
1400	37.030	11.213	3.544×10^{-3}	2.3839	3.7101	1.546×10^{-1}
1600	32.539	6.5780	3.651×10^{-2}	2.0904	3.4049	1.803×10^{-1}
1800	29.042	2.955	2.261×10^{-1}	1.8625	3.1893	2.009×10^{-1}
2000	26.244	0.04420	9.780×10^{-1}	1.6803	3.0005	2.209×10^{-1}

studies of the carbon tetrachloride solutions of the halogens and interhalogens. An experimental heat capacity of gaseous ICl of 8.27 cal mole^{-1} deg^{-1} was reported by Strecker[51] as a mean value for the range of 100°C to 203°C, whereas we have calculated a value of 8.75 cal mole^{-1} deg^{-1} in this range. Theoretical heat capacities, entropies, free energies, and heat contents for gaseous iodine monochloride were calculated from the spectral constants reviewed and summarized by Herzberg;[13] the results of these data are summarized in Table X. The thermodynamic properties of the dissociation reactions to iodine and chlorine molecules and atoms (Table XI) were calculated from the free energies and heat contents of chlorine and iodine used in the foregoing sections on ClF and IF.

7. IODINE MONOBROMIDE

Iodine monobromide was apparently first prepared by Balard in 1826; this interhalide melts at 42°C and is a liquid at atmospheric pressure[52] up to 116°C.

TABLE XII. Heat capacity, entropy, free energy, and heat content of iodine monobromide.

T °K	C_p^0 cal mole^{-1} deg^{-1}	S^0 cal mole^{-1} deg^{-1}	$-(F^0-E_0^0)/T$ cal mole^{-1} deg^{-1}	$(H^0-E_0^0)/T$ cal mole^{-1} deg^{-1}
298.16	8.721	61.752	53.809	7.943
300	8.724	61.805	53.857	7.948
400	8.841	64.334	56.175	8.158
500	8.904	66.313	58.012	8.302
600	8.944	67.940	59.535	8.406
700	8.973	69.322	60.837	8.485
800	8.996	70.521	61.974	8.547
900	9.015	71.581	62.983	8.598
1000	9.032	72.532	63.892	8.641
1200	9.062	74.183	65.474	8.708
1400	9.090	75.581	66.820	8.761
1600	9.116	76.800	67.993	8.804
1800	9.140	77.871	69.032	8.840
2000	9.165	78.836	69.965	8.871

[51] K. Strecker, Ann. Physik u. Chem. **17**, 85 (1882).
[52] P. C. E. M. Terwogt, Z. anorg. u. allgem. Chem. **47**, 203 (1905).

Müller[53] and Bodenstein and Schmidt,[54] respectively, determined equilibrium constants for the reaction

$$\tfrac{1}{2}I_2(g)+\tfrac{1}{2}Br_2(g)=IBr(g)$$

to be 0.114 at 304.8°C and 0.305 at 1222°C. McMorris and Yost[55] obtained the thermodynamic constants of iodine monobromide experimentally from determinations of the equilibrium compositions of the gas phase existing over solid copper bromide in the presence of iodine vapor from which an entropy of IBr(g) of 60.6 eu resulted. Blair and Yost[42] in their studies of equilibria in solution in CCl_4 obtained an entropy of 62.0 cal mole^{-1} deg^{-1} for IBr(g); the free energy of formation of IBr (in CCl_4) and IBr(g) had been determined by Yost, Anderson, and Skoog[56] to be -1746 cal mole^{-1} and -1790 cal mole^{-1}, respectively. Kelley[57] calculated standard entropies for IBr(g) and IBr(s) of 61.8 and 33.0±1.4 cal mole^{-1} deg^{-1}, respectively, from spectroscopic data. For the present calculations of the thermodynamic properties of gaseous iodine monobromide from spectroscopic data, values of ω_e and $\chi_e\omega_e$ of 268.4 and 0.78 cm^{-1} were taken from Herzberg.[13] The rotational constants were estimated from an internuclear distance of 2.434A obtained from the covalent radii of iodine and bromine.[24] The results of these calculations are summarized in Table XII for the species $I^{127}Br^{79}$. The influence of the presence of the $I^{127}Br^{81}$ isotopic species on these properties was shown to be smaller than the probable error introduced by the methods employed to estimate the unknown spectroscopic constants. In the heat capacity at 2000°K, the difference in the numerical values for the heat

[53] W. Müller, Z. physik. Chem. **123**, 1 (1926).
[54] M. Bodenstein and A. Schmidt, Z. physik. Chem. **123**, 28 (1926).
[55] J. McMorris and D. M. Yost, J. Am. Chem. Soc. **53**, 2625 (1931).
[56] Yost, Anderson, and Skoog, J. Am. Chem. Soc. **55**, 552 (1933).
[57] K. K. Kelley, U. S. Department of Interior, Bureau of Mines Bulletin No. 434 (1940).

TABLE XIII. Heats, free energies, and equilibrium constants for the dissociation of iodine monobromide.

	$IBr \rightleftharpoons I + Br$			$IBr \rightleftharpoons \frac{1}{2}I_2 + \frac{1}{2}Br_2$		
T °K	$\Delta H^0/T$	$\Delta F^0/T$	$K = \frac{P_I P_{Br}}{P_{IBr}}$	$\Delta H^0/T$	$\Delta F^0/T$	$K = \frac{P^{\frac{1}{2}}_{I_2} P^{\frac{1}{2}}_{Br_2}}{P_{IBr}}$
298.16	142.49	119.22	8.795×10^{-27}	5.673	5.9719	4.953×10^{-2}
300	141.62	118.35	6.365×10^{-26}	5.649	5.9428	5.026×10^{-2}
400	106.51	82.901	7.623×10^{-19}	4.684	4.7753	9.044×10^{-2}
500	85.416	61.573	3.495×10^{-14}	4.121	4.0749	1.287×10^{-1}
600	71.350	47.321	4.550×10^{-11}	3.752	3.6079	1.627×10^{-1}
700	61.299	37.117	7.729×10^{-9}	3.492	3.2744	1.925×10^{-1}
800	53.761	29.447	3.669×10^{-7}	3.299	3.0243	2.183×10^{-1}
900	47.900	23.466	7.438×10^{-6}	3.150	2.8280	2.410×10^{-1}
1000	43.213	18.671	8.308×10^{-5}	3.031	2.6739	2.604×10^{-1}
1200	36.190	11.452	3.142×10^{-3}	2.855	2.4402	2.929×10^{-1}
1400	31.185	6.269	4.265×10^{-2}	2.730	2.2732	3.186×10^{-1}
1600	27.439	2.3608	3.048×10^{-1}	2.637	2.1464	3.396×10^{-1}
1800	24.533	−0.69630	1.420	2.565	2.0500	3.564×10^{-1}
2000	22.213	−3.1576	4.899	2.508	1.9764	3.699×10^{-1}

capacities of the two species is less than 0.000 cal mole^{-1} deg^{-1}. At 298.16°K the difference in the heat capacities is less than 0.003 cal mole^{-1} deg^{-1}. The entropies and free energies of the higher isotopic species are 0.073 cal mole^{-1} deg^{-1} higher than those of the $I^{127}Br^{79}$ species.

The heats and free energies of dissociation and dissociation constants for the reactions

$$IBr(g) \rightleftharpoons I + Br$$

and

$$IBr(g) \rightleftharpoons \tfrac{1}{2}I_2 + \tfrac{1}{2}Br_2,$$

calculated from a dissociation energy of iodine monobromide of 1.817 ev and from the reported dissociation energies[13] of $I_2(g)$ and $Br_2(g)$, are summarized in Table XIII.

8. CONCLUSIONS

The thermodynamic properties (heat capacity, entropy, free energy, and heat content) have been calculated for the six diatomic interhalogens as a function of temperature from 298.16°K to 2000°K. The standard entropies of ClF, BrF, IF, BrCl, ICl, and IBr were calculated at a pressure of 1 atmosphere for the ideal gaseous state to be 52.080, 54.703, 56.454, 57.339, 59.123, and 61.752 cal mole^{-1} deg^{-1}, respectively. Previously published data in the literature included the heat capacity, entropy, and free energy of ClF and the free energy of BrCl as a function of temperature. These data were revised for subsequent changes in spectral constants and/or were extended to include values for all four thermodynamic properties to 2000°K. From these data the thermodynamic constants of the twelve dissociation reactions of the diatomic interhalogens were calculated as a function of temperature.

Spectroscopic Studies in the Near Ultraviolet of the Three Isomeric Dimethylbenzene Vapors. III. Fluorescence of *Meta*-Dimethylbenzene*

V. Ramakrishna Rao† and Mantrala L. N. Sastri‡
Department of Physics, Duke University, Durham, North Carolina
(Received June 3, 1952)

The fluorescence spectrum of *meta*-xylene has been obtained in low dispersion using Fe spark lines and a mercury arc lamp for excitation. About 26 bands were measured. They are discussed in their relation to the corresponding absorption spectrum.

INTRODUCTION

In part II[1] of this series the absorption spectra of *ortho*- and *meta*-xylene in the near ultraviolet were discussed and analyzed. Marsh[2] has reported on the fluorescence of *ortho*-xylene vapor in this region; and corresponding emission bands had been obtained in a Tesla discharge through *meta*-xylene vapor by McVicker, Marsh, and Stewart.[3] The present paper supplements these studies by adding information on the fluorescence spectrum of *meta*-xylene.

EXPERIMENTAL DETAILS

The *meta*-xylene used in this research came from the same sample used previously in the absorption experiments (II). It was purchased from the National Bureau of Standards and had a 0.17 ± 0.07 mole percent impurity. The fluorescence cell, the procedure of filling it with the substance, and the optical arrangements used have been described in earlier publications.[4,5] The fluorescence of *meta*-xylene was photographed with a Bausch and Lomb medium quartz spectrograph using slit widths of 30 to 50μ. Vapor pressures ranged from 1.7 to 4.5 mm Hg. Excitation was from a Fe spark and an Hg arc lamp. With Eastman II-0 plates, exposures of about 48 hours were found necessary. A microscope of low magnification was used to measure the bands. Because they are diffuse, with no clearly discernible edges, setting was made at the centers of the bands.

EXPERIMENTAL RESULTS

About 26 bands, distributed over a number of groups, were obtained in the region 2700 to 2860A. On account of their diffuseness, which also characterizes the absorption bands,[1] measurements may be in error by 5 and more cm^{-1}; therefore the frequencies are given to the nearest 5 cm^{-1} only. The region in the neighborhood of the 0—0 band, from 2705 to 2758A, is weaker than the succeeding bands at longer wavelengths. This may be explained by reabsorption of the radiation by the vapor in the fluorescence cell. The band at the shortest wavelength which corresponds to the 0—0 band does not coincide exactly with the center chosen by Cooper for the 0—0 band. Since most of the other band centers are close to values measured by Cooper, the separations of the bands from the 0—0 band in the fluorescence spectrum differ slightly from the corresponding values

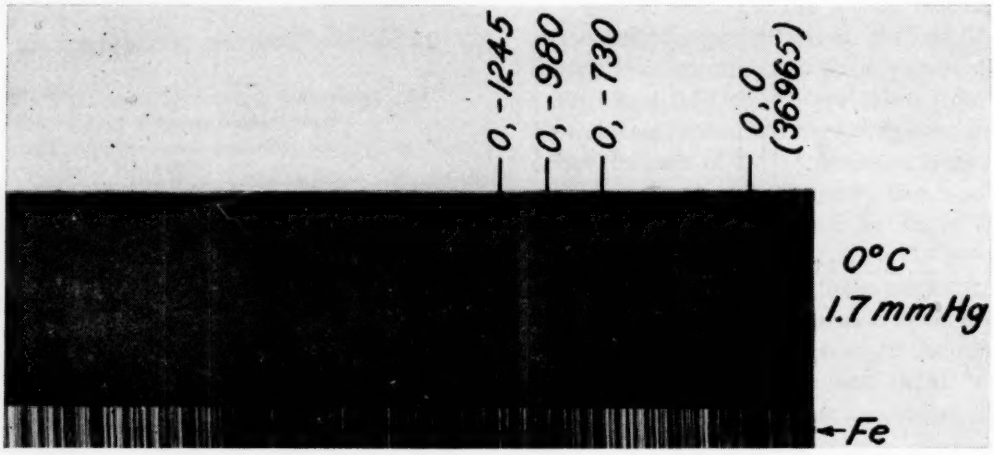

FIG. 1. Fluorescence bands of *meta*-xylene excited by Fe spark.

* This work was supported by the ONR under contract N6ori107, T.O.I., with Duke University.
† Present address: Physics Department, Andhra University, Waltair, India.
‡ Present address: Division of Optics, National Physical Laboratory, New Delhi, India.
[1] C. D. Cooper and H. Sponer, J. Chem. Phys. **20**, 1248 (1952).
[2] J. K. Marsh, J. Chem. Soc. **123**, 3315 (1923); Phil. Mag. **49**, 971 (1925).
[3] McVicker, Marsh, and Stewart, J. Chem. Soc. **125**, 1743 (1924).
[4] A. M. Bass and H. Sponer, J. Opt. Soc. Am. **40**, 389 (1950).
[5] Mantrala L. N. Sastri and H. Sponer, J. Chem. Phys. **20**, 1428 (1952).

in the absorption spectrum. Excitation occurred into the 0−0 band and a few higher absorption bands, but unfortunately the exciting lines were rather weak. The measured fluorescence bands and their assignments are collected in Table I. The intensities are recorded in terms of the scale given in II. There is indication of a few more very faint bands towards longer wavelengths, but they were too diffuse to be measured.

DISCUSSION AND ANALYSIS

The fluorescence bands reported here form the counterpart of the near ultraviolet absorption bands. They result from an allowed transition $^1A_1-{}^1B_1$ if symmetry C_{2v} is assumed for the *meta*-xylene molecule in first approximation. In the region from the 0−0 band

TABLE I. Fluorescence bands of *meta*-xylene.

Wave number cm^{-1}	Intensity	Separation from 0−0 band cm^{-1}	Assignment
36965	*m*	0	0−0
895	*mw*	− 70	0−70
810	*w*	− 155	0−160
790	*w*	− 175	0−160
715	*w*	− 250	0−175−70, 0−250
660	*w*	− 305	0−175−2×70, 0−250−70
635	*ew*	− 330	0−2×160
570	*ew*	− 395	0−2×160−70
450	*w*	− 515	0−515
390	*w*	− 575	0−515−70
320	*vw*	− 645	0−515−2×70
235	*ms*	− 730	0−730
170	*mw*	− 795	0−730−70
105	*vw*	− 860	0−730−160
35985	*m*	− 980	0−980
910	*mw*	−1055	0−980−70
855	*vw*	−1110	0−980−160
720	*mw*	−1265	0−1245
645	*vw*	−1320	0−1245−70
520	*vw*	−1445	0−2×730
465	*ew*	−1500	0−2×730−160
365	*ew*	−1600	0−2×730−160
260 to 115	*w*	−1700	0−980−730 unresolved with faint indication of band 0−980−730−70
35000	*vw*	−1965	0−2×980, 0−1245−730
34930	*ew*	−2035	0−2×980−70

36965 to 35520 absorption and fluorescence bands overlap, and it therefore offers a good check on the analysis presented in II. The groups in this region occur at intervals of 515, 730, 980, 1245, 2×730 cm^{-1} from the 0−0 band. These values check well with those reported in absorption. The 730 and 980 groups are of similar intensity, though the 730 group seems a little stronger. In absorption the group associated with the upper state vibration corresponding to 730 in the ground state is weaker than the group representing the upper state value of 980 cm^{-1}, whereas for the corresponding absorption bands which represent these vibrations in the lower state, the intensity ratio is reversed. This is mainly due to the difference in the respective Boltzmann factors, but the fluorescence results indicate that the transition probabilities for these bands lie in the same order.

TABLE II. Some fundamental frequencies (in cm^{-1}) of *meta*-xylene as obtained from Raman, Tesla luminescence, near ultraviolet absorption and fluorescence spectra.

Raman	Tesla	Fluorescence	Absorption Lower	Absorption Upper
515 (4)	510	515	510	470
536 (8)				
724 (12)	725	730	725	675
999 (14)	995	980	995	965
1249 (5)	1245	1245	1245	1145
1264 (3)				
1375 (6)				1250

The vibrations connected with the wave numbers 730 and 980 occur twice excited and combined in weak fluorescence bands at longer wavelengths. In absorption only the 965 which is the upper state value of the 995 (980 in fluorescence) was found to form definitely a progression. It has been assigned to the totally symmetric carbon "breathing" vibration. Regarding the 730 cm^{-1} separation, there are different opinions in the literature on its assignment to a vibrational mode. They have been mentioned in II and will not be repeated here. The weak band at 515 cm^{-1} from the 0−0 band is associated here, as was done in II, with the β_1 component resulting from the splitting of the $606\epsilon_g{}^+$ benzene vibration in *meta*-xylene.

The 1245, which corresponds to the Raman line at 1249 cm^{-1}, was correlated with the upper state vibration of 1145 cm^{-1} in part II of this series. The assignment of these frequencies to a symmetric carbon or to the $C-CH_3$ valence vibration was left open. The fluorescence results do not contribute additional arguments in favor of one or the other assignment.

The frequency difference of 70 cm^{-1} corresponds to the 65 cm^{-1} reported in absorption and discussed in II. It is connected with a 1−1 transition of a very low vibration. Actually the 65 was obtained in absorption as an average value of five close-lying headless and diffuse bands. Another frequency difference of 160 cm^{-1} was determined in the same fashion, as were the 0−0 band and many of the main bands. The relatively large slit widths used in fluorescence and the fairly small dispersion of the spectrograph did not permit resolution of the broad diffuse bands into subbands as was possible in the absorption work. This accounts for some differences in the numerical values between absorption and fluorescence data. In general, spectral data obtained from the absorption measurements are to be considered more reliable than those from the fluorescence work. Nevertheless, it is not impossible that a faintly indicated splitting of the 160 frequency difference into a 155 and a 175 difference is real.

Table II gives a collection of some fundamental vibrations in *meta*-xylene obtained from various sources.

The authors wish to express their thanks to Dr. H. Sponer for much helpful guidance in the investigation. One of us (V. R. Rao) is grateful to the U. S. Educational Foundation in India for the award of the Fulbright travel grant.

Theoretical Considerations Concerning Hammett's Equation. III. σ-Values for Pyridine and Other Aza-Substituted Hydrocarbons

H. H. JAFFÉ
Venereal Disease Experimental Laboratory, U. S. Public Health Service, School of Public Health, University of North Carolina, Chapel Hill, North Carolina

(Received April 25, 1952)

Electron distributions in pyridine, pyrimidine, quinoline, isoquinoline, acridine, phenazine, and phenanthridine have been calculated by the LCAO MO method, and used to calculate Hammett's σ-values for the different positions in these compounds. The values are compared with the experimental values available for pyridine, quinoline, and isoquinoline, and satisfactory agreement is obtained. Formulas are given for the calculation of σ-values of similar compounds.

IN previous papers from this Laboratory it has been shown that Hammett's substituent constants (σ)* can be correlated with electron densities calculated by molecular orbital (MO) theory.[1] Elderfield and Siegel have recently reported σ-values for all positions in quinoline.[2] σ-values for all three positions of pyridine and one position each in quinoline and isoquinoline can be derived from experimental data in the literature.[3] It seemed of interest to compare these experimental quantities with σ-values calculated theoretically, particularly since only one parameter need be adjusted empirically for the calculation of all the constants.[4]

TABLE I. Comparison of calculated and observed σ-values.

Position[a]	σ_{calc}	σ_{exp}
	1. Pyridine	
2[b]	0.46	0.81[c]; 0.40[d]
3	0.35	0.62[c]
4	1.07	0.93[c]
	2. Quinoline	
2[b]	0.88	0.74[e]; 0.92[c]
3	0.53	0.52[e]; 0.64[c]
4[f]	1.40	0.59[e]; 0.76[c]
5[f]	0.31	0.37[e]
6	0.23	0.23[e]
7	0.45	0.24[e]
8[f]	−0.20	−0.06[e]; −0.11[g]
	3. Isoquinoline	
1[b,f]	0.76	0.70[e]

[a] All compounds are numbered in accordance with A. M. Patterson and L. T. Capell, *The Ring Index* (Reinhold Publishing Corporation, New York, 1940).
[b] These positions are vicinal to the nitrogen atom.
[c] From reference 3a.
[d] From reference 3b.
[e] From reference 2.
[f] These positions are *ortho* to the fused ring system.
[g] From reference 3c.

CALCULATIONS

Electron densities were calculated by standard MO LCAO theory, using the perturbation method of Coulson and Longuet-Higgins.[5] Mutual atom polarizabilities for benzene, naphthalene, anthracene, and phenanthrene, were taken from papers by Coulson and Longuet-Higgins.[5b,6] No assumptions concerning the resonance integrals of the carbon-nitrogen bonds were necessary, since the reference compounds to which the perturbations were applied (benzene, naphthalene, anthracene, and phenanthrene) are alternant hydrocarbons.[7] In such compounds all atom-bond polarizabilities vanish, and the electron densities do not depend on the resonance integrals.[5b,6]

Our calculations differed from those of Longuet-Higgins and Coulson[5] only in the treatment of the inductive effect. In previous work[1] we have justified the introduction of an inductive effect of much larger magnitude than has been used in earlier calculations. Accordingly, we have here treated the inductive effect in the same manner as in our previous papers,[1] i.e., by assigning the Coulomb integrals of the carbon atoms increments (α_n) given by

$$\alpha_n = \epsilon^n \alpha_N, \tag{1}$$

where n is the number of bonds intervening between atom n and the nitrogen atom of Coulomb integral α_N. The constant ϵ has been assigned a value of $\frac{1}{2}$†; the older treatment of the inductive effect has consisted of assigning ϵ a value of $\frac{1}{8}$ and neglecting powers of ϵ higher than the first.

The correlation of electron densities and σ-values has been made on the basis of the assumption that electron density increments induced by a substituent in a given position are proportional to the corresponding σ-values.

* L. P. Hammett, *Physical Organic Chemistry* (McGraw-Hill Book Company, Inc., New York, 1940), Chapter VII.

[1] H. H. Jaffé, J. Chem. Phys. **20**, 279, 778 (1952).

[2] R. C. Elderfield and M. Siegel, J. Am. Chem. Soc. **73**, 5622 (1951).

[3] (a) K. Kindler, Ber. deut. chem. Ges. **69B**, 2792 (1936); (b) C. Walling *et al.*, J. Am. Chem. Soc. **70**, 1537, 1543 (1948); (c) Näsänen, Lumme, and Mukula, Acta Chem. Scand. **5**, 1199 (1951); C. M. Judson and M. Kilpatrick, J. Am. Chem. Soc. **71**, 3110 (1949).

[4] It has previously been pointed out by Elderfield and Siegel (see reference 2) that the rates of the alkaline hydrolysis of the methyl esters of the quinoline carboxylic acids can be roughly correlated with the electron densities calculated by Longuet-Higgins and Coulson (see reference 6).

[5] C. A. Coulson and H. C. Longuet-Higgins, Proc. Roy. Soc. (London), (a) **A191**, 39 (1947); (b) **A192**, 16 (1948).

[6] H. C. Longuet-Higgins and C. A. Coulson, J. Chem. Soc. 971 (1949).

[7] Alternant hydrocarbons are defined as compounds containing no odd-membered rings.

† Equation (1) and the value assigned to ϵ are discussed in detail in reference 1.

The proportionality factor was found to be $\kappa=-15.5$.[1] Accordingly, the σ-values are calculated by the formula

$$\sigma_r=\kappa(q_r-1)=\alpha_N\kappa\sum_s \pi_{r,s}\epsilon^{n_s}. \quad (2)$$

The second equality in Eq. (2) follows from Eq. (2) of the paper by Longuet-Higgins and Coulson.[6]

Thus, the σ-values are expressed in terms of a single parameter, the Coulomb integral of the nitrogen atom (α_N). This parameter was assumed to be identical in all the compounds under consideration; its value was adjusted to give the best correlation of calculated and experimental σ-values. The value thus obtained was $\alpha_N=0.59$‡ in good agreement with a value $\alpha_N=0.6$ derived by Löwdin in calculation of dipole moments.[8]

DISCUSSION

The calculated and experimental σ-values reported in Table I show reasonable agreement with the exception of the values for 4-position of quinoline. This discrepancy finds no ready explanation. It is doubtful that the experimental value could be seriously in error, since fair agreement exists between the σ-value reported by Elderfield and Siegel[2] and that obtained from Kindler's data.[3a] Except for the value for the 4-position of quinoline the calculated and experimental values agree as well or better than duplicate experimental values. This satisfactory agreement may be taken as further evidence for the validity of the hypothesis of the proportionality of electron density increments and σ-values.[9]

No experimental data seem to be available to permit evaluation of substituent constants for other aza-substituted analogs of benzene, naphthalene, anthracene, and phenanthrene. Table II lists the calculated σ-values for pyrimidine, isoquinoline, acridine, phenanthridine and phenazine. These compounds were chosen among the large number of aza-derivatives of the hydrocarbons named as the ones of most importance, and therefore these σ-values were thought to be the most likely to be useful and to find experimental confirmation. Nevertheless, the mutual atom polarizabilities[5b,6] together with Eq. (2) would permit easy calculation of σ-values for further compounds should they become of interest.

‡ In accordance with customary practice in LCAO calculations the Coulomb integrals of the carbon atoms were set equal to zero, thus defining the origin of the energy scale. The resonance integral of the ring carbon-carbon bond (β) was taken as the unit of energy, and all Coulomb integrals are expressed in this unit.

[8] P.-O. Löwdin, J. Chem. Phys. **19**, 1323 (1951).

[9] See reference 1.

TABLE II. Predicted σ-values. (All footnotes refer to footnotes under Table I.)

Position[a]	Pyrimidine	Isoquinoline	Acridine	Phenanthridine	Phenazine
1		0.76[b,f]	0.47[f]	0.16[f]	0.03[f]
2	0.60[b]		0.06	0.28	0.73
3		−0.02[b]	0.64	0.26	
4	1.26[b]	0.47[f]	−0.43[f]	−0.12[f]	
5	0.71	0.07[f]			
6		0.38		1.25[f]	
7		0.23		0.34	
8		0.21		0 12	
9			2.08[f]	0.45	
10				0.05[f]	

Equation (2) can also be used for the calculation of σ-values in other heterocyclic compounds, if the Coulomb integral of the heteroatom is known.

Hammett has shown that a necessary condition for the validity of his equation is that the entropies of activation (when dealing with rate constants) or the entropy changes in the reactions (when dealing with equilibrium constants) are constant in a series of reactions.* Since this condition is not fulfilled by *ortho* substituted compounds Hammett's equation is applicable only to *meta* and *para* substituents. Elderfield and Siegel have pointed out that several positions (4, 6, 8) in quinoline are *ortho* to some part of the fused ring system.[2] They have proceeded on the assumption that the entropy changes in each series of reactions are nevertheless constant, so that Hammett's equation can be applied. Throughout this paper we have implied the same assumption in calculating σ-values. However, the experimental σ-values derived for the 2-position of pyridine from two different reactions[3a,b] do not agree. This fact suggests that Hammett's equation may not be applicable to reactions at side chains vicinal to an aza-nitrogen, which have a formal relation to reactions of *ortho* substituted benzenes. These arguments shed some doubt on the validity of some of the σ-values reported in Tables I and II. Nevertheless, the agreement obtained between the calculated and observed values in Table I suggests that, for the other compounds also, calculated values may be a good approximation to actual σ-values, at least for some reactions, such as the alkaline hydrolyses of the methyl and ethyl esters of the corresponding carboxylic acids.

ACKNOWLEDGMENTS

The author is indebted to Dr. R. L. McKee for several interesting discussions.

Reactions of Methane with Iodine Activated by Radiative Neutron Capture

J. F. Hornig, G. Levey, and J. E. Willard
Department of Chemistry, University of Wisconsin, Madison, Wisconsin
(Received February 1, 1952)

About 50 percent of the I^{128} atoms formed by the $I^{127}(n, \gamma)I^{128}$ reaction in gaseous mixtures of 0.2 mm of iodine and 400 mm of methane enter combination as methyl iodide, whereas much less than 1 percent of iodine atoms produced simultaneously by the photochemical dissociation of the iodine do so. By contrast, about 1 percent of the I^{128} formed by the $I^{127}(n, \gamma)I^{128}$ reaction in gaseous mixtures of iodine and ethyl iodide enters organic combination.

The solubility of iodine in pure liquid methane is less than 10^{-10} m/1 but as much as 3×10^{-5} m/1 may be dissolved when air has been allowed to condense in the methane. In such solutions I^{128} from the $I^{127}(n, \gamma)I^{128}$ reaction is able to enter organic combination as methyl iodide, ethyl iodide, and higher boiling material.

INTRODUCTION

It has been observed by Reid,[1] Friedman and Libby,[2] and more recently in our laboratory,[3,4] that iodine activated by the $I^{127}(n, \gamma)I^{128}$ reaction is able to enter organic combination by reaction with hydrocarbons. This type of reaction is significant because it establishes the fact that an energetic heavy atom can cause the rupture of bonds in a molecule containing only light weight atoms. Such rupture must result from the inelastic transfer of energy to molecules rather than from a billiard ball type of transfer between atoms of approximately equal weight.

As a further step in laying the experimental basis for an understanding of such processes we have investigated the chemical consequences of the $I^{127}(n, \gamma)I^{128}$ reaction in methane. Methane molecules are unique in their low molecular weight and in the fact that they contain only carbon-hydrogen bonds.

In accordance with our expectation, some organic combination occurred in the liquid phase, where the close packing of the molecules favors[4,5] their fragmentation by the energetic iodine atoms. Contrary to all predictions a high organic yield was obtained in the gas phase. This was the case even under conditions which precluded significant combination of the I^{128} with impurities or radiation-produced radicals. The result is unique among studies of gas phase reactions activated by nuclear processes.

EXPERIMENTAL

Gaseous Reaction Mixtures

Known amounts of gaseous iodine (*ca* 0.2 mm) and methane (*ca* 400 mm) were metered into quartz flasks (125 ml and 250 ml) on a vacuum system. In some cases iodine tagged with I^{131} was used in order to determine how much iodine entered organic combination by processes other than those due directly to the $I^{127}(n, \gamma)I^{128}$ reaction. Since methane has an appreciable vapor pressure at liquid air temperatures, a few mm pressure of nitrogen or helium was admitted to the flask just before sealing it in order to flush the methane vapor out of the neck and thus minimize the danger of pyrolysis. Prior to admitting the reactants the evacuated quartz flasks were flamed to red heat with continued pumping.

Purity of Reagents

In order to determine whether the Matheson Chemical Company 99.0 percent pure grade methane contained impurities which would react readily with iodine atoms, a flask containing 400 mm of CH_4 and 0.2 mm of I_2 tagged with I^{131} was irradiated for 60 minutes with a 1000-watt projection lamp under conditions such as to dissociate each iodine molecule about 200 times. Fifteen percent of the I^{131} entered organic combination. Only 0.5 percent of the iodine became organically bound in a similar experiment where the methane was first forced through a sintered glass disk into a 15-inch tower of concentrated sulfuric acid. Methane with and without the sulfuric acid pretreatment and also Phillips Petroleum Company Research grade methane was used in the gas phase neutron irradiations reported. The organic yields of I^{128} with the three types of reagent were indistinguishable. All liquid phase runs were made with the Matheson methane condensed directly from the tank.

Liquid Reaction Mixtures

Liquid methane (mp$-184°$, bp$-162°$) was prepared from methane gas by passing it under atmospheric pressure into a large test tube cooled with liquid nitrogen. Powdered iodine was added to the liquid and stirred periodically for thirty minutes or so, following which the solution was decanted through a Whatman No. 40 filter into a precooled unsilvered soft glass dewar, which was used as the irradiation vessel. Liquid methane which did not contain iodine was added to the filtered solution to make it unsaturated.

[1] A. F. Reid, Phys. Rev. **69**, 530 (1946).
[2] L. Friedman and W. F. Libby, J. Chem. Phys. **17**, 647 (1949).
[3] Goldhaber, Chiang, and Willard, J. Am. Chem. Soc. **73**, 2271 (1951).
[4] S. Goldhaber and J. E. Willard, J. Am. Chem. Soc. **74**, 318 (1952).
[5] G. Levey and J. E. Willard, J. Am. Chem. Soc. (to be published).

Solubility of Iodine in Methane

In an experiment in which air-free liquid methane was placed in contact with finely divided iodine tagged with I^{131} (8 day), the amount of iodine dissolved was found to be less than 6×10^{-9} m/1. In another experiment utilizing inactive iodine, the filtered solution was irradiated for 30 minutes at a flux of 2×10^{11} neutrons cm^{-2} sec^{-1}. Following irradiation the methane was allowed to evaporate in the presence of carrier iodine which was then counted. Negligible I^{128} activity was found, from which it was calculated that the solubility of iodine in liquid methane is less than 10^{-10} m/1. Similar results were always obtained when the liquid methane was protected from contact with air by allowing it to boil continually.

In contrast to these results, solubilities as high as 3×10^{-5} m/1 were obtained when the methane was allowed to stand at temperatures below its boiling point in the presence of air while being saturated with the solid iodine. It was observed that the volume of such methane solutions increased under these conditions. It must be concluded that the vapor pressure of oxygen or nitrogen or both from their moderately concentrated solutions in liquid methane is less than the corresponding atmospheric pressure and that iodine is much more soluble in solutions of these gases in liquid methane than in pure liquid methane.

Neutron Irradiations

All neutron irradiations were made in the thermal column of the CP-3′ pile at the Argonne National Laboratory.[6] The samples were placed at positions of known neutron flux and were exposed for thirty minutes. In cases where it was desired to illuminate a flask during neutron exposure it was mounted about three inches from a G.E. RSP2 reflector photospot lamp and the whole assembly was inserted in the pile with the lamp turned on.

Extraction and Counting of Products

The irradiated flasks of gaseous reaction mixtures were broken at the neck after cooling at the bottom with liquid nitrogen to freeze out the contents. Organic carriers and aqueous sulfite were then added and shaken vigorously, after which they were separated and counted in solution-type Geiger counters. The organic fraction was always given a second sulfite wash before counting. Additional washes did not decrease the organic activity. In several experiments the walls of the quartz reaction flasks were subsequently washed with hot caustic solution which was then counted. The activity obtained in this way was always negligible. The organic yield was calculated as the ratio of the counting rate of the organic phase to the sum of the rates of the organic and inorganic phases after suitable corrections had been made for aliquot sizes, densities of the solutions counted, relative counting efficiency of different counter tubes, and radioactive decay.

In the case of the liquid phase runs the irradiated methane solutions were poured onto a mixture of solid ethyl or methyl iodide and iodine, cooled in liquid nitrogen. The cooling agent was removed, the methane was boiled away slowly, the carriers were washed twice with aqueous sulfite solution, and the organic yield was determined as in the gas phase runs.

In some cases the activity left on the walls of the Dewar used for the liquid phase irradiations was determined by washing with an organic solvent. When this wash was extracted it was found to contain both organic and inorganic activity. An aqueous wash of the Dewar could not be used satisfactorily because of the high level of Na^{24} (15 hr) activity leached from the glass.[7]

Characterization of Products

In the experiments designed to determine the chemical nature of the organic products containing I^{128} the organic carriers added after neutron irradiation of the methane and iodine were usually CH_3I and C_2H_5I; CH_2I_2, which is relatively high boiling and easily separated from the others, was sometimes included. The extracted carriers were distilled through a 12-in. Vigreux column. The refractive index of each $CH_3I-C_2H_5I$ fraction was used to indicate its composition, and the counting rates of all such fractions were plotted against mole fraction. From the intercept of this line at 100 percent mole fraction of each component it was possible to estimate the relative amount of I^{128} in each of the two components. It has previously[5,8] been established that iodine does not exchange with alkyl iodides appreciably during the type of extraction process used in this work and that the alkyl iodide carriers do not exchange iodine with each other.

In those experiments where I^{131} tracer was used, all samples were counted immediately after extraction to obtain the sum of the I^{128} (25 min) and I^{131} (8 day) activities, and again after all I^{128} had decayed to determine the I^{131} alone.

Determination of Gamma-Flux

The flux of gamma-radiation as a function of position in the thermal column was determined from the thermoluminescence of cadmium-wrapped lithium fluoride crystals exposed at several positions in the column.[9]

[6] The pile and space for processing the samples were made available as part of the Participating Institution Program of the Laboratory. We should like to express our especial appreciation to Dr. S. Wexler and Dr. W. H. McCorkle for their cooperation in arranging for these experiments.

[7] A. O. Long and J. E. Willard, Ind. and Eng. Chem. **44**, 916 (1952).

[8] L. H. Gevantman and R. R. Williams, Jr., Ph.D. thesis of L. H. Gevantman, University of Notre Dame (1951).

[9] These samples were kindly supplied and analyzed by Dr. D. Saunders and F. Morehead working on an AEC project under the supervision of Professor Farrington Daniels.

TABLE I. Reaction of gaseous methane with I^{128} activated by the $I^{127}(n, \gamma)I^{128}$ reaction.

Methane used	n flux, cm^{-2} sec^{-1}	Gamma-intensity, r/hr	Photospot	Organic yield, % Total	As CH_3I
a	10^9	1.7×10^4	no	51	
a	10^9	1.7×10^4	no	34	
a	10^9	1.7×10^4	no	55	
b	10^9	1.7×10^4	no	47	47
b	10^{10}	5.2×10^4	no	51	51
c	2×10^{11}	3.7×10^5	yes	49	49
c	10^9	1.7×10^4	yes	43	43

[a] Matheson Company CP methane.
[b] Matheson Company CP methane further purified by dispersing it with a sintered glass disk at the bottom of a column of conc. sulfuric acid and allowing it to rise through 15 in. of the liquid.
[c] Phillips Petroleum Company "research grade" methane.

RESULTS

Organic Yield in Gaseous Methane

The first gas phase irradiations were designed as control experiments for the liquid phase tests because both past experiments on other systems[10] and theoretical considerations indicated that little or no hot atom reaction should occur between gaseous iodine and methane. Therefore, when high organic yields were observed, they were ascribed to impurities or radiation effects. In order to test this interpretation new experiments were conducted with more highly purified methane, with the elemental iodine tagged with I^{131} (8 day) and with the reaction flask illuminated with a photospot lamp during the neutron irradiation which produced the I^{128} (25 min). The illumination was sufficient to dissociate every iodine molecule in the system some 300 times[11] during the neutron irradiation. The rate of production of iodine atoms by the visible light was 10^{11} times as great as the rate of production of I^{128} atoms by the $I^{127}(n, \gamma)I^{128}$ reaction at a neutron flux of 2×10^{11} neutrons cm^{-2} sec^{-1}. It was at least 10^4 times as fast[12] as the production of organic radicals by the gamma-radiation of 3.7×10^5 r/hr which prevailed at this neutron flux. Under these conditions the reaction system contained at all times a high concentration of photochemically produced iodine atoms relative to the I^{128} atoms. Therefore, any reaction of iodine atoms with impurities or with radicals produced by gamma-radiation, would have led to a higher[13] percentage of organically bound I^{131} than I^{128}. On the other hand, a hot atom reaction of I^{128} with methane would lead to methyl iodide tagged with I^{128} but not with I^{131}. Table I shows that in the experiments where the photospot lamp was used during neutron irradiation 49 and 43 percent of the I^{128} were found as methyl iodide. None of the I^{131} entered organic combination in any of the gas experiments.

The neutron fluxes for the two experiments with the photospot lamp differed from each other by a factor of two hundred and the gamma-fluxes by a factor of twenty. The results, in addition to being similar to each other, were similar to those of the five other experiments made with two different sources of methane and without illumination. The I^{128} which did not form CH_3I in the experiments of Table I was in water extractable form; none (i.e., less than 1 percent) was found in higher boiling organic compounds.

Organic Yield of Gaseous Ethyl Iodide

In view of the high organic yield from gaseous iodine in methane, found in the experiments of Table I, similar experiments should be done with other gaseous species. Data which we have obtained on ethyl iodide are of interest in this connection. Eight 25-ml quartz flasks of the gas at 80-mm pressure were irradiated for 30 minutes each, four at a neutron flux of 10^7 cm^{-2} sec^{-1} and a gamma-flux of 3.1×10^3 r/hr and four at a neutron flux of 10^9 cm^{-2} sec^{-1} and a gamma-flux of 1.7×10^4 r/hr. Two samples at each neutron flux contained pure ethyl iodide and two contained 0.2 mm pressure of iodine in addition. The samples without added iodine gave organic yields of 5.5 and 2.9 percent at a neutron flux of 10^7 and 2.0 and 6.8 percent at 10^9. Those with added iodine gave yields of 1.2, 1.3, 1.1, and 1.4 percent.

These results show that organic radicals produced by gamma-radiation in such a system do not lead to a high organic yield. The rather consistent values obtained in the presence of iodine scavenger may represent a true hot atom reaction. They are similar to yields obtained for C_2H_5Br in the presence of HBr scavenger.[10c] The higher and more variable results in the absence of scavenger must be due to a competition between radicals, iodine atoms, impurities, and the walls for thermalized I^{128} atoms.

Liquid Phase Runs

Seven successful neutron irradiations of solutions of iodine and methane were made, two were at a neutron

[10] See, for example: (a) E. G. Bohlmann and J. E. Willard, J. Am. Chem. Soc. **64**, 1342 (1942); (b) W. F. Libby, J. Am. Chem. Soc. **69**, 2523 (1947); (c) R. R. Williams and W. H. Hamill, J. Chem. Phys. **18**, 783 (1950).

[11] For the purpose of this estimate approximate values of the necessary data were taken as follows: (a) 5 percent of the light from the reflector-type photospot lamp fell on the 250-cc reaction flask which was placed at a distance of about 3 inches from it. (b) 5 percent of the input energy of the lamp appeared in the emitted radiation in the wavelength range between 4500 and 6000A [General Electric Review **42**, 540 (1939)]. (c) The average absorption coefficient of gaseous iodine in the 4500–6000A region is 400 [Rabinowitch and Wood, Trans. Faraday Soc. **32**, 540 (1936)].

[12] This rate of production of organic radicals may be estimated to be no more than 5×10^{14} per min from the fact that 1 percent of the I^{131} was found in organic combination. This method of estimation assumes that every organic radical reacts with elemental iodine to form an alkyl iodide. Estimates based on the assumption that 83 ergs are dissipated per gram of matter per roentgen and that one radical is produced per 32 ev of this energy also give very low values for the ratio of radicals produced by gamma-radiation to the iodine atoms produced by light. The largest contribution to the gamma-effect is from photoelectrons originating in the flask walls.

[13] The percentage of I^{131} would be higher than that of I^{128}, rather than equal to it, because all of the I^{131} was present in the reaction vessel throughout the irradiation whereas the I^{128} was formed during the irradiation.

flux of 4×10^{10} cm^{-2} sec^{-1} and a gamma-flux of 2×10^5 r/hr and five at a neutron flux of 2×10^{11} cm^{-2} sec^{-1} and a gamma-flux of 3.7×10^5 r/hr. All irradiations were for thirty minutes. In each run the disintegration rate of organically bound I^{128} at the end of bombardment was 50,000 dis/min or more. The organic yields obtained were 11, 0.25, 30, 13, 20, 59, and 70 percent. Of the 59 percent organic yield, 42 percent was in the form of CH_3I, 9 percent C_2H_5I, and 8 percent some higher boiling compound or compounds. About half of the 70 percent yield was due to CH_3I and half to C_2H_5I. The organic yields reported for liquid methane were all obtained with solutions which contained dissolved nitrogen or oxygen or both from the air, since, as described above, it was impossible to obtain detectable amounts of dissolved iodine activity otherwise.

The fact that I^{128} entered organic combination and that it did so as both methyl iodide and ethyl iodide is significant. The variation in organic yield and in distribution of products is not significant or surprising, when it is remembered that (1) varying amounts of inorganic and organic activity which may have remained on the walls of the irradiation vessel were not included in the analysis; (2) a speck of iodine which escaped removal by the filter when the solution was prepared might raise the inorganic activity greatly; (3) the solutions contained appreciable but different amounts of dissolved oxygen or nitrogen or both.

DISCUSSION

The results reported above show conclusively that approximately 50 percent of the I^{128} atoms formed by the (n, γ) process in gaseous mixtures of iodine (0.2 mm) and methane (400 mm) react to form methyl iodide. The possibility that the observed reaction was due to reactive species formed by the gamma-radiation in the system or to impurities is precluded by the following facts. (1) The organic yield of I^{128} was not altered by the presence in the reaction system of photochemically produced iodine atoms at a concentration 10^{11} times greater than that of the I^{128}. (2) A negligible fraction (<1 percent) of the photochemically produced atoms entered organic combination. (3) All of the organically bound I^{128} was found in the form of methyl iodide. (Methyl iodide could not be formed from any impurity. Likewise it is not the sole product to be expected if the reaction were induced by the ionizing radiation in the system. Gevantman and Williams[8] have shown that the reaction of methane with iodine induced by x-rays or electrons produces a ratio of about 20 percent methylene iodide and 5 percent ethyl iodide to 75 percent methyl iodide.)

It must be concluded, therefore, that I^{128} produced by the $I^{127}(n, \gamma)I^{128}$ process in gaseous methane has the ability to undergo a reaction of the type $I+CH_4\rightarrow CH_3I+H$. This unique reactivity must be due to either the kinetic energy of recoil of the I^{128} or the positive charge acquired as a result of internal conversion[14] accompanying the radiative capture process, or electronic excitation remaining after charge neutralization. Both the reaction $I+CH_4\rightarrow CH_3I+H$ and the reaction $I^+ + CH_4\rightarrow CH_3I+H^+$ are endothermic, the first by some 50 kcal/mole and the second by some 100 kcal/mole.

In seeking a satisfactory concept of how the methyl iodide is produced it is helpful to consider the various possible stages in the life history of an I^{128} atom. Such an atom is usually born with several thousand kcal/mole of kinetic energy as a result of recoil from the gamma-rays emitted in the (n, γ) process. It loses this energy by collisions with methane molecules, the mole ratio of CH_4 to I_2 in the systems studied being 2000. The ratio of the mass of the iodine atom to that of the methane molecule is such that the maximum fraction of the energy which can be lost in a collision is 40 percent. If the average fraction of the energy lost per collision is 20 percent and the initial energy is 200 ev it will require about 20 collisions on the average to reduce the energy to 2 ev and 40 to reduce it to 0.02 ev. Although each I^{128} undergoes some 20 collisions with methane with kinetic energy in excess of the endothermicity of the reaction which would form methyl iodide, it is unlikely for a stable product to result from these collisions for the following reasons. The maximum fraction of the kinetic energy which can go into *internal energy* of the activated complex, and hence be available for breaking the carbon-hydrogen bond, is equal to the ratio of the mass of a methane molecule to the sum of the masses of an iodine atom and a methane molecule, or 0.1. This follows from the requirement of conservation of momentum. Hence, if the 50 kcal/mole needed for reaction is to be available as internal energy of the activated complex, then the kinetic energy of the complex and that of the methyl iodide formed must be about 450 kcal/mole. It is unlikely that the C—I bond in such a molecule would survive the several collisions with other molecules necessary to reduce the methyl iodide to thermal energies.

Because the above reasoning makes it seem improbable that the methyl iodide is formed as a result of the high kinetic energy of the I^{128} atoms it appears likely that reaction results directly or indirectly from the charge.[14] It is not known whether the internal conversion step which produces the charge occurs before or after the kinetic energy of the atom has been lost by collisions (*ca* 10^{-10} sec), but this information is not important for the present purpose. The iodine atom can undergo many collisions with methane molecules without losing its last positive charge since the ionization

[14] It has been observed that 45 percent of the I^{128} recoils from ethyl iodide irradiated at very low pressures are positively charged. S. Wexler and H. Daves, private communication.

potential[15] of methane is 14.4 ev while that of a gaseous iodine atom is 10.6. Eventually the positively charged I^{128} may be expected to undergo a process of the type: (1) $I_2+I^{128+}\rightarrow I_2^{+}+I^{128}$, or (2) $I_2+I^{128+}\rightarrow II^{128+}+I$, since the ionization potential of the iodine molecule is less than that of the atom, i.e., 10.1 volts. On the basis of these considerations, various hypothetical reactions can be suggested to account for the formation of CH_3I^{128}, but as yet, none can be assigned with certainty. They include $I^{128}+CH_4\rightarrow CH_3I^{128}+H$, in which the I^{128} has electronic excitation energy following reaction (1) above, and $II^{128+}+CH_4\rightarrow CH_3I^{128}+HI^{+}$.

It is noteworthy that the high organic yield of the reaction of iodine with methane reported here is unique among studies of reactions activated by radiative neutron capture in the gas phase. Such specificity of molecules for energy transfer has been observed frequently, however, in the quenching of the resonance radiation of cadmium, mercury, and sodium, where wide variations in the effective quenching cross sections of different molecules are observed.[16] In the case of cadmium there is evidence that part of the quenching molecule can combine with the quenched atom, CdH being formed when Cd is quenched with H_2.

In order to investigate further the nature of reactions of the type described in this paper it will be important to observe reactions of bromine with methane when the bromine is activated by the isomeric transition and by neutron capture; reactions of iodine with methane containing added xenon and other additives of different atomic mass, ionization potential, and chemical properties; and reactions of iodine and bromine with other molecules such as ethane.

ACKNOWLEDGMENT

This work was supported in part by the Atomic Energy Commission and in part by the University Research Committee with funds made available by the Wisconsin Alumni Research Foundation.

[15] The ionization potential values used are those given in International Critical Tables.

[16] See, for example: H. C. Lipson and A. C. G. Mitchell, Phys. Rev. **48**, 625 (1935).

THE JOURNAL OF CHEMICAL PHYSICS VOLUME 20, NUMBER 10 OCTOBER, 1952

The Third Virial Coefficient in Polymer Solutions*

WALTER H. STOCKMAYER AND EDWARD F. CASASSA
Department of Chemistry, Massachusetts Institute of Technology, Cambridge, Massachusetts

(Received April 21, 1952)

With the aid of approximate models for the intermolecular potential energy, the third virial coefficient Γ_3 in the virial expansion for the osmotic pressure of a dilute polymer solution has been determined as a function of the second coefficient and one additional parameter obtainable from intrinsic viscosity or light scattering measurements. The theory and experimental results agree in indicating that the ratio Γ_3/Γ_2^2 for most solutions is markedly less than the value of $\frac{5}{8}$ given by the hard sphere molecular model proposed by others for the estimation of Γ_3. The limitations are discussed under which light scattering may be used for evaluation of the virial coefficients.

INTRODUCTION

IT has been recognized for some years that the osmotic pressure π of a high polymer solution may be expressed as a virial expansion in the weight concentration c. In terms of the ratio π/c,

$$\pi/c=(RT/M)[1+\Gamma_2 c+\Gamma_3 c^2+\cdots]. \quad (1)$$

Evaluation of the quantities of interest, the number average molecular weight M and the second virial coefficient Γ_2 requires an extrapolation of experimental data to infinite dilution. Since most measurements are made in fairly dilute solutions, none of the terms beyond the quadratic in Eq. (1) need ordinarily be considered.

To increase the accuracy of the extrapolation procedure it would be desirable to have a relation between Γ_2 and the third coefficient Γ_3. Flory and Krigbaum[1,2] have developed a statistical theory for the second coefficient in solutions of flexible long chain molecules, which can in principle be extended to evaluation of the third; however, the necessary integrations could probably be performed only by laborious numerical methods. Instead, they have assumed, as an approximation, that Γ_2 bears the same relation to Γ_3 as in the case of hard sphere molecules; i.e.,

$$\Gamma_3=\tfrac{5}{8}\Gamma_2^2. \quad (2)$$

Actually, the value of Γ_3/Γ_2^2 is quite sensitive to the nature of the intermolecular potential energy. For "soft" molecules, this ratio is always smaller than $\frac{5}{8}$ and is in general a function of the temperature as well as of

* This work was supported in part by a du Pont Grant-in-Aid of fundamental research.

[1] P. J. Flory, J. Chem. Phys. **17**, 1347 (1949).

[2] P. J. Flory and W. R. Krigbaum, J. Chem. Phys. **18**, 1086 (1950).

parameters characterizing the potential energy of interaction.

The purpose of the present paper is the description of a method, based on a molecular model more realistic than the hard sphere, for calculating the third virial coefficient in terms of the second and of one other quantity obtainable from experiment. The results are then compared with experimental observations.

APPROXIMATE EVALUATION OF THE THIRD VIRIAL COEFFICIENT

To obtain definite results we must assume that the interaction between any pair of polymer molecules in solution separated by a distance r between the centers of mass can be described adequately by a spherically symmetrical mean potential of average force $u(r)$ which is unaffected by the presence of other solute molecules. The osmotic virial coefficients are then given by expressions familiar from the statistical theory of imperfect monatomic gases:[3,4]

$$\Gamma_2 M = 2\pi N_0 \int_0^\infty h(r) r^2 dr, \tag{3}$$

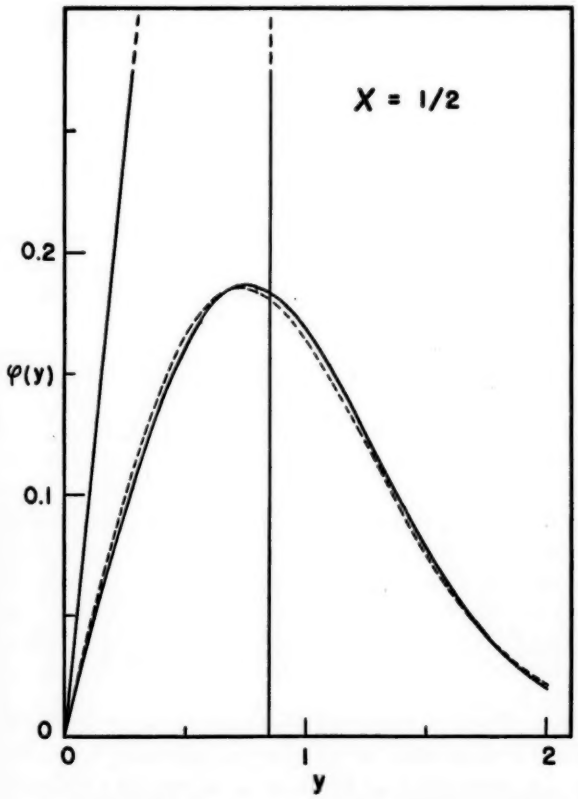

FIG. 1. Plots of $\varphi(y)$ *vs.* y (with $X=\frac{1}{2}$) for different molecular interaction models all giving the same second virial coefficient. Straight line segments, hard sphere; solid curve, Flory-Krigbaum function $\varphi_1(y)$; dashed curve, our function $\varphi_2(y)$ with $A=0.72$.

[3] See, for example, J. E. Mayer and M. G. Mayer, *Statistical Mechanics* (John Wiley and Sons, Inc., New York, 1940), Chapter XIII.

[4] Bird, Spotz, and Hirschfelder, J. Chem. Phys. 18, 1395 (1950).

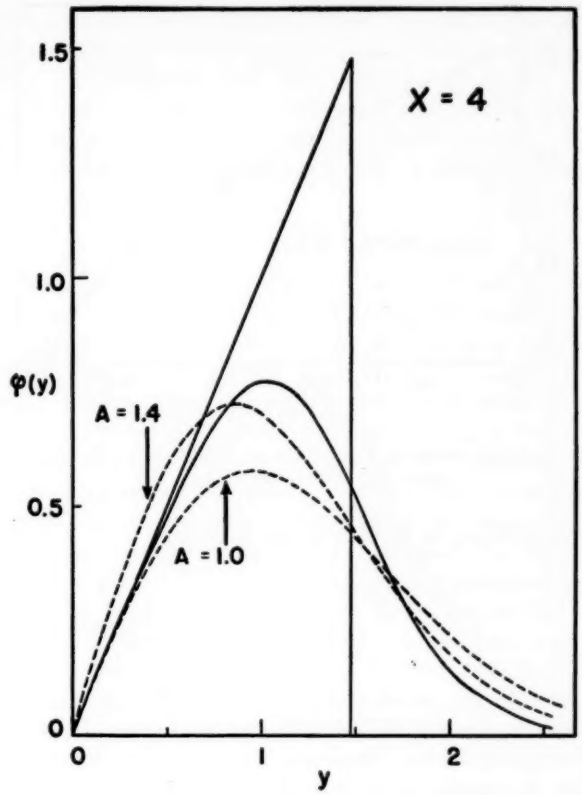

FIG. 2. Plots of $\varphi(y)$ *vs.* y for $X=4$. Triangular figure, hard sphere model; solid curve, $\varphi_1(y)$; dashed curves, $\varphi_2(y)$ for $A=1.0$ and 1.4.

$$\Gamma_3 M^2 = (8\pi^2 N_0^2/3) \times \int\int\int h(r_{12})h(r_{23})h(r_{13}) r_{12} r_{23} r_{13} dr_{12} dr_{23} dr_{13}, \tag{4}$$

where M is the polymer molecular weight, N_0 is Avogadro's number, and

$$h(r) = 1 - \exp(-u(r)/kT). \tag{5}$$

The integration in Eq. (4) extends over all values of the intermolecular distances r_{12}, r_{23}, r_{13} forming a triangle. The approximations inherent in these equations are treated at greater length in the appendix.

The theory of Flory and Krigbaum leads to the function

$$h_1(r) = 1 - \exp[-X \exp(-b^2 r^2)], \tag{6}$$

and the second virial coefficient

$$\Gamma_2 = \pi^{\frac{3}{2}} N_0 X F(X)/2Mb^3. \tag{7}$$

The parameters X and b depend upon temperature, the chemical nature of polymer and solvent, and, it is important to note, upon the molecular weight of the polymer. The function $F(X)$ is a definite integral the evaluation of which is discussed in reference (2).

Since the third virial coefficient is not easily obtained from $h_1(r)$, we have considered another function

$$h_2(r) = A \exp(-\beta^2 r^2), \tag{8}$$

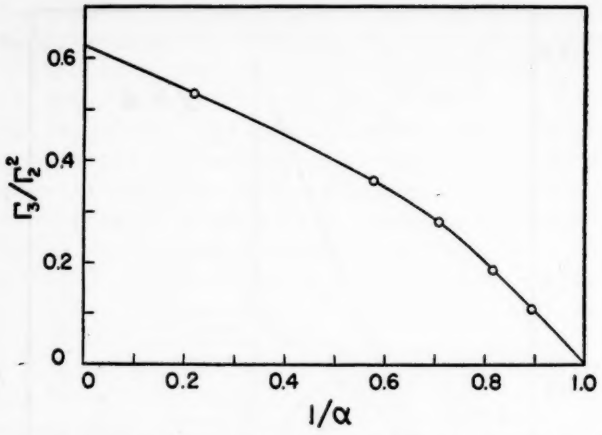

FIG. 3. Graph showing dependence of Γ_3/Γ_2^2 on α. The plotted points are derived from Table I.

corresponding to an interaction potential[5]

$$u(r)=-kT\ln[1-A\exp(-\beta^2r^2)]$$
$$=kT\sum_{n=1}^{\infty}A^n\exp(-n\beta^2r^2)/n. \quad (9)$$

If X in Eq. (6) is sufficiently small, $h_1(r)$ and $h_2(r)$ can be made, by proper choice of A and β, to resemble each other quite closely. Moreover, it is even possible[6] that $h_2(r)$ is superior to $h_1(r)$ on physical grounds although we do not make this claim. For our function, the second virial coefficient is

$$\Gamma_2=\pi^{\frac{3}{2}}N_0A/2M\beta^3, \quad (10)$$

and the third can be evaluated analytically from Eq. (4) by the method of Bird, Spotz, and Hirschfelder.[4] The result of this calculation may be expressed in the form

$$\Gamma_3/\Gamma_2^2=4A/3^{5/2}=0.257A, \quad (11)$$

in which it may be seen that $A\leq 1$, if the physical sense of the model (cf. the logarithmic form of Eq. (9)) is to be preserved.

If it is assumed that the Flory-Krigbaum potential is correct, the values of A and β in our model must be chosen to give the best possible agreement between the two models. The requirement that the second virial coefficients of Eqs. (7) and (10) be the same gives one condition

$$\beta^3XF(X)=Ab^3, \quad (12)$$

but still another is required to fix A and β uniquely. Probably the most trustworthy second condition is obtained in the following manner. It will be recognized that the integrand of Eq. (4) consists of three factors each of the form

$$\varphi(r_{ij})/b=r_{ij}h(r_{ij}).$$

The alternative expressions for φ given by Eqs. (6) and (8) are

$$\varphi_1(y)=y[1-\exp(-Xe^{-y^2})], \quad (13a)$$

$$\varphi_2(y)=Ay\exp\left[-\left(\frac{A}{XF(X)}\right)^{\frac{1}{3}}y^2\right], \quad (13b)$$

where, for convenience, a reduced variable $y=br$ has been introduced, and the condition of Eq. (12) has been applied in writing φ_2. Plots of $\varphi_2(y)$ and $\varphi_2(y)$ against y are then compared and that value of A is chosen which causes the two curves to coincide as nearly as possible.[7]

In Figs. (1) and (2) these graphs are shown for two values of X together with the corresponding functions for hard spheres having the same second virial coefficient as the two soft molecular models. For small values of X, A can be chosen so that φ_1 and φ_2 coincide quite well. This is evident from Fig. (1), which also serves to demonstrate that the Γ_3 calculated from Eq. (11) represents a considerable improvement over the hard sphere approximation. As X increases, the two functions φ_1 and φ_2 cannot be made to agree as well, and it appears advisable to allow A to exceed unity in order to achieve the best fit. At still higher values of X (i.e., greater than about 6) our model ceases to be a useful approximation to that of Flory and Krigbaum; and as X becomes indefinitely large, φ_1 approaches asymptotically the hard sphere case. The results of the graphical evaluation of A, which has been carried out for four values of X, are given in Table I.

TABLE I. Graphical evaluation of Γ_3/Γ_2^2.

X	$F(X)$[a]	A	Γ_3/Γ_2^2
$\frac{1}{2}$	0.912	0.42	0.108
1	0.855	0.72	0.185
2	0.745	1.1	0.28
4	0.605	1.4	0.36
ca. 40	0.221	···	0.53[b]

[a] For $X=\frac{1}{2}$ and 1, $F(X)$ was obtained from a series expansion (Eq. (18.2) of reference (2)), while for the other values of X a graph similar to Fig. (1) of reference (2), but on a somewhat larger scale, was used.
[b] Since for X this large, the function $\varphi_2(y)$ is not a good approximation to the Flory-Krigbaum model, this value of Γ_3/Γ_2^2 was obtained from a repulsive potential proportional to the inverse ninth power of the distance (see Eqs. (14) through (18)).

For values of X much higher than those at which our model is applicable, φ_1 may be approximated fairly well by the corresponding function for a repulsive potential

[5] The special case of this function with $A=1$ has very recently been used as a model for the interaction of protein molecules, P. Doty and R. F. Steiner, J. Chem. Phys. **20**, 85 (1952).

[6] In deriving their form of $h(r)$, Flory and Krigbaum assumed that the total mean density of polymer segments about the center of mass of the molecule is given by a single gaussian function. However, as has been shown by A. Isihara (J. Phys. Soc. Japan **5**, 201 (1950)), the correct result for random-flight chains is actually a sum over Gaussian functions of different moduli. Our Eq. (9) corresponds to such a sum, though not to the correct one.

[7] A more objective procedure for choosing A would be to equalize the areas under the two curves, but this is not strictly correct since the limits of the successive integrations in Eq. (4) are not independent. The requirement of equal areas gives

$$A=\sum_{n\geq 1}(-1)^{n+1}X^n/n!n.$$

However, from the resulting graph of φ_2 it appears that the value of A obtained thus is too large.

energy varying as some inverse power of the distance. The evaluation of the third virial coefficient for a potential of this form requires integration by tedious graphical or numerical methods. However, in the case of the inverse ninth- and twelfth-power potentials, the virial coefficients can be obtained from the work of Kihara,[8] who has made calculations for Lennard-Jones type molecules having these repulsions together with the usual inverse sixth-power attraction. For the model having only repulsive energy proportional to the inverse nth power of the intermolecular distance r,

$$h(r)=1-\exp[-\lambda r^{-n}/kT], \tag{14}$$

$$\Gamma_2=\tfrac{2}{3}\pi(\lambda/kT)^{3/n}\Gamma(1-3/n), \tag{15}$$

$$\Gamma_3/\Gamma_2^2=\tfrac{5}{8}\gamma_0(n)/[\Gamma(1-3/n)]^2, \tag{16}$$

where $\gamma_0(n)$ is a definite integral[8] and Γ without the subscript denotes the gamma-function. For the specific case of $n=9$,

$$\Gamma_3/\Gamma_2^2=\tfrac{5}{8}(1.561)/[\Gamma(5/3)]^2=0.532. \tag{17}$$

Equalizing the second virial coefficients given by the inverse power function and the Flory-Krigbaum model serves to fix λ as a function of X. In the case of the inverse ninth power this stipulation gives

$$\frac{\lambda}{kT}=\left(\frac{3\pi^{\frac{1}{2}}XF(X)}{4b^3\Gamma(2/3)}\right)^3. \tag{18}$$

In order to determine the value of X for which Eq. (18) holds, a plot of $\varphi_1(y)$ as in Figs. (1) and (2) was compared with that of the corresponding variable for the inverse ninth power function. This was repeated for several values of X until the point was found at which the two plots seemed most nearly superimposed. The best fit occurred at roughly $X=40$. A repulsive potential varying as the inverse twelfth power of the distance would presumably be appropriate to some still larger value of X.

Since the third virial coefficient has been evaluated in terms of an intermolecular potential which is a function of the sizes of the molecules interacting, it is clear that our treatment is limited to sharp fractions. For an inhomogeneous polymer, the measured virial coefficients are values averaged over the molecular weight distribution. In this case a calculation does not appear possible; and we can only follow Flory and Krigbaum in suggesting that Γ_3/Γ_2^2 is the same as for a homogeneous polymer, a postulate which is at least not at variance with any experimental evidence.

The parameter X of the Flory-Krigbaum theory is given by

$$X=2(\alpha^2-1). \tag{19}$$

The quantity α, the factor by which the average linear dimensions of the dissolved polymer molecule are increased by intramolecular interference of chain segments, can be evaluated from intrinsic viscosity measurements.[9,10,11] Thus the results given in Table I may be combined with Eq. (19) to express the dependence of Γ_3/Γ_2^2 upon the experimentally obtainable parameter α. The theoretical results are presented graphically in Fig. (3) where Γ_3/Γ_2^2 is plotted against $1/\alpha$.

COMPARISON WITH EXPERIMENT

Unfortunately, there are very few polymer-solvent systems which have been investigated thoroughly enough both with respect to osmotic pressure and intrinsic viscosity to permit anything but a rough estimate of the adequacy of the proposed method for calculating the third virial coefficient. Probably the best osmotic pressure data available for this purpose are those of Flory,[12] who has published results from very careful measurements on a number of polyisobutylene fractions in cyclohexane. For two of these fractions—code numbers, B(0–3), C(4–9)—the limiting value of π/c was determined accurately by extrapolation to infinite dilution from measurements in benzene, a poor solvent, in which Γ_2 is nearly zero. In these two cases the experimental data, given in Table II of reference (12), for the five most dilute solutions were utilized in an empirical evaluation of the coefficients of Eq. (1) terminated after the term in c^2,

$$\pi/c=(\pi/c)_0[1+\Gamma_2 c+\Gamma_3 c^2]. \tag{1a}$$

For this the method of least squares was used with the requirement that $(\pi/c)_0$ given by Eq. (1a) be that

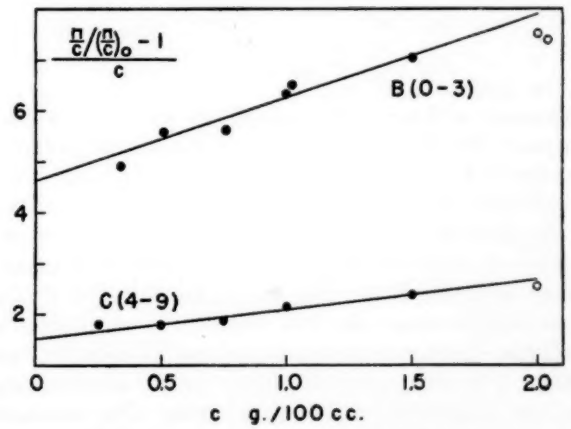

FIG. 4. Osmotic pressure of polyisobutylene fractions in cyclohexane. The straight lines represent the least squares parameters given in Table II. Only those experimental points shown as solid circles were considered in the least squares calculations.

[8] T. Kihara, J. Phys. Soc. Japan 6, 184 (1951).

[9] T. G. Fox, Jr., and P. J. Flory, J. Phys. Coll. Chem. 53, 197 (1949).

[10] P. J. Flory and T. G. Fox, Jr., J. Am. Chem. Soc. 73, 1904 (1951).

[11] Evaluation of α is also possible by light scattering as root mean square end-to-end distances can be obtained from measurements of angular dissymmetry (B. H. Zimm, J. Chem. Phys. 16, 1099 (1948)). The ratio of this length for the solvent in question to that in a very poor one is α.

[12] P. J. Flory, J. Am. Chem. Soc. 65, 372 (1943).

TABLE II. Osmotic pressure of polyisobutylene fractions in cyclohexane (from the data of Flory[12]).

Polymer designation	B(0–3)	C(4–9)
No. average molecular wt.	7.70×10^5	2.56×10^5
α	1.51	1.39
Calculated Γ_3/Γ_2^2	0.31	0.27
Experimental results[a]		
$(\pi/c)_0$	0.33	0.99
Γ_2	4.20	1.51
Γ_3	2.17	0.58
Γ_3/Γ_2^2	0.12	0.25

[a] Dimensions are consistent with π in g/cm² and c in g/100 cm³. The virial coefficients are least squares parameters determined as described in the text.

obtained from the experiments in benzene. The results of this treatment are presented in Fig. (4) in the form of a plot of the quantity

$$[(\pi/c)/(\pi/c)_0-1]/c$$

against c. On the assumption that the quadratic function is adequate for π/c, this graph is evidently a straight line, the intercept giving Γ_2 and the slope Γ_3.

From numerous intrinsic viscosity measurements on polyisobutylene solutions, Fox and Flory[9,13] have deduced the parameters needed for the calculation of α in a number of solvents. For the two polymer fractions discussed above, α in cyclohexane was obtained by solving Eq. (2) of reference (13),

$$\alpha^5-\alpha^3=2\psi_1 C_M(1-\Theta/T)M^{\frac{1}{2}}$$

with the values of the parameters given in the same paper

$$\psi_1 C_M V_1=0.47,$$
$$\Theta=126°\text{K}.$$

The molar volume of the solvent V_1 was taken as 109 cm³/mol. M is the molecular weight of the polymer fraction and T is the temperature at which α is required, in this case 298°K.

The predicted values of Γ_3/Γ_2^2 and those determined empirically from the osmotic pressure measurements are shown in Table II. In the case of fraction C(4–9) the agreement between the two methods is excellent but probably to some extent fortuitous considering the scatter of the experimental data on the one hand and the crudity of the assumptions on the other. The measured Γ_3 for polymer B(0–3), however, appears to be definitely smaller than the calculated value. While these results do not permit a truly quantitative assessment of our calculation of the third coefficient, it does seem to be indicated that our treatment represents an improvement over the hard sphere approximation of Eq. (2).

Further support for this contention may be found in two other cases reported in the literature, in regard to which we shall merely quote the results given without undertaking a new analysis of the experimental data. Schick, Doty, and Zimm[14] measured the osmotic pressure of an unfractionated polystyrene sample (number average molecular weight, 5.24×10^5) in butanone at 27° and 49°C over a very wide concentration range and fitted the experimental data for π/c by quadratic curves giving values of 0.06 and 0.04, respectively, for Γ_3/Γ_2^2. From parameters given by Fox and Flory[15] our method of calculation predicts this ratio to be about 0.1 at both temperatures.

The other example is from the work of Browning and Ferry[16] who determined the osmotic pressure of a polyvinyl acetate fraction (molecular weight, 3.00×10^5) in butanone. They too found that π/c could be fitted well over a large range of concentrations by a quadratic curve, their empirical constants giving 0.06 and 0.07 for Γ_3/Γ_2^2 at 10° and 45°C. From viscosity measurements in this laboratory on polyvinyl acetates of molecular weights both above and below 3×10^5 we have estimated α in butanone at 25°C to be 1.22 for a polymer of this molecular weight. This corresponds to a theoretical value of 0.18 for Γ_3/Γ_2^2.

After examining a considerable amount of osmotic pressure data, including the results for polyisobutylene discussed above, Fox, Flory, and Bueche[17] proposed that Eq. (1a) with $\Gamma_3=\frac{5}{8}\Gamma_2^2$ be adopted as a useful approximation for extrapolation of experimental measurements. Very recently, however, Krigbaum and Flory[18] have concluded from new osmotic pressure experiments on polyisobutylene in cyclohexane and polystyrene in toluene that this hard sphere relation gives a larger value for Γ_3 than the data warrant. Since α is seldom very large (values smaller than 2 apparently including all practical cases for any polymer-solvent pair so far investigated), it can be predicted from Fig. (3) that Γ_3/Γ_2^2 will almost always be considerably smaller than the hard sphere value of $\frac{5}{8}$.

It may be remarked that the various theories based on lattice models[19] also yield unsatisfactory treatments. In the more elaborate of these theories, an experimentally inaccessible parameter, the effective coordination number z of the lattice, is required for a prediction of Γ_3/Γ_2^2. However, if reasonable values of z are taken, the ratio obtained is much too small and furthermore is predicted to be largest in poor solvents or at low molecular weights, in direct contradiction of the experimental results and of our theory.

Flory et al.[2,17] have recommended that the quadratic function for π/c (Eq. (1a)) not be used outside the range $\pi/c\leq3(\pi/c)_0$ because of contributions from the fourth

[13] T. G. Fox, Jr., and P. J. Flory, J. Am. Chem. Soc. **73**, 1909 (1951).

[14] Schick, Doty, and Zimm, J. Am. Chem. Soc. **72**, 530 (1950).

[15] T. G. Fox, Jr., and P. J. Flory, J. Am. Chem. Soc. **73**, 1915 (1951).

[16] G. V. Browning and J. D. Ferry, J. Chem. Phys. **17**, 1107 (1949).

[17] Fox, Flory, and Bueche, J. Am. Chem. Soc. **73**, 285 (1951).

[18] W. R. Krigbaum and P. J. Flory, paper read at the Buffalo, New York, meeting of the Am. Chem. Soc., March 25, 1952.

[19] Consult A. R. Miller, *Theory of Solutions of High Polymers* (Oxford University Press, London, 1948).

and higher virial terms which must render the quadratic curve progressively more inadequate with increasing concentration. This is undoubtedly a valid objection but one circumstance is deserving of note. For any repulsive potential energy, all the virial coefficients are positive if the assumptions of the statistical theory are valid: i.e., any virial coefficient may be expressed as a sum of multiple integrals having integrands of the general form

$$\prod_{ij}(h_{ij}),$$

which are everywhere positive. We should therefore expect that at high concentrations a quadratic curve for π/c would not give enough curvature. Thus, Flory and Krigbaum[2] have anticipated that use of the hard sphere approximation of Eq. (2) for the third coefficient, giving too large a value, and omission of the higher terms would introduce partially compensating errors. Actually, experiments over a wide concentration range seem to indicate a negative deviation at high concentrations from a quadratic curve fitting the data well at lower values. This trend seems to be indicated by the experimental points for fraction $B(0\text{–}3)$ shown in Fig. (4). A clearer instance is provided by the data of Browning and Ferry[16] for polyvinyl acetate in both butanone and trichloropropane, although it is noteworthy in this case that the quadratic appears quite adequate up to concentrations such that $\pi/c=10(\pi/c)_0$. Finally, Schick, Doty, and Zimm[14] report that a negative fourth coefficient appears to be necessary for the benzene solutions of polystyrene which they have investigated. If real, this effect can probably be attributed to the incorrectness of the superposition approximation in the statistical theory, a matter which is discussed in the appendix.

Since it is problematical at what concentration Eq. (1a) ceases to be valid, we have ventured to utilize in our least squares calculations some experimental determinations falling outside the limit $\pi/c\leq 3(\pi/c)_0$. Although the experimental points within this range are very few and probably not as accurate as those at higher concentration, the data presented in Fig. (3) do not indicate that our general conclusions would have been changed had some of the points at greater concentrations not been used.

In the light of the foregoing discussion, it seems to us that the best procedure in extrapolating osmotic pressure data would be to rely on empirical fitting of Eq. (1) to the measured values if these are precise enough and extend over a sufficiently wide concentration range. If the range is short or the precision low, a value of Γ_3 estimated from Fig. (3) should be used in preference to the hard sphere result. An estimate of α is then required; but this need not be extremely precise and, if not otherwise available, can be obtained quickly from simple viscosity measurements.

APPLICATION TO LIGHT SCATTERING

In principle, a third virial coefficient can be evaluated from light scattering measurements as well as from the osmotic pressure. For scattering, the analog of Eq. (1) is

$$Kc/I(90)=(1/M)(1+2\Gamma_2 c+3\Gamma_3 c^2+\cdots), \quad (20)$$

where $I(90)$ is the excess intensity (over that from solvent alone) of radiation scattered by a unit volume of solution through an angle of 90° with respect to the direction of the incident beam, and K is a constant for a given wavelength of light and polymer-solvent system. Except in the case of a homogeneous polymer, the coefficients Γ_2 and Γ_3 are not identical with those of the osmotic pressure Eq. and the solute molecular weight M becomes the weight average M_w.

Equation (20) is valid only if the average dimensions of the dissolved macromolecules are very much smaller than the wavelength of the light used. The experimental criterion of this condition is that $I(\vartheta)$ be symmetrical about 90°. Zimm[20] has developed a more general expression for the scattering, applicable at angles other than 90° and to molecular sizes comparable with the wavelength of the light:

$$Kc/I(\vartheta)=(1/M)\{1/P(\vartheta)+2\Gamma_2 c +[3\Gamma_3 Q(\vartheta)-4(\Gamma_2)^2 P(\vartheta)(1-P(\vartheta))]c^2+\cdots\}. \quad (21)$$

The simple form Eq. (20) is recovered by extrapolation of observations at finite angles to $\vartheta=0$ where the functions $P(\vartheta)$ and $Q(\vartheta)$ are both unity. While $P(\vartheta)$ may be calculated, $Q(\vartheta)$ has not been evaluated completely. Thus the initial slope of Kc/I as a function of c is always Γ_2 regardless of the angle ϑ, even when the intensity of scattering is not symmetrical about 90°; but the curvature of the plot does not generally give Γ_3.[21]

Light scattering data therefore cannot be employed indiscriminately in judging an estimate of Γ_3 nor, conversely, should such an estimate be used in extrapolating the data to infinite dilution except in the cases for which Eq. (20) is valid. For high molecular weights, extrapolation to $\vartheta=0$ is in theory possible, but measurements at small angles are so subject to experimental error that the values of $Kc/I(0)$ resulting would usually not be precise enough to make the term in c^2 significant.

When applied to (unpublished) light scattering measurements carried out in this laboratory for a number of methyl methacrylate polymers in butanone solution, empirical fitting of Eq. (20) gave values for Γ_3/Γ_2^2 considerably smaller than the hard sphere result of $\frac{5}{8}$, provided that angular dissymmetry in the intensity of scattering was unimportant.

APPENDIX

The general statistical mechanical theory of fluids developed by McMillan and Mayer[22] and applied to

[20] B. H. Zimm, J. Chem. Phys. **16**, 1093 (1948).

[21] Equation (21) is not completely rigorous as the derivation involves the "single contact approximation" described in the appendix.

[22] W. G. McMillan, Jr. and J. E. Mayer, J. Chem. Phys. **13**, 276 (1945).

solutions of flexible long chain molecules by Zimm[23] gives the following rigorous expressions for the second and third osmotic virial coefficients:

$$\Gamma_2 = -(N_0/2VM)\int g_2(i,j)d(i)d(j), \tag{A1}$$

$$\Gamma_3 = -(N_0^2/3VM^2) \times \int g_3(i,j,k)d(i)d(j)d(k) + 4(\Gamma_2)^2. \tag{A2}$$

The integrands are defined[22,23] in terms of the molecular distribution functions $F_1(i)$, $F_2(i,j)$, and $F_3(i,j,k)$ for one, two, and three molecules at infinite dilution in the chosen solvent:

$$g_2(i,j) = F_2(i,j) - F_1(i)F_1(j), \tag{A3}$$

$$g_3(i,j,k) = F_3(i,j,k) - F_1(i)F_2(j,k) - F_1(j)F_2(k,i) - F_1(k)F_2(i,j) + 2F_1(i)F_1(j)F_1(k). \tag{A4}$$

In the above expressions, the single symbol i represents all the coordinates specifying the location and configuration of the molecule i, and the quantity $d(i)$ is the corresponding differential element of configuration space. The integrations extend over all configurations consistent with the (arbitrarily large) volume V, and the distribution functions are so normalized that

$$\int F_1(i)d(i) = V; \quad \int F_2(i,j)d(i)d(j) = V^2; \text{ etc.} \tag{A5}$$

In the limit of large volumes, the virial coefficients are independent of V.

To get tractable results for the second coefficient, Zimm factored the pair distribution function in the following way:

$$F_2(i,j) = F_1(i)F_1(j)\exp[-u(i,j)/kT], \tag{A6}$$

and further assumed that the potential of average force $u(i,j)$ thus defined can be written as a sum over all pairwise interactions between the segments of the two polymer chains. This latter assumption is an example of the "superposition" approximation first applied to molecular distribution functions by Kirkwood.[24] For certain problems Zimm adopted the additional simplification of a single contact between pairs of molecules; i.e., that those configurations may be neglected in which more than one segment from each molecule is interacting at one time.

[23] B. H. Zimm, J. Chem. Phys. 14, 164 (1946).
[24] J. G. Kirkwood, J. Chem. Phys. 3, 300 (1935).

If Eqs. (A3) and (A6) are put into (A1), the second virial coefficient becomes

$$\Gamma_2 = -N_0/2VM \times \int F_1(i)F_1(j)[\exp(-u(i,j)/kT) - 1]d(i)d(j). \tag{A7}$$

For monatomic molecules in a fluid, F_1 is everywhere unity and $u(i,j)$ depends only on the separation r between the two molecules, so in this case Eq. (3) is at once obtained. For polymer chains, however, F_1 is a complicated function of the coordinates of all segments, governing the distribution of configurations of a single chain; and $u(i,j)$ is also extremely complicated, even if superposition is assumed to be correct. The theory of Flory and Krigbaum[2] amounts to the assumption that in integrating Eq. (A7) over all coordinates save the separation r of the two centers of mass, the potential $u(i,j)$ may be replaced by an average value $u(r)$ depending only on r, and thus again yields Eq. (3). Formally this average potential is given by

$$u(r) = \int' u(i,j)F_1(i)F_1(j)d(i)d(j) \Big/ \int' F_1(i)F_1(j)d(i)d(j),$$

where the primes indicate integration over all coordinates except r. By expansion of the exponential in Eq. (A7), it is evident that this procedure can be correct only as far as the linear term in the expansion; in the higher terms a false weighting of the various configurations is assured. We shall not comment further on this defect at present, but suppose that the error thus committed can be minimized by judicious choice of $u(r)$.

The third coefficient presents new obstacles unless superposition is again invoked in the well-known form

$$F_3(i,j,k) = F_2(i,j)F_2(j,k)F_2(k,i)/F_1(i)F_1(j)F_1(k).$$

With Eq. (A6) and (A4), and again with a substitution of $u(r)$ for $u(i,j)$, the defining Eq. (A2) then yields Eq. (4) for the third virial coefficient.

We have no means of estimating the error introduced into our calculation of Γ_3 by the use of superposition. It seems likely that superposition of the *average* potentials $u(r)$ rather than of the more specific quantities $u(i,j)$ is the most questionable maneuver employed, and that Γ_3 is thereby somewhat overestimated. Since the assumption of superposition becomes even less accurate for higher distribution functions, it is virtually impossible to conclude anything about the terms in Γ_4 and beyond from a knowledge of Γ_2 alone.

The Self-Diffusion of Liquid Mercury*,†

R. E. HOFFMAN
General Electric Research Laboratory, The Knolls, Schenectady, New York
(Received May 1, 1952)

Self-diffusion coefficients in liquid mercury have been measured by the capillary technique and have been found to be in disagreement with the earlier calculated values of Haissinsky and Cottin. In view of the fact that the present data have been obtained by direct measurement and are also much more compatible with known viscosity data, it is concluded that the data of Haissinsky and Cottin are invalid. An examination of liquid self-diffusion data in general has shown that the Stokes-Einstein equation usually gives a much better correlation of self-diffusion and viscosity coefficients than the Eyring equation.

INTRODUCTION

SELF-DIFFUSION data for liquids should be helpful in the development and testing of theories of the liquid state. Unfortunately, the amount of such data is very limited. Recently Haissinsky and Cottin[1] have calculated self-diffusion coefficients of liquid mercury from measured rates of isotopic exchange between mercury and aqueous solutions of mercurous nitrate, the assumption having been made that diffusion in the mercury was the rate-controlling step of the process. Although attempts were made to justify this assumption experimentally, the evidence is not decisive, and it is therefore of interest to compare their results with what can be predicted from known viscosity data.

In terms of the absolute reaction rate theory, Eyring[2] has shown that the diffusion coefficient, D, and the viscosity coefficient, η, are given by the equations

$$D=\lambda_D^2 K_D, \tag{1}$$

where λ_D and K_D are, respectively, the "jump-distance" and specific rate constant for diffusion, and

$$\eta=\lambda_1 kT/\lambda_2\lambda_3\lambda_v^2 K_v, \tag{2}$$

where λ_3 is the interatomic distance in the direction of motion, λ_1 and λ_2 are interatomic distances in directions perpendicular to λ_3, k is Boltzmann's constant, T the absolute temperature, and λ_v and K_v are, respectively, the "jump-distance" and specific rate constant for viscous flow. Eyring then assumes that

$$\lambda_D^2 K_D=\lambda_v^2 K_v, \tag{3}$$

so that

$$D\eta/kT=\lambda_1/\lambda_2\lambda_3. \tag{4}$$

In the case of simple monatomic liquids such as mercury,

$$\lambda_1=\lambda_2=\lambda_3\cong 2r, \tag{5}$$

where r is the atomic radius, and Eq. (4) then reduces to

$$D\eta/kT=1/2r. \tag{6}$$

Values of r computed from the data of Haissinsky and Cottin's Fig. 3 with the aid of their Eq. (2a), together with the viscosity data of Bingham and Thompson,[3] are given in Table I. These calculated radii are not only much larger than the value obtained from x-ray radial distribution curves,[4] but also change markedly with temperature.

In view of this disagreement and the doubt concerning the validity of the diffusion coefficients calculated by Haissinsky and Cottin, a reinvestigation of the self-diffusion of liquid mercury, using a more conventional technique, was undertaken.

EXPERIMENTAL

The capillary technique first described by Anderson and Saddington[5] was chosen for this work, because of its apparent simplicity and reliability. In this method, diffusion takes place from a capillary tube into an effectively infinite reservoir in which the capillary is immersed. This feature has the advantage that the width of the diffusion zone is small in comparison to its length, thus minimizing the effects of convection currents. In addition, the large reservoir of liquid metal eliminates any thermal gradients along the length of the diffusion zone.

The apparatus used in this work (Fig. 1) consists of a glass vessel of sufficient size to hold approximately one kilogram of mercury, and is provided with two outlets. One of these outlets accommodates, through a mercury seal, a stirrer which rotates at about 250 rpm; the other provides for the insertion and removal of the capillary tube which is supported by a glass rod through a rubber

TABLE I. Atomic radius of mercury calculated from diffusion data of Haissinsky and Cottin.[1]

T, deg K	$10^7 D$, cm² sec⁻¹	$10^2\eta$, g cm sec⁻¹	r_{calc}, A	r_{exp}, A
273	0.38	1.68	3000	1.5
292	0.49	1.56	2600	
366	1.66	1.27	1200	

* Work supported by the U. S. AEC under Contract No. W-31-109-Eng-52.
† Abstract presented before the American Physical Society, New York, January, 1952 [Phys. Rev. 86, 585 (1952)].
[1] M. Haissinsky and M. Cottin, J. phys. radium 11, 611 (1950).
[2] H. Eyring, J. Chem. Phys. 4, 283 (1936).
[3] E. C. Bingham and T. R. Thompson, J. Am. Chem. Soc. 50, 2878 (1928).
[4] P. Debye and E. Mencke, Ergebnisse der technischen Röntgenkunde (Akad. Verlag. Leipzig, Germany, 1931), Vol. II.
[5] J. S. Anderson and K. Saddington, J. Chem. Soc. (London) S381 (1949).

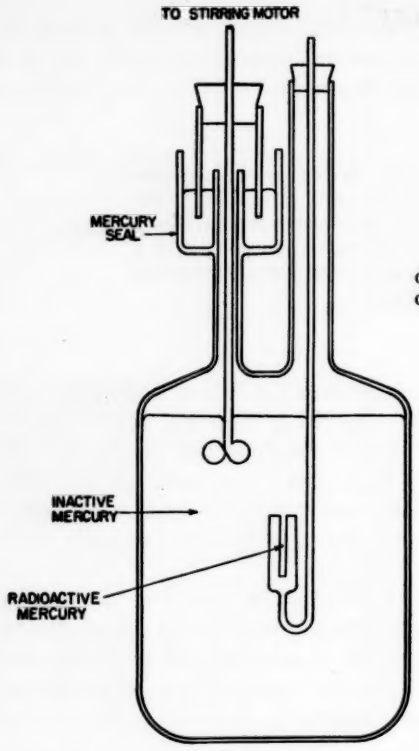

FIG. 1. Schematic diagram of liquid diffusion cell.

stopper. This entire assembly is immersed, up to the bottom of the mercury seal, in a bath whose temperature is held constant within ±0.05°C. The capillary, approximately 0.6 mm in diameter and 2 cm long, was fabricated from tubing of uniform bore. One end was sealed off to form a flat bottom; the open end was ground flat on emery paper. The diameter and length were measured accurately with a slide micrometer and microscope.

Radioactive mercury Hg^{203} was obtained by thermal decomposition, in vacuum, of radioactive HgO furnished by the Isotopes Branch of the United States Atomic Energy Commission. This product was diluted with sufficient inactive mercury to give an initial activity of about 15 cts/min/mg with the counter geometry used.

The capillary is filled with radiomercury and suspended in the cell so that the open end is just above the level of inactive mercury until thermal equilibrium is attained and then completely submerged. After a predetermined length of time, the capillary is removed from the cell and its contents are withdrawn and counted. At the same time, an equal volume of the stock radioactive mercury is counted, in order to correct for decay of the isotope during the time of the experiment.

If the axis of the capillary is taken as the x axis of a coordinate system whose origin is at the bottom of the capillary, the following boundary conditions apply:

$$C=C_0 \quad 0\leq x\leq L \quad \text{at } t=0$$
$$C=0 \quad x>L \quad \text{for all } t,$$

where C is the concentration of the isotope, t the time, and L the length of the capillary. The solution of the diffusion equation,

$$\frac{\partial C}{\partial t}=D\frac{\partial^2 C}{\partial x^2}, \tag{7}$$

under these conditions is given by[6]

$$\frac{C_{av}}{C_0}=\frac{8}{\pi^2}\sum_{n=0}^{\infty}\left\{\frac{1}{(2n+1)^2}\exp\left[\frac{-(2n+1)^2\pi^2 Dt}{4L^2}\right]\right\}, \tag{8}$$

where C_{av} is the average concentration in the capillary after time t. Since L and t are known, measurements of C_0 and C_{av} are sufficient for the calculation of D.

In general, the times were chosen so that C_{av}/C_0 was about 0.3. However, at room temperature several experiments were run for widely varying times. The fact that, within experimental error, the results are independent of time (see Table II below) indicates that convection effects were negligible.

RESULTS AND DISCUSSION

Measurements have been made in the temperature range 0–90°C. The data are summarized in Table II and shown graphically in Fig. 2, wherein $\log D$ is plotted as a function of the reciprocal absolute temperature. The straight line in the figure was calculated by the method of least squares and is described by the equation

$$D=1.26(10)^{-4}\exp(-1160/RT)\ \text{cm}^2\ \text{sec}^{-1}. \tag{9}$$

These diffusion coefficients are larger than those of Haissinsky and Cottin by a factor of several hundred. Since the present data have been obtained by direct measurement and do not depend on the validity of an assumed mechanism, it is concluded that the diffusion coefficients reported by Haissinsky and Cottin are invalid and that some process other than diffusion in the mercury must have controlled the rate of the exchange process studied by them.

Values of the radius evaluated by substituting the data of Table II into Eq. (6) vary between 7.4 and 7.7A, with an average of 7.54±0.09A. The agreement with the experimental value (1.5A), though much better than that obtained with Haissinsky and Cottin's data, is still far from satisfactory. Moreover, it seems reasonable to suppose, as Ewell and Eyring[7] have already suggested, that in liquid metals the unit of flow is the ion rather than the atom. In this case, the agreement of the Eyring equation with the data is even poorer, since the actual radius should then be about 0.7A.‡

It is also of interest to investigate the validity of the Stokes-Einstein equation,

$$r=kT/6\pi D\eta. \tag{10}$$

[6] H. S. Carslaw and J. C. Jaeger, *Conduction of Heat in Solids* (Oxford University Press, London, England, 1947), p. 79.

[7] R. H. Ewell and H. Eyring, J. Chem. Phys. **5**, 726 (1937).

‡ Wycoff (see reference 8) gives 0.72A and 0.66A for the crystal radii of Hg^+ and Hg^{++}, respectively.

[8] R. W. G. Wycoff, *Crystal Structures* (Interscience Publishers, Inc., New York, 1948), Vol. I.

In spite of the theoretical limitation imposed by the fact that its derivation is based on the assumption that the liquid may be treated as a continuous medium, this equation frequently has been found to give a satisfactory description of the data for solutions. Substitution of the diffusion data of Table II into Eq. (10)§ yields a value of 0.80A for r, in good agreement with the expected ionic radius. Also in the case of liquid lead, for which the self-diffusion coefficient has been measured at a single temperature,[9] the Stokes-Einstein equation yields a value of 0.84A, which is intermediate between the bivalent (1.18A) and tetravalent (0.70A) crystal radii.

The only other liquid for which both self-diffusion and viscosity data are available is water. However, it is difficult to apply either the generalized Eyring equation [Eq. (4) above] or the Stokes-Einstein equation to liquids whose molecules are not spherical. With the Eyring theory, the difficulty arises because there is no independent method of evaluating λ_1, λ_2, and λ_3, while the Stokes-Einstein equation can give only one dimension, which is insufficient to describe the shape of the molecule. However, Wang[10] has recently measured self-diffusion coefficients of water, using O^{18} as tracer, and analyzed the data in terms of the Eyring equation. From the diffusion and viscosity data, together with the further approximation that the product $\lambda_1\lambda_2\lambda_3$ is approximately equal to the atomic volume, he calculates $\lambda_1=1.4$A and $(\lambda_2\lambda_3)^{\frac{1}{2}}=4.6$A. However, it does not seem likely that any of the λ's should differ greatly from 2.9A, the average nearest neighbor distance as deduced from radial distribution curves.[11] On the other hand, if the water molecule is considered approximately spherical, the Stokes-Einstein equation gives $r=0.80$A, whereas a value of about 1.4A would be expected. For water, then, it is difficult to decide which equation is in better agreement with the data.

TABLE II. Experimental results.

Temp. deg C	Time, Hrs	10^5D, cm² sec^{-1}	10^5D_{av}
2.5	21.5	1.51	1.52
	23.75	1.53	
16.4	22	1.71	1.68
	24	1.64	
23.0	15	1.81	
	24	1.75	1.79
	63.5	1.80	
31.9	24	1.90	1.88
	26	1.86	
41.5	24	2.00	1.98
	26	1.96	
66.1	19.25	2.23	2.24
	20	2.24	
91.2	16	2.58	2.57
	20	2.56	

§ Actually Eqs. (10) and (6) are identical except for the numerical factors in the denominators, so that radii calculated from the Stokes-Einstein equation will be smaller than those calculated from the simplified Eyring equation by a factor of 3π.

[9] J. Groh and G. von Hevesy, Ann. Physik **63**, 85 (1920).

[10] J. H. Wang, J. Am. Chem. Soc. **73**, 4181 (1951).

[11] J. Morgan and B. E. Warren, J. Chem. Phys. **6**, 666 (1938).

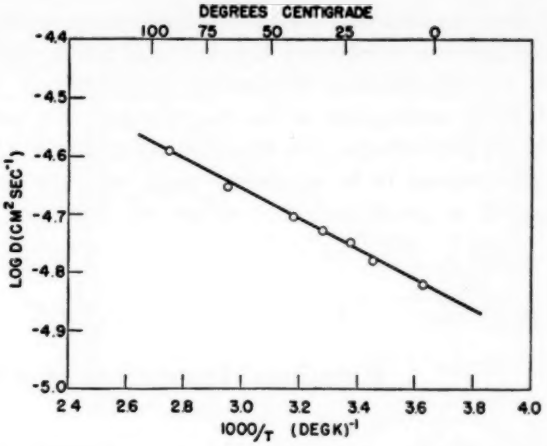

FIG. 2. Temperature dependence of the self-diffusion coefficient of liquid mercury.

The general disagreement between the Eyring equation and the data can be due either to the fact that $\lambda_v\neq\lambda_D$ or that $K_v\neq K_D$. However, since the rate constants are of the form[12]

$$K=e\frac{kT}{h}\exp\left(\frac{\Delta S^{\ddagger}}{R}\right)\exp\left(\frac{-Q}{RT}\right), \tag{11}$$

where e is the base of the Naperian logarithms, $\Delta S^{\ddagger}$ is the entropy of activation, and Q is the experimental activation energy defined by the equation

$$Q=RT^2\frac{(d\ln K)}{dT}, \tag{12}$$

then a difference between K_v and K_D could be due to a difference between $\Delta S_v^{\ddagger}$ and $\Delta S_D^{\ddagger}$ or between Q_v and Q_D. But for both water and mercury, it is found that for the temperature range over which diffusion coefficients have been measured Q_v and Q_D are identical within experimental error. (For water, in the range 0–55°C, $Q_v=4440$ cal/mole,[13] $Q_D=4410$ cal/mole;[10] for mercury between 0° and 90°C, $Q_v=1250$ cal/mole,[14] $Q_D=1160$ cal/mole.)‖ Hence, only a difference between $\Delta S_v^{\ddagger}$ and $\Delta S_D^{\ddagger}$ can cause a difference between K_v and K_D.

[12] Glasstone, Laidler, and Eyring, *The Theory of Rate Processes* (McGraw-Hill Book Company, Inc., New York, 1941).

[13] From data of Bingham and Jackson, Bull. Bur. Standards **14**, 75 (1918).

[14] From data of reference 3.

‖ On the basis of Eqs. (2) and (12), $Q_v=Rd[\ln(\eta/T)]/d[1/T]$. In the literature, it has been customary to refer to the value of $Rd(\ln\eta)/d(1/T)$ as the activation energy for viscous flow. In so far as Eq. (2) is even qualitatively correct, the latter definition seems to be without justification.

It thus appears that the Stokes-Einstein equation in general gives a satisfactory description of the available data on self-diffusion in liquids, even though the underlying assumption of the equation does not seem valid for self-diffusion. On the other hand, the Eyring equation seems to be in disagreement with the data unless it is postulated that either the entropies of activation or the jump-distances for viscous flow and self-diffusion are very different.

ACKNOWLEDGMENT

The author wishes to acknowledge the valuable discussions with various members of the staff of the Metallurgy Department of the Research Laboratory, in particular those with Dr. David Turnbull.

THE JOURNAL OF CHEMICAL PHYSICS VOLUME 20, NUMBER 10 OCTOBER, 1952

Rotational Isomerism as a General Property of Alkyl Nitrites

P. TARTE
University of Liége, Liége, Belgium
(Received March 19, 1952)

The infrared and ultraviolet spectra of 15 alkyl nitrites were studied in the gaseous state. In the infrared, the O−N=O group is characterized by very strong absorption in the three regions 600, 800, and 1650 cm^{-1}, corresponding to O−N=O bending, N−O stretching, and N=O stretching frequencies, respectively. The doubling of the characteristic frequencies and the temperature dependence of the bands of methyl nitrite are explained by rotational isomerism, which appears to be a general property of alkyl nitrites. The influence of the length, shape, and kind of the carbon chain on the frequencies and intensities of the characteristic bands has been studied. The intensity variation of the $\nu_{N=O}$ bands strongly suggests that the relative abundances of the two isomers vary widely from primary to secondary and tertiary nitrites, but depend only to a small extent upon the length and shape of the carbon chain. Application of this property to the diagnosis of primary, secondary, or tertiary alcohols is suggested.

The uv spectra consist essentially of two systems of diffuse bands (and not of one, as stated by previous workers), whose relative intensities vary in the same manner as the relative abundances of the two rotational isomers. The two systems of bands are accordingly assigned to these rotational isomers. This hypothesis has been checked by a study of the temperature dependence of the intensity of the bands.

INTRODUCTION

THE vibration spectra of alkyl nitrites have not yet been extensively studied: only the Raman spectra of a few alkyl nitrites,[1] without frequency assignment, and very incomplete infrared data (between 5 and 8μ only)[2] are to be found in the literature.

The electronic spectra, however, were carefully investigated by Kuhn and co-workers,[3–5] who discovered a characteristic system of diffuse bands between 3000 and 4000A, and by Purkis and Thompson,[6–8] who found a frequency interval of ~1100 cm^{-1} between the bands. A number of facts, however, remained unexplained: the abnormally high frequency interval between the first and the second band of the system,[7] the peculiar intensity distribution in the bands,[6–8] and the abnormal fluctuations of the circular dichroism in the case of optically active nitrites.[5]

This paper deals with the results of the investigation of the infrared and ultraviolet spectra of 15 alkyl nitrites.

Technique

All the nitrites were prepared by the following general method: action of cold diluted H_2SO_4 on the aqueous solution of very pure alcohol and sodium nitrite. The crude product was dessicated and purified by repeated low temperature distillation in vacuum.

The infrared spectra were taken with a Perkin-Elmer spectrometer equipped with KBr and NaCl prisms (length of the cell: 90 mm) and with a Beckman spectrometer with NaCl and LiF prisms (length of the cell: 1 meter). The ultraviolet spectra were taken with a Hilger E1 quartz spectrograph, having a dispersion of about 8A/mm at 3500A and with a one-meter cell. High contrast plates (Ilford Process P 40) were used. All the nitrites were studied in the gaseous state.

RESULTS AND INTERPRETATION

A. Infrared Spectra

(1) General Characteristics

All the nitrites studied are characterized by very strong absorption in the three regions 600, 800, and 1650 cm^{-1}. These bands are attributed to the funda-

[1] K. W. F. Kohlrausch, *Ramanspektren* (Akademische Verlagsgesellshaft, Leipzig, 1943), p. 286.
[2] H. Lenormant and P. Clément, Bull. Soc. Chim. France 1946, pp. 559, 566.
[3] W. Kuhn and H. Lehmann, Z. Elektrochem. **37**, 549, 552 (1931); Z. physik. Chem. **B18**, 32–48 (1932).
[4] W. Kuhn and H. Biller, Z. physik. Chem. **B29**, 1–41 (1935).
[5] H. Elkins and W. Kuhn, J. Am. Chem. Soc. **57**, 296–299 (1935).
[6] H. W. Thompson and C. Purkis, Trans. Faraday Soc. **32**, 674–680 (1936).
[7] C. Purkis and H. W. Thompson, Trans. Faraday Soc. **32**, 1466–1474 (1936).
[8] H. W. Thompson and F. Dainton, Trans. Faraday Soc. **33**, 1546–1555 (1937).

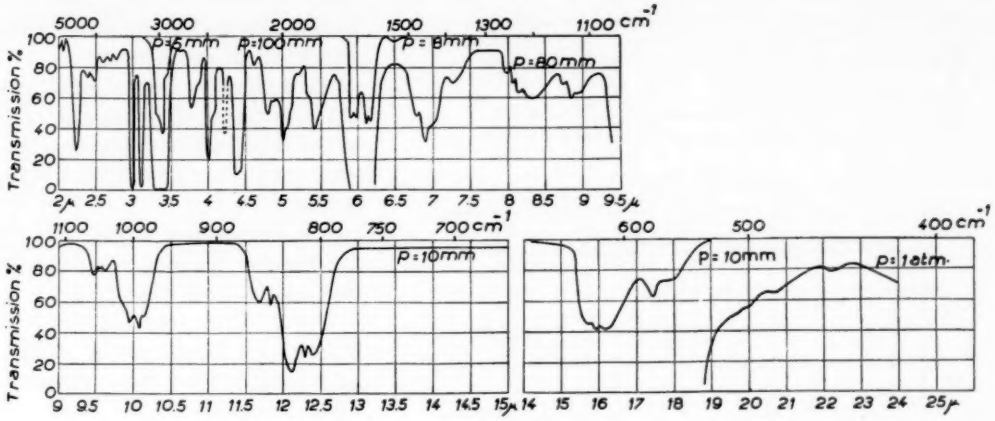

FIG. 1. Infrared spectrum of methyl nitrite. 2–6μ Beckman LiF $d=1$ meter. 6–15μ Perkin Elmer NaCl $d=9$ cm. 14–25μ Perkin Elmer KBr $d=9$ cm.

mental frequencies of the $-O-N=O$ group, namely, the $O-N=O$ bending, $N-O$ stretching, and $N=O$ stretching frequencies, respectively. One of the most important features of these spectra is the doubling of the $O-N=O$ bending and the $N=O$ stretching frequencies in most of the nitrites studied. The $N-O$ stretching frequency appears also to be double, but this can be ascertained only in methyl and ethyl nitrites (in more complex molecules, this spectral region is obscured by bands arising from the carbon chain).

Such a doubling cannot be ascribed to intermolecular association, because the nitrites were studied in the gaseous state at low pressures (intermolecular associations are weak, even in the liquid state, as indicated by the relatively low boiling point of the nitrites). Moreover, the relative intensities of the bands have been found to be independent of pressure.

A much more attractive explanation of the frequency doubling seems to be rotational isomerism. This will be fully demonstrated by the study of the methyl nitrite spectrum.

(2) *The Infrared Spectrum of Methyl Nitrite and the Temperature Dependence of the Intensity of the Bands*

The infrared spectrum of gaseous methyl nitrite is given by Fig. 1, which clearly shows the doubling of the $\delta_{O-N=O}$($\sim$600 cm^{-1}), ν_{N-O}(800 cm^{-1}), ν_{C-O}(1000 cm^{-1}), and $\nu_{N=O}$(1650 cm^{-1}) frequencies.

The temperature dependence of the bands was studied between 3 and 15μ, using the Beckman spectrometer in conjunction with a one meter cell. The cell was surrounded over a 80 cm length by a nearly thermally insulated jacket. This design is very simple and quite sufficient for qualitative measurements.

The spectra were taken, first at room temperature, and then with the jacket filled with dry ice (taking spectra at too high temperatures must be avoided, the alkyl nitrites being thermally unstable).[9]

A temperature dependence has been found for all the pairs of bands between 6 and 15μ (Fig. 2), and also for a number of overtone and combination bands.

[9] E. W. R. Steacie, *Atomic and Free Radical Reactions* (Reinhold Publishing Corporation, 1946), pp. 141–143.

These results strongly support the hypothesis of rotational isomerism. However, no evidence is found about the structure of the isomers: They are possibly *cis*- and *trans*-isomers, which can also be described as chelated and nonchelated form, such as

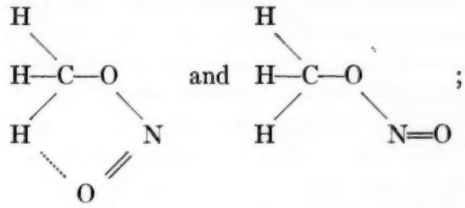

;

but the existence of *trans*- and *gauche*-isomers cannot be excluded.

In this paper, they will be simply referred to as *cis*- and *trans*-isomers.

Table I gives the observed fundamental frequencies, with their assignment to *cis*- and *trans*-isomers, the *cis*- or chelated form being supposed to be the more stable and therefore of decreasing abundance with increasing temperature.

The temperature dependence of the δ_{ONO} fundamental (617–565 cm^{-1}) has not been studied (the frequency of these bands is too low for study with a NaCl spectrometer), and the assignment to *cis*- and *trans*-forms is deduced from the temperature dependence of their first harmonics, at 1234 and 1130 cm^{-1}, respectively. The most important harmonic and combination bands are collected in Table II.

(3) *Rotational Isomerism in Other Alkyl Nitrites*

It is not possible to study the temperature dependence of the bands in all alkyl nitrites in the gaseous state, owing to their low vapor pressure at low temperatures, but the interpretation of the frequency doubling by rotational isomerism is almost obvious. The influence of length, shape, and kind of the carbon chain on the frequencies and intensities of the characteristic bands has been studied. The most important data are collected in Table III.

The $\nu_{N=O}$ pair of bands is by far the most characteristic one. The frequency of these bands undergoes a

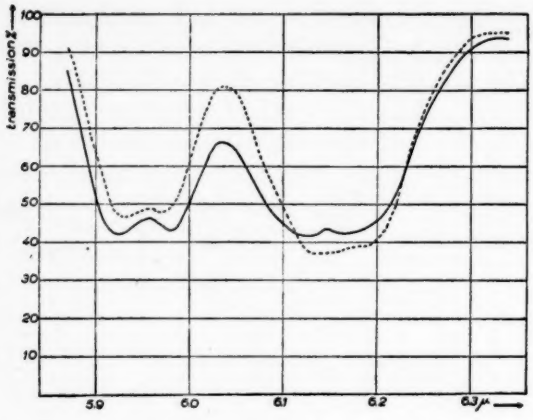

FIG. 2a. Influence of $t°$ on the $\nu_{N=O}$ pair of bands. Beckman LiF $d=1$ meter $p\simeq 0.7$ mm Hg. Curve ————: room temperature (23°C). Curve ----------: dry ice.

small, but systematic shift towards low frequencies when going from methyl nitrite to the nitrites of other primary alcohols, then to nitrites of secondary alcohols, and last to nitrites of tertiary alcohols. But the most important and characteristic feature is the change in the band intensities, which appears clearly in the fifth column of Table III; this column gives the ratio of the extinction $D=\log \cdot I_0/I$ for the *trans*- and the *cis*-forms. The value of this ratio, which is nearly one in methyl nitrite at ordinary temperature, becomes roughly 3 in the other nitrites of primary alcohols, 6 to 10 in the nitrites of secondary alcohols, and finally 35 to 50 in the nitrites of tertiary alcohols; in these last nitrites, the band of the *cis*-form has almost completely disappeared.

In fact, it must be noted that not only the intensity ratio but also the absolute intensity of the bands varies from one class (primary, secondary, or tertiary) nitrites to another, the *trans*-band becoming more and more intense, the *cis*-band, more and more weak. This result is illustrated by Fig. 3, in which the two $\nu_{N=O}$ bands of four characteristic nitrites have been plotted, the spectra

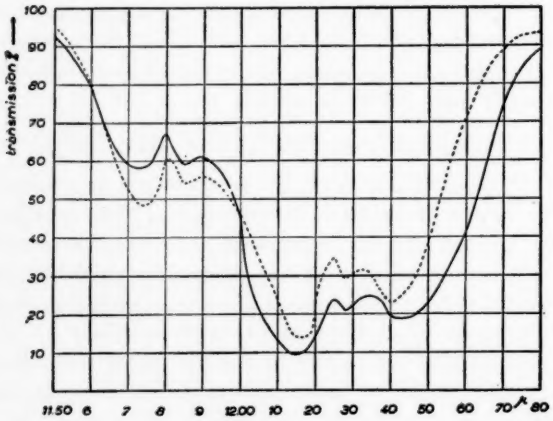

FIG. 2b. Influence of $t°$ on the $\nu_{N=O}$ pair of bands. Beckman NaCl $d=1$ meter $p\simeq 1$ mm Hg. Curve ————: room temperature (23°C). Curve ----------: dry ice.

having been taken under the same conditions of temperature and pressure.

Such changes in the band intensities are most probably the result of a variation of the relative abundances of the two rotational isomers, the *trans*-isomer becoming more and more abundant when going from primary to tertiary nitrites.

It is remarkable indeed that the relative abundance of the isomers depends essentially on the nature (primary, secondary, or tertiary) of the carbon adjacent to the $-O-N=O$ group, and to a much smaller extent on the length and shape of the carbon chain. The study of additional nitrites is necessary for checking the generality of this rule, but if these results are confirmed, their most immediate application would be a new method of identifying primary, secondary, or tertiary alcohols.

The first harmonic of the $\nu_{N=O}$ frequency has also been studied, the bands of the *cis*- and *trans*-forms being near 3200 and 3300 cm^{-1}, respectively. The variations of the frequencies and intensities of these bands are in all respects similar to those of the corresponding fundamentals. The observed frequencies are about 40 cm^{-1} lower than the calculated ones; this lowering is attributed to anharmonicity.

TABLE I. Fundamental frequencies of methyl nitrite.

Vibration	Frequency *cis*	Frequency *trans*
δ_{ONO}	617	565
δ_{CH_3}	1445	1375
ν_{N-O}	844	814
ν_{C-O}	993	1045
$\nu_{N=O}$	1625	1681

The ν_{N-O} fundamental is characterized by the very high intensity of the band of the *trans*-form; in most of the nitrites, this band is by far the strongest of the spectrum. As already stated, the corresponding band of the *cis*-form has been identified with certainty in methyl and ethyl nitrites only, it is much weaker than the band of the *trans*-form, and, in all the other nitrites, superimposed bands of the carbon chain make the assignments quite arbitrary.

The observed frequencies of the ν_{N-O} *trans*-band are reported in Table III. There is a significant shift towards lower frequencies from primary to tertiary nitrites. The frequency values for the third fundamental, δ_{ONO}, are also reported in Table III. Neither the frequencies, nor the intensities exhibit any regularity; this result is not surprising, as the deformation vibration must be affected by the length and shape of the adjacent carbon chain.

In a few cases, the occurrence of other bands in the same spectral region makes assignments uncertain.

B. Ultraviolet Spectra

As previously stated, much experimental work has already been performed on the ultraviolet spectrum of

alkyl nitrites, but the following difficulties still remain:

(1) No attempt has been made to assign the ultraviolet frequency interval to a fundamental frequency in the ground state.

(2) In previous studies, Kuhn[10,11] pointed out, and this was substantiated by many workers,[12,13] that the anisotropy factor remains constant throughout a given electronic transition, being independent of the vibrations and rotations superimposed on the electronic transition. But alkyl nitrites apparently do not follow this rule,[5] and Kuhn postulated the occurrence, in alkyl nitrites, of two superimposed systems of bands, whose detection was quite difficult, owing to their very diffuse nature.

TABLE II. Harmonic and combination bands of methyl nitrite.

ν_{obs} (cm^{-1})	Assignment
1130	$2\delta_{ONO}$ *trans* = 1130 cm^{-1}
1234	$2\delta_{ONO}$ *cis* = 1234 cm^{-1}
1980	$2\nu_{C-O}$ *cis* = 1986
2083	$2\nu_{C-O}$ *trans* = 2090
2252	$\delta_{ONO}+\nu_{N=O}$ = 2245
2451	$\nu_{N-O}+\nu_{N=O}$ *cis* = 2469
2494	$\nu_{N-O}+\nu_{N=O}$ *trans* = 2494
3225	$2\nu_{N=O}$ *cis* = 3250
3333	$2\nu_{N=O}$ *trans* = 3360

(3) The frequency interval of 1100 cm^{-1}, which is characteristic of organic nitrites, was obtained by neglecting the first band of the system.

(1) *Assignment of the Ultraviolet Frequency Interval*

The difficulties arising from this assignment have already been pointed out.[14] The ultraviolet frequency interval can be assigned either to the $\nu_{N=O}$ or to the ν_{N-O} vibration. The latter assignment implies an increase of the frequency from 800 cm^{-1} in the ground state to 1100 cm^{-1} in the excited state. Although unexpected, this is not impossible; such an increase has already been found in the fluorine molecule, whose vibration frequency increases from 891.8 cm^{-1} in the electronic ground state to 1139.8 cm^{-1} in one of the excited states.[15]

TABLE III. Characteristic bands of alkyl nitrites.

Nitrite	$\nu_{N=O}$ *cis* (cm^{-1})	$\nu_{N=O}$ *trans* (cm^{-1})	ν *trans* $-\nu$ *cis* (cm^{-1})	$\frac{D\ trans}{D\ cis}$ ($t°=23°C$)	ν_{N-O} *trans* (cm^{-1})	$\delta_{O-N=O}$ *cis* (cm^{-1})	$\delta_{O-N=O}$ *trans* (cm^{-1})
CH_3ONO	1625	1681	56	0.95 ±0.05	814	617	565
C_2H_5	1621	1675	54	2.3 ±0.1	~800	691	581
C_3H_7	1621	1672	51	3.0 ±0.2	802	687	602
n-C_4H_9	1618	1669	51	3.3 ±0.2	790	689	610
iso-C_4H_9	1618	1669	51	3.5 ±0.2	794	680	625
iso-C_5H_{11}	1618	1669	51	3.5 ±0.2	800	687	617
allyle	1623	1681	58	2.8 ±0.2	796	680?	598
benzyle	1621	1678	57	3.1 ±0.2	793		
sec-C_3H_7	1615	1667	52	6.0 ±0.4	783	688	605
sec-C_4H_9	1615	1665	50	7.2 ±0.4	776	678	600?
sec-C_5H_{11}	1618	1664	46	10 ±0.7	775	678	594?
cyclo-C_5H_9	1613	1664	51	4.7 ±0.3	780	682	604
cyclo-C_6H_{11}	1615	1664	49	9.3 ±0.6	775		
tert-C_4H_9	1610	1655	45	~35	764		621?
tert-C_5H_{11}	~1613	1653	40	~50	751		613?

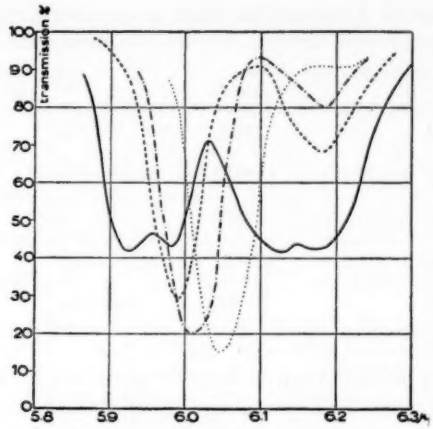

FIG. 3. $\nu_{N=O}$ pair of bands, for 4 characteristic nitrites. ——— methyl nitrite. ---------- *n*-butyl nitrite. -.-.-.-.-.- sec. butyl nitrite. ····· tert. butyl nitrite. Beckman LiF $d=1$ meter $p\simeq 0.6$ mm Hg $T°=23°C$.

An alternative explanation would be the occurrence of fractional valences, with the formation of an $O^{\cdots}N^{\cdots}O$ group in the excited state. This would explain the fact that the uv band system seems to be characteristic, not of an NO single or double bond, but of the O−N=O group as a whole, as it is missing in the spectra of other substances with N−O or N=O bonds (inorganic and organic nitrates, inorganic nitrites, nitro- and nitroso-compounds).

(2) *Occurrence of Two Bands Systems*

As the infrared spectra, the ultraviolet spectra are characteristic (but to a lesser extent) of primary, secondary, and tertiary nitrites: all these spectra exhibit diffuse bands, but these bands are much broader in

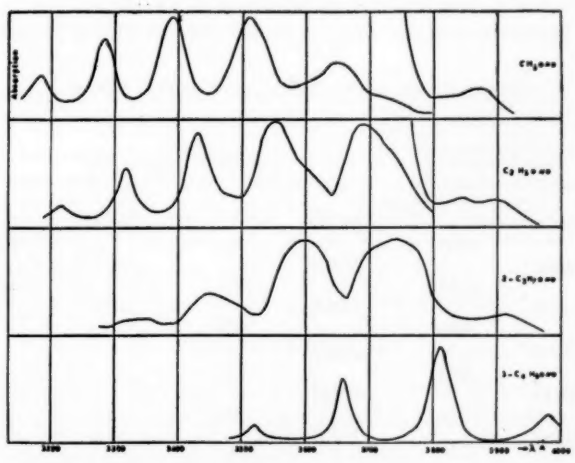

FIG. 4. Microphotometer tracings of the uv spectra of four alkyl nitrites (absorption in arbitrary units).

[10] W. Kuhn and E. Braum, Z. physik. Chem. **B8**, 445–454 (1930).
[11] W. Kuhn and H. Gore, Z. physik. Chem. **B12**, 389–397 (1931).
[12] S. Mitchell and S. Cormack, J. Chem. Soc. London, 415–419 (1932).
[13] T. Lowry and H. Hudson, Trans. Roy. Soc. (London) **232A**, 117 (1933).
[14] L. D'Or and P. Tarte, Bull. Soc. Roy. Sci. Liège, 685–692 (1951).
[15] D. Andrychuk, Can. J. Phys. **29**, 151–158 (1951).

TABLE IV. Ultraviolet spectrum of tert-butyl nitrite.

Wavelength measurements (A)	(cm^{-1})	Frequency interval (cm^{-1})
3982	25106	
		1126
3811	26232	
		1097
3658	27329	
		1088
3518	28417	
		1073
3390	29490	

secondary nitrites than in the primary ones; in tertiary nitrites, however, they are surprisingly much narrower.

Microphotometer tracings of the uv spectra of methyl, ethyl, sec-propyl, and tert-butyl nitrites are reproduced in Fig. 4. If we first consider the spectrum of tert-butyl nitrite, we find a very regular frequency interval (Table IV); the bands although diffuse, are not broad and their contour is very symmetrical. It is quite obvious that one, and only one, band system is present here. This is not the case with methyl nitrite, and the following facts must be pointed out:

(1) The first band is extremely broad, with an irregular contour. Moreover, the frequency interval between this first band and the following one is abnormally high according to Thompson:[7] 1700 cm^{-1} (Table V, A).

(2) A faint band appears near 3740A. This band cannot be fitted into the main band system.

(3) A small hump on the high frequency side of the 3651A band seems to show the existence of another band, which also cannot be fitted into the main band system.

All these irregularities are well explained by the existence of a second, weak band system, occurring on the low frequency side of the main band system. This leads to the new band classification of Table V, B.

In ethyl nitrite, the first four bands are obviously asymmetric, a fact which can be interpretated by an increase of the intensity of the second band system. This new band classification is reported in Table VI.

In sec-propyl nitrite, the bands are extremely broad,

TABLE V. Ultraviolet spectrum of methyl nitrite.

A.—Thompson's classification		B.—New classification			
		1st system		2nd system	
ν (cm^{-1})	$\Delta\nu$ (cm^{-1})	ν	$\Delta\nu$	ν	$\Delta\nu$
25674		26240		25770	
	1708		1142		960
27382		27382		26730	
	1116		1116		1040
28498		28498		27770	
	990		990		
29488		29488			
	953		953		
30441		30441			
	926		926		
31367		31367			
.					
.					
.					

and the contour asymmetry is now at the top of the bands. This is explained by the increased intensity of the second band system, which is now strong as the first one. Frequency measurements are quite fallacious, owing to the broad and diffuse nature of the bands. In tert-butyl nitrite, the only band system to be found is the second one, as shown by the low frequency of the bands.

Summarizing, the ultraviolet spectra of alkyl nitrites seem to consist essentially of two bands systems with approximately the same frequency interval, the relative intensities of the two systems varying strongly from one class of nitrites to another, but remaining roughly constant within a given class.

This is to be compared with the results, obtained in the infrared, on the existence and relative abundance of rotational isomers. This comparison, summarized in Table VII, strongly suggests that the two rotational isomers are responsible for the appearance of two band systems in the ultraviolet, the first system (on the high

TABLE VI. Ultraviolet spectrum of ethyl nitrite.

A.—Thompson's classification		B.—New classification			
		1st system		2nd system	
ν (cm^{-1})	$\Delta\nu$ (cm^{-1})	ν	$\Delta\nu$	ν	$\Delta\nu$
25582		~26000		~25630	
	1518		1100		1030
27100		27100		~26660	
	1060		1060		900
28169		28169		~27650	
	985		985		1040
29154		29154		~28690	
	994		994		
30148		30148			
	956		956		
31104		31104			

frequency side) being related to the *cis*-isomers. This hypothesis is confirmed by the fact that the relative intensities of the two systems depend on temperature, the first system being more intense at lower temperatures. (The experiments were made with gaseous methyl and ethyl nitrites, spectra being taken at $-78°$, $+20°$, and $+70°C$. The pressure was about 1 mm Hg, with an optical path of 3 meters.)

Two objections can however be put forward: (1) The frequency difference between the two rotational isomers is of the order of 50 cm^{-1} or less in the ground state; it becomes 400 or 500 cm^{-1} in the excited state. Although the rotational isomers should possess different electronic transition energies, such a difference is unexpected. (2) The relative intensities of the bands of *cis*- and *trans*-isomers are very different in the infrared and in the ultraviolet.

This objection is not serious because the *cis*- and *trans*-isomers should have different electronic transition probabilities, but the effect is much greater than expected.

It is worth while to remark that a very close analogy exists between alkyl nitrites and nitrous acid itself:

(1) The ir spectrum of the latter in the gaseous state[16,17] has shown that (a) The three characteristic frequencies of the O−N=O group are found also in nitrous acid. (b) The six fundamental frequencies of nitrous acid appear to be double;[16] this doubling is explained, as in alkyl nitrites, by rotational isomerism.

(2) The uv spectrum of nitrous acid[14,18,19] is essentially composed of three systems of diffuse bands, which exhibit a frequency interval of $\sim 1100\ cm^{-1}$.

TABLE VII.

Nitrite	Infrared	Ultraviolet
CH_3ONO	Two rotational isomers *cis* and *trans*.	Two band systems 1 and 2.
Primary nitrites	The relative abundance of the *trans*-isomer is greater than in CH_3ONO. It remains approximately constant in all the primary nitrites.	The relative intensity of the second system is greater than in CH_3ONO. It remains roughly constant in all the primary nitrites.
Secondary nitrites	The relative abundance of the *trans*-isomer is much greater.	The relative intensity of the 2nd system is also much greater.
Tertiary nitrites	The *trans*-isomer is by far the most abundant one. The *cis*-isomer has almost completely disappeared.	The second band system only is present.

ACKNOWLEDGMENTS

We wish to express our deep gratitude to Professor D'Or, under whose kind direction this work was carried out. We wish also to thank the Fonds National de la Recherche Scientifique and the Centre National Belge de Chimie Physique Moléculaire for financial support given to our laboratory for this work.

[16] L. D'or and P. Tarte, J. Chem. Phys. **19**, 1064 (1951); Bull. Soc. Roy. Sc. Liège, 1951, 478–496.
[17] Jones, Badger, and Moore, J. Chem. Phys. **19**, 1599–1604 (1951).
[18] P. Tarte, Bull. Soc. Chim. Belges **59**, 365–376 (1950).
[19] G. Porter, J. Chem. Phys. **19**, 1278–1281 (1951).

THE JOURNAL OF CHEMICAL PHYSICS VOLUME 20, NUMBER 10 OCTOBER, 1952

Approximate Treatment of the Effect of Centrifugal Distortion on the Rotational Energy Levels of Asymmetric-Rotor Molecules*

DANIEL KIVELSON AND E. BRIGHT WILSON, JR.
Mallinckrodt Chemical Laboratory, Harvard University, Cambridge, Massachusetts
(Received May 15, 1952)

A first-order treatment yields the relation

$$W=W_0+A_1W_0^2+A_2W_0J(J+1)+A_3J^2(J+1)^2+A_4J(J+1)\langle \mathbf{P}_z^2\rangle+A_5\langle \mathbf{P}_z^4\rangle+A_6W_0\langle \mathbf{P}_z^2\rangle$$

for the rotational energy W of a nonrigid asymmetric rotor. The A's are constants independent of the rotational quantum numbers (J, K_{-1}, K_{+1}) while W_0 is the rigid-rotor energy. $\mathbf{P}_z$ is the operator for the component of angular momentum along the axis of quantization. Formulas are given for $\langle \mathbf{P}_z^2\rangle$ and $\langle \mathbf{P}_z^4\rangle$, based on continued fractions, as well as expansions useful for nearly symmetric cases. As a special case, the corrections are derived for transitions between the components of asymmetry doublets.

INTRODUCTION

THE theory of centrifugal distortion in the rotational spectra of asymmetric rotor molecules has been formulated by several authors.[1] The exact solution of the problem involves the diagonalization of a Hamiltonian matrix which has off-diagonal elements $(K|\mathbf{H}|K\pm 2)$ and $(K|\mathbf{H}|K\pm 4)$ in a symmetric-rotor representation. In order to have a practical method with which to analyze rotational spectra, an approximate solution must be obtained which dispenses with the necessity of diagonalizing this complicated matrix directly. Golden[2] has devised such an approximate solution for the case in which the Mathieu function approximation for the rigid rotor applies,[3] while Cross[4] and Lawrance and Strandberg[5] have proposed a semiclassical analysis of the problem. In this paper a general quantum-mechanical approach based on first-order perturbation theory is proposed. An explicit correction term to the rigid-rotor energy levels is obtained.

GENERAL THEORY

Let $\mathbf{P}_\mu$ be the μ-component ($\mu=x$, y or z) of the angular-momentum operator, in units of $\hbar$, in the molecule-

* The research reported in this paper was made possible by support extended Harvard University by the ONR under ONR Contract N5ori-76, Task Order V.
[1] (a) E. B. Wilson, Jr., and J. B. Howard, J. Chem. Phys. **4**, 260 (1936); (b) E. B. Wilson, Jr., J. Chem. Phys. **5**, 617 (1937); (c) H. H. Nielsen, Revs. Modern Phys. **23**, 90 (1951).
[2] S. Golden, J. Chem. Phys. **16**, 250 (1948).
[3] S. Golden, J. Chem. Phys. **16**, 78 (1948).
[4] P. C. Cross, Phys. Rev. **47**, 7 (1935).
[5] R. B. Lawrance and M. W. P. Strandberg, Phys. Rev. **83**, 363 (1951).

fixed coordinate system, and let α', β', γ', and $\tau_{\mu\nu\xi\zeta}$ be constants independent of the rotational quantum numbers; then the Hamiltonian for the semirigid rotor is[6]

$$\mathbf{H}=\mathbf{H}_0'+\mathbf{H}_1', \tag{1}$$

$$\mathbf{H}_0'=\alpha'\mathbf{P}_x^2+\beta'\mathbf{P}_x^2+\gamma'\mathbf{P}_y^2, \tag{2}$$

$$\mathbf{H}_1'=\tfrac{1}{4}\hbar^4\sum\tau_{\mu\nu\xi\zeta}\mathbf{P}_\mu\mathbf{P}_\nu\mathbf{P}_\xi\mathbf{P}_\zeta. \tag{3}$$

Here $\mathbf{H}_0'$ is the Hamiltonian of an effective rigid rotor with

$$\alpha'=\hbar^2/2I_x;\quad \beta'=\hbar^2/2I_x;\quad \gamma'=\hbar^2/2I_y,$$

I_x, I_y, and I_z being the effective principal moments of inertia for the given vibrational state. $\mathbf{H}_1'$ is the centrifugal distortion term, the parameters of which depend upon the geometry and force constants of the molecule.[1(b)] It will be assumed that the effect of $\mathbf{H}_1'$ is small so that it may be treated by first-order perturbation theory. The solution for the eigenvalues of $\mathbf{H}_0'$, the zeroth-order approximation to $\mathbf{H}$, has been discussed by King, Hainer, and Cross.[7]

In most cases of interest, many of the constants in $\mathbf{H}_1'$ vanish. For the case of orthorhombic symmetry there are twenty-one nonvanishing coefficients in $\mathbf{H}_1'$: $\tau_{\mu\mu\mu\mu}$, $\tau_{\mu\mu\nu\nu}=\tau_{\nu\nu\mu\mu}$, $\tau_{\mu\nu\mu\nu}=\tau_{\mu\nu\nu\mu}=\tau_{\nu\mu\mu\nu}=\tau_{\nu\mu\nu\mu}$, where $\nu\neq\mu$.[1(b)] This leaves nine different coefficients, although in an H_2O type molecule only four of the coefficients are linearly independent. For nonorthorhombic molecules there are other nonvanishing coefficients which multiply operators that introduce $(K|K\pm1)$ and $(K|K\pm3)$ elements into the Hamiltonian in the symmetric-rotor basis. However, these terms alter the rigid-rotor energy levels in second order only and so can be neglected in this treatment. To show this, first consider the effect of a unitary transformation of the energy matrix by means of the Wang matrix.[8] In particular if the energy matrix is that of a rigid rotor, the transformation factors it into four submatrices designated as $\mathbf{E}^+$, $\mathbf{E}^-$, $\mathbf{O}^-$, and $\mathbf{O}^+$ by KHC. This factoring fails if the energy matrix is that of a general nonrigid asymmetric rotor.[1(c)] In this case, the transformed energy matrix consists of four submatrices along the diagonal with only $(K|K)$, $(K|K\pm2)$, and $(K|K\pm4)$ elements, these blocks corresponding to the $\mathbf{E}^\pm$ and $\mathbf{O}^\pm$ matrices of KHC, and only $(K|K\pm1)$ and $(K|K\pm3)$ elements outside these blocks. If the energy matrix is now transformed to the rigid-asymmetric-rotor basis, no $(K|K\pm1)$ or $(K|K\pm3)$ elements will enter the diagonal blocks, and so in first order they will not affect the energy even in the symmetric rotor limit.

[6] There are cases where the effect of terms in the sixth power of $\mathbf{P}$ must be considered. See W. S. Benedict, Phys. Rev. 75, 1317A (1949).

[7] King, Hainer, and Cross, J. Chem. Phys. 11, 27 (1943), referred to as KHC; King, Hainer, and Cross, J. Chem. Phys. 17, 826 (1949), referred to as KHC II.

[8] S. C. Wang, Phys. Rev. 34, 243 (1929).

Reduction of Distortion Terms

The commutation rules for angular momentum,[9]

$$\mathbf{P}_\nu\mathbf{P}_\mu-\mathbf{P}_\mu\mathbf{P}_\nu=-i\mathbf{P}_\rho \tag{4}$$

(where ν, μ, ρ are in cyclic order), can be used to eliminate the $\mu\nu\mu\nu$ terms in $\mathbf{H}_1'$. The result of this procedure is a change in the coefficients of the remaining terms and the introduction of terms in $\mathbf{P}_\mu^2$ which can be absorbed into $\mathbf{H}_0'$. The new form of $\mathbf{H}$ is then

$$\mathbf{H}=\mathbf{H}_0+\mathbf{H}_1, \tag{5}$$

$$\mathbf{H}_0=\alpha\mathbf{P}_x^2+\beta\mathbf{P}_x^2+\gamma\mathbf{P}_y^2, \tag{6}$$

$$\mathbf{H}_1=\tfrac{1}{4}\sum_{\mu\nu}\tau'_{\mu\mu\nu\nu}\mathbf{P}_\mu^2\mathbf{P}_\nu^2. \tag{7}$$

The relations between the new coefficients α, β, γ, $\tau'_{\mu\mu\nu\nu}$ and the old ones are given in the appendix.

The total angular momentum

$$\mathbf{P}^2=\mathbf{P}_x^2+\mathbf{P}_y^2+\mathbf{P}_z^2 \tag{8}$$

commutes with $\mathbf{H}$, and with $\mathbf{H}_0$, and so is a constant matrix as far as the present problem is concerned, with diagonal values $J(J+1)$. Since $\mathbf{P}^2$ commutes with $\mathbf{P}_x^2$ and $\mathbf{P}_y^2$, we can form the useful operator products, $\mathbf{P}_x^2\mathbf{P}^2+\mathbf{P}^2\mathbf{P}_x^2$ and $\mathbf{P}_y^2\mathbf{P}^2+\mathbf{P}^2\mathbf{P}_y^2$:

$$\begin{aligned}\mathbf{P}_x^2\mathbf{P}^2+\mathbf{P}^2\mathbf{P}_x^2&=2J(J+1)\mathbf{P}_x^2\\&=2\mathbf{P}_x^4+(\mathbf{P}_x^2\mathbf{P}_y^2+\mathbf{P}_y^2\mathbf{P}_x^2)+(\mathbf{P}_z^2\mathbf{P}_x^2+\mathbf{P}_x^2\mathbf{P}_z^2);\end{aligned} \tag{9}$$

$$\begin{aligned}\mathbf{P}_y^2\mathbf{P}^2+\mathbf{P}^2\mathbf{P}_y^2&=2J(J+1)\mathbf{P}_y^2\\&=2\mathbf{P}_y^4+(\mathbf{P}_y^2\mathbf{P}_x^2+\mathbf{P}_x^2\mathbf{P}_y^2)+(\mathbf{P}_z^2\mathbf{P}_y^2+\mathbf{P}_y^2\mathbf{P}_z^2).\end{aligned} \tag{10}$$

Another relation which will be of use is the expression for $\mathbf{H}_0^2$ obtained by squaring Eq. (6):

$$\begin{aligned}\mathbf{H}_0^2=&\alpha^2\mathbf{P}_x^4+\beta^2\mathbf{P}_x^4+\gamma^2\mathbf{P}_y^4+\alpha\beta(\mathbf{P}_x^2\mathbf{P}_x^2+\mathbf{P}_x^2\mathbf{P}_x^2)\\&+\beta\gamma(\mathbf{P}_x^2\mathbf{P}_y^2+\mathbf{P}_y^2\mathbf{P}_x^2)+\gamma\alpha(\mathbf{P}_y^2\mathbf{P}_x^2+\mathbf{P}_x^2\mathbf{P}_y^2).\end{aligned} \tag{11}$$

Next we can use Eq. (8) in order to eliminate $\mathbf{P}_y^2$ in the expression for $\mathbf{H}_0$, Eq. (6). We then square $\mathbf{H}_0$ and differentiate with respect to α, thus obtaining

$$\begin{aligned}\partial\mathbf{H}_0^2/\partial\alpha=&2(\alpha-\gamma)\mathbf{P}_z^4\\&+(\beta-\gamma)(\mathbf{P}_x^2\mathbf{P}_x^2+\mathbf{P}_x^2\mathbf{P}_x^2)+2\gamma J(J+1)\mathbf{P}_z^2.\end{aligned} \tag{12}$$

We can also derive a similar expression in which $\mathbf{P}_z^2$ rather than $\mathbf{P}_y^2$ has been eliminated:

$$\begin{aligned}\partial\mathbf{H}_0^2/\partial\alpha=&2(\alpha-\beta)\mathbf{P}_z^4\\&+(\gamma-\beta)(\mathbf{P}_y^2\mathbf{P}_x^2+\mathbf{P}_x^2\mathbf{P}_y^2)+2\beta J(J+1)\mathbf{P}_z^2.\end{aligned} \tag{13}$$

If W_0 is the energy of the rigid rotor $\mathbf{H}_0$, it has been shown[10] that

$$\langle\mathbf{P}_z^2\rangle=\langle\partial\mathbf{H}_0/\partial\alpha\rangle=\partial W_0/\partial\alpha, \tag{14}$$

where the brackets $\langle\ \rangle$ stand for the diagonal elements (average values) of the enclosed operators in a basis

[9] O. Klein, Z. Physik 58, 730 (1929).

[10] J. K. Bragg and S. Golden, Phys. Rev. 75, 735 (1949).

which diagonalizes $\mathbf{H}_0$. Similarly it can be shown that

$$\langle\partial(\mathbf{H}_0^2)/\partial\alpha\rangle=\partial W_0^2/\partial\alpha=2W_0\langle\mathbf{P}_z^2\rangle. \quad (15)$$

Since the present treatment is a first-order one, the desired energies will involve only the diagonal values of the perturbing operators. Consequently, the equations above relating the various operators appearing in $\mathbf{H}_1$ will ultimately be used only for their diagonal values. With the aid of Eq. (15) and the fact that $\langle\mathbf{H}_0^2\rangle=W_0^2$, we can consider Eqs. (9) through (13) as average value equations which can be solved so that $\langle\mathbf{P}_x^4\rangle$, $\langle\mathbf{P}_y^4\rangle$, $\langle\mathbf{P}_x^2\mathbf{P}_y^2+\mathbf{P}_y^2\mathbf{P}_x^2\rangle$, $\langle\mathbf{P}_y^2\mathbf{P}_z^2+\mathbf{P}_z^2\mathbf{P}_y^2\rangle$, and $\langle\mathbf{P}_z^2\mathbf{P}_x^2+\mathbf{P}_x^2\mathbf{P}_z^2\rangle$ can be expressed in terms of $J(J+1)\langle\mathbf{P}_x^2\rangle$, $J(J+1)\langle\mathbf{P}_y^2\rangle$, $J(J+1)\langle\mathbf{P}_z^2\rangle$, $\langle\mathbf{P}_z^4\rangle$, W_0^2, and $W_0\langle\mathbf{P}_z^2\rangle$. Furthermore, we can use Eqs. (6) and (8) to solve for $\langle\mathbf{P}_x^2\rangle$ in terms of $\langle\mathbf{P}_z^2\rangle$,

$$\langle\mathbf{P}_x^2\rangle=[W_0-\gamma J(J+1)-(\alpha-\gamma)\langle\mathbf{P}_z^2\rangle]/(\beta-\gamma). \quad (16)$$

A similar expression may be obtained for $\langle\mathbf{P}_y^2\rangle$. If we substitute all these results into $\mathbf{H}_1$, we obtain the following expression for the energy of the nonrigid rotor to first order:

$$W=W_0+A_1W_0^2+A_2W_0J(J+1)+A_3J^2(J+1)^2 +A_4J(J+1)\langle\mathbf{P}_z^2\rangle+A_5\langle\mathbf{P}_z^4\rangle+A_6W_0\langle\mathbf{P}_z^2\rangle. \quad (17)$$

The values of the constants A_j in terms of the original τ's are given in the appendix. It should be noted that the A's are independent of the rotational quantum numbers. W_0 is the rigid-rotor energy and can be solved by well-known methods.[7] The evaluation of $\langle\mathbf{P}_z^2\rangle$ has been treated by Golden and Bragg,[10] and is discussed further below. If force constants and fairly good structural parameters are available, the constants A_j can be calculated, although this is often a laborious procedure. The evaluation of $\langle\mathbf{P}_z^4\rangle$ will be taken up in the following section.

We note that although there may be nine relevant distortion constants, only six linear combinations of them enter into the final result. It may often be desirable to evaluate the constants A_j empirically from rotational spectra. The general procedure would be to calculate the rigid-rotor parameters from lines with small rotational quantum numbers, hence with little centrifugal distortion. With these parameters we can calculate W_0 for the various higher levels and thus determine the frequencies the absorption lines would have if the molecule were a rigid rotor. The difference between observed and calculated frequencies is attributed to the effect of centrifugal distortion. If enough absorption lines with appreciable centrifugal distortion are observed, we can evaluate the A's by fitting them to these frequency differences. If more accuracy is desired, these distortion constants may be used to recalculate the lines of low rotational quantum numbers, thus yielding more accurate structural parameters, and the entire process can be repeated.

The difference between Eqs. (2) and (6) introduces an additional ambiguity into the definition of the moment of inertia besides that which arises from the vibrational effects[1(b)]; this ambiguity is transmitted to the interatomic parameters. If we are to keep the classical model of a rigid rotor with centrifugal distortion in analogy with classical mechanics, the quantities α', β', γ' should define the moments of inertia. However, in practice the quantities α, β, γ are measured.

EVALUATION OF $\langle P_z^4\rangle$

As a general approach consider

$$\mathbf{H}''=a\mathbf{P}_a^2+b\mathbf{P}_b^2+c\mathbf{P}_c^2+\tfrac{1}{2}(a-c)q\mathbf{\Pi} =\mathbf{H}_0+\tfrac{1}{2}(a-c)q\mathbf{\Pi}, \quad (18)$$

where a, b, c are parameters corresponding to α, β, γ with the additional condition that $a\geqslant b\geqslant c$, q is independent of the rotational quantum numbers and $\mathbf{\Pi}$ is an operator which is diagonal in the limiting symmetric-rotor basis. $\mathbf{H}''$ can be re-expressed as

$$\mathbf{H}''=\tfrac{1}{2}(a+c)J(J+1)+\tfrac{1}{2}(a-c)\mathfrak{X}'(\kappa,q) +\tfrac{1}{2}(a-c)FJ(J+1), \quad (19)$$

where F is a constant defined by KHC, $\kappa=(2b-a-c)/(a-c)$ and $\mathfrak{X}'(\kappa,q)=\mathfrak{X}(\kappa)+q\mathbf{\Pi}$. In a manner similar to that used in the preceding section, we have

$$\langle\mathbf{\Pi}\rangle=[2/(a-c)](\partial W''/\partial q)_{q=0}=[\partial\lambda'(\kappa,q)/\partial q]_{q=0}, \quad (20)$$

where W'' and λ' are the eigenvalues of $\mathbf{H}''$ and $\mathfrak{X}'$, respectively. Using a notation and method similar to that employed by KHC we can write down an expression for λ' in terms of continued fractions:

$$\lambda'=k_m+q\Pi_m - \cfrac{b_m}{k_{m-1}-\lambda'+q\Pi_{m-1}-\cfrac{b_{m-1}}{k_{m-2}-\lambda'+q\Pi_{m-2}-\cdots}} - \cfrac{b_{m+1}}{k_{m+1}-\lambda'+q\Pi_{m+1}-\cfrac{b_{m+2}}{k_{m+2}-\lambda'+q\Pi_{m+2}-\cdots}}. \quad (21)$$

Here Π_m stands for the mm element of $\mathbf{\Pi}$ in the limiting symmetric-rotor basis. We now introduce the symbols R_n and R_n', where

$$R_n=b_{n+1}/[k_n-\lambda-b_n/(k_{n-1}-\lambda-\cdots)]^2,$$
$$R_n'=b_n/[k_n-\lambda-b_{n+1}/(k_{n+1}-\lambda-\cdots)]^2.$$

The differentiation of λ' with respect to q yields, in combination with Eq. (20),

$$[\partial\lambda'/\partial q]_{q=0}=\langle\mathbf{\Pi}\rangle=\Pi_m+R_{m-1}\{(\Pi_{m-1}-\langle\mathbf{\Pi}\rangle) +R_{m-2}[(\Pi_{m-2}-\langle\mathbf{\Pi}\rangle)+R_{m-3}(\cdots)]\} +R'_{m+1}\{(\Pi_{m+1}-\langle\mathbf{\Pi}\rangle)+R'_{m+2} \times[(\Pi_{m+2}-\langle\mathbf{\Pi}\rangle)+\cdots]\}. \quad (22)$$

This series should have convergence properties similar

to those of the continued fraction above. This gives upon rearrangement

$$\langle \Pi \rangle = \{1+R_{m-1}[1+R_{m-2}(1+\cdots)] + R'_{m+1}[1+R'_{m+2}(1+\cdots)]\}^{-1} \times \{\Pi_m + R_{m-1}[\Pi_{m-1}+R_{m-2}(\cdots)] + R'_{m+1}[\Pi_{m+1}+R'_{m+2}(\cdots)]\}. \quad (23)$$

Except when $E/J(J+1)$, the reduced energy ratio defined by King[11], is nearly equal to κ; only a few terms in the series should be required, particularly since $\langle \Pi \rangle$ enters in a correction term to the rigid-rotor energy and so need not be known as accurately as the latter. The actual calculation of $\langle \Pi \rangle$ is rendered simpler by the fact that it requires only one arithmetic step to evaluate R_n or R_n' from the data obtained when the continued-fraction method is used to calculate rigid-rotor energy levels. By substituting K^2 for Π_m and $(K\pm 2n)^2$ for $\Pi_{m\pm n}$, and choosing the appropriate submatrix (see KHC), the procedure above yields $\langle \mathbf{P}_z^2 \rangle$; by substituting K^4 for Π_m and $(K\pm 2n)^4$ for $\Pi_{m\pm n}$, we get $\langle \mathbf{P}_z^4 \rangle$.

In certain cases, where the asymmetry is slight, it is useful to expand Eq. (23) in terms of an asymmetry parameter. For a slightly asymmetric prolate molecule we use the asymmetry parameter $\delta=(b-c)/(a-c)$, where $0 \leqslant \delta \leqslant 1$. The result is

$$\langle \mathbf{P}_z^2 \rangle = K^2 + \{f(J,K-1)/16(1-K) + f(J,K+1)/16(1+K)\}\delta^2 + 0(\delta^3) + \cdots, \quad (24)$$

$$\langle \mathbf{P}_z^4 \rangle = K^4 + 2\{(K^2-2K+2)f(J,K-1)/16(1-K) + (K^2+2K+2)f(J,K+1)/16(1+K)\}\delta^2 + 0(\delta^3) + \cdots, \quad (25)$$

where K is the quantum number of the limiting prolate rotor and

$$f(J,n) = \tfrac{1}{4}[J(J+1)-n(n-1)][J(J+1)-n(n+1)],$$

except that

$$f(J,1) = \tfrac{1}{2}[J(J+1)][J(J+1)-2].$$

For not too great asymmetry this formula is very satisfactory since it is easy to use and the accuracy required for the correction term is not too stringent. In certain cases rougher approximations will do. Thus for very slight asymmetry

$$\langle \mathbf{P}_z^4 \rangle \cong \langle \mathbf{P}_z^2 \rangle^2 \cong K^4.$$

In the region where $E/J(J+1)$ is very different from κ, K_{-1} large, and the asymmetry slight, a somewhat better approximation is

$$\langle \mathbf{P}_z^4 \rangle \cong \langle \mathbf{P}_z^2 \rangle^2 = (\partial W_0/\partial \alpha)^2.$$

If this approximation is inserted in Eq. (17), the semi-classical relation of Lawrence and Strandberg[5] is obtained.

Thus with these methods of evaluating $\langle \mathbf{P}_z^2 \rangle$ and $\langle \mathbf{P}_z^4 \rangle$, Eqs. (23), (24), and (25), the expression for the energy (17) may be used either by calculating the distortion constants from infrared force-constant data[12] or by obtaining them empirically from the rotational spectrum.

Special Case—Doublet Splitting

An important case consists of transitions where $\Delta J=0$ and $\Delta K=0$, K being the quantum number associated with the limiting symmetric rotor, it being understood that $E/J(J+1)$ and κ differ greatly. In the notation of KHC, for even K, the frequency ν_0 of the transition for a rigid rotor is the difference of the appropriate eigenvalues of the $\mathbf{E}^+$ and $\mathbf{E}^-$ submatrices, except for a factor $\frac{1}{2}(a-c)$. This difference becomes non-vanishing in the Kth order perturbation. To this order ν_0 is given by

$$\nu_0 = \tfrac{1}{2}(a-c)(E_{K:K-2}E_{K-2:K-4}\cdots E_{20}E_{02}\cdots E_{K-2:K})/ (E_{K:K}-E_{K-2:K-2})(E_{K:K}-E_{K-4:K-4})\cdots \times (E_{K:K}-E_{00})\cdots(E_{K:K}-E_{K-2:K-2}). \quad (26)$$

If the explicit expressions for the elements in this equation are inserted, Eq. (26) becomes the Wang[8] splitting formula. Now consider matrices $\mathbf{E}^{\pm}+q\mathbf{\Pi}$. The transition frequency in this system is similar to that above except that the denominator has factors of the form $(E_{KK}-E_{K-2n:K-2n}+q\Pi_m-q\Pi_{m-n})$ instead of those in (26). We can now expand the denominators, retaining terms only through the first power in q. Subtracting ν_0 from this result and expressing the difference in terms of ν_0, we get

$$q\Delta\langle \mathbf{\Pi} \rangle = q\langle \mathbf{\Pi} \rangle^+ - q\langle \mathbf{\Pi} \rangle^- = -\frac{2\nu_0 q}{a-c}\left[\frac{\Pi_m-\Pi_0}{E_{KK}-E_{00}} + 2\left\{\frac{\Pi_m-\Pi_1}{E_{KK}-E_{22}} + \frac{\Pi_m-\Pi_2}{E_{KK}-E_{44}} + \cdots \frac{\Pi_m-\Pi_{m-1}}{E_{KK}-E_{K-2:K-2}}\right\}\right]. \quad (27)$$

Next both sides are divided by q. From KHC we see that $(E_{K:K}-E_{K-2n:K-2n}) = (G-F)[(K-2n)^2-K^2]$, where G and F are given in terms of asymmetry parameters. After making these substitutions and letting Π_{m-n} equal $(K-2n)^2$ for $\langle \mathbf{P}_z^2 \rangle$ and $(K-2n)^4$ for $\langle \mathbf{P}_z^4 \rangle$, we can sum Eq. (27) with the results

$$\Delta\langle \mathbf{P}_z^2 \rangle = [2/(a-c)]\nu_0(1-K)/(G-F), \quad (28)$$

$$\Delta\langle \mathbf{P}_z^4 \rangle = -[2/(a-c)]\nu_0 \tfrac{2}{3}K(K-1)(2K-1)/(G-F). \quad (29)$$

We now have to consider the case of odd K. Here the frequency of transition is the difference between the eigenvalues of the $\mathbf{O}^+$ and $\mathbf{O}^-$ submatrices of KHC. This difference also becomes nonzero in the Kth-order perturbation. However, while for even K the $\mathbf{E}^-$ matrix had a vanishing Kth-order term, both $\mathbf{O}^+$ and $\mathbf{O}^-$ have

[11] G. W. King, J. Chem. Phys. 15, 820 (1947).

[12] M. H. Sirvetz, J. Chem. Phys. 19, 938 (1951). (SO_2).

finite Kth-order terms. These terms are similar in form to the expression in (26) except that we have odd-numbered elements here. The $\mathbf{O}^+$ and $\mathbf{O}^-$ terms differ from each other in that the $(K|K)-(1|1)$ terms in the denominators are $(E_{K:K}-E_{1:1}+E_{1:-1})$ and $(E_{K:K}-E_{1:1}-E_{1:-1})$, respectively. Expanding these terms in the denominators in powers of $E_{1:-1}$ and retaining only the linear ones, we obtain for the rigid rotor energy

$$\nu_0=\tfrac{1}{2}(a-c)(E_{K:K-2}E_{K-2:K-4}\cdots \times E_{3:1}E_{1:3}\cdots E_{K-2:K})2E_{1:-1} \times[(E_{K:K}-E_{K-2:K-2})\cdots(E_{K:K}-E_{1:1})]^{-2}. \quad (30)$$

From here we proceed exactly as for even K, the results being the same.

We now turn back to Eq. (17) for the energy of the nonrigid rotor. The difference between two energy levels i and j is formed ($\nu=W^{(i)}-W^{(j)}$ and $\nu_0=W_0{}^{(i)}-W_0{}^{(j)}$), yielding

$$\nu=\nu_0+2A_1W_0\nu_0+A_2J(J+1)\nu_0+A_4J(J+1)\Delta\langle\mathbf{P}_z^2\rangle +A_5\Delta\langle\mathbf{P}_z^4\rangle+A_6[W_0\Delta\langle\mathbf{P}_z^2\rangle+\langle\mathbf{P}_z^2\rangle\nu_0]. \quad (31)$$

The distinction between $W_0{}^{(i)}$ and $W_0{}^{(j)}$ and between $\langle\mathbf{P}_z^2\rangle^{(i)}$ and $\langle\mathbf{P}_z^2\rangle^{(j)}$ has been dropped except where they enter as differences. Let $W_0=\frac{1}{2}(b+c)[J(J+1)-K^2]+aK^2$ and introduce Eqs. (28) and (29) into (31). We then get

$$\nu=\nu_0\{1+[2KJ(J+1)\delta_J/H +(K-1)J(J+1)D_{JK}/(G-F) -(4/3)K(K^2+2)R_5/H +\tfrac{2}{3}K(K-1)(2K-1)D_K/(G-F) +(8/3)K(K^2-1)R_6(G-F)/H^2]2/(a-c)\}. \quad (32)$$

The distortion constants appearing in (32) are given in the appendix. Terms of the form $R_6/(G-F)$ have been dropped in (32), since under the conditions for which the formula is valid, these terms will be small compared to those of the form $R_6(G-F)/H^2$ which appear in the equation. (See KHC and KHC II for the definition of H and the relative magnitudes of these quantities.) Equation (32) is similar to the relation given by Hillger and Strandberg[13] though not exactly the same.

APPENDIX

The relations of the coefficients of Eqs. (6) and (7) to those of (2) and (3) are

$$\tau'_{zzzz}=\tau_{zzzz}\hbar^4, \quad \tau'_{xxyy}=(\tau_{xxyy}+2\tau_{xyxy})\hbar^4,$$
$$\tau'_{xxxx}=\tau_{xxxx}\hbar^4, \quad \tau'_{yyzz}=(\tau_{yyzz}+2\tau_{yzyz})\hbar^4, \quad (33)$$
$$\tau'_{yyyy}=\tau_{yyyy}\hbar^4, \quad \tau'_{zzxx}=(\tau_{zzxx}+2\tau_{zxzx})\hbar^4,$$

and

$$\alpha=\alpha'+(3\tau_{xyxy}-2\tau_{xxxx}-2\tau_{yzyz})\hbar^4/4,$$
$$\beta=\beta'+(3\tau_{yzyz}-2\tau_{xyxy}-2\tau_{zxzx})\hbar^4/4, \quad (34)$$
$$\gamma=\gamma'+(3\tau_{zxzx}-2\tau_{xyxy}-2\tau_{zyzy})\hbar^4/4.$$

After suitable manipulations of Eqs. (6) through (16) we obtain Eq. (17), where

$$A_1=16R_6/(\beta-\gamma)^2,$$
$$A_2=-[16R_6(\beta+\gamma)/(\beta-\gamma)^2+4\delta_J/(\beta-\gamma)],$$
$$A_3=-D_J+2R_6+16R_6\beta\gamma/(\beta-\gamma)^2 +2\delta_J(\beta+\gamma)/(\beta-\gamma), \quad (35)$$
$$A_4=-[D_{JK}-2\delta_J\sigma-16R_6(\alpha^2-\beta\gamma)/(\beta-\gamma)^2 +4R_6\sigma^2+4R_5(\gamma+\beta)/(\beta-\gamma)],$$
$$A_5=-(D_K+4R_5\sigma+2R_6-4R_6\sigma^2),$$
$$A_6=(8R_5-16R_6\sigma)/(\beta-\gamma),$$

and

$$\sigma=(2\alpha-\beta-\gamma)/(\beta-\gamma),$$
$$D_J=-(1/32)(3\tau_{xxxx}+3\tau_{yyyy} +2\tau_{xxyy}+4\tau_{xyxy})\hbar^4,$$
$$D_K=D_J-\tfrac{1}{4}(\tau_{zzzz}-\tau_{zzxx}-\tau_{yyzz} -2\tau_{zxzx}-2\tau_{yzyz})\hbar^4, \quad (36)$$
$$D_{JK}=-D_J-D_K-\tfrac{1}{4}\tau_{zzzz}\hbar^4,$$
$$R_5=-1/32[\tau_{xxxx}-\tau_{yyyy}-2(\tau_{xxzz}+2\tau_{zxzx}) +2(\tau_{yyzz}+2\tau_{yzyz})]\hbar^4,$$
$$R_6=1/64[\tau_{xxxx}+\tau_{yyyy}-2(\tau_{xxyy}+2\tau_{xyxy})]\hbar^4,$$
$$\delta_J=-1/16(\tau_{xxxx}-\tau_{yyyy})\hbar^4.$$

The last five constants are those used by Nielsen,[1(c)] in energy units, in terms of the τ's given by Wilson.[1(b)]

In the limit of the symmetric rotor R_5, R_6, and δ_J vanish and $\beta=\gamma$. Making use of the equations used in deriving (17), we can show that the factors multiplying R_5, R_6, and δ_J are finite. With these results and remembering that $\langle\mathbf{P}_z^4\rangle=\langle\mathbf{P}_z^2\rangle^2=K^4$ in the symmetric rotor limit, we find that equation (17) becomes

$$W=W_0-D_JJ^2(J+1)^2-D_{JK}J(J+1)K^2-D_KK^4, \quad (37)$$

which is the result given by Dennison and Slawsky[14] for this limit.

[13] R. E. Hillger and M. W. P. Strandberg, Phys. Rev. **83**, 575 (1951).

[14] Z. I. Slawsky and D. M. Dennison, J. Chem. Phys. **7**, 509 (1939).

Solutions of Some Problems Concerning Long Random Coils

C. A. HOLLINGSWORTH
Department of Chemistry, University of Pittsburgh, Pittsburgh, Pennsylvania
(Received April 14, 1952)

The problem of random flights in boundary value form is used to determine certain probabilities related to the probability that a long random coil passes within a given distance of one or more given points.

INTRODUCTION

SUPPOSE that an object starts at the origin of a coordinate system and makes N successive displacements $\mathbf{r}_i$ $(i=1, \cdots, N)$. The total displacement of the object is then given by

$$\mathbf{R}=\sum_{i=1}^{N}\mathbf{r}_i. \tag{1}$$

Suppose also that the individual displacements are independent of each other in magnitude and direction and are governed statistically by the function

$$\tau(\xi, \eta, \zeta)d\xi d\eta d\zeta, \tag{2}$$

which gives the *a priori* probability that the components of the displacements are in the range

$$\xi, \xi+d\xi; \eta, \eta+d\eta; \zeta, \zeta+d\zeta. \tag{3}$$

The *problem of random flights* is the following problem: Determine the probability density $W(N, \mathbf{R})$ such that

$$W(N, \mathbf{R})dv=W(N, x, y, z)dxdydz \tag{4}$$

is the probability that the vector sum $\mathbf{R}$, given by Eq. (1), has components in the range

$$x, x+dx; y, y+dy; z, z+dz. \tag{5}$$

This problem was treated by Lord Rayleigh[1] in 1880 and has received considerable attention since. The treatments of various aspects of the problem have been recently reviewed and in some cases extended by S. Chandrasekhar.[2]

In problems where the individual steps are not independent of each other in direction or length, it is often possible to determine a number s such that $\tau_i(\mathbf{r}_i)$ can be considered to be independent of $\mathbf{r}_{i-s}$. The problem then becomes one of random flights in which the total number of "random" displacements is N/s, and the length of each "random" displacement is the average of the vector sum of s "dependent" displacements. This method has been introduced into the treatment of polymer molecules by W. Kuhn.[3,4]

The solution of the problem of random flights takes the following simple form in the important case where the number of displacements N is large[2,5] $(N>10)$:

$$W(N, \mathbf{R})=1/(8\pi^3N^3\langle\xi^2\rangle\langle\eta^2\rangle\langle\zeta^2\rangle)^{\frac{1}{2}} \times\exp\left[\frac{-(x-N\langle\xi\rangle)^2}{2N\langle\xi^2\rangle}-\frac{(y-N\langle\eta\rangle)^2}{2N\langle\eta^2\rangle}-\frac{(z-N\langle\zeta\rangle)^2}{2N\langle\zeta^2\rangle}\right], \tag{6}$$

where $\langle\xi\rangle, \cdots, \langle\zeta^2\rangle$, denote the various first and second moments of (ξ, η, ζ). The coordinate system (ξ, η, ζ) has been so chosen that the second moments of the type $\langle\xi\eta\rangle, \cdots, \langle\eta\xi\rangle$ do not appear.

It can be shown that Eq. (6) is a solution of the following differential equation:

$$\frac{\partial W}{\partial N}=\tfrac{1}{2}\left[\langle\xi^2\rangle\frac{\partial^2W}{\partial x^2}+\langle\eta^2\rangle\frac{\partial^2W}{\partial y^2}+\langle\zeta^2\rangle\frac{\partial^2W}{\partial z^2}\right] -\left[\langle\xi\rangle\frac{\partial W}{\partial x}+\langle\eta\rangle\frac{\partial W}{\partial y}+\langle\zeta\rangle\frac{\partial W}{\partial z}\right]. \tag{7}$$

In case $\tau(\xi, \eta, \zeta)$ is spherically symmetric, Eqs. (6) and (7) simplify to

$$W(N, \mathbf{R})=\left(\frac{3}{2\pi Nl^2}\right)^{\frac{3}{2}}\exp[-3|\mathbf{R}|^2/2Nl^2] \tag{8}$$

and to the diffusion equation,

$$\frac{\partial W}{\partial N}=\frac{l^2}{6}=-\nabla^2W, \tag{9}$$

where l^2 is the mean square of $|\mathbf{r}|$ given by

$$l^2=4\pi\int r^2\tau(r)dr. \tag{10}$$

Equation (7) or (9) is useful for obtaining the solution of the random flight problem for large values of N when boundary conditions apply.

In this paper Eqs. (8) and (9) are used to obtain approximate solutions to some problems concerned with the probability that an object undergoing random flight passes by one or more given points during N flights. Since the path of an object undergoing random flight is a "random chain" or a "random coil," the problems can be stated in terms of the probability that a random coil

[1] Lord Rayleigh, Phil. Mag. **10**, 73 (1880) or *Scientific Papers of Lord Rayleigh*, Vol. I.
[2] S. Chandrasekhar, Revs. Modern Phys. **15**, 1 (1943).
[3] W. Kuhn, Kolloid-Z. **68**, 2 (1934).
[4] W. Kuhn and H. Kuhn, J. Colloid Sci. **3**, 11 (1948).
[5] M. H. Quenouille, Proc. Cambridge Phil. Soc. **43**, 581 (1947).

passes by one or more given points. This terminology is used in the statements of the problems treated here.

PROBLEM 1

Determine the probability $\beta(N, \mathbf{R}; \mathbf{P})\rho dv$ *that a random coil of N links, which starts at the origin, passes within a distance* ρ *of the point* $\mathbf{P}$ *at least once and then ends in the volume element* dv *at* $\mathbf{R}(|\mathbf{P}| \ll Nl, |\mathbf{R}| \ll Nl, l \ll \rho \ll |\mathbf{P}|)$.

An approximate solution to this problem, for the conditions stated, can be obtained by solving the approximate boundary value problem. The method, which is not new in principle, is similar to that used previously by the author to obtain approximately some "boundaries" of the random coil.[6,7]

The restriction that $l \ll \rho$ must be imposed to take care of the fact that this random flight problem cannot be represented by a boundary value problem when ρ is not sufficiently large relative to l. This is due to the discrete nature of the random flight phenomenon. In random flight l is the average length of discrete, linear flights, while in the boundary value problem l has no such discrete significance.

We place an "absorbing" sphere of radius ρ at $\mathbf{P}$ and consider the function $W(N, \mathbf{R}; \mathbf{P}, \rho)$, which represents a solution of Eq. (9) corresponding to $W(N, \mathbf{R})$ but modified by the presence of the "absorbing" sphere at $\mathbf{P}$. This means that $W(N, \mathbf{R}; \mathbf{P}, \rho)$ is zero when $\mathbf{R}$ is the position vector of any point on the surface of the sphere. Physically this requires that a random flight end once it strikes the sphere.[2] It follows that $W(N, \mathbf{R}; \mathbf{P}, \rho)dv$ is the probability that the random coil ends in the volume element dv at $\mathbf{R}$ *without* passing within a distance ρ of $\mathbf{P}$. Therefore, the solution to our problem is given by $\beta(N, \mathbf{R}; \mathbf{P}, \rho)dv$ in the following equation:

$$\beta(N, \mathbf{R}; \mathbf{P}, \rho)dv = W(N, \mathbf{R})dv - W(N, \mathbf{R}; \mathbf{P}, \rho)dv. \quad (11)$$

$\beta(N, \mathbf{R}; \mathbf{P}, \rho)$ is a solution of Eq. (9) and must satisfy the following boundary condition:

$$\beta(N, \mathbf{R}; \mathbf{P}, \rho) = W(N, \mathbf{R}) \quad (12)$$

on the surface of the absorbing sphere centered at $\mathbf{P}$.

It is convenient to make a substitution for $\mathbf{R}$ as follows:

$$\mathbf{R} = \mathbf{r} + \mathbf{P}, \quad (13)$$

and then $\beta(N, \mathbf{R}; \mathbf{P}, \rho)$ becomes $\beta'(N, \mathbf{r}; \mathbf{P}, \rho)$. Since we are dealing with the case where

$$\rho \ll |\mathbf{P}|, \quad (14)$$

we can use the approximation that

$$W(N, \mathbf{P} + \boldsymbol{\varrho}) \simeq W(N, \mathbf{P}), \quad (15)$$

where $\boldsymbol{\varrho}$ is the vector $\mathbf{r}$ for points on the sphere. As a result of this approximation, $\beta'(N, \mathbf{r}; \mathbf{P}, \rho)$ is spherically symmetric. Note that $\beta'(N, \mathbf{r}; \mathbf{P}, \rho)$ is approximately spherically symmetric, and Eq. (15) can be applied in a case for which condition (14) does not hold, and that is when

$$\rho \leq |\mathbf{P}| \ll |\mathbf{R}|. \quad (16)$$

The reason for this is that the effects of the various positions of the absorbing sphere "blend" and produce more symmetry at greater distance from the origin. Also $\beta'(N, \mathbf{r}; \mathbf{P}, \rho)$ is exactly spherically symmetric in the special case $\mathbf{P} = \mathbf{0}$, but the solution $\beta'(N, \mathbf{r}; \mathbf{0}, \rho) = W(N, \mathbf{r})$ for this case is trivial; this merely means that all chains must pass through a sphere enclosing the origin.

Before the boundary value problem can be set up completely, it is necessary to determine the "initial" condition. That is, we must have the expression for $\beta'(N, \mathbf{r}; \mathbf{P}, \rho)$ for some fixed value of N. The exact relationship would seem to be

$$\beta'(N, \mathbf{r}; \mathbf{P}, \rho) = 0 \quad \text{when} \quad Nl \leq |\mathbf{P}| + |\mathbf{r}|. \quad (17)$$

If a change of variable is made as follows:

$$N'l = Nl - |\mathbf{P}| + |\mathbf{r}|, \quad (18)$$

so that

$$\beta^*(N', \mathbf{r}; \mathbf{P}, \rho) = 0 \quad \text{when} \quad N' = 0, \quad (19)$$

then to a first approximation we can take

$$N' = N, \quad (20)$$

and to a second approximation

$$N' = N - |\mathbf{P}|/l. \quad (21)$$

The first approximation given by Eq. (20) will be used. The result for the better approximation can be obtained if desired by substituting from Eq. (21) in the final result.

In this connection it is interesting to observe that according to Eq. (8), which we will use,

$$W(N, \mathbf{R}) \to 0 \quad \text{when} \quad N \to 0, \quad (22)$$

when actually the function $W(N, \mathbf{R})$ which would hold for the case where $|\mathbf{R}| \to Nl$ should satisfy the condition that

$$W(N, \mathbf{R}) = 0 \quad \text{when} \quad Nl \leq |\mathbf{R}|. \quad (23)$$

This is a reason, of course, that the values given by Eq. (8) are too high[5] when N is not large compared to $|\mathbf{R}|/l$.

Returning now to the determination of $\beta'(N, \mathbf{r}; \mathbf{P}, \rho)$, we will take

$$u(N, r) = r\beta'(N, \mathbf{r}; \mathbf{P}, \rho), \quad (24)$$

where $r = |\mathbf{r}|$, and then $u(N, r)$ is the solution of the following boundary value problem:

$$\frac{\partial u(N, r)}{\partial N} = \frac{l^2}{6} \frac{\partial^2 u(N, r)}{\partial r^2}, \quad (25)$$

$$u(0, r) = 0, \quad (26)$$

$$u(N, \rho) = \rho W(N, \mathbf{P}), \quad (27)$$

$$\lim_{r \to \infty} u(N, r) = 0. \quad (28)$$

[6] C. A. Hollingsworth, J. Chem. Phys. **16**, 544 (1948).
[7] C. A. Hollingsworth, J. Chem. Phys. **17**, 97 (1949).

Since we desire the solution outside the sphere ($r \geq \rho$), the problem corresponds exactly to that of determining the temperature of a semi-infinite solid $x \geq \rho$ when the initial temperature is zero, and the face is kept at a temperature given by a prescribed function of the time (N corresponding to time). The formal solution can be given in the following form:[8,9]

$$u(N, r) = \left(\frac{3}{2\pi l^2}\right)^{\frac{1}{2}} (r-\rho) \times \int_0^N \frac{W(N-\tau, \mathbf{P})}{\tau^{\frac{3}{2}}} \exp\left[\frac{-3(r-\rho)^2}{2l^2\tau}\right] d\tau. \quad (29)$$

If we substitute for $W(N-\tau, \mathbf{P})$ from Eq. (8) and make the changes of variables, first $\tau = N/z^2$, then $z^2 = \lambda^2 + 1$, and finally $\lambda^2 = 2Nl^2x^2/[3(r-\rho)^2]$, we obtain

$$u(N, r) = 2\rho(r-\rho)\left(\frac{3}{2\pi Nl^2}\right)^2 \int_0^\infty (1+1/\lambda^2) \times \exp\left[\frac{-3(\lambda^2+1)}{2Nl^2}\left(\frac{P^2}{\lambda^2} + (r-\rho)^2\right)\right] d\lambda$$

$$= 2\rho(r-\rho)\left(\frac{3}{2\pi Nl^2}\right)^2 \times \exp\left\{\frac{-3}{2Nl^2}[P^2 + (r-\rho)^2]\right\} \cdot \times \left(\frac{2Nl^2}{3(r-\rho)^2}\right)^{\frac{1}{2}} J(a) - \left(\frac{3(r-\rho)^2}{2Nl^2}\right)^{\frac{1}{2}} \frac{\partial J(a)}{\partial a}, \quad (30)$$

where

$$J(a) = \int_0^\infty \exp\left[\frac{-a}{x^2} - x^2\right] dx = (\sqrt{\pi}/2) \exp(-2\sqrt{a}), \quad (31)$$

$$a = \left(\frac{3(r-\rho)P}{2Nl^2}\right)^2, \quad (32)$$

and

$$P = |\mathbf{P}|.$$

Thus,

$$u(N, r) = \left(\frac{3}{2\pi Nl^2}\right)^{\frac{3}{2}} \frac{\rho}{P}(P+r-\rho) \times \exp\left[\frac{-3}{2Nl^2}(P+r-\rho)^2\right] \quad (33)$$

$$\simeq \left(\frac{3}{2\pi Nl^2}\right)^{\frac{3}{2}} \frac{\rho}{P}(P+r) \exp\left[\frac{-3}{2Nl^2}(P+r)^2\right], \quad (33a)$$

and, therefore,

$$\beta(N, \mathbf{R}; \mathbf{P}, \rho) \simeq \rho\beta(N, \mathbf{R}; \mathbf{P}), \quad (34)$$

where

$$\beta(N, \mathbf{R}; \mathbf{P}) = \left(\frac{3}{2\pi Nl^2}\right)^{\frac{3}{2}} \frac{1}{|\mathbf{R}-\mathbf{P}|} + \frac{1}{|\mathbf{P}|} \times \exp\left[\frac{-3}{2Nl^2}(|\mathbf{P}| + |\mathbf{R}-\mathbf{P}|)^2\right]$$

$$= \left(\frac{3}{2\pi Nl^2}\right)^{\frac{3}{2}} \frac{|\mathbf{P}| + |\mathbf{R}-\mathbf{P}|}{|\mathbf{R}| \cdot |\mathbf{R}-\mathbf{P}|} \times \exp\left[\frac{-3}{2Nl^2}(|\mathbf{P}| + |\mathbf{R}-\mathbf{P}|)^2\right]. \quad (35)$$

The function given by Eq. (35) assumes the following limiting forms:

$$\rho\beta(N, \mathbf{R}; \mathbf{P}) \to W(N, \mathbf{P}) \quad \text{when} \quad |\mathbf{R}-\mathbf{P}| \to \rho \quad (36)$$

and

$$\rho\beta(N, \mathbf{R}; \mathbf{P}) \to W(N, \mathbf{R}) \quad \text{when} \quad |\mathbf{P}| \to \rho, \quad \text{and} \quad \rho \ll |\mathbf{R}|. \quad (37)$$

The limiting relation given by Eq. (37) is a correct result obtained in spite of the use of approximation (15) when condition (14) does not apply. This is because condition (16) applies in this case.

The symmetry of Eq. (35) with respect to interchange of $\mathbf{P}$ and $\mathbf{R}-\mathbf{P}$ expresses the fact that it is immaterial which end of the coil we consider to be the beginning and, therefore, situated at the origin.

It is interesting to observe that when $\beta'(N, \mathbf{r}; \mathbf{P})$ is expressed in integral form, namely,

$$\beta'(N, \mathbf{r}; \mathbf{P}) = \left(\frac{3}{2\pi l^2}\right)^{\frac{3}{2}} \int_0^N \frac{W(N-\tau, \mathbf{P})}{\tau^{\frac{3}{2}}} \times \exp\left[\frac{-3r^2}{2l^2\tau}\right] d\tau, \quad (38)$$

it takes the form of the field due to a *continuous point source*[9] of strength

$$\Phi(N) = \frac{2\pi l^2}{3} W(N, \mathbf{P}) \quad (39)$$

at the origin, $\mathbf{r}=\mathbf{0}$. In this connection it is also interesting to note that $W(N, \mathbf{R})$ as given by Eq. (8) is the field due an *instantaneous point source*[9] of unit strength at the origin, $\mathbf{R}=\mathbf{0}$.

It will be noted that the dimensions of $\beta(N, \mathbf{R}; \mathbf{P})$ are L^{-1}, and $\rho\beta(N, \mathbf{R}; \mathbf{P})$ is dimensionless, as it must be in order to be identified with a probability.

PROBLEM 2

Determine the probability $\alpha(N, \mathbf{R}; \mathbf{P})\rho$ that a random coil of N links, which starts at the origin and ends at $\mathbf{R}$,

[8] R. V. Churchill, *Modern Operational Mathematics in Engineering* (McGraw-Hill Book Company, Inc., New York, 1944).

[9] H. S. Carslaw and J. C. Jaeger, *Conduction of Heat in Solids* (Oxford University Press, London E. C. 4, 1947).

passes at least once within a distance ρ of the point $\mathbf{P}$ ($|\mathbf{P}| \ll Nl$; $|\mathbf{R}| \ll Nl$; $l \ll \rho \ll |\mathbf{P}|$).

In this case it is known that the coil starts at the origin and ends at $\mathbf{R}$, and we seek the probability that the coil passes through a sphere of radius ρ centered at $\mathbf{P}$. The solution is obtained immediately from the result of Problem 1. For, it is clear that

$$\beta(N, \mathbf{R}; \mathbf{P})\rho = W(N, \mathbf{R})\alpha(N, \mathbf{R}; \mathbf{P})\rho, \tag{40}$$

or

$$\alpha(N, \mathbf{R}; \mathbf{P}) = \frac{\beta(N, \mathbf{R}; \mathbf{P})}{W(N, \mathbf{R})} = \frac{|\mathbf{P}| + |\mathbf{R}-\mathbf{P}|}{|\mathbf{P}| \cdot |\mathbf{R}-\mathbf{P}|} \exp\left\{\frac{-3}{2Nl^2} \times [(|\mathbf{P}| + |\mathbf{R}-\mathbf{P}|)^2 - |\mathbf{R}|^2]\right\}. \tag{41}$$

Of course, for the cases represented by Eqs. (36) and (37), $\rho\alpha(N, \mathbf{R}; \mathbf{P}) \to 1$.

PROBLEM 3

Determine the probability $\eta(k, \mathbf{P})\rho$ that a random coil of N links, which starts at the origin, passes within a distance ρ of $\mathbf{P}$ *for the first time at the kth link* ($|\mathbf{R}|, |\mathbf{P}| \ll Nl$; $l \ll \rho \ll |\mathbf{P}|$).

Consider a large number of particles which start at the origin and undergo random flight. It can be shown[2] that the fraction of those particles that would strike an element of surface of the absorbing sphere for the first time during the kth displacement is given by

$$f(k, \mathbf{P}, \rho)ds = \frac{l^2}{6} \operatorname{grad}_R W(k, \mathbf{R}; \mathbf{P}, \rho) \cdot d\mathbf{s}, \tag{42}$$

where $d\mathbf{s}$ is the vectorial element of surface and is taken to be positive when it is pointing away from the center of the sphere. $W(k, \mathbf{R}; \mathbf{P}, \rho)$ is defined by Eq. (11). The function that we seek is, therefore, given by

$$\eta(k, \mathbf{P}) = \int_S f(k, \mathbf{P}, \rho)ds = \frac{l^2}{6} \int \{\operatorname{grad}[W(k, \mathbf{R})] - \operatorname{grad}_R[\rho\beta(k, \mathbf{R}; \mathbf{P})]\} \cdot ds, \tag{43}$$

where the integration is taken over the surface of the absorbing sphere. Use of the symmetry properties of $W(k, \mathbf{R})$ and $\beta'(k, \mathbf{r}; \mathbf{P})$ leads to

$$\operatorname{grad} W(k, \mathbf{R}) = \frac{\partial W(k, \mathbf{R})}{\partial R}\left(\frac{\mathbf{R}}{R}\right) = \frac{-3}{kl^2} W(k, \mathbf{R})\mathbf{R}, \tag{44}$$

where $R = |\mathbf{R}|$; and

$$\operatorname{grad}_R[\rho\beta(k, \mathbf{R}; \mathbf{P})] = \frac{\rho\partial\beta'(k, r, P)}{\partial r}\frac{\mathbf{r}}{r} = -\left(\frac{3}{2\pi kl^2}\right)^{\frac{3}{2}} \rho\left(\frac{1}{r^2} + \frac{3}{kl^2}\frac{(P+r)^2}{rP}\right) \times \exp\left[\frac{3}{2kl^2}(P+r)^2\right]\frac{\mathbf{r}}{r}. \tag{45}$$

On the surface of the sphere, $r = \rho$, we can use the following approximations:

$$\frac{\partial W}{\partial R} \simeq \frac{-3P}{kl^2} W(k, \mathbf{P}), \tag{46}$$

and

$$\rho\frac{\partial\beta'(k, \mathbf{r}; \mathbf{P})}{\partial r} \simeq -\left(\frac{1}{\rho} + \frac{3P}{kl^2}\right) W(k, \mathbf{P}) \simeq -\left(\frac{1}{\rho}\right) W(k, \mathbf{P}), \tag{47}$$

where the last approximation was obtained by neglecting the term of order $1/(kl^2)^{\frac{1}{2}}$ compared to $1/\rho$. It will be noted that $W(k, \mathbf{P}) \simeq 0$ except for cases in which $(kl^2)^{\frac{1}{2}} \simeq P$. Thus we have to a first approximation

$$\eta(k, \mathbf{P})\rho = -\left(\frac{l^2}{6}\right)\frac{3PW(k, \mathbf{P})}{kl^2} \times \int_0^\pi 2\pi\rho^2 \sin\theta \cos\theta d\theta + \frac{l^2}{6\rho} W(k, \mathbf{P}) 4\pi\rho^2, \tag{48}$$

where θ is the angle between $\mathbf{r}$ and $\mathbf{P}$. This gives

$$\eta(k, \mathbf{P})\rho = \left(\frac{2\pi l^2}{3}\right)\rho W(k, \mathbf{P}). \tag{49}$$

PROBLEM 4

Determine the probability $\eta(k, N, \mathbf{R}; \mathbf{P})\rho dv$ that a random coil of N links, which starts at the origin, passes within a distance ρ of $\mathbf{P}$ *for the first time at the kth link and then ends in dv at* $\mathbf{R}$ ($|\mathbf{R}|, |\mathbf{P}| \ll Nl$; $l \ll \rho \ll |\mathbf{P}|$).

We have immediately that

$$\eta(k, N, \mathbf{R}; \mathbf{P})dv = \eta(k, \mathbf{P})W(n-k, \mathbf{R}-\mathbf{P})dv. \tag{50}$$

It is easy to extend this result to obtain other probabilities. For example,

$$\rho^2\eta(k_1, k_2, N, \mathbf{R}; \mathbf{P}_1, \mathbf{P}_2)dv = \rho\eta(k, \mathbf{P}_1)\rho\eta(k_2, \mathbf{P}_2 - \mathbf{P}_1)W(N-k_1-k_2, \mathbf{R}-\mathbf{P}_2)dv \tag{51}$$

expresses the probability that a coil of N links passes by $\mathbf{P}_1$ at the k_1th link for the first time, then by $\mathbf{P}_2$ at the

k_2th link for the first time after the k_1th link, and then ends in dv at $\mathbf{R}$. The following relations hold:

$$\eta(k, \mathbf{P}) = \int \eta(k, N, \mathbf{R}; \mathbf{P}) dv, \tag{52}$$

$$\eta(k_1, k_2; P_1, P_2) = \int \eta(k_1, k_2, N, \mathbf{R}; \mathbf{P}_1, \mathbf{P}_2) dv, \text{ etc.} \tag{53}$$

Also,

$$\sum_{k=0}^{N} \eta(k, \mathbf{R}; \mathbf{P}) = \beta(N, \mathbf{R}; \mathbf{P}). \tag{54}$$

Equations (52) and (53) can be obtained directly by the use of Eqs. (50) and (51). Equation (54) can be proved as follows: Because N is large we have to a sufficiently good degree of approximation

$$\sum_{k=0}^{N} \eta(k, \mathbf{R}; \mathbf{P}) = \int_0^N \eta(k, \mathbf{R}; \mathbf{P}) dk, \tag{55}$$

and then we use

$$\begin{aligned}
&\int_0^N \eta(k, \mathbf{R}; \mathbf{P}) dk \\
&= \int_0^N \eta(k, \mathbf{P}) W(N-k, \mathbf{R}-\mathbf{P}) dk \\
&= \frac{2\pi l^2}{3} \int_0^N W(k, \mathbf{P}) W(N-k, \mathbf{R}-\mathbf{P}) dk \\
&= \left(\frac{3}{2\pi l^2}\right)^{\frac{3}{2}} \int_0^N \frac{W(N-\tau, \mathbf{P}) \exp[-3r^2/2\tau l^2]}{\tau^{\frac{3}{2}}} d\tau,
\end{aligned} \tag{56}$$

where $\tau = N-k$. Equation (54) now follows from Eq. (38).

PROBLEM 5

Determine the probability $\rho\gamma(N, \mathbf{P})$ *that a random coil of* N *links, which starts at the origin, passes at least once within a distance* ρ *of* $\mathbf{P}$ ($|\mathbf{P}| \ll Nl$; $l \ll \rho \ll |\mathbf{P}|$).

This function can be obtained easily by two methods, one using $\beta'(N, \mathbf{r}; \mathbf{P})$ and the other using $\eta(k, \mathbf{P})$. The first method is the following: We have at once

$$\begin{aligned}
\gamma(N, \mathbf{P}) &= \int \beta'(N, \mathbf{r}; \mathbf{P}) dv \\
&= 4\pi \int_0^\infty \beta'(N, \mathbf{r}; \mathbf{P}) r^2 dr \\
&= \frac{4\pi}{P} \left(\frac{3}{2\pi N l^2}\right)^{\frac{3}{2}} \int_0^\infty r(P+r) \\
&\qquad \times \exp\left[\frac{-3}{2Nl^2}(P+r)^2\right] dr.
\end{aligned} \tag{57}$$

Letting $P+r=x$, we obtain

$$\begin{aligned}
\gamma(N, \mathbf{P}) &= \frac{4}{\pi^{\frac{1}{2}}} \frac{a^{\frac{3}{2}}}{P} \left[\int_P^\infty x^2 \exp[-ax^2] dx - P \right. \\
&\qquad \left. \times \int_P^\infty x \exp[-ax^2] dx \right] \\
&= \frac{-2a^{\frac{3}{2}}}{P} \frac{\partial J(a, P)}{\partial a} - 2\left(\frac{a}{\pi}\right)^{\frac{3}{2}} \exp[-aP^2],
\end{aligned} \tag{58}$$

where

$$a = \frac{3}{2Nl^2}, \tag{59}$$

and

$$\begin{aligned}
J(a, P) &= \frac{2}{\pi^{\frac{1}{2}}} \int_P^\infty \exp[-a\lambda^2] d\lambda \\
&= (1/a^{\frac{1}{2}}) \operatorname{erfc}(aP),
\end{aligned} \tag{60}$$

where $\operatorname{erfc}(x)$ is the *complementary error function*. It follows that

$$\gamma(N, \mathbf{P}) = (1/P) \operatorname{erfc}[(3/2N)^{\frac{1}{2}}(P/l)]. \tag{61}$$

This function can be obtained by the use of $\eta(k, \mathbf{P})$ in the following manner: We have

$$\gamma(N, \mathbf{P}) = \sum_{k=0}^{N} \eta(k, P), \tag{62}$$

or approximately

$$\gamma(N, \mathbf{P}) = \int_0^N \eta(k, \mathbf{P}) dk, \tag{63}$$

and this gives

$$\begin{aligned}
\gamma(N, \mathbf{P}) &= \left(\frac{3}{2\pi l^2}\right)^{\frac{3}{2}} \int_0^N \exp\left[\frac{-3P^2}{2kl^2}\right] \frac{dk}{k^{\frac{3}{2}}} \\
&= \frac{2}{P\sqrt{\pi}} \int_{(3/2N)^{\frac{1}{2}}(P/l)}^\infty \exp[-x^2] dx \\
&= (1/P) \operatorname{erfc}[(3/2N)^{\frac{1}{2}}(P/l)].
\end{aligned} \tag{64}$$

It is interesting to compare $\rho\gamma(N, \mathbf{P})$ with Simha's function[10]

$$\int_\gamma^N f_c(P) dv,$$

defined by

$$\begin{aligned}
\int_\gamma^N f_c(P) dv &= \sum_{i=\gamma}^{N} W(i, \mathbf{P}) dv \simeq \frac{3}{2\pi l^2 P} \\
&\times \left\{ \operatorname{erf}\left[\left(\frac{3}{2\gamma}\right)^{\frac{1}{2}} \left(\frac{P}{l}\right)\right] - \operatorname{erf}\left[\left(\frac{3}{2N}\right)^{\frac{1}{2}} \left(\frac{P}{l}\right)\right] \right\} dv,
\end{aligned} \tag{65}$$

[10] R. Simha, J. Polymer Sci. 3, 227 (1948).

where $W(i, \mathbf{P})$ is given by Eq. (8), and $\operatorname{erf}(x)$ is the *error function* defined by

$$\operatorname{erf}(x)=\frac{2}{\pi^{\frac{1}{2}}}\int_0^x \exp[-\lambda^2]d\lambda. \tag{66}$$

From Eq. (65) we have

$$\Big|_0^N f_c(P)=\frac{3}{2\pi l^2 P}\left\{1-\operatorname{erf}\left[\left(\frac{3}{2N}\right)^{\frac{1}{2}}\left(\frac{P}{l}\right)\right]\right\}$$

$$=\frac{3}{2\pi l^2 P}\left\{\operatorname{erfc}\left[\left(\frac{3}{2N}\right)^{\frac{1}{2}}\left(\frac{P}{l}\right)\right]\right\}, \tag{67}$$

from which comes the relation

$$\Big|_0^N f_c(P)=\frac{3}{2\pi l^2}\gamma(N, \mathbf{P}), \tag{68}$$

or

$$\Big|_0^N f_c(P)dv_P=\frac{2\rho^2}{l^2}\gamma(N, \mathbf{P})\rho, \tag{69}$$

wherein we have taken

$$dv_P=(4/3)\rho^3. \tag{70}$$

In obtaining Eq. (67), $W(i, \mathbf{P})$ as defined by Eq. (8) was used for values of i down to zero regardless of the fact that Eq. (8) usually does not apply except for higher values of i. The use of Eq. (8) is permissible here, however, as long as P is large enough to cause $W(i, \mathbf{P})$ to approach zero for the lower values of i.

At first sight, Eq. (68) may be surprising. For it may seem that $\rho\gamma(N, \mathbf{P})$ and

$$\Big|_0^N f_c(P)$$

should be the same function obtained in different manners. However, a simple analysis of

$$\Big|_0^N f_c(P)dv_P$$

such as the one which will be given below will explain why this function increases more rapidly with increasing ρ than does $\rho\gamma(N, P)$.

It will be convenient to use the following terminology: The number of configurations possible for a coil of i links which starts at $\mathbf{r}_1$ and ends at $\mathbf{r}_2$ will be expressed as $Q(i, \mathbf{r}_1, \mathbf{r}_2)$. The number of configurations possible for a coil of i links which starts at a given point and ends anywhere will be designated $Q(i)$. Since the configurations are continuously variable, these expressions can represent only the relative number of configurations. Some simple relationships follow directly:

$$Q(i, \mathbf{r}_1, \mathbf{r}_2)=Q(i, \mathbf{0}, \mathbf{r}), \tag{71}$$

where $\mathbf{r}=\mathbf{r}_2-\mathbf{r}_1$,

$$Q(i)Q(k)=Q(i+k), \tag{72}$$

$$Q(i, \mathbf{0}, \mathbf{r})/Q(i)=Q(i, \mathbf{0}, \mathbf{r})Q(N-i)/Q(N), \tag{73}$$

and

$$W(i, \mathbf{r})=Q(i, \mathbf{0}, \mathbf{r})/Q(i). \tag{74}$$

We have, therefore,

$$\Big|_\gamma^N f_c(P)dv_P=\sum_{i=0}^{N} W(i, \mathbf{P})dv_P$$

$$=\frac{dv_P}{Q(N)}\sum_{i=0}^{N} Q(i, \mathbf{0}, \mathbf{P})Q(N-i). \tag{75}$$

The ith term in the summation is the number of configurations of a coil of N links which starts at the origin, has the ith link ending at $\mathbf{P}$, and has the last link anywhere. It can now be seen that some coil configurations are counted more than once in the summation in Eq. (75). For example, all configurations which have both the jth and the kth links in dv_P are included in term $Q(j, \mathbf{0}, \mathbf{P})Q(N-j)$ as well as in the term $Q(k, \mathbf{0}, \mathbf{P})Q(N-k)$. Likewise all configurations which have the ith, jth, and kth links in dv_P are counted three times; and so on for the cases in which larger numbers of links are in dv_P. It follows that the sum in Eq. (75) is larger than the number of configurations in which one or more of the N links are in dv_P.

Thus

$$\Big|_0^N f_c(P)>\gamma(N, \mathbf{P})$$

when $\rho>l$, and the difference between the two functions increases rapidly with increasing ρ. For when ρ is large compared to l many of the configurations which have the jth link in dv_P will also have links which neighbor the jth in dv_P. When dv_P becomes so large that it must contain the entire coil, each configuration is counted N times, and this explains why

$$\int \Big|_0^N f_c(P)dv_P=N. \tag{76}$$

When $\rho<l$, the function

$$\Big|_0^N f_c(P)$$

should approach the probability that at least one link of the coil ends in dv_P. This is smaller, however, than the probability that at least one link passes through dv_P, and for this reason when ρ becomes small compared to l,

$$\Big|_0^N f_c(P)dv_P$$

becomes smaller than the probability that the coil

passes through dv_P at least once. By a geometric consideration it can be shown that when $\rho \ll l$ the ratio of the number of links that end in dv_P to the number of links that pass through dv_P is $4\rho/3l$. For $\rho \simeq l$ the relationship is more complex (see Appendix). Therefore,

$$\frac{3l}{4\rho}\Big|_0^N f_c(P)dv_P = \pi l \rho^2 \Big|_0^N f_c(P) = \frac{3}{2}\frac{\rho}{l}\gamma(N, \mathbf{P})\rho \quad (77)$$

should give approximately the probability that the coil passes through dv_P when $\rho \ll l$.

The function $\gamma(N, \mathbf{P})\rho$ as obtained by the boundary value method is too large when $\rho \leq l$, because this method does not take care of the discrete nature of the random flight phenomenon.

PROBLEM 6

Determine the probability $\epsilon(N, \mathbf{R}; \mathbf{P})dv$ *that a random coil of N links, which starts at the origin and passes within a distance* ρ *of point* $\mathbf{P}$ *at least once, ends in dv at* $\mathbf{R}$ ($|\mathbf{P}| \ll Nl$; $|\mathbf{R}| \ll Nl$; $l \ll \rho \ll |\mathbf{P}|$).

In this case we know that the coil starts at the origin and passes "through" $\mathbf{P}$. We seek the probability that the coil ends in dv at $\mathbf{R}$. This probability can be obtained in terms of two functions which have already been calculated. For

$$\beta(N, \mathbf{R}; \mathbf{P})\rho dv = \gamma(N, \mathbf{P})\rho\epsilon(N, \mathbf{R}; \mathbf{P})dv, \quad (78)$$

$$\epsilon(N, \mathbf{R}; \mathbf{P}) = \beta(N, \mathbf{R}; \mathbf{P})/\gamma(N; \mathbf{P}). \quad (79)$$

PROBLEM 7

Determine the probability $\beta^*(N, \mathbf{R}; \mathbf{P}_1, \mathbf{P}_2, \cdots, \mathbf{P}_n)\rho^n dv$ *that a coil of N links, which starts at the origin, passes at least once within a distance* ρ *of the point* $\mathbf{P}_1$, *then at least once within a distance* ρ *of the point* $\mathbf{P}_2$, *etc., until it finally passes within a distance* ρ *of the point* $\mathbf{P}_n$ *and then ends in dv at* $\mathbf{R}$ ($|\mathbf{R}| \ll Nl$; $l \ll \rho \ll |\mathbf{P}_{i+1} - \mathbf{P}_i| \ll Nl$).

We have already solved this problem for $n=1$. The solution will now be obtained for $n=2$, and the result will then be extended to the general case.

By the same process that led to Eqs. (25) to (28) in the determination of $\beta(N, \mathbf{R}; \mathbf{P})$, we arrive at the following boundary value problem in this case:

$$\frac{\partial \omega(N, r)}{\partial N} = \frac{l^2}{6}\frac{\partial^2 \omega(N, r)}{\partial r^2}, \quad (80)$$

$$\omega(0, r) = 0, \quad (81)$$

$$\omega(N, \rho) = \rho^2 \beta(N, \mathbf{P}_2; \mathbf{P}_1), \quad (82)$$

$$\lim_{r \to \infty} \omega(N, r) = 0, \quad (83)$$

where in analogy to Eq. (24)

$$\omega(N, r) = r\beta'(N, r; \mathbf{P}_1, \mathbf{P}_2)\rho, \quad (84)$$

and

$$\mathbf{r} = \mathbf{R} - \mathbf{P}_2. \quad (85)$$

Since

$$\beta(N, \mathbf{P}_2; \mathbf{P}_1) = \frac{1}{|\mathbf{P}_2 - \mathbf{P}_1|} + \frac{1}{|\mathbf{P}_1|} W(N, \mathbf{X}), \quad (86)$$

where

$$|\mathbf{X}| = |\mathbf{P}_1| + |\mathbf{P}_2| - |\mathbf{P}_1|, \quad (87)$$

we have, by using Eq. (38),

$$\begin{aligned}
&\beta^*(N, \mathbf{R}; \mathbf{P}_1, \mathbf{P}_2) \\
&= \left(\frac{3}{2\pi l^2}\right)^{\frac{1}{2}} \frac{|\mathbf{P}_1| + |\mathbf{P}_2 - \mathbf{P}_1|}{|\mathbf{P}_1| \cdot |\mathbf{P}_2 - \mathbf{P}_1|} \int_0^N \left\{ \frac{W(N-\tau, \mathbf{X})}{\tau^{\frac{3}{2}}} \right. \\
&\qquad \left. \times \exp\left[\frac{-3}{2Nl^2\tau}|\mathbf{R} - \mathbf{P}_2|^2\right]\right\} d\tau \\
&= \left(\frac{3}{2\pi N l^2}\right)^{\frac{3}{2}} \frac{|\mathbf{X}|}{|\mathbf{P}_1| \cdot |\mathbf{P}_2 - \mathbf{P}_1|} \frac{|\mathbf{X}| + |\mathbf{R} - \mathbf{P}_2|}{|\mathbf{X}| \cdot |\mathbf{R} - \mathbf{P}_2|} \\
&\qquad \times \exp\left[\frac{-3}{2Nl^2}(|\mathbf{X}| + |\mathbf{R} - \mathbf{P}_2|)^2\right] \\
&= \left(\frac{3}{2\pi N l^2}\right)^{\frac{3}{2}} \left(\frac{|\mathbf{P}_1| + |\mathbf{P}_2 - \mathbf{P}_1| + |\mathbf{R} - \mathbf{P}_2|}{|\mathbf{P}_1| \cdot |\mathbf{P}_2 - \mathbf{P}_1| \cdot |\mathbf{R} - \mathbf{P}_2|}\right) \\
&\qquad \times \exp\left[\frac{-3}{2Nl^2}(|\mathbf{P}_1| + |\mathbf{P}_2 - \mathbf{P}_1| + |\mathbf{R} - \mathbf{P}_2|)^2\right]. \quad (88)
\end{aligned}$$

This result can be extended by a process of mathematical induction to obtain the probability that the coil passes by n different points "in succession" at least once. The result is

$$\begin{aligned}
&\beta^*(N, \mathbf{R}; \mathbf{P}_1, \mathbf{P}_2, \cdots, \mathbf{P}_n) \\
&= \left(\frac{3}{2\pi N l^2}\right)^{\frac{3}{2}} \frac{\sum_{i=0}^{n} |\mathbf{P}_{i+1} - \mathbf{P}_i|}{\prod_{i=0}^{n} |\mathbf{P}_{i+1} - \mathbf{P}_i|} \\
&\qquad \times \exp\left[\frac{-3}{2Nl^2}\left(\sum_{i=0}^{n} |\mathbf{P}_{i+1} - \mathbf{P}_i|\right)\right)^2\Bigg], \quad (89)
\end{aligned}$$

where $\mathbf{P}_{n+1} = \mathbf{R}$, and $\mathbf{P}_0 = \mathbf{0}$.

Equation (89) can also be obtained by using a function of the type given by Eq. (51). For

$$\beta^*(N, \mathbf{R}; \mathbf{P}_1, \cdots, \mathbf{P}_n) = \sum_{k_1=0}^{N} \sum_{k_2=0}^{N_1} \cdots \times \sum_{k_n=0}^{N_{n-1}} \eta(k_1, \cdots, k_n, N, \mathbf{R}; \mathbf{P}_1, \cdots, \mathbf{P}_n), \quad (90)$$

where

$$N_1=N-k_1,$$
$$\cdots\cdots\cdots$$
$$N_i=N-k_1-k_2-\cdots-k_i. \quad (91)$$

Equation (90) can be expressed approximately by

$$\beta^*(N, \mathbf{R}; \mathbf{P}_1, \cdots, \mathbf{P}_n)=\int_0^N \cdots \int_0^{N_{n-1}} \times\eta(k_1, \cdots, k_n, N, \mathbf{R}; \mathbf{P}_1, \cdots, \mathbf{P}_n)dk_n, \cdots dk_1, \quad (92)$$

or

$$\begin{aligned}\beta^*(N, \mathbf{R}; \mathbf{P}_1, \cdots, \mathbf{P}_n)&=\int_0^N \cdots \int_0^{N_{n-1}} \eta(k_1, \mathbf{P}_1)\eta(k_2, \mathbf{P}_2-\mathbf{P}_1)\cdots \\ &\quad\times\eta(k_n, \mathbf{P}_n-\mathbf{P}_{n-1})W(N_n, \mathbf{R})dk_n\cdots dk_1 \\ &=\int_0^N \eta(k_1, \mathbf{P}_1-\mathbf{P}_0)\int_0^{N_1}\eta(k_2, \mathbf{P}_2-\mathbf{P}_1)\cdots \\ &\quad\times\int_0^{N_{n-1}}\eta(k_n, \mathbf{P}_n-\mathbf{P}_{n-1}) \\ &\quad\times W(N_n, \mathbf{R}-\mathbf{P}_n)dk_n\cdots dk_1. \quad (93)\end{aligned}$$

Evaluation of these integrals by use of Eqs. (56), (49), (38), and (35) gives Eq. (89). The following relationship should hold:

$$\begin{aligned}\beta^*(N, \mathbf{R}; \mathbf{P}_1, \cdots, \mathbf{P}_n)&=\sum_{k_1=0}^{N}\sum_{k_2=0}^{N_1}\cdots\sum_{k_{n-m}=0}^{N_{n-m-1}} \\ &\quad\times[\eta(k_1, \mathbf{P}_1)\eta(k_2, \mathbf{P}_2)\cdots\eta(k_{n-m}, \mathbf{P}_{n-m}) \\ &\quad\times\beta^*(N_{n-m}, \mathbf{R}; \mathbf{P}_{n-m+1}-\mathbf{P}_{n-m}, \cdots, \mathbf{P}_n)]. \quad (94)\end{aligned}$$

Indeed Eq. (93) gives

$$\begin{aligned}\beta^*(N, \mathbf{R}; \mathbf{P}_1, \cdots, \mathbf{P}_n)&=\int_0^N \cdots \int_0^{N_{n-m-1}} \eta(k_1, \mathbf{P}_1)\eta(k_2, \mathbf{P}_2)\cdots \\ &\quad\times\eta(k_{n-m}, \mathbf{P}_{n-m})\beta^*(N_{n-m}, \mathbf{R}; \mathbf{P}_{n-m+1} \\ &\quad-\mathbf{P}_{n-m}, \cdots, \mathbf{P}_n)dk_{n-m}\cdots dk_1. \quad (95)\end{aligned}$$

A special case arises when all of the vectors $\mathbf{P}_{i+1}-\mathbf{P}_i$ are equal in magnitude. Then

$$\rho^n\beta^*(N, \mathbf{R}; \mathbf{P}_1, \cdots, \mathbf{P}_n)=\left(\frac{3}{2\pi Nl^2}\right)^{\frac{3}{2}}\left(\frac{\rho}{s}\right)^n(n+1) \times\exp\left[\frac{-3(n+1)^2s^2}{2Nl^2}\right], \quad (96)$$

where $s=|\mathbf{P}_{i+1}-\mathbf{P}_i|$. It is to be recalled that Eq. (94) holds only in case $\rho\ll s$.

Equation (89) applies in cases for which $\mathbf{P}_i=\mathbf{P}_j$, where $j-i\geq 2$. It does not apply when $P_i=P_{i+1}$.

PROBLEM 8

Determine the probability $\rho\delta(N, \mathbf{R}; \mathbf{P}, \mathbf{X})dv$ *that a coil of N links, which starts at the origin, passes at least once within a distance* ρ *of the point* $\mathbf{P}$, *without having passed within a distance* ρ *of the point* $\mathbf{X}$ *prior to any of the one or more passages within a distance* ρ *of point* $\mathbf{P}$, *and then ends in dv at* $\mathbf{R}(|\mathbf{R}|, |\mathbf{P}|, |\mathbf{X}|\ll Nl; l\ll\rho; \rho\ll|\mathbf{P}|, |\mathbf{X}|, |\mathbf{P}-\mathbf{X}|)$.

This probability can be obtained by solving the boundary value problem given by Eqs. (25) to (24) with the $W(N, \mathbf{P})$ in Eq. (27) replaced by $W(N, \mathbf{P}; \mathbf{X}, \rho)$. However, the result can be written down directly in terms of some of the probabilities which we have already obtained. Thus

$$\delta(N, \mathbf{R}; \mathbf{P}, \mathbf{X})=\beta(N, \mathbf{R}; \mathbf{P})-\rho\beta^*(N, \mathbf{R}; \mathbf{X}, \mathbf{P}). \quad (97)$$

Since we are considering the cases for which $\rho\ll|\mathbf{P}-\mathbf{X}|, |\mathbf{X}|$, we have for a first approximation

$$\delta(N, \mathbf{R}; \mathbf{P}, \mathbf{X})\simeq\beta(N, \mathbf{R}; \mathbf{P}). \quad (98)$$

PROBLEM 9

Determine the probability $\rho^2\beta(N, \mathbf{R}; \mathbf{P}_1, \mathbf{P}_2)dv$ *that a coil of N links, which starts at the origin, passes within a distance* ρ *of each of two points* $\mathbf{P}_1$ *and* $\mathbf{P}_2$ *at least once and then ends in dv at* $\mathbf{R}(|\mathbf{R}|, |\mathbf{P}_1|, |\mathbf{P}_2|\ll Nl; l\ll\rho\ll|\mathbf{P}_1|, |\mathbf{P}_2|, |\mathbf{P}_2-\mathbf{P}_1|)$.

This probability can be expressed as a rapidly converging series of solutions to Problem 7 as follows:

$$\begin{aligned}\beta(N, \mathbf{R}; \mathbf{P}_1, \mathbf{P}_2)&=\beta^*(N, \mathbf{R}; \mathbf{P}_1, \mathbf{P}_2)+\beta^*(N, \mathbf{R}; \mathbf{P}_2, \mathbf{P}_1) \\ &\quad-\rho\beta^*(N, \mathbf{R}; \mathbf{P}_2, \mathbf{P}_1, \mathbf{P}_2)-\rho\beta^*(N, \mathbf{R}; \mathbf{P}_1, \mathbf{P}_2, \mathbf{P}_1) \\ &\quad+\rho^2\beta^*(N, \mathbf{R}; \mathbf{P}_1, \mathbf{P}_2, \mathbf{P}_1, \mathbf{P}_2) \\ &\quad+\rho^2\beta^*(N, \mathbf{R}; \mathbf{P}_2, \mathbf{P}_1, \mathbf{P}_2, \mathbf{P}_1), \text{ etc.} \quad (99)\end{aligned}$$

For the cases that we are considering a first approximation is

$$\beta(N, \mathbf{R}; \mathbf{P}_1, \mathbf{P}_2)\simeq\beta^*(N, \mathbf{R}; \mathbf{P}_1, \mathbf{P}_2)+\beta^*(N, \mathbf{R}; \mathbf{P}_2, \mathbf{P}_1). \quad (100)$$

Extension of this problem to obtain the probability of passage by more than two given points is straight forward in principle, but the number of terms forming the coefficient of a given power of ρ goes up very rapidly with the number of points.

PROBLEM 10

Determine the probability $\rho\beta^\dagger(N, \mathbf{R}; \mathbf{P}_1; \mathbf{P}_2)dv$ *that a coil of N links, which starts at the origin, passes within a distance* ρ *of at least one of the points* $\mathbf{P}_1$ *and* $\mathbf{P}_2$ *at least once and then ends in dv at* $\mathbf{R}(|\mathbf{R}|, |\mathbf{P}_1|, |\mathbf{P}_2|\ll Nl; l\ll\rho\ll|\mathbf{P}_1|, |\mathbf{P}_2|, |\mathbf{P}_2-\mathbf{P}_1|)$.

If we just add $\beta(N, \mathbf{R}; \mathbf{P}_1)$ and $\beta(N, \mathbf{R}, \mathbf{P}_2)$, we count twice all those coils that pass by both points. Making correction for this, we have

$$\beta^\dagger(N, \mathbf{R}; \mathbf{P}_1; \mathbf{P}_2)dv=\beta(N, \mathbf{R}; \mathbf{P}_1) +\beta(N, \mathbf{R}; \mathbf{P}_2)-\rho\beta(N, \mathbf{R}; \mathbf{P}_1, \mathbf{P}_2). \quad (101)$$

Under the conditions which we are assuming, the first approximation is

$$\beta^\dagger(N, \mathbf{R}; \mathbf{P}_1; \mathbf{P}_2)\simeq\beta(N, \mathbf{R}; \mathbf{P}_1)+\beta(N, \mathbf{R}; \mathbf{P}_2). \quad (102)$$

DISCUSSION

The problems in the preceding sections can be considered to be general problems in three independent stochastic variables. Extention of these problems to n independent variables is straight foreward. The vectors become n-dimensional, and Eq. (8) will be

$$W(N, R)=\left(\frac{n}{2\pi Nl^2}\right)^{n/2}\exp\left[-\frac{n|\mathbf{R}|^2}{2Nl^2}\right], \quad (103)$$

and Eq. (9) becomes

$$\frac{\partial W}{\partial N}=\frac{l^2}{2n}\nabla^2 W, \quad (104)$$

where ∇^2 is the n-dimensional Laplacian. Of course, all volume elements become n-dimensional hypervolume elements.

In addition to this general concept of the problems they have analogies in diffusion, heat flow, Brownian motion, and shapes of large molecules. Let us consider briefly some diffusion and heat flow analogies.

Suppose that at time zero a quantity of substances A is introduced at the origin into an unstirred suspending medium. The substance A diffuses from the origin, the origin being an instantaneous point source. Assume that an adsorbing sphere of radius ρ is situated at $\mathbf{P}$, and for the present, assume that a constant fraction of the A that diffuses to the surface of the sphere is adsorbed. Then $Q(t, \mathbf{P})$, the number of particles of A adsorbed upon the sphere between time zero and time t, is given to a first approximation in terms of $\rho\gamma(N, \mathbf{P})$ of Problem 5 by

$$Q(t, \mathbf{P})=g\rho\gamma(t, \mathbf{P}), \quad (105)$$

where N has been replaced by nt and $l^2/6$ has been replaced by D/n, the diffusion coefficient of the suspending medium divided by the number of "flights" per second n. Equation (105) neglects the time dependence of the probability that a particle is adsorbed only after diffusing to the sphere two or more times. The proportionality to ρ is in contrast with proportionality to ρ^2 which holds for the case in which equilibrium exists between the A adsorbed and the A in the surrounding medium. This weaker dependence upon ρ for the non-equilibrium case is due to the competition for A among the various portions of the adsorbing surface. When equilibrium exists there is no such competition since adsorption and de-adsorption are taking place at equal rates.

This diffusion problem can be extended by assuming that there are n similar spheres at points $\mathbf{P}_1, \mathbf{P}_2, \cdots, \mathbf{P}_1$. If the spheres are far apart we have to a good approximation that the total amount of A adsorbed on all the spheres between times zero and t is given by

$$Q(t, \mathbf{P}_1, \cdots, \mathbf{P}_n)=g\rho\sum_{i=1}^{n}\gamma(t, \mathbf{P}_i). \quad (106)$$

If the spheres are not sufficiently far apart they interfere with one another, and a better approximation is

$$Q(t, \mathbf{P}_1, \cdots, \mathbf{P}_n)=g\rho\Big[\sum_{i=1}^{n}\gamma(t, \mathbf{P}_i) -\rho g\sum_{i=1}^{n}{}'\sum_{j=1}^{n}\int\beta(t, \mathbf{R}; \mathbf{P}_i, \mathbf{P}_j)dv\Big], \quad (107)$$

where the integration is over all $\mathbf{R}$-space, $\sum_{i=1}^{n}{}'$ means summation over i with the term $i=j$ excluded, and $\beta(t, \mathbf{R}; \mathbf{P}_i, \mathbf{P}_j)$ is defined in Problem 9. The second term on the right of Eq. (107) corrects for the fact that a particle which is absorbed on one sphere cannot be adsorbed on another.

Other extensions of this problem can be immediately obtained. For example, instead of having only one source of particles we might have m instantaneous sources at points $\mathbf{S}_i, \cdots, \mathbf{S}_m$. Then the amount adsorbed by one sphere at $\mathbf{P}$ by time t is

$$Q(t; \mathbf{P})=g\rho\sum_{i=1}^{m}\gamma(t, \mathbf{P}-\mathbf{S}_i). \quad (108)$$

If we have, instead of an instantaneous source, a continuous source where A enters continuously at a rate $r(t)$, which is a function of the time, we have, instead of Eq. (105),

$$Q(t; \mathbf{P})=g\rho\int_0^t r(t-\tau)\gamma(\tau, \mathbf{P})d\tau. \quad (109)$$

When the fraction of those particles of A striking the surface which are adsorbed depends upon the amount of A already adsorbed we have instead of g, a function $g(Q)$. $Q(t, \mathbf{P})$ is then not given by Eq. (105) but as the solution of

$$\int_{Q(0,\mathbf{P})}^{Q(t,\mathbf{P})}\frac{dQ}{g(Q)}=\rho\gamma(t, P). \quad (110)$$

Combinations of the preceding extensions of the original problem can be made to obtain the formal solutions of still more general diffusion problems.

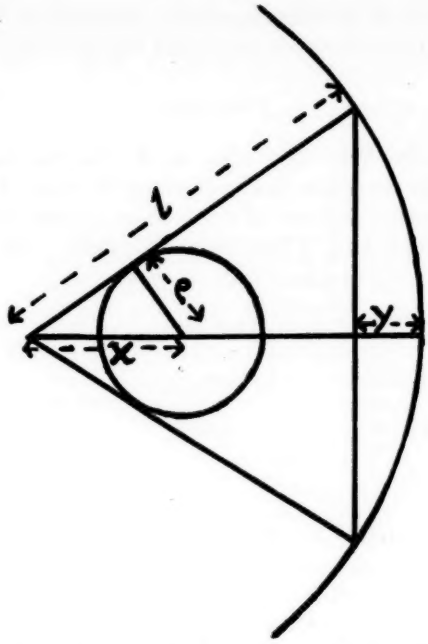

FIG. 1. Spherical segment for links that pass through a sphere of radius ρ.

In the analogous heat flow problems, $W(N, \mathbf{R})$ becomes the temperature at time N at point $\mathbf{R}$, and $l^2/6$ becomes the thermal diffusivity κ of the medium surrounding the sphere and is given by

$$\kappa = K/dc, \tag{111}$$

where K is the thermal conductivity, d is the density, and c is the heat capacity. Equation (105) gives the heat adsorbed between times zero and t by a sphere situated at $\mathbf{P}$ and kept at constant temperature by continual removal of the heat absorbed—the heat having been introduced at the origin into the surrounding medium at time zero, and the medium having been originally (zero time) at the same temperature as the sphere. When the rate of transfer of heat from the medium to the sphere is sufficiently rapid to cause the temperature of the medium in contact with the sphere to be the same as that of the sphere (or nearly so) g can be taken as a constant. If this last simplification does not apply, then Eq. (110) holds. Likewise if the temperature of the sphere is not kept constant Eq. (110) holds.

Concerning Brownian particles, one interpretation of $\rho\gamma(t, \mathbf{P})$ is the following: A particle undergoing Brownian motion is at the origin at time zero. If a spherial "counter" of radius ρ is at $\mathbf{P}$, then the probability that the particle will be "counted" by time t is given by $\rho\gamma(t, \mathbf{P})$. Also $\rho\alpha(t, \mathbf{R}; \mathbf{P})$ of Problem 2 gives the probability that a particle, known to be at the origin at time zero and at $\mathbf{R}$ at time t, has been counted at $\mathbf{P}$ between times zero and t—the assumption being made that the process of counting does not destroy the Brownian motion of the particle. Other interpretations of the problems (or modifications thereof) in the preceding sections can be made. However, it is noteworthy that none of these problems can give us the probability that a particle is counted twice by a counter at $\mathbf{P}$. We can obtain only the probability that the particle is counted at least once at $\mathbf{P}$, or the probability that it is counted at least once at $\mathbf{P}_1$, then at least once at $\mathbf{P}_2$, and then again at least once at $\mathbf{P}_1$ (Problem 7)—or simple modifications of these probabilities.

The failure of the boundary value method to give us the probability of counting a particle twice with the same counter shows up as a failure to give us the answer to an interesting problem in polymers. This is the problem of the "volume effect," which has received considerable attention recently.[10–15] The problem is that of determining how much the shape of a molecule is modified by the inability of the molecule to pass through a volume element of atomic size more than once. The boundary value method fails here for a second reason: Spheres of atomic size require consideration of the discrete nature of the random flight.

Problems 3 and 4 are special "first time passage problems." The one-dimensional problem of this type has been of interest for some time.[16] Wasow[17] has recently treated three- and n-dimensional problems to obtain *mean duration* of random walks.

APPENDIX

We will develop here the relationship between the number of links that pass through a sphere of radius ρ and the number of links that end in the sphere when $\rho < l$. The main purpose of presenting this derivation is to show clearly what approximations are involved.

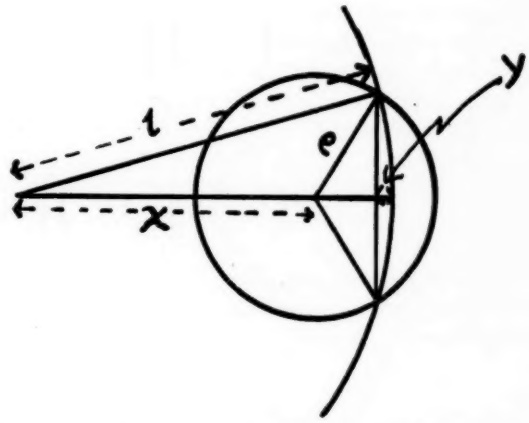

FIG. 2. Spherical segment for links that end in a sphere of radius ρ

[11] P. J. Flory, J. Chem. Phys. **17**, 303 (1949).
[12] Elliott W. Montroll, J. Chem. Phys. **18**, 734 (1950).
[13] Weissberg, Simha, and Rothman, J. Research Natl. Bur. Standard **47**, 298 (1951).
[14] Frisch, Collins, and Freedman, J. Chem. Phys. **19**, 1402 (1951).
[15] Gilbert W. King, Natl. Bur. Standards, Applied Mathematics Series **12**, U. S. Government Printing Office, Washington 25, D. C. (1951), p. 12.
[16] Arnold J. F. Siegert, Phys. Rev. **81**, 617 (1951).
[17] Wolfgang Wasow, J. Research Natl. Bur. Standards **46**, 462 (1951), RP 2215.

Of those links that start at a point **P** the fraction $F_T(\mathbf{P})$ that pass through the sphere of radius ρ is the ratio of the area of a spherical segment of one base on a sphere of radius l to the total area of the sphere of radius l (see Fig. 1). The area A_T of the spherical segment is

$$A_T=2\pi ly, \tag{A1}$$

where y is the altitude of the segment and is given by

$$y=l\left[1-\frac{1}{x}(x^2-\rho^2)^{\frac{1}{2}}\right], \tag{A2}$$

where x is the distance of the center of sphere of radius ρ from **P** (Fig. 1). Therefore,

$$F_T(\mathbf{P})=\frac{A_T}{4\pi l^2}=1/2\left[1-\frac{1}{x}(x^2-\rho^2)^{\frac{1}{2}}\right], \tag{A3}$$

and the total number of links ϕ_T that either end in the sphere or pass through the sphere is

$$\phi_T=\int_{\rho}^{l+\rho} f(\mathbf{P})F_T(\mathbf{P})4\pi x^2dx, \tag{A4}$$

where $f(\mathbf{P})$ is the number of links starting from **P**. If the point **P** is sufficiently far from the origin (say, $\langle OP\rangle>10l$), then we can use the approximation that $f(\mathbf{P})$ is a constant f, and we have

$$\begin{aligned}\phi_T&=f\int_{\rho}^{l+\rho}F_T(\mathbf{P})4\pi x^2dx\\&=2\pi f\int_{\rho}^{l+\rho}[x^2-x(x^2-\rho^2)^{\frac{1}{2}}]dx\\&=\frac{2\pi f}{3}\left[l^3+3l^2\rho+3l\rho^2-l^3\left(1+2\frac{\rho}{l}\right)^{\frac{3}{2}}\right]\\&=\frac{2\pi f}{3}\left[l^3+3l^2\rho+3l\rho^2-l^3\left(1+\frac{3\rho}{l}+\frac{3}{2}\frac{\rho^2}{l^2}+\cdots\right)\right].\end{aligned} \tag{A5}$$

In case ρ is sufficiently small compared to l we can neglect terms of order $(\rho/l)^3$ and higher. Then

$$\phi_T\simeq\pi fl\rho^2. \tag{A6}$$

Of those links that start at **P**, the fraction $F_E(\mathbf{P})$ ending in the sphere is also given by the ratio of the area of a spherical segment of one base on a sphere of radius l to the total area of the sphere of radius l (see Fig. 2). The area A_E of this spherical segment is

$$A_E=2\pi ly, \tag{A7}$$

where (Fig. 2)

$$y=l-\frac{l^2-\rho^2}{2x}-x^2. \tag{A8}$$

The probability $F_E(\mathbf{P})$ that a link starting at point **P** ends in the sphere is therefore

$$F_E(\mathbf{P})=\frac{A_E}{4\pi l^2}=\frac{1}{2l}\left(l-\frac{l^2-\rho^2}{2x}-\frac{x^2}{2}\right). \tag{A9}$$

The number of links ϕ_E that end in the sphere is

$$\begin{aligned}\phi_E&=f\int_{l-\rho}^{l+\rho}F_E(\mathbf{P})4\pi x^2dx\\&=f\frac{4}{3}\pi\rho^3.\end{aligned} \tag{A10}$$

The ratio Z of the number of links that end in the sphere to the number that pass through is

$$Z=\phi_E/(\phi_T-\phi_E). \tag{A11}$$

For the case in which ρ is small compared to l,

$$Z\simeq 4/3(\rho/l). \tag{A12}$$

Calculation of Vibrational Relaxation Times in Gases

R. N. SCHWARTZ, Z. I. SLAWSKY, *Naval Ordnance Laboratory, White Oak, Silver Spring, Maryland*

AND

K. F. HERZFELD, *Catholic University of America, Washington, D. C.*

(Received May 9, 1952)

Vibrational relaxation times in gases are calculated with the method of Zener using an exponential repulsion in a one-dimensional model. The constants of the interaction potential are determined by fitting it to the data of Hirschfelder, *et al.* The great effect which some impurities have is accounted for either by their low mass and resultant high velocity or by "near resonance" transfers in which the vibrational quantum of the substratum is used partly to excite the vibration of the impurity, only the difference being transferred to translation. However, there are other impurities, the action of which cannot be explained in this manner. The theoretical values for the relaxation times are 10 to 30 times shorter than the experimental ones, which difference may be accounted for by the use of the one-dimensional model. Macroscopic equations governing the more complex relaxation processes in polyatomic gases and gas mixtures are developed.

INTRODUCTION

CONTINUED interest in the study of relaxation phenomena in gases over the last 20 years has resulted in the accumulation of a large body of experimental data concerning the relaxation time of pure gases as well as gas mixtures. The dependence of the relaxation time on density over moderate ranges is now well known; the dependence on the temperature not as well known. The only theoretical calculation on the vibrational relaxation time of gases that has found any general acceptance to date was made by Landau and Teller[1] in 1936. This was refined somewhat by Bethe and Teller[2] in 1940. These calculations give the general character of dependence of the relaxation time of a pure diatomic gas on the density and temperature. No calculation of the effect of mixing different gases has been attempted.

With the advance in our knowledge of the force constants between molecules, it becomes possible to attempt a more quantitative calculation of the relaxation time and to even extend the calculations to mixtures of gases. The objective of this paper will be to make a quantitative calculation of the relaxation time in gases. The method of calculation given here is generally applicable to diatomic gases, to chemically nonreactive gas mixtures, and gas molecules with several normal vibrational modes. The theory of the macroscopic behavior of gases with relaxation times, such as sound dispersion and absorption, is then extended to include the cases of gas mixtures and polyatomic gases.

The behavior of a material volume of gas in a sound field or gas flow can be described by the standard equations: (1) equation of state of the gas; (2) law of conservation of mass; (3) momentum equation; and (4) energy equation. With relaxation phenomena present in the gas flow, these equations are not sufficient. The internal energy of the gas can no longer be expressed as a function of a single temperature. It is customary to write for a perfect gas the internal energy as the sum of energies of translation, rotation, vibration, etc.,

$$E=E_{\text{trans}}(T)+E_{\text{rot}}(T_r)+E_{\text{vib}}(T_v)+\cdots, \qquad (1)$$

where T, T_r, T_v, etc., are "temperatures," but not necessarily equal to one another.

For a pure diatomic gas the lack of adjustment of the vibrational degrees of freedom may be described by the equation derived by Landau and Teller:[1]

$$\frac{dE_{\text{vib}}(T_v)}{dt}=\frac{1}{\tau}\{E_{\text{vib}}(T)-E_{\text{vib}}(T_v)\}, \qquad (2)$$

where T is the temperature of the translational degrees of freedom, T_v is the temperature of the vibrational degrees of freedom, and τ is called the relaxation time of the gas. As energy is transferred between degrees of freedom only during a molecular collision, the rate of energy transfer is inversely proportional to the number of collisions a molecule experiences per second, $M_{a,a}$, and thus to density. Furthermore, not every collision is effective in transferring a quantum of vibrational energy to translation or vice versa, so that the relaxation time must also be proportional to the probability of such an energy exchange, denoted by P. For the relaxation time we may write

$$\tau=1/M_{a,a}P.$$

Here, P is, roughly speaking, the probability that upon a collision, a quantum of vibrational energy is removed from the vibrating system and converted to translational energy. For a gas composed of polyatomic molecules or mixtures of different types of molecules, there arises the possibility of energy exchange between the different vibrational degrees of freedom during a collision as well as exchanges with the translational degrees of freedom. A separate relaxation time must now be ascribed to each of these energy transfers.

[1] L. Landau and E. Teller, Phys. Z. Sowietunion **10**, 34 (1936).
[2] H. A. Bethe and E. Teller, Aberdeen Proving Ground Report X-117.

Additional equations more complicated than Eq. (2) must be used to describe the behavior of the gas system.

GENERAL THEORY OF COLLISION PROCESS

We will first develop formulas for the numerical computation of the probability of a vibrational energy jump taking place during a molecular collision. Let $p^{i\to f}(v_0)$ denote the probability that the system made up of a pair of colliding molecules, originally of relative velocity v_0 and vibrational states $i_1, i_2, \cdots, i_n$, will, after a collision, arrive at vibrational states $f_1, f_2, \cdots, f_n$. The method of calculating $p^{i\to f}(v_0)$ given by Zener[3] will be applied here. Zener assumed that the problem may be treated one-dimensionally. The molecules are taken as rotationless and approach each other along a straight line. This motion can be described in terms of the coordinate r, the distance between centers of gravity of the collision pair, and the normal vibrational coordinates $s_1, s_2, \cdots, s_n$. It is further assumed that the zero-order wave functions describing the collision are separable in these coordinates. Then, if the interaction potential between the molecules is also approximated by a product of functions of the coordinates,

$$V=V_0\cdot V_r(r)\cdot V_1(s_1)\cdots V_n(s_n), \tag{3}$$

it becomes possible to express the probability $p^{i\to f}(v_0)$ in a product form. Here V_0 is a constant with dimensions of energy.

$$p^{i\to f}(v_0)=\frac{16\pi^2V_0^2}{v_0v_F h^2}[\mathbf{V}(i_1\to f_1)\cdots\mathbf{V}(i_n\to f_n)R]^2, \tag{4}$$

where R, $\mathbf{V}(i_1\to f_1)$, $\cdots\mathbf{V}(i_n\to f_n)$ are defined as follows:

$$R\equiv\int_{-\infty}^{\infty}F_0F_FV_r dr, \tag{5}$$

where F_0, F_F are solutions of the Schrödinger equation for the motion of a free particle in the potential field V_r.

$$\frac{d^2}{dr^2}F_F+\frac{8\pi^2\mu}{h^2}\left(\frac{\mu v_F^2}{2}-V_0V_r\right)F_F=0.$$

μ is the reduced mass of the molecules. The matrix elements $\mathbf{V}(i_n\to f_n)$ are defined

$$\mathbf{V}(i_n\to f_n)\equiv\int_{-\infty}^{\infty}\psi_i^{(n)}V_n^{(s_n)}\psi_f^{(n)}ds_n, \tag{6}$$

where $\psi_i^{(n)}$, $\psi_f^{(n)}$ are normalized oscillator wave functions for the s_nth normal vibrational coordinate. v_0 is the relative velocity of the molecules before collision, v_F the velocity after collision.

[3] C. Zener, Phys. Rev. **37**, 556 (1931). Since this paper was finished C. F. Curtiss and F. T. Adler, J. Chem. Phys. **20**, 249 (1952), have applied group theoretical arguments to extend Zener's method of approximation to the three-dimensional collision of a nonspherical molecule and an atom. No actual evaluation of probabilities was carried out.

Jackson and Mott[4] evaluated the integral R in a closed form for a potential $V_r=e^{-\alpha r}$. Making use of their results, $p^{i\to f}$ assumes the form

$$p^{i\to f}=\mathbf{V}^2(i_1\to f_1)\cdots\mathbf{V}^2(i_n\to f_n)\frac{1}{16\pi^2}(\theta_0^2-\theta_F^2)^2\times\frac{(e^{\theta_0}-e^{-\theta_0})(e^{\theta_F}-e^{-\theta_F})}{(e^{\theta_0}+e^{-\theta_0}-e^{\theta_F}-e^{-\theta_F})^2}, \tag{7}$$

where $\theta_0\equiv 4\pi^2\mu v_0/\alpha h$. Here v_0 and v_F are related by the fact that the total energy of the collision system is conserved in the collision, i.e.,

$$\mu/2v_0^2-v_F^2=\Delta E, \tag{8}$$

where ΔE is the total energy exchanged between vibration and translation during a collision. Those energy exchanges for which $\Delta E=0$ are called resonance exchanges; such occur when one molecule looses a quantum of vibrational energy to another molecule without changing their translational energies.

Equation (7) tells us that the probability of an energy exchange during collision depends on the linear momentum gained or lost in the collision. The probability is largest for a resonant exchange but may become exceedingly small for a typical nonresonant exchange in which the linear momentum is changed by a large fraction. Equation (7) may be simplified under these two limiting conditions of resonance or large nonresonance.

The probability $p^{i\to f}$, given in Eq. (7) is dependent on the initial velocity v_0. We must therefore average over all initial velocities to arrive at a probability, $P^{i\to f}$. Assuming the velocities are distributed according to Maxwell's law at a temperature T,

$$P^{i\to f}=2\left(\frac{\mu}{2kT}\right)^2\int_0^{\infty}v_0^3p^{i\to f}\exp(-\mu v_0^2/2kT)dv_0. \tag{9}$$

This integral may be evaluated in the limiting cases mentioned in the paragraph above. For a nonresonant energy exchange, in Appendix A we evaluated Eq. (9) to yield

$$P^{i\to f}=\mathbf{V}^2(i_1\to f_1)\cdots\mathbf{V}^2(i_n\to f_n)0.39\times\left[\frac{8\pi^3\mu\Delta E}{(\alpha^*)^2h^2}\right]^2\frac{\sigma^{\frac{1}{2}}e^{-\sigma}}{1-e^{-\frac{1}{2}\sigma}}, \tag{A7}$$

where

$$\sigma\equiv 3\left(\frac{2\pi^4(\Delta E)^2\mu}{(\alpha^*)^2h^2kT}\right)^{\frac{1}{3}}\pm\frac{\Delta E}{2kT},$$

and $\mathbf{V}(i_n\to f_n)$ is defined by Eq. (6) and evaluated in Appendix A; α^*, further specified in the following paragraphs, is the reciprocal of a length, the measure of the "hardness" of the molecule on impact. The upper

[4] J. M. Jackson and N. F. Mott, Proc. Roy. Soc. (London) **A137**, 703 (1932).

sign appearing in σ applies if the total vibrational energy decreases during collision, the lower if the vibrational energy increases.

Equation (A7) is valid as long as we limit ourselves to those molecular excitations and temperatures for which

$$\exp\left(-\frac{4\pi^2\Delta E}{\alpha^* h v_0^*}\right)\ll 1,$$

$$\Delta E\ll\frac{\mu}{2}(v_0^*)^2,$$

$$\Delta E\ll\frac{\mu}{2}(v_F^*)^2,$$

[as shown in Appendix A, Eqs. (A3) and (A6)], where v_0^* is a "most favorable" velocity for bringing about the excitation and is further specified in Appendix A. It is interesting to note that the classical estimate made by Landau and Teller gave a result

$$P\sim\exp\left(\frac{\pi^2(\Delta E)^2\mu}{2\alpha^2 h^2 kT}\right)^{\frac{1}{3}},$$

which agrees with the quantum-mechanical calculations of the dependence of $P^{i\to f}$ on ΔE, μ, α, and T but misses a factor of $(4\pi^2)^{\frac{1}{3}}$ in the exponents. The Eq. (A7) may be used for numerical computation of P once α^* is given. There is nothing in the development which restricts us to simple diatomic gases. Polyatomic gases and gas mixtures may be treated. As the quantum-mechanical development is one-dimensional, values of $P^{i\to f}$ so determined would be for molecular collisions in which the molecules are "pre-oriented" in a most favorable manner for the excitation to occur; $P^{i\to f}$ should be multiplied by a geometrical factor less than unity. This factor, denoted by $C^{i\to f}$, can be expected to be fairly constant from molecule to molecule and over a wide range of temperatures.

A number of general conclusions as to relaxation phenomena can be drawn from a brief examination of Eq. (A7). The probability of an excitation is seen to be $\exp(-\Delta E/kT)$ of the reverse process as demanded by general statistical principles. If a number of gases and gas mixtures are compared at the same temperature, the only factors in Eq. (A7) causing large variation in the calculated $P^{i\to f}$ from gas to gas are μ and ΔE. Since $P^{i\to f}$ decreases very rapidly with an increase in σ, small energy jumps, ΔE, and small masses, μ (i.e., high translational velocities), are favorable to energy transfer. As ΔE becomes small, however, condition (A6) mentioned above is not satisfied. Under conditions of exact resonance, $\Delta E=0$, $p^{i\to f}$ reduces to a simple expression and $P^{i\to f}$ is given:

$$P^{i\to f}=\mathbf{V}^2(i_1\to f_1)\cdots\mathbf{V}^2(i_n\to f)\frac{8\pi^2\mu kT}{(\alpha^*)^2h^2}$$

(see (A9) in Appendix A).

THE POTENTIAL FIELD BETWEEN MOLECULES

It is customary to represent the field by the Lennard-Jones function:[5]

$$V=4\epsilon\{(r_0/r)^{12}-(r_0/r)^6\}. \tag{10}$$

This is made up of an attractive component as well as a short-range, repulsive component. For reasons already given by Landau and Teller,[6] only short-range forces are of importance in energy transfer. Since Mott and Jackson have solved the Schrödinger equation for an exponential repulsive potential, we approximate the interaction between the individual atoms of different molecules by a similar function:

$$V=Ce^{-\alpha_x\chi}. \tag{11}$$

Here, χ is the distance between atoms A and A', and α_x may be taken as a measure of the effective extent of their mutual repulsive force field. In practice, the extent of the repulsive field is much smaller than the distance between the atoms in a molecule, i.e.,

$$\alpha_x^{-1}\ll d, \tag{12}$$

so that influence of molecules B and B' (Fig. 1) on the collision may be neglected. Equation (11), therefore, may be used to approximate the intermolecular field for a collision such as illustrated by Fig. 1.

THE EVALUATION OF THE CONSTANTS IN $V=V_0e^{-\alpha(r+A_1s_1+\cdots)}$

In general, we may write the distance of separation of the nearest atoms of the two molecules, χ, in terms of the distance of separation of the centers of gravity of the molecules, r, and the normal coordinates of vibration, s_1, s_2, $s_3+\cdots s_n$:

$$\chi=r+A_0+A_1s_1+A_2s_2+\cdots.$$

The potential function may be written as

$$V=V_0e^{-\alpha(r+A_1s_1+\cdots+A_ns_n)}, \tag{13}$$

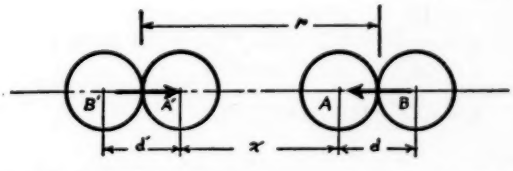

FIG. 1. Schematic drawing of the one-dimensional collision.

[5] R. H. Fowler, *Statistical Mechanics* (The Cambridge University Press, New York, 1936), Chap. X; Hirschfelder, Bird, and Spotz, *Transport Properties of Gases* (University of Wisconsin Press, Madison, Wisconsin, 1948), II" CM-508, contain a compilation of constants ϵ and r_0 for many gases from viscosity and diffusion data.

[6] In general, long-range forces distort, adiabatically, the internal and external wave functions without inducing transitions. (See Appendix.) For a discussion of the role of certain long-range forces, see Slawsky, De Wette, and De Groot, Supplemento Al Volume VII, Serie IX Del Nuovo cimento, N. 2 (1950). The effect of the centrifugal term appearing in a three-dimensional treatment is being evaluated as a long-range interaction.

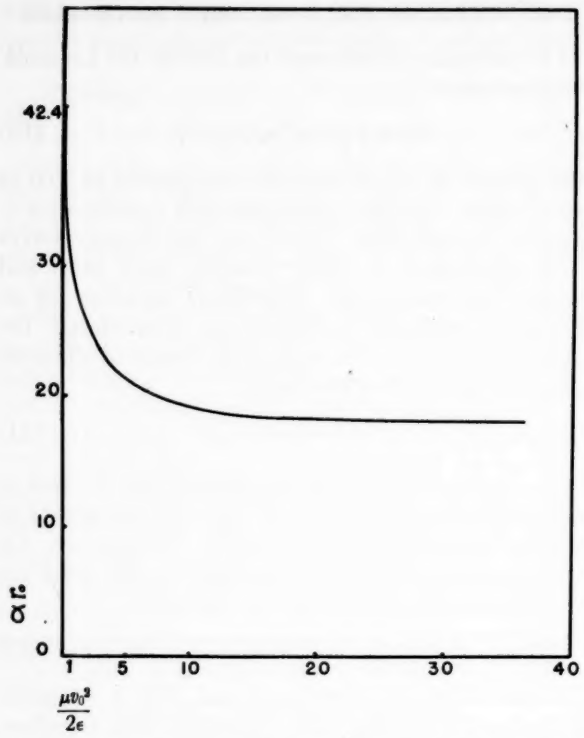

FIG. 2. The reciprocal of the effective extent of the repulsive molecular field, α^{-1}, as a function of the initial translational energy of the colliding molecules. ϵ and r_0 are constants for a given molecule appearing in the Lennard-Jones potential, Eq. (10).

which is of the form of Eq. (3). In order to determine α, the first term of Eq. (13),

$$V \cong V_0 e^{-\alpha r}, \tag{14}$$

is fitted to the Lennard-Jones potential curve (Eq. (10)) at the point $r=r_1$. This is done by setting V and dV/dr of Eqs. (10) and (14) equal and adding the condition $V \to -\epsilon$ as $r \to \infty$. The point $r=r_1$ is somewhat arbitrary. We have taken r_1 as the classical point of closest approach of the two molecules moving towards each other with relative velocity v_0. Then,

$$\alpha = \frac{12}{r_0 D}[\tfrac{1}{2}+\tfrac{1}{2}(1+D)^{\frac{1}{2}}]^{1/6}[1+(1+D)^{\frac{1}{2}}+D],$$
$$r_1 = r_0[\tfrac{1}{2}+\tfrac{1}{2}(1+D)^{\frac{1}{2}}]^{-1/6}, \tag{15}$$

where

$$D \equiv \frac{(\mu/2)v_0^2+\epsilon}{\epsilon}.$$

The function αr_0 is plotted as a function of D in Fig. 2.

In treating unlike molecules, the effective values of α and r_0 used in Eq. (15) are approximated by

$$r_0(1,2) \cong \tfrac{1}{2}(r_0(1)+r_0(2)),$$
$$\epsilon(1,2) \cong (\epsilon(1)\epsilon(2))^{\frac{1}{2}}, \tag{16}$$

for those cases in which experimental values of $r_0(1,2)$ and $\epsilon(1,2)$ are not available.

Two points of interest will be pointed out before closing the discussion of the molecular field. One is that from Fig. (2), it can be seen that, for molecules whose value of ϵ is not too great, we can make the approximate generalization that $\alpha \cong 17.5/r_0$. Secondly, that in the rather arbitrary manner we have chosen to compute α, the numerical value of α is slightly dependent on initial molecular velocities and consequently on temperature. In Eqs. (A7) and (A9), the value of α at $v_0=v_0^*$ is used.

DIATOMIC MOLECULES

Landau and Teller[1] have shown that the P appearing in Eq. (3) when applied to diatomic molecules is

$$P = P^{1\to 0}(1-e^{-h\nu/kT}). \tag{17}$$

Numerical results from (A7) are given in Table I as $P^{1\to 0}(a, a)$.

POLYATOMIC MOLECULES AND GAS MIXTURES

In these cases, two problems have to be considered: The numerical value of $P^{i\to f}$ as given by (A7), and the equation connecting P and $P^{i\to f}$, which will replace (17).

It is clear from the form of $P^{i\to f}$ that it makes no difference whether the gas is composed of molecules with several normal modes (CO_2, COS, etc.) or a mixture of diatomic gases. It becomes possible, therefore, to calculate the adjustment rate of the vibrational energy for these complex situations and the acoustical relaxation times that should be assigned to them. The form of (A7) explains the great effect some impurities may have on the relaxation time. The addition of hydrogen to a heavier gas will decrease μ and thus increase $P^{i\to f}$. This may be termed a *mass effect* and further illustrations of it will be given later. This effect has been experimentally verified. On the other hand, an impurity, which permits the exchange of vibrational energy among two or more vibrational degrees of freedom with a consequent decrease in the amount of energy, ΔE, exchanged with translation, will again increase the probability $P^{i\to f}$. We will call this effect the near *resonance effect;* examples of such an effect will be given later. The existence of such an effect in ultrasonics has not been pointed out previously.[7]

THE MACROSCOPIC EQUATIONS

In the calculation of the resultant P of Eq. (3) from the $P^{i\to f}$ as computed above, we have to write differential equations which express the change of internal energy as a difference between the effect of deactivating and of exciting collisions for all possible transitions.

Our attention shall be limited to a gas whose molecules display but two different, active frequencies of internal vibration ν_a and ν_b; the internal energy is the sum of energies $E_{\text{vib }1}$ and $E_{\text{vib }2}$, hereafter written E_a

[7] It was pointed out by E. Patat and E. Bartholome, Z. physik. Chem. **32**, 396 (1936), that in the study of reaction kinetics, gas mixtures, for which a transfer of energy between vibrational degrees of freedom is easy, promote the reaction. However, they concluded that in ultrasonics, only the translational to vibrational energy transfer was important.

and E_b. We will further limit ourselves to cases where a change of two or more quanta in either vibrational mode during a collision is so improbable as to be negligible. This is most often the case. An exception, wherein a jump of two quanta in a particular mode must be considered will be treated separately.

In the following, we may picture the gas as being made up of two kinds of molecules, molecules a with frequency ν_a, and molecules b of frequency ν_b, a being the fraction of kind a and b the fraction of kind b.

Energy is being fed into the ν_a vibration of molecules a by collision with other molecules a (number per second $M_{a,a}$) and also by collision with molecules b (number per sec $M_{a,b}$). Each effective collision feeds in an amount $h\nu_a$. The fraction of effective collisions with other molecules a, is given by a sum of terms of transition probabilities, $P^{\lambda\to\lambda+1}(a,a)$, each weighted by the relative population of states λ. Similarly, the fraction of effective collisions with molecules b is given by a double sum of terms $P_{l\to l-1}{}^{\lambda\to\lambda+1}(a,b)$ weighted by the product of the relative populations of states λ (molecules a) and l (molecules b). The total change of energy in vibration is then

$$\frac{daE_a}{dt}=Nh\nu_a\Big\{M_{a,a}\Big(P^{0\to1}(a,a)\frac{n_0}{N}+P^{1\to2}(a,a)\frac{n_1}{N}+\cdots-P^{1\to0}(a,a)\frac{n_1}{N}-\cdots\Big)+M_{a,b}\Big(P_{0\to0}{}^{0\to1}(a,b)\frac{n_0}{N}\frac{m_0}{N}+\cdots+P_{1\to0}{}^{0\to1}(a,b)\frac{n_0}{N}\frac{m_1}{N}+\cdots\Big)\Big\}$$
$$+\text{terms involving } 2h\nu_a \text{ changes which are not considered at the moment.} \tag{18}$$

The probability functions $P^{0\to1}(a,a)\cdots$, $P_{1\to0}{}^{0\to1}(a,b)$, etc., have already been defined. The transition indicated by the superscript will refer to change in ν_a vibration, the subscript to the simultaneous transition in ν_b vibration. n_0/N, n_1/N, $\cdots$, n_k/N are the fractions of all molecules that are in the zeroth, first, etc., quantum levels of the ν_a vibration. m_0/N, m_1/N, $\cdots$ are fractions in the quantum levels of the ν_b vibration.

Equation (18) can be considerably simplified by the use of relation (A11). It follows that

$$\begin{aligned}P^{\lambda\to\lambda-1}(a,a)&=\lambda P^{1\to0}(a,a),\\ P_{l\to l}{}^{\lambda\to\lambda-1}(a,b)&=\lambda P_{0\to0}{}^{1\to0}(a,b),\\ P_{l\to l-1}{}^{\lambda\to\lambda+1}(a,b)&=(\lambda+1)lP_{1\to0}{}^{0\to1}(a,b).\end{aligned} \tag{19}$$

Furthermore, the relationship (A7) tells us that

$$P_{1\to0}{}^{0\to1}(a,b)=P_{0\to1}{}^{1\to0}\exp\Big[-\frac{h(\nu_a-\nu_b)}{kT}\Big].$$

When the above relations are introduced into Eq. (18), it becomes

$$\frac{daE_a}{dt}=Nh\nu_a\Big\{M_{a,a}\sum_{\lambda=0}^{\infty}\frac{n_\lambda}{N}\Big(P^{0\to1}(a,a)\sum_{\lambda=0}^{\infty}(\lambda+1)\frac{n_\lambda}{N}-P^{1\to0}(a,a)\sum_{\lambda=0}^{\infty}\frac{\lambda n_\lambda}{N}\Big)+M_{a,b}\sum_{l=0}^{\infty}\frac{m_l}{N}\times\Big(P_{0\to0}{}^{0\to1}(a,b)\sum_{\lambda=0}^{\infty}(\lambda+1)\frac{n_\lambda}{N}-P_{0\to0}{}^{1\to0}(a,b)\sum_{\lambda=0}^{\infty}\frac{\lambda n_\lambda}{N}\Big)+M_{a,b}\Big(P_{1\to0}{}^{0\to1}(a,b)\sum_{\lambda=0}^{\infty}(\lambda+1)\frac{n_\lambda}{N}\sum_{l=0}^{\infty}l\frac{m_l}{N}-P_{0\to1}{}^{1\to0}(a,b)\sum_{\lambda=0}^{\infty}\sum_{l=0}^{\infty}\lambda\frac{n_\lambda}{N}(l+1)\frac{m_l}{N}\Big)\Big\}. \tag{20}$$

In this form the expression can readily be applied to the calculation of the adjustment rate of pure polyatomic gases or gas mixtures.

When a mixture of two gases is considered, the following relations hold

$$\begin{aligned}&N=\sum_{\lambda=0}^{\infty}n_\lambda+\sum_{l=0}^{\infty}m_l \qquad h\nu_a\sum_{\lambda=0}^{\infty}\lambda n_\lambda=aE_a\\ &\sum_{\lambda=0}^{\infty}n_\lambda=aN \qquad h\nu_b\sum_{l=0}^{\infty}lm_l=bE_b,\\ &\sum_{l=0}^{\infty}m_l=bN\end{aligned} \tag{21}$$

and reduce Eq. (20) to

$$a\frac{dE_a}{dt}=[aM_{a,a}P^{1\to0}(a,a)+bM_{a,b}P_{0\to0}{}^{1\to0}(a,b)]\times[E_a(T)-E_a]+M_{a,b}abP_{0\to1}{}^{1\to0}(a,b)\times\Big[\frac{E_a(T)-E_a}{E_b(T)}\Big\{\frac{1-e^{-h\nu_a/kT}}{1-e^{-h\nu_b/kT}}\Big\}-E_a\frac{E_b(T)-E_b}{E_b(T)}\Big]. \tag{22}$$

TABLE I. Probability of the simple excitation of vibration in a pure gas and a gas mixture.

Gases a	Gases b	T	$P^{1\to0}(a,a)$ Exp.	$P^{1\to0}(a,a)$ Theory	$P^{1\to0}(a,b)$ Exp.	$P^{1\to0}(a,b)$ Theory
Cl_2	N_2	288°A	[a] 3×10^{-5}	10^{-4}	[a] 2.3×10^{-5}	6×10^{-4}
Cl_2	H_2	288°A	3×10^{-5}	10^{-4}	[a] 1.3×10^{-3}	1.7×10^{-2}
CO_2	N_2	288°A	[a] 2×10^{-5}	4×10^{-4}	...	7.5×10^{-4}
CO_2	H_2	288°A	2×10^{-5}	4×10^{-4}	[a] 2×10^{-3}	4.5×10^{-2}
N_2	A	600°A	[b] 3×10^{-8}	7×10^{-9}	...	3×10^{-8}
N_2	H_2	600°A	3×10^{-8}	7×10^{-9}	...	9×10^{-4}

[a] A. Eucken and R. Becker, Z. physik. Chem. **27**(B), 235 (1934).
[b] P. W. Huber and A. Kantrowitz, J. Chem. Phys. **15**, 275 (1947).

TABLE II. Probability of a complex excitation of vibration in a gas mixture.

Gases a	Gases b	T	$P^{1\to 0}(a,a)$ Exp.	$P^{1\to 0}(a,a)$ Theory	$P_{1\to 0}(b,b)$ Exp.	$P_{1\to 0}(b,b)$ Theory	$P_{0\to 1}{}^{1\to 0}(a,b)$ Exp.	$P_{0\to 1}{}^{1\to 0}(a,b)$ Theory
O_2	N_2	288°K	4×10^{-8}	8.5×10^{-8}	0	0	3×10^{-6}	3×10^{-7}
CO	N_2	600°K	···	6×10^{-8}	[a] 3×10^{-8}	7×10^{-9}	···	1.5×10^{-3}
O_2	CO	288°K	4×10^{-8}	8.5×10^{-8}	···	7×10^{-10}	1.2×10^{-4}	2×10^{-6}

[a] P. W. Huber and A. Kantrowitz, J. Chem. Phys. **15**, 275 (1947).

Here $E_a(T)$ is the well-known Einstein function for the energy of a harmonic oscillator at temp. (T):

$$E_a(T)=\frac{Nh\nu_a}{e^{h\nu_a/kT}-1}.$$

A similar expression may be given for dE_b/dt. The first terms of Eq. (22) describes the adjustment of E_a by a simple excitation process and was originally proved by Landau and Teller.[1] One finds that the effective relaxation time of the simple process is

$$\frac{1}{\tau_a(\text{eff.})}=\frac{a}{\tau_a(a,a)}+\frac{b}{\tau_a(a,b)},$$

where

$$[\tau_a(a,a)]^{-1}\equiv M_{a,a}P^{1\to 0}(a,a)(1-e^{-h\nu_a/kT})$$
$$[\tau_a(a,b)]^{-1}\equiv M_{a,b}P_{0\to 0}{}^{1\to 0}(a,b)(1-e^{-h\nu_a/kT}).$$

The complex excitation process, one in which two degrees of freedom are involved, will have its own relaxation time,

$$(\tau_{a,b})^{-1}=abM_{a,b}P_{0\to 1}{}^{1\to 0}(a,b),$$

and is described by the second term of Eq. (22).

In treating a pure polyatomic gas instead of a mixture as above, we substitute the following in Eq. (20) in place of relationships (21):

$$N=\sum_{\lambda=0}^{\infty}n_\lambda=\sum_{l=0}^{\infty}m_l,$$

$$E_a=K_ah\nu_a\sum_{\lambda=0}^{\infty}\lambda n_\lambda, \qquad (23)$$

$$E_b=K_bh\nu_b\sum_{l=0}^{\infty}lm_l,$$

where K_i is the degree of degeneracy of ith degree of freedom. The resulting expression is similar to Eq. (20) except that here

$$a=b=1$$
$$M_{a,b}=M \qquad (24)$$
$$M_{a,a}=0.$$

APPLICATION OF THE RELAXATION EQUATIONS TO ACOUSTICS

As the measurements of relaxation times in gases have usually been made by acoustical methods, an approximate equation applicable to these measurements will be given. In a sound field, we may write

$$T\cong T_0+\Delta T+\cdots$$
$$T_a\cong T_0+\Delta T_a+\cdots$$
$$T_b\cong T_0+\Delta T_b+\cdots$$
$$\Delta E_a\cong C_a\Delta T_a.$$

Then, making use of the equation for the energy of an oscillator, the more general Eq. (22) reduces to[8]

$$\frac{d\Delta T_a}{dt}=\frac{1}{\tau_a(\text{eff.})}(\Delta T-\Delta T_a)+\frac{1}{\tau_{a,b}}\frac{1-e^{-h\nu_a/kT}}{1-e^{-h\nu_b/kT}}$$
$$\times\left\{(\Delta T-\Delta T_a)-\frac{h\nu_b}{h\nu_a}(\Delta T-\Delta T_b)\right\}, \qquad (25)$$

and a similar equation for ΔT_b. $\tau_{a,b}$ and $\tau_a(\text{eff.})$ have been defined already.

SOME SPECIFIC EXAMPLES

Cl_2-He Type Mixture

From Table I it can be seen that in mixtures in which the reduced mass μ of the two kinds of molecules is much smaller than for the pure gas, the effective relaxation time corresponding to the simple adjustment is markedly changed by the addition of the second gas. An excellent example of this "mass effect" is afforded by the addition of helium to chlorine gas. Equation (20) (without the second term describing a complex adjustment) may be used to describe the relaxation process.

$CO-N_2$ Type Mixture

This mixture should be an example of a mixture exhibiting the "resonance" effect mentioned in an earlier paragraph and should have a very short relaxation time because the vibrational frequencies of CO and N_2 are very close to one another. The frequencies are $\nu=6.50\times10^{13}$/sec for CO and 7.05×10^{13}/sec for N_2. These frequencies are quite large and the probability of a simple vibrational excitation of either CO or N_2 is small.[9] On the other hand, the energy exchange involved in a complex process is small. That process whereby a N_2 molecule is de-excited simultaneously with each

[8] This equation differs from each of the systems of equations proposed by Schafer, Z. physik. Chem. **B46**, 212 (1940) for a polyatomic gas with two active vibrational degrees of freedom.

[9] At room temperature, there is no appreciable excitation of either CO or N_2. However, at 600°K, the temperature of the experiments, the effect is measurable.

excitation of a CO molecule will dominate the energy adjustment. Table II shows that for every adjustment involving a CO or N_2 singly, there will be 25,000 adjustments of energy between vibration and translation which involve simultaneous changes in CO and N_2. This means that for nearly equal amounts of the two gases, the second term in Eq. (20) is the dominant term and only the complex relaxation time will be observable. Where only small amounts of one gas are contained in the other, i.e., a or b small, the effective relaxation times of the simple and complex adjustment processes may be of the same order of magnitude, and two independent relaxation times should be observable in the gas.

Air is another case where the measured relaxation time can be attributed to a complex process. At room temperature the E_v of N_2 is essentially zero; the E_v of O_2 very small. Calling O_2 the a component of the gas, and N_2 the b component, we set E_b in Eq. (22) equal to zero. Then the vibrational adjustment of O_2 in air is given by

$$\frac{dE_a}{dt}=\frac{1}{\tau_a(\text{eff.})}(E_a(T)-E_a), \tag{26}$$

where now

$$[\tau_a(\text{eff})]^{-1}\equiv aM_{a,a}P^{1\to 0}(a,a) +bM_{a,b}(P_{0\to 0}{}^{1\to 0}(a,b)+P_{0\to 1}{}^{1\to 0}(a,b)e^{\Delta E/kT}).$$

The most effective process of deactivating an O_2 molecule consists in exciting an N_2 molecule and supplying the difference of the quanta of N_2 and O_2 from translational energy. The value of $\tau_a(\text{eff})$ of Eq. (26) is smaller than for pure O_2. The calculated values of these probabilities are given in Table II.

COS Type Gas

Equation (20), as modified by relations (24), is applicable to a polyatomic gas such as COS. In COS, there are three fundamental frequencies, only two of which are active at temperatures of a few hundred degrees centigrade. The active frequencies are $\nu_1=2.57\times10^{13}$/sec and $\nu_2=1.576\times10^{13}$/sec. The ν_2 vibration is doubly degenerate. As ν_2 is much lower than ν_1, the probability of the simple process $P^{1\to 0}(\nu_1)$ is much smaller than $P_{1\to 0}(\nu_2)$, and so, not observable. But the difference $(\nu_1-\nu_2)$ is much less than ν_2 and the probability $P_{0\to 1}{}^{1\to 0}(\nu_1,\nu_2)$ (for which the ΔE of Eq. (A7) is $h(\nu_1-\nu_2)$) cannot be neglected. A computation of $P_{0\to 1}{}^{1\to 0}(\nu_1,\nu_2)$ shows it to be somewhat less than $P_{1\to 0}(\nu_2)$. Values of these probabilities are given in Table III. The experiments of Schafer seem to indicate two observable relaxation times. This is in keeping with the present analysis which identifies these two times as that of the simple ν_2-adjustment and a complex adjustment of the ν_1- and ν_2-frequencies (see Table III).

CO_2 Type Gas

Whenever a harmonic of one of the fundamental frequencies lies close to another fundamental, we might suspect a "resonance" transfer of energy between degrees of freedom in which the probability of a jump of two quantum levels in one vibrational mode may be relatively high. An extreme example is CO_2, a gas which has been extensively studied. In CO_2, the ν_1- and ν_2-vibrations are accidentally degenerate, i.e., $2\nu_2-\nu_1=0$. A resonant exchange between the ν_1- and ν_2-vibrations during a collision is very probable. It seems not unlikely that two competing excitation processes may be observed in CO_2. These are the simple excitation of the ν_2-vibration and the resonant exchange between the ν_1- and ν_2-vibrations. The direct excitation of ν_1-vibration is much less probable than these. Thus, for the case of CO_2, the variation in E_1 (which then receives its energy from E_2 and not from translation) is given by

$$\frac{dE_1}{dt}=2MNh\nu_2\Big[\Big(P_{2\to 0}{}^{0\to 1}\frac{n_0}{N}\frac{m_2}{N}+\cdots +P_{l\to l-2}{}^{\lambda\to\lambda+1}\frac{n_\lambda}{N}\frac{m_l}{N}+\cdots\Big)-\Big(P_{0\to 2}{}^{1\to 0}\frac{n_1}{N}\frac{m_0}{N} +\cdots P_{l\to l+2}{}^{\lambda\to\lambda-1}\frac{n_\lambda}{N}\frac{m_l}{N}+\cdots\Big)\Big], \tag{27}$$

and

$$\frac{dE_2}{dt}=MP_{1\to 0}(\nu_2)(1-e^{-h\nu_2/kT})(E_2(T)-E_2)-2\frac{dE_1}{dt}.$$

The various terms have the same meaning as in Eq. (20), except that both modes now reside in the same molecule. The fractions n_0/N, n_1/N, etc., and subscripts λ refer to the ν_1-vibration, and m_0/N, etc., and subscripts l refer to the ν_2-vibration. Since here $E=0$ for the resonance transition,

$$P_{0\to 2}{}^{1\to 0}=P_{2\to 0}{}^{0\to 1},$$

and

$$P_{l\to l+2}{}^{\lambda\to\lambda-1}=(l+2)(l+1)\lambda P_{0\to 2}{}^{1\to 0}.$$

TABLE III. Probability of a complex excitation in a polyatomic gas.

Gas	T	Quantum change in ν_1-vib.	Quantum change in ν_2-vib.	Theory	Observed
COS	288°K	+1	0	10^{-7}	Not observed
COS	288°K	0	+1	10^{-3}	10^{-4} [b]
COS	288°K	−1	+1	6×10^{-2}	10^{-4}
CO_2	288°K	0	1	4×10^{-4}	2×10^{-5} [a]
CO_2	288°K	1	0	10^{-9}	Not observed
CO_2	288°K	−1	+1	10^{-7}	Not observed
CO_2	288°K	±1	∓2	1.5×10^{-3}	10^{-5} [a]

[a] K. F. Buschmann and K. Schafer, Z. physik. Chem. (B)50, 73–99 (1941).
[b] K. Schafer, Z. physik. Chem. (B)46, 212 (1940).

Equation (27) is reduced to

$$\frac{dE_1}{dt}=2MP_{2\to0}{}^{0\to1}Nh\nu_2\left[\sum_{l=0}^{\infty}l(l-1)\frac{m_l}{N}\sum_{\lambda=0}^{\infty}\frac{n_\lambda}{N}\lambda\right.$$

$$\sum_{l=0}^{\infty}l(l-1)\frac{m_l}{N}\sum_{\lambda=0}^{\infty}\frac{n_\lambda}{N}$$

$$\left.-\sum_{l=0}^{\infty}(l+2)(l+1)\frac{m_l}{N}\sum_{\lambda=0}^{\infty}\frac{n_\lambda}{N}\lambda\right]. \quad (28)$$

Assuming the ν_2-vibration can exchange energy freely among its own vibrational levels, and making use of the accidental degeneracy between ν_1- and ν_2-vibrations, we have

$$E_1(T_2)=2\frac{Nh\nu_2e^{-2h\nu_2/kT_2}}{1-e^{-2h\nu_2/kT_2}},$$

$$=\frac{e^{-h\nu_2/kT_2}}{1+e^{-h\nu_2/kT_2}}E_2(T_2).$$

So that we can write Eq. (28) finally as

$$\frac{dE_1}{dt}=2P_{2\to0}{}^{0\to1}M\frac{E_2(T_2)}{E_2(T_2)-2E_1(T_2)}(E_1(T_2)-E_1). \quad (29)$$

Equation (29) describes the adjustment of the ν_1-vibration with the ν_2-vibration. The effective relaxation time is given as

$$(\tau_{1,2})^{-1}\equiv2P_{2\to0}{}^{0\to1}M\frac{E_2(T_2)}{E_2(T_2)-2E_1(T_2)}.$$

Under the approximation permissible in the applications of these equations to an acoustic field, we obtain for CO_2,[10]

$$\frac{d\Delta T_2}{dt}=\frac{1}{\tau_2}(\Delta T-\Delta T_2)-\frac{2}{\tau_{1,2}}\frac{C_1}{C_2}(\Delta T_2-\Delta T_1),$$

$$\frac{d\Delta T_1}{dt}=\frac{1}{\tau_{1,2}}(\Delta T_2-\Delta T_1),$$

where τ_2 is defined as above and $\tau_{1,2}$ is given by

$$(\tau_{1,2})^{-1}=2MP_{2\to0}{}^{0\to1}\frac{1+e^{-h\nu_2/kT}}{1-e^{-h\nu_2/kT}}.$$

AGREEMENT OF THEORY AND EXPERIMENT

The authors have presented a method for calculating relaxation times in gases which has been applied to pure gases, mixtures, and polyatomic gases. A comparison of some results of these calculations and experiments are shown in Tables I–III. The agreement of calculated and experimental results are considered better than expected. The predicted probability $P^{1\to0}$ for N_2 and for a Cl_2-H_2 mixture differ by a factor of 10^6 and yet they each check with experiment within a factor of 25. The Tables I–III were computed assuming the geometrical factor $C^{i\to f}$ mentioned above to be unity, while in reality, this factor may be expected to be 1/3 and perhaps as small as 1/30 in particular cases. Gas mixtures which react chemically as CO and Cl_2, as well as gases such as HCl and Cl_2 where the rotation-vibration interaction is important, cannot be treated by these methods.

[10] These equations are similar in form to one of two proposed sets of equations given by Schafer, see reference 8.

APPENDIX A

Nonresonant Energy Exchanges

The contribution of low speed particles to the overall probability integral Eq. (9) is small for typical nonresonant energy exchanges, since $p^{i\to f}(v_0)$ will be extremely small. While only molecules of appreciable velocity have any reasonable value for $p^{i\to f}(v_0)$, the number of molecules having these velocities diminish sharply with increasing velocity, due to the Boltzmann factor $\exp(-\mu v_0{}^2/2kT)$. Thus, the integrand is expected to go through a maximum value at some velocity $v_0{}^*$. Assume for the moment: (a) That the factor appearing in Eq. (7) evaluated at $v_0=v_0{}^*$

$$\exp\left(\frac{4\pi^2\mu v_0{}^*}{\alpha h}\right)\gg1. \quad (A1)$$

Then Eq. (9) becomes approximately

$$p^{i\to f}=\mathbf{V}^2(i_1\to f_1)\cdots\frac{\pi^2}{16}\left(\left[\frac{4\pi\mu v_0}{\alpha h}\right]^2-\left[\frac{4\pi\mu v_F}{\alpha h}\right]^2\right.$$

$$\times\frac{\exp\left[\pm\dfrac{4\pi^2\mu(v_0-v_F)}{\alpha h}\right]}{\left\{1-\exp\left[\dfrac{-4\pi^2\mu(v_0-v_F)}{\alpha h}\right]\right\}^2}, \quad (A2)$$

in the neighborhood of $v_0=v_0{}^*$. In this paragraph the upper sign applies if $v_F>v_0$; the lower sign applies if $v_0>v_F$. (b) That the translational energies $(\mu/2)v_0{}^{*2}$ and $(\mu/2)v_F{}^{*2}$ are much greater than ΔE, i.e.,

$$\begin{aligned}(\mu/2)v_0{}^{*2}&\gg\Delta E,\\(\mu/2)v_F{}^{*2}&\gg\Delta E.\end{aligned} \quad (A3)$$

Then Eq. (10) may be approximated by a series

$$v_F\cong v_0\pm\frac{\Delta E}{\mu v_0}-\frac{1}{2}\frac{(\Delta E)^2}{\mu^2v_0{}^3}+\cdots,$$

and the complete exponent appearing in Eq. (9), when the expression for $p^{i\to f}$ given by Eq. (A2) is inserted in

Eq. (4), becomes

$$\frac{\mu}{2kT}v_0^2-\frac{4\pi^2}{\alpha h}\frac{\Delta E}{v_0}\pm\frac{2\pi^2(\Delta E)^2}{\alpha h\mu v_0^3}+\cdots. \quad \text{(A4)}$$

The maximum value of this expression and thus approximately the maximum of the integrand of Eq. (9) occurs at

$$v_0^*=\left(\frac{4\pi^2kT\Delta E}{\alpha^*h\mu}\right)^{\frac{1}{4}}\mp\frac{\Delta E}{2\mu}\left(\frac{4\pi^2kT\Delta E}{\alpha^*h\mu}\right)^{-\frac{1}{4}}+\cdots \quad \text{(A5)}$$

and has the value

$$\sigma=\frac{3\mu}{2kT}v_0^{*2}\pm\frac{\Delta E}{2kT}+\cdots.$$

Here α^* denotes the value of α at $v_0=v_0^*$. As long as the denominator in Eq. (A2) is nearly equal 1, i.e.,

$$\exp\left[-\frac{4\pi^2\mu}{\alpha h}(v_F-v_0)\right]\approx 0, \quad \text{(A6)}$$

the major contribution to the total probability $P^{i\to f}$ comes from the neighborhood of $v_0=v_0^*$. $P^{i\to f}$ may be approximated by substituting the approximate $p^{i\to f}$ of Eq. (A2) into Eq. (9). Using the saddlepoint method of evaluating the integral,[11] $P^{i\to f}$ then becomes

$$P^{i\to f}=0.394\mathbf{V}^2(i_1\to f_1)\cdots\left[\frac{8\pi^3\mu\Delta E}{\alpha^{*2}h^2}\right]^2\sigma^{\frac{1}{2}}e^{-\sigma}, \quad \text{(A7)}$$

where

$$\sigma=\frac{3\mu}{2kT}v_0^{*2}\pm\frac{\Delta E}{2kT}=3\left[\frac{2\pi^4(\Delta E)^2\mu}{\alpha^{*2}h^2kT}\right]^{\frac{1}{4}}\pm\frac{\Delta E}{2kT}.$$

Assuming realistic values of α^*, μ, and ΔE for specific cases, inequalities (A1) and (A3) are indeed satisfied and Eq. (A5) may be used to find v_0^*.

Likewise the assumed inequality (A1) is usually well satisfied. The deBroglie wavelength of the oncoming beam of particles for v_0^* is

$$\lambda^*=h/2\pi\mu v_0^*.$$

The inequality (A1) then means that we are dealing with the case for which $(\alpha^*)^{-1}$ is at least several times the deBroglie wavelength λ^*. *A collision for which the extent of the intermolecular force field is large compared to λ^* would be "adiabatic" in nature and an energy "jump" unlikely.* We see now that this is nearly the case even for the relatively short-range, repulsive field we have chosen. *The near "adiabatic" nature of the collision is the cause of the very low probability of energy transfer for vibration.*[12] The conditions placed upon Eq. (A7) are not independent. If the conditions

$$\exp\left(-\frac{4\pi^2\Delta E}{\alpha^*hv_0^*}\right)\ll 1 \quad \text{(A6)}$$

and

$$(\mu/2)(v_0^*)^2\gg\Delta E \quad \text{(A3)}$$

are satisfied, then inequality (A1) is automatically satisfied.

Resonant Energy Exchanges

From Eq. (19) it can be seen that the above development fails as $\Delta E\to 0$. Under conditions of exact resonance, Eq. (7) takes the form

$$p^{i\to f}=\mathbf{V}^2(i_1\to f_1)\cdots\left(\frac{2\pi\mu v_0}{\alpha h}\right)^2 \quad \text{(A8)}$$

and Eq. (9) may be integrated immediately to yield

$$P^{i\to f}=\mathbf{V}^2(i_1\to f_1)\cdots\frac{8\pi^2\mu kT}{\alpha^2h^2}. \quad \text{(A9)}$$

Evaluation of the $\mathbf{V}(i_n\to f_n)$ for an Exponential Field

If $V_n=e^{-\alpha A_n s_n}$ is expanded in an infinite series, $\mathbf{V}(i_n\to f_n)$ may be written

$$\mathbf{V}(i_n\to f_n)=\int_{\infty}^{\infty}\psi_i^{(n)}\left(1-\alpha A_n s_n+\left(\frac{\alpha A_n s_n}{2!}\right)^2+\cdots\right)\psi_f^{(n)}ds_n. \quad \text{(A10)}$$

This integral is well known and has been evaluated in standard textbooks on quantum mechanics:

$$\mathbf{V}(i_n\to i_n)=1;$$

$$\mathbf{V}(i_n\to i_n\pm 1)=-\alpha A\left[\frac{h(i_n+\frac{1}{2}\pm\frac{1}{2})}{8\pi^2M_n\nu_n}\right]^{\frac{1}{2}}, \quad \text{(A11)}$$

where M_n is the reduced mass of the oscillator vibrating at the frequency ν_n. Similarly

$$\mathbf{V}(i_n\to i_n\pm 2)=\alpha^2A^2\left[\frac{(i_n+1\pm 1)(i_n\pm 1)h}{16\pi^2M_n\nu_n}\right]^{\frac{1}{2}}. \quad \text{(A12)}$$

[11] H. Jeffreys and B. C. Jeffreys, *Methods of Mathematical Physics* (The Cambridge University Press, New York, 1950), p. 504, Eq. (12).

[12] This point was made by J. M. Jackson and N. F. Mott, Proc. Roy. Soc. (London) **A137**, 703 (1932).

Semilocalized Orbitals. IV.* Relationship of n-Center Orbitals, Two-Center Orbitals, and Bond Properties

CHARLES R. MUELLER
Chemistry Department, Purdue University, Lafayette, Indiana
(Received April 17, 1952)

The relationship between n-center orbitals, two-center orbitals, and bond properties is discussed from the standpoint of atomic, molecular, and semilocalized orbital theory.

The necessary restrictions on the transformation from the more general n-center to the two center orbitals is also discussed and a practical computational method for molecular problems is suggested.

The relationship of the atomic and molecular orbital theories of the excited electronic states of molecules is also investigated.

ONE of the most important questions of chemical valency theory is to establish the relationship of the most general electronic orbitals to the two-center orbitals. Questions of chemical reactivity and structure can be more easily discussed from the standpoint of the simpler orbitals; in other words, the formalism of the two-center orbitals is much closer to the language of empirical chemistry.

It is interesting to consider the restrictions on an eigenfunction and the approximations that one must make in order to shape the quantum-mechanical formalism in such a way as to more or less coincide with the ideas of bond properties.

Besides these questions which are chiefly concerned with the ground state of the molecule, the transformation of n-center orbitals to simpler bond orbitals can be utilized as a tool in understanding the relationship of atomic and molecular theories of excited electronic states of molecules.

In the course of these investigations we shall discuss the validity of a Coulombic approximation which greatly reduces the labor of molecular computation.

I. TRANSFORMATION FROM n-CENTER TO TWO-CENTER ORBITALS

In order to establish the relationship of n-centered to two-centered orbitals, we must begin with some assumptions as to the nature of the most general electronic orbitals. For the sake of convenience we shall confine ourselves to systems in which the individual one-electron orbitals are written as linear combinations of atomic orbitals. We shall also restrict ourselves to those specific forms of orbitals which fall under the classifications of atomic, molecular, and semilocalized orbital theory.

The question of the relationship of n-center and two-center or equivalent orbitals has been thoroughly investigated by Lennard-Jones[1] for molecular orbitals, and the extension of the theory to other systems will follow his work rather closely. We shall begin with a brief description of this method for molecules of type XY_n, where X is a central atom with atoms of Y symmetrically distributed around it.

In this case each of the n-center orbitals in the molecular orbital picture belongs to an irreducible representation of the point symmetry group of the molecule. Orbitals belonging to different irreducible representations are automatically orthogonal. Orthogonality is thus obtained without loss of generality since any set of n-center orbitals can be transformed by means of a unitary transformation into a set of orbitals each belonging to an irreducible representation of the point symmetry group of the molecule.

For the case of molecular orbitals Lennard-Jones has shown that one can transform such a set of n-centered orbitals to two-centered orbitals by means of a unitary transformation matrix t which is found from the point symmetry group of the molecule. We shall illustrate this transformation for methane.

The individual n-centered one-electron orbitals are

$$\left.\begin{aligned}
\psi_1&=\varphi_{c1s}\\
\psi_2&=\varphi_{c2s}+\lambda(\varphi_{h1}+\varphi_{h2}+\varphi_{h3}+\varphi_{h4})\\
\psi_3&=\varphi_{c2p_x}+\lambda(\varphi_{h1}+\varphi_{h2}-\varphi_{h3}-\varphi_{h4})\\
\psi_4&=\varphi_{c2p_y}+\lambda(\varphi_{h1}-\varphi_{h2}+\varphi_{h3}-\varphi_{h4})\\
\psi_5&=\varphi_{c2p_z}+\lambda(\varphi_{h1}-\varphi_{h2}-\varphi_{h3}+\varphi_{h4})
\end{aligned}\right\}. \qquad (1)$$

In the ground state a pair of electrons is assigned to each one of these orbitals.

When the product of these orbitals is antisymmetrized, a molecular eigenfunction consisting of a single Slater determinantal eigenfunction is formed.

If one then subjects this set of five orbitals to the unitary transformation

$$t=\tfrac{1}{2}\begin{bmatrix}2&0&0&0&0\\0&1&1&1&1\\0&1&1&-1&-1\\0&1&-1&1&-1\\0&1&-1&-1&1\end{bmatrix}, \qquad (2)$$

we obtain another set of five orbitals composed of the $1S$ carbon atomic orbital, and four two-center molecular orbitals, $\varphi_{cte}+\lambda\varphi_h$, each of the latter projecting to the corners of a tetrahedron.

* The preceding papers in this series are C. Mueller and H. Eyring, J. Chem. Phys. **19**, 1491 (1951); C. Mueller, J. Chem. Phys. **19**, 1495 (1951); C. Mueller, J. Am. Chem. Soc. **74**, 3466 (1952).

[1] J. Lennard-Jones, Proc. Roy. Soc. (London) **A198**, 14 (1949).

A similar transformation can be carried out for semilocalized orbital theory for molecules of type XY_n, but we must first discuss briefly the n-centered orthogonalized semilocalized orbitals.

The orginal criteria for the functional form of these orbitals was that they should assume either atomic or molecular orbital form for certain values of the variational parameters.

For the n-center case this means, for example, instead of two electrons with opposite spins being assigned to the same orbitals, as they are in molecular orbital theory, one would be assigned to an orbital, $\psi_2=\varphi_{c2s}+\lambda_1(\varphi_{h1}+\varphi_{h2}+\varphi_{h3}+\varphi_{h4})$, and the other to the orbital, $(\lambda_2\varphi_{c2s}+\varphi_{h1}+\varphi_{h2}+\varphi_{h3}+\varphi_{h4})$.

The latter can be written for the sake of convenience as $\varphi_{c2s}+\lambda'(\varphi_{h1}+\varphi_{h2}+\varphi_{h3}+\varphi_{h4})$ and will be designated as ψ_2'.

If we now antisymmetrize the product of the ten one-electron eigenfunctions we obtain a sum of 16 Slater determinants for the molecular eigenfunction. If we operate on this set with the transformation matrix

$$A=\begin{bmatrix}2 & 0 & 0\\ 0 & t' & 0\\ 0 & 0 & t'\end{bmatrix}, \tag{3}$$

after arranging the column matrix in the form

$$(\psi_1\psi_2\cdots\psi_n\psi_1'\psi_2'\cdots\psi_n'),$$

we obtain a set of nine two-center semilocalized orbitals. t' is the minor of the matrix element 2 in t'.

These orbitals have the forms, apart from a normalization factor,

$$\left.\begin{aligned}\tau_1&=\varphi_{c1s}\\ \tau_2&=\varphi_{ctc}+\lambda\varphi_h\\ \tau_2'&=\varphi_{ctc}+\lambda'\varphi_h\end{aligned}\right\}. \tag{4}$$

In the notation used previously by the author

$$\lambda_1=\lambda,\quad \lambda_2=\frac{1}{\lambda'}.$$

Since, when λ_2 and λ_1 are zero, we pass to the atomic orbital form, one might consider the orbital φ_{2s}, and $\varphi_{h1}+\varphi_{h2}+\varphi_{h3}+\varphi_{h4}$, etc., as n-centered atomic orbitals. Such a set when subjected to the transformation (3) would pass into the ordinary atomic orbital form.

We can now see the relationship between at least some of the excited states of methane as seen from the standpoints of the atomic and molecular orbital theories.

Suppose an electron is excited from the

$$\varphi_{c2s}+\lambda\sum_{i=1}^{4}\varphi_{ni}$$

orbital to the

$$\varphi_{c3s}+\lambda\sum_{i=1}^{4}\varphi_{ni}$$

orbital, then a transition occurs from one A_1 orbital to a second A_1 orbital. An excitation from the $2s$ to $3s$ state in atomic orbital method, viewed as an n-center problem is also a transition from one A_1 to a second A_1 orbital. Similar considerations apply to other transitions.

The proof of the invariance of the total electronic energy of a single Slater determinantal orbital under a unitary transformation has been given by Lennard-Jones[1] and Roothan.[2]

The proof for the many determinant case is straightforward because the value of a determinant is unchanged by a unitary transformation. Actually, the preceding proofs apply to the case of orthogonalized localized orbitals and the energy invariance is not quite exact for the L.C.A.O. approximation.

Up to this point we have not taken cognizance of any limitation on the n-centered orbitals. Lennard-Jones[3] has pointed out that in the case of the most general n-centered molecular orbitals, the coefficient of the linear combination of hydrogen atom orbital in ψ_2 need not be equal to the coefficient in ψ_3, ψ_4, and ψ_5. The transformation cannot be carried out unless this equality holds. However, it is easily seen than this restriction is simply equivalent to requiring tetrahedral character in the carbon atomic orbitals in the two-centered case, and there is no reason to suppose that this restriction is serious. Similar considerations apply to molecules of the type XY_n.

Other restrictions have been noted by Mulliken and Parr.[4]

For butadiene the localized molecular orbitals for the electrons are written as

$$\tau_1=N(\chi_1+\chi_2)\tau_2=N(\chi_3+\chi_4)\quad N=[2(1+S_{12})]^{-\frac{1}{2}}. \tag{5}$$

These orbitals can be transformed by means of a unitary matrix to the n-center orbitals

$$\begin{aligned}\Phi_{k1}&=[2(1+S_{23})]^{-\frac{1}{2}}(\tau_1+\tau_2),\\ \Phi_{k2}&=[2(1-S_{23})]^{-\frac{1}{2}}(\tau_1-\tau_2).\end{aligned} \tag{6}$$

Mulliken and Parr then point out that the most general n-center orbital is not of this form but is

$$\Phi_{1,2}=(a_j\chi_1+b_j\chi_2)\pm(b_j\chi_3+a_j\chi_4). \tag{7}$$

The difficulty here again is not serious. If we wrote the original molecular orbitals as

$$\tau_1=a_j\chi_1+b_j\chi_2\quad \tau_2=b_j\chi_3+a_j\chi_4,$$

we would obtain (7) as the n-center orbitals. Similar considerations apply to the semilocalized orbitals where a second set of orbitals τ_1' and τ_2' are required. As in the previous case, the unitary transformation matrix is into the most general 2-centered set of orbitals:

$$A=\begin{pmatrix}t & 0\\ 0 & t\end{pmatrix},\quad \text{where}\quad t=\begin{pmatrix}1 & 1\\ 1 & -1\end{pmatrix}. \tag{8}$$

[2] C. Roothan, Revs. Modern Phys. **23**, 69 (1951).
[3] J. Lennard-Jones, Proc. Roy. Soc. (London) **A198**, 1 (1949).
[4] R. Mulliken and R. Parr, J. Chem. Phys. **19**, 1271 (1951).

However, Mulliken and Parr have pointed out similar restrictions in the case of benzene which are not so easily disposable, and it appears that there is no means of transforming the most general n-centered set of orbitals into the most general 2-centered set of orbitals.

In summary, it appears that in many cases the transformation from n-centered to two-centered orbitals implies no important restrictions. The importance of such transformations are that they connect the n-centered orbitals, which are better for a treatment of excited electronic states, with the two-centered orbitals which are better for the treatment of chemical valency problems. We shall now turn to the second problem.

II. TWO-CENTERED ORBITALS AND THE COULOMBIC APPROXIMATION

In this section we will confine ourselves largely to two-centered semilocalized orbitals. Since the localized molecular and atomic orbital orbitals are special cases of the former, the results will be of a more or less general character.

The semilocalized orbitals are characterized by a large degree of nonorthogonality. As a consequence, the usual question of multiple exchange integrals arises. Because of the nonorthogonality, each of the $n!$ permutations of the n-electron problem give rise to exchange integrals, and the formalism becomes exceedingly complex. We shall attempt to overcome this problem by means of a reasonable approximation. We shall further limit ourselves to molecules in which configuration interaction is not important.

We shall initially neglect multiple permutations and later show the reasonableness of this ommission.

Applying the Dirac vector model,[5] the energy of a molecule is

$$E=\frac{Q+\sum_{\triangleright i'}K(i,i')-\frac{1}{2}\sum_{\triangleright j\neq i}K(i,j)}{1+\sum_{\triangleright i'}S^2(i,i')-\frac{1}{2}\sum_{\triangleright j\neq i}S^2(i,j)}, \tag{9}$$

where $K(i,i')$ represents an exchange integral between bonding electrons, $K(i,j)$ between nonbonding electrons.

If we add and subtract

$$Q\{\sum_{\triangleright i'}S^2(i,i')-\tfrac{1}{2}\sum_{\triangleright j\neq i}S^2(i,j\}$$

to the numerator, (9) reduces to

$$E=Q+\frac{\sum_{\triangleright i'}\{K(i,i')-S^2(i,i')Q\}-\frac{1}{2}\sum_{\triangleright j\neq i}\{K(i,j)-S^2(i,j)Q\}}{1+\sum_{\triangleright i'}S^2(i,i')-\frac{1}{2}\sum_{\triangleright j\neq i}S^2(i,j)}. \tag{10}$$

[5] E. Corson, *Perturbation Methods in the Quantum Mechanics of n-Electron Systems* (Hafner Publishing Company, Inc., New York, 1951), Chap. 10.

Now let us examine a typical term in the numerator for a system of n electrons and a nuclei. There are $n(1+a)$ one-electron terms in the Hamiltonian. For a given exchange integral there are only $2(1+a)$ one-electrons terms involved in the exchange. The rest of the $(n-2)(1+a)$ terms vanish on subtraction by the same term in $S^2(k,l)Q$.

There are $n(n-1)/2$ two-electron terms in the Hamiltonian. Of these one involves both of the exchanged electrons. $2(n-2)$ involves one of the exchanged electrons and the rest cancel because of subtraction by $S^2(k,l)Q$ terms.

Out of $n(n+2a+1)/2$ terms only $2(n+2a-1)$ terms remain. Suppose we now turn our attention to the remaining terms. We shall designate the portions of the Hamiltonian containing the coordinates of electrons 1 and 2 by H_1 and H_2.

This part of $K(k,l)$ is

$$K'(k,l)=\int\tau_k(1)\tau_l(2)\{H_1+H_2\}\tau_k(2)\tau_l(1)d\tau_1d\tau_2$$

$$=S(kl)\left\{\int\tau_k(1)H_1\tau_l(1)d\tau_1+\int\tau_k(2)H_2\tau_l(2)d\tau_2, \right. \tag{11}$$

$$K'(k,l)-S^2(k,l)Q'$$

$$=S(kl)\left[\int\tau_k(1)H_1\tau_l(1)d\tau_1-\frac{S(k,l)}{2}\right.$$

$$\times\left\{\int\tau_k(1)H_1\tau_k(1)d\tau_1+\int\tau_l(2)H_2\tau_l(2)d\tau_2\right\}$$

$$+\int\tau_k(2)H_2\tau_l(2)d\tau_2-\frac{S(k,l)}{2}$$

$$\left.\left.\times\left\{\int\tau_k(1)H_1\tau_k(1)d\tau_1+\int\tau_l(2)H_2\tau_l(2)d\tau_2\right\}\right] . \tag{12}$$

Because of the symmetry of the Hamiltonian in electrons one and two we have

$$K'(k,l)-S^2(k,l)Q'$$

$$=S(k,l)\left[\int\tau_k(1)2H_1\tau_l(1)d\tau_1\right.$$

$$-\frac{S(k,l)}{2}\left\{\int\tau_k(1)2H_1\tau_k(1)d\tau_1\right.$$

$$\left.\left.+\int\tau_l(1)2H_1\tau_l(1)d\tau_1\right\}\right]. \tag{13}$$

The second term on the right is just a generalization of Mulliken's overlap-average approximation.[6]

[6] R. Mulliken, J. Chem. Phys. **46**, 497 (1949).

If we adopt this approximation, the one-electron terms all vanish.

If we indicate the two-electron term involving both exchanged electrons by a double prime,

$$K''(k,l)-S^2(k,l)Q''=(\tau_k\tau_l|\gamma_{12}^{-1}|\tau_l\tau_k) -S^2(k,l)(\tau_k\tau_k|\gamma_{12}^{-1}|\tau_l\tau_l). \quad (14)$$

The second term is just the approximation used by Heitler and London in the first application of quantum mechanics to molecules.[7]

For two-electron terms involving one exchanged electron, an extension of Mulliken's approximation is again involved.

In addition to these reductions in the numerator, the denominator becomes increasingly large with an increase in the complexity of the molecule. In small molecules such as hydrogen one might expect a considerable error. In a more complex molecule such as methane we would expect the error to be much less.

Table I summarizes the results found for methane using Slater atomic orbitals.

In calculations of this sort it is customary to neglect multiple exchange integrals. If we include these integrals we can again utilize the same sort of procedure and show that omitting them from the energy expression is simply equivalent to their replacement by the approximations previously mentioned. In addition, these integrals are undoubtedly small and one has every reason to suspect that the error involved is much less than for the single exchange integrals.

Superficially the results appear to be good except for K_{1SH} and K_{1SC}. The discrepancy here is due to the nonorthogonality of the Slater 1s and 2s orbitals, and could be almost entirely removed by using orthogonalized atomic orbitals.

However, this superficial agreement can be shown to be partially the result of a fortunate cancellation of errors.

In Tables II, III, and IV in the Appendix we have listed some comparisons of individual integrals and the approximations which replace them, and the agreement is not too good. There is some internal compensation even here with kinetic energy terms compensating for error in J_{hs}, $J_{h\sigma}$ and $J_{s\sigma}$ terms. The notation is that of Kotani, Amemiya, and Simose.[8] The values of the integrals are from Kotani and Amemiya[9] or from the tables of Kopeneck.[10]

In many cases the overlap integral between two bonding orbitals is extremely large. In the case of methane the value is about 0.99 and, hence, the error involved in the approximation should be quite small, since as the overlap integral approaches one, the exchange integral between bonding electrons should approach the value of the Coulombic integral.

Wherever the approximations have been used they have seemed to have given satisfactory results, even though the individual integrals have values different from the corresponding approximation. Since the reduction of labor is so remarkable, it seems likely that we must, in any case, adopt these approximations.

TABLE I. Coulombic approximation.

	K_{CH}	K_{CH_1}	K_{CC_1}	K_{HH_1}	K_{1SH}	K_{1SC}
$K(i,j)$	12.48014	0.56704	0.43278	0.73188	0.14785	0.19411
$S^2(i,j)Q$	12.50887	0.54805	0.41340	0.69487	0.11768	0.13454

III. BOND PROPERTIES

So long as the energy is expressed in the form of Eqs. (9) or (10), the task of calculating molecular properties is quite complicated. If we tried to set up a secular equation for a system where the nonorthogonality corrections are large, the final expression would be very complex. If we adopt the approximations suggested in the previous paragraph, then the solution for the two-center orbitals is quite straightforward. In the course of solving the secular equation we find that we can utilize previous self-consistent field calculations for the molecule and we may regain some of the accuracy which we lost in the Coulombic approximation.

The problem will differ in two ways from the customary molecular orbital treatment. First, we must set up a secular equation for each different semilocalized two-center orbital. In general, there will be twice as many of these equations as in the localized molecular orbital treatment. Second, the Hamiltonion will involve only Coulombic interactions. It is customary in molecular orbital treatments to ignore nonorthogonality corrections and to include exchange terms. It should be noted from the form of Eq. (10) that this gives too much emphasis to the exchange interactions.

Suppose we write the one electron orbital in the form

$$\tau=a\chi_1+b\chi_2. \quad (15)$$

If we use the notation of Mulliken,[6] the secular equation becomes

$$\begin{vmatrix} \alpha_1-\epsilon & \gamma_{12}-S_{12}\epsilon \\ \gamma_{12}-S_{12}\epsilon & \alpha_2-\epsilon \end{vmatrix}=0; \quad (16)$$

ϵ is the energy of an electron in the orbital τ;

$$\left.\begin{aligned} \alpha_i&=\int \chi_i\mathfrak{H}\chi_i d\tau \\ \gamma_{ij}&=\int \chi_i\mathfrak{H}\chi_j d\tau \end{aligned}\right\}. \quad (17)$$

$\mathfrak{H}$ is a Hamiltonion containing the kinetic energy operator and the Coulombic potentials arising from all the nuclei and the other electrons in the molecule.

[7] W. Heitler and F. London, Z. Physik 44, 455 (1927).
[8] Kotani, Amemiya, and Simose, Proc. Phys. Math. Soc. Japan 20, Extra No. (1938).
[9] M. Kotani and A. Amemiya Proc. Phys. Math. Soc. Japan 22, Extra No. (1940).
[10] H. Kopeneck, Z. Naturforsh. 5a, 420 (1950).

If we make the substitution

$$\gamma_{12}=\beta_{12}+S_{12}\bar{\alpha}_{12} \tag{18}$$

where

$$\bar{\alpha}_{12}=\tfrac{1}{2}(\alpha_1+\alpha_2)=\bar{\alpha}_{21},$$

the secular equation becomes

$$\begin{vmatrix} \alpha_1-\epsilon & \beta_{12}-S_{12}(\epsilon-\bar{\alpha}_{12}) \\ \beta_{12}-S_{12}(\epsilon-\bar{\alpha}_{12}) & \alpha_2-\epsilon \end{vmatrix}=0. \tag{19}$$

Following Mulliken, we introduce the following definitions:

$$\delta_{12}=\tfrac{1}{2}(\alpha_2-\alpha_1) \quad \rho_{12}=\delta_{12}/\beta_{12}.$$

We obtain the solution

$$\epsilon=\bar{\alpha}_{12}+[\beta(1-S^2)][-S\pm(1+(1-S^2)\delta^2/\beta^2)]^{\frac{1}{2}}. \tag{20}$$

The coefficients are

$$a(2\pm 2S)^{\frac{1}{2}}=\pm 1-\tfrac{1}{2}(1\pm S)\rho\mp(1-S^2)\rho^2/8+\cdots,$$
$$b(2\pm 2S)^{\frac{1}{2}}=1\pm\tfrac{1}{2}(1\pm S)\rho-(1-S^2)\rho^2/8+\cdots.$$

The upper sign corresponds to a bonding orbital, the lower sign to an antibonding orbital.

Since $\alpha_i=\int\chi_i\mathfrak{H}\chi_i d\tau$ and $\bar{\alpha}=\frac{1}{2}(\alpha_1+\alpha_2)$ we can separate α into two terms, ϵ_{at} and W, where ϵ_{at} is the Coulombic energy of an electron in the separated atom. Since the coefficients a and b are functions of ρ and the latter depend on the difference $(\alpha_2-\alpha_1)$, it is important that we have good values of the atomic energies. These Coulombic atomic energies can be obtained directly from the self-consistent field calculation for the atoms. In the case of methane the ϵ_{at} for carbon and hydrogen are about 4 times as large as the W's. Since the carbon-hydrogen bond energy is high compared to other bonds, one suspects that the ratio of ϵ_{at} and W for most bonds is at least as high, and the difference $(\alpha_2-\alpha_1)$ depends to a large extent on the atoms involved in bonding. This is certainly confirmed by the experimental data.

The integral β has been investigated by Mulliken[6] and has been called the bond integral. It seems to determine to a large extent the bond energy and is remarkably insensitive to extra-bond environment.

Certainly these considerations of the integrals α and β suggest very strongly the empirical concept of binding that the chemist has used with great success.

APPENDIX

TABLE II. Validity of Coulombic approximation.

α[a] =	4.0	4.5	5.0	5.5
$S_{\sigma\sigma}J_{\sigma\sigma}Z^{-1}$	0.06355	0.06894	0.06387	0.05294
$S_{\sigma\sigma}J_{\sigma\sigma}'Z^{-1}$	0.05315	0.06222	0.06117	0.05339
$A_{\sigma\sigma\sigma\sigma}Z^{-1}$	0.10472	0.10593	0.09493	0.07777
$A_{\sigma\sigma\sigma\sigma}'Z^{-1}$	0.03715	0.04185	0.03907	0.03210

[a] $\alpha=ZR/2$. Primes indicate approximation.

TABLE III. Validity of Coulombic approximation.

α[a] = β =	2.00 −0.50	2.25 −0.25	2.50 0.00	2.75 0.25	3.00 0.50
$S_{sh}J_{sh}$	0.09635	0.1346	0.1507	0.1502	0.1403
$S_{sh}J_{sh}'$	0.1076	0.1553	0.1781	0.1802	0.1697
$S_{sh}J_{hs}$	0.1491	0.1975	0.2070	0.1907	0.1632
$S_{sh}J_{hs}'$	0.1780	0.2308	0.2387	0.2190	0.1879
N_{ss}'	0.06454	0.09586	0.1071	0.1030	0.09108
N_{ss}	0.09624	0.1314	0.1434	0.1389	0.1260
$4SZ^{-2}(1S_a$ $\vert -1/2\Delta\vert 2S_b)$	0.0839	0.1196	0.1304	0.1223	0.1047
$4SZ^{-2}(1S_a\vert$ $-1/2\Delta\vert 2S_b)'$	0.1248	0.1667	0.1753	0.1623	0.1398

[a] $\alpha=R[(Z/2)+1]$. $\beta=R/2[(Z/2)-1]$.

TABLE IV. Validity of Coulombic approximation.

α = β =	2.00 −0.50	2.25 −0.25	2.50 0.00	2.75 0.25	3.00 0.50
$S_{\sigma h}J_{\sigma h}$	0.1011	0.1320	0.1372	0.1259	0.1076
$S_{\sigma h}J_{\sigma h}'$	0.1213	0.1665	0.1801	0.1707	0.1496
$S_{\sigma h}J_{h\sigma}$	0.2129	0.2728	0.2743	0.2407	0.1947
$S_{\sigma h}J_{h\sigma}'$	0.2137	0.2645	0.2573	0.2196	0.1742
$N_{\sigma\sigma}$	0.1427	0.1874	0.1950	0.1790	0.1528
$N_{\sigma\sigma}'$	0.08233	0.1169	0.1225	0.09753	0.08872
$4SZ^{-2}(2p\sigma_a$ $\vert -1/2\Delta\vert 1S_b)$	0.1579	0.2146	0.2238	0.2008	0.1643
$4SZ^{-2}(2p\sigma_a$ $\vert -1/2\Delta\vert 1S_b)'$	0.1591	0.2029	0.1998	0.1710	0.1354

The Induction Period in Chain Reactions*

SIDNEY W. BENSON†
Laboratoire de Chimie Physique, Paris, France
(Received December 20, 1951)

The conditions for the establishment of a stationary state in a system of consecutive reactions can be investigated quantitatively in a sufficient number of cases to permit precise criteria to be formulated generally for the length of the induction period (i.e., prestationary state period) in chain reactions. These are given as functions of the individual rate constants for the separate reactions, the extent of the reaction and the percent of stationary state concentrations achieved. Such relations provide a means for the evaluation of the self-consistency of experimental data with proposed mechanisms and also provide numerical limits on the values of individual rate constants.

Various chain reactions are examined in the light of these criteria. Of the hydrogen-halogen reactions, the H_2-Cl_2 reaction mechanism does not fulfill the stationary state requirements, and it is probable that many of the discordant results found in this reaction arise from this difficulty.

INTRODUCTION

THE mathematical technique currently employed for the integration of the system of dependent, differential equations involved in consecutive or chain reactions rests upon an assumption, popularly known as the "steady-state hypothesis" [Bodenstein method]. This latter states that during a negligibly short time interval at the beginning of a chain reaction, the concentrations of intermediate substances will rise until they reach a limiting value which is then maintained for the duration of the reaction. These limiting or "steady-state" concentrations can be calculated mathematically by equating the rates of formation and destruction of the intermediate substances.

Implicit in such a hypothesis and indeed a necessary and sufficient condition for its validity[1] is the idea that the steady-state concentrations of radicals are "negligibly small" compared to the concentrations of both reacting materials and stable products.[2,3]

It is the purpose of the present paper to explore quantitatively the conditions that must be imposed upon the various specific rate constants involved in the steps of the chain in order to fulfill the requirements of a "stationary state," and also to describe quantitatively the chain "induction period." This analysis is made possible by the exact integration of the original kinetic system of differential equations, a procedure which though generally impossible becomes possible in a sufficient number of simple cases to illustrate the behavior in the more complex systems.

There has been a long history of investigations of this type of problem, and references will be made to such work in the course of the manuscript. However, the results have been obtained either for very particular systems or else where a more general approach has been taken[2,3] the conclusions have not been reducible to the quantitative form reported here.

I. CONSECUTIVE REACTIONS INVOLVING ONLY A SINGLE INTERMEDIATE

Case 1. The simplest case of a chain reaction is the well-known first-order sequence

$$\left.\begin{array}{l} A \xrightarrow{k_1} B \\ B \xrightarrow{k_2} C \end{array}\right\}, \tag{1}$$

for which the differential equations are

$$\frac{dA}{dt}=-k_1A\,;\quad \frac{dB}{dt}=k_1A-k_2B\,;\quad \frac{dC}{dt}=k_2B. \tag{2}$$

The exact solutions of this system are known[4] and have the form:[5]

$$\left(\frac{A}{A_0}\right)=e^{-k_1t};\quad B=\alpha(e^{-k_1t}-e^{-k_2t});$$
$$C=A_0(1-e^{-k_1t})-\alpha(e^{-k_1t}-e^{-k_2t}). \tag{3}$$

We can express the solution for B as

$$\frac{B}{A}=\frac{1}{(K-1)}\left[1-e^{-(k_2-k_1)t}\right], \tag{4}$$

where $K=k_2/k_1$.

---

* Presented before the Division of Physical Chemistry at the XII[th] International Congress of the Union of Pure and Applied Chemistry, New York City, September, 1951.

† Present address: Chemistry Department, University of Southern California, Los Angeles 7, California. The present work was done during a sabbatical leave from the University of Southern California.

[1] S. W. Benson, unpublished work.

[2] D. A. Frank-Kamenetskii, J. Phys. Chem. U.S.S.R. **14**, 695 (1940) has analyzed the criteria in terms of the mean life times of the intermediates.

[3] N. N. Semenov, J. Phys. Chem. U.S.S.R. **17**, 187–214 (1943) has extended such discussions to all types of branching chain reactions.

[4] Very general discussions of this and related systems have been given by (a) Jen-Yuan Chien, J. Am. Chem. Soc. **70**, 2256 (1948); (b) F. A. Matsen and J. L. Franklin, J. Am. Chem. Soc. **72**, 3337 (1950); (c) B. Zwolinski and H. Eyring, J. Am. Chem. Soc. **69**, 2702 (1947); (d) Denbigh, Hicks, and Page, Trans. Faraday Soc. **44**, 479 (1948); (e) A. A. Balandin and D. N. Vaskevich, J. Gen. Chem. U.S.S.R. **6**, 1870 (1936); (f) W. Esson, Phil. Trans. Roy. Soc. (London) **156**, 220 (1866).

[5] The boundary conditions are $A=A_0$; $B=C=0$ at $t=0$, and $\alpha=A_0/K-1$.

Application of the steady-state hypothesis involves setting $dB/dt=0$ from which we obtain (from Eq. (2)) the steady-state concentration of B in the form

$$(B/A)_S=k_1/k_2=1/K. \tag{5}$$

We can now examine the ratio of the actual value of B/A (Eq. (4)) to that required by the steady-state hypothesis (Eq. (5)):

$$R=\frac{(B/A)}{(B/A)_S}=\left[\frac{1}{1-(1/K)}\right]\left[1-e^{-(k_2-k_1)t}\right]. \tag{6}$$

It can be seen that R will be close to unity only when K is large and $(k_2-k_1)t$ is also large. In a more direct fashion we can calculate for various values of the ratio, $K=k_2/k_1$, what fraction of A_0 will have been consumed for a certain proportion of the steady-state concentrations to be achieved. By elimination of the time we can express R directly in terms of A/A_0:

$$R=\frac{1}{[1-(1/K)]}\left[1-\frac{A}{A_0}\right]^{K-1}. \tag{7}$$

Table I gives the values of R computed from this equation, and Fig. 1 shows the behavior graphically.

It can be seen from Table I that the fraction of A consumed before 99 percent of the steady-state concentrations are reached will be between 2 and 5 times $1/K$. For values of K in excess of 1000, the induction period is experimentally negligible while for values of K less than 100 it is certainly a measurable region.

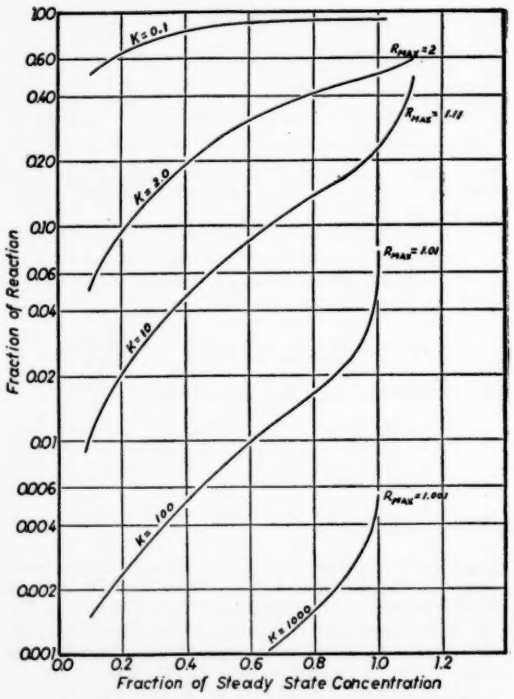

FIG. 1. Fraction of steady-state concentration achieved as a function of fraction of reaction for different rate constants. Cases 1 and 4 (see Eqs. (7) and (21), Table I).

TABLE I. The extent of reaction of initial reactant as a function of the fraction of steady-state concentration achieved (Cases 1 and 4).

	R = fraction of steady-state concentrations						% reaction at
$K=k_2/k_1$	0.1	0.5	0.9	0.95	0.99	R_{max}[a]	$0.99R_{max}$
0.1	0.51	0.85	0.914	0.919	0.922	∞	...
2.0	0.05	0.25	0.45	0.475	0.495	2.00	0.99
10.0	0.010	0.064	0.168	0.193	0.218	1.11	0.400
100	0.0015	0.0070	0.022	0.028	0.038	1.01	0.046
1000	0.00011	0.00069	0.0023	0.0030	0.0046	1.001	0.0046

Values given in the table are of $[1-(A/A_0)]$ = extent of reaction.

[a] It is important to point out that R_{max} is not unity for values of $K>1$ but only approaches unity as K becomes very large. The reason for this paradoxical behavior is that whereas the intermediate B certainly reaches an absolute maximum when the steady-state conditions are reached, the ratio (B/A) reaches a maximum value only at the end of the reaction (when $A\to 0$). This happens when $K>1$ since although B is then always disappearing relatively faster than A, the ratio B/A is always increasing. For large values of K the difference is negligible, but for small values it is appreciable.

Case 2. A second system different only in order from the first is[6,7]

$$\begin{aligned} A+A &\xrightarrow{k_1} B \\ B+B &\xrightarrow{k_2} C \end{aligned} \tag{8}$$

for which the equations are

$$\frac{dA}{dt}=-k_1A^2;\quad \frac{dB}{dt}=\tfrac{1}{2}k_1A^2-k_2B^2;\quad \frac{dC}{dt}=\tfrac{1}{2}k_2B^2. \tag{9}$$

This system[8] is most simply discussed after the elimination of the time as a dependent variable. On dividing the expression for dB/dt by that for dA/dt we obtain

$$\frac{dB}{dA}=-\tfrac{1}{2}+\left(\frac{k_2}{k_1}\right)\left(\frac{B}{A}\right)^2, \tag{10}$$

and substituting $y=B/A$; $K=k_2/k_1$ we have

$$\frac{dy}{d\ln A}=Ky^2-y-\tfrac{1}{2}. \tag{11}$$

The solution of this equation is

$$\ln\left\{\frac{1-(y/y_1)}{1-(y/y_2)}\right\}=(1+2K)^{\frac{1}{2}}\ln\left(\frac{A}{A_0}\right), \tag{12}$$

where y_1 is the positive root and y_2 the negative root of the equation $y^2-(y/K)-(1/2K)=0$.[8] For various choices of K it is possible to calculate the values of

[6] The formal explicit solution for A and B involves a Riccati equation. This has been solved by Jen-Yuan Chien (reference 4a) and by (a) A. D. Stepukhovich and L. M. Timonin, Zhur. Fiz. Khim. **25**, 143 (1951). Solutions for special boundary conditions have been obtained by (b) J. Hirniak, Acta Physiochim. U.R.S.S. **14**, 613 (1941).

[7] S. Ya. Pshezbatskii and R. N. Rubinshteen, J. Phys. Chem. U.S.S.R. **21**, 659 (1947) have applied methods similar to the ones used here for sequences of second and higher order reactions.

[8] Boundary conditions are $A=A_0$, $y=0$ at $t=0$.

(A/A_0) corresponding to different values of y (which will always have a value less than y_1). In this way another table of values of the ratio of B/A to its steady-state concentration,

$$\left(\frac{B}{A}\right)_s = \left(\frac{k_1}{2k_2}\right)^{\frac{1}{2}} = (2K)^{-\frac{1}{2}},$$

can be calculated as a function of the extent of reaction. These values are shown in Table II. The data are presented graphically in Fig. 2.

The most significant difference between this and the preceding system is that the induction period is extended here to larger regions for comparable values of K. The reason is that the higher order of this system (Case 2) involves not k_2/k_1 but the square root of this ratio. Thus the induction period will extend to measurable regions unless K exceeds 10^5.

Case 3. A simple case of a mixed order sequence is

$$\begin{matrix} A \xrightarrow{k_1} B \\ A+B \xrightarrow{k_2} C. \end{matrix} \qquad (13)$$

The differential equations are

$$\frac{dA}{dt} = -k_1A - k_2AB; \quad \frac{dB}{dt} = k_1A - k_2AB; \quad \frac{dC}{dt} = k_2AB. \qquad (14)$$

Eliminating the time as before we obtain the equation

$$\frac{dB}{dA} = \frac{B-K}{B+K}, \qquad (15)$$

where $K = k_1/k_2$. This integrates directly to give ($B=0$ when $A=A_0$)

$$\frac{B}{K} + 2\ln\left(1-\frac{B}{K}\right) = -\frac{A_0}{K}\left(1-\frac{A}{A_0}\right). \qquad (16)$$

The steady-state concentration of $B=K$ so that we can here calculate directly values of $R=B/K$, the ratio of B to its steady-state value. The results are presented in Table III for different values of the ratio A_0/K.

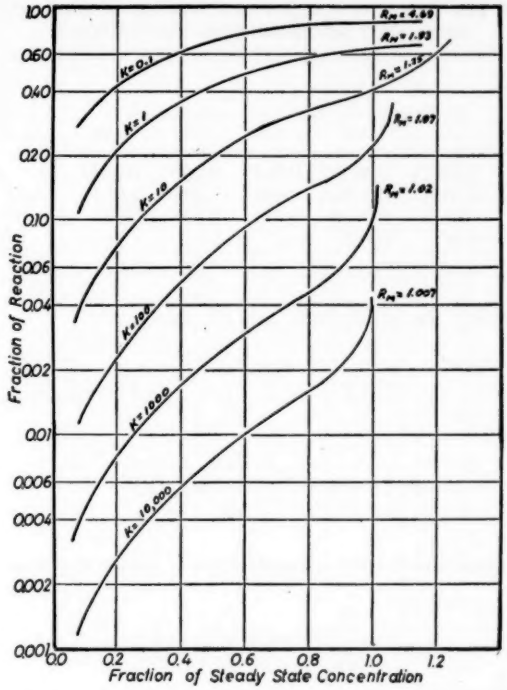

FIG. 2. Fraction of steady-state concentration achieved as a function of fraction of reaction for different rate constants. Case 2 (see Eq. (12), Table II).

In this case K actually does represent a limiting value for B which is identical with its stationary state value. Owing to the mechanism employed B may reach a finite limiting value at the end of the reaction ($A=0$) which is less than K (e.g., when $A_0/K=1$, a substantial amount of B remains although A is completely used up; see last column, Table III). This case is also different from the previous cases in that the value of B reached depends on the initial concentration of A, namely, A_0.

Case 4. A final illustrative example of this type of system is[9]

$$\begin{matrix} A+B \xrightarrow{k_1} C \\ B+C \xrightarrow{k_2} D \end{matrix} \qquad (17)$$

TABLE II. Extent of reaction as a function of the fraction of steady-state concentrations achieved (Case 2).

$K=k_2/k_1$	R=fraction of steady-state concentration 0.1	0.5	0.9	0.95	0.99	Roots of quadratic y_1[a]	$-y_2$	Y_S	y_1/y_S	Extent of reaction at 0.99 y_1
0.1	0.311	0.702	0.820	0.827	0.825	10.48	0.475	2.24	4.69	0.9991
1.0	0.124	0.430	0.611	0.629	0.643	1.366	0.366	0.707	1.93	0.967
10	0.043	0.20	0.36	0.39	0.41	0.279	0.179	0.224	1.25	0.70
100	0.013	0.072	0.161	0.184	0.206	0.0759	0.0659	0.0707	1.07	0.315
1000	0.0044	0.023	0.060	0.072	0.089	0.0229	0.0219	0.0224	1.02	0.112
10000	0.0014	0.0077	0.021	0.026	0.032	0.00712	0.00702	0.00707	1.007	0.036

Values given are $[1-(A/A_0)]$ = extent of reaction.
[a] y_1 represents limiting value of B/A when $A/A_0 \to 0$. Note that the limiting value at $t=\infty$, namely y_1 is always greater than y_S.

[9] This system which resembles the initial step in catalytic polymerizations has been solved by the above methods for these systems by (a) G. Natta, Rend. Inst. Lombardo Sci. 78, No. 1, 307 (1945) and (b) C. Potter and W. C. MacDonald, Can. J. Research 25B, 415 (1947).

TABLE III. Extent of reaction as a function of the fraction of steady-state concentrations achieved (Case 3).

A_0/K	Fraction of steady-state concentration 0.1	0.5	0.9	0.95	0.99	Value of $(1-B/K)$ when $A/A_0=0$
1000	0.00011	0.00089	0.0037	0.0050	0.0082	0
100	0.0011	0.00886	0.0371	0.0504	0.082	3.4×10^{-22}
10	0.0110	0.0886	0.371	0.504	0.822	0.0065
1	0.110	0.886	···	···	···	0.535

for which the differential equations are

$$\frac{dA}{dt}=-k_1AB; \qquad \frac{dB}{dt}=-k_1AB-k_2BC;$$
$$\frac{dC}{dt}=k_1AB-k_2BC; \qquad \frac{dD}{dt}=k_2BC. \tag{18}$$

The equation for the intermediate C is best expressed as

$$\frac{dC}{dA}=-1+\frac{k_2}{k_1}\left(\frac{C}{A}\right). \tag{19}$$

On substituting $y=C/A$; $K=k_2/k_1$ we obtain

$$\frac{dy}{d\ln A}=-1+(K-1)y, \tag{20}$$

which has for its solution ($y=0$ when $A=A_0$)

$$y=\left(\frac{C}{A}\right)=\frac{1}{K-1}\left[1-\left(\frac{A}{A_0}\right)^{K-1}\right]. \tag{21}$$

It may be seen that C/A has the same dependence on A that the intermediate B/A had in Case 1 (Eq. (7)). For the steady-state concentrations we have

$$(C/A)_S=\frac{k_1}{k_2}=\frac{1}{K} \tag{22}$$

so that the ratio $R=(C/A)/(C/A)_S$ is given by Eq. (7). The values of R can then be taken from Table I.

TABLE IV. Roots of the quadratic $z^2-(1+K_1+K_3)z+K_1K_3$ for different values of K_1 and K_3 (Case 5).

K_3	Values of K_1 0.001	0.01	0.10	1.00	10	100	1000	
0.001	1.002	1.011	1.101	2.001	11.00	101.0	1001	z_1
	0.0100	0.099	0.909	5.00	9.09	9.90	9.99	$Z_2\times10^4$
0.01	···	1.020	1.109	2.005	11.00	101.0	1001	z_1
	···	0.980	9.02	49.9	90.9	99.0	99.9	$z_2\times10^4$
0.100	···	···	1.192	2.052	11.01	101.0	1001	z_1
	···	···	8.39	48.7	90.8	99.0	99.9	$z_2\times10^3$
1.00	···	···	···	2.618	11.10	101.0	1001	z_1
	···	···	···	38.2	90.1	99.0	99.9	$z_2\times10^2$
10	···	···	···	···	13.71	101.1	1001	z_1
	···	···	···	···	7.29	9.89	9.99	z_2
100	···	···	···	···	···	110.6	1001	z_1
	···	···	···	···	···	90.4	99.9	z_2
1000	···	···	···	···	···	···	1032	z_1
	···	···	···	···	···	···	969	z_2

II. SYSTEMS INVOLVING EQUILIBRIA

The simplest equilibrium system is

$$A\underset{k_2}{\overset{k_1}{\rightleftarrows}}B \qquad B\xrightarrow{k_3}C. \tag{23}$$

This system is representative of the state of affairs in a unimolecular reaction at constant pressure.[10,11]

The differential equations are

$$\frac{dA}{dt}=-k_1A+k_2B; \qquad \frac{dB}{dt}=k_1A-(k_2+k_3)B;$$
$$\frac{dC}{dt}=k_3B. \tag{24}$$

Dividing dB/dt by dA/dt we have on making the substitution $y=B/A$; $K_3=k_3/k_2$; $K_1=k_1/k_2$:

$$\frac{dy}{d\ln A}=-(1+y)+\frac{K_3y}{K_1-y}. \tag{25}$$

Replacing $z=K_1-y$ this can be rearranged:

$$\frac{zdz}{z^2-(1+K_1+K_3)z+K_1K_3}=-d\ln A. \tag{26}$$

Since the discriminant of the quadratic in z (Eq. (26)) is always positive, there will be two real positive roots[12] which we can write as $z_1>z_2$. The solution to the equation then takes the form ($z=K_1$ when $A=A_0$)

$$\ln\left[\frac{z-z_1}{K_1-z_1}\right]-\left(\frac{z_2}{z_1}\right)\ln\left[\frac{z-z_2}{K_1-z_2}\right]$$
$$=-\left(1-\frac{z_2}{z_1}\right)\ln\left(\frac{A}{A_0}\right) \tag{27}$$

[10] A detailed analysis of the second-order mechanism corresponding to the Lindemann Hypothesis has been carried out and will be published shortly. R. H. Fowler, *Statistical Mechanics* (Cambridge University Press, Cambridge, 1936), gives a treatment of this system and an approximate treatment of the Lindemann mechanism.

[11] For the most general treatment of this type of first-order coupled system, see Zwolinski and Eyring (reference 4c) and Matsen and Franklin (reference 4b). Particular systems have been treated by A. Skrabal, Sitz. Ber. Akad. Wiss. Wien. **137**, 1045 (1928); Z. Physik. Chem. **B6**, 382 (1929) and A. E. Korvezee, Rec. Trav. Chim. **59**, 913 (1940).

[12] $(1+K_1+K_3)^2-4K_1K_3>0$ since it can be written as $1+2(K_1+K_3)+(K_1-K_3)^2$. When K_1 and K_3 are both large, then the roots are approximately K_1 and K_3, respectively.

or in terms of $y=B/A$:

$$\ln\left[1-\frac{y}{K_1-z_1}\right]-\left(\frac{z_2}{z_1}\right)\ln\left[1-\frac{y}{K_1-z_2}\right]=-\left(1-\frac{z_2}{z_1}\right)\ln\frac{A}{A_0}. \quad (28)$$

Table IV gives the roots z_1 and z_2 for various choices of the ratios K_3 and K_1. It should be noted that the quadratic for these roots (Eq. (26)) is symmetrical with respect to K_1 and K_3. As in the previous cases the maximum concentration ratio of the intermediate $B/A=y$ may exceed the stationary state concentration given by $y_S=k_1/(k_2+k_3)=K_1/(1+K_3)$. The values of y_{max}/y_S are shown in Table V. In Table VI is listed the extent of reaction required to achieve various fractions of the stationary state concentrations. Values are listed for selected choices of K_1 and K_3.

It will be noticed from Table VI that the length of the induction period is sensitive to the choice of K_3 (for given K_1) only when K_3 is greater than 1. For values of K_3 less than 1, there is little relative effect.

TABLE V. Values of (y_{max}/y_S) (Case 5).[a]

K_3	K_1 0.001	0.01	0.10	1.00	10	100	1000
0.001	1.000	1.000	1.0001	1.0005	1.0009	1.001	1.001
0.01	1.000	1.000	1.001	1.002	1.001	1.009	1.010
0.1	1.000	1.001	1.008	1.046	1.090	1.099	1.100
1.00	1.00	1.002	1.026	1.236	1.820	1.98	1.998
10.0	1.001	1.002	1.012	1.089	2.981	9.91	10.89
100	1.010	1.010	1.010	1.010	1.111	9.70	90.9
1000	1.001	1.001	1.001	1.001	1.001	1.001	31.0

[a] $y_{max}=K_1-z_2$. $y_S=K_1/(1+K_3)$. $y_{max}/y_S=[1-(z_2/K_1)](1+K_3)$.

In general it can be said that the length of the induction period is dominated by the ratio $k_1/(k_2+k_3)=K_1/(1+K_3)$ which may be looked upon as the ratio of the rate of the production of intermediate to the rates of destruction. If we call this ratio α, then (for small α) the minimum fraction of reaction occurring during the induction period is α and it is generally greater than α by a small factor. We can see that this same generalization holds true for the earlier cases studied as well.

From this viewpoint we can estimate the role of the reverse reaction (k_2). For k_2 small compared to k_1 and k_3 the present case resembles the earlier cases. However, when k_2 is large, then the equilibrium reaction has the effect of a feedback mechanism, tending to bring the induction period close to its minimum duration. The graphical behavior of the induction period is shown in Fig. 3.

III. SYSTEMS INVOLVING MORE THAN ONE INTERMEDIATE

To extend our discussion we now consider the case of more than one intermediate. This is illustrated by the

TABLE VI. Extent of reaction as a function of fraction of steady-state concentrations achieved (Case 5).

$k_1/(k_2+k_3)$	K_1	K_3	Fraction of steady-state concentration 0.1	0.5	0.9	0.95	0.99	Extent of reaction at $0.99y_{max}$
0.909	10	10	0.0837	0.366	0.565	0.586	0.603	0.998
0.500	1	1	0.049	0.228	0.399	0.424	0.445	0.688
0.909	1	0.1	0.084	0.318	0.472	0.489	0.506	0.540
0.00099	0.1	100	0.0001	0.001	0.002	0.003	0.004	0.004
0.0091	0.1	10	0.001	0.006	0.018	0.023	0.033	0.038
0.050	0.1	1	0.005	0.029	0.072	0.084	0.101	0.129
0.0909	0.1	0.1	0.009	0.045	0.085	0.095	0.104	0.128
0.099	0.1	0.01	0.010	0.049	0.084	0.089	0.093	0.093
0.00091	0.01	10	0.0006	0.002	0.002	0.003	0.004	0.004
0.005	0.01	1	0.0005	0.003	0.008	0.010	0.014	0.015
0.0091	0.01	0.1	0.001	0.0055	0.011	0.012	0.014	0.014
0.0099	0.01	0.01	0.001	0.005	0.009	0.010	0.011	0.011

following:

$$\text{Case 6} \qquad A \underset{k_2}{\overset{k_1}{\rightleftarrows}} B \qquad B \xrightarrow{k_3} C \qquad C \xrightarrow{k_4} D. \quad (29)$$

For A, D, and the two intermediates B and C we have the differential equations

$$\frac{dA}{dt}=-k_1A+k_2B; \quad \frac{dB}{dt}=k_1A-(k_2+k_3)B;$$
$$\frac{dC}{dt}=k_3B-k_4C; \quad \frac{dD}{dt}=k_4C. \quad (30)$$

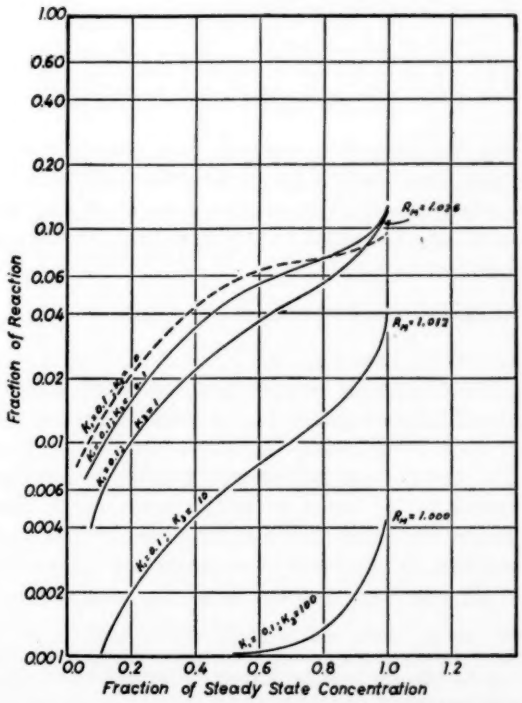

FIG. 3. Fraction of steady-state concentration achieved as a function of fraction of reaction for different rate constants. Effect of equilibrium (see Eq. (28), Tables IV, V, VI).

The equations for A and B are independent of C and so have been treated under Case 5. We shall here be concerned only with the behavior of C. To solve the system exactly is a considerable labor[13] and so we shall restrict the discussion to the behavior of C after the intermediate B has reached its stationary state concentration

$$(B/A)_S=\frac{k_1}{k_2+k_3}=\frac{K_1}{1+K_3}, \tag{31}$$

when $K_1=k_1/k_2$ and $K_3=k_3/k_2$. Under these conditions the equations for A and C become,

$$\begin{aligned}\frac{dA}{dt}&=-k_1\left(\frac{k_3}{k_2+k_3}\right)A,\\ \frac{dC}{dt}&=\frac{k_1k_3}{(k_2+k_3)}A-k_4C.\end{aligned} \tag{32}$$

It may be recognized from the form of these equations that the effect of the assumption that B has reached a stationary concentration is to reduce the system to one of two consecutive, first-order reactions (Case 1) where the composite constant $k_1k_3/(k_2+k_3)$ plays the role of the first rate constant. This is clear since the effect of a steady state for B is to eliminate it from the scheme.

Under such circumstances, C will now have the relation to A that the single intermediate B had in Case 1. We can now say something about the induction period for C. The duration of this period is determined by the ratio (see Table I for K):

$$\left(\frac{C}{A}\right)_S=\frac{1}{K}=\frac{k_1k_3}{k_4(k_2+k_3)}=\frac{k_1}{k_4}\left(\frac{1}{1+(k_2/k_3)}\right). \tag{33}$$

When K is large, then the induction period for C/A is small and from Table I we can say that C/A will reach $0.99C/A_S$ after a fraction which is roughly $4/K$ of A has been used up. There are two different conditions under which K can be large:

Condition 1: $k_2/k_3<1$ and $k_1\ll k_4$.

Since (k_2+k_3) must exceed k_1 for B to reach a steady state (Eq. (31)), this implies that the influence of the back equilibrium reaction (k_2) is small compared to k_3. Under these conditions B is removed rapidly by formation of C and C must be removed rapidly by forming D (compared to A) since k_1 is less than k_4. A simple calculation will show that if $k_4\gtrsim k_3$, then by the time B has reached its stationary concentration C will have also.[14] If, however, $k_3>k_4$, then the total induction period for B and C is approximately the sum of the independently calculated induction periods.

Condition 2:

$$k_2/k_3\gg 1 \quad \text{and} \quad k_1\gtrsim k_4 \text{ (such that } k_1/k_2\cdot k_3/k_4\ll 1).$$

Again $(k_2+k_3)\gg k_1$ to keep B stationary and under the above conditions it is the equilibrium reaction (k_2) that is responsible for bringing C quickly to a stationary value. The combination of these conditions, however, still requires that k_4 be of the same order of magnitude as k_3 or greater. That is, the rate of removal of C must be as fast or faster than its rate of production. It is of interest to note how a fast equilibrium involving the first intermediate B can considerably loosen the requirements for a rapid approach to a stationary state for the subsequent intermediates.

We can generalize from this system to a system of "n" consecutive intermediates as follows:

(A) In the absence of fast reverse reactions the stationary state is achieved only if the collective rate constants[15] for the destruction of each intermediate are much greater than the rate constant for the production of the first intermediate. Under these conditions the collective rate constant for the production of each intermediate must be of about the same order of magnitude or smaller than the collective rate constant for the destruction of this intermediate.[16]

(B) If the first intermediate decomposes much more rapidly to give the initial reactants than it reacts to give the second intermediate, the main requirement on the collective rate constants for the destruction of this and subsequent intermediates is that they be of the same order of magnitude or greater than the collective rate constants for the production of the intermediates. A corollary of this condition, however, is that the constant for this reverse reaction of the first intermediate must then be much greater than all subsequent collective constants for production of intermediates.

IV. REGENERATIVE MECHANISMS

To complete our discussion of the induction period we must consider one additional mechanism which occurs commonly in chain reactions, namely, the chain propagation mechanism. Of the various chain propagation mechanisms the one which demands further analysis is the type we shall describe as regenerative. A regenerative mechanism will be defined as one in which an intermediate may react to form a second intermediate which may further react to recreate the initial species. A typical such cycle is exemplified by the propagation mechanism in the hydrogen-halogen reactions where X may represent Cl or Br or I and B_2 is hydrogen.

$$\begin{aligned}&\overset{k_3}{\longrightarrow}\\ &X+B_2\quad BX+B\\ &\overset{k_4}{\longrightarrow}\\ &B+X_2\quad BX+X.\end{aligned} \tag{34}$$

[13] For this and more complicated, coupled systems of linear equations, the exact solutions can be written but the computation obscures the inherent relations looked for between rate constants and induction period (see reference 4b, c).

[14] When $k_4\gg k_3$ then this means that C will quickly reach a steady state with respect to B so that it presents no problem as a secondary intermediate.

[15] Collective rate constants may be used in the sense that if there are processes of different order occurring then the "constant" that must be used is the regular rate constant multiplied by an initial concentration (see Case 3 and also Sec. IV).

[16] These conditions are generally satisfied in chain reactions and polymerization schemes when there is considerable activation energy required to produce the first intermediate.

The feature of such a regenerative cycle is that while it does not change the total concentration of radicals $(X+B)$ it may permit a considerable amount of reaction to occur. To avoid confusion, let us discuss a simplified scheme for a chain reaction of X_2 and B_2.[17]

$$\begin{aligned} &M+X_2 \underset{k_2}{\overset{k_1}{\rightleftarrows}} 2X+M \\ &X+B_2 \underset{k_5}{\overset{k_3}{\rightleftarrows}} BX+B \\ &B+X_2 \xrightarrow{k_4} BX+X. \end{aligned} \tag{35}$$

The regeneration mechanism is only of importance as a consideration separate from the cases previously discussed when it is very fast, that is, when in the process of building the intermediate concentrations to their stationary values, these intermediates can account for a good deal of reaction. In such a case an ordinarily short induction period may be extended considerably.

For this condition to occur it must mean that reactions 3, (k_3) and 4, (k_4) are each much faster than 2, (k_2) the chain terminating step. But they must also be much faster than the reverse reaction 5, (k_5) or the effect will be nullified.

The precise mathematics of the induction period are difficult to formulate.[18] However, it is possible to state precisely what conditions must be satisfied for the induction period to be restricted to a specified interval.

The simplest case to treat is that in which $k_4 \gg k_3$ so that we can say that the (B) atoms quickly reach a steady state with respect to (X) atoms. In this case we find the equation for $d(X)/dt$ reduces to

$$\frac{d(X)}{dt}=2k_1(X_2)(M)-2k_2(X)^2(M). \tag{36}$$

The steady-state concentration of (X) will be given by P:

$$P=(X)_S=\left[\frac{k_1}{k_2}(X_2)\right]^{\frac{1}{2}}. \tag{37}$$

Since we are looking for conditions under which the induction period is short (i.e., X_2 is not appreciably used up in establishing $(X)_S$) we can make the approximation of considering (X_2) constant. Under these conditions Eq. (36) may be integrated to give

$$t=\frac{1}{4Mk_2P}\ln\left(\frac{P+X}{P-X}\right) \tag{38}$$

or

$$\frac{X}{P}=\frac{(X)}{(X)_S}=\frac{e^{ct}-1}{e^{ct}+1}, \tag{39}$$

where $C=4MPk_2=4M(k_1k_2X_2)^{\frac{1}{2}}$.

The time required for (X) to reach any fraction of its stationary concentration P is then equal to‡

$$t=\frac{1}{k_2{}^*P}\ln\left(\frac{1+\alpha}{1-\alpha}\right)\underset{(\alpha\to 1)}{\approx}\frac{1}{k_2{}^*P}\ln\left(\frac{2}{1-\alpha}\right). \tag{40}$$

It is seen that the relative error in t, made by considering (X_2) a constant will only amount to about one-half the relative difference between the initial and final values since t depends only on the square root of X_2.

We now turn to the equation for $d(B_2)/dt$ which, under our assumption, becomes

$$\frac{d(B_2)}{dt}=\frac{-k_3(B_2)(X)}{1+(k_5/k_4)\cdot(BX/X_2)}. \tag{41}$$

On neglecting the second term in the denominator[19] we obtain the expression for the maximum rate of disappearance of B_2:

$$\frac{d(\ln B_2)}{dt}=-k_3(X). \tag{42}$$

On substituting the value of X (Eq. (39)) and integrating we obtain:

$$\ln\left(\frac{B_2}{B_{20}}\right)=\frac{k_3}{k_2{}^*}\ln(1-\alpha^2) \tag{43}$$

$$\underset{\alpha\to 1}{\xrightarrow{\approx}}\frac{k_3}{k_2{}^*}\ln[2-2\alpha]. \tag{44}$$

In order that the ratio B_2/B_{20} be close to unity (i.e., be equal to $(1-x)$ where x is small) which would imply a short induction period we have the condition that

$$\frac{k_3}{k_2{}^*}\leqslant\frac{\ln(B_2/B_{20})}{\ln(2-2\alpha)}\approx-\frac{x}{\ln(2-2\alpha)}. \tag{45}$$

Thus for $\alpha=0.99$ and an induction period of 1 percent $(x=0.01)$ we have

$$\frac{k_3}{k_2{}^*}\leqslant\frac{0.01}{\ln 50}=\frac{0.01}{3.9}\approx 0.002. \tag{46}$$

This result is not unexpected since it says that the rate of the termination reaction 2 must be fast compared to the rate of the chain propagation reaction 3 (note that

[17] The addition of further steps such as $B+X\to BX$(3 Body); $B\to 1/2B_2$ (diffusion); $X\to 1/2X_2$ (diffusion) does not change the essential aspects of the discussion.

[18] Matsen and Franklin (reference 4b) have made an approximate solution of this system.

‡ We have absorbed the quantity $4M$ into k_2; $k_2{}^*=4Mk_2$.

[19] This will certainly be valid in the early stages of reaction when $BX=0$. Otherwise, it may be observed that as previously noted (Case 5) the effect of the equilibrium reaction $5(k_5)$ is to shorten the induction period.

we have assumed that $k_4 > k_3$ so that k_3 is the slow step) in order to have a short induction period.

While these conditions are fulfilled in the case of the analogous H_2-Br_2 reaction where the ratio k_3/k_2^* is about 10^{-4} at 1-atmosphere pressure[20] they are not fulfilled in the case of the H_2-Cl_2 reaction[20] where this ratio is about unity.[21] It becomes clear in the latter case why this reaction follows a different kinetics and shows such remarkable sensitivity to small amounts of inhibitors or impurities.[20]

In general it may be shown that for a regenerative mechanism not to enhance the induction period, that the slowest of the rate constants of the regenerative steps[22] must be smaller than the termination rate constant. For an induction period equal to a fraction α of the original reactants the ratio of these constants must be at least α and roughly about 0.2α.[23]

It can thus be concluded that the stationary state hypothesis can be justifiably employed in the case of fast chain reactions only when there are termination mechanisms available which are fast compared to the slowest rate in a regenerative cycle.[24]

V. CONCLUSIONS

The most important behavior of chain intermediates are best considered from the viewpoint of the following terminology: (1) initiation reactions, (2) termination reactions, (3) restorative or equilibrium reactions, and (4) regenerative or propagation reactions.

From this standpoint we can make the following statements:

(1) The stationary concentration of a single intermediate is essentially determined by the ratio of its termination rates to its initiation rates. In order for the induction period (leading to the establishment of the stationary state) to be smaller than a fraction α where α represents the fraction of reaction, this ratio must be at least greater than $1/\alpha$ and usually greater than $4/\alpha$ (for $\alpha < 0.1$).

(2) The existence of an equilibrium between intermediate and initial reactants may reduce the induction period if the back reaction (itself a termination reaction) is of the same order or faster than the other termination reactions. The extent of this effect is to reduce the factor of $4/\alpha$ (above) to nearer $1/\alpha$.

(3) The above criteria apply also to systems in which more than one intermediate is produced. In such systems it is the ratio of the termination reaction rates for each intermediate to the rate of the *first* initiation rate for the entire system which must be employed in formulating the criterion.

(4) For systems in which propagative chain mechanisms are present, the criterion is that the mean rate or slowest rate in the cycle must be less than $4/\alpha$ times the rate of the termination reaction for radicals capable of starting such cycles.

ACKNOWLEDGMENTS

The author would like to express his appreciation to the John Simon Guggenheim Memorial Foundation and to the Fulbright Commission for a joint Fellowship which made possible the present work. He also wishes to thank Professor E. Bauer and Dr. M. Magat, of the Laboratoire de Chimie Physique, for the hospitality which they extended and for the many interesting discussions in connection with this work.

[20] K. J. Laidler, *Chemical Kinetics* (McGraw-Hill Book Company, Inc., New York, 1950), Chapter 8.

[21] There is an additional point worth noting in the case of photochemical reactions. Here the initial intermediate (X) will start out at values higher than its photostationary state, namely, $2I_{abs}/V$, and decay to this latter value. The mathematical analysis is the same (Eq. (38)) except for a constant of integration and high initial rates. The principal point of interest is that the induction period will be characterized by a faster rate of reaction than occurs in the thermal reaction. If now a thermal and photochemical reaction are unwittingly compared during their induction periods rather large discrepancies may be found either in rate constants or in apparent order. In either case calculated activation energies or frequency factors will turn out to be in error.

[22] When the steps in the chain have about the same rate then we can employ a reduced rate constant $\bar{k}$ in formulating our criterion. $\bar{k}$ is defined by $\bar{k}^{-1} = \Sigma\, k_i^{-1}$ where k_i are the rates for the steps in the chain propagation mechanism (see Semenov, reference 3).

[23] The approximate solution of (41) under conditions that the neglected term in the denominator is large compared to unity only slightly weakens this condition. The new condition then becomes

$$k_3/k_2^* \leqslant 0.002(k_5/k_4)(BX/X_2).$$

When k_4/k_5 is about unity (as it is for the hydrogen-halogen reactions) this would require a large initial ratio of (BX/X_2) to be satisfied, i.e., for the denominator to be important.

[24] Such reactions, when studied photochemically, are characterized by very high quantum yields. An extended discussion of the application of the preceding material to specific, fast, chain reactions will be made later.

The Compressibility of Krypton. I. An Equation of State for Krypton and the Weight of a Liter of Krypton

JAMES A. BEATTIE, JAMES S. BRIERLEY, AND ROLAND J. BARRIAULT
Department of Chemistry, Massachusetts Institute of Technology, Cambridge, Massachusetts

(Received June 18, 1952)

The compressibility of krypton containing 0.90 mole percent xenon has been measured from 0° to 300°C and over the density range 1 to 10 mole per liter. The constants of the Beattie-Bridgeman equation of state for the sample and for pure krypton were determined. The constants for pure krypton are $R=0.08206$, $A_0=2.4230$, $a=0.02865$, $B_0=0.05261$, $b=0$, $c=14.89\times10^4$ in units of standard atmos, liter per mole, and °K (T°K$=t$°C$+273.13$). The equation for the sample studied reproduced the observed pressures with an average deviation of 0.16 percent. The weight of one liter of Kr at a pressure of one standard atmosphere is calculated from the molecular weight (83.7) and the above constants to be 3.745 g per liter at 0°C and 3.474 g per liter at 70°F.

RECENTLY[1] we published the results of a study of the compressibility of gaseous xenon. The present paper deals with the compressibility of gaseous krypton over the temperature range 0° to 300°C and from 1 to 10 mole per liter, the maximum pressure reached being about 415 atmos.

Ramsay and Travers[2] studied the volumetric behavior of krypton at the two temperatures 11.2° and 237.3°C.

The experimental method employed in the present investigation has been described elsewhere.[3] For krypton we used the steel bomb having a volume of about 200 ml, the weight of the gas sample being 14.1043 g.

The compressor settings were originally made on the basis that the gas was pure krypton having a molecular weight of 83.7. A plot of the function

$$B(V, T)=V(pV-RT) \qquad (1)$$

against $1/V$ did not extrapolate to zero density in a rational manner; the curve bent sharply instead of approaching linearity as $1/V$ approached zero. A preliminary analysis of some of the unused gas was made by Dr. R. G. Gillette and showed about 0.63 mole percent xenon but no detectable amount of Ne, A, O_2, or N_2. The pressures were then interpolated through the function $B(V, T)$ *without smoothing* for integer and half-integer values of density corresponding to the molecular weight 84.100 in the manner described in the paper on xenon. These values of pressure are listed in Table II. Subsequently an accurate analysis of some of the gas removed from the compressibility bomb gave a xenon content of 0.90 ± 0.01 mole percent. This would correspond to a molecular weight for the gas sample of $84.128(=0.991\times83.7+0.009\times131.3)$ on the basis of the accepted atomic weights (83.7 for krypton and 131.3 for xenon), and to a change of 0.03329 percent in the densities of Table II or 0.03 percent to 0.04 percent in the pressures, which is outside the experimental error of the compressibility measurements. This latter correction was not applied.

The constants of the Beattie-Bridgeman equation of state of the mixture are given in Table I together with those for pure krypton computed from the relations for the combination of constants given in the paper[1] on xenon, and the constants for xenon. The deviations of the pressures calculated from the equation of state with the constants for the mixture from the observed pressures are listed in Table II. The equation of state gives a better representation of the pressures of krypton than those of xenon. In fitting the equation of state to the observations we used the value 273.13° for the Kelvin temperature of the ice point and computed the Kelvin temperature corresponding to other temperatures on the International Temperature Scale from the relation given in Table I. This was done for the sake of consistency of the present work with the constants for the many other gases previously studied.

WEIGHT OF A LITER OF KRYPTON AT ONE ATMOSPHERE PRESSURE

The results of the calculation of the weight of one liter of pure krypton under a pressure of one standard atmosphere at 0°C and 70°F are given in Table III. One calculation was based on RT and T_0 obtained from $R=0.08206$ and $T_0=273.13$. The second employed the same values of the virial coefficients, but the leading term RT was evaluated from Birge's[4] value $RT_0=22.4140$ liter-atmos per mole and the Kelvin tempera-

TABLE I. Constants of the Beattie-Bridgeman equation of state for krypton.

$p=[RT(1-\epsilon)/V^2][V+B]-A/V^2$
$A=A_0(1-a/V)$ $B=B_0(1-b/V)$ $\epsilon=c/VT^3$
Units: standard atmosphere, liter per mole, °K (T°K$=t$°C$+273.13$)

Composition in mole percent	R	A_0	a	B_0	b	c	Molecular weight
99.10% Kr, 0.90% Xe	0.08206	2.4400	0.02869	0.05280	0	15.00×10^4	···
100% Kr	0.08206	2.4230	0.02865	0.05261	0	14.89×10^4	83.7

[1] Beattie, Barriault, and Brierley, J. Chem. Phys. **19**, 1219 (1951).
[2] W. Ramsay and M. W. Travers, Trans. Roy. Soc. (London) **A197**, 47 (1901).
[3] J. A. Beattie, Proc. Am. Acad. Arts Sci. **69**, 389 (1934).
[4] R. T. Birge, Revs. Modern Phys. **13**, 233 (1941).

TABLE II. Comparison of the pressures calculated from the equation of state with the observed pressures for gaseous krypton containing 0.90 mole percent xenon. For each temperature the first line gives the observed pressure and the second line gives the observed pressure minus the pressure calculated from the equation of state given in Table I. For the critical constants of krypton J. J. Meihuizen and C. A. Crommelin (Leiden Comm., No. 245*c*, 1937) give $t_c = -63.75°C$, $p_c = 54.18$ atmos and S. F. Pickering (Sci. Paper of the Bureau of Standards, No. 541, 1926) selects $d_c = 9.3$ mole per liter.

Density, mole/liter Temp., °C (Int.)	1.0	1.5	2.0	2.5	3.0	3.5	4.0	4.5	5.0	6.0	7.0	8.0	9.0	10.0
							Pressure, standard atmosphere							
0 obsd.	21.058	30.660	39.663	48.199	56.239	63.849	71.066	77.833	84.416	96.78	108.37	119.62	130.88	142.47
obsd.-calc.	0.005	0.032	0.033	0.094	0.139	0.190	0.237	0.176	0.229	0.24	0.11	−0.08	−0.37	−0.79
25 obsd.	23.221	34.048	44.353	54.202	63.636	72.700	81.443	89.901	98.115	114.00	129.45	144.80	160.52	177.04
obsd.-calc.	−0.020	0.035	0.069	0.103	0.130	0.149	0.161	0.155	0.125	−0.01	−0.25	−0.66	−1.14	−1.62
50 obsd.	25.432	37.425	48.988	60.153	70.985	81.505	91.762	101.825	111.672	131.09	150.37	169.86	190.04	211.50
obsd.-calc.	0.010	0.041	0.077	0.103	0.135	0.148	0.141	0.137	0.065	−0.10	−0.39	−0.82	−1.31	−1.66
75 obsd.	27.614	40.787	53.596	66.078	78.277	90.232	102.008	113.623	125.156	148.03	171.07	194.76	219.43	245.84
obsd.-calc.	0.015	0.042	0.077	0.107	0.128	0.131	0.132	0.101	0.068	−0.14	−0.45	−0.75	−1.11	−1.16
100 obsd.	29.789	44.139	58.193	71.973	85.543	98.925	112.189	125.379	138.507	164.90	191.70	219.54	248.71	280.00
obsd.-calc.	0.016	0.041	0.079	0.103	0.127	0.126	0.119	0.102	0.038	−0.11	−0.37	−0.51	−0.64	−0.35
125 obsd.	31.958	47.485	62.771	77.852	92.772	107.581	122.319	137.066	151.818	181.66	212.24	244.12	277.86	314.03
obsd.-calc.	0.014	0.040	0.073	0.100	0.115	0.118	0.101	0.094	0.044	−0.06	−0.22	−0.26	−0.01	0.69
150 obsd.	34.126	50.823	67.334	83.700	99.974	116.194	132.411	148.679	165.054	198.30	232.68	268.67	306.84	347.79
obsd.-calc.	0.013	0.036	0.061	0.079	0.095	0.095	0.082	0.059	0.033	−0.05	−0.04	0.14	0.66	1.74
175 obsd.	36.293	54.154	71.883	89.532	107.141	124.767	142.458	160.230	178.233	214.85	252.92	292.93	335.58	381.41
obsd.-calc.	0.012	0.027	0.040	0.053	0.054	0.053	0.045	−0.002	0.011	−0.07	0.03	0.37	1.28	2.87
200 obsd.	38.464	57.469	76.418	95.345	114.286	133.314	152.450	171.761	191.304	231.39	273.14	317.19	364.27	415.17
obsd.-calc.	0.017	0.006	0.011	0.015	0.004	0.001	−0.024	−0.054	−0.083	−0.03	0.16	0.72	1.97	4.32
225 obsd.	40.598	60.780	80.940	101.131	121.398	141.799	162.408	183.211	204.350	247.81	293.09	341.08	392.57	
obsd.-calc.	−0.015	−0.017	−0.027	−0.042	−0.069	−0.099	−0.110	−0.165	−0.173	−0.08	0.08	0.77	2.39	
250 obsd.	42.754	64.090	85.466	106.926	128.512	150.310	172.318	194.678	217.372	264.12	313.18	365.07		
obsd.-calc.	−0.023	−0.039	−0.058	−0.086	−0.133	−0.163	−0.228	−0.239	−0.262	−0.20	0.19	1.00		
275 obsd.	44.908	67.400	89.989	112.699	135.622	158.793	182.216	206.052	230.260	280.38	333.08	388.96		
obsd.-calc.	−0.033	−0.060	−0.089	−0.147	−0.194	−0.245	−0.347	−0.391	−0.467	−0.33	0.15	1.18		
300 obsd.	47.058	70.703	94.495	118.480	142.717	167.262	192.158	217.486	243.301	296.69	353.04	412.68		
obsd.-calc.	−0.057	−0.086	−0.134	−0.197	−0.265	−0.334	−0.412	−0.469	−0.502	−0.40	0.21	1.23		
Ave. dev. (atmos)	0.019	0.039	0.064	0.095	0.122	0.142	0.165	0.165	0.162	0.140	0.204	0.653	1.088	1.689
Ave. percent dev.	0.052	0.079	0.100	0.122	0.132	0.132	0.132	0.112	0.096	0.074	0.107	0.250	0.420	0.596

Total average deviation (atmos) 0.295; total average percent deviation, 0.158.

ture computed from the relation given in the paper on xenon. For both computations the same values of the second virial coefficient $\beta(=RTB_0-A_0-Rc/T^2)$ and the third virial coefficient $\gamma(=-RTB_0b+A_0a-RB_0c/T^2)$ were used. Both calculations gave the same weight of a liter to the number of significant places retained.

We are grateful to the Linde Air Products Company for a Grant-in-Aid that made this work possible. We are indebted to the Linde Company and Dr. John M. Gaines for the gift of the sample of krypton and to Dr. Roger H. Gillette of the same company for the careful analyses of the samples.

TABLE III. Weight of one liter of krypton at a pressure of one standard atmosphere.

Temp.	β atmos-liter^2/mole^2	γ atmos-liter^3/mole^3	m g/liter
0°C	−1.4076	+0.061	3.745
70°F	−1.2938	+0.062	3.474

THE JOURNAL OF CHEMICAL PHYSICS VOLUME 20, NUMBER 10 OCTOBER, 1952

The Compressibility of Gaseous Krypton. II. The Virial Coefficients and Potential Parameters of Krypton

JAMES A. BEATTIE, JAMES S. BRIERLEY, AND ROLAND J. BARRIAULT
Department of Chemistry, Massachusetts Institute of Technology, Cambridge, Massachusetts

(Received June 18, 1952)

The second and third virial coefficients of a sample of krypton containing 0.90 mole percent xenon have been determined from our compressibility measurements over the temperature range 0° to 300°C and to a density of 10 mole per liter. They are listed in Table II. The parameters of the Lennard-Jones (6, 12) potential for krypton are $\mu=2.044\times10^{-58}$ erg-cm^6, $\lambda=0.438\times10^{-102}$ erg-cm^{12}, $\epsilon=238.4\times10^{-16}$ erg, $b_0=58.40$ cm^3 per mole, $\theta=172.7$°K, $\sigma=3.591\times10^{-8}$ cm, $r_0=4.030\times10^{-8}$ cm. The representation of the second virial coefficient is quite satisfactory. The third virial coefficients diverge more than those of xenon from the theoretical values for a Lennard-Jones (6, 12) potential as tabulated by Bird, Spotz, and Hirschfelder. The observed second virial coefficients agree moderately well with the tabulated values of Buckingham and Corner for an inverse sixth and inverse eighth power attractive and an exponential repulsive potential when the tables are used in conjunction with the values of the arguments derived by Kane from data on the solid state of krypton and Born and Mayer's value of the exponent derived for neon.

RECENTLY[1] we published the results of a study of the compressibility of xenon and of the parameters of various potential functions of gaseous xenon. In the first paper[2] of the present series on krypton we presented measurements of the compressibility of gaseous krypton from 0° to 300°C and over the density range 1 to 10 moles per liter. The gas contained 0.90 mole percent xenon, and all of the results given in the present paper apply to this mixture. The effects of this impurity, errors in the early analyses of the gas sample, and how the observations were treated are discussed in the first paper on krypton.

The values of $B(V, T)$,

$$B(V, T)=V(pV-RT), \tag{1}$$

where V is the molar volume of the gas sample at p and T, were computed as described in the earlier paper on krypton and are listed in Table I as observed values.

For this calculation we took

$$RT=22.4140(T/T_0) \text{ liter-atmos/mole}, \tag{2}$$

as given by Birge,[3] and the value[4] found in this laboratory for the Kelvin temperature T corresponding to t°C (Int.):

$$T=t+273.16+\frac{t}{100}\left(\frac{t}{100}-1\right)\times(0.04217-7.481\times10^{-5}t). \quad 0°<t<450°. \tag{3}$$

To compute the second and third virial coefficients, $B(T)$ and $C(T)$, we used the closed form,

$$B(V, T)=B(T)+\frac{C(T)}{V}+\frac{D(T)}{V^3}, \tag{4}$$

and applied the method of least squares to the values of $B(V, T)$ entered in Table I. The values of the parameters of Eq. (4) are presented in Table II, and the deviations of the values of $B(V, T)$ computed by Eq. (4) from those observed appear in Table I.

The virial coefficients of Eq. (4) are usually divided by RT for purposes of the statistical mechanics discussion; thus,

$$B'(T)=[B(T)/RT], \quad C'(T)=[C(T)/RT]. \tag{5}$$

[1] Beattie, Barriault, and Brierley, J. Chem. Phys. **19**, 1219 (1951); **19**, 1222 (1951).
[2] Beattie, Brierley, and Barriault, J. Chem. Phys. **20**, 1613 (1952).
[3] R. T. Birge, Revs. Modern Phys. **13**, 233 (1941).
[4] See report on International Temperature Scale of 1948, H. F. Stimson, J. Research Natl. Bur. Standards **42**, 209 (1949).

TABLE I. Values of $B(V, T)$ for krypton. $B(V, T) = V(pV - RT)$ (obs.) $B(V, T) = B(T) + (C(T)/V) + (D(T)/V^2)$ (calc., see Table II).

Temp., °C (Int.)		0	25	50	75	100	125	150	175	200	225	250	275	300
Temp., °K		273.16	298.152	323.150	348.153	373.160	398.170	423.183	448.198	473.214	498.231	523.248	548.264	573.278
RT, liter-atmos/mole		22.4140	24.4647	26.5159	28.5675	30.6194	32.6716	34.7241	36.7767	38.8293	40.8821	42.9348	44.9875	47.0400
Density, mole/liter							$B(V, T)$, liter²-atmos/mole²							
1	obs.	−1.35587	−1.24348	−1.08368	−0.95330	−0.83032	−0.71365	−0.59830	−0.48407	−0.36485	−0.28395	−0.18096	−0.07986	+0.00837
	obs.-calc.	−0.00650	−0.02629	−0.00919	−0.00669	−0.00605	−0.00711	−0.00603	−0.00388	0.00503	−0.00752	−0.00631	−0.00772	−0.01313
1.5	obs.	−1.31607	−1.17713	−1.04396	−0.91731	−0.79583	−0.67674	−0.56147	−0.44941	−0.34455	−0.24157	−0.13892	−0.03595	+0.06367
	obs.-calc.	0.00245	0.00822	0.00059	−0.00039	−0.00138	−0.00040	0.00018	−0.00007	−0.00557	0.00121	0.00076	0.00091	0.00423
2	obs.	−1.29135	−1.14418	−1.01092	−0.88486	−0.76151	−0.64310	−0.52866	−0.41748	−0.31013	−0.20612	−0.10083	+0.00345	+0.10382
	obs.-calc.	−0.00362	0.00941	0.00369	0.00234	0.00307	0.00297	0.00226	0.00087	−0.00224	0.00289	0.00378	0.00488	0.00638
2.5	obs.	−1.25371	−1.11351	−0.98180	−0.85444	−0.73206	−0.61240	−0.49763	−0.38557	−0.27650	−0.17190	−0.06583	+0.03688	+0.14083
	obs.-calc.	0.00331	0.00845	0.00289	0.00301	0.00258	0.00329	0.00241	0.00161	0.00004	0.00317	0.00358	0.00269	0.00531
3	obs.	−1.22254	−1.08423	−0.95135	−0.82510	−0.70172	−0.58252	−0.46654	−0.35429	−0.24460	−0.13871	−0.03255	0.07331	+0.17741
	obs.-calc.	0.00387	0.00625	0.00344	0.00256	0.00288	0.00266	0.00245	0.00148	0.00028	0.00221	0.00149	0.00326	0.00371
3.5	obs.	−1.19186	−1.05520	−0.92252	−0.79627	−0.67285	−0.55264	−0.43597	−0.32259	−0.21132	−0.10517	+0.00312	+0.10908	+0.21402
	obs.-calc.	0.00406	0.00397	0.00239	0.00154	0.00161	0.00187	0.00176	0.00149	0.00150	0.00135	0.00161	0.00289	0.00203
4	obs.	−1.16184	−1.02598	−0.89382	−0.76638	−0.64305	−0.52298	−0.40536	−0.29052	−0.17920	−0.07000	+0.03614	+0.14163	+0.24991
	obs.-calc.	0.00373	0.00209	0.00123	0.00153	0.00114	0.00067	0.00087	0.00153	0.00112	0.00182	−0.00116	−0.00103	−0.00052
4.5	obs.	−1.13729	−0.99705	−0.86402	−0.73731	−0.61276	−0.49170	−0.37429	−0.26002	−0.14670	−0.03747	+0.07266	+0.17820	+0.28674
	obs.-calc.	−0.00191	0.00017	0.00121	0.00063	0.00102	0.00089	0.00015	−0.00036	0.00061	−0.00069	−0.00068	−0.00131	−0.00228
5	obs.	−1.10615	−0.96834	−0.83628	−0.70726	−0.58359	−0.46161	−0.34264	−0.22602	−0.11373	−0.00240	+0.10793	+0.21291	+0.32405
	obs.-calc.	−0.00079	−0.00171	−0.00085	0.00064	−0.00039	−0.00032	−0.00030	0.00081	−0.00001	−0.00103	−0.00174	−0.00387	−0.00374
6	obs.	−1.04729	−0.91083	−0.77794	−0.64923	−0.52276	−0.39922	−0.27904	−0.16130	−0.04409	+0.06997	+0.18091	+0.29050	+0.40134
	obs.-calc.	−0.00134	−0.00445	−0.00199	−0.00169	−0.00127	−0.00135	−0.00200	−0.00157	0.00048	−0.00079	−0.00243	−0.00230	−0.00461
7	obs.	−0.99044	−0.85312	−0.71930	−0.58982	−0.46192	−0.33589	−0.21192	−0.09214	+0.02725	+0.14110	+0.25784	+0.37073	+0.48483
	obs.-calc.	−0.00294	−0.00556	−0.00265	−0.00303	−0.00301	−0.00270	−0.00186	−0.00177	−0.00041	−0.00381	−0.00072	−0.00037	−0.00023
8	obs.	−0.93262	−0.79565	−0.66038	−0.52774	−0.39718	−0.26954	−0.14257	−0.02003	+0.10237	+0.21912	+0.33742	+0.45400	+0.56814
	obs.-calc.	−0.00246	−0.00524	−0.00284	−0.00218	−0.00186	−0.00250	−0.00147	−0.00165	−0.00111	−0.00229	0.00183	0.00196	0.00286
9	obs.	−0.87468	−0.73653	−0.60005	−0.46515	−0.33166	−0.19978	−0.07003	+0.05666	+0.18274	+0.30409			
	obs.-calc.	−0.00059	−0.00136	−0.00139	−0.00135	−0.00108	−0.00058	−0.00013	0.00004	−0.00065	0.00348			
10	obs.	−0.81674	−0.67603	−0.53658	−0.39836	−0.26181	−0.12684	+0.00553	+0.13647	+0.26881				
	obs.-calc.	0.00272	0.00606	0.00346	0.00307	0.00272	0.00262	0.00169	0.00146	0.00091				

SECOND AND THIRD VIRIAL COEFFICIENTS FROM THE LENNARD-JONES (6, 12) POTENTIAL

Proceeding as in the case of xenon we determined the parameters of the Lennard-Jones[5] potential for krypton. The potential energy $u(r)$ of a pair of molecules is taken to be

$$u(r)=\lambda r^{-12}-\mu r^{-6}, \tag{6}$$

$$=4\epsilon\left[\left(\frac{\sigma}{r}\right)^{12}-\left(\frac{\sigma}{r}\right)^{6}\right]=\epsilon\left[\left(\frac{r_0}{r}\right)^{12}-2\left(\frac{r_0}{r}\right)^{6}\right], \tag{7}$$

where ϵ is the depth of the potential well, σ the separation of a pair of molecules at $u(r)=0$, and r_0 the separation at $u(r)$ a minimum. It has been found[6] that the expression for the second virial coefficient yielded by Eq. (6) can be represented quite well by the expression

$$\frac{B'(T)}{b_0}=\left(\frac{\theta}{T}\right)^{\frac{1}{4}}\left[1.0591-3.5891\left(\frac{\theta}{T}\right)\right],\quad 0.20\lesssim\frac{\theta}{T}\lesssim 1.00, \tag{8}$$

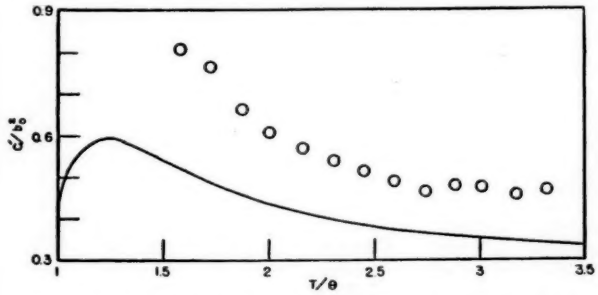

FIG. 1. Plot of C'/b_0^2 against T/θ for krypton. The circles are the observed values, and the curve represents the theoretical values for a Lennard-Jones (6, 12) potential.

where

$$b_0=2\pi N\sigma^3/3,\quad \theta=\epsilon/k, \tag{9}$$

N is Avogadro's number, and k the Boltzmann constant.

From the values of $B(T)$ given in Table II we found by the method of least squares:

$$T^{\frac{1}{4}}B'(T)=0.22419-(131.18/T). \tag{10}$$

The deviations of the values of $T^{\frac{1}{4}}B'(T)$ calculated from this equation from those observed are given in Table III. The representation of the experimental values is quite satisfactory except perhaps at the highest temperature. Comparison of Eqs. (8) and (10) gives the parameters b_0 and θ listed in Table IV. The other parameters of the Lennard-Jones potential in this table are calculated from these two and the usual relations, which are given in the xenon paper.[1] Hirschfelder, Bird, and Spotz[7] find

[5] J. E. Lennard-Jones, Proc. Roy. Soc. (London) **A106**, 463 (1924); R. H. Fowler, *Statistical Mechanics* (Macmillan Company, New York, 1936), Chap. X.

[6] W. H. Stockmayer and J. A. Beattie, J. Chem. Phys. **10**, 476 (1942). For the values of the constants used here see the second paper under reference 1.

[7] Hirschfelder, Bird, and Spotz, Chem. Revs. **44**, 205 (1949).

TABLE II. Second and third virial coefficients of krypton. $pV=RT+(B(T)/V)+(C(T)/V^2)+(D(T)/V^4)$.

Temp. °C (Int.)	$B(T)$ liter²-atmos per mole²	$C(T)$ liter⁴-atmos per mole³	$D(T)\times10^5$ liter⁶-atmos per mole⁴
0	−1.411 1705	+0.06182 4965	−2.653 7449
25	−1.281 0210	0.06387 3404	−3.979 9745
50	−1.134 4024	0.05991 3508	−0.477 4084
75	−1.005 9535	0.05933 1420	+1.120 6558
100	−0.883 8115	0.05951 9458	2.408 3663
125	−0.766 7970	0.06022 4256	3.509 2339
150	−0.653 3492	0.06102 9387	4.689 4233
175	−0.541 6458	0.06139 4739	6.270 7328
200	−0.431 3650	0.06139 5359	8.531 2104
225	−0.343 5068	0.06702 4467	5.609 9322
250	−0.244 4420	0.06974 4884	4.311 8780
275	−0.142 4780	0.07027 2916	6.315 7660
300	−0.054 2743	0.07575 1903	2.645 3185

for krypton $\sigma=3.61$A, $\theta=190$°K from viscosity data, $\theta=169$° from the boiling point and 158° from the critical temperature, and $\sigma=3.96$A from the critical volume.

The expression for the third virial parameter given by classical statistical mechanics has been evaluated for a Lennard-Jones (6, 12) potential by Montroll and Mayer,[8] de Boer and Michels,[9] and Bird, Spotz, and Hirschfelder.[10] The latter give $C'(T)/b_0^2$ to five decimal places over the range in T/θ from 0.70 to 400. These are plotted as the solid curve in Fig. 1. The circles are our values of $C'(T)$ derived from Table II divided by b_0^2 from Table IV.

THE SECOND VIRIAL COEFFICIENT FOR AN EXPONENTIAL REPULSIVE POTENTIAL

If we add a term in r^{-8} for the dipole-quadrupole interaction to the Slater[11] potential, we find for the mutual potential energy $u(r)$ of a pair of molecules:

$$u(r)=ae^{-r/\rho}-br^{-6}(1+cr^{-2}) \tag{11}$$

$$=\epsilon\left[f_1e^{-\alpha(s-1)}-f_2s^{-6}(1+\beta s^{-2})\right], \tag{12}$$

TABLE III. Representation of $T^{\frac{1}{4}}B'(T)$ by Eq. (10).

T °K	$T^{\frac{1}{4}}B'(T)$ (obs.) °K$^{\frac{1}{4}}$-liter/mole	obs.-calc. (in percent)
273.160	−0.255955	+0.04
298.152	−0.217583	−0.82
323.150	−0.181389	+0.21
348.153	−0.152107	+0.33
373.160	−0.126864	+0.39
398.170	−0.104840	+0.42
423.183	−0.085339	+0.54
448.198	−0.067766	+1.09
473.214	−0.051814	+2.35
498.231	−0.039697	−1.48
523.248	−0.027230	−2.60
548.264	−0.015325	−1.59
537.278	−0.005646	−17.80

[8] E. Montroll and J. E. Mayer, J. Chem. Phys. **9**, 626 (1941).

[9] J. de Boer and A. Michels, Physica **6**, 97 (1939).

[10] Bird, Spotz, and Hirschfelder, J. Chem. Phys. **18**, 1395 (1950).

[11] J. C. Slater, Phys. Rev. **32**, 349 (1928).

TABLE IV. Values of the parameters in the Lennard-Jones (6, 12) potential for krypton.

b_0 (cm³ per mole)	58.40
θ (°K)	172.7
$\epsilon\times10^{16}$ (erg)	238.4
σ (A)	3.591
r_0 (A)	4.030
$\mu\times10^{58}$ (erg-cm⁶)	2.044
$\lambda\times10^{102}$ (erg-cm¹²)	0.438
$\theta/T_{critical}$	0.825

where

$$\left.\begin{aligned} &\alpha=\frac{r_0}{\rho},\quad s=\frac{r}{r_0},\quad f_1=\frac{6+8\beta}{\alpha(1+\beta)-6-8\beta},\\ &f_2=\frac{\alpha}{\alpha(1+\beta)-6-8\beta},\\ &\epsilon=\frac{br_0^{-6}}{f_2}=\frac{a}{f_1}e^{-\alpha},\quad \beta=cr_0^{-2},\quad r_0^6=\frac{6b}{a\alpha}e^{\alpha}\left(1+\frac{4}{3}\beta\right). \end{aligned}\right\} \quad (13)$$

Here ϵ is the depth of the potential well and r_0 the separation of a pair of molecules at the minimum potential. The function (11) depends on the four parameters which may be taken as a, b, c, ρ or β, α, ϵ, r_0.

Kane[12] has evaluated the constants a/b, b, and bc of Eq. (11) from the lattice distances and heat of sublimation of solid krypton on the basis of two assumptions for ρ: $\rho=0.345$A taken from the calculations of Born and Mayer[13] for alkali halide crystals, and $\rho=0.2091$A from those of Bleick and Mayer[14] for neon atoms. For the first value of ρ he gives two sets of parameters, for one of which c (or β) is taken to be zero; for the second value of ρ he gives only one set of values in which c is taken to be zero. These are listed in Table V together with the other parameters that can be computed from these values. The values of r_0 and ϵ do not deviate too far from those for the Lennard-Jones potential derived from our experimentally determined second virial coefficients.

TABLE V. Values of the parameters of Eqs. (12) and (13) for krypton given by Kane.

		% deviation[a]		% deviation[a]		% deviation[a]
ρ (A)	0.345[b]		0.345[b]		0.2091[b]	
$(a/b)\times10^{-48}$ (cm⁻⁶)	15.0		18.7		14,700	
$b\times10^{60}$ (erg-cm⁶)	209		190		148	
$bc\times10^{76}$ (erg-cm⁸)	0		587		0	
r_0 (A)	4.0775	−1.2	4.0767	−1.2	3.9813	+1.2
β	0		0.1859		0	
$\epsilon\times10^{16}$ (erg)	223.9	+6.1	228.6	+4.1	254.5	−6.8
θ (°K)	162.2		165.6		184.4	
α	11.819		11.817		19.040	

[a] From the values of Table IV.
[b] Assumed.

[12] G. Kane, J. Chem. Phys. **7**, 603 (1939).
[13] M. Born and J. E. Mayer, Z. Physik **75**, 1 (1932).
[14] W. E. Bleick and J. E. Mayer, J. Chem. Phys. **2**, 252 (1934).

Buckingham and Corner[15] have tabulated values of the function $B'(T)/2\pi Nr_0^3$ derived from the potential (11) for $s\geq1$. For $s<1$ they multiply the last term by $\exp[-4(s^{-1}-1)^3]$ which need not concern us here. They also include a correction for quantum effects which can be neglected for krypton above 0°C. Two tables are given: In one the function is given for $\beta=0$, $\alpha=12$ to $\alpha=14$ in steps of 0.5, and various values of $x(=\epsilon/kT)$; in the other the function is listed for $\beta=0.2$ and the same values of α and x. In the first table we extrapolated each line of constant x to $\alpha=11.819$, and in both tables to $\alpha=11.817$. From these we interpolated the function with the proper value of θ given in Table V to the values of x corresponding to our measured temperatures as given in Table VI. The values of $B'(T)$ so obtained for $\beta=0$ are listed in the third column of Table VI; those for $\beta=0.1859$ are in the fifth column. The differences of these values of $B'(T)$, which were computed from

TABLE VI. Comparison of the values of the second virial coefficients calculated from Buckingham and Corner's tables and Kane's values of r_0, α, ϵ/k, and β with the observed values.

T°K	B'(T) (obs.) liter/mole	B'(T) (calc.), liter/mole β=0		β=0.1859	
			obs.-calc.		obs.-calc.
273.160	−0.0630	−0.0656	+0.0026	−0.0649	+0.0019
298.152	−0.0524	−0.0549	0.0025	−0.0541	0.0017
323.150	−0.0428	−0.0461	0.0033	−0.0454	0.0026
348.153	−0.0352	−0.0387	0.0035	−0.0380	0.0028
373.160	−0.0289	−0.0325	0.0036	−0.0318	0.0029
398.170	−0.0235	−0.0272	0.0037	−0.0265	0.0030
423.183	−0.0188	−0.0226	0.0038	−0.0219	0.0031
448.198	−0.0147	−0.0186	0.0039	−0.0179	0.0032
473.214	−0.0111	−0.0151	0.0040	−0.0144	0.0033
498.231	−0.0084	−0.0120	0.0036	−0.0113	0.0029
523.248	−0.0057	−0.0092	0.0035	−0.0086	0.0029
548.264	−0.0032	−0.0067	0.0035	−0.0061	0.0029
573.278	−0.0012	−0.0045	0.0033	−0.0039	0.0027

Kane's parameters, from those experimentally determined are also given. The differences of both sets of calculated values from those measured are always positive and roughly by a constant amount in each case. The same comparison for xenon gave about the same deviations (in absolute amount) above 75°C, but the calculated values crossed those observed at about 35°C.

The tables of Buckingham and Corner could not be extrapolated to $\alpha=19.040$ corresponding to Kane's calculations for $\rho=0.2091$A.

We are grateful to the Linde Air Products Company for a Grant-in-Aid that made this work possible. We are also indebted to the Company and to Dr. J. M. Gaines and Dr. R. J. Gillette for the gift of the krypton and for the analyses of the sample. We wish to express our appreciation of the continued interest and the many valuable suggestions of Professor W. H. Stockmayer and Professor I. Amdur.

[15] R. A. Buckingham and J. Corner, Proc. Roy. Soc. (London) **A189**, 118 (1947).

The Compressibility of and an Equation of State for Gaseous Neopentane

JAMES A. BEATTIE, DONALD R. DOUSLIN, AND SAMUEL W. LEVINE
Department of Chemistry, Massachusetts Institute of Technology, Cambridge, Massachusetts

(Received June 16, 1952)

The compressibility of gaseous neopentane (2-2-dimethyl propane) has been measured from 160.60°, the critical temperature, to 275° over a density range from 1 to 7 mole per liter, the maximum pressure being about 300 atmos. The constants of the Beattie-Bridgeman equation of state for the gas phase are $R=0.08206$, $A_0=23.3300$, $a=0.15174$, $B_0=0.33560$, $b=0.13358$, $c=400\times10^4$ in units of normal atmos, liter per mole, °K(T°K$=t$°C$+273.13$), the molecular weight being taken as 72.0924 g per mole. The second virial coefficients were determined graphically at each temperature.

THE compressibilities of a number of gaseous hydrocarbons have been studied in this laboratory.[1] Neopentane $C(CH_3)_4$ is of interest because of its symmetrical structure. The experimental method used has been published[2] earlier. For neopentane the bomb with a glass liner was employed.

TABLE I. Values of the constants of the Beattie-Bridgeman equation of state for gaseous neopentane (2-2-dimethyl propane).

$$p=[RT(1-\epsilon)/V^2][V+B]-A/V^2$$
$$A=A_0(1-a/V)$$
$$B=B_0(1-b/V)$$
$$\epsilon=c/VT^3$$

Units: normal atmospheres, liter per mole, °K (T°K$=t$°C$+273.13$°).

$R=0.08206$	$b=0.13358$
$A_0=23.3300$	$c=400\times10^4$
$a=0.15174$	Mol. wt.$=72.0924$
$B_0=0.33560$	

The sample of neopentane was the same used for a study of the vapor pressure and critical constants[3] and was supplied through the courtesy of Dr. Frederick D. Rossini. It was a sample of API–NBS hydrocarbon made available by the American Petroleum Institute and the U. S. National Bureau of Standards through the API Research Project 44, and purified by the API Research Project 6 from materials supplied by the California Research Corporation. The stated purity was 99.982±0.012 mole percent neopentane. The behavior of the substance in the vapor pressure runs indicated that it was of high purity.

The weight of the sample used in the compressibility measurements was 7.04873 g, while the internal volume of the glass liner was about 120 ml. After the completion of the measurements of the compressibility at each temperature, the pressure at the lowest density—1 mole per liter—was repeated. In no case did this pressure vary

TABLE II. Comparison of the pressures calculated from the equation of state with the observed pressures for gaseous neopentane (C_5H_{12}). For each temperature the first line gives the observed pressure in normal atmospheres and the second gives the observed minus the calculated pressure. The calculated pressures are computed from the equation given in Table I. The critical constants of neopentane are $t_c=160.60$°C (Int.), $p_c=31.57$ normal atmosphere, $v_c=0.303$ liter/mole, $d_c=3.30$ mole/liter.

Density, mole/liter Temp., °C (Int.)		1.0	1.5	2.0	2.5	3.0	3.5	4.0	4.5	5.0	6.0	7.0
		Pressure, normal atmosphere										
160.60	obsd.	23.73	28.73	30.84	31.48	31.56	31.58	31.73	33.12	38.56	85.36	258.30
	obsd.-calcd.	−0.17	−0.10	+0.06	+0.28	+0.07						
175	obsd.	25.46	31.62	35.13	37.12	38.46	39.70	41.77	46.03	55.45	114.62	297.92
	obsd.-calcd.	−0.11	−0.05	+0.16	+0.23	−0.45						
200	obsd.	28.35	36.51	42.25	46.59	50.43	54.63	60.38	69.68	85.78	165.35	
	obsd.-calcd.	−0.08	0.00	+0.15	+0.07	−0.77						
225	obsd.	31.21	41.29	49.18	55.92	62.44	69.85	79.60	94.10	117.24	217.08	
	obsd.-calcd.	−0.06	+0.01	+0.11	0.00	−0.70						
250	obsd.	33.96	45.90	55.95	65.11	74.43	85.15	99.10	118.84	149.00	268.83	
	obsd.-calcd.	−0.11	−0.08	+0.02	+0.01	−0.36						
275	obsd.	36.71	50.49	62.65	74.25	86.41	100.58	118.85	144.02	181.08	320.93	
	obsd.-calcd.	−0.15	−0.15	−0.04	+0.10	+0.21						
Ave. deviation (atmos)		0.11	0.06	0.09	0.12	0.43						
Ave. percent deviation		0.39	0.17	0.22	0.30	0.78						

Total average deviation (atmos) 0.16 Total average percent deviation 0.37

[1] For the last reports on this work see Beattie, Marple, and Edwards, J. Chem. Phys. **18**, 127 (1950); J. A. Beattie and S. Marple, Jr., J. Am. Chem. Soc. **72**, 4143 (1950).
[2] J. A. Beattie, Proc. Am. Acad. Arts Sci. **69**, 389 (1934).
[3] Beattie, Douslin, and Levine, J. Chem. Phys. **19**, 948 (1951).

TABLE III. Second virial coefficients of neopentane.

t, °C (Int.)	$B_V = \lim_{1/V \to 0} V[(pV/RT)-1]$, B_V, liter/mole
160.60	−0.383
175	−0.354
200	−0.312
225	−0.273
250	−0.243
275	−0.216

from that measured at the beginning of the series of runs by more than 0.006 atmos, the average difference being 0.002 atmos. This indicates that no decomposition occurred even at 275°, where the pressure measured after the runs was 0.002 atmos less than that measured at the beginning.

RESULTS

The observed pressures for a series of densities from 1 to 7 mole per liter and from 160.60°, the critical temperature, to 275° are listed in Table II together with the deviations of the pressure calculated from the equation of state given in Table I from the measured values. The constants of the equation were determined from the values below the critical density which is 3.30 mole per liter. The average deviation of the calculated from the observed pressure is 0.16 atmos or 0.37 percent.

The molecular weight of neopentane was taken to be 72.0924 (H=1.0077, C=12.000) for the purpose of computing the compressor settings to obtain a desired gas density (in mole per liter), and the Kelvin temperature of the ice point was taken to be 273.13 (rather than 273.16) for the purpose of determining the constants of the equation of state. These values were used in conformity with those employed in the earlier work on hydrocarbons which extends back more than 20 years.

The second virial coefficient B_V of neopentane in the equation $pV=RT[1+(B_V/V)+(C_V/V^2)+\cdots]$ was determined graphically at each temperature from plots of $V[(pV/RT)-1]$ against $1/V$. These are listed in Table III.

We are very grateful to the United States Rubber Company for a fellowship held by one of us (D.R.D.).

THE JOURNAL OF CHEMICAL PHYSICS VOLUME 20, NUMBER 10 OCTOBER, 1952

Intermolecular Potentials for the Systems CO_2-CO_2 and CO_2-N_2O

I. AMDUR, J. ROSS, AND E. A. MASON
Department of Chemistry, Massachusetts Institute of Technology, Cambridge, Massachusetts

(Received April 21, 1952)

Experimental values of self-diffusion and mutual diffusion coefficients, in the range −78° to 90°C, have been used to determine the intermolecular potentials for the systems CO_2-CO_2 and CO_2-N_2O. It has been assumed that a spherically symmetric potential of the form $V(r)=4\epsilon[(\sigma/r)^{12}-(\sigma/r)^6]$ may be used and that the dynamics of the diffusion process are adequately described by the classical Chapman-Enskog transport relations, which consider only elastic, binary collisions.

The potential parameters derived from diffusion measurements have been compared with those obtained from measurements of viscosity, compressibility, the critical temperature, and the critical volume. It was not possible, for either system, to obtain a single set of parameters which could satisfactorily reproduce all the gaseous properties. It has been concluded that, for the present systems, the failure is due to one or both of the following: (1) inadequacy of the assumed potential form, (2) importance of inelastic collisions.

EXPERIMENTAL values have been reported[1] for the self-diffusion coefficient of CO_2 and the mutual diffusion coefficient of the system CO_2-N_2O in the temperature range −78° to 90°C. Results of this type may be used to obtain information concerning intermolecular forces for the systems CO_2-CO_2 and CO_2-N_2O. Such information is helpful in understanding a variety of properties of these systems in the gaseous, liquid, and solid states.

The relation between the diffusion coefficient for a binary system and the intermolecular potential has been investigated by Enskog[2] and by Chapman,[3] who obtained the expression

$$D=\frac{3}{16}\left(\frac{2\pi kT}{\mu}\right)^{\frac{1}{2}}\frac{1}{nQ_D(1-\Delta)}, \quad (1)$$

where D is the diffusion coefficient, k the Boltzmann constant, T the absolute temperature, μ the reduced mass, n the total molecular density, and Δ a second-order correction term which can be calculated from collision theory. (For the potential model used in the present case, Δ increases from 2×10^{-4} to 3×10^{-3} between −78° and 90°C.) Q_D is the temperature dependent cross section for diffusion for molecules of a Maxwellian gas and is defined by

$$Q_D=2\left(\frac{\mu}{2kT}\right)^3\int_0^\infty v^5 S_D \exp\left(-\frac{\mu v^2}{2kT}\right)dv, \quad (2)$$

[1] Amdur, Irvine, Mason, and Ross, J. Chem. Phys. **20**, 436 (1952).
[2] D. Enskog, Inaug. Diss. Upsala (1917).
[3] S. Chapman, Phil. Trans. Roy. Soc. (London) **A211**, 433 (1912); **A216**, 279 (1916); **A217**, 115 (1917).

where v is the absolute value of the relative initial velocity of a pair of molecules whose collision is under consideration. S_D is the velocity dependent cross section for diffusion and is given by

$$S_D=2\pi\int_0^\infty[1-\cos\theta(v,b)]bdb, \tag{3}$$

where b, the collision parameter, is the perpendicular distance between one of the molecules and the initial line of relative approach of the other. The angle $\theta(v,b)$, through which the relative initial velocity vector is rotated by the collision, may be expressed by[4]

$$\theta(v,b)=\pi-2b\int_{r_0}^\infty\frac{dr}{r\{[1-(2V(r)/\mu v^2)]r^2-b^2\}^{\frac{1}{2}}}, \tag{4}$$

where $V(r)$ is the potential energy of the molecules at the separation distance r, and r_0 is the distance of closest approach, which may be defined by the relation

$$\left(1-\frac{2V(r_0)}{\mu v^2}\right)r_0^2=b^2. \tag{5}$$

Equations (1)–(5) are strictly applicable only when the following conditions are fulfilled: (1) The effects of ternary and higher order collisions must be negligible; (2) the binary collisions must be elastic; (3) the potential $V(r)$ must be spherically symmetric; and (4) classical mechanics must be capable of representing the dynamics of the collision process. The extent to which the equations do not apply when these conditions are not met is not yet known.

The procedure for calculating the intermolecular potential from experimental values of the diffusion coefficient requires the assumption of an analytical form for $V(r)$ in order to calculate Q_D as a function of temperature and the parameters of the potential. Final numerical values of the parameters are determined from comparisons of these calculated values of Q_D with those obtained through Eq. (1) from observed values of D.

Since the exact calculation of Q_D usually requires extensive numerical integrations, relatively few potential forms have been thoroughly investigated. The four parameter potential

$$V(r)=p/r^s-q/r^t, \tag{6}$$

which was first used by Lennard-Jones[5] in calculating viscosity coefficients, has probably been studied more than any other. Kihara and Kotani,[6] and Hirschfelder, Bird, and Spotz[7] have independently evaluated the integrals in Eqs. (2) and (3) for a form of the Lennard-Jones potential, which may be written as

$$V(r)=4\epsilon[(\sigma/r)^{12}-(\sigma/r)^6], \tag{7}$$

where σ is the value of r for which $V(r)$ is zero, and $-\epsilon$ is the minimum potential energy. These two investigations, which are the most extensive to date for this potential, are in excellent agreement.[8] For the present calculations, it was decided to use the results of Hirschfelder and his co-workers, who have tabulated a dimensionless quantity which they designate $W^{(l)}(n;x)$. This quantity is used to obtain values of the temperature dependent cross section for a particular transport property or for a second-order correction term, such as Δ in Eq. (1), since the indices l and n are those appearing in generalized expressions for S and Q, which may be written

$$S=2\pi\int_0^\infty[1-\cos^l\theta(v,b)]bdb \tag{8}$$

and

$$Q=2\left(\frac{\mu}{2kT}\right)^{n+2}\int_0^\infty v^{2n+3}S\exp-\left(\frac{\mu v^2}{2kT}\right)dv. \tag{9}$$

Thus, for the case of diffusion, $l=n=1$, and $W^{(l)}(n;x)$ becomes $W^{(1)}(1;x)$, which is defined as

$$W^{(1)}(1;x)=Q_D/2\pi\sigma^2, \tag{10}$$

where

$$x=\epsilon/(kT). \tag{11}$$

Various methods may be used to obtain numerical values of σ and ϵ from observed values of D. The present procedure is similar to that used by Buckingham[9] in deriving potential energy information from second virial coefficients. If Q_D in Eq. (1) is replaced by $2\pi\sigma^2W^{(1)}(1;x)$, a function X may be defined as

$$X=\log\sigma^2=-\log[16/3(2\pi\mu/kT)^{\frac{1}{2}}nD]-\log(1-\Delta)W^{(1)}(1;x). \tag{12}$$

From Eq. (11) a second function Y may be defined as

$$Y=\log(\epsilon/k)=\log x+\log T. \tag{13}$$

For every pair of observed values of D and T, a curve of X *vs* Y is obtained by introducing a number of values of $\log(1-\Delta)W^{(1)}(1;x)$ and $\log x$ into Eqs. (12) and (13). Two such curves should intersect at those values of $\log\sigma^2$ and $\log(\epsilon/k)$ which, through Eqs. (10) and (1), are capable of reproducing the two measured values of D. The degree of localization of all such intersections is an indication of the suitability of Eq. (7) as an analytical representation of the potential energy.

The $X-Y$ plots for the systems CO_2-CO_2 and CO_2-N_2O are shown in Fig. 1. Although the intersections are not particularly well localized, it is possible to obtain mean values of σ and ϵ, which agree with those

[4] E. H. Kennard, *Kinetic Theory of Gases* (McGraw-Hill Book Company, Inc., New York, 1938), pp. 115–122.
[5] J. E. Lennard-Jones, Proc. Roy. Soc. (London) **A106**, 441 (1924).
[6] T. Kihara and M. Kotani, Proc. Phys.Math. Soc. Japan **25**, 602 (1943).
[7] Hirschfelder, Bird, and Spotz, J. Chem. Phys. **16**, 968 (1948).
[8] Hirschfelder, Bird, and Spotz, J. Chem. Phys. **17**, 1343 (1949).
[9] R. A. Buckingham, Proc. Roy. Soc. (London) **A168**, 264 (1938).

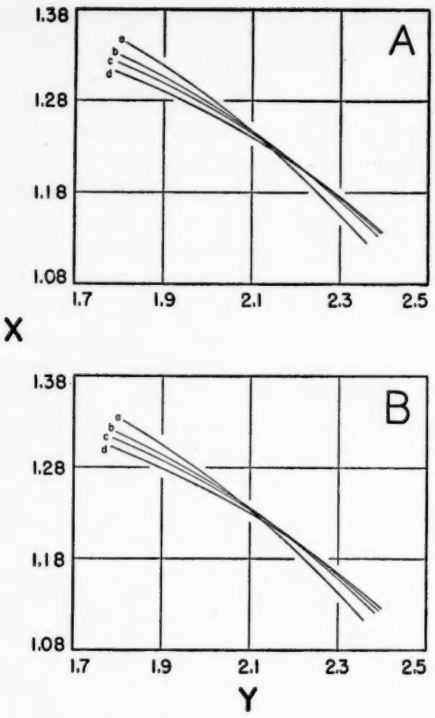

FIG. 1. Graphical determination of potential parameters: A. CO_2-CO_2; B. CO_2-N_2O. Curves *a*, *b*, *c*, and *d* refer to 194.8°, 273.2°, 312.8°, and 362.6°K, respectively.

calculated by an alternative method[10] and which are capable of reproducing the observed values of D within the estimated accuracy of 1.5 percent. The results are summarized in Table I which gives the mean values of the potential parameters (according to the usual practice, values of ϵ/k, rather than ϵ, are given), the experimental values of D which were used for the curves in Fig. 1, values of D calculated from Eqs. (10) and (1), and the percentage deviations between the observed and calculated values. In so far as the potential form of Eq. (7) and the relations given in Eqs. (1)–(5) are suitable for the system CO_2-CO_2, the parameters $\sigma=4.07$A and $\epsilon/k=150$°K, appear to be well established. For example, the diffusion coefficients obtained by Winn[11] for this system over a comparable range of temperature, lead to values of $\sigma=4.09$A and $\epsilon/k=153$°K.

[10] If Q_D is replaced by $2\pi\sigma^2 W^{(1)}(1;x)$, Eq. (1) may be transformed into

$$\log\left[\frac{16}{3}\left(\frac{2\pi\mu}{kT}\right)^{\frac{1}{2}}nD\right]=-\log(1-\Delta)W^{(1)}(1;x)-2\log\sigma.$$

Similarly, Eq. (11) may be transformed into

$$\log T=-\log x+\log(\epsilon/k).$$

Thus, a plot of the experimentally known quantities

$$\log\left[\frac{16}{3}\left(\frac{2\pi\mu}{kT}\right)^{\frac{1}{2}}nD\right]$$

and $\log T$ should be superposable on a plot of the tabulated quantities $-\log(1-\Delta)W^{(1)}(1;x)$ and $-\log x$ by a translation of axes if Eq. (7) is a proper representation of the potential. The amount of translation parallel to the axes determines $-2\log\sigma$ and $\log(\epsilon/k)$.

[11] E. B. Winn, Phys. Rev. **80**, 1024 (1950).

MacCormack and Schneider[12] have recently reviewed the potential energy information for the system CO_2-CO_2, which has been obtained from measurements of viscosity,[7,13] second[12] and third[14,15] virial coefficients, and the critical temperature and volume.[16,17] For the system CO_2-N_2O there are few accurate measurements of transport properties or compressibilities of the binary mixture over an adequate range of composition, temperature, or pressure. Accordingly, except for the values of σ and ϵ/k obtained directly from the mutual diffusion coefficients in Table I, it is necessary to combine potential parameters obtained from experimental results on pure CO_2 and pure N_2O to obtain parameters for the intermolecular potential between CO_2 and N_2O. The usual combination procedure,[18] which is semi-empirical in character, uses the arithmetic mean of the σ values and the geometric mean of the ϵ/k values from the systems of like molecules to obtain the parameters for the unlike molecule system. It is possible, in this way, to derive potential energy information for the system CO_2-N_2O, from experimental values of the coefficient of viscosity,[13] and of the second virial coefficients[7,12] of CO_2 and N_2O. For the two systems of present interest, values of σ and ϵ/k from various sources are given in Table II.

The agreement among the sets of parameters in Table II is not considered satisfactory. For example, for the system CO_2-CO_2, if the values of σ and ϵ/k obtained from self-diffusion are used to predict the other properties, it is not possible to obtain agreement between calculated and observed values. Calculated viscosities average 6 percent greater than measured values which are known to at least 0.8 percent, and calculated second virial coefficients are between 44.8 and 77.8 cc/mole greater than values derived from compressibility measurements −71.85 to −145.0 cc/mole.

TABLE I. Comparison between calculated and observed diffusion coefficients.

	A. The system CO_2-CO_2 $\sigma=4.07$A, $\epsilon/k=150$°K			B. The system CO_2-N_2O $\sigma=4.02$A, $\epsilon/k=150$°K		
T, °K	D, cm²/sec (obs.)	D, cm²/sec (calc.)	Percent deviation	D, cm²/sec (obs.)	D, cm²/sec (calc.)	Percent deviation
194.8	0.0516	0.0511	+1.0	0.0531	0.0524	+1.3
273.2	0.0970	0.0973	−0.3	0.0996	0.0997	−0.1
312.8	0.1248	0.1251	−0.2	0.1280	0.1282	−0.2
362.6	0.1644	0.1639	+0.3	0.1683	0.1680	+0.2

[12] K. E. MacCormack and W. G. Schneider, J. Chem. Phys. **19**, 849 (1951).

[13] H. L. Johnston and K. E. McCloskey, J. Phys. Chem. **44**, 1038 (1939).

[14] Bird, Spotz, and Hirschfelder, J. Chem. Phys. **18**, 1395 (1950).

[15] Michels, Michels, and Wouters, Proc. Roy. Soc. (London) **A153**, 214 (1935); A. Michels and C. Michels, Proc. Roy. Soc. (London) **A160**, 348 (1937).

[16] Wentorf, Buehler, Hirschfelder, and Curtiss, J. Chem. Phys. **18**, 1484 (1950).

[17] Michels, Blaisse, and Michels, Proc. Roy. Soc. (London) **A160**, 358 (1937).

[18] Hirschfelder, Bird, and Spotz, Chem. Revs. **44**, 205 (1949); Trans. Am. Soc. Mech. Engrs. **71**, 921 (1949).

In the case of third virial coefficients, calculated values are 0.60 to 0.67 of experimental values. Finally, calculated values of the critical temperature and volume of CO_2 are 114 degrees smaller and 31 cc/mole greater than the corresponding measured quantities. When the calculation procedure is reversed, that is, when values of σ and ϵ/k from viscosity, virial coefficients, and critical temperature and volume, are used to calculate self-diffusion coefficients, the average percentage deviations between observed and calculated coefficients have the following values: 5.9 (viscosity); 24.2 (second virial coefficients, 0°–200°C); 4.2 (second virial coefficients, 300°–600°C); 16.4 (third virial coefficients); and 1.9 (critical temperature and volume). The good agreement in the case of the self-diffusion coefficients calculated with σ and ϵ/k values obtained from the critical temperature and volume must be considered fortuitous in view of the highly empirical and approximate nature of the relations between these critical constants and the parameters of the potential.

For the system CO_2-N_2O, measured viscosities of the pure components and of mixtures are equal to within about 0.5 percent above room temperature. Below room temperature only measurements on the pure components are available, and these differ by only 1.8 percent at the lowest temperature, 190°K. In the case of compressibility, there appears to be no experimental measurements on mixtures which can be used to calculate reliable second virial coefficients. However, in view of the viscosity results and the isostere character of the system, it should be safe to assume that second virial coefficients for the mixture would be equal to those for CO_2 within a percent or so, in the range of temperature of present interest. Accordingly, the values of σ and ϵ/k derived from mutual diffusion coefficients will be used to calculate viscosities and second virial coefficients, and these values will be compared with the corresponding experimental values for CO_2 for the purpose of judging the adequacy of the parameters. The agreement is poor, since the calculated viscosities average 8 percent greater than the measured values and the calculated second virial coefficients are between 45.8 and 80.2 cc/mole greater than the values obtained from experiment. When the σ and ϵ/k values, obtained by combining parameters for the systems CO_2-CO_2 and N_2O-N_2O, are used to calculate mutual diffusion coefficients, the average percentage deviation between observed and calculated values are 8.2 (viscosity) and 28.1 (second virial coefficients).

MacCormack and Schneider[12] have postulated the existence of binary association in order to account for the fact that it was necessary to use two different sets of potential parameters to reproduce their experimental virial coefficients for CO_2 over the complete range of temperature, 0° to 600°C. Since association of the labeled molecules with normal molecules could result in anomalous diffusion coefficients in experiments involving radioactive tracers, the effect of such association on D was investigated. From the theory of diffusion in multicomponent systems[19] and the degree of association given by MacCormack and Schneider, it is possible to show that the maximum uncertainty in the experimental diffusion coefficients which can be attributed to association is less than 0.5 percent. It would appear, therefore, that there are other reasons why a single set of σ and ϵ/k values cannot reproduce, within the experimental limits, all the gas properties of the present system over an appreciable range of temperature.

TABLE II. Values of σ and ϵ/k from various sources.

Source	A. The system, CO_2-CO_2 σ, A	A. The system, CO_2-CO_2 ϵ/k, °K	B. The system, CO_2-N_2O σ, A	B. The system, CO_2-N_2O ϵ/k, °K
Diffusion	4.07	150	4.02	150
Viscosity	4.00	190	3.94	204
Second virial coefficient	4.47[a] 3.91[b]	187.5[a] 203.3[b]	4.53	188
Third virial coefficient	4.11	221		
Critical temperature and volume	3.70	240.3		

[a] From measurements between 0° and 200°C.
[b] From measurements between 300° and 600°C.

The failure might be due to the fact that the potential energy function represented by Eq. (7) may be inadequate in form. For example, the use of an inverse power in the repulsion term, and the assumption of a central force field may not be completely justified. Further, the Chapman-Enskog relations, in addition to requiring spherically symmetrical force fields, apply only to systems where all the collisions of interest are elastic. It is doubtful whether either of these conditions are satisfactorily fulfilled for the CO_2-CO_2 and CO_2-N_2O systems. Until such time as additional experimental or theoretical information indicates the proper form of the potential, or of the transport relations for systems of polyatomic gases, it would seem desirable to consider the form of Eq. (7) as useful for the representation of any one property over a limited range of temperature.[20]

[19] C. F. Curtiss and J. O. Hirschfelder, J. Chem. Phys. **17**, 550 (1949).

[20] Other potential models which are physically less plausible, however, may serve nearly as well for this purpose. For example, the van der Waals model, hard spheres with forces of attraction, which Kihara and Kotani preferred for the viscosity of N_2 and of CH_4, can be used to reproduce the present diffusion results within ±2 percent. The parameters which must be used, however, are quite unrealistic as evidenced by abnormally deep minima in the potential energy functions.

Tables of the Lennard-Jones and Devonshire Equation of State at High Temperatures and Densities

W. FICKETT AND WM. W. WOOD
Los Alamos Scientific Laboratory, Los Alamos, New Mexico

(Received April 28, 1952)

The Lennard-Jones and Devonshire equation of state is computed for the following ranges of the reduced variables: temperature, kT/ϵ^*, 20 to 150 in steps of 10; volume, v/v^*, 0.3 to 0.7 in steps of 0.05 and 0.7 to 1.3 in steps of 0.1.

AN attempt is under way at this laboratory to develop a theoretical equation of state applicable to the products of detonation in a solid explosive. A free volume equation of state for mixtures has recently been given by Prigogine and Garikian.[1] Kirkwood's recent statistical mechanical derivation of the free volume equation of state[2] has made it possible to obtain their result as a first approximation in a more rigorous treatment.[3] The use of this mixture equation of state requires a tabulation of the Lennard-Jones and Devonshire (LJD) equation of state in the region of interest.

The LJD equation of state has been presented in tabular form by Wentorf *et al.*[4] These tables are not sufficient for our purposes for two reasons: they do not extend to sufficiently low values of the reduced volume, and the intervals in both reduced temperature and reduced volume are unsatisfactory for interpolation in the region of interest to us.

Accordingly, we have prepared a tabulation of the equation of state which extends to lower reduced

TABLE I. A tabulation of G.

θ \ τ	0.30	0.35	0.40	0.45	0.50
20	1.3974 (−5)	3.5436 (−5)	7.8929 (−5)	1.5865 (−4)	2.9305 (−4)
30	2.5404 (−5)	6.3853 (−5)	1.4045 (−4)	2.7771 (−4)	5.0264 (−4)
40	3.8708 (−5)	9.6496 (−5)	2.0983 (−4)	4.0887 (−4)	7.2740 (−4)
50	5.3540 (−5)	1.3245 (−4)	2.8498 (−4)	5.4811 (−4)	9.6080 (−4)
60	6.9688 (−5)	1.7110 (−4)	3.6454 (−4)	6.9284 (−4)	1.19891(−3)
70	8.6961 (−5)	2.1199 (−4)	4.4753 (−4)	8.4152 (−4)	1.43935(−3)
80	1.0522 (−4)	2.5478 (−4)	5.3326 (−4)	9.9289 (−4)	1.68059(−3)
90	1.2437 (−4)	2.9919 (−4)	6.2108 (−4)	1.14608(−3)	1.92159(−3)
100	1.4432 (−4)	3.4500 (−4)	7.1075 (−4)	1.30046(−3)	2.1612 (−3)
110	1.6498 (−4)	3.9203 (−4)	8.0182 (−4)	1.45555(−3)	2.3997 (−3)
120	1.8630 (−4)	4.4012 (−4)	8.9403 (−4)	1.61097(−3)	2.6362 (−3)
130	2.0821 (−4)	4.8914 (−4)	9.8713 (−4)	1.76643(−3)	2.8707 (−3)
140	2.3067 (−4)	5.3898 (−4)	1.08095(−3)	1.92172(−3)	3.1029 (−3)
150	2.5362 (−4)	5.8953 (−4)	1.17533(−3)	2.07666(−3)	3.3327 (−3)

θ \ τ	0.55	0.60	0.65	0.70	0.80
20	5.0377 (−4)	8.1403 (−4)	1.24644(−3)	1.8205 (−3)	3.4501 (−3)
30	8.4415 (−4)	1.32997(−3)	1.98348(−3)	2.8203 (−3)	5.0760 (−3)
40	1.19892(−3)	1.85204(−3)	2.7068 (−3)	3.7754 (−3)	6.5537 (−3)
50	1.55874(−3)	2.3690 (−3)	3.4085 (−3)	4.6825 (−3)	7.9083 (−3)
60	1.91891(−3)	2.8770 (−3)	4.0857 (−3)	5.5442 (−3)	9.1606 (−3)
70	2.2762 (−3)	3.3738 (−3)	4.7385 (−3)	6.3641 (−3)	1.03269(−2)
80	2.6299 (−3)	3.8586 (−3)	5.3679 (−3)	7.1462 (−3)	1.14198(−2)
90	2.9787 (−3)	4.3313 (−3)	5.9753 (−3)	7.8941 (−3)	1.24492(−2)
100	3.3222 (−3)	4.7920 (−3)	6.56201(−3)	8.6107 (−3)	1.34231(−2)
110	3.6602 (−3)	5.2412 (−3)	7.12946(−3)	9.2991 (−3)	1.43481(−2)
120	3.9924 (−3)	5.6793 (−3)	7.67894(−3)	9.9615 (−3)	1.52294(−2)
130	4.3191 (−3)	6.1068 (−3)	8.21164(−3)	1.06001(−2)	1.60715(−2)
140	4.6401 (−3)	6.5241 (−3)	8.72865(−3)	1.12168(−2)	1.68783(−2)
150	4.9556 (−3)	6.9317 (−3)	9.23098(−3)	1.18133(−2)	1.76529(−2)

θ \ τ	0.90	1.00	1.10	1.20	1.30
20	5.7596 (−3)	8.72641(−3)	1.22723(−2)	1.62921(−2)	2.06759(−2)
30	8.0889 (−3)	1.17704(−2)	1.59936(−2)	2.06249(−2)	2.55424(−2)
40	1.01207(−2)	1.43411(−2)	1.90591(−2)	2.41280(−2)	2.94228(−2)
50	1.19315(−2)	1.65830(−2)	2.16889(−2)	2.70963(−2)	3.26809(−2)
60	1.35709(−2)	1.85805(−2)	2.40040(−2)	2.96860(−2)	3.55046(−2)
70	1.50726(−2)	2.03877(−2)	2.60793(−2)	3.19914(−2)	3.80053(−2)
80	1.64611(−2)	2.20419(−2)	2.79646(−2)	3.40741(−2)	4.02550(−2)
90	1.77543(−2)	2.35698(−2)	2.96952(−2)	3.59770(−2)	4.23034(−2)
100	1.89661(−2)	2.49913(−2)	3.12969(−2)	3.77313(−2)	4.41861(−2)
110	2.01075(−2)	2.63220(−2)	3.27894(−2)	3.93603(−2)	4.59299(−2)
120	2.11870(−2)	2.75739(−2)	3.41879(−2)	4.08823(−2)	4.75552(−2)
130	2.22120(−2)	2.87568(−2)	3.55046(−2)	4.23114(−2)	4.90782(−2)
140	2.31881(−2)	2.98787(−2)	3.67494(−2)	4.36592(−2)	5.05117(−2)
150	2.41205(−2)	3.09460(−2)	3.79304(−2)	4.49352(−2)	5.18662(−2)

Note: The number in parentheses is the power of 10 by which the entry is to be multiplied.

TABLE II. A tabulation of g_L.

θ \ τ	0.30	0.35	0.40	0.45	0.50
20	2.915 (−7)	1.3736 (−6)	5.2184 (−6)	1.6717 (−5)	4.6548 (−5)
30	7.890 (−7)	3.6668 (−6)	1.3653 (−5)	4.2604 (−5)	1.1501 (−4)
40	1.5919 (−6)	7.3004 (−6)	2.6693 (−5)	8.1459 (−5)	2.1441 (−4)
50	2.7353 (−6)	1.23844(−5)	4.4543 (−5)	1.3329 (−4)	3.4339 (−4)
60	4.2442 (−6)	1.89891(−5)	6.7288 (−5)	1.9791 (−4)	5.0042 (−4)
70	6.1402 (−6)	2.7177 (−5)	9.4943 (−5)	2.7491 (−4)	6.8395 (−4)
80	8.4400 (−6)	3.6964 (−5)	1.2748 (−4)	3.6393 (−4)	8.9258 (−4)
90	1.1157 (−5)	4.8375 (−5)	1.6487 (−4)	4.6455 (−4)	1.1250 (−3)
100	1.4306 (−5)	6.1422 (−5)	2.0699 (−4)	5.7638 (−4)	1.3786 (−3)
110	1.7888 (−5)	7.6108 (−5)	2.5380 (−4)	6.9901 (−4)	1.6540 (−3)
120	2.1915 (−5)	9.2432 (−5)	3.0519 (−4)	8.3210 (−4)	1.9493 (−3)
130	2.6392 (−5)	1.10388(−4)	3.6108 (−4)	9.7527 (−4)	2.2637 (−3)
140	3.1324 (−5)	1.29968(−4)	4.2137 (−4)	1.12821(−3)	2.5962 (−3)
150	3.6714 (−5)	1.51158(−4)	4.8598 (−4)	1.29060(−3)	2.9459 (−3)

θ \ τ	0.55	0.60	0.65	0.70	0.80
20	1.1524 (−4)	2.5793 (−4)	5.2951 (−4)	1.0086 (−3)	3.0394 (−3)
30	2.7506 (−4)	5.9368 (−4)	1.1759 (−3)	2.1571 (−3)	6.0754 (−3)
40	4.9901 (−4)	1.0485 (−3)	2.0175 (−3)	3.6121 (−3)	9.7168 (−3)
50	7.8180 (−4)	1.6056 (−3)	3.0279 (−3)	5.3167 (−3)	1.38230(−2)
60	1.1188 (−3)	2.2554 (−3)	4.1820 (−3)	7.2302 (−3)	1.83034(−2)
70	1.5035 (−3)	2.9873 (−3)	5.4618 (−3)	9.3229 (−3)	2.30952(−2)
80	1.9344 (−3)	3.7932 (−3)	6.8527 (−3)	1.15716(−2)	2.81516(−2)
90	2.4072 (−3)	4.6664 (−3)	8.3431 (−3)	1.39583(−2)	3.34377(−2)
100	2.9189 (−3)	5.6012 (−3)	9.9233 (−3)	1.64681(−2)	3.89256(−2)
110	3.4669 (−3)	6.5927 (−3)	1.15852(−2)	1.90890(−2)	4.45932(−2)
120	4.0489 (−3)	7.6364 (−3)	1.33220(−2)	2.18109(−2)	5.04222(−2)
130	4.6627 (−3)	8.7287 (−3)	1.51277(−2)	2.46253(−2)	5.63973(−2)
140	5.3066 (−3)	9.8663 (−3)	1.69972(−2)	2.75244(−2)	6.25058(−2)
150	5.9788 (−3)	1.1046 (−2)	1.89261(−2)	3.05021(−2)	6.87366(−2)

θ \ τ	0.90	1.00	1.10	1.20	1.30
20	7.5301 (−3)	1.60831(−2)	3.06599(−2)	5.35096(−2)	8.71106(−2)
30	1.41960(−2)	2.88684(−2)	5.28479(−2)	8.92163(−2)	1.41328(−1)
40	2.18513(−2)	4.30695(−2)	7.68762(−2)	1.27150(−1)	1.98096(−1)
50	3.02361(−2)	5.82858(−2)	1.02203(−1)	1.66643(−1)	2.56648(−1)
60	3.91918(−2)	7.42830(−2)	1.28518(−1)	2.07319(−1)	3.16553(−1)
70	4.86127(−2)	9.09087(−2)	1.55623(−1)	2.48936(−1)	3.77536(−1)
80	5.84236(−2)	1.08056(−1)	1.83381(−1)	2.91330(−1)	4.39407(−1)
90	6.85684(−2)	1.25647(−1)	2.11691(−1)	3.34381(−1)	5.02027(−1)
100	7.90041(−2)	1.43622(−1)	2.40479(−1)	3.77997(−1)	5.65289(−1)
110	8.96964(−2)	1.61935(−1)	2.69685(−1)	4.22108(−1)	6.29103(−1)
120	1.00617(−1)	1.80547(−1)	2.99260(−1)	4.66657(−1)	6.93391(−1)
130	1.11745(−1)	1.99428(−1)	3.29168(−1)	5.11597(−1)	7.58078(−1)
140	1.23059(−1)	2.18552(−1)	3.59375(−1)	5.56886(−1)	8.23090(−1)
150	1.34544(−1)	2.37897(−1)	3.89854(−1)	6.02489(−1)	8.88354(−1)

[1] Prigogine and Garikian, Physica **16**, 239 (1950).
[2] J. G. Kirkwood, J. Chem. Phys. **18**, 380 (1950).
[3] Z. W. Salsburg and J. G. Kirkwood, J. Chem. Phys. **20**, 1538 (1952).
[4] Wentorf, Buehler, Hirschfelder, and Curtiss, J. Chem. Phys. **18**, 1484 (1950).

TABLE III. A tabulation of g_M.

θ \ τ	0.30	0.35	0.40	0.45	0.50
20	6.894 (−8)	3.2222 (−7)	1.2095 (−6)	3.812 (−6)	1.0392 (−5)
30	1.8573 (−7)	8.531 (−7)	3.123 (−6)	9.531 (−6)	2.5026 (−5)
40	3.7304 (−7)	1.6852 (−6)	6.033 (−6)	1.7913 (−5)	4.5609 (−5)
50	6.381 (−7)	2.8374 (−6)	9.953 (−6)	2.8855 (−5)	7.1572 (−5)
60	9.859 (−7)	4.3197 (−6)	1.4876 (−5)	4.2222 (−5)	1.02385(−4)
70	1.4204 (−6)	6.140 (−6)	2.0779 (−5)	5.7859 (−5)	1.37574(−4)
80	1.9445 (−6)	8.295 (−6)	2.7634 (−5)	7.5624 (−5)	1.7674 (−4)
90	2.5602 (−6)	1.0787 (−5)	3.5413 (−5)	9.5381 (−5)	2.1957 (−4)
100	3.270 (−6)	1.3612 (−5)	4.4074 (−5)	1.17003(−4)	2.6517 (−4)
110	4.073 (−6)	1.6766 (−5)	5.3587 (−5)	1.40377(−4)	3.1396 (−4)
120	4.972 (−6)	2.0244 (−5)	6.3921 (−5)	1.65402(−4)	3.6542 (−4)
130	5.966 (−6)	2.4041 (−5)	7.5041 (−5)	1.9199 (−4)	4.1932 (−4)
140	7.055 (−6)	2.8150 (−5)	8.6918 (−5)	2.2006 (−4)	4.7547 (−4)
150	8.240 (−6)	3.2566 (−5)	9.9521 (−5)	2.4954 (−4)	5.3368 (−4)

θ \ τ	0.55	0.60	0.65	0.70	0.80
20	2.5078 (−5)	5.4482 (−5)	1.08159(−4)	1.9861 (−4)	5.5221 (−4)
30	5.7922 (−5)	1.2047 (−4)	2.2925 (−4)	4.0236 (−4)	1.03250(−3)
40	1.02150(−4)	2.0578 (−4)	3.7798 (−4)	6.4465 (−4)	1.56569(−3)
50	1.56114(−4)	3.0583 (−4)	5.4849 (−4)	9.1384 (−4)	2.12982(−3)
60	2.1855 (−4)	4.1848 (−4)	7.3538 (−4)	1.20241(−3)	2.71274(−3)
70	2.8757 (−4)	5.4130 (−4)	9.3511 (−4)	1.50539(−3)	3.3071 (−3)
80	3.6306 (−4)	6.7260 (−4)	1.14508(−3)	1.81925(−3)	3.9081 (−3)
90	4.4394 (−4)	8.1102 (−4)	1.36332(−3)	2.14141(−3)	4.5126 (−3)
100	5.2957 (−4)	9.5550 (−4)	1.58829(−3)	2.46993(−3)	5.1184 (−3)
110	6.1938 (−4)	1.10520(−3)	1.81879(−3)	2.80336(−3)	5.7240 (−3)
120	7.1290 (−4)	1.25931(−3)	2.05384(−3)	3.14053(−3)	6.3283 (−3)
130	8.0974 (−4)	1.41726(−3)	2.29266(−3)	3.4806 (−3)	6.9304 (−3)
140	9.0954 (−4)	1.57855(−3)	2.53461(−3)	3.8227 (−3)	7.5297 (−3)
150	1.01200(−3)	1.74275(−3)	2.77915(−3)	4.1664 (−3)	8.1260 (−3)

θ \ τ	0.90	1.00	1.10	1.20	1.30
20	1.25428(−3)	2.44759(−3)	4.2568 (−3)	6.7768 (−3)	1.00706(−2)
30	2.18755(−3)	4.0252 (−3)	6.6656 (−3)	1.01877(−2)	1.46335(−2)
40	3.16732(−3)	5.6100 (−3)	9.0035 (−3)	1.34103(−2)	1.88551(−2)
50	4.1651 (−3)	7.1766 (−3)	1.12621(−2)	1.64686(−2)	2.28061(−2)
60	5.1671 (−3)	8.7158 (−3)	1.34441(−2)	1.93850(−2)	2.65357(−2)
70	6.1661 (−3)	1.02245(−2)	1.55549(−2)	2.21780(−2)	3.00795(−2)
80	7.1580 (−3)	1.17019(−2)	1.76005(−2)	2.48627(−2)	3.34642(−2)
90	8.1406 (−3)	1.31487(−2)	1.95861(−2)	2.74512(−2)	3.67104(−2)
100	9.1126 (−3)	1.45659(−2)	2.15168(−2)	2.99536(−2)	3.98344(−2)
110	1.00733(−2)	1.59549(−2)	2.33969(−2)	3.23783(−2)	4.28494(−2)
120	1.10224(−2)	1.73170(−2)	2.52301(−2)	3.47323(−2)	4.57662(−2)
130	1.19599(−2)	1.86535(−2)	2.70200(−2)	3.70217(−2)	4.85935(−2)
140	1.28858(−2)	1.99658(−2)	2.87695(−2)	3.92517(−2)	5.13386(−2)
150	1.38003(−2)	2.12549(−2)	3.04813(−2)	4.14267(−2)	5.40078(−2)

TABLE IV. The compressibility factor pv/NkT.

θ \ τ	0.30	0.35	0.40	0.45	0.50
20	140.759	76.064	45.323	29.329	20.3877
30	96.145	52.977	32.423	21.6791	15.6251
40	73.819	41.400	25.925	17.7938	13.1729
50	60.411	34.431	21.9935	15.4224	11.6551
60	51.459	29.766	19.3490	13.8142	10.6122
70	45.056	26.4227	17.4419	12.6433	9.8452
80	40.246	23.9022	15.9972	11.7491	9.2534
90	36.498	21.9324	14.8630	11.0408	8.7807
100	33.495	20.3487	13.9455	10.4641	8.3891
110	31.032	19.0462	13.1866	9.9838	8.0618
120	28.976	17.9551	12.5475	9.5767	7.7820
130	27.231	17.0267	12.0011	9.2265	7.5395
140	25.733	16.2266	11.5277	8.9214	7.3267
150	24.431	15.5291	11.1131	8.6528	7.1379

θ \ τ	0.55	0.60	0.65	0.70	0.80
20	15.084	11.7672	9.5937	8.1066	6.2651
30	11.9874	9.6722	8.1260	7.0330	5.6356
40	10.3598	8.5444	7.3015	6.4150	5.2474
50	9.3357	7.8145	6.7618	5.9987	4.9740
60	8.6224	7.2977	6.3715	5.6921	4.7667
70	8.0861	6.9066	6.0717	5.4535	4.6018
80	7.6689	6.5971	5.8317	5.2605	4.4661
90	7.3315	6.3442	5.6337	5.0997	4.3515
100	7.0516	6.1324	5.4664	4.9630	4.2530
110	6.8144	5.9516	5.3224	4.8447	4.1669
120	6.6102	5.7945	5.1968	4.7408	4.0908
130	6.4318	5.6566	5.0858	4.6486	4.0227
140	6.2742	5.5340	4.9867	4.5660	3.9614
150	6.1337	5.4241	4.8974	4.4913	3.9056

θ \ τ	0.90	1.00	1.10	1.20	1.30
20	5.2018	4.51787	4.04135	3.68940	3.41813
30	4.7887	4.22220	3.81596	3.50972	3.27025
40	4.5176	4.01831	3.65450	3.37715	3.15850
50	4.3200	3.86584	3.53141	3.27457	3.07101
60	4.16681	3.74564	3.43320	3.19198	3.00005
70	4.04293	3.64735	3.35222	3.12344	2.94084
80	3.93975	3.56479	3.28378	3.06522	2.89034
90	3.85187	3.49399	3.22479	3.01486	2.84651
100	3.77568	3.43229	3.17319	2.97065	2.80792
110	3.70871	3.37781	3.12746	2.93137	2.77352
120	3.64915	3.32918	3.08652	2.89613	2.74252
130	3.59568	3.28537	3.04955	2.86423	2.71432
140	3.54727	3.24559	3.01592	2.83513	2.68842
150	3.50314	3.20924	2.98512	2.80843	2.66445

volumes and covers the region of interest with considerably finer intervals in reduced temperature and more regular intervals in reduced volume. The potential of intermolecular force was the same as that used in reference 4, $V(r)=4\epsilon^*[(r_0/r)^{12}-(r_0/r)^6]$. The calculations were quite similar to those described previously[4] and were carried out on an International Business Machines Corporation Model II CPEC combination. The numerical integrations were carried out with Simpson's rule and a nominal 64 to 72 values of the integrand. Shortening of the range of integration was carried out as required so that the number of non-negligible values was always at least two-thirds of the nominal number. We believe these results to be somewhat more accurate than those of Wentorf *et al.*, who state that they used Simpson's rule with 15 to 30 non-negligible values of the integrand. An estimate of the error involved in the numerical evaluation of the integrals was obtained by comparing the results with those obtained by using Simpson's rule with half the original number of points. The number of figures to be included in the tabular entries was decided on the basis of this comparison. Although the last figure in each entry is thought to have some significance, it is not necessarily a "significant figure" in the strict sense.

The results of the calculation are presented in Tables I–VI. The reduced volume and temperature are defined as follows: $\tau=v/v^*$ and $\theta=kT/\epsilon^*$, where $v^*=Nr_0^3$ and ϵ^* are the molecular parameters defining the Lennard-Jones potential of intermolecular force. The symbols G, g_l, and g_m represent integrals needed for the evaluation of the compressibility factor pv/RT, the reduced internal energy of gas imperfection $E'/N\epsilon^*$, and the reduced entropy of gas imperfection S'/R. Precise definitions of and expressions for these quantities may be found in reference 4.[5]

[5] The complete expression for the entropy is

$$S=S^0(T)-R\log(RT/v^*)+R\log(v/v^*)+S'(v,T)+R\log(\sigma/e)+RT\left(\frac{\partial\log\sigma}{\partial T}\right),$$

$$S'(v,T)=[12N\epsilon^*/T][(v^*/v)(g_l/G)-2(v^*/v)(g_m/G)]+R\log(G/G_\infty),$$

$$G_\infty=\lim_{v\to\infty}G=(2\sqrt{2}\pi)^{-1}.$$

The parameter σ has been precisely defined by Kirkwood (see reference 2).

In Eq. (21) of reference 4 it has apparently been assumed that the communal entropy ($R\log\sigma+RT(\partial\log\sigma/\partial T)$) is equal to R, or that σ is temperature-independent and equal to e.

Since present knowledge has not led to general agreement on the value of σ (except in the limits of low and high density), this assumption may not be justified throughout the range of density covered in their tables.

We are inclined to believe that σ is quite temperature-dependent and closer to unity than to e through most of the range of the tables presented here. Thus the contribution of the terms con-

TABLE V. The reduced internal energy of gas imperfection $E'/N\epsilon^*$.

θ \ τ	0.30	0.35	0.40	0.45	0.50
20	617.84	315.44	175.30	104.53	66.328
30	632.32	329.52	188.84	117.37	78.390
40	646.61	343.30	201.92	129.65	89.811
50	660.75	356.79	214.63	141.47	100.705
60	674.70	370.02	227.00	152.91	111.177
70	688.50	383.06	239.08	164.00	121.294
80	702.15	395.86	250.89	174.78	131.112
90	715.65	408.45	262.48	185.30	140.673
100	729.07	420.86	273.82	195.58	149.93
110	742.30	433.09	284.95	205.65	159.01
120	755.41	445.00	295.90	215.53	167.90
130	768.40	457.06	306.66	225.23	176.61
140	781.28	468.82	317.27	234.78	185.17
150	794.05	480.44	327.72	244.17	193.58

θ \ τ	0.55	0.60	0.65	0.70	0.80
20	44.554	31.530	23.398	18.112	12.032
30	55.793	41.947	33.057	27.004	19.661
40	66.328	51.665	41.943	35.219	26.702
50	76.333	60.803	50.347	42.955	33.333
60	85.928	69.543	58.355	50.321	39.656
70	95.104	77.942	66.045	57.394	45.735
80	104.010	86.057	73.471	64.226	51.613
90	112.657	93.928	80.672	70.852	57.321
100	121.076	101.588	87.679	77.301	62.883
110	129.293	109.064	94.516	83.596	68.318
120	137.330	116.370	101.202	89.754	73.640
130	145.204	123.527	107.753	95.790	78.861
140	152.930	130.550	114.180	101.714	83.991
150	160.521	137.448	120.497	107.538	89.038

θ \ τ	0.90	1.00	1.10	1.20	1.30
20	8.8603	6.9966	5.7941	4.9620	4.3558
30	15.4864	12.8358	11.0137	9.6879	8.6825
40	21.6171	18.2619	15.8873	14.1211	12.7584
50	27.406	23.4027	20.5202	18.3486	16.6563
60	32.939	28.3285	24.9709	22.4193	20.4175
70	38.268	33.0836	29.2760	26.3644	24.0686
80	43.431	37.6980	33.4610	30.2051	27.6277
90	48.452	42.1935	37.5439	33.9570	31.1084
100	53.352	46.5863	41.5387	37.6319	34.5203
110	58.145	50.8891	45.4559	41.2389	37.8710
120	62.845	55.1121	49.3041	44.7853	41.1658
130	67.460	59.2635	53.0904	48.2770	44.4085
140	72.000	63.3500	56.8205	51.7189	47.6016
150	76.469	67.3775	60.4994	55.1147	50.7466

TABLE VI. The reduced entropy of gas imperfection $-S'/Nk$.

θ \ τ	0.30	0.35	0.40	0.45	0.50
20	7.5145	6.6025	5.8279	5.1649	4.5961
30	6.9274	6.0310	5.2785	4.6436	4.1060
40	6.5161	5.6346	4.9018	4.2899	3.7772
50	6.2005	5.3334	4.6181	4.0260	3.5339
60	5.9461	5.0921	4.3924	3.8174	3.3429
70	5.7335	4.8910	4.2062	3.6465	3.1868
80	5.5512	4.7202	4.0485	3.5025	3.0557
90	5.3922	4.5719	3.9121	3.3786	2.9431
100	5.2509	4.4411	3.7926	3.2702	2.8457
110	5.1248	4.3246	3.6865	3.1742	2.75911
120	5.0107	4.2200	3.5912	3.0883	2.68175
130	4.9068	4.1243	3.5050	3.0106	2.61199
140	4.8113	4.0371	3.4264	2.9399	2.54858
150	4.7232	3.9570	3.3543	2.8750	2.49056

θ \ τ	0.55	0.60	0.65	0.70	0.80
20	4.1065	3.6852	3.3216	3.0069	2.49454
30	3.6498	3.2617	2.9289	2.64517	2.18421
40	3.3463	2.9817	2.67319	2.40846	1.98132
50	3.1229	2.7778	2.48549	2.23568	1.83321
60	2.9478	2.6184	2.33939	2.10129	1.71786
70	2.80653	2.48885	2.22079	1.99221	1.62411
80	2.68756	2.38046	2.1216	1.90096	1.54561
90	2.58569	2.28773	2.03676	1.82290	1.47836
100	2.49697	2.20701	1.96291	1.75493	1.41974
110	2.41863	2.13575	1.89774	1.69493	1.36793
120	2.34869	2.07216	1.83955	1.64134	1.32162
130	2.28566	2.01487	1.78711	1.59302	1.27982
140	2.22840	1.96283	1.73947	1.54911	1.24180
150	2.17602	1.91523	1.69589	1.50893	1.20698

θ \ τ	0.90	1.00	1.10	1.20	1.30
20	2.09945	1.78771	1.53613	1.32891	1.15510
30	1.82995	1.55025	1.32391	1.13680	0.97925
40	1.65331	1.39392	1.18351	1.00910	0.86185
50	1.52400	1.27911	1.08005	0.91469	0.77481
60	1.42307	1.18925	0.99886	0.84044	0.70620
70	1.34088	1.11592	0.93247	0.77960	0.64990
80	1.27193	1.05428	0.87657	0.72830	0.60236
90	1.21277	1.00132	0.82847	0.68410	0.56136
100	1.16114	0.95503	0.78637	0.64537	0.52540
110	1.11544	0.91401	0.74903	0.61099	0.49346
120	1.07455	0.87726	0.71555	0.58013	0.46479
130	1.03760	0.84403	0.68524	0.55218	0.43883
140	1.00396	0.81374	0.65759	0.52667	0.41517
150	0.97312	0.78596	0.63221	0.50324	0.39347

TABLE VII. Comparison with previous results.

		This report			Wentorf *et al.*[a]		
θ	τ	G	$\frac{pv}{RT}$	$\frac{E'}{N\epsilon^*}$	G	$\frac{pv}{RT}$	$\frac{E'}{N\epsilon^*}$
20	0.5657		13.8798	39.758		13.735	39.08
	0.9899		4.5756	7.1479		4.576	7.150
	1.2728	1.94535(−2)[b]	3.48559[b]	4.5036[b]	1.945(−2)	3.486	4.504
50	0.5657	1.78914(−3)[b]	8.7920	70.732	1.823(−1)	8.717	69.86
			8.7918[b]	70.731[b]			
	0.9899		3.90534	23.7470		3.905	23.75
100	0.5657		6.72775	114.175		6.733	114.29
	0.9899		3.46255	47.1791		3.462	47.18

[a] See reference 4.
[b] Calculated directly.

In order to facilitate interpolation, tables of $pv/N\epsilon^*$, $\log[(pv/RT)-1]$, and $\log(E'/N\epsilon^*)$ were prepared. With these, five-point interpolation in τ and three-point interpolation in θ were found to give satisfactory results.

A comparison of our results for G, pv/RT, and $E'/N\epsilon^*$ with those of Wentorf *et al.*[4] is made in Table VII. The discrepancies between our results and theirs become larger for the lower values of θ and τ, where the integrands become sharply peaked, and are probably due to their use of a smaller number of points in the integration. The values of pv/RT and $E'/N\epsilon^*$ from this work presented in Table VII were obtained by seven-point centered interpolation in the tables of $\log[(pv/RT)-1]$ and $\log(E'/N\epsilon^*)$ previously mentioned, except as otherwise indicated.

taining it to the values of the thermodynamic functions probably cannot be neglected.

Infrared and Raman Spectroscopy Studies of Light and Heavy Trifluoroacetic Acids*

NELSON FUSON AND MARIE-LOUISE JOSIEN, *Fisk University, Nashville 8, Tennessee*
ERNEST A. JONES, *Vanderbilt University, Nashville, Tennessee*
AND
JAMES R. LAWSON, *Tennessee A & I State University, Nashville, Tennessee*
(Received March 17, 1952)

An infrared and Raman spectroscopic study of light and heavy trifluoroacetic acids shows that their vapors at room temperature are composed of a mixture of monomeric and associated molecules. The principal bands corresponding to vibrations of the COOH and COOD groups have been identified for both the monomeric and the associated molecules by means of a comparative study of the two acids (a) in the vapor state at different pressures, (b) in CCl_4 solutions at various concentrations, and (c) in the liquid state. The monomeric carbonyl frequencies, influenced by the presence of the perfluoromethyl group, are the highest yet reported in the literature; this is true not only for CF_3COOH (1826 cm^{-1}, vapor), CF_3COOD (1823 cm^{-1}, vapor), but also for the ethyl ester, $CF_3COOC_2H_5$ (1802 cm^{-1}, vapor), the sodium salt, CF_3COONa (1687 cm^{-1}, solid), and the anhydride $(CF_3CO)_2O$ (1884 cm^{-1} and 1818 cm^{-1}, vapor). On the basis of a comparative study of the spectra of all these compounds, as well as of other perfluoromethyl compound spectra reported in the literature, the C—F stretching vibrations for the two acids have been assigned to the strong infrared absorptions at 1244 cm^{-1} and 1185 cm^{-1}. The corresponding Raman bands are very weak.

I. INTRODUCTION

As far as we know no spectroscopic study of the trifluoroacetic acids has been made. Nevertheless, several of the physical properties of the light acid have been investigated.[1–4] Since the effect of fluorine atoms in molecules is still under discussion,[5] it is of interest to apply infrared and Raman spectroscopy to the study of these molecules.

II. EXPERIMENTAL

A. Raman

The Raman spectra of the liquid trifluoroacetic acids from 100 cm^{-1} to 2000 cm^{-1} were obtained using the Vanderbilt University Physics Department's model 612 Hilger spectrograph and an irradiation unit consisting of eight single-jacketed General Electric type AH-2 mercury arcs arranged symmetrically about the vertical Raman tube. Eastman 103-J and 103-O plates were used, and the excitation was by means of the 4358A line of mercury.

B. Infrared

The Fisk University infrared spectrometer, described elsewhere,[6] was equipped with a sodium chloride prism for the region between 4μ and 15μ and with a lithium fluoride prism for the 2μ to 4μ region. All the work was done at room temperature (25°C). Individual sharp bands were reproducible with an uncertainty of ± 1 cm^{-1} in the 3300 cm^{-1} region using the lithium fluoride prism and ± 2 cm^{-1} at 1700 cm^{-1} and ± 1 cm^{-1} at 1000 cm^{-1} with the sodium chloride prism. The spectrometer calibration has already been described.[6,7] Spectral slit widths are indicated on the spectra illustrated in the figures.

Spectrograms of the two trifluoroacetic acids[8] were recorded from 3600 cm^{-1} to 660 cm^{-1} as liquid capillary films and in the vapor state at several different pressures between 2 mm and 25 mm of mercury. In addition spectra were obtained in solution in CCl_4 from 3600 cm^{-1} to 1000 cm^{-1} for trifluoroacetic acid and at 1400 cm^{-1} for the deuterated acid.

In order to help in determining the assignments of the observed bands, spectrograms were made of ethyltrifluoroacetate[9] (both vapor and liquid film), sodium trifluoroacetate[10] (solid film), trifluoroacetic anhydride[11] (vapor), and trichloroacetic acid[12] (solution in CCl_4).

III. RESULTS

Table I and Fig. 1 summarize the results obtained for trifluoroacetic acid. Table II and Fig. 2 do the same for deutero-trifluoroacetic acid.

The intensity symbols have the usual meanings: vw = very weak, w = weak, Mw = medium weak, M = medium, MS = medium strong, S = strong, VS = very strong, (sh) = shoulder, (br) = broad. Regions not studied are indicated in the table columns by vertical

* A preliminary Note has been published in Compt. rend. **234**, 1163 (1952). This paper was reported upon in part at the Annual Symposium on Molecular Structure and Spectroscopy held at Ohio State University, Columbus, Ohio, June 9–13, 1952.

[1] J. H. Simons and K. E. Lorentzen, J. Am. Chem. Soc. **72**, 1426 (1950).

[2] J. H. Gibbs and C. P. Smith, J. Am. Chem. Soc. **73**, 5115 (1951).

[3] A. L. Henne and C. J. Fox, J. Am. Chem. Soc. **73**, 2323 (1951).

[4] J. Karle and L. O. Brockway, J. Am. Chem. Soc. **66**, 574 (1944).

[5] J. Leonard and L. E. Sutton, J. Am. Chem. Soc. **70**, 1564 (1948).

[6] Josien, Fuson, and Cary, J. Am. Chem. Soc. **73**, 4445 (1951).

[7] Fuson, Josien, Powell, and Utterback, J. Chem. Phys. **20**, 145 (1952).

[8] The deutero trifluoroacetic acid was prepared from trifluoroacetic anhydride and 99.8 percent heavy water. Its freedom from any nondeuterated acid was evident from the absence of absorption bands in the 2700–3700 cm^{-1} region. This compound was prepared for us by Dr. Carl M. Hill, Department of Chemistry, Tennessee A & I State University, Nashville, Tennessee. The light trifluoroacetic acid was obtained from Minnesota Mining and Manufacturing Company, St. Paul, Minnesota.

[9] The ethyl trifluoroacetate was obtained from Dr. A. L. Henne, Department of Chemistry, Ohio State University, Columbus, Ohio.

[10] The sodium trifluoroacetate was prepared for us by Dr. Carl Hill, Department of Chemistry, Tennessee A & I State University, Nashville, Tennessee.

[11] Reagent grade commercial sample from Halogen Chemical Inc., Columbia, S. Carolina.

[12] Reagent grade commercial sample from Allied Chemical & Dye Corporation, New York, New York.

lines. Frequencies linked together by brackets indicate bands not completely resolved. It is to be noted that the infrared spectra are much richer in absorption bands than the Raman spectra in the 4000–700 cm^{-1} region.

IV. ASSIGNMENTS

Vibrations in which different atomic subgroups are mainly responsible will be considered in turn, in each case the light and heavy acids being discussed together. The correlation between the spectra of the two compounds and the assignments made are summarized in Table III.

A. Bands Assigned to the Carboxylic Group

Six major bands at approximately 3500, 3000, 1700, 1400, 1250, and 900 cm^{-1} have been suggested as characteristic of the COOH group.[13–16] As far as we know a similar general statement has not been made in the literature for the bands of COOD. It has been assumed that carboxylic acids exist generally as dimers,

TABLE I. Infrared and Raman frequencies (cm^{-1}) and relative intensities of trifluoroacetic acid.

Vapor	Infrared CCl_4 solution	Liquid	Raman Liquid
3587 M	3500 Mw		
3248 }			
3144 }	3112 }		
3084 }	3068 } M		
2985 } S	2980 }		
2950 }			
2905 }			
2838 }			
2700 }			
2598 M	2580 w		
1826 MS	1810 Mw		
1788 S	1787 M	1785 S	1770 S (br)
1465 M	1465 w	1452 w	1445 S
1300 Mw	1292 w	1288 vw (sh)	
1244 S	1232 M		1241 w
1203 VS		1200 VS[a]	
1182 VS	1173 MS		1174 w
1130 M		1130 vw (sh)	
1123 M	1123 w		
1010 vw			
967 w			
904 M		893 w (br)	
825 Mw		810 MS	813 S
800 w (sh)			794 vw
782 w			
708 Mw		707 MS	
		688 M	689 vw
			598 w
			525 vw
			436 MS
			419 MS
			401 MS
			260 S

[a] 100 percent absorption 120 cm^{-1} wide.

[13] J. Lecomte, "Structure des molecules" in *Traite de Chimie Organique* (Masson et Cie, Paris, 1936), Tome II.
[14] M. M. Davies and G. B. B. M. Sutherland, J. Chem. Phys. **6**, 755 (1938).
[15] M. St. C. Flett, J. Chem. Soc., 962 (1951).
[16] Buswell, Rodebush, and Roy, J. Am. Chem. Soc. **60**, 2239 (1938).

with the following structure:

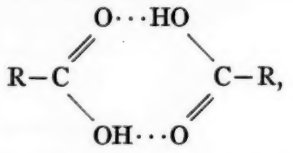

because of particularly strong hydrogen bonding.[13,14,16] Electron diffraction studies show that trifluoroacetic acid molecules behave in a similar fashion.[4]

1. The OH *and* OD *Stretching Vibrations*

In the vapor spectrum of CF_3COOH the sharp band at 3587 cm^{-1} (3500 cm^{-1} in the CCl_4 solution spectrum) is assigned to the free OH stretching vibration while the broad bands centered at about 3000 cm^{-1} correspond to the associated OH stretching vibrations. The two bands coexist at room temperature in the vapor at the pressures studied and in the solution spectra showing that some monomer is still present. This is in agreement with the dissociation constant studies of Karle and Brockway.[4] A CCl_4 solution study was also made. Several different concentrations were used, the cell path length being so chosen that the path length times concentration (i.e., the total number of molecules in the path) remained constant within the uncertainty range of ±10 percent. The two main sources of error lie in the cell thicknesses[7] and in the high volatility of the compounds studied. The results given in Table IV show that the percentage of the monomer is increased by dilution. This effect appears very much like that obtained by Davies and Sutherland[14] with a fixed

TABLE II. Infrared and Raman frequencies (cm^{-1}) and relative intensities of deutero-trifluoroacetic acid.

Vapor	Infrared CCl_4 solution	Liquid	Raman Liquid
2648 MS			
2457 }			
2413 }			
2366 } S (br)		2370 VS (br)	
2290 }		2260 S	
2203 }			
2164 }		2165 w (sh)	
2077 M		2050 Mw	
1823 S			
1784 S		1780 S	1760 M (br)
1690 w			
1432 Mw	1428 M	1430 S	1427 S
1384 M	1388 M		
1243 S			1241 Vs
1187 S		1220 VS[a]	1170 Vw
1155 M		1150 M	
1039 S		1027 MS	
993 M			
798 VS		785 MS	792 VS
778 w (sh)			
667 M			648 w
			596 w
			434 S
			417 MS
			399 MS
			260 S

[a] 100 percent absorption 100 cm^{-1} wide.

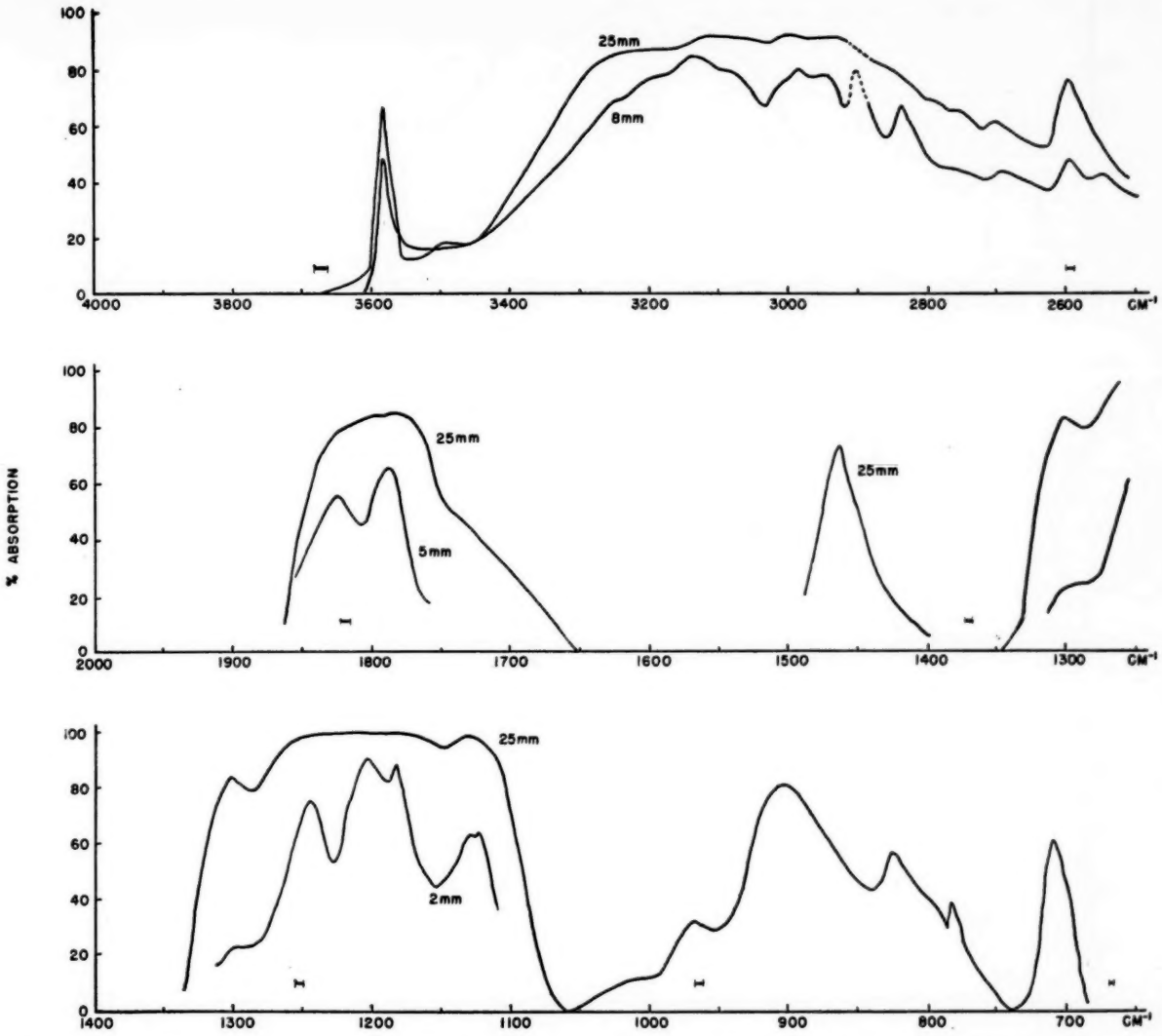

FIG. 1. Infrared spectrum of trifluoroacetic acid vapor at the several pressures indicated on the curves. The dotted curve at 2900 cm^{-1} is uncertain due to background interference. In spectral regions of no absorption the curve is absent. Spectral slit widths are indicated by horizontal lines (|—|).

concentration of CH_3COOH in CCl_4 solution studied at different temperatures.

Table V compares the OH frequencies and acid dissociation constants of a group of carboxylic acids.[15,17,18] The values found for the free OH stretching frequency in CF_3COOH is in agreement with its strong acid properties.

For CF_3COOD in the vapor state the absorption of the OD valence vibration is the sharp band at 2648 cm^{-1} for the monomer and the broad band in the neighborhood of 2370 cm^{-1} for the associated molecules. The corresponding frequency ratios $\nu(OH)/\nu(OD)$ are 1.36 and 1.33, respectively.

The broad OH and OD associated bands in both solution and gas forms, particularly in the latter, seems to have some kind of structure. This band's width and structure have already been noted for trichloroacetic acid and acetic acid[14,19,20] and other carboxylic acids.[21] The band profile in the trifluoroacetic acids is too complex to allow meaningful comparison with Chulanovskii's data and analysis of formic, acetic, and trichloroacetic acids.[20] This author's analysis has, moreover, already been contradicted by the findings of Hadzi and Sheppard,[21] who noticed that there is no change in relative intensity of these bands at room temperature and liquid oxygen temperature.

The CF_3COOH spectrum contains a band of medium intensity at 2598 cm^{-1}. A similarly placed band at 2077 cm^{-1} appears in the CF_3COOD spectrum, the

[17] R. H. Gillette, J. Am. Chem. Soc. **58**, 1143 (1936).
[18] R. E. Richards, Trans. Faraday Soc. **44**, 40 (1948).
[19] M. Davies, Trans. Faraday Soc. **86**, 116 (1940).
[20] V. M. Chulanovskii and P. D. Simova, Doklady Akad. Nank. SSSR **68**, 1033 (1949).
[21] D. Hadzi and N. Sheppard, "The Assignment of the Infrared Frequencies of the COOH Group in Carboxylic Acid Dimers." Paper given at the International Meeting of Spectroscopists in Basel, Switzerland, June 28–30, 1951.

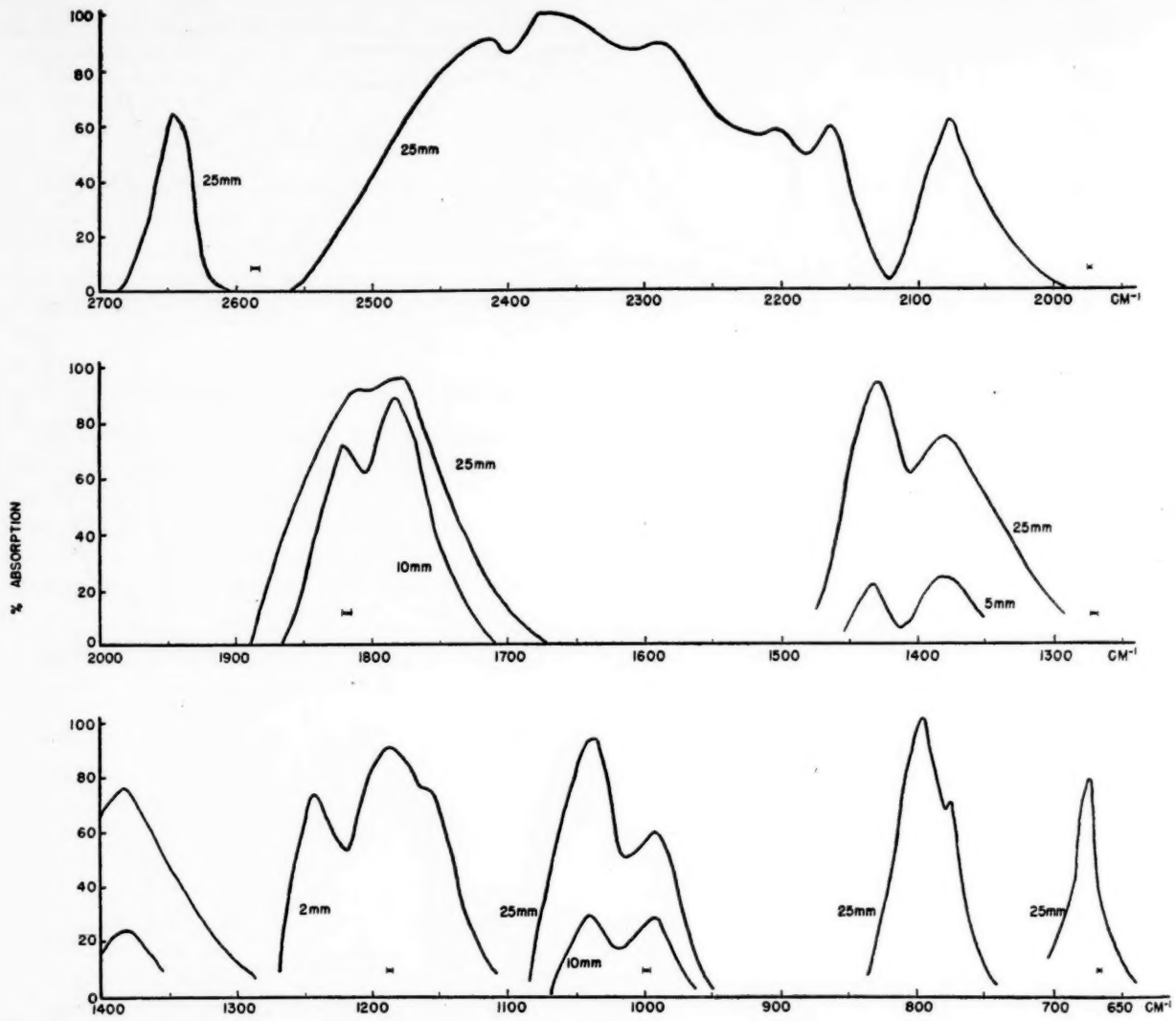

FIG. 2. Infrared spectrum of deutero-trifluoroacetic acid vapor at the several pressures indicated on the curves. In spectral regions of no absorption the curve is absent. Spectral slit widths are indicated by horizontal lines (|—|).

frequency ratio being 1.25. Flett[15] has already stressed the importance of this band at 2500–2700 cm^{-1} for the identification of carboxylic acids because it is not overlaid by CH stretching bands even in Nujol mulls.

2. *The* C=O *Stretching Vibration*

The strong absorption band observed at about 1825 cm^{-1} in the vapor spectrum of CF_3COOH is assigned to the C=O linkage. It remains almost unchanged (1823 cm^{-1}) in the spectrum of the deuterated acid. The two corresponding Raman bands are a strong one at 1770 cm^{-1} in CF_3COOH, having a band width of about 110 cm^{-1}, and a 40 cm^{-1} broad medium band at 1760 cm^{-1} in CF_3COOD. In the infrared spectrogram of the gas recorded at low pressure this band is resolved into two bands at 1826 cm^{-1} and 1788 cm^{-1}; the infrared spectrum in solution shows the corresponding absorptions at 1810 cm^{-1} and 1787 cm^{-1}. The lowering of the "free" carbonyl vibration frequency by 16 cm^{-1} in going from vapor to solution state is the usual shift observed. The associated vibration frequency does *not* shift as the state is changed, which indicates that the polymerization in some way insulates the carbonyl vibration from any influence of the surrounding medium. The coexistence of these two bands is to be attributed again to the presence of the two forms, free and associated, of CF_3COOH molecules. The effect of dilution on the intensity ratio of bands due to these two kinds of molecules may be observed by a similar technique to that used for the OH band, the results being qualitatively the same.

Table VI is a comparison of the location of the free and associated bands of CF_3COOH and CCl_3COOH with those found by Davies and Sutherland[14] for CH_3COOH. The C=O frequency increases with increase in acid strength,[22] while at the same time the

[22] M. St. C. Flett, Trans. Faraday Soc. **44**, 767 (1948).

TABLE III. Infrared frequencies, relative intensities, frequency ratios, and assignments for CF_3COOH and CF_3COOD in the vapor state.

CF_3COOH			Frequency ratio**	CF_3COOD		
Assignment*	Intensity	Frequency (cm^{-1})		Frequency (cm^{-1})	Intensity	Assignment*
m ν(OH)	MS	3587				
		3248				
a ν(OH)	S	3144	1.36			
		2985				
		2950				
		2905	1.33			
		2830				
		2700				
				2648	MS	m ν(OD)
	M	2598				
				2457		
				2413		
				2366	S	a ν(OD)
				2290		
				2203		
				2164		
				2077	M	
m ν(C=O)	S	1826	1.00	1823	S	m ν(C=O)
a ν(C=O)	S	1788	1.00	1784	S	a ν(C=O)
				1690	vw	
m,a δ(C-O)	M	1465	1.02	1432	MS	a δ(C-O)
			1.06	1384	M	m δ(C-O)
m ν(C-O)	Mw	1300	1.04			
m,a ν_1(C-F)	S	1244	1.00	1243	S	m,a ν_1(C-F); m ν(C-O)
a ν(C-O)	VS	1203	1.04			
a δ(OH in-plane)						
m,a ν_2(C-F)	VS	1182	1.00	1187	S	m,a ν_2(C-F)
				1155	M	a ν(C-O)
m δ(OH) in-plane	M	1130	1.15			
a δ(OH) out-of-plane	M	1123	1.14	1039	S	a δ(OD) in-plane
	vw	1010				
			1.40	993	M	m δ(OD) in-plane
	w	967				
m δ(OH) out-of-plane	M	904				
m,a ν(C-C)	Mw	825	1.03			
	w	800		798	VS	a δ(OD) out-of-plane; m,a ν(C-C)
	w	782		778	w	
$\delta(C\overset{O}{\diagdown})$	Mw	708	1.34			
				667	M	m $\delta(C\overset{O}{\diagdown})$ (OD) out-of-plane

* m = monomer; a = associated; ν = stretching vibration; δ = deformation vibration.
** The number close to each line in this column indicates the CF_3COOH/CF_3COOD frequency ratio for the two frequencies linked together by the line.

difference between the free and the associated frequencies decreases.

The C=O frequencies for CF_3COOH are significantly higher than for CCl_3COOH whereas the OH frequencies are essentially the same. This striking influence of the CF_3 group on the carbonyl frequency persists also in the ester and anhydride carbonyls and in the carboxylate ion of the salt, as may be seen in Table VII.

The position of the ester carbonyl absorption may be compared with the range given by Hartwell, Richards, and Thompson[23] in

[23] Hartwell, Richards, and Thompson, J. Chem. Soc., 1436 (1948).

TABLE IV. Effect of dilution upon the 3-micron region spectrum of CF_3COOH in CCl_4 solution.

Concentration: volume ratio (solute/solvent)	Cell thickness (mm)	Percent absorption ν(OH) Monomer	ν(OH) Assoc.
1:200	1.0	24	38
1:20	0.1	15	55

which the average position for alkyl esters is 1765 cm^{-1}, the highest being 1786 cm^{-1} for $CCl_3COOC_2H_5$. The carboxylate ion frequency of the salt is much higher than the maximum of the range (1625 cm^{-1}) for this ion frequency given in the literature.[24,25]

Both Lecomte[26] and Davies and Sutherland[14] have discussed the fact that for carboxylic acids the difference between the infrared and Raman carbonyl frequencies is about 60 cm^{-1}. It is interesting to note that the C=O frequency in the Raman spectra of CF_3COOH (1770 cm^{-1}) and the associated C=O frequency in the corresponding infrared spectrum (1785 cm^{-1}) are much closer together than is generally found for carboxylic acids. This is also true for CF_3COOD.

3. *The* C—O *Deformation Vibration*

The strong band in the 1400 cm^{-1} region of carboxylic acids has already been designated as a COOH band by Lecomte,[13] Davies and Sutherland,[14] and Flett.[15] However, some of these authors differ with each other in its more detailed assignment.

Davies and Sutherland[14] proposed a correlation of this band with the stretching vibration ν(C—O). Davies[27] ten years later proposed the deformation vibration δ(C—O). Recently Hadzi and Sheppard,[21] on the basis of a study of eighteen carboxylic acids in normal and deuterated form, assign this 1450 cm^{-1} band to the deformation vibration δ(OH) in-plane.

The results in the 1400 cm^{-1} region obtained for the trifluoroacetic acids are most easily seen in Table III and Table VII. We suggest the assignment of these 1400 cm^{-1} region bands to the C—O deformation vibration for the following reasons:

(a) The frequency shift is slight in going from CF_3COOH to CF_3COOD as one would expect for a C—O vibration in which C—OH is replaced by C—OD.

TABLE V. Free OH stretching frequencies and acid dissociation constants of several carboxylic acids in CCl_4 solution.

	Free ν(OH) (cm^{-1})	Acid dissociation constant[a]
CH_3COOH	3533[b]	1.86×10^{-5}
CCl_3COOH	3504[b]	2.0×10^{-1}
CF_3COOH	3504	5.0×10^{-1}

[a] The dissociation constants for CH_3COOH and CCl_3COOH are given by Davies and Sutherland (reference 14); for CF_3COOH by Henne (reference 3).
[b] These values obtained by us agree well with previous measurements of Davies and Sutherland (reference 14) and Buswell (reference 16).

[24] Randall, Fowler, Fuson, and Dangl, *Infrared Determination of Organic Structures* (D. Van Nostrand Company, Inc., New York, 1949).
[25] N. B. Colthup, J. Opt. Soc. Am. **40**, 396 (1950).
[26] J. Lecomte, *Le Rayonnement Infrarouge* (Gauthier-Villars, Paris, 1949), Tome II.
[27] M. Davies, J. Chem. Phys. **16**, 267 (1948).

TABLE VI. Comparison of the (C=O) stretching frequencies for several carboxylic acids in CCl_4 solution.

	Frequencies (cm^{-1}) Free	Associated	$\Delta\nu$	Acid dissociation constant
CH_3COOH	1768[a]	1701[a]	67	1.86×10^{-5} [a]
CCl_3COOH	1784	1750	34	2.0×10^{-1} [a]
CF_3COOH	1810	1787	23	5.0×10^{-1} [b]

[a] Reference 14.
[b] Reference 3.

(b) In the deuterated compound it has been possible to resolve the band into two components. Changes in solution concentration and in vapor pressure (Figs. 1 and 2) affect the relative intensity of these CF_3COOD bands, the band at the higher frequency becoming dominant at higher pressures and greater concentrations, conditions conducive to maximum association. Furthermore, the higher frequency band is the only one remaining in spectrum of the liquid (Table VII). Since the higher frequency component is thus the associated band, this absorption cannot result from stretching vibrations but must be produced by bending vibrations.[28]

The results here obtained thus lead to an assignment in agreement with the suggestion of Davies.[27] The frequency ratio (δ(C—O) associated)/(δ(C—O) monomer) in CF_3COOD is 1.035, which may be compared with the ratios for CD_3COOD (1.064) and C_2H_5COOD (1.015) obtained by Davies.[27] The position of this absorption band in the spectrum of liquid CF_3COOH (1452 cm^{-1}) is higher than the corresponding frequency in any of the sixty carboxylic acids reported by Flett.[15]

4. *The* OH *and* OD *Bending Vibrations*

In the spectrum of a carboxylic acid monomer are to be expected two absorption bands associated with the deformation of the hydroxyl group, one being described as the in-plane vibration, the other as the out-of-plane vibration. Association should shift both these bending vibrations to higher frequencies. Four bands should be looked for in a mixture containing molecules in both the monomeric and the associated forms.

Major bands in the 1250 cm^{-1} region and the 900 cm^{-1} region generally have been assigned to the COOH group. Both Hadzi and Sheppard[21] and Davies[27] agree that the *ca* 930 cm^{-1} band of the COOH group in the latter region is due to the δ(OH) out-of-plane vibration. The position of the associated band in the former region varies widely between 1200 cm^{-1} and 1300 cm^{-1} as has been shown by Flett.[15] Davies and Sutherland[14] and Davies[27] assign the 1250 cm^{-1} region bands to δ(OH) in-plane. Hadzi and Sheppard[21] assign a *ca* 1300 cm^{-1} band in carboxylic dimers to ν(C—O). Herman and Hofstadter[29] in their study of light and heavy acetic acids also assign this band to ν(C—O).

The tentative band assignments listed in Table III for the hydroxyl deformation vibrations in the trifluoroacetic acids have been made for the following reasons:

(a) The other bands in the 1200 cm^{-1} region (*ca* 1244 cm^{-1} and 1185 cm^{-1}) are assigned to valence vibrations of the CF_3 group for reasons given later in this paper.

(b) The order of magnitude of the deuterization shifts is what

[28] G. B. B. M. Sutherland, Trans. Faraday Soc. **38**, 889 (1940).
[29] R. C. Herman and R. Hofstadter, J. Chem. Phys. **6**, 534 (1938).

is to be expected. For the trifluoroacetic acids the out-of-plane frequency ratio $\delta(OH)/\delta(OD)$ is about 1.35. The in-plane frequency ratio $\delta(OH)/\delta(OD)$ for these acids is about 1.15. Davies[27] finds ratios ranging from 1.16 to 1.23 for the corresponding in-plane vibrations of CD_3COOH and C_2H_5COOH.

(c) The intensities of both the monomer and the associated bands vary in the expected way as the pressure of the vapor is increased and as the state of the compound is changed from vapor to liquid. The 993 cm^{-1} band, assigned to the CF_3COOD monomeric form, is relatively intense in the vapor at 2 mm and 5 mm pressure, weakens at 25 mm pressure and disappears for the liquid state. The monomeric out-of-plane band at 667 cm^{-1} in CF_3COOD disappears in the pure liquid spectrum and the corresponding band at 904 cm^{-1} in CF_3COOH becomes of negligible intensity in the liquid spectrum. A similar comparison in CF_3COOH at 1130 cm^{-1} is not possible because of the strength of neighboring absorption bands. In contrast to these monomeric bands the four bands assigned to the vibration of the associated molecules in the two acids grow relatively more intense in the liquid phase.

(d) The relative intensities of the bands assigned to the monomeric and associated vibrations remain unchanged in going from the ordinary to the deuterated acid. The strong 1203 cm^{-1} band shifts upon deuterization to a strong band at 1039 cm^{-1} while the medium band at 1130 cm^{-1} is transformed into a medium band at 993 cm^{-1}. The medium band at 1123 cm^{-1} shifts upon deuterization such that it is responsible for part of the strong band at 798 cm^{-1}, while the medium band at 904 cm^{-1} goes over into the medium band at 667 cm^{-1}.

(e) The ratio (δ(OH) monomer)/(δ(OH) associated) in-plane for both the two trifluoroacetic acids is about 1.06. This is of the same order of magnitude as the corresponding ratios for CD_3COOH and C_2H_5COOH (1.10) and their deuterated counterparts (1.06) which we have calculated from the data listed by Davies.[27]

It is interesting to note that the ratio, (δ(OH) monomer)/(δ(OH) associated) out-of-plane, for trifluoroacetic acid is about 1.20 which indicates that the out-of-plane vibration is more affected by association than is the in-plane vibration. As has already been indicated the out-of-plane vibration is also more sensitive to deuterization than is the in-plane vibration.

5. *The* C—O *Stretching Vibration*

The region where the band due to ν(C—O) is to be expected is a crowded one in both the molecules under consideration, so that the assignments made below are less unambiguous than the previous ones. The only band left for assignment to the ν(C—O) vibrations in the vapor spectrum of CF_3COOH is the medium weak band at 1300 cm^{-1}. It becomes much weaker in the spectrum of liquid CF_3COOH as would be expected of a monomer band. No distinct unassigned band was found at the point in the spectrum of CF_3COOH where the corresponding ν(C—O) associated band would be expected or in the spectrum of CF_3COOD where the deuterated ν(C—O) monomer band would appear. However, a consideration of the effect of deuterization on the reduced mass suggests a ratio of ν(C—OH)/ν(C—OD) = 1.06 and the strong 1243 cm^{-1} band which will be assigned to C—F is approximately at the expected position. Similarly the strong 1203 cm^{-1} band in CF_3COOH, already assigned to the δ(OH) in-plane associated vibration, is at the correct position to account also for the ν(C—O) associated vibration.

The only important band left for assignment in CF_3COOD is the medium band at 1155 cm^{-1} in the vapor spectrum. This band is rightly placed both with respect to the 1203 cm^{-1} in CF_3COOH and the 1243 cm^{-1} band in CF_3COOD to be considered as the other ν(C—O) associated band thus completing the set of four ν(C—O) vibration bands; furthermore, its intensity remains unchanged in the spectrum of liquid CF_3COOD after the fashion of bands due to associated vibrations.

B. Bands Assigned to the CF_3 Group

Of the molecules containing CF_3 for which assignments have been reported, hexafluoroethane (C_2F_6),[30] methylfluoroform (CF_3CH_3),[31,32] and sodium trifluoro-

TABLE VII. Comparison of important frequencies (cm^{-1}) in the 1000–2000 cm^{-1} region for fluorinated compounds and for trichloroacetic acid.

CF_3COOH			CF_3COOD			$CF_3COOC_2H_5$		$(CF_3CO)_2O$	CF_3COONa	CCl_3COOH
Vapor	CCl_4 Sol'n	Liquid	Vapor	CCl_4 Sol'n	Liquid	Vapor	Liquid	Vapor	Solid	CCl_4 Sol'n
								1884 S		
1826 MS	1810 Mw		1823 S			1802 S	1780 S	1818 S		1784 w
1788 S	1787 M	1785 S	1734 S		1780 S					1750 S
									1687 Mw	
1465 M	1465 w	1452 w	1432 Mw	1428 M	1430 S		1467			1413 MS
							1405			
			1384 M	1388 M		1390 Mw	1385 M			1395 M
						1352 M	1351 MS	1336 M		
1300 Mw	1292 w									
										1257 Mw
1244 S	1232 M		1243 S			1238 S	1222 S	1251 VS	1227 w	
1203 VS		1200 VS[a]			1220 VS[a]					
1182 VS	1173 MS		1187 S			1188 VS	1162 VS	1205 VS	1186 Mw	
			1155 M		1150 M	1149 VS				1146 w
1130 M										
1123 M							1113 w			
			1039 S		1027 MS		1011 M		1067 vw	

[a] 100 percent absorption *ca* 100 cm^{-1} wide.

[30] Nielsen, Richards, and McMurry, J. Chem. Phys. **16**, 67 (1948).
[31] Cowan, Herzberg, and Sinha, J. Chem. Phys. **18**, 1538 (1950).
[32] Nielsen, Classen, and Smith, J. Chem. Phys. **18**, 1471 (1950).

acetate (CF_3COONa)[33] are structurally the closest to the trifluoroacetic acids. Using the assignments for CF_3CH_3 as a guide, we searched the 600 cm^{-1} and 1200 cm^{-1} regions for the CF_3 group vibrations in CF_3COOH. We did not find it possible to make any definite assignments in the 600 cm^{-1} region, although there are several weak bands which might be considered in the Raman spectrum of the liquid.

Because the 1200 cm^{-1} region in the spectra of CF_3COOH is crowded with bands, we made a spectroscopic study not only of CF_3COOH and CF_3COOD in this region but also of $CF_3COOC_2H_5$, $(CF_3CO)_2O$, CF_3COONa, and CCl_3COOH. The spectra are compared in Table VII. We decided to assign the two C—F stretching vibrations to the bands at 1244 cm^{-1} and 1182 cm^{-1} in CF_3COOH and at 1243 cm^{-1} and 1187 cm^{-1} in CF_3COOD for the following two reasons:

(a) These bands have the clearest counterparts in the spectra of the four other compounds we studied (see Table VII). Strong absorption bands are also present at these points in the following four compounds' infrared spectra which have been published in the literature without analysis: perfluoropropane (C_3F_8),[34] trifluoroacetaldehyde (CF_3CHO),[35] trifluorotrichloroethane CF_3CCl_3,[36] and 1,1,1-trifluoro-3-nitropropane ($CF_3CH_2CH_2NO_2$).[36]

(b) These bands are not shifted by changes in vapor pressure or solution concentration, and are thus unaffected by association as is to be expected of vibrations in which the CF_3 group plays the dominant part.

Our assignment of the C—F stretching vibrations to the 1200 cm^{-1} region is incompatible with the assignments to the 400–600 cm^{-1} range which Fonteyne[33] made for these vibrations in the Raman spectra of CF_3COONa. In this connection it is interesting to note that the C—F vibration bands are among the strongest in the infrared spectra of CF_3COOH and CF_3COOD while the corresponding Raman bands are very weak.

While we are not able to resolve the disagreement as to which CF stretching vibration, the symmetric or the asymmetric, should be assigned to the band at higher of the two frequencies,[31,32] we believe that for molecules in which the perfluoromethyl group is attached to another carbon atom, the two C—F stretching vibrations are about 50 cm^{-1} apart and are to be found in the range 1150–1300 cm^{-1}.

C. Miscellaneous Band Assignments

In line with assignments made in the literature[31,32] a possible candidate for the C—C stretching vibration in CF_3COOH is the medium weak infrared band at 825 cm^{-1} in the vapor state, the medium strong absorption at 810 cm^{-1} in the liquid and the strong Raman band at 813 cm^{-1} in the liquid. The corresponding bands in CF_3COOD lie at 798 cm^{-1}, 785 cm^{-1}, and 791 cm^{-1}, respectively.

The 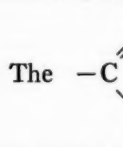 skeletal deformation vibration in monomeric formic acid has been assigned by Thomas[37] to a band at 658 cm^{-1}. Hadzi and Sheppard[21] assign to this vibration mode a band of medium intensity in the spectra of stearic acid and the dicarboxylic acids. A candidate for this vibration mode in CF_3COOH is the medium band at 708 cm^{-1}. Its counterpart in CF_3COOD may account for part of the intensity of the band at 667 cm^{-1}.

The CF_3 twisting vibration[32] may be responsible for the strong Raman line at 260 cm^{-1} in both CF_3COOH and CF_3COOD.

Three medium strong Raman bands in the 400–450 cm^{-1} region of CF_3COOH remain almost unchanged in the Raman spectrum of the deuterated acid. These are possible candidates for the asymmetrical CF_3 rocking frequency which Cowan, Herzberg, and Sinha[31] assign to the 368 cm^{-1} Raman band in CF_3CH_3.

ACKNOWLEDGMENTS

We would like to thank Dr. Carl M. Hill of Tennessee A & I State University and Dr. A. A. Henne of Ohio State University for the compounds which we received from them. Mr. Lawrence K. Akers of Vanderbilt University aided in obtaining the Raman data. Miss Jeanne-Marie Lebas and Mr. Brandt G. Kuperstock of Fisk University helped in the infrared measurements.

The work at Fisk University on this problem has been supported by a Frederick Gardner Cottrell Grant from the Research Corporation.

[33] R. Fonteyne, Natrw. Tijdschr. Belg. **24**, 161 (1942); Chem. Abstracts **38**, 48667 (1944).
[34] Edgell, Mallory, and Weiblen, J. Am. Chem. Soc. **72**, 4858 (1950).
[35] H. Schechter and F. Conrad, J. Am. Chem. Soc. **72**, 3371 (1950).
[36] G. Glockler and W. F. Edgell, J. Chem. Phys. **9**, 387 (1941).
[37] O. Thomas, Disc. Faraday Soc. **9**, 339 (1950).

THE JOURNAL OF CHEMICAL PHYSICS VOLUME 20, NUMBER 10 OCTOBER, 1952

Two-Center Heteronuclear Hybrid Coulomb-Exchange Integrals

R. O. BRENNAN AND J. F. MULLIGAN
*Woodstock College, Woodstock, Maryland**

(Received April 14, 1952)

The method introduced by Sklar and Lyddane, and used by Parr and Crawford, to evaluate two-center hybrid Coulomb-exchange integrals involving atoms with equal effective nuclear charges has been extended to include the case of unequal effective nuclear charges. Formulas for all thirty nonvanishing integrals of this type involving $2s$ and $2p$ Slater atomic orbitals (assuming that the $2s$ and $2p$ orbitals on the same atom have the same screening) are given in a form convenient for numerical calculations. These formulas are valid for both the homonuclear and the heteronuclear cases. The method here given has the advantage that all the integrals are expressed in terms of natural logarithms, exponentials, and exponential integrals, adequate tables of which are readily available. Exact numerical values obtained by this method for thirty hybrids involving carbon and oxygen atomic orbitals in CO_2 are given. These exact values have been used as a check on the validity of an approximation previously employed for these integrals.

I. INTRODUCTION

QUANTUM-MECHANICAL discussions of molecular properties have always been hindered by the large number of cumbersome integrals that occur in the calculations. Up till a few years ago it was customary to obtain approximate values for these integrals by semi-empirical methods. In recent years, however, there has been a shift towards what Mulliken[1] calls "approximate theoretical methods" in the solution of molecular problems. These methods employ exact values for the integrals that turn up, although the wave functions used are still, of course, approximations. As a result, there has recently been a revival of interest in the exact determination of these molecular integrals.

Much progress has been made in the last few years in accumulating formulas and numerical tables for these basic integrals of molecular theory. Important contributions have been made by Kopineck and by Coulson and Barnett. Kopineck[2] has given complete formulas and tables for all two-center molecular integrals involving $2s$ and $2p$ atomic orbitals with equal effective nuclear charges. In this work Kopineck made use of the methods and auxiliary tables given by Kotani, Amemiya, and Simose[3] in 1938–40, but for many years neglected in the literature. Barnett and Coulson[4] have developed a new method of evaluating molecular integrals which is equally valid for equal and unequal effective nuclear charges. They have given formulas for all needed two-center integrals, except exchange integrals, involving atomic orbitals with total quantum number n equal to 1 or 2. The most comprehensive attack on these integrals has been made by the University of Chicago Spectroscopic Laboratory, which has undertaken to prepare formulas and numerical tables for all necessary two-center integrals. To date they have published tables of overlap integrals,[5] and formulas for overlap[5] and other one-electron integrals[6] and for two-electron Coulomb[6] and exchange[7] integrals. Furthermore, formulas for hybrid Coulomb-exchange integrals have been prepared by Rüdenberg and Roothaan and are soon to be published.[8]

In view of the proximate appearance of Roothaan and Rüdenberg's formulas and the existence of the formulas of Coulson and Barnett for these hybrids, the publication of the present paper requires some justification. This is especially true since their work is wider in scope than ours. In place of the thirty nonvanishing integrals for which we have obtained formulas, they have given formulas for all ninety hybrid integrals involving $1s$, $2s$, and $2p$ atomic orbitals. Then also, their integrals are functions of four parameters, i.e., apply to cases in which each of the four wave functions in the integral may have a different effective nuclear charge. The ones published here are functions of two parameters, i.e., all the $n=2$ atomic orbitals on a given atom are assumed to have the same screening.[9] Our case is thus intermediate between the simplest (all nuclear charges equal) and the most general (all nuclear charges different).

Despite these considerations our formulas may be useful for the following reasons: (a) The sooner formulas for hybrid integrals appear in a form suitable for computation,[10] the sooner the work already done by the

* This work was begun while the authors were at the Department of Physics of The Catholic University of America, Washington, D. C.

[1] R. S. Mulliken, Chem. Revs. **41**, 201 (1947).

[2] H.-J. Kopineck, Z. Naturforsch. **5a**, 420 (1950); **6a**, 177 (1951).

[3] Kotani, Amemiya, and Simose, Proc. Phys.-Math. Soc. Japan **20**, extra number 1 (1938); **22**, extra number (1940). Some supplementary formulas and numerical tables of integrals have been given by G. Araki and W. Watari, Prog. Theoret. Phys. **6**, 961 (1951).

[4] M. P. Barnett and C. A. Coulson, Trans. Roy. Soc. (London) **A243**, 221 (1951).

[5] Mulliken, Rieke, Orloff, and Orloff, J. Chem. Phys. **17**, 1248 (1949).

[6] C. C. J. Roothaan, J. Chem. Phys. **19**, 1445 (1951).

[7] K. Rüdenberg, J. Chem. Phys. **19**, 1459 (1951).

[8] Private communication from K. Rüdenberg.

[9] For the thirty hybrids involving $2s$ and $2p$ atomic orbitals given in this paper the more general formulation is required only if it is supposed that the $2s$ and $2p$ orbitals on the same atom have different screening. This refinement has not been given much consideration up to the present, but it may be of importance for future work. Of course, as soon as both $n=1$ and $n=2$ orbitals appear in the same integral, the assumption of three, or four, different effective nuclear charges becomes necessary.

[10] For numerical work the formulas given by Barnett and Coulson require generalized exponential integrals and Bessel functions of half-integral order and imaginary argument, adequate

TABLE I. Identities relating hybrid integrals or parts of hybrid integrals.

$$[2s_a2s_b|2p\sigma_b2p\sigma_b]=[2s_a2s_b|2s_b2s_b]+[2s_a2s_b|Q_{\sigma\sigma}]$$
$$[2s_a2s_b|2p\pi_b2p\pi_b]=[2s_a2s_b|2s_b2s_b]+[2s_a2s_b|Q_{\pi\pi}]$$
$$[2p\sigma_a2s_b|2p\sigma_b2p\sigma_b]=[2p\sigma_a2s_b|2s_b2s_b]+[2p\sigma_a2s_b|Q_{\sigma\sigma}]$$
$$[2p\sigma_a2s_b|2p\pi_b2p\pi_b]=[2p\sigma_a2s_b|2s_b2s_b]+[2p\sigma_a2s_b|Q_{\pi\pi}]$$
$$[2s_a2p\sigma_b|2p\sigma_b2p\sigma_b]=[2s_a2p\sigma_b|2s_b2s_b]+[2s_a2p\sigma_b|Q_{\sigma\sigma}]$$
$$[2s_a2p\sigma_b|2p\pi_b2p\pi_b]=[2s_a2p\sigma_b|2s_b2s_b]+[2s_a2p\sigma_b|Q_{\pi\pi}]$$
$$[2p\sigma_a2p\sigma_b|2p\sigma_b2p\sigma_b]=[2p\sigma_a2p\sigma_b|2s_b2s_b]+[2p\sigma_a2p\sigma_b|Q_{\sigma\sigma}]$$
$$[2p\sigma_a2p\sigma_b|2p\pi_b2p\pi_b]=[2p\sigma_a2p\sigma_b|2s_b2s_b]+[2p\sigma_a2p\sigma_b|Q_{\pi\pi}]$$
$$[2p\pi_a2p\pi_b|2p\sigma_b2p\sigma_b]=[2p\pi_a2p\pi_b|2s_b2s_b]+[2p\pi_a2p\pi_b|Q_{\sigma\sigma}]$$
$$[2p\pi_a2p\pi_b|2p\pi_b2p\pi_b]=[2p\pi_a2p\pi_b|2s_b2s_b]+[2p\pi_a2p\pi_b|Q_{\pi\pi}]$$

$$[2s_a2s_b|Q_{\sigma\sigma}]+2[2s_a2s_b|Q_{\pi\pi}]=0$$
$$[2p\sigma_a2s_b|Q_{\sigma\sigma}]+2[2p\sigma_a2s_b|Q_{\pi\pi}]=0$$
$$[2s_a2p\sigma_b|Q_{\sigma\sigma}]+2[2s_a2p\sigma_b|Q_{\pi\pi}]=0$$
$$[2p\sigma_a2p\sigma_b|Q_{\sigma\sigma}]+2[2p\sigma_a2p\sigma_b|Q_{\pi\pi}]=0$$
$$[2p\pi_a2p\pi_b|Q_{\sigma\sigma}]+[2p\pi_a2p\pi_b|Q_{\pi\pi}]+[2p\bar{\pi}_a2p\bar{\pi}_b|Q_{\pi\pi}]=0$$
$$[2p\bar{\pi}_a2p\bar{\pi}_b|2p\pi_b2p\pi_b]+2[2p\bar{\pi}_a2p\pi_b|2p\pi_b2p\bar{\pi}_b]=[2p\pi_a2p\pi_b|2p\pi_b2p\pi_b]$$
$$[2p\pi_a2p\sigma_b|2s_b2p\pi_b]=[2p\pi_a2p\pi_b|2s_b2p\sigma_b]$$

Chicago group will become useful. In this matter it is a question of all or nothing. (b) An important by-product of the present work are some numerical results which serve at least as a spot-check on an approximation for heteronuclear hybrid integrals proposed by Mulligan.[11] Until adequate numerical tables of these integrals exist in the literature, it is likely that in many cases resort will still be had to approximations in applications to heteronuclear problems. (c) The method used in the present paper differs from that used by the other workers in this field. Barnett and Coulson's work[4] is based on the expansion of exponentials in terms of so-called ζ functions, which involve modified Bessel functions. Rüdenberg and Roothaan[8] have used elliptical coordinates, which had previously been used by Kotani, Amemiya, and Simose,[3] and by Kopineck.[2] The method of the present paper is a generalization of the method used by Sklar and Lyddane[12] and Parr and Crawford[13] for hybrid integrals involving $n=2$ atomic orbitals with equal effective nuclear charges. Although the demonstration of the analytic equivalence of formulas obtained by these different methods would be a herculean task, the numerical evaluation of some cases by these different methods will be a good check on the published formulas.

II. DEFINITIONS AND METHOD

The two-center hybrid Coulomb-exchange integrals (called "ionic integrals" by Kopineck[2] and others) considered in this paper form a class intermediate between the two-center Coulomb integrals and the two-center exchange integrals. This can be seen from the following definitions, in which χ, χ', $\bar{\chi}$, $\bar{\chi}'$ are four different real

TABLE II. Hybrid integrals containing four $2p$ functions. Integrals at column heads are given by the sums of the terms in column 7 multiplied by the coefficients in the table and the power of ρ indicated in column 6. The terms in column 7 are defined in Tables IV and V. Integrals containing four $2p$ functions not listed here may be found by the identities of Table I. $P_6=Z_2^{-1}\xi^{-5/2}\rho^5e^{\rho/2}$.

$4608P_6$ $[2p\sigma_a2p\sigma_b\|Q_{\sigma\sigma}]$	$36864P_6$ $[2p\pi_a2p\pi_b\|Q_{\pi\pi}]$	$36864P_6$ $[2p\bar{\pi}_a2p\bar{\pi}_b\|Q_{\pi\pi}]$	$3072P_6$ $[2p\sigma_a2p\pi_b\|2p\sigma_b2p\pi_b]$	$3072P_6$ $[2p\pi_a2p\sigma_b\|2p\pi_b2p\sigma_b]$		
3	− 9	− 3	−1	1	ρ^0	$J(9,1)+6J(9,0)$
−12	36	12	4	−4		$J(7,3)+6J(7,2)+24J(7,1)+72J(7,0)$
18	−54	−18	−6	6		$J(5,5)+6J(5,4)+24J(5,3)+72J(5,2)+144J(5,1)+144J(5,0)$
−12	36	12	4	−4		$J(3,7)+6J(3,6)+24J(3,5)+72J(3,4)+144J(3,3)+144J(3,2)$
3	− 9	− 3	−1	1		$J(1,9)+6J(1,8)+24J(1,7)+72J(1,6)+144J(1,5)+144J(1,4)$
− 6	36	12	2	−4	ρ^2	$J(7,1)+6J(7,0)$
14	−52	−28	−2	8		$J(5,3)+6J(5,2)+24J(5,1)+72J(5,0)$
−10	− 4	20	−2	−4		$J(3,5)+6J(3,4)+24J(3,3)+72J(3,2)+144J(3,1)+144J(3,0)$
2	20	− 4	2	0		$J(1,7)+6J(1,6)+24J(1,5)+72J(1,4)+144J(1,3)+144J(1,2)$
0	−54	−18	0	6	ρ^4	$J(5,1)+6J(5,0)$
0	− 4	20	0	−4		$J(3,3)+6J(3,2)+24J(3,1)+72J(3,0)$
0	−22	14	0	−2		$J(1,5)+6J(1,4)+24J(1,3)+72J(1,2)+144J(1,1)+144J(1,0)$
6	36	12	−2	−4	ρ^6	$J(3,1)+6J(3,0)$
− 2	20	− 4	−2	0		$J(1,3)+6J(1,2)+24J(1,1)+72J(1,0)$
− 3	− 9	− 3	1	1	ρ^8	$J(1,1)+6J(1,0)$
−1296	3888	1296	432	−432	ρ^0	$6I(5,0)-4I(3,2)+I(1,4)$
4320	1728	−8640	864	1728	ρ^2	$I(3,0)$
− 864	−8640	1728	−864	0		$I(1,2)$
0	9504	−6048	0	864	ρ^4	$I(1,0)$
−1296	3888	1296	432	−432	ρ^0	$\gamma^4(4,4)$
−2592	0	0	864	0	ρ^2	$\gamma^4(3,3)$
5184	−15552	−5184	−1728	1728	ρ^0	$\gamma^2(3,3)$
9504	−24192	−3456	−4320	1728	ρ^2	$\gamma^2(2,2)$
3456	0	0	−3456	0	ρ^4	$\gamma^2(1,1)$

TABLE III. Hybrid integrals containing at least one $2s$ function. For integrals not listed here see Table I. $P_n=Z_2^{-1}\xi^{-n/2}\rho^ne^{\rho/2}$.

tables of which are not readily available. In contrast to this our formulas require only tables of natural logarithms, exponentials, and exponential integrals.

[11] J. F. Mulligan, J. Chem. Phys. **19**, 347 (1951).
[12] A. L. Sklar and R. H. Lyddane, J. Chem. Phys. **7**, 374 (1939).
[13] R. G. Parr and B. L. Crawford, Jr., J. Chem. Phys. **16**, 1049 (1948).

TABLE III. Hybrid integrals containing at least one $2s$ function. For integrals not listed here see Table I. $P_n = Z_2^{-1}\xi^{-5/2}\rho^n e^{\rho/2}$.

A. Coefficients of the terms $\rho^0 J(s,t)$

(s,t)	(7,2)	(7,1)	(7,0)	(5,4)	(5,3)	(5,2)	(5,1)	(5,0)	(3,6)	(3,5)	(3,4)	(3,3)	(3,2)	(3,1)	(1,8)	(1,7)	(1,6)	(1,5)	(1,4)	(1,3)
$1536\sqrt{3}\ P_4[2p\pi_a 2p\sigma_b \mid 2s_b 2p\pi_b]$	−1	−6	−20	3	18	60	120	120	−3	−18	−60	−120	−120		1	6	20	40	40	
$1536\sqrt{3}\ P_4[2p\sigma_a 2p\pi_b \mid 2s_b 2p\pi_b]$	1	6	20	−3	−18	−60	−120	−120	3	18	60	120	120		−1	−6	−20	−40	−40	
$768\sqrt{3}\ P_4[2p\sigma_a 2p\sigma_b \mid 2s_b 2p\sigma_b]$	−1	−6	−20	3	18	60	120	120	−3	−18	−60	−120	−120		1	6	20	40	40	
$1536\sqrt{3}\ P_4[2p\pi_a 2s_b \mid 2p\pi_b 2p\sigma_b]$	−1	−6	−24	3	18	72	216	432	−3	−18	−72	−216	−432	−432	1	6	24	72	144	144
$2304\sqrt{3}\ P_4[2p\sigma_a 2s_b \mid Q_{\sigma\sigma}]$	−3	−18	−72	9	54	216	648	1296	−9	−54	−216	−648	−1296	−1296	3	18	72	216	432	432
$1152\ P_3[2p\sigma_a 2p\sigma_b \mid 2s_b 2s_b]$					1	6	18	24		−2	−12	−36	−48			1	6	18	24	
$2304\ P_3[2p\pi_a 2p\pi_b \mid 2s_b 2s_b]$					1	6	18	24		−2	−12	−36	−48			1	6	18	24	
$1152\ P_3[2p\sigma_a 2s_b \mid 2s_b 2p\sigma_b]$					1	6	20	40		−2	−12	−40	−80	−80		1	6	20	40	40
$2304\ P_3[2p\pi_a 2s_b \mid 2s_b 2p\pi_b]$					1	6	20	40		−2	−12	−40	−80	−80		1	6	20	40	40
$576\sqrt{3}\ P_3[2p\sigma_a 2s_b \mid 2s_b 2s_b]$											−1	−6	−18	−24			1	6	18	24
(s,t)	(8,1)	(8,0)	(6,3)	(6,2)	(6,1)	(6,0)	(4,5)	(4,4)	(4,3)	(4,2)	(4,1)	(4,0)	(2,7)	(2,6)	(2,5)	(2,4)	(2,3)	(2,2)	(2,1)	
$2304\sqrt{3}\ P_4[2s_a 2p\sigma_b \mid Q_{\sigma\sigma}]$	3	18	−9	−54	−216	−648	9	54	216	648	1296	1296	−3	−18	−72	−216	−432	−432		
$1536\sqrt{3}\ P_4[2s_a 2p\pi_b \mid 2p\sigma_b 2p\pi_b]$	−1	−6	3	18	72	216	−3	−18	−72	−216	−432	−432	1	6	24	72	144	144		
$3456\ P_3[2s_a 2s_b \mid Q_{\sigma\sigma}]$				−3	−18	−72		6	36	144	432	864		−3	−18	−72	−216	−432	−432	
$1152\ P_3[2s_a 2p\sigma_b \mid 2s_b 2p\sigma_b]$				−1	−6	−20		2	12	40	80	80		−1	−6	−20	−40	−40		
$2304\ P_3[2s_a 2p\pi_b \mid 2s_b 2p\pi_b]$				1	6	20		−2	−12	−40	−80	−80		1	6	20	40	40		
$576\sqrt{3}\ P_3[2s_a 2p\sigma_b \mid 2s_b 2s_b]$									1	6	18	24			−1	−6	−18	−24		
$576\sqrt{3}\ P_2[2s_a 2s_b \mid 2s_b 2p\sigma_b]$									1	6	20	40			−1	−6	−20	−40	−40	
$864\ P_1[2s_a 2s_b \mid 2s_b 2s_b]$																−1	−6	−18	−24	

B. Coefficients of the terms $\rho^2 J(s,t)$

(s,t)	(5,2)	(5,1)	(5,0)	(3,4)	(3,3)	(3,2)	(3,1)	(3,0)	(1,6)	(1,5)	(1,4)	(1,3)	(1,2)	(1,1)
$1536\sqrt{3}\ P_4[2p\pi_a 2p\sigma_b \mid 2s_b 2p\pi_b]$	3	18	60	−2	−12	−40	−80	−80	−1	−6	−20	−40	−40	
$1536\sqrt{3}\ P_4[2p\sigma_a 2p\pi_b \mid 2s_b 2p\pi_b]$	−1	−6	−20	−2	−12	−40	−80	−80	3	18	60	120	120	
$768\sqrt{3}\ P_4[2p\sigma_a 2p\sigma_b \mid 2s_b 2p\sigma_b]$	1	6	20	−2	−12	−40	−80	−80	1	6	20	40	40	
$1536\sqrt{3}\ P_4[2p\pi_a 2s_b \mid 2p\pi_b 2p\sigma_b]$	3	18	72	−2	−12	−48	−144	−288	−1	−6	−24	−72	−144	−144
$2304\sqrt{3}\ P_4[2p\sigma_a 2s_b \mid Q_{\sigma\sigma}]$	3	18	72	−2	−12	−48	−144	−288	−1	−6	−24	−72	−144	−144
$1152\ P_3[2p\sigma_a 2p\sigma_b \mid 2s_b 2s_b]$														
$2304\ P_3[2p\pi_a 2p\pi_b \mid 2s_b 2s_b]$					−2	−12	−36	−48		−2	−12	−36	−48	
$1152\ P_3[2p\sigma_a 2s_b \mid 2s_b 2p\sigma_b]$														
$2304\ P_3[2p\pi_a 2s_b \mid 2s_b 2p\pi_b]$					−2	−12	−40	−80		−2	−12	−40	−80	−80
$576\sqrt{3}\ P_2[2p\sigma_a 2s_b \mid 2s_b 2s_b]$											−1	−6	−18	−24
(s,t)	(6,1)	(6,0)	(4,3)	(4,2)	(4,1)	(4,0)	(2,5)	(2,4)	(2,3)	(2,2)	(2,1)	(2,0)		
$2304\sqrt{3}\ P_4[2s_a 2p\sigma_b \mid Q_{\sigma\sigma}]$	−9	−54	14	84	336	1008	−5	−30	−120	−360	−720	−720		
$1536\sqrt{3}\ P_4[2s_a 2p\pi_b \mid 2p\sigma_a 2p\pi_b]$	3	18	−2	−12	−48	−144	−1	−6	−24	−72	−144	−144		
$3456\ P_3[2s_a 2s_b \mid Q_{\sigma\sigma}]$				6	36	144		−2	−12	−48	−144	−288		
$1152\ P_3[2s_a 2p\sigma_b \mid 2s_b 2p\sigma_b]$				2	12	40		−2	−12	−40	−80	−80		
$2304\ P_3[2s_a 2p\pi_b \mid 2s_b 2p\pi_b]$				−2	−12	−40		−2	−12	−40	−80	−80		
$576\sqrt{3}\ P_2[2s_a 2p\sigma_b \mid 2s_b 2s_b]$									−1	−6	−18	−24		
$576\sqrt{3}\ P_2[2s_a 2s_b \mid 2s_b 2p\sigma_b]$									−1	−6	−20	−40		
$864\ P_1[2s_a 2s_b \mid 2s_b 2s_b]$														

TABLE III.—(*Continued*).

C. Coefficients of the terms $\rho^4 J(s,t)$

(s,t)	(3,2)	(3,1)	(3,0)	(1,4)	(1,3)	(1,2)	(1,1)	(1,0)
$1536\sqrt{3}\ P_4[2p\pi_a 2p\sigma_b \mid 2s_b 2p\pi_b]$	−3	−18	−60	−1	−6	−20	−40	−40
$1536\sqrt{3}\ P_4[2p\sigma_a 2p\pi_b \mid 2s_b 2p\pi_b]$	−1	−6	−20	−3	−18	−60	−120	−120
$768\sqrt{3}\ P_4[2p\sigma_a 2p\sigma_b \mid 2s_b 2p\sigma_b]$	1	6	20	−1	−6	−20	−40	−40
$1536\sqrt{3}\ P_4[2p\pi_a 2s_b \mid 2p\pi_b 2p\sigma_b]$	−3	−18	−72	−1	−6	−24	−72	−144
$2304\sqrt{3}\ P_4[2p\sigma_a 2s_b \mid Q_{\sigma\sigma}]$	3	18	72	1	6	24	72	144
$1152\ P_3[2p\sigma_a 2p\sigma_b \mid 2s_b 2s_b]$					−1	−6	−18	−24
$2304\ P_3[2p\pi_a 2p\pi_b \mid 2s_b 2s_b]$					1	6	18	24
$1152\ P_3[2p\sigma_a 2s_b \mid 2s_b 2p\sigma_b]$					−1	−6	−20	−40
$2304\ P_3[2p\pi_a 2s_b \mid 2s_b 2p\pi_b]$					1	6	20	40
$576\sqrt{3}\ P_2[2p\sigma_a 2s_b \mid 2s_b 2s_b]$								
(s,t)	(4,1)	(4,0)	(2,3)	(2,2)	(2,1)	(2,0)		
$2304\sqrt{3}\ P_4[2s_a 2p\sigma_b \mid Q_{\sigma\sigma}]$	9	54	−5	−30	−120	−360		
$1536\sqrt{3}\ P_4[2s_a 2p\pi_b \mid 2p\sigma_b 2p\pi_b]$	−3	−18	−1	−6	−24	−72		
$3456\ P_3[2s_a 2s_b \mid Q_{\sigma\sigma}]$				−3	−18	−72		
$1152\ P_3[2s_a 2p\sigma_b \mid 2s_b 2p\sigma_b]$				−1	−6	−20		
$2304\ P_3[2s_a 2p\pi_b \mid 2s_b 2p\pi_b]$				1	6	20		
$576\sqrt{3}\ P_2[2s_a 2p\sigma_b \mid 2s_b 2s_b]$								
$576\sqrt{3}\ P_2[2s_a 2s_b \mid 2s_b 2p\sigma_b]$								
$864\ P_1[2s_a 2s_b \mid 2s_b 2s_b]$								

D. Coefficients of the terms $\rho^6 J(s,t)$

(1,2)	(1,1)	(1,0)
1	6	20
1	6	20
−1	−6	−20
1	6	24
−3	−18	−72
(2,1)	(2,0)	
−3	−18	
1	6	

E. Coefficients of the terms $\rho^n I(s,t)$

	$\rho^0 I(s,t)$					$\rho^2 I(s,t)$			$\rho^4 I(s,t)$
(s,t)	(5,0)	(3,2)	(3,1)	(1,4)	(1,3)	(3,0)	(1,2)	(1,1)	(1,0)
$1536\sqrt{3}\ P_4[2p\pi_a 2p\sigma_b \mid 2s_b 2p\pi_b]$	−360	360		−120		240	120		120
$1536\sqrt{3}\ P_4[2p\sigma_a 2p\pi_b \mid 2s_b 2p\pi_b]$	360	−360		120		240	−360		360
$768\sqrt{3}\ P_4[2p\sigma_a 2p\sigma_b \mid 2s_b 2p\sigma_b]$	−360	360		−120		240	−120		120
$1536\sqrt{3}\ P_4[2p\pi_a 2s_b \mid 2p\pi_b 2p\sigma_b]$			1296		−432			432	
$2304\sqrt{3}\ P_4[2p\sigma_a 2s_b \mid Q_{\sigma\sigma}]$			3888		−1296			432	
$1152\ P_3[2p\sigma_a 2p\sigma_b \mid 2s_b 2s_b]$	−72	144		−72					72
$2304\ P_3[2p\pi_a 2p\pi_b \mid 2s_b 2s_b]$	−72	144		−72		144	144		−72
$1152\ P_3[2p\sigma_a 2s_b \mid 2s_b 2p\sigma_b]$			240		−120				
$2304\ P_3[2p\pi_a 2s_b \mid 2s_b 2p\pi_b]$			240		−120			240	
$576\sqrt{3}\ P_2[2p\sigma_a 2s_b \mid 2s_b 2s_b]$			72		−72			72	
(s,t)	(4,0)	(2,2)	(2,1)			(2,0)			
$2304\sqrt{3}\ P_4[2s_a 2p\sigma_b \mid Q_{\sigma\sigma}]$	−3888	1296				2160			
$1536\sqrt{3}\ P_4[2s_a 2p\pi_b \mid 2p\sigma_b 2p\pi_b]$	1296	−432				432			
$3456\ P_3[2s_a 2s_b \mid Q_{\sigma\sigma}]$			1296						
$1152\ P_3[2s_a 2p\sigma_b \mid 2s_b 2p\sigma_b]$	−240	120				240			
$2304\ P_3[2s_a 2p\pi_b \mid 2s_b 2p\pi_b]$	240	−120				240			
$576\sqrt{3}\ P_2[2s_a 2p\sigma_b \mid 2s_b 2s_b]$	−72	72				72			
$576\sqrt{3}\ P_2[2s_a 2s_b \mid 2s_b 2p\sigma_b]$			120						
$864\ P_1[2s_a 2s_b \mid 2s_b 2s_b]$			72						

Slater atomic orbitals, a and b indicate the atoms concerned, and 1 and 2 number the electrons:[14]

Coulomb integral—

$$[\chi_a\chi_a' \mid \bar{\chi}_b\bar{\chi}_b'] = \int\int \chi_a(1)\bar{\chi}_b(2)(2/r_{12})\chi_a'(1)\bar{\chi}_b'(2)dv_1dv_2;$$

exchange integral—

$$[\chi_a\chi_b' \mid \bar{\chi}_a\bar{\chi}_b'] = \int\int \chi_a(1)\bar{\chi}_a(2)(2/r_{12})\chi_b'(1)\bar{\chi}_b'(2)dv_1dv_2;$$

hybrid, or hybrid Coulomb-exchange (or "ionic") integral—

$$[\chi_a\chi_b' \mid \bar{\chi}_b\bar{\chi}_b'] = \int\int \chi_a(1)\bar{\chi}_b(2)(2/r_{12})\chi_b'(1)\bar{\chi}_b'(2)dv_1dv_2.$$

The Coulomb integral measures the classical Coulomb interaction of two electron distributions $\chi_a\chi_a'$ and $\bar{\chi}_b\bar{\chi}_b'$ centered on atom a and atom b, respectively. The ex-

[14] Throughout this paper atomic units are used: distances in units of the first Bohr radius $a_0 = 0.5292$ A, energies in units of $e^2/2a_0 = 13.602$ ev. The definitions of these integrals differ from those given by Roothaan and Rüdenberg in the presence of $(2/r_{12})$ instead of $(1/r_{12})$ in the integrand. This corresponds to our use of atomic energy units which are one-half the units they employed.

TABLE III.—(*Continued*).

F. Coefficients of the terms $\rho^n\gamma^j(s,t)$

	$\gamma^3(3,3)$	$\rho^2\gamma^3(2,2)$	$\gamma^2(3,3)$	$\rho^2\gamma^2(2,2)$	$K(5)$	$\rho^2K(3)$	$\rho^4K(1)$
$1536\sqrt{3}\ P_4[2p\pi_a2p\sigma_b\|2s_b2p\pi_b]$			120				
$1536\sqrt{3}\ P_4[2p\sigma_a2p\pi_b\|2s_b2p\pi_b]$			−120	−240			
$768\sqrt{3}\ P_4[2p\sigma_a2p\sigma_b\|2s_b2p\sigma_b]$			120	240			
$1536\sqrt{3}\ P_4[2p\pi_a2s_b\|2p\pi_b2p\sigma_b]$	432				−1296	864	432
$2304\sqrt{3}\ P_4[2p\sigma_a2s_b\|Q_{\sigma\sigma}]$	1296	2592			−3888	864	−432
$1152\ P_3[2p\sigma_a2p\sigma_b\|2s_b2s_b]$							
$2304\ P_3[2p\pi_a2p\pi_b\|2s_b2s_b]$							
$1152\ P_3[2p\sigma_a2s_b\|2s_b2p\sigma_b]$					−120		120
$2304\ P_3[2p\pi_a2s_b\|2s_b2p\pi_b]$					−120	240	−120
$576\sqrt{3}\ P_2[2p\sigma_a2s_b\|2s_b2s_b]$							
	$[\gamma^4(4,3)+\gamma^4(3,4)]$	$[\gamma^3(3,2)+\gamma^3(2,3)]$	$[\gamma^2(3,2)+\gamma^2(2,3)]$	$\rho^2[\gamma^2(2,1)+\gamma^2(1,2)]$	$K(4)$		$\rho^2K(2)$
$2304\sqrt{3}\ P_4[2s_a2p\sigma_b\|Q_{\sigma\sigma}]$	−648		1944	864			
$1536\sqrt{3}\ P_4[2s_a2p\pi_b\|2p\sigma_b2p\pi_b]$	216		−648	−864			
$3456\ P_3[2s_a2s_b\|Q_{\sigma\sigma}]$		648			−2592		864
$1152\ P_3[2s_a2p\sigma_b\|2s_b2p\sigma_b]$			60				
$2304\ P_3[2s_a2p\pi_b\|2s_b2p\pi_b]$			−60				
$576\sqrt{3}\ P_2[2s_a2p\sigma_b\|2s_b2s_b]$							
$576\sqrt{3}\ P_2[2s_a2s_b\|2s_b2p\sigma_b]$					−120		120
$864\ P_1[2s_a2s_b\|2s_b2s_b]$							

change integral measures the interaction of two electrons, each of which is exchanged between the two atoms. The hybrid integral measures the interaction of one electron exchanged between the two atoms, and the charge distribution $\bar{\chi}_b\bar{\chi}_b'$ of the second electron on atom b. From this definition it is clear why the name "ionic integral" is an apt one.

The atomic orbitals used in the calculations are the following Slater[15] $2s$ and $2p$ atomic orbitals:

$$(2s)=(Z^5/96\pi)^{\frac{1}{2}}r\exp(-Zr/2),$$
$$(2p\sigma)=(Z^5/32\pi)^{\frac{1}{2}}r\cos\theta\exp(-Zr/2),$$
$$(2p\pi)=(Z^5/32\pi)^{\frac{1}{2}}r\sin\theta\cos\phi\exp(-Zr/2),$$
$$(2p\bar{\pi})=(Z^5/32\pi)^{\frac{1}{2}}r\sin\theta\sin\phi\exp(-Zr/2).$$

The Slater $2s$ orbital is a nodeless atomic orbital which is not orthogonal to the $1s$ orbital on the same atom. For orbitals centered on atom a the effective nuclear charge (Z) is denoted by Z_1, for those on atom b by Z_2.

The integration over the coordinates of electron 2 may be carried out easily in polar coordinates. The results of the first integration have been summarized by Mulligan[11] for all the cases needed here. For the subsequent integration over the coordinates of electron 1 the dipolar coordinate system used by Sklar and Lyddane[12] and Parr and Crawford[13] has been used. They used the coordinates $\alpha=r_aZ$, $\beta=r_bZ$, and ϕ, the azimuthal angle. In our case, however, we now have not a single Z but two different Z's. Hence we use a coordinate system consisting of $\alpha=r_aZ_2$, $\beta=r_bZ_2$, and ϕ, and define a new parameter $\xi=Z_1/Z_2$. We also introduce the quantity $\rho=Z_2R$, where R is the internuclear distance in atomic units.[16] All the formulas given below are functions of these two parameters, ξ and ρ. For simplicity this dependence is not explicitly included in the notation adopted, but is presumed throughout.

The derivation of the formulas now proceeds in a manner very similar to that used by Parr and Crawford,[13] but slightly more complicated due to the unequal effective nuclear charges. We shall not go into the tedious algebraic work involved in the derivations, but shall merely give the new definitions of the functions required, and the resulting formulas for the 30 nonvanishing hybrid integrals involving $2s$ and $2p$ Slater functions. In the case of equal effective nuclear charges, our formulas of course reduce to those of Parr and Crawford for the comparatively few cases they give. This was used as a check on our final formulas.

III. RESULTS

A. Integrals Involving Four $2p$ Atomic Orbitals

Though the integrals involving four $2p$ atomic orbitals are the most complicated, the many relations existing among them help to simplify the calculations. It was mentioned above that the hybrid integrals arise from the interaction of an exchanged electron in the field of an electronic charge distribution confined to a single atom. It has been noted that in the case of $2p$ functions the potential of these charge distributions consists of one or two terms which become classical pole and quadrupole terms in the limit of large distances.[6,11] The pole term of the $(2p)^2$ distribution is the

[15] J. C. Slater, Phys. Rev. **36**, 57 (1930).

[16] This definition of ρ is the one used by Sklar and Lyddane and by Parr and Crawford. It differs from the corresponding variable used in the more recent papers in that it does not include the principal quantum number n (equal to 2 in this case).

TABLE IV. Definitions and recurrence relations for the component integrals occurring in Tables II and III. For the expansions of the $\gamma^j(s,t)$ see Table V. The parameters that occur here are defined as follows: $\eta=\frac{1}{2}(\xi+1)$, $\nu=\frac{1}{2}(\xi+3)$, $\epsilon=\frac{1}{2}(1-\xi)$, $\mu=\frac{1}{2}(3-\xi)$; γ is Euler's constant.

Integral	Starting Value	Recurrence Formula	Range of Parameters
$A_s=e^{\nu\rho}\int_\rho^\infty e^{-\nu\alpha}\alpha^s d\alpha$	$A_0=1/\nu$	$A_s=(1/\nu)[\rho^s+sA_{s-1}]$	
$B_s=e^{-\rho}\int_0^\rho e^{\mu\alpha}\alpha^s d\alpha$	$B_0=(1/\mu)(e^{\epsilon\rho}-e^{-\rho})$	$B_s=(1/\mu)[e^{\epsilon\rho}\rho^s-sB_{s-1}]$	
$C_s=e^{\eta\rho}\int_\rho^\infty e^{-\eta\alpha}\alpha^s d\alpha$	$C_0=1/\eta$	$C_s=(1/\eta)[\rho^s+sC_{s-1}]$	
$D_s=e^{\mu\rho}\int_0^\rho e^{-\mu\alpha}\alpha^s d\alpha$	$D_0=(1/\mu)(e^{\mu\rho}-1)$	$D_s=(1/\mu)[sD_{s-1}-\rho^s]$	$s=0, 1, \cdots, 9$
$G_s=\int_0^\rho e^{\epsilon\alpha}\alpha^s d\alpha$	$G_0=(1/\epsilon)(e^{\epsilon\rho}-1)$	$G_s=(1/\epsilon)[e^{\epsilon\rho}\rho^s-sG_{s-1}]$	
$H_s=e^{\epsilon\rho}\int_0^\rho e^{-\epsilon\alpha}\alpha^s d\alpha$	$H_0=(1/\epsilon)(e^{\epsilon\rho}-1)$	$H_s=(1/\epsilon)[sH_{s-1}-\rho^s]$	
$I(s,t)=\frac{1}{2}e^{\rho/2}\int\int e^{-\frac{1}{2}(\xi\alpha+\beta)}\alpha^s\beta^t d\alpha d\beta$	$I(s,0)=i(s,0)+j(s,0)$	$I(s,t)=2tI(s,t-1)+i(s,t)+j(s,t)$	$(s,t)=(1,0)\ (2,0)\ (3,0)\ (4,0)\ (5,0)$ $(1,1)\ (2,1)\ (3,1)$ $(1,2)\ (2,2)\ (3,2)$ $(1,3)$ $(1,4)$
$i(s,t)=-\int_0^\infty e^{-\eta\alpha}\alpha^s(\rho+\alpha)^t d\alpha+e^\rho\int_\rho^\infty e^{-\eta\alpha}\alpha^s(\alpha-\rho)^t d\alpha$	$i(s,0)=-s!/\eta^{s+1}+e^{\epsilon\rho}C_s$ $i(0,t)=e^{\epsilon\rho}t!/\eta^{t+1}-C_t$	$i(s,t)=(1/\eta)[si(s-1,t)+ti(s,t-1)]$	
$j(s,t)=\int_0^\rho e^{\epsilon\alpha}\alpha^s(\rho-\alpha)^t d\alpha$	$j(s,0)=G_s$	$j(s,t)=(1/\epsilon)[tj(s,t-1)-sj(s-1,t)]$	$\xi\neq 1$
	$j(0,t)=H_t$	or $j(s,t)=[t/(s+1)]j(s+1,t-1)$	$\xi=1$
$J(s,t)=\frac{3}{2}e^{\rho/2}\int\int e^{-\frac{1}{2}(\xi\alpha+3\beta)}\alpha^s\beta^t d\alpha d\beta$	$J(s,0)=f(s,0)+g(s,0)$	$J(s,t)=(2t/3)J(s,t-1)+f(s,t)+g(s,t)$	$(s,t)=(1,0)\ (2,0)\ \cdots\ (8,0)\ (9,0)$ $(1,1)\ (2,1)\ \cdots\ (8,1)\ (9,1)$ $(1,2)\ (2,2)\ \cdots\ (8,2)\ (9,2)$ $(1,3)\ (2,3)\ \cdots\ (7,3)$ $\cdots\ \cdots\ \cdots$ $(1,8)\ (2,8)$ $(1,9)$
$f(s,t)=e^{-\rho}\int_0^\rho e^{\mu\alpha}\alpha^s(\rho-\alpha)^t d\alpha$	$f(s,0)=B_s$ $f(0,t)=e^{-\rho}D_t$	$f(s,t)=(1/\mu)[tf(s,t-1)-sf(s-1,t)]$	
$g(s,t)=-e^{-\rho}\int_0^\infty e^{-\nu\alpha}\alpha^s(\alpha+\rho)^t d\alpha+e^{2\rho}\int_\rho^\infty e^{-\nu\alpha}\alpha^s(\alpha-\rho)^t d\alpha$	$g(s,0)=e^{\epsilon\rho}A_s-e^{-\rho}s!/\nu^{s+1}$ $g(0,t)=-e^{-\rho}A_t+e^{\epsilon\rho}t!/\nu^{t+1}$	$g(s,t)=(1/\nu)[sg(s-1,t)+tg(s,t-1)]$	
$K(s)=\frac{1}{2}e^{\rho/2}\int\int e^{-\frac{1}{2}(\xi\alpha+3\beta)}\alpha^s(e^\beta-1)\beta^{-1}d\alpha d\beta$	$K(0)=m(0)+n(0)$	$K(s)=(2s/\xi)K(s-1)+m(s)+n(s)$	
$m(s)=(e^{\eta\rho}/\xi)\int_\rho^\infty e^{-\nu\beta}(e^\beta-1)(\beta-\rho)^s\beta^{-1}d\beta$	$m(0)=(e^{\eta\rho}/\xi)[Ei(-\nu\rho)-Ei(-\eta\rho)]$	$m(s)=[(s-1)!/\xi][1/\eta^s-e^{-\rho}/\nu^s]-\rho m(s-1)$	
$n(s)=(e^{\epsilon\rho}/\xi)\Big[-\int_0^\infty e^{-\nu\beta}(e^\beta-1)\beta^{-1}(\rho+\beta)^s d\beta$ $+\int_0^\rho e^{-\mu\beta}(e^\beta-1)\beta^{-1}(\rho-\beta)^s d\beta\Big]$		$n(s)=(1/\xi)[e^{\epsilon\rho}A_{s-1}+B_{s-1}-e^{\epsilon\rho}C_{s-1}-G_{s-1}]$ $+\rho n(s-1)$	$s=0, 1, \cdots, 9$
	$n(0)=(e^{\epsilon\rho}/\xi)[\ln(\eta\mu/\epsilon\nu)+Ei(-\epsilon\rho)$ $-Ei(-\mu\rho)]$		$\xi<1$
	$n(0)=\ln(\rho/2)+\gamma-Ei(-\rho)$		$\xi=1$
	$n(0)=(e^{\epsilon\rho}/\xi)[\ln(\eta\mu/\lvert\epsilon\rvert\nu)+Ei(\lvert\epsilon\rho\rvert)$ $-Ei(-\mu\rho)]$		$1<\xi<3$
	$n(0)=(e^{-\rho}/3)[\ln(2/3\rho)-\gamma+Ei(\rho)]$		$\xi=3$
	$n(0)=(e^{\epsilon\rho}/\xi)[\ln(\eta\mu/\epsilon\nu)+Ei(\lvert\epsilon\rho\rvert)$ $-Ei(\lvert\mu\rho\rvert)]$		$\xi>3$

$\gamma^j(s,t)=\frac{1}{2}e^{\rho/2}\int\int e^{-\frac{1}{2}(\xi\alpha+3\beta)}(\alpha+\rho)^s(\alpha-\rho)^t\left[e^\beta-\left(1+\beta+\frac{1}{2}\beta^2+\cdots+\frac{\beta^{j-1}}{(j-1)!}\right)\right]\beta^{-j}d\alpha d\alpha d\beta$ See Table V.

TABLE V. Expansion of the integrals $\gamma^j(s,t)$. For definitions see Table IV.

$$
\begin{aligned}
48\gamma^4(4,4) = &-K(9)+4\rho^2K(7)-6\rho^4K(5)+4\rho^6K(3)-\rho^8K(1)\\
&+\{-8(C_6+H_6)+2(C_7+H_7)-(C_8+H_8)-e^{-\rho}[-8(A_6+D_6)-6(A_7+D_7)-3(A_8+D_8)]\}\\
&+\rho\{72(C_5+H_5)-18(C_6+H_6)+9(C_7+H_7)-e^{-\rho}[72(A_5+D_5)+54(A_6+D_6)+27(A_7+D_7)]\}\\
&+\rho^2\{-256(C_4+H_4)+64(C_5+H_5)-32(C_6+H_6)-e^{-\rho}[-256(A_4+D_4)-192(A_5+D_5)-96(A_6+D_6)]\}\\
&+\rho^3\{448(C_3+H_3)-112(C_4+H_4)+56(C_5+H_5)-e^{-\rho}[448(A_3+D_3)+336(A_4+D_4)+168(A_5+D_5)]\}\\
&+\rho^4\{-384(C_2+H_2)+96(C_3+H_3)-48(C_4+H_4)-e^{-\rho}[-384(A_2+D_2)-288(A_3+D_3)-144(A_4+D_4)]\}\\
&+\rho^5\{128(C_1+H_1)-32(C_2+H_2)+16(C_3+H_3)-e^{-\rho}[128(A_1+D_1)+96(A_2+D_2)+48(A_3+D_3)]\}\\
&+e^{\epsilon\rho}\{-5760/\nu^7-30240/\nu^8-120960/\nu^9+5760/\eta^7-10080/\eta^8+40320/\eta^9\\
&+\rho(-8640/\nu^6-38880/\nu^7-136080/\nu^8+8640/\eta^6-12960/\eta^7+45360/\eta^8)\\
&+\rho^2(-6144/\nu^5-23040/\nu^6-69120/\nu^7+6144/\eta^5-7680/\eta^6+23040/\eta^7)\\
&+\rho^3(-2688/\nu^4-8064/\nu^5-20160/\nu^6+2688/\eta^4-2688/\eta^5+6720/\eta^6)\\
&+\rho^4(-768/\nu^3-1728/\nu^4-3456/\nu^5+768/\eta^3-576/\eta^4+1152/\eta^5)+\rho^5(-128/\nu^2-192/\nu^3-288/\nu^4+128/\eta^2-64/\eta^3+96/\eta^4)\}.
\end{aligned}
$$

$$
\begin{aligned}
48[\gamma^4(4,3)+\gamma^4(3,4)] = &-2K(8)+6\rho^2K(6)-6\rho^4K(4)+2\rho^6K(2)\\
&+\{-16(C_5-H_5)+4(C_6-H_6)-2(C_7-H_7)-e^{-\rho}[-16(A_5-D_5)-12(A_6-D_6)-6(A_7-D_7)]\}\\
&+\rho\{128(C_4-H_4)-32(C_5-H_5)+16(C_6-H_6)-e^{-\rho}[128(A_4-D_4)+96(A_5-D_5)+48(A_6-D_6)]\}\\
&+\rho^2\{-400(C_3-H_3)+100(C_4-H_4)-50(C_5-H_5)-e^{-\rho}[-400(A_3-D_3)-300(A_4-D_4)-150(A_5-D_5)]\}\\
&+\rho^3\{608(C_2-H_2)-152(C_3-H_3)+76(C_4-H_4)-e^{-\rho}[608(A_2-D_2)+456(A_3-D_3)+228(A_4-D_4)]\}\\
&+\rho^4\{-448(C_1-H_1)+112(C_2-H_2)-56(C_3-H_3)-e^{-\rho}[-448(A_1-D_1)-336(A_2-D_2)-168(A_3-D_3)]\}\\
&+\rho^5\{128(C_0-H_0)-32(C_1-H_1)+16(C_2-H_2)-e^{-\rho}[128(A_0-D_0)+96(A_1-D_1)+48(A_2-D_2)]\}\\
&+e^{\epsilon\rho}\{-1920/\nu^6-8640/\nu^7-30240/\nu^8+1920/\eta^6-2880/\eta^7+10080/\eta^8\\
&+\rho(-3072/\nu^5-11520/\nu^6-34560/\nu^7+3072/\eta^5-3840/\eta^6+11520/\eta^7)\\
&+\rho^2(-2400/\nu^4-7200/\nu^5-18000/\nu^6+2400/\eta^4-2400/\eta^5+6000/\eta^6)\\
&+\rho^3(-1216/\nu^3-2736/\nu^4-5472/\nu^5+1216/\eta^3-912/\eta^4+1824/\eta^5)\\
&+\rho^4(-448/\nu^2-672/\nu^3-1008/\nu^4+448/\eta^2-224/\eta^3+336/\eta^4)+\rho^5(-128/\nu-96/\nu^2-96/\nu^3+128/\eta-32/\eta^2+32/\eta^3)\}.
\end{aligned}
$$

$$
\begin{aligned}
6\gamma^4(3,3) = &-\gamma^3(3,3)-\{C_4+H_4-e^{-\rho}[(A_4+D_4)+(A_5+D_5)+\tfrac{1}{2}(A_6+D_6)]\}+7\rho\{C_3+H_3-e^{-\rho}[(A_3+D_3)+(A_4+D_4)+\tfrac{1}{2}(A_5+D_5)]\}\\
&-18\rho^2\{C_2+H_2-e^{-\rho}[(A_2+D_2)+(A_3+D_3)+\tfrac{1}{2}(A_4+D_4)]\}+20\rho^3\{C_1+H_1-e^{-\rho}[(A_1+D_1)+(A_2+D_2)+\tfrac{1}{2}(A_3+A_3)]\}\\
&-8\rho^4\{C_0+H_0-e^{-\rho}[(A_0+D_0)+(A_1+D_1)+\tfrac{1}{2}(A_2+D_2)]\}-e^{\epsilon\rho}\{24(1/\nu^5+5/\nu^6+15/\nu^7-1/\eta^5)\\
&+42\rho(1/\nu^4+4/\nu^5+10/\nu^6-1/\eta^4)+36\rho^2(1/\nu^3+3/\nu^4+6/\nu^5-1/\eta^3)\\
&+20\rho^3(1/\nu^2+2/\nu^3+3/\nu^4-1/\eta^2)+8\rho^4(1/\nu+1/\nu^2+1/\nu^3-1/\eta)\}.
\end{aligned}
$$

$$
\begin{aligned}
4\gamma^3(3,3) = &-\gamma^2(3,3)-\{C_5+H_5-e^{-\rho}[(A_5+D_5)+(A_6+D_6)]\}+7\rho\{C_4+H_4-e^{-\rho}[(A_4+D_4)+(A_5+D_5)]\}\\
&-18\rho^2\{C_3+H_3-e^{-\rho}[(A_3+D_3)+(A_4+D_4)]\}+20\rho^3\{C_2+H_2-e^{-\rho}[(A_2+D_2)+(A_3+D_3)]\}\\
&-8\rho^4\{C_1+H_1-e^{-\rho}[(A_1+D_1)+(A_2+D_2)]\}-e^{\epsilon\rho}\{120(1/\nu^6+6/\nu^7-1/\eta^6)+168\rho(1/\nu^5+5/\nu^6-1/\eta^5)\\
&+108\rho^2(1/\nu^4+4/\nu^5-1/\eta^4)+40\rho^3(1/\nu^3+3/\nu^4-1/\eta^3)+8\rho^4(1/\nu^2+2/\nu^3-1/\eta^2)\}.
\end{aligned}
$$

$$
\begin{aligned}
2\gamma^2(3,3) = &-K(7)+3\rho^2K(5)-3\rho^4K(3)+\rho^6K(1)-\{C_6+H_6-e^{-\rho}(A_6+D_6)\}+7\rho\{C_5+H_5-e^{-\rho}(A_5+D_5)\}\\
&-18\rho^2\{C_4+H_4-e^{-\rho}(A_4+D_4)\}+20\rho^3\{C_3+H_3-e^{-\rho}(A_3+D_3)\}-8\rho^4\{C_2+H_2-e^{-\rho}(A_2+D_2)\}\\
&-e^{\epsilon\rho}\{720(1/\nu^7-1/\eta^7)+840\rho(1/\nu^6-1/\eta^6)+432\rho^2(1/\nu^5-1/\eta^5)+120\rho^3(1/\nu^4-1/\eta^4)+16\rho^4(1/\nu^3-1/\eta^3)\}.
\end{aligned}
$$

$$
\begin{aligned}
4[\gamma^3(3,2)+\gamma^3(2,3)] = &-[\gamma^2(3,2)+\gamma^2(2,3)]-2\{C_4-H_4-e^{-\rho}[(A_4-D_4)+(A_5-D_5)]\}+12\rho\{C_3-H_3-e^{-\rho}[(A_3-D_3)+(A_4-D_4)]\}\\
&-26\rho^2\{C_2-H_2-e^{-\rho}[(A_2-D_2)+(A_3-D_3)]\}+24\rho^3\{C_1-H_1-e^{-\rho}[(A_1-D_1)+(A_2-D_2)]\}\\
&-8\rho^4\{C_0-H_0-e^{-\rho}[(A_0-D_0)+(A_1-D_1)]\}-e^{\epsilon\rho}\{48(1/\nu^5+5/\nu^6-1/\eta^5)+72\rho(1/\nu^4+4/\nu^5-1/\eta^4)\\
&+52\rho^2(1/\nu^3+3/\nu^4-1/\eta^3)+24\rho^3(1/\nu^2+2/\nu^3-1/\eta^2)+8\rho^4(1/\nu+1/\nu^2-1/\eta)\}.
\end{aligned}
$$

$$
\begin{aligned}
2[\gamma^3(3,2)+\gamma^3(2,3)] = &-2K(6)+4\rho^2K(4)-2\rho^4K(2)-2\{C_5-H_5-e^{-\rho}(A_5-D_5)\}+12\rho\{C_4-H_4-e^{-\rho}(A_4-D_4)\}\\
&-26\rho^2\{(C_3-H_3-e^{-\rho}(A_3-D_3)\}+24\rho^3\{C_2-H_2-e^{-\rho}(A_2-D_2)\}-8\rho^4\{C_1-H_1-e^{-\rho}(A_1-D_1)\}\\
&-e^{\epsilon\rho}\{240(1/\nu^6-1/\eta^6)+288\rho(1/\nu^5-1/\eta^5)+156\rho^2(1/\nu^4-1/\eta^4)+48\rho^3(1/\nu^3-1/\eta^3)+8\rho^4(1/\nu^2-1/\eta^2)\}.
\end{aligned}
$$

$$
\begin{aligned}
4\gamma^3(2,2) = &-\gamma^2(2,2)-\{C_3+H_3-e^{-\rho}[(A_3+D_3)+(A_4+D_4)]\}+5\rho\{C_2+H_2-e^{-\rho}[(A_2+D_2)+(A_3+D_3)]\}\\
&-8\rho^2\{C_1+H_1-e^{-\rho}[(A_1+D_1)+(A_2+D_2)]\}+4\rho^3\{C_0+H_0-e^{-\rho}[(A_0+D_0)+(A_1+D_1)]\}\\
&-e^{\epsilon\rho}\{6(1/\nu^4+4/\nu^5-1/\eta^4)+10\rho(1/\nu^3+3/\nu^4-1/\eta^3)+8\rho^2(1/\nu^2+2/\nu^3-1/\eta^2)+4\rho^3(1/\nu+1/\nu^2-1/\eta)\}.
\end{aligned}
$$

$$
\begin{aligned}
2\gamma^2(2,2) = &-K(5)+2\rho^2K(3)-\rho^4K(1)-\{C_4+H_4-e^{-\rho}(A_4+D_4)\}+5\rho\{C_3+H_3-e^{-\rho}(A_3+D_3)\}-8\rho^2\{C_2+H_2-e^{-\rho}(A_2+D_2)\}\\
&+4\rho^3\{C_1+H_1-e^{-\rho}(A_1+D_1)\}-e^{\epsilon\rho}\{24(1/\nu^5-1/\eta^5)+30\rho(1/\nu^4-1/\eta^4)+16\rho^2(1/\nu^3-1/\eta^3)+4\rho^3(1/\nu^2-1/\eta^2)\}.
\end{aligned}
$$

$$
\begin{aligned}
2[\gamma^2(2,1)+\gamma^2(1,2)] = &-2K(4)+2\rho^2K(2)-2\{C_3-H_3-e^{-\rho}(A_3-D_3)\}+8\rho\{C_2-H_2-e^{-\rho}(A_2-D_2)\}-10\rho^2\{C_1-H_1-e^{-\rho}(A_1-D_1)\}\\
&+4\rho^3\{C_0-H_0-e^{-\rho}(A_0-D_0)\}-e^{\epsilon\rho}\{12(1/\nu^4-1/\eta^4)+16\rho(1/\nu^3-1/\eta^3)+10\rho^2(1/\nu^2-1/\eta^2)+4\rho^3(1/\nu-1/\eta)\}.
\end{aligned}
$$

$$
\begin{aligned}
2\gamma^2(1,1) = &-K(3)+\rho^2K(1)-\{C_2+H_2-e^{-\rho}(A_2+D_2)\}+3\rho\{C_1+H_1-e^{-\rho}(A_1+D_1)\}-2\rho^2\{C_0+H_0-e^{-\rho}(A_0+D_0)\}\\
&-e^{\epsilon\rho}\{2(1/\nu^3-1/\eta^3)+3\rho(1/\nu^2-1/\eta^2)+2\rho^2(1/\nu-1/\eta)\}.
\end{aligned}
$$

potential of the $(2s)^2$ distribution. This fact has been used in tabulating formulas. For example,

$$[2s_a2s_b|2p\pi_b2p\pi_b]=[2s_a2s_b|2s_b2s_b]+[2s_a2s_b|Q_{\pi\pi}], \quad (1)$$

where $Q_{\pi\pi}$ is used to indicate the quadrupole part of the potential of the $(2p\pi)^2$ distribution. Relations of this kind and some others, perhaps not so obvious, are listed in Table I. In Table II are listed the formulas for hybrid integrals or parts of integrals containing four $2p$ functions, except for some which can be obtained from the identities of Table I. The fact that all the integrals of Table II come from the quadrupole part of the potential makes them rather uniform. Of course, to get the final value of some of these integrals the values obtained for the quadrupole term from Table II must be added to the pole contributions given in Table III.

The integrals given by Parr and Crawford[13] agree exactly with the corresponding integrals given here except for the factor $\xi^{-5/2}$ in P_n. The terms $J(s,t)$, $I(s,t)$, and $\gamma^j(s,t)$, as defined in Tables IV and V, however, are slightly more complicated than in the homonuclear case. The functions $\gamma^j(s,t)$ are not defined in Parr and Crawford's published paper but are to be found in an extended version of the same which was circulated privately. The γ's are combinations of the functions $K(s)$, A_s, C_s, D_s, defined by Sklar and Lyddane,[12] and of powers of ρ. In the heteronuclear case the γ's preserve essentially the same form, but now many of the powers of ρ are replaced by the integrals H_s defined in Table IV. Complete formulas for the γ's are given in Table V.

B. Integrals Involving at Least One 2s Wave Function

Such large groups of similar integrals do not occur among the remaining integrals. It is therefore more convenient to list them term by term. This is done in Table III. Those which are alike are listed together so that the computer may make use of many short cuts. Note that the same integrals occur in all five parts of this table. Hence to obtain the final value of any integral, the contributions listed in each part must be added.

IV. THE COMPONENT INTEGRALS AND THEIR CALCULATION

The formulas given in Tables II and III are all in terms of the component integrals $I(s,t)$, $J(s,t)$, and $\gamma^j(s,t)$. These are tedious to calculate, but once they have been obtained for a particular integral, they can be used for all the remaining integrals corresponding to the same values of ξ and ρ.

Definitions and recurrence formulas for $I(s,t)$ and $J(s,t)$ are given in Table IV. The recurrence formulas are somewhat complicated and in each case require two auxiliary functions which must be calculated in turn by their own recurrence formulas.

In the case of $J(s,t)$ and its auxiliary functions $f(s,t)$ and $g(s,t)$, a two-dimensional array of numbers is required. The starting values $f(s,0)$, $f(0,t)$, $g(s,0)$, $g(0,t)$ enable the first row and first column of the array to be calculated.[17] Then using two adjacent entries, the array can be filled in until the diagonal is reached, as indicated in Table IV in the column headed "Range of Parameters."

The number of integrals $I(s,t)$ is considerably smaller, and the procedure for calculating them is very similar to that outlined for $J(s,t)$.

To obtain the functions $\gamma^j(s,t)$ the auxiliary integrals A_s, C_s, D_s, H_s, and $K(s)$ must be calculated. This is done from the recurrence formulas given in Table IV. The recurrence formula for $K(s)$ requires the two auxiliary functions $m(s)$ and $n(s)$, which must be calculated in turn by their own recurrence formulas. These recurrence formulas and the starting values $m(0)$ and $n(0)$ are given in Table IV. Formulas for the γ's are given in Table V. The γ's themselves can be obtained from recurrence relations, and this has been done in those cases where the intermediate terms are also of interest for integrals given in Tables II and III. In other cases we have simply stated the final results.

A number of identities that the γ's must satisfy are given in Table VI. Because of these identities the expression of the hybrid integrals in terms of the γ's is not unique. These identities were used as a check on the accuracy of the algebraic work involved in deriving the formulas for the γ's given in Table V.

Though the derivation of the formulas here presented was very tedious, we feel that all errors have been eliminated, since the formulas for the integrals for equal effective nuclear charges were obtained completely independently by the two authors in the course of work on two papers previously published,[11,18] and the extension to the case of unequal effective nuclear charges required but a redefinition of terms, while the basic formulas remained the same. The fact that the numerical values given by one of us agree so well in all cases with those obtained by Kopineck by an entirely different method, indicates the essential correctness of both sets of formulas.[19]

TABLE VI. Some identities connecting the functions $\gamma^j(s,t)$.

$$\gamma^4(5,3)+\gamma^4(3,5)=2\gamma^4(4,4)+4\rho^2\gamma^4(3,3)$$
$$\gamma^2(5,1)+\gamma^2(1,5)=2\gamma^2(3,3)+16\rho^2\gamma^2(2,2)+16\rho^4\gamma^2(1,1)$$
$$\gamma^2(4,2)+\gamma^2(2,4)=2\gamma^2(3,3)+4\rho^2\gamma^2(2,2)$$
$$\gamma^2(4,1)+\gamma^2(1,4)=\gamma^2(3,2)+\gamma^2(2,3)+4\rho^2[\gamma^2(2,1)+\gamma^2(1,2)]$$

[17] There is a typographical error in the formula for $g(0,t)$ given by Sklar and Lyddane (reference 12). The correct formula is $g(0,t)=-e^{-\rho}\rho^t/2+(t/2)g(0,t-1)$.

[18] R. O. Brennan, J. Chem. Phys. **20**, 40 (1952).

[19] Compare the values given in Table XVI of reference 11 with those given in the second of Kopineck's articles cited in reference 2. For comparison purposes the values given in reference 11 must be divided by $2Z$.

TABLE VII. Carbon-oxygen hybrid Coulomb-exchange integrals for CO_2.
($Z_1=4.55$; $Z_2=3.25$; $\xi=1.400$; $\rho=7.1332$[a])

Integral	Exact value (atomic units[b])	Approx. value[c] from Eq. (2)	Integral	Exact value (atomic units[b])	Approx. value[c] from Eq. (2)
$[2s_a2s_b\|2s_b2s_b]$[d]	0.42024	0.423	$[2p\bar{\pi}_a2p\bar{\pi}_b\|2p\pi_b2p\pi_b]$	0.22429	0.227
$[2p\sigma_a2s_b\|2s_b2s_b]$[d]	0.41392	0.404	$[2s_a2s_b\|2s_b2p\sigma_b]$	0.10482	0.077
$[2s_a2p\sigma_b\|2s_b2s_b]$[d]	0.48141	0.472	$[2p\sigma_a2s_b\|2s_b2p\sigma_b]$	0.09486	0.058
$[2p\sigma_a2p\sigma_b\|2s_b2s_b]$[d]	0.39722	0.407	$[2s_a2p\sigma_b\|2s_b2p\sigma_b]$	0.15903	0.168
$[2p\pi_a2p\pi_b\|2s_b2s_b]$[d]	0.23788	0.239	$[2p\sigma_a2p\sigma_b\|2s_b2p\sigma_b]$	0.14593	0.180
$[2s_a2s_b\|2p\sigma_b2p\sigma_b]$	0.44929	0.438	$[2p\pi_a2p\pi_b\|2s_b2p\sigma_b]$	0.05407	0.041
$[2p\sigma_a2s_b\|2p\sigma_b2p\sigma_b]$	0.43761	0.418	$[2p\pi_a2s_b\|2s_b2p\pi_b]$	0.05184	0.050
$[2s_a2p\sigma_b\|2p\sigma_b2p\sigma_b]$	0.53301	0.514	$[2p\pi_a2p\sigma_b\|2s_b2p\pi_b]$	0.05407	0.050
$[2p\sigma_a2p\sigma_b\|2p\sigma_b2p\sigma_b]$	0.44273	0.447	$[2s_a2p\pi_b\|2s_b2p\pi_b]$	0.05798	0.056
$[2p\pi_a2p\pi_b\|2p\sigma_b2p\sigma_b]$	0.24720	0.241	$[2p\sigma_a2p\pi_b\|2s_b2p\pi_b]$	0.07052	0.065
$[2s_a2s_b\|2p\pi_b2p\pi_b]$	0.40572	0.415	$[2p\pi_a2s_b\|2p\sigma_b2p\pi_b]$	0.02335	0.017
$[2p\sigma_a2s_b\|2p\pi_b2p\pi_b]$	0.40208	0.397	$[2p\pi_a2p\sigma_b\|2p\sigma_b2p\pi_b]$	0.03183	0.030
$[2s_a2p\sigma_b\|2p\pi_b2p\pi_b]$	0.45561	0.450	$[2s_a2p\pi_b\|2p\sigma_b2p\pi_b]$	0.01968	0.013
$[2p\sigma_a2p\sigma_b\|2p\pi_b2p\pi_b]$	0.39117	0.387	$[2p\sigma_a2p\pi_b\|2p\sigma_b2p\pi_b]$	0.02067	0.012
$[2p\pi_a2p\pi_b\|2p\pi_b2p\pi_b]$	0.24213	0.250	$[2p\bar{\pi}_a2p\pi_b\|2p\pi_b2p\bar{\pi}_b]$	0.00892	0.008

[a] See footnote 16.
[b] See footnote 14.
[c] Some of the values given here differ slightly from those given in Table XV of reference 11, since orthogonalized Slater $2s$ functions were used there instead of the present non-orthogonal Slater $2s$ functions.
[d] These integrals were also calculated exactly using elliptical coordinates, with identical results.

V. NUMERICAL RESULTS

Exact numerical values were calculated by the method of this paper for thirty hybrid integrals that occur in molecular orbital calculations on the carbon dioxide molecule. These integrals are those in which one electron is exchanged between the carbon and oxygen atoms in the field of the second electron on the carbon atom. The calculations were found to be quite straightforward. The W.P.A. Tables of logarithms, exponentials, and exponential integrals[20] were used to obtain the starting values of the auxiliary functions. These starting values together with the recurrence relations of Table IV led to tables of values of the I's, J's, and γ's. These tables were then used together with Tables II and III to obtain all the desired hybrid integrals.

No serious computational difficulties occurred in the course of these calculations. This is in contrast to the experience of Barnett and Coulson[4] with their method for these hybrids, where "differencing effects" complicated the use of recurrence formulas for the auxiliary functions required. In calculating the functions $\gamma^j(s,t)$ it was found that more significant figures had to be carried through the calculations than were required in the final values of the integrals, since two or three significant figures were lost as the result of a final subtraction of nearly equal quantities. The values obtained for these thirty integrals are given in Table VII.

In a previous molecular orbital treatment of the ground state of the carbon dioxide molecule,[11] many hybrid integrals involving the carbon and oxygen atoms were approximated in terms of overlaps and hybrids between atoms with equal effective nuclear charges. In the notation of the present paper this approximation takes the form

$$[\chi_a\chi_b'|\bar{\chi}_b\bar{\chi}_b']=\frac{(\chi_a|\chi_b')}{(\bar{\chi}_a|\chi_b')}[\bar{\chi}_a\chi_b'|\bar{\chi}_b\bar{\chi}_b'], \qquad (2)$$

where $\bar{\chi}_a$ indicates an atomic orbital centered on atom a, but having the same effective nuclear charge as the corresponding orbital on atom b; and $(\chi_a|\chi_b')$ is the overlap integral $\int\chi_a(1)\chi_b'(1)dv_1$. This approximation breaks down for certain integrals involving π-functions, where the overlap integrals vanish because of the presence of a single π-function in the integrand. In this case the overlap integrals in Eq. (2) were replaced by integrals of the form $\int\chi_a(1)\chi_b'(1)xdv_1$, where x (or y) is a coordinate chosen to correspond with the π-function occurring in the integral. These integrals can be evaluated easily in the same way as the overlap integrals.[5]

The approximation of Eq. (2) is physical, not mathematical, in nature and is based on the supposition that the field in which the exchanged electron moves does not change with the nature of atom a, but depends only on the charge distribution on atom b. If this assumption is true, the ratio of the integral for unequal effective nuclear charges to that for equal effective nuclear charges should be equal to the ratio of the overlap integrals corresponding to the exchange. That this assumption is fairly close to the physical facts is seen from the agreement shown in Table VII between approximate values obtained from Eq. (2) and the exact values calculated by the method of this paper. The agreement is best for π-functions, less good for σ-functions. This is due to the concentration of the σ-functions

[20] Works Progress Administration, Mathematical Tables Project, *Table of Natural Logarithms* (New York, 1941); *Tables of the Exponential Function* (New York, 1947); *Tables of the Sine, Cosine, and Exponential Integrals* (New York, 1940).

along the internuclear axis, and the resultant distortion they produce. It is to be expected that for this reason the approximation will be better for greater internuclear distances. How useful it will be in a particular case depends on the accuracy required in the molecular property being calculated. Because of the availability of Kopineck's tables of hybrids for equal effective nuclear charges, and the overlap tables of Mulliken *et al.*, this approximation is extremely simple to use. It may be useful, at least for rough calculations, until the time when tables of hybrids for unequal effective nuclear charges become available.

VI. ACKNOWLEDGMENT

The authors would like to express their gratitude to Dr. Klaus Rüdenberg, to Dr. M. P. Barnett, and to Dr. Robert G. Parr, for their encouragement and helpful advice concerning the publication of this paper.

THE JOURNAL OF CHEMICAL PHYSICS VOLUME 20, NUMBER 10 OCTOBER, 1952

The Thermal Dimerization of Butadiene, and the Equilibrium between Butadiene and Vinylcyclohexene

N. E. DUNCAN* AND G. J. JANZ
Walker Laboratory, Department of Chemistry, Rensselaer Polytechnic Institute, Troy, New York
(Received May 9, 1952)

The kinetics of the dimerization of butadiene and of the dissociation of vinylcyclohexene have been considered in the light of thermodynamic equilibrium calculations. The lack of accord between the results is resolved if the dissociation of vinylcyclohexene is given by the rate expression

$$k_d = 5.02\times10^{15}\exp(-61{,}800/RT)\ \text{sec}^{-1}.$$

THREE major kinetic investigations, two on the thermal dimerization of butadiene and one on the depolymerization of dimeric butadiene, have recently been described in the literature. From 446 to 660°K, Kistiakowsky and Ransom[1] found the dimerization to be second order, proceeding by the rate equation

$$k_a = 9.20\times10^{9}\exp(-23{,}690/RT)\ \text{cc mole}^{-1}\ \text{sec}^{-1}.$$

It appeared also that with increasing temperature the activation energy for the dimerization increased. The work of Rowley and Steiner[2] in the temperature range 690–925°K substantiated this. At these temperatures the rate expression obtained was

$$k_a = 1.38\times10^{11}\exp(-26{,}800/RT)\ \text{cc mole}^{-1}\ \text{sec}^{-1}.$$

Depolymerization of dimeric butadiene was reported by Doumani[3] and associates to proceed by a first-order mechanism according to the relation

$$k_a = 2.35\times10^{8}\exp(-36{,}000/RT)\ \text{sec}^{-1}$$

in the temperature range 783–977°K. From these data the heat of reaction and equilibrium constants for the reaction

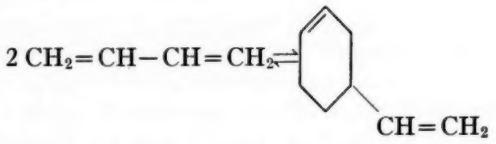

can be calculated. From 750 to 950°K the equilibrium constant is given by the ratio of the forward and reverse rates, and in terms of partial pressure is

$$K_p = 5.87\times10^{2}/RT\exp(9200/RT).$$

The equilibrium constants and free energy changes for this equilibrium from this expression are as shown in Table I.

TABLE I.

T(°K)	750°	775°	800°	825°	850°	875°	900°	925°	950°
K_p	188.6	149.6	120.2	97.9	80.5	67.0	56.2	47.6	40.6
$\Delta F°$(kcal)	−7.81	−7.71	−7.62	−7.52	−7.42	−7.31	−7.21	−7.10	−7.00

The temperature dependence of the free energy change is exceedingly small according to these results. The heat of reaction, is predicted as 9.2 kcal/mole in this temperature range.

Comparison of these data with results from the thermodynamic method shows that only at 800°K is there approximate agreement. The free energy changes for the butadiene-vinylcyclohexene equilibrium were calculated using the van't Hoff Isochore in the modified form

$$\Delta F_T{}^0 = I_H + (\Delta a - I_s)T = \Delta aT\ln T - \tfrac{1}{2}\Delta bT^2 - \tfrac{1}{6}\Delta cT^3,$$

where the constants I_H and I_S are evaluated from the

TABLE II.

T(°K)	298.1	300	400	500	600	700	800	900	1000
$\Delta F°$(kcal)	−25.7	−25.6	−21.9	−17.9	−14.7	−11.5	−7.9	−4.7	−1.3

* Cyanamid Research Fellow (Department of Chemistry).

[1] G. B. Kistiakowsky and W. W. Ransom, J. Phys. Chem. **7**, 725 (1939).

[2] D. Rowley and H. Steiner, Disc. Faraday Soc. **10**, 198 (1951).

[3] Doumani, Deering, and McKinnis, Ind. Eng. Chem. **39**, 89 (1947).

data at 298.1°K. For this purpose the following data were used for vinylcyclohexene: $\Delta H^0 f_{298.1} = 16.8$ kcal, $S^\circ_{298.1} = 96.4$ cal/deg/mole, $C_p{}^0 = -2.22 + 148.2 \times 10^{-3} T - 62.38 \times 10^{-6} T^2$. These data were calculated from reference compounds, ethylbenzene,[4] cyclohexane,[4] cyclohexene,[5,6] for which the data are well established, and the method of group increments or contributions.[7,8] The thermodynamic properties of butadiene have been reported elsewhere.[9] The free energy changes thus calculated for the dimerization of butadiene for temperatures up to 1000°K are given in Table II.

In Fig. 1 a comparison is shown of the results from the thermodynamic method and the experimentally established rate equations. The lack of agreement between the two methods is much greater than the errors inherent in the above calculation. The heat of reaction at 25°C calculated from heats of formation is -36.7 ± 0.5 kcal.

The cause of disagreement observed for the two methods is found to lie in the equation[3] for the thermal dissociation of vinylcyclohexene. The frequency factor can be calculated using the statistical expression of the theory[10] of reaction rates:

$$a = Ke^2 kT/h(\exp \Delta S_c^*/R).$$

The entropy value for this activated complex has been calculated by Wassermann[11] as $S^\circ_{c600} = 120.44$ eu per mole, and the entropy of vinylcyclohexene[1] at 600°K is 112.6 eu. Thus for the dissociation ΔS_c^* is 7.8 eu, and the frequency factor is $10^{15.7}$ if the transmission coefficient is taken as approximately unity (true in many first-order reactions). The energy of activation can be obtained from a knowledge of the heat of reaction at 800°K and the energy of activation for the forward reaction.[2] Using the data for butadiene,[9] and the heat of formation of vinylcyclohexene corrected to 800°K, the heat of reaction $\Delta E^\circ_{800} = 35.0$ kcal. The value for the latter from experimental kinetic data was 9.2 kcal. It is unlikely that the calculated value is in error by more than 2 or 3 kcal. The energy of activation for the dissociation reaction is thus 61.8 kcal/mole. This value is in accord with the order of magnitude for the energy of activation reported[12] for the dissociation of cyclohexene (57.5 kcal) and that previously estimated[1] for dissociation of vinycyclohexene (64 kcal). Accordingly, the rate of dissociation of 3-vinylcylohexene is given by

$$k_a = 5.02 \times 10^{15} \exp(-61{,}800/RT) \text{ sec}^{-1}.$$

The expression for the equilibrium constant for the butadiene-vinylcyclohexene reaction is

$$K_p = 2.76 \times 10^{-5}/RT \exp(35{,}000/RT),$$

if the rate equation above is used with the data of Rowley and Steiner. The free energy changes and $\log K_p$ calculated from this equation are in good agreement with the results of the thermodynamic calculation as is shown in Fig. 1.

The frequency factor and activation energy reported by Doumani, Deering, and McKinnis[3] seem to be unusually low for the homogeneous thermal dissociation of vinylcyclohexene and do not lend themselves to equilibrium calculations as seen by the criterion of the thermodynamic methods. The low values may possibly be accounted for by a catalysis or wall effect present but not reported in the investigation.

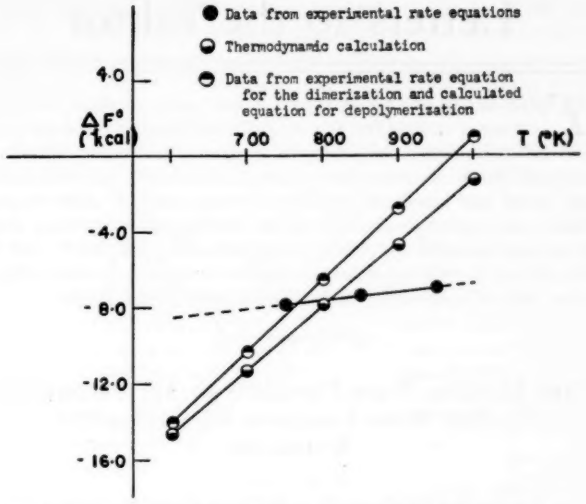

FIG. 1. The free energy change-temperature relation for the equilibrium: $2(CH_2{=}CH{-}CH{=}CH_2) \rightleftharpoons C_8H_{12}$.

[4] "Selected Values of Properties of Hydrocarbons," Natl. Bur. Standards, Circular 461 (1947).
[5] Beckett, Freeman, and Pitzer, J. Am. Chem. Soc. **70**, 4227 (1948).
[6] Epstein, Pitzer, and Rossini, J. Research Natl. Bur. Standards **42**, 379 (1946).
[7] I. G. M. Bremner and G. D. Thomas, Trans. Faraday Soc. **43**, 779 (1947).
[8] Andersen, Beyer, and Watson, Natl. Pet. News R476 (1944).
[9] Brickwedde, Moskow, and Aston, J. Research Natl. Bur. Standards **37**, 263 (1946).
[10] Glasstone, Laidler, and Eyring, *Theory of Rate Processes* (McGraw Hill Book Company, Inc., New York, 1941).
[11] A. Wassermann, J. Chem. Soc. (London) 612 (1942).
[12] L. Kuchler, Trans. Faraday Soc. **35**, 874 (1939); Nach. Ges. Wiss. Göttingen **1**, 231 (1939).

Letters to the Editor

THIS section will accept reports of new work, provided these are terse and contain few figures, and especially few half-tone cuts. The Editorial Board will not hold itself responsible for opinions expressed by the correspondents. Contributions to this section should not exceed 600 words in length and must reach the office of the Editor not later than the 15th of the second month preceding that of the issue in which the Letter is to appear. No proof will be sent to the authors. A publication charge of $10.00 per Letter is made which, when honored, will entitle the Institution to 100 free reprints.

Free Electron Wave Functions as Approximations To MO Wave Functions for Conjugated Molecules

H. H. JAFFÉ
V. D. Experimental Laboratory, U. S. Public Health Service School of Public Health, University of North Carolina, Chapel Hill, North Carolina
(Received August 8, 1952)

THE Free Electron Model (FEM) has recently been used extensively for calculations of spectra of conjugated organic compounds. The results of such calculations have been compared with similar results obtained by molecular orbital (MO) theory. Platt[1] has made a detailed comparison of energies and symmetry characteristics of wave functions (WF) of aromatic compounds obtained from FEM and MO theory. He find sa one-to-one correspondence of low energy WF. Although the energies of corresponding pairs do not agree too closely, the symmetry characteristics are identical. The FEM, however, leads to an infinite number of high energy WF which have no analogy in MO theory unless atomic orbitals of energy higher than the $2p\pi$-orbitals are considered.

The FEM has been used even more successfully for acyclic compounds than for the aromatic systems.[2] Again there exists a one-to-one correspondence of FEM and MO WF. An approximate graphic representation of the MO WF can be obtained by plotting the distances along the conjugated chain against the values of the AO coefficients (c_{ik}). A smooth curve through the points thus obtained is identical with the FEM WF, if the free electron path is assumed to extend one bond length beyond the last nucleus on either end.[3] Such a graph is given in Fig. 1 for all the MO WF of the free radical, $CH_2=CH-CH=CH-CH_2$. The vertical lines represent the magnitudes and signs of the c_{ik}'s, and the solid curves represent the FEM WF. Each MO WF in Fig. 1 is accurately represented by a FEM WF. This correspondence remains unchanged by inclusion of hetero-atoms in the conjugated system.[4] As in aromatic systems, higher energy FEM WF can be constructed, which may be interpreted as corresponding to MO WF involving excited AOs. The energies of corresponding FEM and MO WF in the open chain compounds also do not agree. In spite of this disagreement, Fig. 1 shows that FEM WF give a good approximation in shape to the MO WF and that the AO coefficients (c_{ik}) in a MO may be obtained from FEM WF. Thus, it is possible to calculate electron densities, bond orders, and free valences from FEM WF; therefore, the cumbersome procedure of solving the secular equations of the MO method can be avoided.

A similar use of the FEM WF in cyclic molecules is less straightforward. Since the quantization of FEM WF arises from continuity rather than boundary conditions, the location of nuclei with respect to nodes must be achieved by judicious choice. Furthermore, in condensed ring systems the FEM introduces an additional assumption by ignoring the bridge bonds.

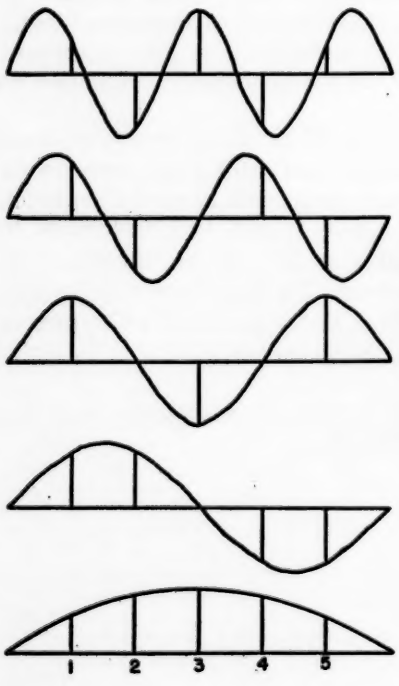

FIG. 1. The correspondence of FEM and MO WF for $CH_2=CH-CH=CH-CH_2$. The energy of the WF increases in ascending order. The vertical lines are the c_{ik} for the atoms k given at the bottom. These numbers also specify the position of the nuclei for the FEM WF. The amplitude is plotted as ordinate.

[1] J. R. Platt, J. Chem. Phys. **17**, 484 (1949).
[2] Cf. e.g., H. Kuhn, Helv. Chim. Acta **31**, 1441, 1780 (1948); **32**, 2247 (1949); **34**, 1308, 2371 (1951).
[3] This assumption is due to Kuhn (reference 2); it seems to receive a better theoretical basis from the present discussion.
[4] For the FEM treatment cf. H. Kuhn, Helv. Chim. Acta **34**, 2371 (1951).

The Absolute Intensity of the ν_4 Infrared Absorption Band of Methane and Its Enhancement by Nitrogen at High Pressures

H. L. WELSH AND P. J. SANDIFORD*
McLennan Laboratory, University of Toronto, Toronto, Canada
(Received August 8, 1952)

EXPERIMENTS previously reported[1] showed that the integrated absorption coefficient of the ν_3-(3.3μ) band of methane, after a rapid initial increase caused by pressure-broadening of the rotational lines, continues to increase linearly with the density of the foreign gases helium, argon, and nitrogen. The enhancement is greatest with nitrogen; at 360 amagat units of density (600 atmos) the absorption coefficient is 20 percent greater than that of the free methane molecule. If one assumes that the vibrating dipole of the absorbing molecule (polarizability α_1) is augumented by the reaction field of the foreign gas molecules (polarizability α_2), the fractional increase in the absorption coefficient is $16\pi\alpha_1\alpha_2 N/3R_0^3$, where N is the number of foreign gas molecules per cc and R_0 is the distance of closest approach of the two types of molecules. With this simple theory the values of R_0 required to fit the experimental data are only about one-half of the sum of the gas kinetic molecular radii. Since the constants in the above expression are independent of frequency, it follows that, for a given foreign gas, the fractional increase for ν_4, the other infrared active fundamental, should be the same as for ν_3. Experiments have now been carried out to check this prediction of the theory.

The high pressure absorption cell previously described[1] was used. A calcium fluoride window, 1.0-cm thick, was sufficiently transparent in the 7.6μ-region, but its mechanical strength limited the highest pressure to 300 atmos. The apparent integrated absorption coefficients B for four base pressures of methane with nitrogen as the foreign gas are plotted against the density of nitrogen in Fig. 1. The sharp initial rise is followed at the higher

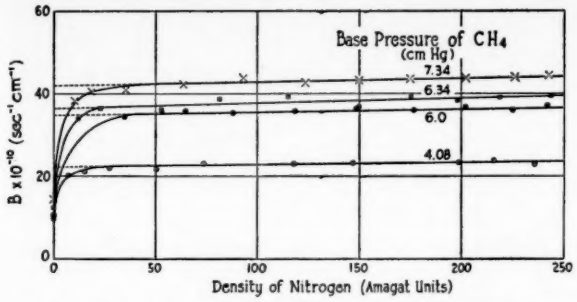

FIG. 1. Variation of the apparent absorption coefficient B of the ν_4 band of methane, in methane-nitrogen mixtures.

pressures by a very small linear increase which is almost obscured by the experimental error. However, a statistical analysis showed that the increase is significantly greater than zero. The reduction of the results gave for the induced absorption coefficient 0.12×10^{10} cm^{-1} sec^{-1} at NTP per amagat of nitrogen. Extrapolation of the integrated absorption coefficients to zero density of nitrogen gave for the absolute intensity of the band 472×10^{10} cm^{-1} sec^{-1} at NTP, about 5 percent greater than that found by Thorndike.[2]

The fractional increase in the absorption coefficient caused by the induction effect is thus 2.5×10^{-4} per amagat of nitrogen, which is only one-half as great as the value 5.4×10^{-4} found for the ν_3-band.[1] Using the values $\alpha_1=2.61\times10^{-26}$ cm^3, $\alpha_2=8.1\times10^{-26}$, and $R_0=3.6\times10^{-8}$ cm, the sum of the kinetic theory radii,[3] the calculated fractional increase for both bands is 0.60×10^{-4}. The theory is thus inadequate in two respects: (a) It predicts equal enhancements for both bands, and (b) the theoretical value of the enhancement, assuming a reasonable value of R_0, is much less than that observed. It is therefore concluded that the major part of the enhancement is due, as in the case of normally inactive infrared bands,[4,5] to a distortion of the electron distribution of the absorbing molecule during close collisions. However, the enhancement of the active bands of methane by nitrogen is an order of magnitude greater than the absorption induced in hydrogen by nitrogen, the coefficient for which is 0.0185×10^{10}.

The authors are indebted to the National Research Council of Canada for financial assistance in the construction of high pressure apparatus.

* Present address: Hydro-Electric Power Commission of Ontario, Toronto, Canada.

[1] Welsh, Pashler, and Dunn, J. Chem. Phys. **19**, 340 (1951).
[2] A. M. Thorndike, J. Chem. Phys. **15**, 868 (1947).
[3] M. Trautz, Ann. Physik **15**, 198 (1932).
[4] Crawford, Welsh, and Locke, Phys. Rev. **75**, 1607 (1949); **76**, 580 (1949).
[5] Crawford, Welsh, MacDonald, and Locke, Phys. Rev. **80**, 469 (1950).

Paramagnetic Resonance in Liquids

M. A. GARSTENS AND S. H. LIEBSON
Electricity Division, Naval Research Laboratory, Washington, D. C.
(Received July 28, 1952)

WE have been interested in observing the effects of exchange in hyperfine structure in paramagnetic liquids. When a crystal containing divalent Mn ion in a $^6S_{5/2}$ ground state, present in sufficient dilution, is placed within a magnetic field it is possible to observe its hyperfine structure because of the interaction of the nucleus of the Mn ion, which has spin 5/2, with the 5 electrons in its 3*d* shell. Six hyperfine lines may thus be observed. Additional splitting due to asymmetry in the electric field can produce as many as 30 different lines due to both hyperfine and fine structure. In liquids hyperfine structure has been observed, but thus far no fine structure has been observed.

Solutions of $Mn(NO_3)_2$ in water were chosen for our experiment. $Mn(NO_3)_2$ is capable of being dissolved in large quantities in water. It is thus possible to obtain a wide range of Mn^{++} ion concentration from a low value where the hyperfine lines are clearly visible and the line width varies, owing to changes of the reorientation time in the Brownian motion of the liquid, to a very high concentration where the effects of exchange among the electrons become dominant. At the same time by using solutions, gradual variations in concentration are possible.

Our experimental apparatus consisted of a rectangular one-cm cavity operating in the $TE_{01.2}$ mode, the rf magnetic field being at right angles to the steady external magnetic field. This field was swept magnetically at 280 cycles per second. The presence of water in the cavity drastically affects its Q, so that at low concentrations great sensitivity is necessary for observation of the absorption lines. The samples were kept in that portion of the cavity where the electric field was at a minimum. A narrow band amplifier with a phase detector operated at 280 cycles, and a time constant of about 5 seconds was used to detect the slope at every point of the absorption curve, the external field being moved slowly through the absorption line. A nuclear resonance arrangement was used to measure the magnetic field at every point.

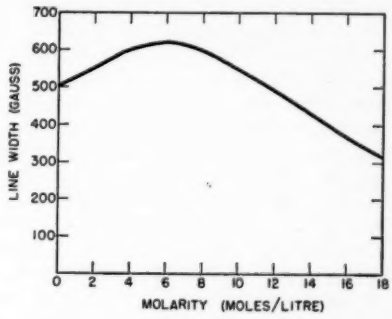

FIG. 1. Plot of line width *versus* concentration

In paramagnetic resonance two kinds of mechanisms can produce narrowing effects on line widths. In paramagnetic crystals exchange among the electrons is found to narrow the resonance lines, and in paramagnetic liquids the Brownian motion can also do so. Our experiment indicates that exchange effects can be effective in liquids as well as in solids.

Where exchange occurs, Van Vleck[1] has shown that the resultant narrowing can be understood in terms of its effect in increasing the value of the fourth moment of the absorption line. In this case he shows too that a reorientation time $\tau\sim h/J$, where J is the exchange integral, can be assigned to the varying magnetic environment of an ion just as in the case of liquids;[2] and when this time is shorter than the lifetime associated with the inverse width of the resonance line (i.e., when $\langle\Delta\nu^2\rangle_{Av}\tau^2\ll1$), the half-width is reduced to $\tau\langle\Delta\nu^2\rangle_{Av}$ in order of magnitude, where $\langle\Delta\nu^2\rangle_{Av}$ is the mean square absorption frequency. In the case of highly concentrated solutions both of these narrowing effects may occur simultaneously and their effects on the hyperfine structure be observed.

Figure 1 is a plot of the over-all line width against concentration measured in moles per liter. Below the maximum, six hyperfine

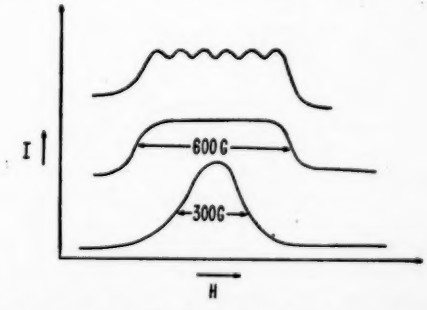

FIG. 2. Appearance of the lines at various concentrations: top-low concentrations; middle—intermediate concentrations; bottom—high concentrations.

lines are observed. At the maximum the hyperfine lines are no longer visible, and beyond the maximum the effects of exchange appear as a narrowing of the over-all width. At the highest concentration the liquid becomes very viscous and glasslike. Figure 2 shows in order from top to bottom, the appearance of the absorption line at low, intermediate, and high concentration. The individual hyperfine lines widen with increasing concentration due both to the diminution of the Brownian motion, and to the increasing dipolar interaction. The latter is, however, the more dominant effect. At larger concentrations, as both figures indicate, exchange becomes important; the widening action, due both to dipolar interaction and to the decreased effects of the Brownian motion in diminishing the intensity of "zero" frequency components in the varying magnetic field of an ion due to the motion of its neighbors,[2] is overcome, and the line width diminishes.

Of particular interest is the effect of exchange in averaging the structure due to the hyperfine interaction. The over-all width due to this interaction is about 500 gauss, whereas the line width when the exchange effects are strong is less than half of this. At low concentrations, however, there seems to be no observable averaging effect due to the liquid motion on the hyperfine spacing.

It is still not entirely certain as to what redistribution of hyperfine lines is involved in reducing the absorption line to its final low value when the M_n^{++} ion concentration is high. This can occur in two ways. Either the individual lines are drawn together (i.e., the hyperfine spacing diminishes), or the intensities of the inner lines are built up at the expense of the outer ones. There appears to be some experimental evidence for the first hypothesis. Thus in most cases where both the hyperfine structure and the fine structure of the M_n^{++} ion has been fully revealed (as in the 30 lines observed by Schneider and England)[3] the individual peaks in each set of hyperfine lines seem to be of equal intensity. A superposition of such peaks when the fine structure lines are very close to each other would give six hyperfine lines with no variation of intensity among them. This is actually observed when the hyperfine lines are seen. If this is still the case when the M_n^{++} ion concentration is high, then even when dipolar broadening smears out the six lines, a line broader than 500 gauss should be observed.

[1] J. H. Van Vleck, Phys. Rev. **74**, 1168 (1948).
[2] Bloembergen, Purcell, and Pound, Phys. Rev. **73**, 679 (1948).
[3] E. E. Schneider and T. S. England, Physica **XVII**, 221 (1951).

Photoelectric Emission Associated with β-Band Absorption in Alkali Iodides

E. Taft and L. Apker
General Electric Research Laboratory, Schenectady, New York
(Received August 6, 1952)

DELBECQ, Pringsheim, and Yuster[1] have carefully studied a new short-wave optical absorption, termed the β-band, in KI. They attribute it to a perturbed form of fundamental absorption that occurs in the disturbed lattice at an F-center.

Professor F. Seitz, who kindly called these results to our attention, pointed out the following implication of this interpretation: β-absorption leads to an excited state that may conveniently be viewed as an exciton trapped at an F-center (or alternatively, as a hole trapped at an F'-center). This configuration has a total energy appreciably exceeding that of an electron at rest in the vacuum outside the crystal. Thus, it may decay to a state consisting of a negative ion vacancy and an electron of appreciable kinetic energy in the vacuum. This is a special kind of exciton-induced photoelectric emission from an F-center. It differs from the normal variety[2] in that the exciton is initially trapped at its point of decay. The photon energy involved is therefore lower, peaking with the β-band at $h\nu = 5.48$ ev instead of with the first fundamental exciton absorption peak at 5.80 ev (temperature, ~80°K). Further, the over-all transition probabilities should be different from those for ordinary exciton-induced emission.[3]

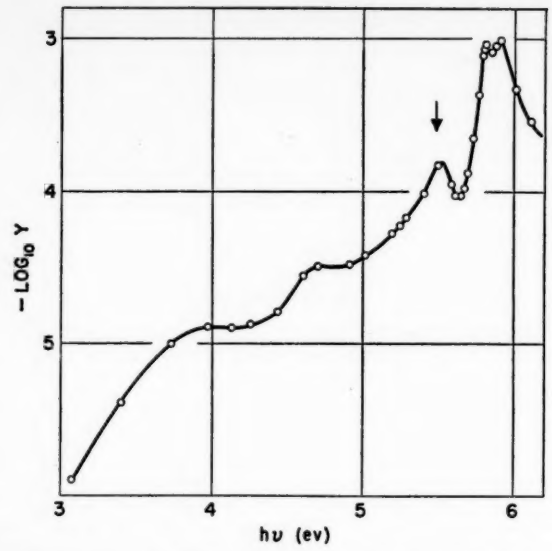

FIG. 1. Photoelectric yield Y (electron/incident quantum) from evaporated KI containing F-centers at ~80°K. Arrow marks position of β-band optical absorption as given in reference 1. To the right is the split peak due to normal exciton-induced emission. Between 4 and 5 ev is an example of less pronounced structure due to variations in optical constants, in this case arising from Tl impurity added to the sample. The yield from pure samples varies smoothly in this region, but in addition to the β-peak may show a slight inflection (probably of optical origin) near 5.2 ev.

The data in Fig. 1, taken on an evaporated layer of KI at ~80°K, support Seitz's hypothesis. There is indeed a well-resolved peak in the external photoelectric yield at $h\nu \sim 5.5$ ev, the position of the β-band in KI.[1] This effect, which also appears in earlier work on RbI,[2,3] can be associated with decay of the excited state resulting from β-absorption.

The photoelectric yield shows other structure in this same spectral region because of the rapidly changing optical constants. Prior to the work of Delbecq, Pringsheim, and Yuster, we attributed the entire structure for RbI to this effect. As pointed out in the original paper,[2] however, the explanation was not a satisfying one because the observed peaks were too pronounced. Further work with doped samples having additional absorption bands has convinced us that the optical effects are always more gradual than the observed structures. Seitz's suggestion removes the difficulty and leads to the conclusion that the sharp peak at $h\nu \sim 5.4$ ev in the photoemission from RbI containing F-centers at ~80°K is induced by β-band absorption.

[1] Delbecq, Pringsheim, and Yuster, J. Chem. Phys. **19**, 574 (1951); **20**, 746 (1952); W. Martienssen, Naturwiss. **38**, 482 (1951).
[2] L. Apker and E. Taft, Phys. Rev. **79**, 964 (1950); **81**, 698 (1951); **82**, 814 (1951).
[3] For a theoretical discussion, see D. L. Dexter and W. R. Heller, Phys. Rev. **84**, 377 (1951); D. L. Dexter, Phys. Rev. **83**, 1044 (1951).

Dielectric Relaxation in *d*-Camphor*

J. G. Powles†
Frick Chemical Laboratory, Princeton University, Princeton, New Jersey
(Received July 31, 1952)

AT 179°C *d*-camphor solidifies to a cubic form which transforms to rhombohedral at 97°C and to another more birefringent rhombohedral form at about −30°C.[1-3] The dielectric properties in the frequency range 1–100 kc/sec and at 18 Mc/sec have been measured[4] and the dielectric constant values are shown in Fig. 1. The dielectric loss was low except near the melting point, and the dielectric constant remained unchanged up to 18 Mc/sec.

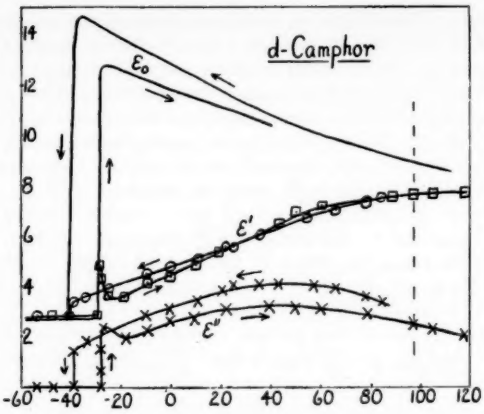

FIG. 1. Static dielectric constant, ϵ_0, and dielectric constant ϵ' and loss ϵ'' at 9,330 Mc/sec *versus* temperature in °C for *d*-camphor.

d-Camphor has therefore a high dielectric constant in the solid state over the unusually large range of about 200° and shows no dielectric dispersions below 18 Mc/sec.

We have measured the dielectric constant ϵ' and loss ϵ'' of *d*-camphor at 9330 Mc/sec (3.22-cm wavelength) over the temperature range −54°C to +118°C by a method which depends on the measurement of the complex reflection coefficient of an air-dielectric interface in a wave guide which is described elsewhere.[5] The observed values of ϵ' and ϵ'' at 9330 Mc/sec given in Fig. 1 for rising and falling temperature show that there is considerable dielectric dispersion at this frequency.

Although measurements at only one frequency in the dispersion region have been made, a rough estimate of the critical frequency for dielectric dispersion (frequency for maximum of ϵ'') may be obtained provided this frequency is near enough to the critical one and the static dielectric constant ϵ_0 and the high frequency value ϵ_∞ are available. We have used Yager and Morgan's values for ϵ_0 although these were for pressed disks and may be somewhat high for our samples which were obtained by solidification of the liquid. We take $\epsilon_\infty = 2.8$, the value of the dielectric constant below the transition. The Cole-Cole plots[6] for three temperatures are shown in Fig. 2 together with estimates of the critical frequencies. These values of critical frequency vary exponentially with inverse temperature, and if the rate expression[7] is used, one finds an activation energy of 3.2 kcal/mole and an activation entropy of 5 cal/°C/mole. These figures may be compared with the values for the substituted benzenes in the solid state[7(c),8] which are of the order 10 kcal/mole and several units of cal/°C/mole, respectively. The lower energy of activation results in much higher critical frequencies in camphor. These results again suggest that the dielectric phenomena in camphor are the result of the movement of the molecule as a whole[3,9] and not of internal motions of the molecule as has been tentatively suggested,[10] although the latter effect, if present, may well facilitate the movement and help to explain the low activation energy for this large molecule.

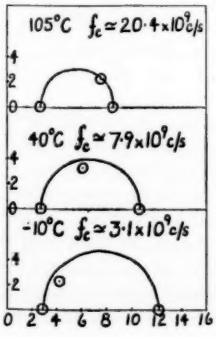

FIG. 2. Plots of ϵ'' *versus* ϵ' at three temperatures for *d*-camphor. The curves are semicircles on the diameter $\epsilon_0 - \epsilon_\infty$.

There was no evidence in our measurements of any change in properties near 97°C. This transition therefore appears to have little effect on either the static dielectric constant[4] or the critical frequency. The small peak in ϵ' for rising temperature near the lower transition, and the somewhat retarded rise in ϵ'' may indicate that the dispersion does not move in the normal way with temperature near the transition. This effect is also found in other materials.[5]

* This research has been supported in part by the ONR. Reproduction, translation, publication, use, or disposal in whole or in part by or for the United States Government is permitted.

† Visiting Research Fellow supported by a grant from E. I. du Pont de Nemours and Company, to the Department of Chemistry of Princeton University.

[1] F. Wallerant, Compt. rend. **158**, 597 (1914).
[2] P. W. Bridgeman, Proc. Am. Acad. Arts Sci. **52**, 91 (1916).
[3] C. Finbak, Arch. Math. Naturvidenskab **B42**, 71 (1938). C. Finbak and H. Viervoll, Tids. Kjemi Bergvesen **2**, 35 (1942); Chem. Zentr. II 113, 2780 (1942).
[4] W. A. Yager and S. O. Morgan, J. Am. Chem. Soc. **57**, 2071 (1935).
[5] Powles, Williams, and Smyth (to be published).
[6] K. S. Cole and R. H. Cole, J. Chem. Phys. **9**, 341 (1941).
[7] (a) F. C. Frank, Trans. Faraday. Soc. **32**, 1634 (1936); (b) H. Eyring, J. Chem. Phys. **4**, 283 (1936); (c) W. Kauzmann, Revs. Modern Phys. **14**, 12 (1942).
[8] White, Biggs, and Morgan, J. Am. Chem. Soc. **62**, 16 (1940).
[9] A. H. White and W. S. Bishop, J. Am. Chem. Soc. **62**, 8 (1940).
[10] A. H. White and S. O. Morgan, J. Am. Chem. Soc. **57**, 2078 (1935).

Equilibrium and the Rate Laws

C. A. HOLLINGSWORTH
Department of Chemistry, University of Pittsburgh, Pittsburgh 13, Pennsylvania
(Received August 7, 1952)

CONSIDER the reaction

$$aA+bB+\cdots \rightleftharpoons mM+nN+\cdots.$$

One necessary and sufficient condition for equilibrium is given by the equilibrium constant, *viz.*,

$$g[(A),(B),\cdots,(M),(N),\cdots] = (M)^m(N)^n\cdots/(A)^a(B)^b\cdots = K[T], \quad (1)$$

where $(A), (B), \cdots, (M), (N), \cdots$ are the activities, and $K[T]$ is a function of the absolute temperature.

Another necessary and sufficient condition for equilibrium may be expressed in terms of the forward and reverse rate expressions r_f and r_b as follows:

$$\frac{r_f}{r_b} = f[(A),(B),\cdots,(M),(N),\cdots,T,u,v,\cdots] = 1, \quad (2)$$

where $u, v, \cdots$ are nonthermodynamic variables, which enter into the rate expressions but do not enter into the equilibrium constant expression g.

In a previous letter[1] it was pointed out that a *sufficient* condition for Eq. (2) to hold for all activities and temperatures for which Eq. (1) holds is that the function f be expressible as a function of $g/K[T]$ such that

$$f[(A),(B),\cdots,(M),(N),\cdots,T,u,v,\cdots] = \mathfrak{F}[\theta] \quad (3)$$

and

$$\mathfrak{F}[1] = 1, \quad (4)$$

where $\theta = g/K[T]$. Equations (3) and (4) do not express a *necessary* condition, however. In fact, another *sufficient* condition is expressed by the following relationships:

$$f[(A),(B),\cdots,(M),(N),\cdots,T,u,v,\cdots] = \mathfrak{F}[\theta,u,v,\cdots], \quad (5)$$

such that

$$\mathfrak{F}[1,u,v,\cdots] \equiv 1, \quad (6)$$

where the last expression is an identity in the nonthermodynamic variables $u, v, \cdots$. Even these last relationships are not *necessary*.

A condition that *is necessary* when f has continuous derivatives of all orders at $\theta = 1$ is the following: It must be possible to express $f-1$ as a function which is divisible by the function $\theta-1$ in the neighborhood of $\theta = 1$.

This condition can be established in the following manner: Using the expression for θ, one can substitute θ for one of the variables (A), (B), $\cdots(M)$, (N), $\cdots$, T in the function f, thus obtaining a function f^* of θ and the remaining variables. At equilibrium (i.e., when $\theta=1$) $f^*\equiv 1$ must become an identity in the remaining variables. If we expand f^* about $\theta=1$ keeping all the other variables fixed at any *arbitrary* values, we obtain

$$f^*[1+\Delta\theta, \cdots]=1+\left(\frac{\partial f^*}{\partial\theta}\right)_{\theta=1}\Delta\theta+\frac{1}{2}\left(\frac{\partial^2 f^*}{\partial\theta^2}\right)_{\theta=1}\Delta\theta^2+\cdots, \quad (7)$$

or

$$f^*[\theta, \cdots]-1=(\theta-1)\psi^*, \quad (8)$$

where

$$\psi^*=\left(\frac{\partial f^*}{\partial\theta}\right)_{\theta=1}+\frac{1}{2}\left(\frac{\partial^2 f}{\partial\theta^2}\right)_{\theta=1}\Delta\theta. \quad (9)$$

Therefore, by replacing θ in f^* and ψ^* by the original variable we obtain

$$f-1=(\theta-1)\psi[(A), (B), \cdots, (M), (N), \cdots, T, u, v, \cdots]. \quad (10)$$

This constitutes the proof of the necessary condition, and the condition is obviously sufficient.

On the other hand, a necessary condition for f to be unity *only when θ is unity* is that ψ have no zeros in the neighborhood of $\theta=1$ in which Eq. (9) holds.

It follows that *when f has continuous derivative of all orders at $\theta=1$, a necessary and sufficient condition for f to be unity when and only when θ is unity is that Eq. (9) hold in the neighborhood of $\theta=1$ and that ψ have no zeros in that neighborhood.*

[1] C. A. Hollingsworth, J. Chem. Phys. **20**, 921 (1952).

Contact Angles and Boundary Energies of a Low Energy Solid

F. M. Fowkes and W. M. Sawyer
Shell Development Company, Emeryville, California
(Received August 8, 1952)

FUNDAMENTAL quantities associated with the wetting of solids are the free energies of the solid/vapor boundary (γ_{SV}) and the solid/liquid boundary (γ_{SL}). These have been obtained for the special case of a glassy solid fluorocarbon on which the contact angles (θ) have been measured for liquids of widely different surface tension (γ_{LV}). The excellent agreement between the observed angles and those calculated from the theoretical relation,

$$\gamma_{SV}-\gamma_{SL}=\gamma_{LV}\cos\theta,$$

is offered as experimental verification of this equation.

Measurements were made on a series of fractions obtained from the vacuum distillation of a perfluorinated lubricating oil.[1] At 25°C these varied from fluid liquids to a brittle solid with increase in boiling range. The surface and interfacial tensions of the liquid fractions presented in Table I were measured by the drop-volume technique. These show no significant dependence on molecular weight as indicated by boiling range. A similar insensitivity of surface tension to molecular weight is reported for lubricating oils[2] and relatively high molecular weight hydrocarbons.[3] The transition from liquid to solid involves no essential structural change in the amorphous oil, and no contribution to the surface energy of the solid would be expected as a result of crystallinity.[4] Mean values of the surface and interfacial tensions obtained with the liquid fractions were then taken as equal to γ_{SV} and γ_{SL}, respectively, for the solid and used to calculate θ by the above equation. Values of θ (advancing) for drops of the several liquids on the solid fraction were measured with a simple goniometer and are compared with the calculated values in Table I. The use of the above equation for calculating contact angles from boundary tensions gives values in excellent agreement with those determined by direct measurement. This agreement also indicates that this low energy surface is not appreciably modified by adsorption of these vapors.[5,6]

TABLE I. Surface and interfacial properties of perfluorinated lubricating oil fractions at 25°C.

Boiling range at 5 mm Hg, °C	Surface tension, dynes/cm	Interfacial tension *vs* Water (γ_{LV}=72.0)	α-Methylnaphthalene (γ_{LV}=37.2)	Benzene (γ_{LV}=28.5)
124–135	21.8	57.0	12.7	7.8
135–145	22.3	56.3	12.5	7.8
145–155	22.8	58.4	12.9	7.9
155–165	22.6	59.3	···	7.5
Mean value	22.4	57.7	12.7	7.7
Observed contact angle *vs* solid		117°±3°	76°±2°	57°±2°
Calculated contact angle *vs* solid		119°	75°	59°

The contact angles on this surface are higher than those observed on polytetrafluoroethylene.[6] This results in smaller values of $\gamma_{LV}\cos\theta$; thus, γ_{SV} is lower and/or γ_{SL} is higher for the several liquids. The value of 22.4 dynes/cm for γ_{SV} is in agreement with that estimated for the "$-CF_3$ surface" of adsorbed perfluorocapric acid.[7] The approximation of γ_{SV} obtained by the application of Antonoff's rule[8] yields 18.3, 23.5, and 21.8 dynes/cm with water, α-methylnaphthalene, and benzene, respectively.

[1] Supplied by E. I. du Pont de Nemours and Company and designated FCX-412.
[2] M. Z. Freund, Petroleum **35**, 269 (1939).
[3] M. P. Doss, *Physical Constants of Pure Hydrocarbons* (The Texas Company, New York, 1943).
[4] J. W. Gibbs, *Collected Works* (Yale University Press, New Haven, 1928), p. 315.
[5] G. E. Boyd, and H. K. Livingston, J. Am. Chem. Soc. **64**, 2383 (1942); see also J. W. Gibbs, *Collected Works* (Yale University Press, New Haven, 1928), p. 329.
[6] H. W. Fox and W. A. Zisman, J. Colloid Sci. **5**, 514 (1950).
[7] F. Schulman and W. A. Zisman, Presented at the Buffalo meeting of the American Chemical Society, March, 1952.
[8] G. A. H. Elton, J. Chem. Phys. **19**, 1066 (1951).

The Nature of the Thermal Color Change in Zinc Oxide

C. K. Coogan and A. L. G. Rees
Chemical Physics Section, Division of Industrial Chemistry, Commonwealth Scientific and Industrial Research Organization, Melbourne, Australia
(Received August 12, 1952)

SOME confusion exists in the literature on the nature of the color change produced in pure zinc oxide by heating.[1,2] The reversible change from white to yellow with increasing temperature has been ascribed to partial decomposition of the ZnO at high temperatures to give a zinc-rich nonstoicheiometric oxide having a defect absorption band at 4000–4300A. On cooling, the nonstoicheiometric oxide is thought to recombine with oxygen.

Color change takes place at quite low temperatures ($<0.25T_m$, where T_m is the melting point in °K) and is completely reversible on cooling to room temperature, unless the heating has been prolonged at temperatures $>0.25T_m$. The absence of lag in the color change at such low temperatures suggests that solid and surface diffusion do not take place[3] and that the color change should not be ascribed to defects.

Nicholl[4] has pointed out that the color change may be ascribed to a thermal shift of the ultraviolet absorption band of ZnO. A recent measurement by Miller[5] of the shift in the absorption edge for a single crystal of ZnO in air with change in temperature shows a shift of about 1.4A/°C towards the red in the range 26–77°C. There is some evidence that the thermal shift of the absorption edge frequency will be a linear function of temperature.[6] An extrapolation of Miller's results on this basis places the absorption edge at about 4700A at 425°C, which would produce a pronounced yellow appearance in the solid.

To prove that the color change is of thermal origin, ZnO was heated in vacuum to 400–500°C, a barium getter fired to remove any oxygen evolved, and the temperature allowed to fall. The oxide regained its white color immediately. The reversible color change of ZnO must, therefore, be ascribed to a thermal shift of the absorption band into the visible region and not to a stoicheiometric defect. Only after prolonged heating under nonoxidizing conditions does ZnO attain a permanent yellow color due to stoicheiometric excess of Zn.

It is possible that color changes induced by heating in other oxides (e.g., CeO_2, In_2O_3) may be of similar origin.

[1] H. H. Baumbach and C. Wagner, Z. phys. Chem. **22B**, 199 (1933).
[2] J. S. Anderson, Ann. Repts. Chem. Soc. **43**, 110 (1947).
[3] Bevan, Shelton, and Anderson, J. Chem. Soc. **1947**, 1729.
[4] F. H. Nicholl, J. Opt. Soc. Am. **38**, 817 (1948).
[5] P. H. Miller, *Semi-Conducting Materials* (Butterworth Scientific Publications Ltd., London, 1951), p. 172.
[6] I. C. Cheeseman, Proc. Phys. Soc. (London) **A65**, 25 (1952).

Infrared Emission and Absorption of Thermally Excited Carbon Dioxide*

RICHARD H. TOURIN
Industrial Scientific Company, New York, New York
(Received August 14, 1952)

MEASUREMENTS have been made of the infrared emission and absorption of carbon dioxide under controlled conditions of temperature, pressure, and composition, at temperatures up to 1100°C. This work is aimed towards obtaining precise information on the spectral emissivities of combustion gases at high temperatures. Very few measurements of this type have been carried out heretofore[1,2] and no reliable values of emissivities obtained. Carbon dioxide was selected as a suitable gas for initial study, since its absorption spectrum is well known, its molecular structure has been established, and it is an important product of hydrocarbon combustion.

The apparatus used comprises a special gas cell, heating equipment, and an infrared spectrophotometer. The gas cell constructed was a fused quartz tube equipped with windows and connections to the gas line and manometer. The heating equipment consists of a tube furnace, in which the gas cell is placed, and a power supply unit which includes a controller to maintain constant temperature in the furnace. The spectrophotometer is a modified Perkin-Elmer 12-C infrared spectrometer with supplementary optics designed to permit both absorption and emission measurements with the furnace.

Figure 1 shows an example of the emission from carbon dioxide in the 2.8-micron and 4.3-micron regions, measured with the

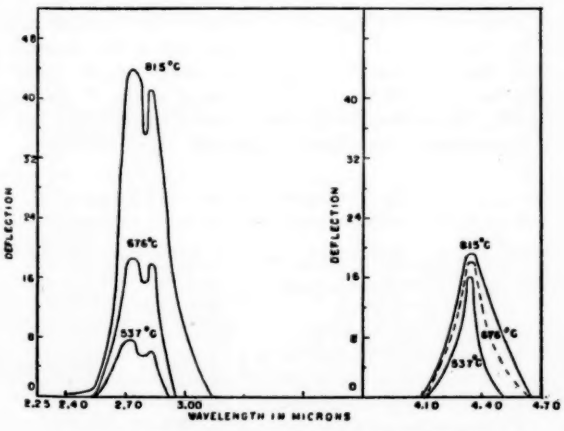

FIG. 1. Infrared emission of heated carbon dioxide.

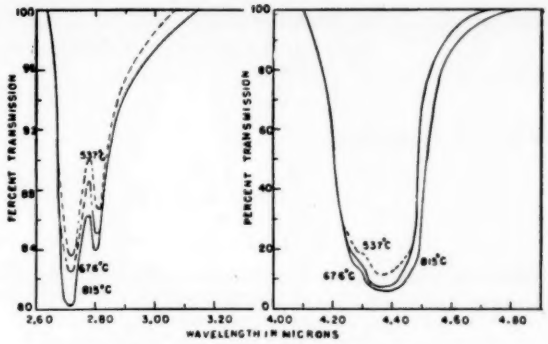

FIG. 2. Infrared absorption of heated carbon dioxide.

setup described above, using a rocksalt prism. The gas cell was filled to a pressure of 62 mm Hg, with commercial 99.96 percent pure "bone-dry" carbon dioxide, having water vapor as a trace impurity. This spectrum has been corrected for the effect of atmospheric absorption. However, no correction has been made for the fact that the quartz windows absorb more strongly in the 4.3-micron than in the 2.7-micron region, and the intensities in the two sets of curves are therefore not comparable. The 3716 cm^{-1} and 3609 cm^{-1} combination bands of carbon dioxide appear at the left. These are the bands which are difficult to observe in flame spectra, due to overlapping by the water vapor fundamental bands. In these measurements the slit width was about 50 cm^{-1}. On the right in Fig. 1 we have the 2349 cm^{-1} CO_2 fundamental, which is not resolved. The slit width used here was about 30 cm^{-1}. The absorption spectrum of heated carbon dioxide appears in Fig. 2 measured under the same conditions as the emission.

Further measurements have been made, with higher resolution, and will be reported on in the near future.

* Flight Research Laboratory, Wright Air Development Center, Air Research and Development Command. Presented at the Symposium on Energy Transfer in Hot Gases, National Bureau of Standards, Washington, D. C., September 17–18, 1951.

[1] See Schmidt, Ann. Physik **42**, 415 (1913).
[2] C. Tingwaldt, Physik Z. **39**, 1 (1938).

Modified Distribution Functions for Ethylene Oxide-Type Polymerizations

LOUIS GOLD
Research Laboratory of Electronics, Massachusetts Institute of Technology, Cambridge, Massachusetts
(Received August 8, 1952)

THE class of polymerization commonly associated with ethylene oxide is distinguished by invariancy of the number of propagating species, a condition, which for identical reaction rates of monomer with diverse sized species, Flory[1] has demonstrated leads to a Poisson distribution of molecular size for the resultant polymer.

The present communication is the forerunner of a detailed report of an investigation related to the identification of the size distribution functions where the restriction of identical reaction rates no longer prevails, a consideration which has important practical implications. The basic formulation of the problem employed is such as to yield a solution which holds for any degree of polymerization. Thus, for the instance of an initiation rate distinct from identical propagation rates the distribution may be expressed in the form

$$N_x/I_0=\frac{1}{r}\cdot P(Y,x)\cdot F(Z,x), \qquad (1)$$

where N_x is the number of x-mers for a prescribed amount of initiator I_0, and r is the ratio of propagation and initiation rates,

$kp/k_i=r$; $P(Y, x)$ is the Poisson function

$$P(Y, x)=(Y^x/x!)e^{-Y} \quad (2)$$

with

$$Y=r\ln(I_0/I); \quad (3)$$

while for $F(Z, x)$ we have

$$F(Z, x)=1+\sum_{p=1}^{\infty}\frac{Z^p}{(p/II)_{m=1}(x+m)}, \quad (4)$$

with

$$Z=(r-1)\ln(I_0/I). \quad (5)$$

I denotes the residual amount of initiator for specified quantities of monomer consumed according to the relation

$$M=M_0+(1-r)(I-I_0)+rI_0\ln(I/I_0), \quad (6)$$

where M and M_0 are the instantaneous and initial concentrations of monomer, respectively.

It is clearly evident that $r\to\infty$ enhances the likelihood of securing high polymers even where relatively high concentrations of initiator are present. The time-dependent Flory solution derives from $r=1$.

[1] P. J. Flory, J. Am. Chem. Soc. **62**, 1561 (1940).

The Infrared Spectra of PF_3, POF_3, and PF_5*

H. S. Gutowsky and A. D. Liehr†
Noyes Chemical Laboratory, University of Illinois, Urbana, Illinois
(Received July 25, 1952)

THE Raman spectrum of PF_3 has been reported and a frequency assignment proposed.[1] However, polarization data were not obtained, and our observations of the infrared spectrum demonstrate an inversion in the assignment of the two low frequency fundamentals. The spectrum in Fig. 1, of the gas, shows that the bands at 486 and 891 cm^{-1} have the *PQR* structure characteristic of parallel bands of a symmetric top and correspond therefore to the A_1 species.[2] Table I summarizes the Raman and infrared data, the frequency assignments, and gives recalculated valence type force constants.

POF_3 is a C_{3v} molecule with six fundamentals, five of which have been found[3] in the Raman spectrum. The infrared band structures, combined with the Raman polarization data, locate the other fundamental and verify the frequency assignment. The data and assignments are summarized in Table II. In addition, there are listed force constants computed by Wilson's matrix methods,[4] neglecting off-diagonal terms in F and the $f_{\alpha\beta}$ terms in F_{33}. The P—F stretching constant f_d is considerably higher in POF_3, 6.18, than in PF_3, 4.64, while f_{dd} remains unchanged. However, f_α, the FPF angle bending is weaker in POF_3 than in PF_3, and the angle interactions also appear to differ.

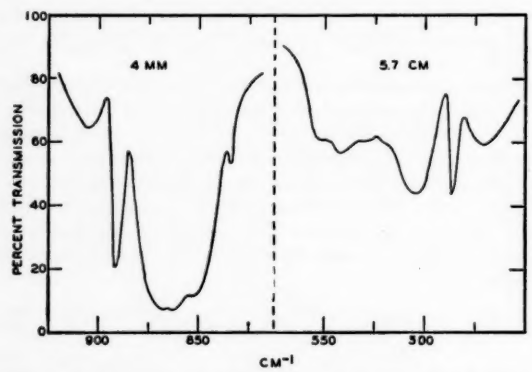

FIG. 1. The infrared spectrum of PF_3 gas, at room temperature, in a cell 10 cm long.

TABLE I. Raman and infrared spectra of PF_3, frequency assignment, and force constants.

Spectra: Raman[1] (g), cm^{-1}	Spectra: Raman[1] (1), cm^{-1}	Spectra: Infrared[a] (g), cm^{-1}	Frequency assignment: Fundamental	Frequency assignment: Ref. (1)	Frequency assignment: This research
487 (7)	486 (3)	486 ∥	$A_1\nu_1$ stretching	890 cm^{-1}	892 cm^{-1}
···	531 (3)	532 ⊥	(∥)ν_2 bending	531	487
851 (5)	840 (10)	844 ⊥	$E\nu_3$ stretching	840	848
893 (5)	890 (10)	891 ∥	(⊥)ν_4 bending	486	532
Force Constants[b]			f_d	f_α	f_{dd}	$f_{\alpha\alpha}$
10^5 dynes/cm			4.64	1.15	0.78	−0.09

[a] The separation of P and R branch maxima in parallel bands is about 32 cm^{-1}.
[b] See reference 2, p. 188. The calculations assume α, the FPF angle, is 104° [Brockway and Wall, J. Am. Chem. Soc. **56**, 2373 (1934)]. Fundamental constants were taken from Beardon and Watts, Phys. Rev. **81**, 73 (1951).

No prior spectroscopic observations of PF_5 seem to have been reported. Electron diffraction indicates a D_{3h} trigonal bipyramid structure[5] which would lead to five infrared active fundamentals, two parallel A_2'' bands and three perpendicular E' bands. Preliminary infrared data obtained on the gas are listed in Table III, with tentative assignment of four fundamentals. The fifth infrared active fundamental is probably below the limit of the KBr optics used. The band at 1025 cm^{-1} suffered inteference from the intense 1031 cm^{-1} band of SiF_4, a trace of which was in the sample. The band at 534 cm^{-1}, has structure rather similar to the definitely parallel band at 576 cm^{-1}, but is assigned as the E' PF_3 deformation by elimination. Additional infrared observations of PF_5, including longer wavelengths, are planned.

TABLE II. Raman and infrared spectra of POF_3, frequency assignments, and force constants.

Raman[a] (1), cm^{-1}	Infrared[a] (g), cm^{-1}	Assignment	Frequency assignment and force constants
			A_1 species (∥; R, p)
337 dp		ν_6	ν_1 PO stretching 1415 cm^{-1}
	473 s, ∥	ν_3	ν_2 PF stretching 873
476 dp	485 ms, ⊥	ν_5	ν_3 PF_3 deformation 473
	690 vw	$2\nu_6$	E species (⊥; R, dp)
	830 w	$\nu_5+\nu_6$	ν_4 PF stretching 990
875 p	873 ms, ∥	ν_2	ν_5 PF_3 bending 485
	946 w	$2\nu_3$	ν_6 PF_3 rocking 345
	957 w	$\nu_3+\nu_5$	
982 dp	990 vs, ⊥	ν_4	
	1275 w, ∥	$2\nu_3-\nu_3$	f_B 11.4×10^5 dynes/cm
	1330 m	$\nu_4+\nu_6$	f_d 6.18
	1345 m	$\nu_2+\nu_3$	f_{dd} 0.79
	1360 w	$\nu_2+\nu_5$	$f_\alpha-f_{\alpha\alpha}$ 0.84
1395 p	1415 ms, ∥	ν_1	$f_\beta-f_{\beta\beta}$ 0.365
	1462 w	$\nu_3+\nu_4$	$f_{\alpha\alpha}+f_{\beta\beta}$ 0.052
	1472 w	$\nu_4+\nu_5$	
	1740 vw	$2\nu_2$	PO[b] is $D=1.48$ A°
	1855 m	$\nu_2+\nu_4$	PF is $d=1.52$ A°
	2295 w	$\nu_1+\nu_2$	∠FPF is $\alpha=109°28'$
	2815 vw	$2\nu_1$	∠OPF is $\beta=109°28'$

[a] The separation of P and R branch maxima in parallel bands is about 22 cm^{-1}.
[b] The structural data are discussed by Hawkins, Cohen, and Koski, J. Chem. Phys. **20**, 528 (1952). The assumed tetrahedral angles simplify the calculations and are close enough to the observed 107°±2°, for α, to give accurate results.

TABLE III. The infrared spectrum of PF_5 gas.

cm^{-1}	Assignment	cm^{-1}	Assignment
534 ms (⊥?)	E' PF_3 deformation	938, 948, 957 s ∥	A_2'' PF_2 stretch
		985 w	
565, 576, 585 ms ∥	A_2'' PF_3 inversion		
		1025 vs ⊥	E' PF_3 stretch
870 w		1590 w	
898 w ⊥		1670 vw	
		1760 vw	

The spectra were obtained at room temperature with Perkin-Elmer spectrometers, Models 12B and 21, equipped with NaCl and KBr optics. PF_3 was prepared by the fluorination of distilled PCl_3 with AsF_3;[1] PF_5, by the similar reaction of PCl_5.[6]

We thank Dr. C. J. Hoffman and Mr. D. W. McCall for several of the preparations. POF_3 was produced by the moisture catalyzed reaction of PF_5 with silica[7] in the gas handling system; the SiF_4, also formed in the reaction, and unreacted PF_5 were identified by their spectra and removed by fractional distillation. Several spurious bands were caused by interaction between samples, particularly POF_3, and the gas cell windows; they were identified readily by comparing spectra in cells with NaCl and KBr windows.

* Based in part on an undergraduate thesis submitted by A. D. Liehr to the Department of Chemistry, University of Illinois.
† Now at Harvard University, Cambridge, Massachusetts.
[1] D. M. Yost and T. F. Anderson, J. Chem. Phys. **2**, 624 (1934).
[2] G. Herzberg, *Infrared and Raman Spectra of Polyatomic Molecules* (D. Van Nostrand Company, Inc., New York, 1945), p. 416.
[3] M. L. Delwaulle and F. Francois, Compt. rend. **222**, 550 (1946).
[4] E. B. Wilson, Jr., J. Chem. Phys. **7**, 1047 (1939); **9**, 76 (1941); A. G. Meister and F. F. Cleveland, Am. J. Phys. **14**, 13 (1946).
[5] L. O. Brockway and J. Y. Beach, J. Am. Chem. Soc. **60**, 1836 (1938).
[6] R. Linke and W. Rohrmann, Z. phys. Chem. **B35**, 256 (1937).
[7] A. B. Burg, "Volatile inorganic fluorides," in *Fluorine Chemistry* (Academic Press, Inc., New York, 1950), p. 98.

Molecular Orbital Theory of Reactivity in Aromatic Hydrocarbons

H. H. GREENWOOD
Sir John Cass College, Aldgate, London, E.C. 3, England
(Received July 31, 1952)

IN a recent paper Fukui *et al.*[1] have suggested that the reactions of conjugated hydrocarbons are associated in particular with the density distribution of the two π-electrons which occupy the highest occupied energy level of the ground state configuration. These they term the "frontier" electrons.

We have recently obtained results of quite a different kind. These may best be illustrated briefly by reference to reactions involving attack by electrophilic reagents. The investigation shows that the two π-electrons which tend to be localized at the position of attack are those which occupy the lowest i.e., the deepest energy level. The remaining π-electrons, including the "frontier" electrons, are simultaneously removed from this region. The energy required to bring about this partial or complete localization may be looked upon as being used partly in localizing the two π-electrons concerned, and partly in removing the remaining π-electrons from the region of localization. It is therefore not strictly logical to attempt to correlate experimentally observed rates of reaction with the density distribution of a particular pair of π-electrons, i.e., with the pair which tend to become localized.

It is hoped to publish the detailed results of this investigation shortly.

[1] Fukio, Yonezawa, and Shingo, J. Chem. Phys. **20**, 722 (1952).

On the Use of Unfiltered Light in Determining Molecular Weights by Light Scattering*

MILTON KERKER
Department of Chemistry, Clarkson College of Technology, Potsdam, New York
(Received August 8, 1952)

THE determination of molecular weights by light scattering is generally carried out with the 5461A line of a mercury vapor lamp isolated with the aid of Corning Glass filters. These filters reduce the visible light intensity by a factor of about 25. For dilute solutions the intensity of scattered radiation may be so small that measurements become difficult and it is desirable to either increase the sensitivity of the instrument or the intensity of the incident beam. The latter can be effected by using unfiltered light. This paper will demonstrate that with unfiltered light the data can be used to obtain the same information about molecular weights as with monochromatic light.

For monochromatic light, the molecular weight is related to the turbidity by[1]

$$\tau_\lambda=\frac{16}{3}\pi r^2(i_\lambda/I_\lambda)=H_\lambda cM, \tag{1}$$

where

$$H_\lambda=(32\pi^3\mu_0^2/3N\lambda^4)\left(\frac{\mu-\mu_0}{c}\right)^2, \tag{2}$$

τ_λ = excess turbidity, i_λ = intensity of light scattered at 90° to the incident direction, I_λ = intensity of incident light beam, c = concentration in g/cc, M = molecular weight, N = Avogadro's number, λ = wavelength in cm, μ_0 = refractive index of solvent, μ = refractive index of solution, and r = distance of observer from scatterer in cm.

The intensity scattered at 90° is

$$i_\lambda=\frac{3}{16\pi r^2}H_\lambda cMI_\lambda=H_\lambda{}^1cMI_\lambda, \tag{3}$$

where $H_\lambda{}^1$ includes the numerical factor $3/16\pi r^2$. For unfiltered light consisting of discrete wavelengths, the total intensity scattered at 90° is

$$i=\Sigma\, i_\lambda=cM\,\Sigma\, H_\lambda{}^1I_\lambda, \tag{4}$$

where the summation is extended over each of the wavelengths in the spectrum. In practice it will probably be necessary to include only two or three wavelengths when the mercury vapor lamp is used.

Let the response of the phototube as recorded by the deflection of a galvanometer to light of wavelength λ and unit intensity be R_λ and the response of the phototube to the entire spectrum of scattered radiation at 90° be d. Then

$$d=\Sigma\, i_\lambda R_\lambda=cM\,\Sigma\, H_\lambda{}^1I_\lambda R_\lambda, \tag{5}$$

and the molecular weight is given by

$$M=\frac{d}{c}\left[\frac{1}{\Sigma\, H_\lambda{}^1I_\lambda R_\lambda}\right]. \tag{6}$$

It is now necessary to evaluate the square bracket above, which means evaluating the individual quantities $I_\lambda R_\lambda$. In order to do this, the incident beam should be directed through a monochromator. The monochromator of the Beckmann spectrophotomer which is found in most laboratories can be used. The beam emerging from the monochromator is permitted to fall upon the same phototube used in the light scattering apparatus. Let F be a factor by which the incident beam is reduced on passing through the monochromator, and let us assume it is independent of wavelength. In the event there is a dispersion of F with wavelength, only the relative values of F as a function of wavelength need be determined.

The response of the phototube to each wavelength in the monochromator experiment is given by

$$d_\lambda{}^1=FI_\lambda R_\lambda. \tag{7}$$

Let D be the phototube response when the incident beam used in the light scattering experiment shines directly on the phototube. Then D is given by

$$D=\Sigma\, I_\lambda R_\lambda. \tag{8}$$

But from Eq. (7),

$$\frac{\Sigma\, d_\lambda{}^1}{F}=\Sigma\, I_\lambda R_\lambda=D, \tag{9}$$

so that

$$F=\frac{\Sigma\, d_\lambda{}^1}{D}. \tag{10}$$

By Eqs. (7) and (10) we obtain

$$I_\lambda R_\lambda=\frac{d_\lambda{}^1}{\Sigma\, d_\lambda{}^1}D, \tag{11}$$

which when substituted in Eq. (6) gives

$$M=\frac{d}{c}\left\{\frac{1}{\Sigma[H_\lambda{}^1(d_\lambda{}^1/\Sigma d_\lambda{}^1)D]}\right\}. \tag{12}$$

The quantities d and D, the galvanometer deflections produced by the light scattered at 90° and the transmitted light are those usually obtained in a light-scattering experiment. The quantities $d_\lambda{}^1$ are the galvanometer deflections obtained in the auxiliary experiment with the monochromator. These quantities could alternatively be determined by multiplying together the relative output of the lamp and response of the phototube at the respective wavelengths. These data are usually obtainable from the manufacturers of the equipment.

For nonideal solutions where the following equation is applicable,

$$H_\lambda\frac{c}{\tau_\lambda}=\frac{1}{M}+2\frac{Bc}{RT}, \tag{13}$$

the appropriate expression for unfiltered light is

$$c\frac{\Sigma[H_\lambda{}^1(d_\lambda{}^1/\Sigma d_\lambda{}^1)D]}{d}=\frac{1}{M}+\frac{2BC}{RT}. \tag{14}$$

The molecular weight is given by the reciprocal of the intercept on the ordinate when the left-hand side of (13) is plotted against concentration.

* The work reported herein was supported by Office of Ordnance Research, U. S. Army, Contract Number DA-30-115-ORD-309.

[1] G. Oster, Chem. Revs. **43**, 319 (1949).

On the Statistical Theory of Crystallite Length

ROBERT SIMHA
Department of Chemical Engineering, New York University, University Heights, New York, New York

(Received July 21, 1952)

RECENTLY a thermodynamic investigation of solid polyethylene has been presented.[1] In connection with the crystallinity of this branched polymer, the size distribution of (crystallizable) sequences between branch points was considered. It is the purpose of this note to comment on the statistical results obtained by these authors.

The problem at hand involves the distribution of two species, branched and unbranched units, over a fixed number of sites. Hence it is completely analogous to two other questions previously treated, namely, the size distribution of a randomly degrading polymer[2] and the sequence distribution in a random copolymer.[3] Translated into the language of the present problem, the nature of the calculation involved may be summarized as follows: First we assume that one of the N chains carries an arbitrary number y of branch points and compute $N_\zeta(y)/N$, the number of sequences of length ζ in that chain, as a function of y. Now there are altogether B branched units in the sample which can be distributed in a variety of ways over the N chains and S units forming the backbone of a molecule. Consequently $N_\zeta(y)$ must next be multiplied by a weighing factor, that is, the probability that one out of N chains has y out of a total of B branch points. Finally the product must be summed over all possible values of y, $0\leqq y\leqq S-\zeta$. Assuming the formation of branches to have occurred at random, we find for N_ζ, the total number of ζ-sequences in N molecules with B branch points:

$$\left.\begin{aligned}N_\zeta/N&=\alpha(1-\alpha)^\zeta\\ N_S/N&=(1-\alpha)^S[2+(S-\zeta-1)\alpha];\quad 0\leqq\zeta\leqq S-1\end{aligned}\right\}. \tag{1}$$

Here $\alpha=B/NS=\bar{y}/S$ represents the average fraction of branched units in the main chain. Equation (1) is identical with a familiar result in degradation theory.

The results in reference 1 are at variance with Eq. (1) because the authors erroneously assumed that there are $\bar{y}$ branch units in each chain without making allowance for fluctuations. Thus only the first step in the calculation outlined above is carried out. Indeed, their Eq. (11) for C_ζ corresponds exactly, as it should, to the intermediate quantity f_{tr} in Eq. (2) of reference 2, taking into consideration differences in definitions and symbols. Thus, with $S\to p$, $y\to r$, $\zeta\to t-1$,

$$C_\zeta\to f_{tr}\binom{p}{r}\times(p+1)/t.$$

Following the notation of reference 1, one finds from Eq. (1) for the number and weight fractions,

$$\bar{\nu}_\zeta=N_\zeta/\sum_{\zeta=0}^{S}N_\zeta=N_\zeta/(1+\bar{y}),$$

$$\bar{W}_\zeta=\zeta N_\zeta/\sum_{1}^{S}\zeta N_\zeta=\zeta\bar{\nu}_\zeta(1+\bar{y})/(S-\bar{y}),$$

and the number average length of a sequence

$$\langle\zeta\rangle=\Sigma\,\zeta N_\zeta/\Sigma\,N_\zeta=(S-\bar{y})/(1+\bar{y}).$$

The formula

$$N_\zeta/N=S\alpha^2(1-\alpha)^\zeta, \tag{1a}$$

frequently used, is valid and follows from (1) for $S-\bar{y}\gg\zeta$, $\bar{y}\gg1$. These conditions are fulfilled for the relatively high degrees of branching normally encountered in polyethylene. When α is small, say, of the order of 10^{-2} for a molecular weight $\sim3\times10^4$, it follows that $S<2\times10^3$, $\langle\zeta\rangle\sim10^2$, and the exact Eq. (1) must be used.

[1] Dole, Hettinger, Larson, and Wethington, J. Chem. Phys. **20**, 781 (1952).
[2] E. W. Montroll and R. Simha, J. Chem. Phys. **8**, 721 (1940).
[3] R. Simha, J. Am. Chem. Soc. **63**, 1479 (1941).

Luminescence of Ice and Tritiated Ice

LEONARD I. GROSSWEINER AND MAX S. MATHESON
Chemistry Division, Argonne National Laboratory, Chicago, Illinois

(Received July 25, 1952)

WORK currently in progress at this laboratory has shown that pure ice at low temperatures emits ultraviolet radiation when excited by filtered 50-kv tungsten x-rays. To our knowledge, this luminescence has not been previously reported.[1,2]

The ice samples were prepared by distilling in vacuum, in the absence of grease, 10 cc of triply distilled water[3] into scrupulously clean 26-mm Pyrex tubes and slowly freezing from the bottom up by placing the tubes on a cooled aluminum rod. Immediately before use the sample tubes were opened on a dry box and the ice samples transferred to the sample holder.

The sample holder was a 7-in.×1¼-in. cylindrical brass rod, hollowed out at the upper end to form a 1½-in.×1-in. well. The luminescence was transmitted through a conical side tube attached to a ¾-in. hole in the side of the well. A 2 mm thick quartz window closed the side tube. The top of the well was made vacuum-tight with a flange using 2-mil aluminum foil through which the exciting x-rays were passed. Cooling was effected by immersing the sample holder base in liquid nitrogen and temperatures were measured by a copper-constantan thermocouple soldered into the sample holder wall adjacent to the sample.

Light transmitted by the quartz window was collected by a 100-mm front-surface aluminized mirror and focused by a similar mirror on either a 1P28 photomultiplier tube or Eastman 103-0 plate. A 50-kv, 50-ma tungsten target beryllium window x-ray machine was used with a 100-mg/cm² aluminum filter which permitted x-rays of 0.24 to 1.2A to reach the ice. The x-ray dosage was measured with the ferrous sulfate oxidation reaction[4] to be 116,000 r/hr at 40-ma x-ray current.

A steady luminescence from the ice was detected under steady excitation in the temperature range of −170 to −100°C. The spectral distribution as determined with a series of Corning filters showed a peak at 3400A. The intensity of steady luminescence was linear with x-ray current over a dosage range of 400 to 100,000 r/hr. The intensity of luminescence decreased with increasing

temperature, and in the range −160 to −130°C the Arrhenius equation was followed with an activation energy of 0.20 ev. Other aspects of this luminescence, including the build-up and decay, are being investigated and will be reported in detail.

Another aspect of this effect which has been investigated is the luminescence (self-induced) of tritiated ice.[5] An important feature of self-excitation is that the efficiency of conversion of absorbed energy to luminous energy can be estimated since the absorbed energy can be calculated when the tritium concentration is known.

A sample holder similar to, but smaller than, the one previously described was used except that the top of the well was sealed with a quartz window and a magnet was located above the ice level to deflect beta-particles from the quartz. The experiment was performed by distilling 0.5 cc of tritiated water (10 curies per cc) into the sample holder, freezing to liquid nitrogen temperature, and exposing an Eastman Type 103*a*-0 plate to the sample for 24 hours while maintaining a vacuum of 5×10^{-5} mm Hg. The result was a sharp, intense image (which must originate from the sample) over a lighter, diffuse background. From the sensitivity of the plate, the absorbed energy, and the geometry factor we estimate the efficiency of conversion is about 3×10^{-5} quanta emitted per ion pair (assuming 33 ev per ion pair) formed at liquid nitrogen temperature.

It is a pleasure to acknowledge valuable discussions concerning this work with Professor Paul L. Copeland, Department of Physics, Illinois Institute of Technology.

[1] L. H. Gray, J. chim. phys. **48**, 172 (1951), reports a failure to find any light emission from water bombarded with electrons, excepting the Cerenkov spectrum.
[2] Greenfield, Kratz, and Dowdy, UCLA-127 (April 23, 1951), report ultraviolet emission in distilled water exposed to radium gamma-rays, but it appears that this is at least partly Cerenkov radiation from the energetic secondary electrons.
[3] E. J. Hart, J. Am. Chem. Soc. **73**, 69 (1951).
[4] E. J. Hart, J. Am. Chem. Soc. **73**, 1891 (1951).
[5] A. O. Allen and J. A. Ghormley, ORNL-128 (September 1, 1948) report visual luminescence from 20 percent tritiated water when contained in quartz capillaries at both room and liquid nitrogen temperatures, but they point out that such luminescence may be due to either the water or the quartz.

The Average Energy of $Sr^{90}-Y^{90}$ as a Function of Absorber

ROBERT H. GOECKERMANN AND WALTER H. SEITZER
Palmer Physical Laboratory, Princeton University, Princeton, New Jersey
(Received August 6, 1952)

THE average energy of an equilibrium mixture of Sr^{90} and Y^{90} as a function of aluminum absorber has been determined for low absorber by the use of a magnetic lens spectrometer. $Sr^{90}-Y^{90}$ is a good β-source in that it is a pure β-emitter, has fairly high energy (2.24 Mev for Y^{90}), has a long half-life (19.9 yrs), and is available essentially carrier-free.

The variation in average energy was determined by measuring the spectrum, using aluminum foil absorbers; then the average energy $\bar{E}$ was calculated from the ratio

$$\bar{E}=\int_0^{E_{max}}N_E E dE/\int_0^{E_{max}}N_E dE.$$

The values of the integrals were obtained graphically. Table I and Fig. 1 show the results.

TABLE I. Energy *vs* aluminum absorber for $Sr^{90}-Y^{90}$

Al absorber (mg/cm²)	Average energy per count (Mev)	Normalized count	Total average energy (Mev)
0.0	0.558[a]	1.000	0.558
1.6	0.562	0.965	0.543
6.2	0.576	0.870	0.501
10.3	0.591	0.789	0.466
17.2	0.610	0.706	0.431
27.4	0.656	0.603	0.396
41.2	0.705	0.508	0.358

[a] Determined from Fig. 1.

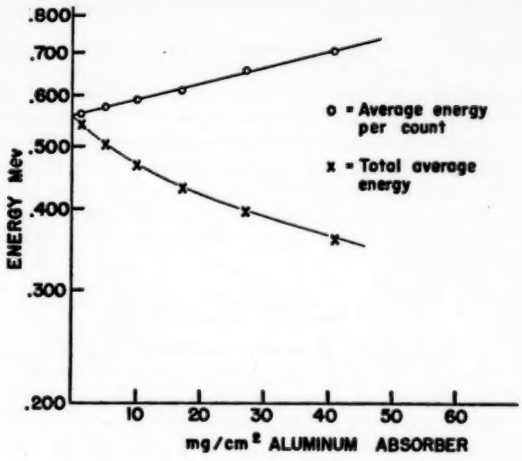

FIG. 1. Plot of logarithm of energy *vs* thickness of aluminum foil for $Sr^{90}-Y^{90}$.

The normalized count was taken from an absorption curve plotted from counts with standard deviations of 0.3 percent to 0.5 percent. The counts from which the β-spectra were plotted had average standard deviations of approximately 2 percent.

The Radiation Decomposition of Organic Molecules

J. B. BIRKS
Physics Department, Rhodes University, Grahamstown, South Africa
(Received July 29, 1952)

ALDER and Eyring[1] have recently reviewed the current experimental data on the decomposition of various organic molecules in solution, induced by ionizing radiation. It is generally observed that the solute concentration $[S]$ decreases from its initial value $[S_0]$ with increased radiation dose It. The disappearance-dose curve is either exponential

$$[S]=[S_0]e^{-\gamma It}, \quad (1)$$

or, when the fraction of solute decomposed is small, it is linear

$$[S]=[S_0](1-\gamma It). \quad (2)$$

The ionic yield, defined as

$$\phi=\gamma[S_0], \quad (3)$$

increases and approaches a constant value as $[S_0]$ increases, according to the relation

$$\phi=(A[S_0])/(1+B[S_0]), \quad (4)$$

where A and B are constants, for a given type of solution and a particular ionizing radiation.

Alder and Eyring propose a general mechanism to account for the behavior of aqueous solutions, involving interactions between H, OH, and HO_2 radicals and the solute molecules, which leads after certain simplifying assumptions to theoretical relations in agreement with the experimental data.

The purpose of this note is to propose an alternative, simpler mechanism of radiation decomposition, in terms of primary photon emission by the molecules ionized and excited by the ionizing radiation. Dee, Richards, and Cole[2,3] have obtained direct experimental evidence for this process, and it has been applied by the author to various radiation phenomena in scintillation crystals and solutions[4] and to photographic emulsions.[5] It is suggested that the primary photons are reabsorbed preferentially by the organic solute molecules, which have an absorption coefficient B relative to those of the solution and which decompose photochemically. On this theory the fraction of the primary photons absorbed by an

initial concentration $[S_0]$ of solute molecules/solvent molecule will be

$$f=(B[S_0])/(1+B[S_0]). \quad (5)$$

If an additional factor A/B is introduced into (5) to describe (a) the efficiency of primary photon production by the particular ionizing radiation and (b) the quantum efficiency of the photochemical decomposition, an expression for the ionic yield in agreement with (4) is obtained.

The definition of ϕ is based on the low dosage yield when $[S]\sim[S_0]$, and (5) is only strictly valid in this region. In general, (5) becomes

$$f=\frac{B[S]}{1+B[S]+B'([S_0]-[S])}, \quad (6)$$

where B' is the relative absorption coefficient of the decomposed molecules, concentration $([S_0]-[S])$. If it is assumed that $B\sim B'$, the validity of (4) may be extended to higher dosages. In their theory, Alder and Eyring equate three parameters describing interactions of radicals and decomposed molecules to unity, to obtain a similar result. It is doubtful, however, that such an extension is either necessary or justified by the present experimental data.

The ionic yield ϕ depends on the specific energy loss of the ionizing radiation, and is reduced by a factor of the order of 100 when the more strongly ionizing α-particles, rather than electrons or x-rays, are used for irradiation. A similar effect occurs with the specific fluorescence of organic crystals and liquids, and it is attributed to local "quenching" of the primary photons by molecules damaged directly by the incident radiation.[4] It is to be expected, however, according to the photon theory, that the factor B in (4) will be independent of the nature of the radiation.

For carboxypeptidase in water, the only solution for which a comparison is made,[1] the experimental values of B for x-rays and α-particles agree within 10 percent.

The photon emission and reabsorption mechanism is not restricted to aqueous solutions. The similar effects reported[1] with solutions of β-carotene in petroleum ether can therefore be explained in terms of the same process, which is of general application.

[1] M. G. Alder and H. Eyring, Nucleonics **10**, No. 4, 54 (1952).
[2] P. I. Dee and E. W. T. Richards, Nature **168**, 736 (1951).
[3] E. W. T. Richards and J. F. I. Cole, Nature **167**, 286 (1951).
[4] J. B. Birks, S.A.A.A.S. Congress, Cape Town, July, 1952; Proc. Phys. Soc. (London) (to be published); Phys. Rev. (to be published).
[5] J. B. Birks, Phys. Rev. **86**, 791 (1952).

Exchange Coupling and the Curie-Weiss Law*

ROALD K. WANGSNESS
U. S. Naval Ordnance Laboratory, White Oak, Maryland
(Received August 15, 1952)

THE fact that the high temperature susceptibility of a pair of exchange-coupled spins can be approximated by a Curie-Weiss law has apparently not been previously pointed out.

The energy levels of the pair in a field H are given by $E_{Sm}=2\mu Hm-JS(S+1)$, where J is the exchange integral, μ the Bohr magneton and $S=0.1$. A straightforward statistical calculation shows that the relative magnetization $m=M/2n\mu$ is given by $m=\sinh h[\cosh h+e^{-j}\cosh j]^{-1}$, where $h=2\mu H/kT$ and $j=J/kT$.

If $h\ll 1$, the susceptibility is

$$\chi=(4C/T)(3+e^{-4\theta/T}+h^2)^{-1}, \quad (1)$$

where $C=2n\mu^2/k$ is the Curie constant and $\theta=J/2k$. If, in addition, $|\theta|/T\ll 1$, one finds from (1) that

$$\chi=C\{T-\theta+(k^2T)^{-1}[(\mu H)^2+\tfrac{1}{2}J^2]\}^{-1} \quad (2)$$

(for simplicity, only the quadratic term in J has been kept). This result shows that θ is the characteristic temperature of the Curie-Weiss law and that its value agrees with that given by the molecular field theories of ferro- and antiferromagnetism, $zJ/2k$, since z, the number of nearest neighbors, is unity in this case. It has been found experimentally that the susceptibilities of certain organic biradicals for which the above considerations may have some relevance do show a Curie-Weiss dependence on temperature.[1]

There are two other interesting results which can be found for the case $\theta<0$. If $h\ll 1$, the susceptibility (which is zero at $T=0$) has a maximum at $T_m=-2.5\theta$. At $T=0$, m is zero if H is less than a critical field $H_c=-J/\mu$, while for H equal to or greater than H_c, m equals $\frac{1}{2}$ and 1, respectively. This is reminiscent of a result recently obtained by Ziman and Garrett.[2]

* Supported in part by the ONR.
[1] Kuhn, Katz, and Franke, Naturwiss. **22**, 808 (1934); Müller, Müller-Rodloff, and Bunge, Ann. Chem. **520**, 235 (1935); E. Müller and I. Müller-Rodloff, Ann. Chem. **521**, 81 (1935); G. Foëx, Le Magnétisme III (Collect. Scientif. Inst. Intern. de Coop. Intellect., Paris, 1940), p. 191.
[2] J. M. Ziman, Proc. Phys. Soc. (London) **64A**, 1108 (1951); C. G. B. Garrett, J. Chem. Phys. **19**, 1154 (1951).

Evidence for a Completely Planar Structure of Pyrrole from Its Microwave Spectrum*

W. S. WILCOX AND J. H. GOLDSTEIN
Department of Chemistry, Emory University, Emory University, Georgia
(Received July 30, 1952)

DESPITE a number of investigations of the structure of the pyrrole molecule, the question of the inclination of the N−H bond to the plane of the ring seems not to have been definitely established. Recently Kofod, Sutton, and Jackson,[1] using dipole moment data, have been able to place a limit of 7° to this inclination. These authors also summarize the experimental work done to date on the structure of pyrrole, and point out that the theoretical treatment of Coulson and Longuet-Higgins[2] predicts a completely coplanar structure.

We have been studying the pure rotational spectrum of pyrrole in the region of 22,000–32,000 mc, using a Stark-effect spectrograph. While our investigations are not yet complete, we feel that sufficient data are at hand to permit us to make a reasonable argument in favor of the coplanar structure.

In all, some 80 lines have been observed in this region, of which about 30 have been identified. In the analysis of the spectrum we have made use of approximate rotational constants calculated from the structural parameters furnished by the electron diffraction data of Schomaker and Pauling.[3] These constants, together with other considerations, have enabled us to identify eight pairs of Q-type lines falling in the K-band which are pertinent to the present argument. Data on these lines are reproduced in Table I. In columns 3 and 4 are listed the frequencies, accurate to about one megacycle, of the lines identified in columns 1 and 2. Columns 5 and 6 give the observed relative intensities of the members of each pair.

If the molecule is indeed entirely coplanar, it falls in point group C_{2v}, and a rotation through 180° about the symmetry axis exchanges two pairs of protons. Hence, a nuclear spin statistical weight factor must be included in the computation of the relative intensities of the rotational absorption lines. In this case the factor is 10 for those lines arising from levels symmetric in the

TABLE I. Portion of Q-type rotational spectrum of pyrrole.

Transition pair		Observed frequency		Observed relative intensity	
$3_{03}-3_{22}$	$3_{13}-3_{12}$	22,674	22,660	10	5.5
$4_{13}-4_{32}$	$4_{23}-4_{22}$	22,681	22,639	7.5	10
$5_{23}-5_{42}$	$5_{33}-5_{32}$	22,696	22,597	[a]	[a]
$6_{33}-6_{52}$	$6_{43}-6_{42}$	22,722	22,530	[a]	[a]
$7_{43}-7_{62}$	$7_{53}-7_{52}$	22,772	22,420	10	5
$8_{53}-8_{72}$	$8_{63}-8_{62}$	22,843	22,259	6	10
$9_{63}-9_{82}$	$9_{73}-9_{72}$	22,947	22,037	10	6
$10_{73}-10_{92}$	$10_{83}-10_{82}$	23,097	21,742	5	10

[a] Incompletely resolved doublets occur at 22,597 and 22,722, rendering uncertain the relative intensities of these pairs.

nuclei and 6 for those from antisymmetric levels.[4] Apart from this factor, the members of each pair of lines in Table I would be expected to have very nearly equal intensities.

If the molecule were not entirely coplanar, it would not fall in group C_{2v}, the nuclear spin statistical weight factor would not apply, and the two lines of each pair would be of the same intensity. The observed relative intensities, within the experimental error, are in agreement with the 10 to 6 ratio predicted for the completely coplanar model. We therefore conclude that the N−H bond of pyrrole lies in the plane of the ring.

* This work supported in part by the Office of Ordnance Research.
[1] Kofod, Sutton, and Jackson, J. Chem. Soc. 1467 (1952).
[2] C. A. Coulson and H. C. Longuet-Higgins, Trans. Faraday Soc. **43**, 87 (1947).
[3] V. Schomaker and L. Pauling, J. Am. Chem. Soc. **61**, 2922 (1939).
[4] G. Herzberg, *Infra-Red and Raman Spectra* (D. Van Nostrand Company, Inc., New York, 1945), p. 53.

Thermodynamic Properties of Diacetylene*

SALVADOR M. FERIGLE AND ALFONS WEBER
Spectroscopy Laboratory, Department of Physics, Illinois Institute of Technology, Chicago 16, Illinois
(Received August 6, 1952)

THE molecular structure of diacetylene has been the object of controversy due to the apparent inconsistency between the values obtained for the bond length and the stretching potential constant of the central carbon-carbon bond.[1,2] The recent experimental work of Jones[3] and a correlation study with dimethyldiacetylene carried out in this laboratory[4] revealed that the anomaly was the result of a misinterpretation of the observed spectrum. Now that this problem is settled, it seems desirable to calculate the thermodynamic properties by using the new assignment of the vibrational frequencies. The values of the fundamentals given by Jones[3] and their corresponding degeneracies are listed in Table I. The moment of inertia also has been calculated by Jones[5] from an analysis of the rotation-vibration spectrum as $I_0=191.13\cdot10^{-40}$ g cm^2 ($B_0=0.14641$ cm^{-1}), which agrees with the value calculated from the electron diffraction data of Pauling *et al.*[6]

TABLE I. Wave numbers and degeneracies corresponding to the fundamental frequencies of diacetylene ($H-C\equiv C-C\equiv C-H$).[a]

Designation	Wave number (cm^{-1})	Degeneracy
ν_1	3329[b]	1
ν_2	2184	1
ν_3	874	1
ν_4	2020	1
ν_5	3329	1
ν_6	627	2
ν_7	482	2
ν_8	630	2
ν_9	220[b]	2

[a] A. V. Jones, reference 3.
[b] Not observed.

TABLE II. Heat content, free energy, entropy, and heat capacity of diacetylene for the ideal gaseous state at 1-atmos pressure.

T(°K)	$(H^0-E_0^0)/T$	$-(F^0-E_0^0)/T$	S^0	C_p^0
100	7.54[a]	38.30	45.84	9.05
200	9.44	44.07	53.51	13.73
273.16	11.02	47.24	58.26	16.76
298.16	11.53	48.23	59.76	17.60
400	13.43	51.89	65.32	20.17
500	14.96	55.06	70.02	21.86
600	16.22	57.90	74.12	23.14
700	17.28	60.49	77.77	24.20
800	18.21	62.86	81.07	25.11
900	19.02	65.07	84.09	25.90
1000	19.74	67.09	86.83	26.61

[a] Cal deg^{-1} mole^{-1}.

Using the above data, the heat content, free energy, entropy, and heat capacity of diacetylene have been calculated for temperatures from 100° to 1000°K, to a rigid rotor, harmonic oscillator approximation. Nuclear spins and the effect of isotopic mixing have been neglected. The calculated values are for the ideal gaseous state at 1-atmos pressure. Birge's 1941 values for the physical constants[7] have been used throughout the calculations. The calculated values are given in Table II.

* Part of a research program which has been aided by grants from the Research Corporation, the American Academy of Arts and Sciences, and by a contract (DA-11-022-ORD-464) with the Office of Ordnance Research.
[1] G. Herzberg, *Infrared and Raman Spectra of Polyatomic Molecules*, (D. Van Nostrand and Company, Inc., New York, 1945), first edition, p. 324.
[2] T. Y. Wu, *Vibrational Spectra and Structure of Polyatomic Molecules*, (J. W. Edwards, Ann Arbor, 1946) second edition, p. 259.
[3] A. V. Jones, Proc. Roy. Soc. (London) **A211**, 285 (1952).
[4] Ferigle, Cleveland, and Meister, Phys. Rev. **81**, 302 (1951); J. Chem. Phys. **20**, 526 (1952); J. Chem. Phys. (to be published).
[5] A. V. Jones, J. Chem. Phys. **20**, 860 (1952).
[6] Pauling, Springall, and Palmer, J. Am. Chem. Soc **61**, 927 (1939).
[7] R. T. Birge, Revs. Modern Phys. **13**, 233 (1941).

Separation of High Specific Activity Sodium^{22} from Large Quantities of Magnesium

V. J. LINNENBOM
Nucleonics Division, Naval Research Laboratory, Washington, D. C.
(Received August 6, 1952)

RADIOACTIVE sodium of high specific activity has usually been separated from bombarded magnesium by hot water extraction of either MgO,[1,2] or $MgCO_3$.[3] Another method involves the precipitation of magnesium ammonium carbonate, which does not carry the sodium activity.[4] For the separation from small quantities of magnesium (14 mg) an ion-exchange technique has been employed.[5]

We have extended the ion-exchange technique to include situations where large quantities (15 g or more) of magnesium must be processed. The advantages of the ion-exchange technique over the hot water extraction method are several, among which may be mentioned cleanness of separation, quantitativeness of recovery, and in the case where large amounts of activity are involved, decreased exposure of the worker to radiation hazards. For example, preliminary experiments carried out in this laboratory in which hot water extraction of MgO was used resulted in the recovery of only 85 percent of the activity regardless of whether the MgO was obtained by ignition of either the nitrate or oxalate. The formation of colloidal MgO is also an objectionable feature of the hot water extraction method.

The ion-exchange column which was used was prepared in the following manner: 100-mesh Dowex-50 resin was first conditioned by slurrying in a large beaker with alternate portions of 3*N* HCl and 3*N* NaCl until the washings were color-free, then given a final rinse with water, and air-dried. About 850 g of this air-dried resin was then slurried with water into a large polystyrene column and allowed to rest on a mat of polyethylene fiber supported on a fine-mesh tantalum screen, which in turn was supported by a hollow Lucite plug cemented into the bottom of the column. No glass was used in the construction of the column. After settling, the resin was given a final wash with 3*N* HCl, then washed thoroughly with water until the washings were neutral. The resin bed as thus prepared measured in water 115 cm in height and 3.8 cm in diameter; it had a theoretical capacity of approximately 4.2 equivalents, about 3.5 times the amount of magnesium which was put through.

Fifteen grams of deuteron-bombarded magnesium metal was dissolved in a slight excess of dilute HCl. After solution was complete, the excess acidity was neutralized by addition of a few pieces of inactive magnesium metal turnings. After dilution to approximately 2.5 liters with water, the solution was allowed to flow at room temperature through the column at a rate of 2.5 ml/min. Both the magnesium and the sodium activity were completely adsorbed on the column. Elution was then carried out

with $N/10$ HCl, at a rate of 1 ml/min (0.09 ml/cm²/min). At this rate, it had been found previously that the position of the adsorbed magnesium remained relatively fixed while the active Na moved down the column. After about 72 hours of elution, activity began to appear in the eluate. A total of 3.5 liters was then collected, at which point elution of activity was complete. This solution was evaporated to dryness by first heating in a large beaker, then in a small platinum dish after the volume had been reduced. Adsorption of radioactive sodium on Pyrex glass from an HCl solution is negligible; it is, however, appreciable from a neutral or alkaline medium. The small residue left after evaporation was treated with a few drops of concentrated HNO_3 to destroy traces of organic matter which seemed to have been picked up from the resin, then again evaporated to dryness. The weight of residue at this point was about 16 mg. This was taken up in water and reprocessed again on a much smaller column (20 cm high, 0.8 cm in diameter) in the same manner. The final residue after evaporation weighed about 3 mg. The recovery of activity was quantitative and separation from Mg was complete; the residue is due to the small amount of sodium impurity in the original magnesium.

Thanks are due M. Tetenbaum and A. Knudsen for assistance in the preliminary stages of this work.

[1] V. Drehmann, Naturwiss. **33**, 24 (1946).
[2] J. H. Wang and J. W. Kennedy, J. Am. Chem. Soc. **72**, 2080 (1950).
[3] J. Govaerts Bull. Soc. Roy. Sci. Liege **9**, 38 (1940).
[4] J. W. Irvine, Jr., and E. T. Clarke, J. Chem. Phys. **16**, 686 (1948).
[5] R. Bouchez and G. Kayas, Compt. rend. 228, 1222 (1949).

On the Relaxation Time of Equilibrium Systems as Related to Ultrasonic Absorption and Reaction Kinetics

MILTON MANES*
Synthetic Fuels Research Branch, Fuels Technology Division, U. S. Bureau of Mines, Region VIII, Bruceton, Pennsylvania
(Received August 11, 1952)

LAMB and Pinkerton[1] have recently published data on the velocity and absorption of ultrasonic waves in acetic acid. Freedman[2] has showed that these data are consistent with the postulate that the absorption is due to perturbation of the equilibrium between monomeric and dimeric acetic acid,

$$2\mathrm{HOAc} \underset{k_2}{\overset{k_1}{\rightleftarrows}} (\mathrm{HOAc})_2,$$

and with the postulate that the reaction is second order in the forward direction and first order in the reverse direction. The data are not reconcilable with a rate law, which is first order in both directions. Freedman[2] defined the relaxation time τ as equal to k_1.

It can be shown[3] that the approach of a perturbed (one-phase) system to chemical equilibrium from small displacements is a first-order process and that the kinetics of the reaction at equilibrium affect the magnitude of the rate constant for this process. Furthermore, near chemical equilibrium,

$$-d\frac{(a-a^*)}{dt}=\frac{(a-a^*)}{\tau}, \tag{1}$$

where a is any parameter of the system, such as pressure, temperature, or activity of a component, a^* is its value when the system attains equilibrium, and τ is the reciprocal of the first-order rate constant for the process. It is therefore a true relaxation time in the physical sense, characteristic of the particular state of equilibrium and independent of the type of perturbation.† One can substitute τ into the stress-strain differential equation of Hall[4] and find the absorption of sound due to the relaxation of the reaction in the general case:

$$\mu(\nu)=2\pi\cdot\frac{c^2}{c_0^2}\cdot\frac{\beta_0-\beta_\infty}{\beta_0}\cdot\frac{\omega\tau}{1+\omega^2\tau^2}, \tag{2}$$

where μ is the energy absorption coefficient per wavelength, β_0 is the static compressibility ($\nu\to 0$), β_∞ is the instantaneous compressibility ($\nu\to\infty$), $\omega=2\pi\nu$, and c and c_0 are the observed velocities at $\nu=\nu$ and $\nu=0$. Substitution of τ into the quasi-thermodynamic derivation of E. Bauer[5] gives an almost identical result at low values of the absorption.‡ The relaxation time can be related to the kinetics of the reaction

$$aA+bB+\cdots\rightleftarrows qQ+rR+\cdots,$$

by the equation

$$1/\tau=h_f[(a^2/n_A)+\cdots+(q^2/n_Q)+\cdots], \tag{3}$$

provided that the forward and reverse reactions are of the form

$$r_f=k_fG_f(n_A\cdots,n_Q\cdots),\quad r_b=k_bG_b(n_A\cdots,n_Q\cdots),$$

and, at equilibrium,

$$G_b/G_f=K.$$

The concept of the relaxation time for an equilibrium system therefore enables one to calculate expressions for $\mu(\nu)$ for a wide variety of postulated rate laws. Tabuchi[6] has, in effect, done this for ideal gas systems, although he assumed the Guldberg-Waage mass-action law.

The derivation of the equations and a discussion of the implications of these results to possible studies of kinetics by ultrasonic absorption is in preparation.

* Now with Koppers Company, Inc., Pittsburgh, Pennsylvania.
[1] J. Lamb and J. M. M. Pinkerton, Proc. Roy. Soc. (London) **A199**, 114 (1949).
[2] E. Freedman, J. Chem. Phys. **19**, 1318 (1951).
[3] M. Manes (to be published).
[4] L. Hall, Phys. Rev. **73**, 775 (1948).
† It follows that the reaction rate, $r_f=r_b$, at equilibrium, can be measured in terms of the first-order decay constant for any parameter.
[5] E. Bauer, Proc. Phys. Soc. (London) **A62**, 141 (1949).
[6] Tabuchi, J. Chem. Soc. Japan **71**, 329 (1950).
‡ It will be shown (see reference 3) that Eq. (1) is more accurate than the one derived from the quasi-thermodynamic approach.

Transition Temperatures in Solid Solutions of Ammonium Chloride and Ammonium Bromide. A New Transition in Pure Ammonium Bromide

C. C. STEPHENSON AND H. E. ADAMS
Department of Chemistry, Massachusetts Institute of Technology, Cambridge, Massachusetts
(Received July 28, 1952)

THE temperatures at which gradual transitions occur in solid solutions of ammonium chloride and ammonium bromide were determined dilatometrically by Mandleberg and Staveley.[1] Differing results for the same system were given graphically by Cochet-Muchy and Paris,[2] who followed the transformation by differential thermal analysis. This disagreement prompts us to report some measurements on this system made with a simple cooling-curve apparatus. The results are summarized in the following table. All of the temperatures are averages of values obtained on both cooling and warming, except for the lower of the two transitions in the sample containing 9.0 mole percent am-

TABLE I. Results of measurements made with a simple cooling-curve apparatus.

NH_4Br, mole %	Transition temperature, °K
0	242.3±0.3
1.2	239.5±0.3
3.5	234.3±0.2
9.0	202.0−217.5
	241.1±0.3
19.3	256.7±0.3
37.6	269.5±0.3
64.4	267.0±0.3
81.1	255.4±0.3
89.6	246.8±0.3
95.6	240.0±0.2
100.0	234.6±0.2

monium bromide, where marked hysteresis was observed. These results are in satisfactory agreement with those of Mandleberg and Staveley, although at small concentrations of ammonium bromide our temperatures are somewhat lower.

In a more recent investigation[3] of the heat capacity of pure ammonium bromide, another transition was found at about 78°K on cooling, and 108.5°K on warming. This transition corresponds to the transformation at 169°K in ND_4Br.[4]

[1] C. J. Mandleberg and L. A. K. Staveley, J. Chem. Soc. 2736 (1950).
[2] B. Cochet-Muchy and R. A. Paris, Compt. rend. **232**, 1930 (1951).
[3] Stephenson, Cole, and Landers (to be published).
[4] Clusius, Kruis, and Schanzer, Z. anorg. u. allgem. Chem. **236**, 26 (1938).

Spectra of Material Ejected from Plaster by the Impact of Ultraspeed Pellets

WILLIAM C. WHITE AND JOHN S. RINEHART
Michelson Laboratory, U. S. Naval Ordnance Test Station, Inyokern, China Lake, California
(Received August 11, 1952)

As part of the experimentation conducted to study the shapes of craters formed in plaster of paris by ultraspeed pellets,[1] several spectrograms were taken of the impact of the pellet on the plaster to observe the vaporization, if any, of the plaster material. The experimental arrangement was the same as that used for the examination of the spectra of ultraspeed pellets[2] except that a plaster block was placed adjacent to the slit and perpendicular to the face of the spectrograph. With this arrangement, pellets were fired across the slit into the plaster block.

Two types of pellets were fired; one type was made of a special magnesium-lithium-aluminum alloy and the other was of aluminum. The velocity of impact was 5.5 km/sec and 4.5 km/sec, respectively.

Along with the lines and bands of the spectrum of the ultraspeed pellet, calcium lines and calcium oxide bands were identified. These were λλ4227 due to Ca; λλ5473 to 5602 due to Ca and CaO; and λλ5983 to 6097 and λλ6183 to 6362, both due to CaO.

It is evident from the spectrograms that there is a considerable amount of vaporization of the plaster material.

[1] J. S. Rinehart and Wm. C. White, Am. J. Phys. **20**, 14 (1952).
[2] White, Rinehart, and Allen, J. Appl. Phys. **23**, 198 (1952).

Phase Transitions of the Barium Dicalcium *n*-Butyrate

SEI-ICHI KONDO AND TSUTOMU ODA
Laboratory of Physical Chemistry, Osaka Liberal Arts University, Osaka, Japan
(Received August 7, 1952)

We have reported[1] the crystal structure of cubic barium dicalcium *n*-butyrate, $BaCa_2(CO_2CH_2CH_2CH_3)_6$, in which alkyl groups within ionic radicals are rotating, and we have suggested phase transitions which might be attributed to possible changes in rotational modes. We have recently found two phase transitions on this crystal and will give a brief account of our investigation.

The observation under the polarizing microscope shows that by slow cooling the cubic modification changes into an anisotropic one at 5.2°C without remarkable shattering, and by heating it from room temperature up to about 100°C it shows no appreciable changes in appearance. By means of the usual dilatometry, we found two volume changes at about 5.2°C and 50.2°C (Fig. 1), the dilatometer liquids used being evacuated mercury, liquid paraffin, and xylene. The results of the differential thermal analysis, using pure rock salt as standard material, are illustrated in Fig. 2. The

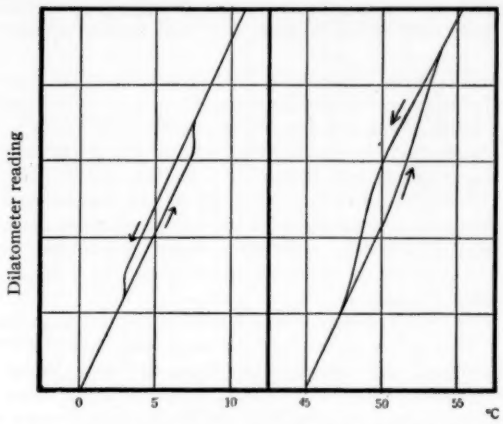

FIG. 1. The dilatometry of $BaCa_2(CO_2CH_2CH_2CH_3)_6$. The cubic thermal expansion coefficient is about 0.2 cc/1 gr mole. The volume change for the lower transition is about 0.3 and for the upper 1.0 cc/1 gr mole, respectively.

double peaks of the lower transition somewhat resemble those in the transition of barium dicalcium propionate at −6.0°C. The peak of the upper transition is very small and flat. The dielectric constant of the powdered sample at 50 kc increases a little, on heating, at 5.2°C, whereas at 50.2°C there is no detectable change.

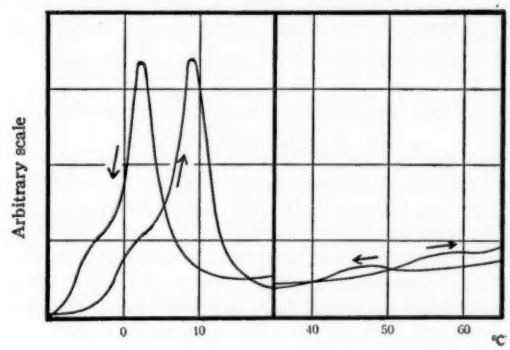

FIG. 2. Differential thermal analysis of barium dicalcium *n*-butyrate. The heating rate of the specimen is about 10 min/deg.

From these results we may deduce a tentative explanation of the mechanism of the transitions as follows: In the lowest anisotropic phase the rotational motion of the *n*-butyrate ion at room temperature is frozen and assumes a lower symmetry. The weak upper transition which is of the higher order type may be looked upon as related to the positional transfer of the carboxyl oxygen atoms between two alternatives.

We thank Professor I. Nitta, Professor T. Watanabe, and Professor S. Seki for their kind encouragement.

[1] Oda, Sakata, and Kondo, J. Chem. Phys. **19**, 1314 (1951).
[2] Seki, Momotani, and Nakatsu, J. Chem. Phys. **19**, 1061 (1951).

Photobromination of Pentane

M. S. KHARASCH, WERNER ZIMMT, AND WALTER NUDENBERG
George Herbert Jones Laboratory, The University of Chicago, Chicago 37, Illinois
(Received August 4, 1952)

It is claimed by Williams and Hamill[1] that "in the photobromination of gaseous *n*-pentane with visible light at 80°, the ratio of all the lower bromides to amyl bromide appears to be approximately 30:70." This ratio was arrived at by addition of

appropriate carrier substances to the bromination mixture obtained when radioactive bromine of a high specific activity was used.

It seemed highly improbable that organic chemists had overlooked the formation of such large quantities of lower bromides, as claimed by Williams and Hamill, in the bromination of normal hydrocarbons. A study was therefore made of the products formed in the vapor phase bromination of *n*-pentane at 80°. Over 94 percent of the theoretically possible amount of bromine used was recovered as amyl bromides, with the rest probably swept out of the apparatus with the hydrogen bromide gas formed in the reaction. A very careful but unsuccessful search was made for low boiling alkyl bromides.

Therefore, it appears to us that the statement of these investigators,[1] "In conclusion, we wish to emphasize that the experimental evidence for considerable fragmentation of the carbon chain in photobromination of *n*-pentane at 80°C seems to us quite inescapable," must be regarded with considerable reserve by organic chemists, and that the technique which led to their erroneous conclusion should be critically examined.

[1] Williams and Hamill, J. Am. Chem. Soc. **72**, 1857 (1950); Hamill, Williams, and Voiland, Brookhaven Conference Report No. 4, p. 90 (1950).

Reduction Potentials and Unsaturation Energy Changes in Electrode Reactions Leading to the Formation of Acridyl Radicals

N. S. Hush
Department of Physical Chemistry, The University of Manchester, Manchester, England
(Received July 31, 1952)

THE occurrence of stable semiquinones as intermediates in the reduction of some phenazines has been studied in detail,[1] mainly by potentiometric methods; but although it has often been proposed that semiquinone formation occurs in reactions involving the corresponding mono-aza hydrocarbons, the acridines,[2] quantitative data for these systems have only recently become available.

I II

FIG. 1. Radical types considered.

The two-step reduction of a series of aminoacridines at the mercury capillary electrode has been studied by Kaye and Stonehill[3] under conditions such that specific adsorption effects (complications arising from which often obscure the significance of current-potential data for systems involving semiquinones) are absent, or are at least greatly minimized. The aminoacridines, in general, reduce in two one-electron steps, both of which may be *p*H-dependent; the first step leads to the formation of radicals of types I or II (Fig. 1), depending on the acidity of the solution.

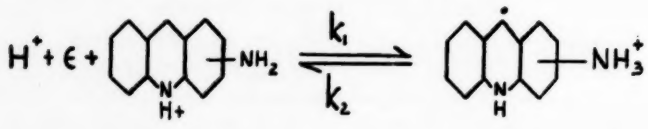

III II

FIG. 2. Reaction of ionized aminoacridine II from radical of type II.

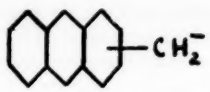

IV

FIG. 3. Anthracenemethyl anion, type IV.

These measurements are useful, as they constitute the only case where quantitative information on semiquinone formation is available over a range of systems of which the oxidants are conjugated molecules which are iso-π-electronic with each other. This being so, it is of interest to inquire whether there is a correlation between the observed reduction potentials and the changes in π-electron energy accompanying the electrode reaction.

In this preliminary treatment, attention is confined to the reaction in which ionized aminoacridine (III) is reduced to an ionized acridyl of type II, as in Fig. 2. Where the rates of all other reactions affecting the concentration of III and II at the electrode interface are small compared to the (composite) rates $k_1(\mathrm{III})(\mathrm{H}^+)$ and $k_2(\mathrm{II})$ at potentials in the vicinity of the half-wave point, we may write,* for a series of aminoacridines,

$$F\delta V_{\frac{1}{2}} = -\delta(\Delta G_a) \simeq \delta Q_a, \qquad (1)$$

where $V_{\frac{1}{2}}$ is the half-wave potential, F is the Faraday, and ΔG_a and Q_a are, respectively, the free energy change and the exothermicity of the reaction in Fig. 2.

The conditions under which (1) is valid are not completely fulfilled for these systems; but, on the assumption that H^+ participates in the transition state of reaction, it may be assumed[4] that partial irreversibility of Fig. 2 will modify the relationship

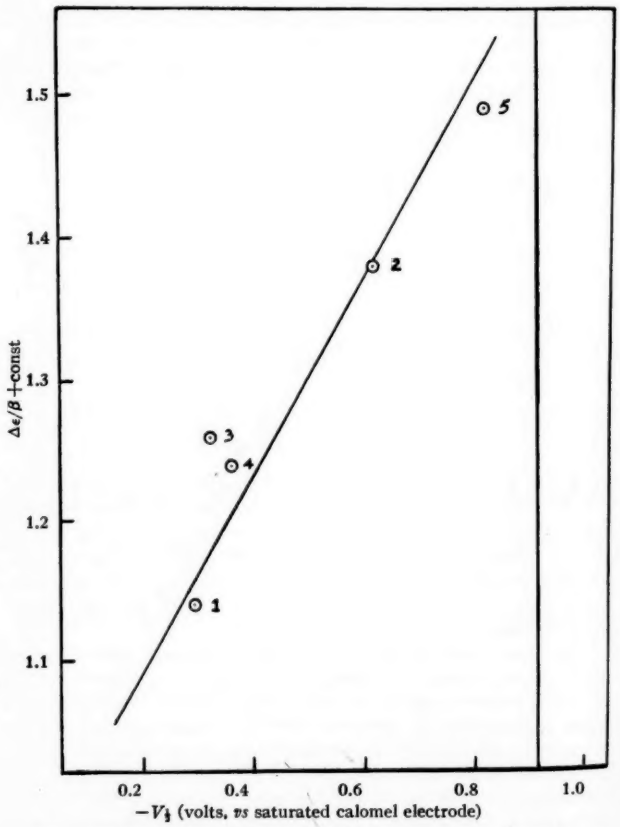

FIG. 4. Observed value of half-wave potential plotted against $\Delta\epsilon/\beta$.

between V_j and Q_a in such a way that (1) may now be reformulated as

$$F\delta V_j \simeq \alpha(\delta Q_a) \quad (1>\alpha>0), \tag{2}$$

so that in either case a linear relationship between V_j and Q_a should obtain.

Variations in $-Q_a$ for the systems we are considering can to a reasonably good approximation be equated to the change of unsaturation energy $\Delta\epsilon$ accompanying the reaction shown in Fig. 2. This may be calculated quite simply by the LCAO MO method, in combination with first-order perturbation theory.[5] Noting that the hydrocarbon iso-π-electronic with III is an anthracenemethyl anion of type IV (see Fig. 3), while that iso-π-electronic with the acridyl II is an anthracene molecule with one electron placed in the lowest unoccupied MO, and taking into account only the effects arising from perturbations of Coulomb integrals of the hydrocarbon species on nitrogen substitution, the energy change $\Delta\epsilon$ may be expressed as

$$\Delta\epsilon = \text{const} - \epsilon_{\text{conj}} - q_1'x - q_2'y, \tag{3}$$

where III is a monoaminoacridine; in Eq. (3), ϵ_{conj} is the conjugation energy of the $-CH_2$ group to the aromatic nucleus in IV, q_1' and q_2' are the net π-electron charge densities at the position of aza-substitution and at the extracyclic atom, respectively, in IV, x is the difference in Coulomb integral of $\diagdown\!\!=\!\!\diagup$N and carbon in the aromatic $\diagdown\!\!=\!\!\diagup$CH grouping, and y is the corresponding difference in Coulomb integral for $-NH_2$ and $-CH_2^-$ in the extracyclic positions. Since q_1' and q_2' are always ≥ 0[6] and the Coulomb terms for nitrogen are more negative than those for the carbon centers, the variable terms in (3) are all of the same sign. The terms x and y should be of comparable orders of magnitude, and for the purposes of this approximate correlation we shall assume $x=y=\beta_{CC}$, where β_{CC} is the $C-C$ resonance integral.

From Eqs. (2), (3), and the foregoing discussion, it follows that the plot of $\Delta\epsilon/\beta$ against $-V_j$ for reactions of the type in Fig. 2 should be roughly linear, with a positive slope. The observed values of $-V_j$ (measured in fifty percent $E+OH$) are plotted against $\Delta\epsilon/\beta$, calculated according to Eq. (3),† in Fig. 4, and it is seen that these predictions are borne out. Although more detailed calculations are desirable, there can be little doubt that the order of reduction potentials correlates simply with the change of unsaturation energy involved in passing from ionized aminoacridine to ionized acridyl radical.

[1] L. Michaelis, Ann. N. Y. Acad. Sci., 40 (1940).
[2] A. Albert, *The Acridines* (Edward Arnold and Company, London, 1951).
[3] R. Kaye and H. Stonehill, (a) J. Chem. Soc. **1951**, 27; (b) **1951**, 2638.
[4] Differences in entropy of reduction are assumed to be small.
[4] M. G. Evans and N. S. Hush, J. chim. phys. **49**, 159 (1952).
[5] H. C. Longuet-Higgins, J. Chem. Phys. **18**, 265, 275 (1950).
[6] C. A. Coulson and H. C. Longuet-Higgins, Proc. Roy. Soc. (London) **A191**, 39 (1947); **192**, 16 (1947).

† For the 2- and 5-isomers, the values of V_j at PHO for the reaction in Fig. 2 have been determined by extrapolation in Fig. 4 and other figures as in Table 2 of Kaye and Stonehill's paper [see reference 3(b)]. In calculating $\Delta\epsilon$, the small effect due to variation in Coulomb integral for aromatic carbon at the point of attachment of the $-NH_3^+$ group in II has been neglected.

Theory of Absorption Spectra of Carotenoids According to Tomonaga-Gas Model of π-Electrons

GENTARO ARAKI AND TOMOKAZU MURAI
Faculty of Engineering, Kyoto University, Yosida, Kyoto, Japan
(Received July 28, 1952)

AN explanation of the relation between absorption spectra and molecular structure of organic dyes was attempted by Kuhn[1] on the basis of quantum mechanics. His theoretical result was not in good agreement with experiment. He neglected interactions between electrons. We have calculated the first excitation energy for carotenoid molecules fully taking into account the interactions, and we have been able to greatly improve the agreement of theory with experiment. A short account of our result will be given in the following:

We consider a one-dimensional longitudinal motion of N electrons in a pipe with a rectangular section. The length and sectional area of the pipe are denoted by L and A, respectively. Tomonaga[2] showed that this system of fermions can be considered as a system of bosons (the Tomonaga gas), and he derived a formula for energy levels of the system in terms of numbers of excited bosons and the one-dimensional potential of two-electron forces. We assume that the one-dimensional potential of Tomonaga is given by an average of the Coulomb potential, of two-electron

TABLE I. Absorption maxima of Carotenoids (λ is measured in mμ).

Carotenoids	N	λ_{obs}	λ_{calc}	δ
Dibenzylbutadiene[a]	4	235	246	0.1078
Dibenzylhexatriene[a]	6	270	272	0.1818
Isodesmethylaxerophtene[b]	8	306	304	0.2873
Isoaxerophtene[b]	8	308	304	0.2873
Axerophtene[c]	10	346	339	0.4209
Desmethylaxerophtene[c]	10	346	339	0.4209
Isoanhydrovitamin A[d]	10	347	339	0.4209
Anhydrovitamin A[d]	12	370	370	0.5819
	14		397	0.7700
Dihydro-β-Carotene[e]	16	420	420	0.9852
	18		438	1.227
Antheraxanthin[f]	20	450	454	1.497
γ-Carotene[g]	22	462	468	1.793
Rubixanthin[h]	22	462	468	1.793
Lycopene[a]	22	472	468	1.793
Rhodoxanthin[i]	24	480	479	2.116
Rhodoviolascin[i]	26	492	489	2.466
	28		497	2.843
Dehydrolycopene[j]	30	504	504	3.247
Decapreno-β-Carotene[k]	30	508	504	3.247

[a] K. W. Hausser and A. Smakula, Angew. Chem. **47**, 657 (1934).
[b] Karrer, Karanth, and Benz, Helv. Chim. Acta **32**, 1036 (1949).
[c] P. Karrer and J. Benz, Helv. Chim. Acta **31**, 1607 (1948).
[d] Isler, Huber, Ronco, and Kofler, Helv. Chim. Acta **30**, 1911 (1947).
[e] P. Karrer and A. Rüegger, Helv. Chim. Acta **23**, 955 (1940).
[f] G. Tappi and P. Karrer, Helv. Chim. Acta **32**, 50 (1949).
[g] Zechmeister, Le Rosen, Schroeder, Polgar, and Pauling, J. Am. Chem. Soc. **65**, 1940 (1943).
[h] R. Kuhn and C. Grundmann, Ber. deut. chem. Ges. **67**, 339 (1934).
[i] P. Karrer and E. Würgler, Helv. Chim. Acta **26**, 116 (1943).
[j] P. Karrer and J. Rutschmann, Helv. Chim. Acta **28**, 793 (1945).
[k] P. Karrer and C. H. Eugster, Helv. Chim. Acta **34**, 28 (1951).

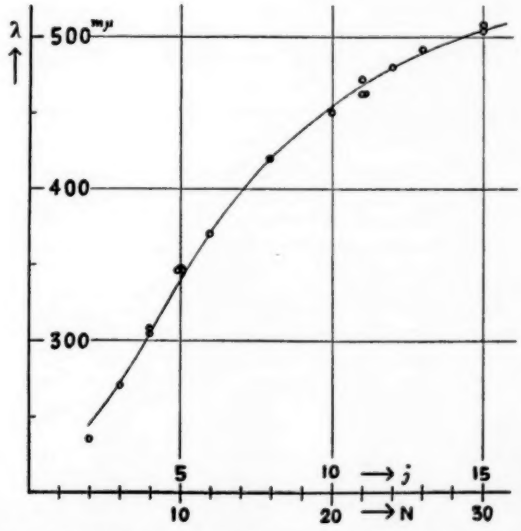

FIG. 1. Relation between absorption maxima and number π-electrons of carotenoids. λ: absorption maximum; j: number of conjugated double bonds; N: number of π-electrons; full curve: present theory; circles: observed values. (See references a–k, Table I.)

repulsive forces, over a transverse section of the pipe. The first excitation energy of the system is then given by

$$\Delta E=(\pi/L)^2(N-2)(1+\delta)^{\frac{1}{2}}, \quad (1)$$

where

$$\delta=(L/\pi)^3(2/A)(N-2)^{-1} \quad (2)$$

indicates a strength of interactions between electrons. (All quantities are measured in atomic units.)

We can apply the equations to carotenoid molecules if we assume that L is the length of a chain of conjugated double bonds in the molecule and that N is the number of π-electrons belonging to the chain. Further, we assume that $L=N(l_1+l_2)/2$, where l_1 and l_2 are the lengths of single and double bonds, respectively. The number of conjugated double bonds is equal to $j=N/2$. The wavelengths of absorption maxima for carotenoids are then given by $\lambda=2\pi c(\Delta E)^{-1}$. The calculated values of λ are compared with experiment in Table I and Fig. 1, where the theoretical values are computed for $l_1+l_2=2.8\text{A}=5.2915$ atomic units and $A=354.8$ atomic units. The comparison is extended to shorter molecules, although the present theory cannot reasonably be applied to such cases. The values of δ are given in the last column. We see that the agreement between theory and experiment is very good and that the effect of the Coulomb interactions between electrons is very large for long carotenoids. A full report of the present theory and result will shortly be published in Progress of Theoretical Physics.

[1] H. Kuhn, J. Chem. Phys. **17**, 1198 (1949).
[2] S. Tomonaga, Prog. Theoret. Phys. **5**, 544 (1950).

Calculated Thermodynamic Properties of GeF_4*

FRED. L. VOELZ
Spectroscopy Laboratory, Department of Physics, Illinois Institute of Technology, Chicago 16, Illinois
(Received July 24, 1952)

THE infrared spectrum of GeF_4 was recently published by Woltz and Nielsen.[1] By using their values of the fundamentals, the heat content, free energy, entropy, and heat capacity of GeF_4 were calculated for 12 temperatures from 100° to 1000°K to a rigid rotator, harmonic oscillator approximation. The calculated values are for the ideal gaseous state at 1 atmos pressure. The masses of the atoms were taken as $m_{Ge}=72.60$ and $m_F=19.00$ awu. Assuming tetrahedral angles and using a Ge−F bond length of 1.67 ± 0.03A as given by Caunt, Mackle, and Sutton,[2] one finds that the moments of inertia are $I_{xx}=I_{yy}=I_{zz}=136.26$ awu A.[2] Birge's 1941 values[3] of the physical constants and a symmetry number of 12 were used throughout the calculations.

The wave numbers corresponding to the fundamental frequencies, and the degeneracies, are given in Table I, and the calculated values of the thermodynamic properties are given in Table II.

TABLE I. Wave numbers and degeneracies for the GeF_4 molecule.

Designation	Wave number (cm^{-1})	Degeneracy
ν_1	740[a]	1
ν_2	200[a]	2
ν_3	800	3
ν_4	260	3

[a] Calculated by Woltz and Nielsen from overtone and combination bands.

TABLE II. Heat content, free energy, entropy, and heat capacity of GeF_4 for the ideal gaseous state at 1 atmos pressure (cal $mole^{-1}$ deg^{-1}).

T(°K)	$(H^0-E_0^0)/T$	$-(F^0-E_0^0)$K	S^0	C_p^0
100	9.17	45.93	55.11	12.12
200	11.92	53.17	65.09	16.70
273.16	13.51	57.13	70.64	18.94
298.16	13.99	58.09	72.08	19.57
300	14.02	58.42	72.44	19.61
400	15.68	62.69	78.37	21.55
500	16.99	66.34	83.33	22.78
600	18.03	69.54	87.57	23.58
700	18.86	72.37	91.24	24.11
800	19.54	74.94	94.48	24.48
900	20.11	77.27	97.38	24.74
1000	20.58	79.41	99.99	24.94

* Part of a research program which is supported in part by the Office of Ordnance Research, Contract No. DA-11-022-ORD-464.
[1] P. J. H. Woltz and A. H. Nielsen, J. Chem. Phys. **20**, 307 (1952).
[2] Caunt, Mackle, and Sutton, Trans. Faraday Soc. **47**, 943 (1951).
[3] R. T. Birge, Revs. Modern Phys. **13**, 233 (1941).

A New Effect of Cold Work on Powder X-Ray Patterns

SHOICHI ANNAKA
Physical Institute, Tokyo University of Education, Tokyo, Japan
(Received July 28, 1952)

THE plastic deformation of metals due to cold work has been long investigated by means of x-ray[1,2] and electron diffraction,[3] as well as by the examination of the change of physical properties such as electric resistance, magnetic susceptibility, etc. According to the x-ray study, the cold work is known to cause the broadening of diffraction lines of powder pattern, and the line broadening is ascribed to the following causes:[2,4] (1) the reduction in the crystal size; (2) uniform and nonuniform strains left in the crystals. Most of the results obtained by the other methods also seem to be consistent with these conclusions, and these phenomena have been generally explained by the repeated slipping or slip band of microscopic and ultramicroscopic steps.

We have recently studied the structural change, caused by cold work, of $AuCu_3$ and AuCu having ordered lattices and found a new type of structure change. Annealed $AuCu_3$ and AuCu were gently filed at room temperature and one-half of each filing was annealed in N_2 gas at 350°C. The x-ray photographs of the filings of $AuCu_3$ and AuCu were taken and compared with those of the annealed filings in ordered state (Figs. 1 and 2). In the case of $AuCu_3$ the changes in the fundamental lines were nearly the same as those of brass studied by Warren.[2] The dimension of coherent region of cold-worked crystal was estimated as about 120A from the broadening of (200) line of $AuCu_3$. A quite different result was obtained with the superlattice lines. The superlattice lines were

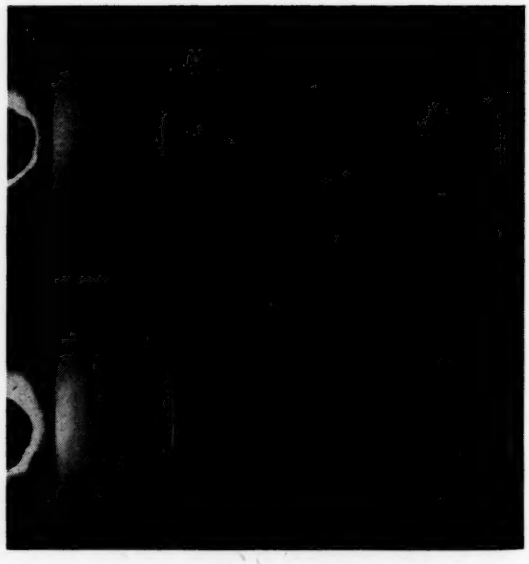

FIG. 1. $AuCu_3$: (a) annealed, (b) filing.

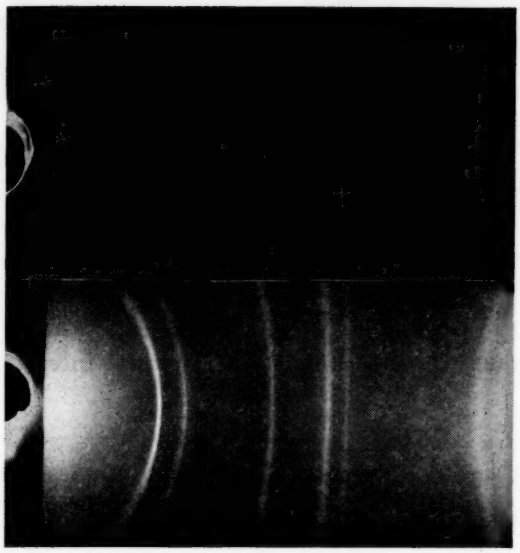

FIG. 2. AuCu: (a) annealed, (b) filing.

hardly found in the cold-worked sample. In the case of AuCu the diffuse lines of face-centered cubic lattice, instead of tetragonal, were obtained in the cold-worked sample, and the superlattice lines again disappeared completely.

These phenomena can hardly be explained by the hypothesis stated above, and we came to the conclusion that the filings of $AuCu_3$ and AuCu were in disordered state. As to the mechanism of disordering due to filing, we may now take two causes into consideration, although the latter cause seems more probable than the former: (1) Atoms exchange their positions randomly. (2) The slipping of extremely small steps occurs parallel to the (111) plane, for example.

The study is now in progress.

In conclusion, the author wishes to express his sincere thanks to Professor Mitsuo Miwa for his encouragement and discussion throughout this work. He is also indebted to the Ministry of Education for financial aids.

[1] G. W. Brindley and F. W. Spiers, Proc. Phys. Soc. (London) **46**, 841 (1934).
[2] B. L. Averbach and B. E. Warren, J. Appl. Phys. **20**, 1066 (1949).
[3] R. D. Heidenreich and W. Shockley, J. Appl. Phys. **18**, 1029 (1947).
[4] P. B. Hirsh, Acta Cryst. **5**, 162, 168, and 172 (1952).

Polarized Infrared Spectrum of Sodium Formate*

ROGER NEWMAN†
Gates and Crellin Laboratories, California Institute of Technology, Pasadena, California
(Received August 8, 1952)

ALTHOUGH the Raman spectrum of the formate ion has been studied by several authors,[1-3] its infrared spectrum has, to our knowledge, not been previously reported. It was hoped that a study of the polarized infrared spectra of single crystals of sodium formate could perhaps remove some of the uncertainty with regard to the assignment of fundamentals and supply additional information of interest. Accordingly, the study whose results are reported here was undertaken.

Sodium formate forms monoclinic crystals of space symmetry, C_{2h}^6, with four molecules/unit cell.[4] Although the positions of the hydrogen atoms are not determined by the x-ray analysis it is assumed, consistent with valence and crystal structure considerations, that the formate ion is planar with symmetry C_{2v}. The two oxygen atoms of the ion are equivalent with the C—O distance,

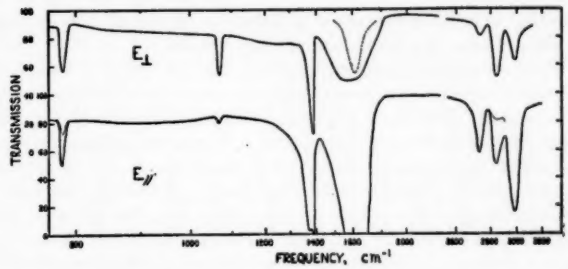

FIG. 1. Polarized spectra of a (010) section of a $NaHCO_2$ single crystal in convergent light (solid curve). Dotted curves show portions of the spectrum of this crystal in unpolarized parallel light. Dashed curve shows a portion of the spectrum of a thin polycrystalline specimen.

1.27A, and the O—C—O angle, 124°. In the crystal the planes of all the formate ions lie parallel to one another and to the **b** axis. In addition the two-fold axes of the ions likewise all lie parallel to **b**. The normal to the molecular planes make an angle of 13° to the **c** axis. In what follows the designations ∥ and ⊥ will refer, respectively, to directions in the (010) plane parallel and perpendicular to the molecular planes.

Evaporation of aqueous solutions of reagent grade sodium formate gives large (usually twinned) fairly thin (010) plates. For use these were further thinned by hand polishing. Spectra were taken with an infrared microscope[5] and a Beckman IR-2 spectrometer. Some observations were made with crystals in the parallel light beam between the source and the monochromator. A silver chloride polarizer was used. The observed spectra are shown in Fig. 1. The frequencies, direction of activity, and assignments are given in Table I.

When a parallel light is incident normal to a (010) crystal plate, it would be expected that only the asymmetric C—O stretch (ν_4) and the in-plane C—H bend (ν_5) would appear for $E_{\parallel}$, and only the out-of-plane C—H bend (ν_6) would appear for $E_{\perp}$. However, with the crystal plate mounted in the convergent beam of the microscope considerable unpolarized contributions from vibrations active parallel to the ions' two-fold axis (i.e., parallel to **b**) will be present.[6] These vibrations are, namely, the C—H stretch (ν_2), the symmetric C—O stretch (ν_1) and the symmetric C—O bend (ν_3). If spectra of a given crystal plate are taken in both the convergent beam of the microscope and in a parallel light beam, these latter bands can be identified. They will show little or no polarization effect in the microscope spectra and will be absent or greatly weakened in the parallel light spectra.

It is on the basis of the method of analysis outlined above and the usual frequency considerations that the assignment of fundamentals given in Table I was obtained. The frequencies found by Fonteyne in his study of the Raman spectrum of solutions of sodium formate are also given Table I. The two sets of data differ in two respects. First, there are perhaps significant differences between some of the frequencies observed for the solid and for the solution. The outstanding example is ν_4. Second, we have ap-

TABLE I. Frequencies (cm^{-1}) observed for $NaHCO_2$.

Activity[a]			Raman effect (ref. 2)	Assignment
∥	⊥	b		
		784	773	ν_3, sym. C—O bend
	1070		1069	ν_6, out-of-plane C—H bend
1365			1386	ν_5, in-plane C—H bend
		1377	1352	ν_2, sym. C—O stretch
1620			1584	ν_4, asym. C—O stretch
2750				$\nu_1+\nu_5$
		2870	2825	ν_2, C—H stretch
2990				$\nu_1+\nu_4$

[a] The designations ∥ and ⊥ refer to the direction in the (010) plane parallel and perpendicular to the plane of the formate ion. The designation b refers to the direction parallel to the **b** axis of the crystal (the C_2 axis of the ion).

parently reversed Fonteyne's assignment of the ν_1 and ν_5 frequencies. These two points are perhaps related.

Our observations in the region from 1350 to 1400 cm^{-1} showed that when the microscope was used, two almost overlapping bands were present. The lower frequency band absorbed only $E_{\perp}$, the higher frequency band was apparently unpolarized. The spectrum in parallel light seemed to indicate the absence of the higher frequency band. (Because of the close spacing of the two bands and the inferior aperture of the crystal, this last feature was not completely established, and no reference to it is shown in Fig. 1.) These results suggested the assignment of ν_1 and ν_5 that we have made. On the other hand, intensity[1] and depolarization[3] measurements of the Raman lines of the solution support Fonteyne's assignment.

If the Raman and infrared frequencies given in the table are taken as correct (the infrared frequencies from 1340 to 1900 are self-calibrated by overlapping H_2O bands), then the difference in frequency for the asymmetric C—O stretch vibration in the two sets of data is perhaps indicative of a strong influence (e.g., hydrogen bonding) of the aqueous solvent on the Raman frequencies. It is then at least conceivable that the frequency of the symetrical C—O stretch could similarly be lowered by solvent action so that a Raman measurement would place it lower than the frequency of the ν_5 vibration.

With respect to the remaining vibrations our results provide an independent, definitive corroboration of Fonteyne's assignments.

* This work was supported by the ONR under contract N-6ori-102, VI.
† Present address: General Electric Research Laboratory, Schenectady, New York. Contribution No. 1719 from the Gates and Crellin Laboratories.
[1] J. T. Edsall, J. Chem. Phys. **4**, 1 (1936).
[2] R. Fonteyne, Naturwiss. **31**, 441 (1943).
[3] J. Gupta, Indian J. Phys. **10**, 313 (1936): **11**, 333 (1937).
[4] W. H. Zachariasen, J. Am. Chem. Soc. **62**, 1011 (1940).
[5] R. M. Badger and R. Newman, Rev. Sci. Instr. **22**, 935 (1951).
[6] The mixing phenomenon was discussed and illustrated in a previous paper, R. Newman, J. Chem. Phys. **20**, 444 (1952).

Erratum: On the Principle of Thermal Interaction

[J. Chem. Phys. **20**, 526 (1952)]

HANS HOLTAN, JR.
Norges Tekniske Hoegskole, Trondheim, Norway

IN the second paragraph, third line, of the above article there is a misprint. It now reads "(no mass concentration)" and it should read "(no bulk mass convection)."